Fluid Mechanics and Machinery

Mohd. Kaleem Khan
Assistant Professor
Department of Mechanical Engineering
Indian Institute of Technology
Patna

OXFORD
UNIVERSITY PRESS

OXFORD
UNIVERSITY PRESS

Oxford University Press is a department of the University of Oxford.
It furthers the University's objective of excellence in research, scholarship,
and education by publishing worldwide. Oxford is a registered trade mark of
Oxford University Press in the UK and in certain other countries.

Published in India by
Oxford University Press
YMCA Library Building, 1 Jai Singh Road, New Delhi 110001, India

First published in 2015

ISBN-13: 978-0-19-945677-2
ISBN-10: 0-19-945677-1

Typeset in BaskervilleMT
by Tata Consultancy Services
Printed in India by Magic International, Greater Noida

Dedicated
to
my family

About the Author

Mohd. Kaleem Khan has been working as an Assistant Professor in the Department of Mechanical Engineering, Indian Institute of Technology Patna (IIT-P) since December 2008. Before joining IIT Patna, he has taught at Thapar University, Patiala and Aligarh Muslim University, Aligarh. He received his Ph D and M Tech. degrees from IIT Roorkee. He has taught many courses and is currently supervising three Ph D students. His areas of interest include mechanics of Newtonian and non-Newtonian fluids, heat transfer and two-phase fluid flow in mini and micro channels, refrigeration and air conditioning, nuclear safety research, solar-thermal systems, and computational fluid dynamics.

Dr Khan has published a number of articles in international peer-reviewed journals and conferences. He is a member of professional bodies of international repute such as the American Society of Mechanical Engineers (ASME) and American Society of Heating, Refrigerating and Air Conditioning Engineers (ASHRAE). In 2012, Dr Khan authored a chapter entitled '*Refrigeration, Air Conditioning and Cold Storage*' in the *Handbook of Food Process Design* published by Wiley-Blackwell, UK. He has successfully completed a sponsored research project funded by the Atomic Energy Regulatory Board (AERB), Government of India. Another sponsored research project funded by Board of Research in Nuclear Science is underway. Besides, he has also reviewed a number of research articles, books, and theses.

Preface

Fluid is a common term used to refer to either a liquid or a gas. The word *fluid* evolved in the 16th century from the Latin word *fluidus* which means *to flow*. From time immemorial, humans, inspired by Mother Nature, have applied the logical approach towards fluids in the making of arks, arrows, spears, irrigation canals, etc. Even today, modern aircraft and submarine designs are inspired by nature's creations such as birds and fishes respectively. Fluid mechanics as a science only dates back to the 17th century, with the beginning of understanding fluids through the fundamental principles of mass, momentum, and energy conservation. The governing equations developed till early 18th century were capable of solving only non-viscous incompressible flow problems. Consequently, there was a major discrepancy between the analytical and experimental results. Only with the advent of Navier–Stokes (N–S) equation by the mid-19th century, were the solutions for viscous incompressible flows made possible. The analytical solutions of N–S equations, except for a few simpler problems, were difficult to achieve.

With the development of numerical techniques and invention of computers in the 20th century, the solutions to many complex flow problems became feasible. In the last few decades, with advancements in high-speed computational devices (i.e., super-computers), the design of rockets, supersonic jets, intercontinental ballistic missiles, and highly efficient turbines are now a reality. However, there are flow problems that are still extremely difficult to formulate and integrate even after using the best available computational facility. Some examples are flow of non-Newtonian fluids, multiphase flows, astrophysical flows, hypersonic flows, etc., whether laminar or turbulent. The development of numerical techniques along with advancements in the existing computational facilities would hopefully give the answers to these challenging problems.

ABOUT THE BOOK

This book is intended to build the fundamental background for undergraduate students in the area of fluid mechanics and machinery. It covers the syllabi of undergraduate courses in fluid mechanics taught at different universities and engineering colleges in India and targets the undergraduate students of mechanical engineering, civil engineering, chemical engineering, physics, and biotechnology.

This book has its own style, especially in the continuity of the topics within the chapter as well as throughout the book. Fluids at rest (fluid statics),

fluids in motion without consideration of forces (fluid kinematics), analyses of forces causing the fluid motion (fluid dynamics), and application of fluids (fluid machinery) is the general pedagogical sequence of the book. The logic behind this sequence is that it is important to understand fluid behaviour at rest before comprehending its motion. The knowledge of features of fluid motion is a prerequisite to understand the visualization of flow. The forces that cause motion in fluids are analysed on the basis of external flow (boundary layer and open channel flows) and internal flow (pipe flow). The compressible flows are introduced after detailed analyses of different types of inviscid and viscous incompressible flows. The design principle of different types of fluid machines working on fluid power is covered only after building the base of different types of flows. The last chapter on dimensional analysis and similitude is included for a thorough understanding of prototypes and their models. This chapter stands alone and can be taught at any point of the course as it does not require complete knowledge of fluid mechanics.

The physical interpretation of different phenomena along with mathematical formulation supported by high-quality figures are the key pedagogic features of this book. Every topic is followed by relevant solved examples for better understanding and clarity. At the end of each chapter, a standout section on the design of laboratory experiments has been included to facilitate learning through experiments among undergraduate students. The methodology adopted in the book not only builds the analytical and numerical skills, but also the experimental design capability of the students.

KEY FEATURES

- Logical sequencing of topics throughout the book
- Physical interpretation of a phenomenon followed by mathematical formulation
- High-quality images to support the concepts discussed
- Practical utility of fluid mechanics fundamentals to real-life situations
- Relevant solved numerical problems of moderate to high difficulty levels after each section
- Chapter-end unsolved numerical problems and review questions requiring critical thinking
- Detailed coverage on flow measurement and pressure measurement techniques
- A unique section on the design of relevant laboratory experiments in each chapter

CONTENT AND STRUCTURE

The book is organized into ten chapters with an intention to develop a systematic understanding of fluid mechanics and machinery in the simplest terms. The following is a brief outline of all the chapters:

Chapter 1 is an introduction to fluids, their properties and classifications, and different computational fluid dynamics (CFD) tools. Fluids and flows are classified on the basis of different parameters. Fluid properties relevant to flows such as density, viscosity, surface tension, etc., are described in detail. This chapter is useful to give a general overview of fluid mechanics.

Chapter 2 deals with fluids at rest. This chapter covers the analyses of submerged planar and curved surfaces, stability of submerged and floating bodies and pressure distribution in rotating and accelerating containers filled with fluids. Evaluation of hydrostatic forces on submerged gates is used to design hydraulic structures like dams. Stability analysis of submerged and floating bodies is useful in the design of boats, ships, and submarines. In addition, the pressure measuring devices such as manometers, bourdon tube and bellow type pressure gauges, and dead weight pressure tester are included.

Chapter 3 deals with fluid kinematics in general and potential flow theory in particular. Flow visualization and salient features of fluid motion are discussed. The concept of stream function and velocity potential functions is introduced, which forms the basis for the potential flow theory. Potential flow is the irrotational flow of ideal (inviscid and incompressible) fluids. Incompressible inviscid flows over a blunt body, and stationary and rotating cylinders are solved analytically in this chapter.

Chapter 4 is dedicated to the development of conservation equations using integral and differential approaches. Laws of conservation of mass, linear and angular momentum, and energy are used to evolve the differential and integral forms of governing equations. The famous Navier–Stokes equation is derived in this chapter. Some simple but important incompressible viscous flow problems such as Hagen Poiseuille flow and Couette flow are solved analytically.

Chapter 5 deals with incompressible viscous external flow over the solid surfaces. The concept of boundary layer is introduced in this chapter. The governing equations for the boundary layer flow are derived. The near-exact and approximate solutions to the laminar boundary layer for a flat plate are obtained. The concept of lift and drag is built by relating it with the development of boundary layer and its separation. A detailed comparison is made between incompressible viscous flow and incompressible inviscid flow past a cylinder to illustrate the role of viscous boundary layer on the overall drag.

Chapter 6 covers incompressible viscous internal flow. Laminar and turbulent flow development inside a pipe and the concept of hydraulic roughness and losses in a pipe are the focus of this chapter. Pipe networks and the methods used for solving flow problems related to them are provided. The concept of hydraulic grade line (HGL) and energy grade line (EGL) are also introduced in this chapter. Moreover, exclusive coverage is given to different types of flow measuring devices such as pitot tube, hotwire anemometer, constriction meters, rotameter and coriolis flow meter for pipes, and mouthpiece, orifice, and siphon for tanks. The phenomenon of water hammer, its causes, and ways to dampen its effect are also featured.

Chapter 7 provides insights into the open channel flows and their classifications. Manning and Chezy correlations for the determination of discharge through the open channels are explained. Evaluation of the most economical section for different channel cross-sections has been presented. The phenomenon of hydraulic jump is elaborated. Flow measurement in open channels using different types of notches/weirs and venturi flume is included.

Chapter 8 covers various aspects of compressible (variable density) flows. A brief section on the review of thermodynamics is included to complement the requirements of compressible flows. Isentropic compressible flows through a varying area duct (i.e., flow through nozzles and diffusers), adiabatic compressible flow through constant area friction duct (i.e., Fanno flow), non-adiabatic flow through the constant area frictionless duct (i.e., Rayleigh flow), and analysis of normal shocks are the key topics in this chapter. Compressible flow over airfoil is also described.

Chapter 9 is dedicated to various types of fluid machinery or more appropriately hydraulic machinery. This chapter is mainly divided under two main categories-power-producing machines (hydraulic turbines) and power-consuming machines (hydraulic pumps). Impact of jets is included as it is a prerequisite to analyse any type of turbo machinery. The chapter has a description of impulse (Pelton) and reaction turbines (Francis and Kaplan) as well as centrifugal and reciprocating pumps. The typical characteristic curves for both pumps and turbines are explained. For the sake of completeness, a section on miscellaneous machines such as hydraulic crane, fluid coupling, torque converter, and hydraulic ram is included.

Chapter 10 introduces the concept of dimensional analysis and similarity between the prototype and its model. A note on physical quantities and their dimensions is incorporated to provide a basis for dimensional analysis using either Rayleigh or Buckingham-pi method. The importance of dimensional analysis is highlighted with the help of GI Taylor's analysis. The concepts of geometric, kinematic, and dynamic similarities are explained to define the complete similarity (similitude) between a prototype and its model.

ONLINE RESOURCES

The following resources are available at the online resources centre for faculty and students using this text:

Faculty:

- PowerPoint slides
- Solutions manual

Students:

- Test generator
- Photographs of certain important experiments and video presentations to supplement concepts discussed

ACKNOWLEDGMENTS

I express my heartfelt gratitude to my Ph D student Mr Siddharth Suman for his constant help and support in the preparation of the manuscript. In fact, he is the first reader who brought the student perspective on the content, which really helped in making this book student-friendly.

I pay my sincere thanks to my colleagues Dr Manabendra Pathak and Dr Akhilendra Singh for providing timely inputs during the preparation of the manuscript. I am also thankful to Dr Nalin Bharti and Dr Rajesh Kumar for their constant motivation.

Last but not the least, I thank my grandfather Dr Mohammed Naimullah Khan, my parents, Mr Mohammed Waseem Khan and Mrs Shamim Rabbani, and my brothers and sisters in the family and my well-wishers whose blessings helped me write this book. I am also thankful to my wife Farah and children Yasir, Rida, and Asjad for their unwavering patience, understanding, and encouragement, as the present work is, in great part, due to their personal sacrifices and support for which I shall ever remain indebted.

Any suggestions for improving this book are welcome. Please send your comments to kalimdme@gmail.com.

MOHD. KALEEM KHAN

Brief Contents

Preface *v*

Features of the Book *x*

Detailed Contents *xiv*

1.	Introduction to Fluids and Fluid Mechanics	1
2.	Fluid Statics	34
3.	Fluid Kinematics	97
4.	Conservation Equations	149
5.	Boundary Layer Flow	211
6.	Pipe Flow	263
7.	Open Channel Flow	333
8.	Compressible Flow	380
9.	Fluid Machinery	459
10.	Dimensional Analysis and Similitude	545

Appendix A: *Properties of Common Fluids* *571*

Appendix B: *Perfect Gas Tables* ($\gamma = 1.4$) *576*

Appendix C: *Uncertainty Analysis* *604*

Appendix D: *Scalar, Vector, and Tensor Quantities* *606*

Glossary *608*

Index *621*

About the Author *627*

Detailed Contents

Preface *v*

Features of the Book *x*

Brief Contents *xiii*

1. Introduction to Fluids and Fluid Mechanics **1**

1.1 Definition of Fluids 1

1.2 Fluid as a Continuum 3

1.3 Classification of Fluids 4

1.4 Properties of Fluids 6

1.4.1 Density *7*

1.4.2 Viscosity *9*

1.4.3 Surface Tension *13*

1.4.4 Capillary Effect *15*

1.4.5 Vapour Pressure *17*

1.5 Classification of Flows 18

1.5.1 Laminar and Turbulent Flows *18*

1.5.2 Viscous and Non-viscous (Inviscid) Flows *19*

1.5.3 Compressible and Incompressible Flows *19*

1.5.4 Subsonic and Supersonic Flows *19*

1.5.5 Steady and Unsteady Flows *20*

1.5.6 Uniform and Non-uniform Flows *20*

1.5.7 One- and Multidimensional Flows *20*

1.5.8 Internal and External Flows *20*

1.6 Introduction to Computational Fluid Dynamics 21

1.6.1 Finite Difference Method *22*

1.6.2 Finite Volume Method *22*

1.6.3 Finite Element Method *23*

2. Fluid Statics **34**

2.1 Pressure 35

2.2 Pascal's Law 36
2.3 Pressure Variation with Depth 38
2.4 Measurement of Pressure 41
2.4.1 Gauge, Vacuum, and Absolute Pressure 41
2.4.2 Bourdon Tube Pressure Gauge 41
2.4.3 Bellows Type Pressure Gauge 42
2.4.4 Dead Weight Pressure Tester 43
2.4.5 Manometers 44
2.4.6 Barometer 52
2.5 Submerged Surfaces 53
2.5.1 Submerged Plane Surface 54
2.5.2 Submerged Curved Surface 63
2.6 Buoyancy and Stability 68
2.6.1 Stability of Submerged Bodies 69
2.6.2 Stability of Floating Bodies 71
2.7 Fluid in a Rigid Body Motion 75
2.7.1 Fluid in an Accelerating Tank 77
2.7.2 Fluid in a Rotating Cylindrical Tank 79

3. Fluid Kinematics 97
3.1 Lagrangian and Eulerian Approaches 97
3.2 Flow Lines 101
3.2.1 Streamline 101
3.2.2 Pathline 102
3.2.3 Streakline 103
3.2.4 Timeline 104
3.3 Features of Fluid Motion 108
3.4 Condition for the Existence of Flow 112
3.5 Stream Function and Velocity Potential Function 114
3.6 Potential Flow 120
3.6.1 Uniform Flow 121
3.6.2 Source and Sink Flows 121

3.6.3 Vortex Flow *123*

3.6.4 Doublet—Combination of Source and Sink of Equal Strengths *125*

3.6.5 Flow over a Blunt Body—Combination of Uniform Flow and Source Flow *128*

3.6.6 Flow Past Circular Cylinder—Combination of Uniform Flow and Doublet *131*

3.6.7 Rotating Circular Cylinder—Combination of Uniform, Doublet, and Vortex Flows *134*

4. Conservation Equations **149**

4.1 Integral Approach 149

4.1.1 Reynolds Transport Theorem *150*

4.1.2 Mass Conservation Principle *153*

4.1.3 Linear Momentum Conservation Principle *154*

4.1.4 Angular Momentum Conservation Principle *164*

4.1.5 Energy Conservation Principle *168*

4.2 Differential Approach 171

4.2.1 Mass Conservation—Continuity Equation *171*

4.2.2 Momentum Conservation—Navier–Stokes Equations *172*

4.3 Steady Incompressible Viscous Flows 182

4.3.1 Flow Between Infinite Parallel Plates *183*

4.3.2 Couette Flow *188*

4.3.3 Fully Developed Laminar Flow through Circular Pipe (Hagen–Poiseuille Flow) *191*

4.4 Energy and Momentum Correction Factors 196

5. Boundary Layer Flow **211**

5.1 Concept of Boundary Layer 211

5.2 Boundary Layer Thicknesses 213

5.2.1 Displacement Thickness *214*

5.2.2 Momentum Thickness *215*

5.2.3 Energy Thickness *215*

5.3 Boundary Layer Equations 219

5.4 Near-exact Solution—Blasius Solution for Boundary Layer Flow over Flat Plate 222
5.5 Approximate Solution—von Karman Momentum Integral Equation 229
5.6 Turbulent Boundary Layer 236
5.7 Boundary Layer Flow over Curved Surface 238
5.8 Boundary Layer Separation 243
5.9 Lift and Drag 247

6. Pipe Flow 263

6.1 Flow Development in Pipe 264
6.2 Losses in Pipe 268
6.2.1 Major Losses 269
6.2.2 Minor Losses 272
6.3 Pipe Networks 279
6.3.1 Pipes in Series 281
6.3.2 Pipes in Parallel 283
6.3.3 Hardy Cross Method 285
6.3.4 Branching Pipes 289
6.4 Hydraulic and Energy Grade Lines 291
6.5 Power Transmission through Pipes 294
6.6 Flow Measurement in Pipes 296
6.6.1 Constriction Meters 296
6.6.2 Pitot-static Tube 301
6.6.3 Rotameter 303
6.6.4 Hot-wire Anemometer 304
6.6.5 Coriolis Flow Meter 305
6.7 Orifice and Mouthpiece 306
6.8 Hydraulic Siphon 309
6.9 Water Hammer 311
6.9.1 Methods to Control Water Hammer 312
6.10 Slurry Flow 314

7. Open-channel Flow **333**

7.1 Classification of Open-channel Flow 333

7.1.1 Classification on the Basis of Reynolds Number *334*

7.1.2 Classification on the Basis of Froude Number *335*

7.1.3 Classification on the Basis of Specific Energy *336*

7.2 Uniform Flow 337

7.2.1 Velocity Distribution *337*

7.2.2 Chezy and Manning Equations *338*

7.2.3 Head Loss due to Friction *340*

7.3 Optimum Hydraulic Cross-section 344

7.4 Non-uniform or Varied Flow 347

7.4.1 Gradually Varied Flow *351*

7.4.2 Rapidly Varied Flow *354*

7.5 Hydraulic Jump 354

7.6 Flow Measurement in Open Channels 359

7.6.1 Notches and Weirs *359*

7.6.2 Venturi Flume *365*

8. Compressible Flow **380**

8.1 Review of Thermodynamics 381

8.1.1 Thermodynamic State Variables *382*

8.1.2 Laws of Thermodynamics *384*

8.2 Velocity of Sound 392

8.2.1 Mach Number *395*

8.2.2 Mach Cone *396*

8.3 Stagnation and Critical Quantities 397

8.4 Non-dimensional Numbers 400

8.5 Effect of Mach Number on Flow Compressibility 405

8.6 Isentropic Flow through Varying Area Ducts 406

8.6.1 Critical Area Ratio *408*

8.6.2 Critical Impulse Function Ratio *409*

8.6.3 Critical Mass Flow Rate *410*

8.6.4 Convergent Nozzles *413*

8.6.5 Convergent–Divergent Nozzles *419*

8.7 Compressible Flow through Constant Area Duct 421

8.7.1 Fanno Flow *421*

8.7.2 Rayleigh Flow *428*

8.8 Shock Waves 435

8.8.1 Prandtl–Meyer Relation *437*

8.8.2 Mach Number Downstream of the Shock *438*

8.8.3 Ratio of Various Quantities across the Shock *439*

8.8.4 Rankine–Hugoniot Relation *442*

8.8.5 Shock Strength *443*

8.9 Compressible Flow over an Airfoil 446

9. Fluid Machinery 459

9.1 Classification of Fluid Machines 459

9.2 Classification of Hydraulic Turbines 461

9.3 Heads and Efficiencies 461

9.4 Impact of Jet 463

9.4.1 Stationary Flat Vertical Plate *463*

9.4.2 Stationary Flat Inclined Plate *464*

9.4.3 Stationary Curved Plate *465*

9.4.4 Moving Flat Plates *465*

9.4.5 Moving Curved Plate *466*

9.5 Pelton Turbine 469

9.5.1 Governing Mechanism *469*

9.5.2 Velocity Triangles and Output Power *472*

9.6 Reaction Turbine 477

9.6.1 Francis Turbine *478*

9.6.2 Kaplan Turbine *483*

9.6.3 Draft Tube *487*

9.6.4 Governing Mechanism of Reaction Turbines *490*

9.7 Unit Quantities 491

9.8 Performance Characteristics of Turbines 494

9.8.1 Main Characteristics 495

9.8.2 Operating Characteristics 496

9.8.3 Muschel Characteristics 498

9.9 Hydroelectric Power Plant 499

9.10 Pumps 500

9.10.1 Centrifugal Pump 500

9.10.2 Pump Characteristics 510

9.10.3 Reciprocating Pump 516

9.11 Miscellaneous Fluid Machines 525

9.11.1 Hydraulic Crane 526

9.11.2 Hydraulic Ram 526

9.11.3 Fluid Coupling 527

9.11.4 Torque Converter 529

10. Dimensional Analysis and Similitude 545

10.1 Dimensional Analysis 545

10.1.1 Dimensions 548

10.1.2 Rayleigh or Indicial Method 548

10.1.3 Buckingham-pi Theorem 551

10.1.4 Taylor Analysis 557

10.2 Similitude 559

10.2.1 Geometric Similarity 559

10.2.2 Kinematic Similarity 560

10.2.3 Dynamic Similarity 561

10.2.4 Distorted Models 565

Appendix A: Properties of Common Fluids 571

Appendix B: Perfect Gas Tables ($\gamma = 1.4$) 576

Appendix C: Uncertainty Analysis 604

Appendix D: Scalar, Vector, and Tensor Quantities 606

Glossary 608

Index 621

About the Author 627

CHAPTER 1

Introduction to Fluids and Fluid Mechanics

LEARNING OBJECTIVES

After studying this chapter, the reader will be able to:

- Infer the concept of fluid, its classification, and common properties
- Get a general understanding of the different types of flow
- Understand when to treat fluid as continuum
- Interpret the basics of the computational fluid dynamics techniques
- Design simple experiments for the measurement of some fluid properties

The chapter gives an introduction to fluids and fluid mechanics. Some of the important fluid properties are also discussed. A chart, shown in Fig. 1.1, has been drawn to understand the various terminologies associated with the broad area of *mechanics*. *Mechanics* is a field of physics that deals with the motion of bodies caused due to the action of forces. It has two sub-categories—*statics* and *dynamics*. *Statics* deals with stationary bodies or bodies at rest, whereas *dynamics* is the study of bodies in motion. In fact, *statics* may be considered as a special case of *dynamics*, when the body is at rest. *Dynamics* has two sub-categories, namely *kinematics* and *kinetics*. *Kinematics* deals with motion only, which is characterized by velocity or/and acceleration, while *kinetics* also takes care of forces that cause motion.

Depending upon the type of matter, the study of mechanics has been grouped into two major areas, viz. *solid mechanics* and *fluid mechanics*. *Fluid mechanics* is a sub-category of mechanics that deals with the behaviour of fluids at rest (*fluid statics*) or in motion (*fluid dynamics*).

A brief introduction to computational fluid dynamics (CFD) has also been included in this chapter.

1.1 DEFINITION OF FLUIDS

Anything that has mass and occupies space is known as *matter*. Matter exists in three forms, namely solid, liquid, and gas. Together liquids and gases are termed as *fluids*. The material's response to applied shear stress also forms

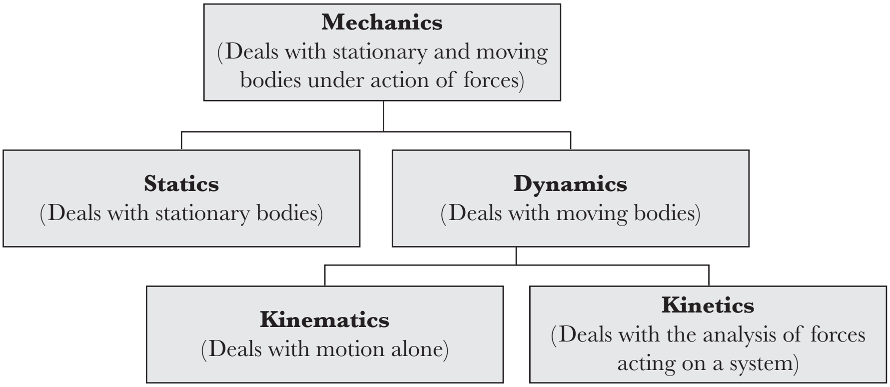

Fig. 1.1 Classification of Mechanics

the basis of distinction between solids and fluids. In solids, the deformation is proportional to the applied stress. The solid body behaves elastically up to a certain value of applied stress, which means that after the removal of stress, the body regains its original shape. According to *Hooke's law*, stress is directly proportional to strain within the elastic limit. Beyond this limit, further loading causes the material to deform permanently. This marks the beginning of the plastic region. Further application of load leads to fracture and failure. *Fluids*, on the other hand, are substances that deform continuously and indefinitely under the action of shear stress. Unlike solids, even the smallest magnitude of shear stress causes deformation in fluids.

According to *Newton's law of viscosity*, shear stress (τ) is directly proportional to strain rate (velocity gradient), that is,

$$\tau = \mu \frac{du}{dy} \tag{1.1}$$

where μ is the constant of proportionality and is a fluid property known as dynamic viscosity (discussed in Section 1.4.2). The term du/dy is known as strain rate or velocity gradient. Figure 1.2 shows the effect of viscous forces on the fluid velocity as it flows over a flat solid surface. Experiments have confirmed that there exists no relative motion between the fluid and the solid surface,

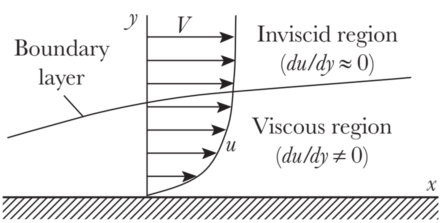

Fig. 1.2 Viscous effects near the surface

that is, the fluid velocity is zero at the surface. This condition is known as *no slip* condition. The fluid velocity starts increasing and approaches main stream velocity V at a certain distance from the surface. At this point, the velocity gradient du/dy approaches zero. Thus, the effect of viscous forces is limited to a thin region near the solid boundary known as the *boundary layer*. Beyond this region, the flow may be treated as *non-viscous* or *inviscid* flow.

1.2 FLUID AS A CONTINUUM

All matter is composed of atoms or molecules. In solids, they are closely packed whereas in fluids, they are widely spaced. In a gas, the molecules are separated by *mean free path*, which may be defined as the average distance travelled by a molecule before its collision with another molecule. The mean free path is dependent upon the pressure and temperature. The concept of continuum disregards the atomic nature of fluids. According to it, the fluids are considered as continuous homogenous matter with no voids or free space. The concept of continuum is valid as long as the characteristic dimension of the system is greater than its mean free path. A non-dimensional number that sets the condition for the applicability of the concept of continuum is *Knudsen number*. It is defined as the ratio of the mean free path of molecules to the characteristic length of the flow channel.

$$Kn = \frac{\lambda}{L} \quad \Rightarrow \quad Kn = \frac{k_B T}{\sqrt{2}\pi d^2 pL} \tag{1.2}$$

where λ is the mean free path, k_B is the Boltzmann constant ($1.3806503 \times 10^{-23}$ J/K), d is the diameter of the fluid particle in metres, T is the temperature in K, p is the total pressure in Pa, and L is the characteristic dimension of the flow system in metres.

The various flow regimes based on Knudsen number are shown in Table 1.1. If the characteristic dimension of the flow system is very small or the gas is available at a very low pressure, the continuum approach cannot be applied. For example, the re-entry of a space shuttle into the earth's atmosphere cannot be analysed using the continuum approach.

Table 1.1 Flow regimes

Range	**Description**
$Kn < 0.01$	Assumption of fluid as continuum is valid
$0.01 < Kn < 0.1$	Slip flow
$0.1 < Kn < 10$	Flow is in transition regime
$Kn > 10$	Free molecular flow governed by kinetic theory of gases

1.3 CLASSIFICATION OF FLUIDS

When a fluid is at rest, the only force that acts on it is pressure force. However, with the flow of fluid, viscous shear stress also comes into picture. The variation of viscous stress with the local strain rate classifies a fluid as *Newtonian* or *non-Newtonian*. This classification is based on the stress–strain behaviour of the fluids as shown in Fig. 1.3. Fluids that follow the Newton's law of viscosity, given by Eq. (1.1), are known as *Newtonian fluids*. That is, in such fluids, shear stress varies linearly with the local deformation rate. Thus, the Newtonian fluid is represented by a straight line passing through the origin in stress–strain graph shown in Fig. 1.3. It should be noted that majority of the fluids (liquids as well as gases) are Newtonian fluids. Water and air are the most common examples of Newtonian fluids.

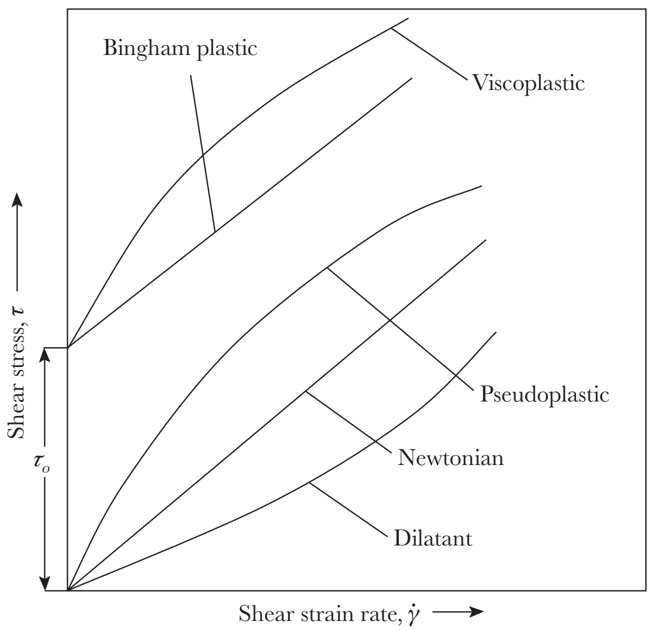

Fig. 1.3 Classification of non-Newtonian fluids

Non-Newtonian fluids do not follow Newton's law of viscosity. In such fluids, shear stress can be related to shear strain rate by the following relationship:

$$\tau = \tau_o + k\left(\frac{du}{dy}\right)^n \tag{1.3}$$

where n is flow behaviour index, k is the consistency index, and τ_o is the minimum shear stress (known as yield stress) required to cause deformation in fluids. Below yield stress, the non-Newtonian fluid behaves like a solid.

All other curves in Fig. 1.3 correspond to different types of non-Newtonian fluids. The following are the examples of non-Newtonian fluids:

1. *Pseudoplastic* (also known as *shear thinning fluids*) ($\tau_o = 0$, $n < 1$), for example, blood, ketchup, syrup, nail polish, etc.
2. *Dilatant* (also known as *shear thickening fluids*) ($\tau_o = 0$, $n > 1$), for example, suspension of corn starch and of sand in water, etc.
3. *Viscoplastic* ($\tau_o \neq 0$, $n < 1$), for example, flubber, nuclear fuel slurries, etc.
4. *Bingham plastic fluids* ($\tau_o \neq 0$, $n = 1$), for example, toothpaste, chocolate, mayonnaise, etc.

It can be seen from Fig. 1.3 that for a given temperature and pressure, the slope of the stress–strain rate curve for non-Newtonian fluids is not constant. The slope of the stress–strain rate curve of such fluids may be written in a similar way as that of Newtonian fluid by expressing Eq. (1.3) as

$$\tau = \eta \frac{du}{dy} \tag{1.4}$$

where $\eta = k(du/dy)^{n-1}$ is known as the *apparent viscosity* and it is greater than the viscosity of water for most of the non-Newtonian fluids.

The detailed description of non-Newtonian fluids is beyond the scope of this book.

Example 1.1 Based on the rheological data provided in the following table, identify the type of fluid.

Deformation rate (s^{-1})	0.0	0.5	1.0	1.5	2.0	2.5	3.0
Shear stress (Pa)	2.00	3.00	3.41	3.73	4.00	4.24	4.45

Solution: Plotting the data in Fig. 1.4.

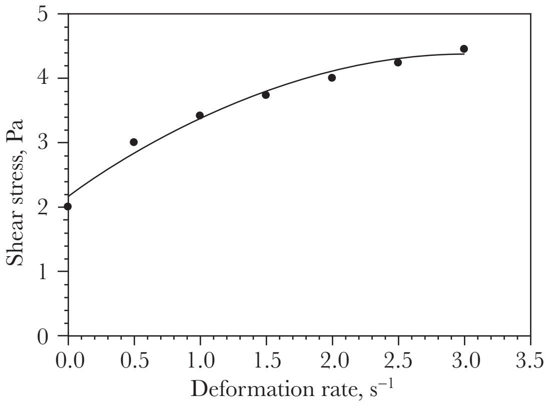

Fig. 1.4

The data in Fig. 1.4 pertain to *viscoplastic fluid*.

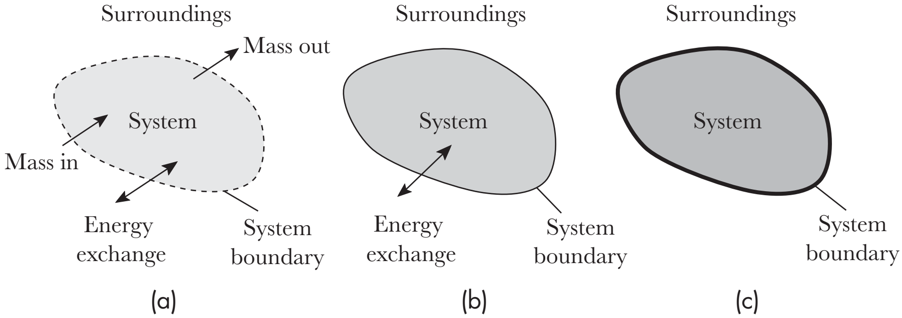

Fig. 1.5 Types of systems (a) Open system (b) Closed system (c) Isolated system

1.4 PROPERTIES OF FLUIDS

A *property* is the characteristic of a *system*. A *system* is defined as a part of the universe consisting of a quantity of matter or region that is under investigation. Anything outside the system is termed as *surroundings*. The system is separated from its surroundings by an imaginary or real surface known as *system boundary*. There are three types of *systems*, namely, *closed system* (also referred as *system*) or *control mass*, *open system* or *control volume*, and *isolated system*, as shown in Fig. 1.5. This classification is based on the interactions of the system with its surroundings. A system is said to be an *open system* if it allows mass to cross its boundaries. However, energy exchange with the surroundings may also take place. The volume of an open system is generally fixed. That is why it is also termed as *control volume*. In a *closed system*, on the other hand, only energy interactions are permissible across the system boundary with no change in the quantity of mass within. In an *isolated system*, the system is completely isolated having no mass or energy interactions with its surroundings. In Fig.1.5, the system boundaries are purposely drawn porous for an open system (to represent the mass exchange), solid and thin for a closed system (to represent no exchange of mass), and solid and thick for an isolated system (to represent no exchange of mass as well as energy).

Pressure, temperature, density, volume, mass, enthalpy, viscosity, etc., are some of the common properties of fluids. These properties are classified as either *intensive* or *extensive* properties. An *intensive property* is independent of the mass of the system, for example, temperature, pressure, density, etc. An *extensive property* is dependent on the size of the system, for example, mass, volume, etc. An easy way to identify whether a property is extensive or intensive can be explained with the help of Fig. 1.6. Consider a system of mass m, volume $\forall$, temperature T, pressure p, and density ρ. On dividing the system into two halves by means of a partition, observe the properties that change due to partitioning. The properties that remain unaffected due to partitioning of the system are

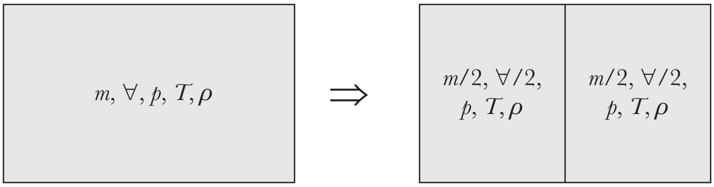

Fig. 1.6 Difference between extensive and intensive properties

temperature, pressure, and density and hence, they are intensive properties. The properties such as mass and volume become half of the original values, that is, they are size dependent. Thus, these properties are termed as extensive properties. Extensive properties per unit mass are known as *specific* properties, for example, specific volume, specific enthalpy, etc.

Some of the important properties of fluids are discussed in the following sections.

1.4.1 Density

Density is defined as mass per unit volume, that is,

$$\rho = \frac{m}{\forall} \tag{1.5}$$

The density of a fluid depends upon temperature and pressure. For most of the gases, the density is directly proportional to pressure and inversely proportional to temperature. An increase in pressure leads to an increase in the density. Similarly, an increase in temperature reduces the density. The density of an ideal gas is related to temperature and pressure by means of the ideal gas law, given by

$$\rho = \frac{p}{RT} \tag{1.6}$$

where R is the specific gas constant. The detailed description for gases is given in Chapter 8. Unlike gases, solids and liquids are incompressible (i.e., density is constant). In fact, solids are essentially incompressible whereas liquids are practically incompressible as the variation in density due to change in pressure and temperature is negligibly small. The SI unit of density is kg/m^3.

Figure 1.7 shows the variation of density of air with temperature and pressure.

Specific volume is another fluid property defined as the reciprocal of density. The term density is more common in fluid mechanics whereas specific volume is preferably used in thermodynamics. The SI unit of specific volume is m^3/kg.

Specific gravity of a fluid is defined as the ratio of density of a given fluid to that of a standard fluid at a specified condition. For liquids, the standard fluid

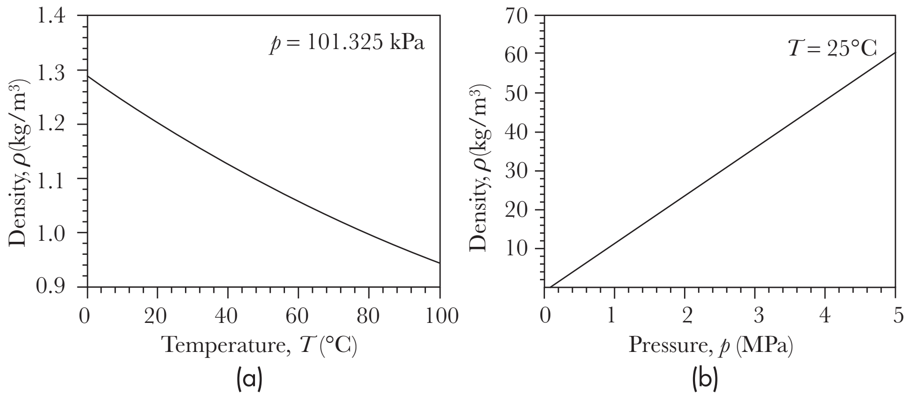

Fig. 1.7 Variation of air density with (a) Temperature (b) Pressure

is water having density 1000 kg/m^3 at 4°C and for gases, the standard fluid is air having density 1.2 kg/m^3 at 20°C temperature and 1 atm pressure. Specific gravity is, thus, given by

$$SG_{\text{liquid}} = \frac{\rho_{\text{liquid}}}{(\rho_{\text{water}})_{4°\text{C}}} \tag{1.7a}$$

$$SG_{\text{gas}} = \frac{\rho_{\text{gas}}}{(\rho_{\text{air}})_{20°\text{C},1\text{ atm}}} \tag{1.7b}$$

Specific weight is defined as the weight of unit volume of a substance, that is,

$$\gamma_s = \rho g \tag{1.8}$$

The SI unit of specific weight is N/m^3.

Example 1.2 If the density of a fluid is 1260 kg/m^3, determine its (a) specific gravity, (b) specific volume, (c) specific weight, and (d) weight for the volume of 7.5 L.

Solution: Given that $\rho = 1260$ kg/m^3

(a) Specific gravity

$$SG = \frac{\rho}{(\rho_w)_{4°\text{C}}} \quad \Rightarrow \quad SG = \frac{1260}{1000} \quad \Rightarrow \quad SG = 1.26$$

(b) Specific volume

$$v = \frac{1}{\rho} \quad \Rightarrow \quad v = \frac{1}{1260} \quad \Rightarrow \quad v = 7.9365 \times 10^{-4} \text{ m}^3/\text{kg}$$

(c) Specific weight

$$\gamma_s = \rho g \quad \Rightarrow \quad \gamma_s = 1260 \times 9.81 \quad \Rightarrow \quad \gamma_s = 12.36 \text{ kN/m}^3$$

(d) Weight

$$W = \gamma_s \forall \quad \Rightarrow \quad W = 12.36 \times 10^3 \times 7.5 \times 10^{-3} \quad \Rightarrow \quad W = 92.7 \text{ N}$$

Example 1.3 Calculate the density and specific weight of nitrogen gas at 25°C and 50 kPa (abs.). If the nitrogen is enclosed in a rigid container, what will be the pressure if the temperature is brought down to −100°C?

Given data: $T_1 = 298$ K, $p_1 = 50$ kPa (abs), and $T_2 = 173$ K

Solution: The specific gas constant for nitrogen can be calculated by dividing the universal gas constant by its molecular mass,

$$R = \frac{R_o}{M} \quad \Rightarrow \quad R = \frac{8.314 \times 10^3}{28} \quad \Rightarrow \quad R = 296.9 \text{ J/kg-K}$$

From ideal gas law (described, in detail in Chapter 8: Compressible flow), the density can be expressed as

$$\rho_1 = \frac{p_1}{RT_1} \quad \Rightarrow \quad \rho_1 = \frac{50 \times 10^3}{296.9 \times 298} \quad \Rightarrow \quad \rho_1 = 0.565 \text{ kg/m}^3$$

The specific weight, from the definition, is

$$\gamma_{s1} = \rho_1 g \quad \Rightarrow \quad \gamma_{s1} = 0.565 \times 9.81 \quad \Rightarrow \quad \gamma_{s1} = 5.544 \text{ N/m}^3$$

Again from the ideal gas law

$$\frac{p_1 V_1}{T_1} = \frac{p_2 V_2}{T_2} \quad \Rightarrow \quad \frac{p_1}{T_1} = \frac{p_2}{T_2}$$

As the container is rigid, volume is not going to change, that is, $V_1 = V_2$

$$p_2 = p_1 \left(\frac{T_2}{T_1} \right) \quad \Rightarrow \quad p_2 = 50 \times \left(\frac{173}{298} \right) \quad \Rightarrow \quad p_2 = 29 \text{ kPa}$$

1.4.2 Viscosity

Viscosity is a measure of fluid friction. When a solid block is dragged over a surface, a friction force appears between the solid and the surface. This force tries to resist the movement of the block on the surface. Similarly, when the body is dragged in a fluid, the fluid also offers a resistance to the motion. It is easy to drag a body in air than in water. The reason being that water is more viscous than air. Thus, *viscosity* is the internal resistance of the fluid to motion. This happens due to the molecular interchange among various layers of fluid and cohesive forces between fluid molecules. When the fluid flows over a solid surface, the velocity of fluid at the solid surface is essentially zero (no-slip condition), and it increases as one moves away from the surface until it approaches free-stream velocity (Fig. 1.2). The flow may be assumed to take place in layers having different velocities. The variation in velocity is attributed to the net rate of molecular interchange from one layer to another. In gases, the molecular interchange with the change in temperature is more predominant than the cohesive forces between

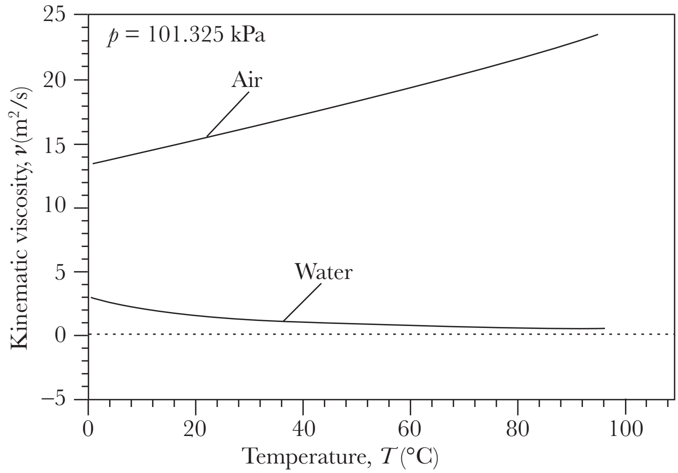

Fig. 1.8 Variation of kinematic viscosity with temperature for air and water

the molecules. With the increase in temperature, the molecular interchange increases leading to an increase in viscosity. In liquids, the cohesive forces are more predominant than the molecular interchange. With the increase in temperature, the cohesive force between the molecules decreases and, thus, the viscosity of liquids decreases. Figure 1.8 shows the variation of viscosity with temperature for air and water. There are two types of viscosity, viz. *dynamic viscosity* and *kinematic viscosity*. The coefficient μ in Newton's law of viscosity, given by Eq. (1.1), is dynamic viscosity. The kinematic viscosity is defined as the ratio of dynamic viscosity to density, that is,

$$\upsilon = \mu/\rho \tag{1.9}$$

The SI units of dynamic and kinematic viscosities are kg/m-s and m^2/s, respectively. Other units are mentioned in Table 1.2.

Table 1.2 Units of viscosity

Dynamic viscosity	
Unit	Equivalent in 'kg/m-s'
1 Pa-s	1
1 N-s/m^2	1
1 poise	0.1
Kinematic viscosity	
Unit	Equivalent in 'm^2/s'
1 stoke	10^{-4}

In addition to the units mentioned in Table 1.2, the viscosity of engine or motor oils is rated in terms of a numerical code system developed by the Society of Automotive Engineers (SAE). The SAE viscosity grading is done in the following way:

1. The SAE is followed with numbers 0, 5, 10, 15, 20, 25, 30, 40, 50, or 60 indicating low to high viscosity.
2. The numbers 0, 5, 10, 15, 20, and 25 are suffixed with the letter 'W' that indicates winter viscosity.
3. The SAE has a separate viscosity rating system for gear, axle, and manual transmission oils.

NOTE

An ideal fluid is one that has zero viscosity (non-viscous/inviscid) and constant density (incompressible).

Example 1.4 If the specific gravity and dynamic viscosity of a fluid at 20°C are 13.6 and 1.526 cP, respectively, determine its (a) specific weight and (b) kinematic viscosity.

Solution: Given that $SG = 1.3$ kg/m^3; $\mu = 1.526 \times 10^{-3}$ kg/m-s

(a) Specific weight

$$\gamma_s = \rho g \quad \Rightarrow \quad \gamma_s = 13.6 \times 1000 \times 9.81 \quad \Rightarrow \quad \gamma_s = 133.4 \text{ kN/m}^3$$

(b) Kinematic viscosity

$$\upsilon = \frac{\mu}{\rho} \quad \Rightarrow \quad \upsilon = \frac{1.526 \times 10^{-3}}{13.6 \times 10^3} \quad \Rightarrow \quad W = 0.112 \times 10^{-6} \text{ m}^2/\text{s}$$

Example 1.5 In Fig. 1.9, if the fluid is SAE 30 at 20°C ($\mu = 0.44$ Pa-s; $\rho = 888$ kg/m^3) and $h = 5$ mm, what shear stress is required to move the upper plate at 5 m/s?

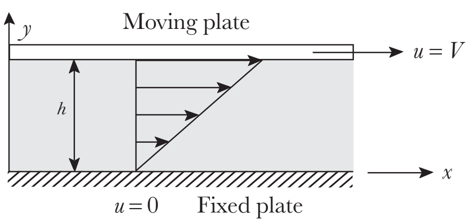

Fig. 1.9

Given data: $T = 293$ K, $\mu = 0.44$ Pa-s, and $h = 5$ mm

Solution: The shear stress can be determined from Newton's law of viscosity

$$\tau = \mu \frac{du}{dy}$$

The velocity gradient du/dy is assumed to be linear if the film thickness is small

$$\frac{du}{dy} = \frac{V}{h}$$

$$\tau = \mu \frac{V}{h}$$

$$\Rightarrow \quad \tau = \frac{0.44 \times 5}{0.005} \quad \Rightarrow \quad \tau = 444 \text{ Pa}$$

Example 1.6 Figure 1.10 shows a circular disk of 80 mm diameter and 1 mm thickness rotating in an oil of viscosity 7×10^{-3} Pa-s in a cylindrical chamber. Determine the damping torque for a rotation speed of 0.5 rad/s.

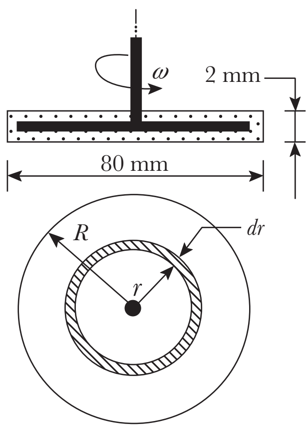

Fig. 1.10

Given data: $\omega = 0.5$ rad/s, $\mu = 0.007$ Pa-s, $R = 40$ mm

Solution: Consider an infinitesimal elemental ring of thickness dr at radius r. The frictional torque by definition is the product of the frictional force and the distance from the axis of rotation. In the present case, the frictional torque on both sides (top and bottom of the disk) of the elemental ring is given by

$$dT_f = 2 \times dF_f r$$

The frictional force on the elemental ring is the product of the elemental area and the shear stress acting on it and thus obtained as

$$dF_f = \tau.dA \quad \Rightarrow \quad dF_f = \tau \times 2\pi r dr$$

From Newton's law of viscosity, the shear stress is given by

$$\tau = \mu \frac{du}{dn}$$

where $\frac{du}{dn} = \frac{\omega r}{\delta}$, where δ is the thickness of the lubrication film on either side of the rotating disk.

The total frictional torque acting on both sides of the disk is obtained by

$$T_f = 2\times \int_0^R \mu\left(\frac{\omega r}{\delta}\right) 2\pi r^2 dr \quad \Rightarrow \quad T_f = \frac{4\pi\mu\omega}{\delta}\int_0^R r^3 dr$$

$$T_f = \frac{\pi\mu\omega R^4}{\delta} \quad \Rightarrow \quad T_f = \frac{\pi \times 0.007\times 0.5\times 0.04^4}{0.5\times 10^{-3}}$$

$$\Rightarrow \quad T_f = \frac{\pi \times 0.007\times 0.5\times 0.04^4}{0.5\times 10^{-3}}$$

$$\Rightarrow \quad T_f = 5.63\times 10^{-5} \text{ N-m}$$

Example 1.7 A 150 mm long sleeve houses a 50 mm diameter rod, shown in Fig. 1.11. The radial clearance between the rod and sleeve is 0.02 mm and is lubricated with an oil of viscosity 800 cP. If the sleeve weighs 15N, determine the sliding velocity of the sleeve when it slides down.

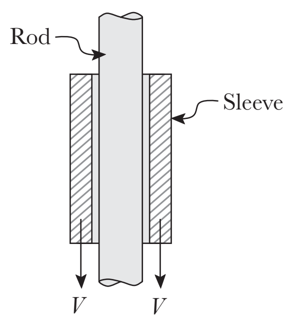

Fig. 1.11

Solution: The viscous shear force acting on the rod is equal to the product of the shear stress acting on the sleeve due to the lubricating oil present in the annulus region and the internal curved surface area of the sleeve, that is,

$$F = \tau(\pi D_i L) = \mu\frac{du}{dr}\pi D_i L \qquad (1)$$

Since the gap between the rod and sleeve is very small, the velocity gradient can be considered as linear. If V is the velocity with which the sleeve comes down, the velocity gradient equals to

$$\frac{du}{dr} = \frac{V}{h}$$

where h is the radial clearance.

The shear force acting on the sleeve balances the effective weight of the sleeve, that is,

$$\Rightarrow \quad 15 = 0.8\times\frac{(\pi\times 50.04\times 10^{-3}\times 0.15)V}{0.02\times 10^{-3}} \quad \Rightarrow \quad V = 0.0159 \text{ m/s}$$

1.4.3 Surface Tension

Surface tension is the consequence of two properties, viz. cohesion and adhesion. *Cohesion* is defined as the intramolecular force of attraction within a liquid whereas *adhesion* is the intermolecular force of attraction at the interface of

a liquid and another fluid or solid. At the interface, a stretched membrane is formed due to cohesive forces between the molecules within the liquid. The molecules in the liquid bulk are pulled equally in all directions by the neighboring molecules. However, the molecules at the interface are pulled only in the downward direction forming a stretched membrane due to the unbalance of forces, as shown in Fig. 1.12.

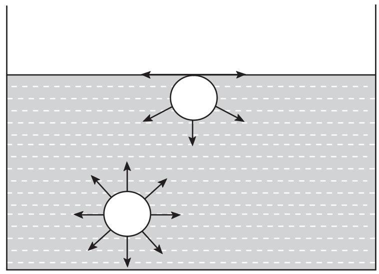

Fig. 1.12 Forces acting on the molecules in different regions of the liquid

The surface tension acts parallel to the surface of liquid and is obtained by dividing the magnitude of the pulling force by the length over which it is acting. Alternatively, the magnitude of the pulling force per unit length is known as *surface tension* and is given by

$$\sigma = F_\sigma / L \tag{1.10}$$

The SI unit of surface tension σ is N/m.

Figure 1.13 shows the cross-section of a pin floating on the surface of a liquid. The liquid surface gets depressed by the pin weight, W. It can be noted

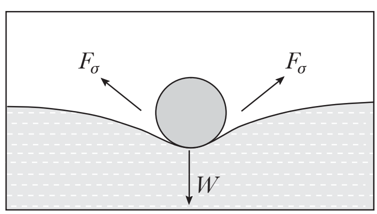

Fig. 1.13 Demonstration of surface tension effect

that the horizontal components of the two surface tension forces F_σ will cancel each other. The weight of the pin is balanced by the vertical components of the two surface tension forces acting on either side of the pin along the liquid surface. The following are a few examples of the surface tension phenomenon:

1. Mercury takes spherical shape
2. Rain droplets are also of spherical shape
3. Razor blades, oil pins, mosquitoes, etc., stay on the water surface

Example 1.8 Consider a vapour bubble of radius $R = 1$ mm in liquid pool as shown in Fig. 1.14. Determine the pressure difference across the liquid–vapour interface if surface tension $\sigma = 0.059$ N/m.

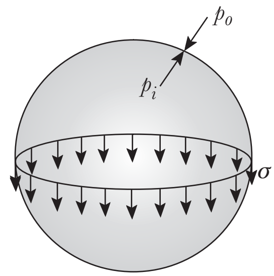

Fig. 1.14

Solution: Under equilibrium conditions, the pressure force will be balanced by the surface tension force.

$$(p_i - p_o)\pi R^2 = \sigma(2\pi R)$$

$$\Rightarrow \quad p_i - p_o = \frac{2\sigma}{R}$$

Substituting the values in the above expression to compute the pressure difference across the liquid–vapour interface.

$$p_i - p_o = \frac{2\sigma}{R} \quad \Rightarrow \quad p_i - p_o = \frac{2\times 0.059}{0.001} \quad \Rightarrow \quad p_i - p_o = 118 \text{ Pa}$$

1.4.4 Capillary Effect

When a liquid droplet falls on a solid surface, it takes a round shape due to its surface tension. The angle formed between the solid surface and the tangent to the liquid droplet periphery at the point of contact is known as *contact* or *wetting angle* φ. This angle is a measure of surface wettability. Depending upon the magnitude of contact angle, the surfaces are classified as *wetting* or *hydrophilic* and *non-wetting* or *hydrophobic* as shown in Fig. 1.15.

For *wetting* or *hydrophilic surface,* $\varphi < 90°$

For *non-wetting* or *hydrophobic surface,* $\varphi > 90°$

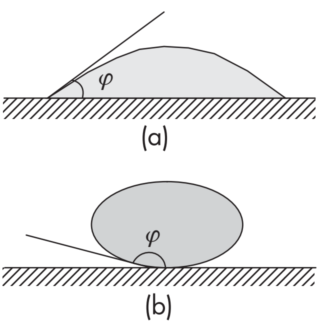

Fig. 1.15 (a) Wetting surface (b) Non-wetting surface

Teflon-coated non-stick cook wares or raincoats have been designed on the basis of the capillary effect.

The rise and fall of a liquid column in a *capillary tube*, a narrow glass tube, when dipped in a pool of liquid is known as *capillary effect* as shown in Fig. 1.16. This is due to the surface tension effect.

As one of the ends of the glass capillary tube is immersed in a wetting liquid such as water, a concave meniscus (shape of the free surface of liquid) is formed. Adhesion forces between the liquid and the solid inner wall of the capillary tube pull the liquid column up until the weight of the lifted liquid column overcomes these intermolecular adhesive forces. The adhesion is stronger than cohesion for a wetting liquid, whereas cohesive forces are stronger than adhesive forces for a non-wetting liquid like mercury. Therefore, there is a capillary fall in non-wetting liquids compared to the more common phenomenon of capillary rise associated with wetting liquids as shown in Fig. 1.16.

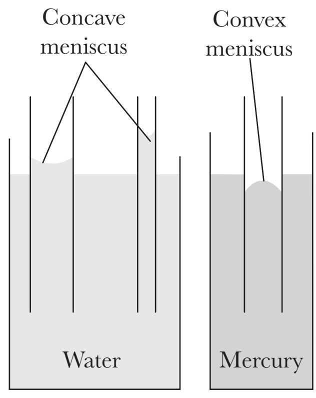

Fig. 1.16 Capillary action

In order to derive the expression of capillary rise, Fig. 1.17 is drawn. If φ is the *contact* (or *wetting*) angle, R is the internal capillary tube radius, and σ is the surface tension, the rise in liquid level h is computed by balancing the weight of liquid rise in the capillary tube with the vertical component of the force due to surface tension (acting between the interface of liquid and internal surface of capillary tube):

$$\rho\pi R^2 hg = \sigma(2\pi R)\cos\varphi \tag{1.11}$$

$$\boxed{h = \frac{2\sigma}{\rho g R}\cos\varphi} \tag{1.12}$$

It should be noted that Eq. (1.12) is applicable to capillary rise (wetting liquids) as well as capillary fall (non-wetting liquids). From this equation, it is clear that a larger diameter tube will have a smaller capillary rise/fall.

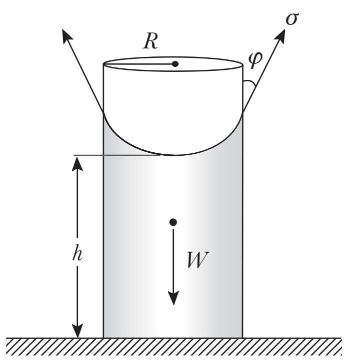

Fig. 1.17 Forces acting on a liquid column during capillary rise

Example 1.9 The surface tension and density of a liquid are 0.063 N/m and 1.260 g/cm^3, respectively. If the liquid rises 5 mm above the outside liquid level in a 3 mm diameter vertical tube, calculate the contact angle.

Solution: The contact angle is obtained from the expression of capillary tube rise

$$\cos\varphi = \frac{\rho g R h}{2\sigma}$$

$$\Rightarrow \quad \cos\varphi = \frac{1260\times 9.81\times 0.0015\times 0.005}{2\times 0.063} = 0.7375$$

$$\varphi = 42.63°$$

Example 1.10 Develop a formula for capillary rise in the annulus region between two concentric glass tubes of radii r_i and r_o and contact angle φ shown in Fig. 1.18.

Solution: Equating the force due to gravity (i.e., weight) of lifted liquid column and force due to surface tension:

$$\rho g h\left(\pi\left(r_o^2 - r_i^2\right)\right) = \sigma(2\pi r_o + 2\pi r_i)\cos\varphi$$

$$h = \frac{2\sigma}{\rho g(r_o + r_i)}\cos\varphi$$

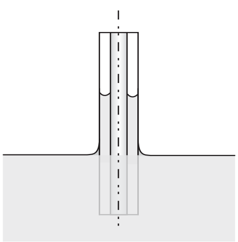

Fig. 1.18

1.4.5 Vapour Pressure

During the evaporation of a liquid in a closed container, the molecules start leaving the free liquid surface and get collected above the interface. In addition, during condensation, the molecules in vapour phase enter into the liquid bulk. At a given temperature, a dynamic equilibrium between liquid and vapour phases is established, that is, the rate of number of molecules leaving the liquid equals the rate of number of molecules entering the liquid. *Vapour pressure* is the pressure exerted by the vapour collected above the liquid surface in a closed container. The vapour pressure corresponding to the dynamic equilibrium is known as the *saturation pressure*. For a pure substance, the *vapour pressure* is same as the *saturation pressure*. The following are the various factors that affect vapour pressure:

Type of fluid Fluids with high intermolecular forces will have low vapour pressure, for example, at 25°C, vapour pressure of water is 3.17 kPa whereas that of ammonia is 1003.2 kPa.

Temperature With the increase in temperature, the vapour pressure increases, for example, at 25°C, vapour pressure of water is 3.17 kPa whereas at 90°C, it is 70.18 kPa.

Surface area Vapour pressure is independent of the surface area of the liquid–vapour interface.

1.5 CLASSIFICATION OF FLOWS

In Section 1.1, the classification of fluids on the basis of stress–strain behaviour has been discussed. In this section, an attempt is made to illustrate the possible ways in which the flow of fluid can be classified as shown in Fig. 1.19. This classification of flow is based on the effect of viscous forces, effect of compressibility, time and space dependence, magnitude of fluid velocity or inertia, flow within bounded and unbounded regions, etc.

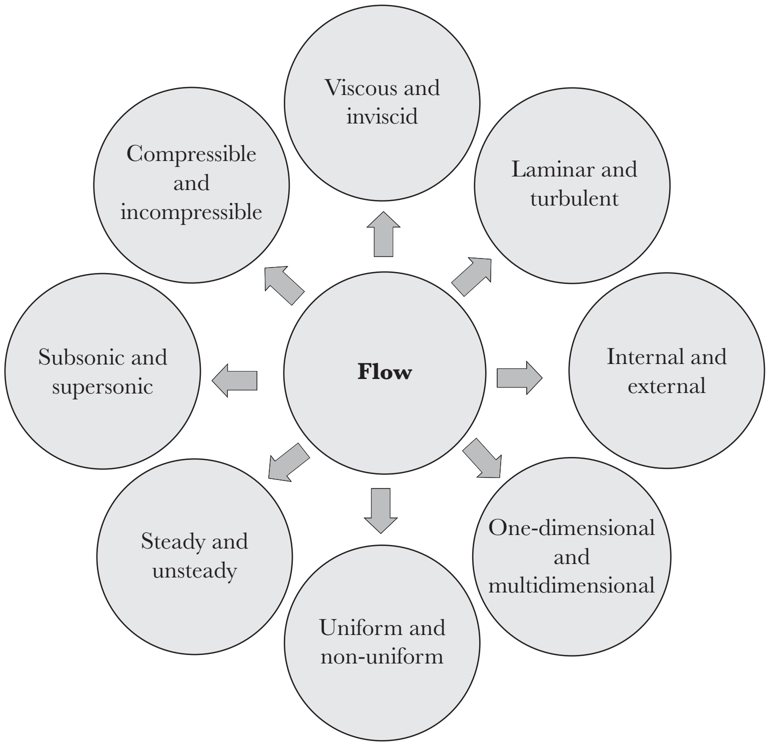

Fig. 1.19 Classification of flows

1.5.1 Laminar and Turbulent Flows

This type of flow classification is based on the relative magnitudes of flow velocity or inertia and viscous shear. A non-dimensional number that relates the inertia force with the viscous force is known as *Reynolds number* (Re), given by the following equation:

$$\mathrm{Re} = \frac{\text{Inertia force}}{\text{Viscous force}} \tag{1.13}$$

Laminar flow is the most ordered flow and is achieved when fluid is flowing at low velocities. In such a case, the flow may be perceived as a movement of laminae (thin planes), one over another. The effect of viscous forces is predominant over inertia forces and as such the value of Reynolds number is small.

Turbulent flow, on the other hand, is a chaotic type of flow where it is difficult to predict the motion of individual fluid particles. The motion is purely random as the effect of inertia forces is predominant. The value of Reynolds number at which the flow transition from laminar to turbulent takes place is known as *critical Reynolds number* (Fig. E3.2).

1.5.2 Viscous and Non-viscous (Inviscid) Flows

An *ideal fluid* is defined as a fluid of constant density and zero viscosity. All the real fluids are viscous in nature. The real fluids also exhibit non-viscous flow phenomena as the effect of viscous forces are limited to a very thin region (known as boundary layer) near the solid surface. The flow within the boundary layer is termed as *viscous flow*. From Newton's law of viscosity, the viscous shear stress is proportional to the velocity gradient or local strain/deformation rate above the solid surface. The velocity gradient becomes negligibly small above the boundary layer. Therefore, the flow of viscous fluids above the boundary layer is treated as *inviscid flow*.

1.5.3 Compressible and Incompressible Flows

The variation in pressure and temperature causes change in the density of fluids. The variation in a material's density due to changes in pressure is explained by a term known as *compressibility*. Solids and liquids are practically incompressible whereas density of gases is susceptible to small variations in pressure and/or temperature. However, it is worth mentioning here that even the flow of compressible fluids, like that of gases, is considered incompressible up to Mach number 0.3. Beyond this value, the effect of compressibility cannot be ignored. The details are available in Chapter 8 of this book.

1.5.4 Subsonic and Supersonic Flows

Compressible flows are further classified on the basis of the magnitude of flow velocity. A non-dimensional number that relates the flow velocity with the velocity of sound in that medium is known as *Mach number*, given by the following equation:

$$M = \frac{\text{Velocity of fluid}}{\text{Velocity of sound}} \tag{1.14}$$

When the fluid velocity equals the sound velocity, the flow is termed as *sonic* flow ($M = 1$). The flow is termed as *subsonic* for $M < 1$ and for $M > 1$, it is known as *supersonic flow*. The passenger and cargo flights generally operate under subsonic flow conditions whereas supersonic fighter jets, ballistic missiles, and rockets operate in a supersonic flow regime. The detailed description is available in Chapter 8.

1.5.5 Steady and Unsteady Flows

Fluid motion is a function of space and time and the fluid velocity is expressed as

$$\vec{V} = \vec{V}(x, y, z, t) \tag{1.15}$$

In general, anything that does not change with time is considered to be in a steady state. If the fluid properties at a point do not change with time, the flow is termed as a *steady flow*. Otherwise, if there is a variation in fluid properties with time, the flow is termed as an *unsteady* or *transient flow*. The turbulent flows are always unsteady by definition.

1.5.6 Uniform and Non-uniform Flows

If at a given instant of time, the magnitude and direction of fluid velocity are same at every point in a flow field, the flow is termed as a *uniform flow*, whereas in *non-uniform flow*, the velocity does not remain the same at every point at a given instant.

1.5.7 One- and Multidimensional Flows

The flow of fluid is said to be *one-dimensional* (1D) if it is taking place in one particular direction. That is, the variation in fluid properties is appreciable in one direction only. The flow domain in such a case is a line and boundaries are the points. A multidimensional flow has appreciable variation in fluid properties in various other directions. For example, a *two-dimensional* (2D) flow is one that takes place in a plane with variation in fluid properties taking place in two different directions. In 2D flows, the domain is plane and boundaries will be represented by lines. In *three-dimensional* (3D) flows, the variation is observed in all the three directions. The flow domain in 3D flows is volume with enclosed planes or surfaces as boundaries.

1.5.8 Internal and External Flows

If the flow is taking place in a region enclosed by a solid surface, it is known as *internal flow*. Flow inside the pipes, ducts, and closed conduits are few examples of internal flows. On the other hand, if the flow is taking place over a solid object, it is termed as *external flow*, for example, flow over an aircraft, submarines, vehicles, etc.

1.6 INTRODUCTION TO COMPUTATIONAL FLUID DYNAMICS

Computational fluid dynamics (CFD) is a computer-based simulation technique used to analyse the problems involving fluid flow and heat transfer. The major applications of CFD are in the fields of aerodynamics, turbo-machinery, internal combustion engines, hydrodynamics, etc. In this technique, governing equations of fluid flow and heat transfer, that is, mass, momentum, and energy conservation equations are solved numerically with the help of computers. In fact, with the development of modern, fast-processing computers and advanced algorithms, CFD has become a versatile technique and a substitute of experimental or analytical techniques for extensive research of fluid dynamics. Moreover, nowadays it is becoming essential to perform a CFD study prior to designing and fabricating costly experimental set-up for reducing the cost and production time. The CFD analysis has several advantages over the experimental approach. The following are some of the advantages:

1. The system performance can be predicted without conducting any experiment on it, resulting in saving huge investments in building models for the test. CFD analysis also helps in saving time.
2. In certain cases, it is difficult to devise laboratory-scale experiments due to problems related to safety or hazardous conditions. Such problems can be solved effectively with the help of CFD.
3. The operating parameters in some of the experiments are difficult or sometimes impossible to control whereas in CFD this can be done very easily.
4. In experimental investigations, the measurements of physical quantities are limited to some specific points of the system where the sensors are placed, whereas the CFD solution provides the magnitude of unknown quantity at any given point in the system. Thus, the results obtained are more versatile and useful.

In CFD analysis, as mentioned earlier, the numerical solution of governing differential equations for a given system geometry is obtained. The three major separate numerical schemes used for performing CFD analysis are the finite difference, finite element, and finite volume methods (FVM) as shown in Fig. 1.20. All these schemes involve conversion of a physical domain (system geometry) into a computational domain. This can be done by discretizing or splitting the physical geometry into a number of infinitesimal elements to form a grid or network. The solution is obtained at nodal points (junctions) in the grid, once the convergence criterion is met.

A small description about each scheme has been provided in the following sections.

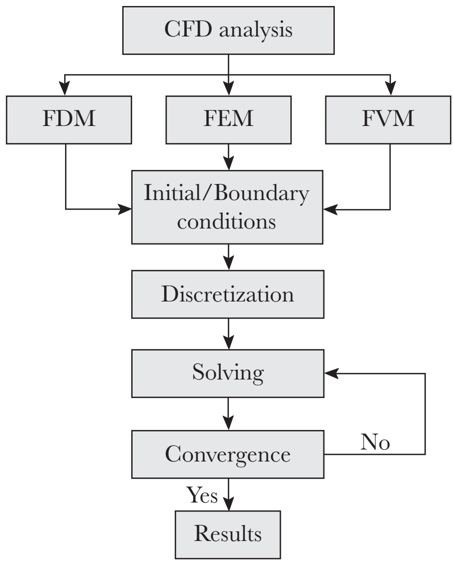

Fig. 1.20 Flowchart for solving a fluid flow problem using any CFD technique

1.6.1 Finite Difference Method

In this technique, the governing differential equations at a particular node (i, j) are converted into difference equations using Taylor series expansion in terms of neighbour nodes, that is, $(i+1, j)$, $(i-1, j)$, $(i, j+1)$, and $(i, j-1)$ as shown in Fig. 1.21, using either of the three backward, forward, and central difference formulation. By this process, a system of simultaneous equations is formed for each node of the computational domain. These simultaneous equations are solved using appropriate numerical methods such as Gauss–Siedel, Gauss elimination, and iterative methods. This technique is simple but limited to only a structured grid, where the connectivity of each node to its neighborhoods is constant.

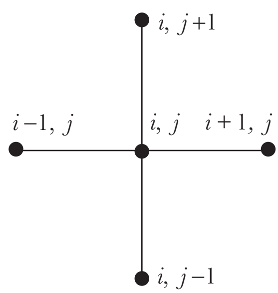

Fig. 1.21 Computational grid for FDM

1.6.2 Finite Volume Method

The FVM is a special category of finite difference methods, where the governing equations are integrated over a small finite or control volumes shown by dotted lines in Fig. 1.22. The integral

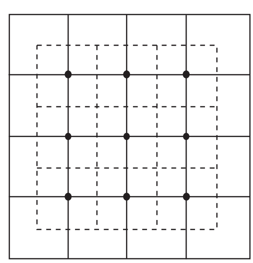

Fig. 1.22 Computational grid for FVM

equations obtained for each control volume is discretized into simultaneous difference equations. The solution for simultaneous system of equations is obtained using the same technique mentioned previously. Since, integral form of equations are used, this method is more versatile than simple finite difference method. The method can be used for a structured as well as an unstructured grid. Some of the commercial softwares based on FVM are ANSYS FLUENT, STAR-CD, PHOENICS, etc.

1.6.3 Finite Element Method

Finite element method (FEM) is a numerical tool to solve partial differential equations obtained as a result of application of laws of conservation of mass, momentum, and energy. Millions of engineers and scientists worldwide use the FEM to predict the behaviour of structural, thermal, fluid, electrical, and chemical systems for design and performance analyses. In this technique, computational domain is discretized in small sub-domains known as finite elements as shown in Fig. 1.23. A solution is approximated in the element for

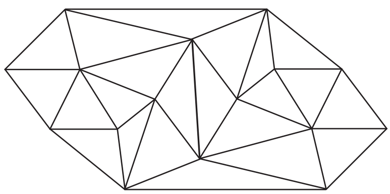

Fig. 1.23 Finite element mesh

the unknown primary variables (velocity, temperatures, displacement, etc.). Over each finite element, approximation functions are derived using the idea that any continuous function can be represented by a linear combination of algebraic polynomials. Element-wise approximation of solution allows modeling of any discontinuous data such as material properties. After approximation, algebraic equations in primary variable are obtained by satisfying the governing equation. The assembly of elements is based on the concept that the solution is continuous at inter-element boundaries. There are many commercially available software packages such as ANSYS, ABAQUS, and NASTRAN that are based on FEM.

A common feature of all the techniques mentioned in Section 1.6 is that they are numerical tools to solve partial differential equations (PDEs). In all these methods, the domain is discretized into smaller parts/elements, and the solution is obtained only at the selected nodal points (junctions). The distinction among these three techniques lies in the way how PDEs are

discretized. It should be remembered that there is nothing like a best method among FDM, FVM, and FEM for any type of problem. The choice is made on the nature of the problem. For example, FDM is popular in solving optimization and flow problems where the domain is regular and simple. In addition, FDM is simpler, easier to implement, and crude compared to FVM and FEM. FVM is popular in fluid flow and heat transfer problems based on discretization of integral form of governing equations solved for control volumes. FEM is popular in structural as well as fluid flow/heat transfer problems and is based on discretization of conservative form of governing equations at nodes. Thus, it has a broader domain compared to the other two techniques and is an obvious choice for dealing with fluid–structure interaction problems.

POINTS TO REMEMBER

- Fluids differ from solids by virtue of their response to applied shear stress. Fluids deform indefinitely whereas solids first deform elastically and then plastically (permanently) until they rupture. In solids, stress is directly proportional to strain whereas in case of fluids stress is directly proportional to strain rate.
- The concept of continuum is applicable when the flow channel dimensions are greater than the mean free path of fluid molecules.
- The easiest way to identify whether a property is extensive or intensive is to divide the chamber containing gas into two parts and see the properties that change due to change in system size. The properties that change are extensive whereas the unchanged properties are intensive properties.
- The effect of viscous forces is limited to the thin region near the solid boundary only. Above this region flow may be treated as non-viscous (inviscid).
- Viscosity increases with temperature in case of gases whereas the opposite happens in case of liquids.
- Surface tension causes the liquid surface to contract to minimal area. This is the reason why the rain drops are spherical and mercury splashes into small balls when fallen on a surface.
- A liquid would wet the surface if forces due to adhesion overcome the forces due to cohesion.
- The capillary rise or fall is a function that is inversely proportional to tube diameter.
- CFD techniques are useful in solving complex flow problems. FVM and FEM are more robust than FDM and they give higher accuracy. FVM is preferred for solving fluid flow/heat transfer problems but FEM is a preferred choice when it comes to solving fluid-structure interaction problems.

SUGGESTED READINGS

Cengel, Y., J.M. Cimbala, *Fluid Mechanics-Fundamentals and Applications*, Tata McGraw-Hill Education, 2010.

Douglas, J.F., J.M. Gasoriek, J.A. Swaffield, L.B. Jack, *Fluid Mechanics*, 5th Ed., Prentice Hall, 2006.

Versteeg, H.K., W. Malalasekera, *An Introduction to Computational Fluid Dynamics-The Finite Volume Method*, 2nd Ed., Prentice Hall, 2007.

MULTIPLE-CHOICE QUESTIONS

1.1 A fluid does not flow
(a) in the presence of pressure
(b) in the presence of shear stress
(c) in the absence of pressure
(d) in the absence of shear stress

1.2 The continuum approach is valid if hydraulic diameter of the flow channel is
(a) less than the mean free path
(b) greater than the mean free path
(c) equal to the mean free path
(d) independent of mean free path

1.3 Mercury forms balls of spherical shape when poured on a flat surface due to the property of
(a) viscosity
(b) density
(c) surface tension
(d) cohesion

1.4 Density of water is 1000 kg/m^3 at a temperature of
(a) 0 K
(b) 273.15 K
(c) 277.15 K
(d) 283.15 K

1.5 Which property will remain unchanged if the system dimensions are changed?
(a) Volume
(b) Mass
(c) Specific enthalpy
(d) Total enthalpy

1.6 Which of the following is a non-Newtonian fluid?
(a) Water
(b) Blood
(c) Beer
(d) Milk

1.7 With temperature, the viscosity of
(a) liquid increases and that of gas decreases
(b) liquid decreases and that of gas increases
(c) both liquids and gases decrease
(d) both liquids and gases increase
(e) remains constant

1.8 The amount of power required to pump a fluid is known as pumping power. It is
(a) more for water and less for air
(b) more for air and less for water
(c) same for both
(d) none of these

1.9 A liquid would wet the solid surface if
(a) adhesion is stronger than cohesion
(b) cohesion is stronger than adhesion
(c) cohesion equals adhesion
(d) independent of cohesion or adhesion

1.10 The non-dimensional number which differentiates a laminar flow from turbulent flow is
(a) Reynolds number
(b) Mach number
(c) Froude number
(d) Knudsen number

1.11 If the specific gravity of a liquid is 1.036, then its density is
(a) 1.036 times that of water
(b) 1036 kg/m^3
(c) 1036 g/m^3
(d) cannot be measured

1.12 The SI unit of surface tension is
(a) N/m^2
(b) N/m
(c) $N\text{-}s/m^2$
(d) $N/m^2\text{-}s$

1.13 Specific weight of water at 4°C at a place, in N/m^3, is
(a) $10g$
(b) $100g$
(c) $1000g$
(d) $981g$
where g is local acceleration due to gravity.

1.14 A liquid will rise in a capillary tube if
(a) diameter is very small
(b) contact angle is less than 90°
(c) liquid density is low
(d) all of these

1.15 The surface tension of a liquid at the critical temperature is
(a) same as that at any other temperature
(b) zero
(c) infinity
(d) indeterminate

1.16 Which of the following is/are true?
(a) The pressure just below the meniscus of water is less than just above it
(b) If the angle of contact is obtuse, the liquid will fall in the capillary tube
(c) Plants suck water from the soil through the roots because of capillarity
(d) All of these

1.17 The non-dimensional number that differentiates subsonic flow from supersonic flow is
(a) Reynolds number
(b) Mach number
(c) Froude number
(d) Knudsen number

1.18 The excess pressure inside a soap bubble is
(a) independent of its radius
(b) directly proportional to its radius
(c) inversely proportional to its radius
(d) inversely proportional to the square root of its radius

1.19 The curve that represents an ideal fluid in Fig. 1.24 is
(a) A
(b) B
(c) C
(d) D
(e) E
(f) F

1.20 The curve that represents a dilatant in Fig. 1.24 is
(a) A
(b) B
(c) C
(d) D
(e) E
(f) F

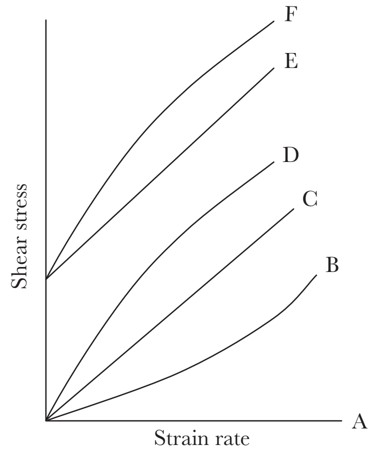

Fig. 1.24

REVIEW QUESTIONS

1.1 Distinguish between the following:
 (a) Fluids and solids
 (b) Shear thinning and shear thickening fluids
 (c) Intensive and extensive properties
 (d) Hydrophilic and hydrophobic surfaces
 (e) Adhesion and cohesion

1.2 When would you apply the continuum approach?

1.3 How would you compute the specific gravity of gases and liquids?

1.4 Why does the kinematic viscosity of liquids decrease and that of gases increase with the increase in temperature?

1.5 What are the methods available for the measurement of dynamic viscosity and kinematic viscosity?

1.6 What are the factors that affect vapour pressure of a fluid?

1.7 Discuss the merits and demerits of CFD techniques namely FDM, FVM, and FEM.

UNSOLVED PROBLEMS

1.1 If the specific gravity of a given liquid is 1.3, determine its (a) specific weight (b) specific volume.

[Ans: (a) 12.753 kN/m^3 (b) 7.692 × 10^{-4} m^3/kg]

1.2 The initial volume of air is 100L in a cylinder fitted with a piston at a pressure of 150 kPa and a temperature of 20°C. If the pressure is doubled and the volume is reduced to 50L, compute the final temperature and density of the air.

[Ans: 293 K, 3.567 kg/m^3]

1.3 Based on the rheological data provided in the following table, identify the type of fluid

Deformation rate (s^{-1})	Shear stress (Pa)
0	1.0
0.5	2.0
1.0	3.0
1.5	4.0
2.0	5.0

[Ans: Bingham fluid]

1.4 The velocity profile for the viscous flow over a flat plate is given by $\mu = 9y - y^2$ for $y \leq 3$. Determine the shear stress at $y = 0$ and $y = 3$ if $\mu = 8.14 \times 10^{-2}$ Pa-s.

[Ans: 0.2442 Pa]

1.5 A 15-kg block, shown in Fig. 1.25, slides on an inclined plane having an angle of inclination of 30° on a 0.1 mm film of SAE 10 oil at 20°C ($\mu = 8.14 \times 10^{-2}$ Pa-s); the area of contact is 0.25 m^2. Find the terminal velocity of the block.

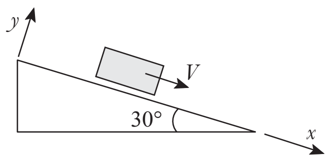

Fig. 1.25

[Ans: 0.36 m/s]

1.6 A 50 mm diameter shaft rotates in a sleeve of 50.3 mm internal diameter and length 100 mm. In the annulus space, a lubricating oil of viscosity $\mu = 0.11$ Pa-s is filled. Calculate the rate of heat generation when the shaft rotates at 200 rpm.

[Ans: 3.157 W]

1.7 A truncated right circular cone with cone angle 60° rotates in a casing at 200 rpm, as shown in Fig. 1.26. A lubricating oil of viscosity 7 mPa-s fills the gap of 2 mm between the cone and the housing. Determine the frictional torque.

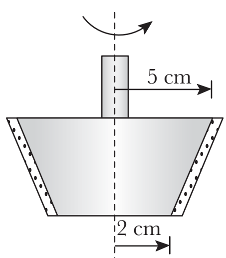

Fig. 1.26

[Ans: 1.4 N-mm]

1.8 Show that the excess pressure in a soap bubble is given by

$$p_i - p_o = \frac{4\sigma}{r}$$

where p_i is the pressure inside the soap bubble, p_o is the pressure outside the bubble, σ is the surface tension, and r is radius of the bubble.

1.9 A glass capillary tube of 1 mm diameter, shown in Fig. 1.27, is used to measure pressure p in the water tank. The temperature of water inside the tank is 30°C. Determine the true water height in the tube to be used for computing the pressure. The surface tension of water corresponding to 30°C is 0.0712 N/m.

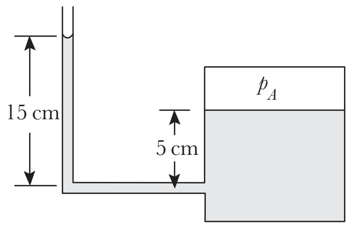

Fig. 1.27

[Ans: 7.78 cm]

1.10 A glass capillary tube of diameter 0.3 mm and length 60 mm is dipped in a water having surface tension 0.017 N/m. The contact angle between the liquid and the tube wall is 40°. Will the water overflow through the tube? If not, comment on the nature and radius of meniscus.

[Ans: No overflow]

Answers to Multiple-choice Questions

1.1 (d)	1.2 (b)	1.3 (c)	1.4 (c)	1.5 (c)
1.6 (b)	1.7 (b)	1.8 (a)	1.9 (a)	1.10 (a)
1.11 (b)	1.12 (c)	1.13 (c)	1.14 (d)	1.15 (b)
1.16 (d)	1.17 (b)	1.18 (c)	1.19 (a)	1.20 (b)

DESIGN OF EXPERIMENTS

Experiment 1.1 Measurement of Surface Tension

Objective

To measure the surface tension of a given liquid using capillary rise method.

Theory

When a narrow glass tube is immersed in the pool of a liquid, there is a rise or fall in the liquid level inside the tube. This phenomenon is called capillary effect, which is due to the liquid property known as surface tension. Surface tension is responsible for the adhesion of liquids onto the contacting solid surfaces. The capillary effect has already been discussed in detail in Section 1.4.4. The rise and fall in liquid level h is given by

$$h = \frac{2\sigma}{\rho g R}\cos\varphi \tag{E1.1}$$

where σ is the surface tension, R is the capillary tube's internal radius, ρ is the liquid density, φ is the contact angle.

Experimental Set-up

The experimental set-up for this experiment is very simple to design, as shown in Fig. E1.1. It consists of glass capillary tubes of different internal diameters fixed on a wooden graduated scale and a beaker containing the liquid whose surface tension is to be measured. If the contact angle between the glass tube and the given liquid is known, Eq. (E1.1) can be used to find out the surface tension of the liquid, that is,

$$\sigma = \frac{\rho g R h}{2\cos\varphi} \tag{E1.2}$$

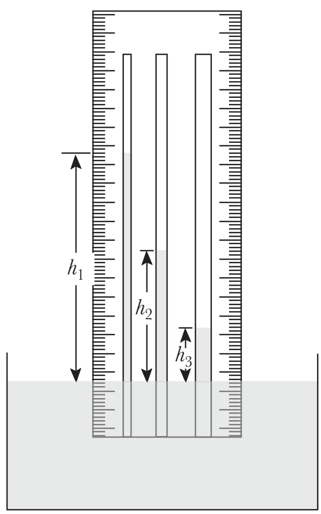

Fig. E1.1 Top view of the test section

Procedure

1. Fill the beaker with the liquid whose surface tension is to be measured.
2. Dip the capillary tube-graduated scale assembly and hold.
3. Note down the meniscus readings in all the tubes.

Observation Table

Density of the given liquid $\rho =$________________________ kg/m^3
Contact angle between the glass tube and the given liquid $\varphi =$__________________

Tube no.	**Radius, R(m)**	**Rise in level, h(m)**	$\sigma_{exp} = \dfrac{\rho g R h}{2\cos\varphi}$ **(Pa)**	$\sigma_{exp} = \dfrac{\sigma_1 + \sigma_2 + \sigma_3}{3}$	**% error** $= \dfrac{\lvert \sigma_{exp} - \sigma_{std} \rvert}{\sigma_{std}} \times 100$
1.					
2.					
3.					

Results and Discussion

Compare the measured value of surface tension with the standard value and discuss the deviation. In addition, plot and discuss the graph σ versus h.

Conclusions

Draw conclusions on the results obtained.

Experiment 1.2 Measurement of Dynamic Viscosity

Objective

To measure the surface tension of a given liquid using Thomas–Stormer viscometer.

Experimental Set-up and Theory

Figure E1.2 shows the schematic diagram of Thomas–Stormer viscometer. It consists of a fixed cylindrical vessel containing the test liquid stirred by a rotating drum. The drum is rotated by a spindle, which is rotated by means of falling weights through a string and pulley arrangement. The principle is that the torque on the rotating drum due to viscous shear is balanced by the thermodynamic work input.

The viscosity of the test liquid filled in a fixed cylindrical vessel stirred by a rotating drum of radius R_D is measured with the help of Newton's law of viscosity Eq. (E1.3), according to which the shear stress is directly proportional to the velocity gradient normal to the solid surface.

$$\tau = \mu \frac{du}{dr} \quad \Rightarrow \quad \tau = \mu C \omega \tag{E1.3}$$

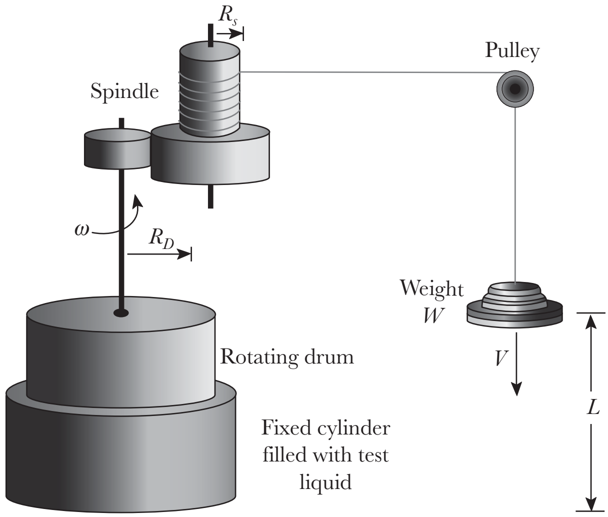

Fig. E1.2 Experimental set-up

where C depends on the viscometer geometry, which sets a particular velocity profile in the liquid, as shown in Fig. E1.3. The frictional (viscous) torque on the rotating drum is given by

$$T_f = (\tau A)R \tag{E1.4}$$

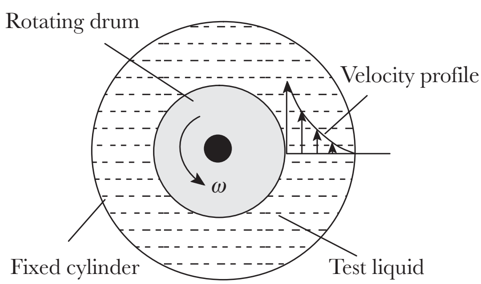

Fig. E1.3

where A is the wetted surface area of the drum and R is mean radius (average of drum radius and cylinder radius). If the losses due to friction in different moving parts are ignored, then viscous power dissipation in the fluid will be equal to the power input of the falling weight.

$$\omega \times T_f = W \times V \quad \Rightarrow \quad \mu C \omega^2 AR = W \times \frac{L}{t}$$

$$\Rightarrow \quad \mu C \omega^2 AR = W \times \frac{2\pi R_s N_s}{t} \tag{E1.5}$$

where N_s is number of turns of the string or number of spindle revolutions and t is the time taken for the weight to cover distance L.

Angular velocity of the drum is given by

$$\omega = \frac{2\pi N_D}{t} \tag{E1.6}$$

where N_D is number of drum revolutions in time t.

From Eqs (E1.5) and (E1.6), the viscosity is obtained as

$$\mu = \frac{R_s N_s}{CARN_D} \frac{W}{\omega} \tag{E1.7}$$

$$\mu = k\frac{W}{\omega} \tag{E1.8}$$

where $k = R_s N_s / CARN_D$. It is evident that k is only dependent upon the geometry of the viscometer.

Procedure

1. Set the Thomas–Stormer viscometer.
2. Fill it with the test liquid (liquid whose viscosity is to be measured).
3. Add the standard weights in a weighing pan and note down the angular velocity of the drum.
4. Repeat the experiment for different weights.

Observation Table

Reading no.	**Weight in the pan, W (N)**	**Drum speed, N (rpm)**	**Angular speed, $\omega = \frac{2\pi N}{60}$ (rad/s)**	**Dynamic viscosity μ_{exp} (kg/m-s)**	**% error** $= \frac{\lvert \mu_{exp} - \mu_{std} \rvert}{\mu_{std}} \times 100$
1.					
2.					
3.					
…					

Results and Discussion

Compare the measured value of viscosity with the standard value and discuss the deviation. In addition, plot and discuss the graph ω versus W/μ.

Conclusions

Draw conclusions on the results obtained.

CHAPTER

2 Fluid Statics

LEARNING OBJECTIVES

After studying this chapter, the reader will be able to:
- Learn the pressure measurement techniques and devices used for the same
- Interpret the concepts of hydrostatic pressure, centre of gravity, centre of pressure, centre of buoyancy, area moment of inertia, metacentre, etc.
- Understand the behaviour of fluids at rest especially in the design of dams, gates, moving and rotating tanks, and stability of floating and submerged bodies

This chapter presents the behaviour of fluids at rest. As discussed in Chapter 1, a fluid is a substance that deforms continuously and indefinitely under the action of shear stresses. Fluid statics deals with motionless fluids, where the forces are solely because of pressure. The forces due to viscous shear stress come into picture only when the fluid is in motion. In this chapter, two situations are analysed: (a) when a fluid may be treated as essentially stagnant and (b) when it behaves like a rigid body. A fluid inside the manometer is essentially stagnant. Likewise, the hydrostatic pressure analysis on submerged surfaces and stability of submerged and floating bodies are done considering the fluid to be motionless. Sometimes the fluid may also be treated as a rigid mass, which means that it does not deform under the action of forces. It is known that shear stresses are responsible for the deformation of any material, whether it is a solid or fluid. No deformation in fluids means the absence of shear stress. Thus, the only stress in such a situation also is the pressure.

A liquid in a uniformly accelerating tank behaves like a rigid mass with each fluid particle having the same acceleration. In addition, the liquid in a tank rotating at a constant angular velocity shows a similar behaviour with each fluid particle rotating at the same angular speed. In these cases, shear stresses are zero because of the absence of relative motion between the fluid particles. The topics covered in this chapter have numerous practical applications, some of which are listed as follows:

1. Pressure measuring devices such as *manometers*, *bourdon tube pressure gauge*, *dead weight pressure gauge tester*, and so on.

2. Design of dams for a water reservoir and design of lock gates by estimating the hydrostatic pressure forces with the help of analyses presented in Section 2.5.
3. Design of a ship, boat, or submarine with the help of analyses presented in Sections 2.6.1 and 2.6.2.
4. Spillage in moving and rotating tanks open from the top with the help of analyses presented in Section 2.7.

2.1 PRESSURE

To define pressure, it is important to understand the concept of stress. When a force is applied on a body, stresses develop inside it. The stress is maximum (theoretical infinite) at the point of application of the force and it diminishes as we move away from it and becomes almost zero at a point far away from it. Therefore, *stress* may be defined as the force per unit area. *Normal stress* is the normal component of force per unit area, whereas *tangential stress* is the tangential component of force per unit area. The force F and its components F_n and F_t are shown in Fig. 2.1. In fluids, the normal stress is known as *pressure* and the tangential stress is called *shear stress*.

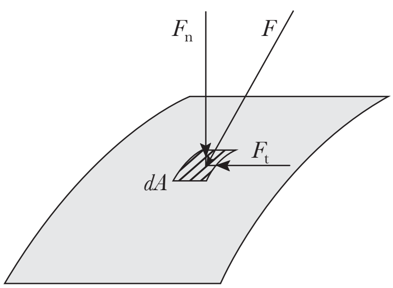

Fig. 2.1 Force acting on a surface

Pressure can also be defined with the help of the kinetic theory of gases, which says that a gas is composed of randomly moving molecules. The root mean square velocity varies as the square root of temperature and is given by

$$v_{rms} = \sqrt{\frac{3k_B T}{m}} \tag{2.1}$$

where k_B is the Boltzmann constant and its value is 1.38066×10^{-23} J/K, T is the temperature in K, and m is the mass of the gas molecule. These molecules collide with each other and with the walls of the container. Therefore, *pressure* may also be defined as the force exerted by the gas molecules colliding the wall

per unit of its area. The SI unit of pressure is pascal (Pa). Pascal is defined as 1 N of force acting on 1 m^2 of area. As 1 N force is almost equal to the weight exerted by a body having mass of 100 g, this means that pascal is a very small unit of pressure. Due to this reason, pressure is usually expressed in kilopascals (kPa) or megapascals (MPa). Various other units of pressure are mentioned in Table 2.1. Commercially available pressure gauges have readings displayed either in pounds per square inch (psi) or in kilogram per square centimetre (kg/cm^2) or in both. The higher values of pressures are usually expressed either in bars or in atms or in MPa. For very low pressures (vacuum), torr is used.

Table 2.1 Units of pressure

Unit	**Equivalent in 'kPa'**
1 kg/cm^2	98.1
1 psi or lb/in^2	6.89
1 mm Hg	0.1333
1 bar	100
1 atm	101.325
1 torr	0.1333 (~1 mm Hg)

2.2 PASCAL'S LAW

Pascal's law is applicable to static fluids, that is, fluids at rest in a container. It states that at a point, a fluid exerts the same pressure in all directions.

Mathematically, it can be proved in the following manner. Consider an infinitesimal wedge-shaped fluid element as shown in Fig. 2.2. The width of

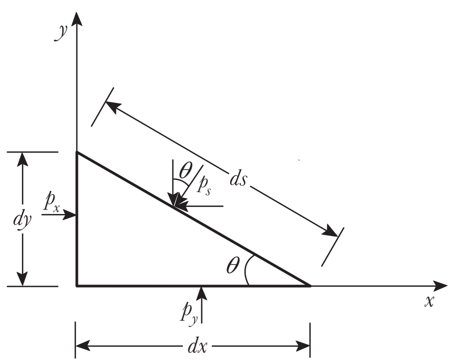

Fig. 2.2 Wedge-shaped fluid element

the wedge (into the paper) is unity. Under equilibrium conditions, the algebraic sum of forces in x and y directions must be zero.

$$\sum F_x = 0 \quad \rightarrow \quad p_x dy = p_s \sin\theta ds \quad \rightarrow \quad p_x dy = p_s dy \quad \rightarrow \quad p_x = p_s$$

$$\sum F_y = 0 \quad \rightarrow \quad p_y dx = p_s \cos\theta ds \quad \rightarrow \quad p_y dx = p_s dx \quad \rightarrow \quad p_y = p_s$$

Hence, $$\boxed{p_x = p_y = p_s} \tag{2.2}$$

This shows that pressure has no direction, that is, it is not a vector quantity. Pressure is thus a scalar quantity. It should be noted that the mass of the wedge-shaped element has not been considered in the analysis due to the fact that the Pascal's law is meant for a point and a point has no mass.

Alternatively, Pascal's law can also be defined as: If the pressure is increased at any point, there is an increase in pressure by the same amount at every other point in the container. Figure 2.3 shows the application of Pascal's law, where two cylinders, fitted with frictionless pistons, are connected through a pipe. The cylinders are filled with a fluid. Subscripts 1 and 2 are used for smaller and larger cylinders, respectively. As the smaller piston is loaded by substituting m_1 kg of weighing mass, the fluid pressure is increased by the same amount at every point in the two cylinders and the connecting line. Thus, the larger piston will also experience the same rise in pressure, and it will be capable of lifting a mass m_2 kg as shown in Fig. 2.3.

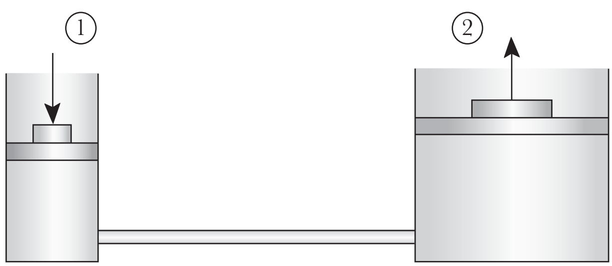

Fig. 2.3 Application of Pascal's law

According to Pascal's law,

$$p_1 = p_2$$

$$\frac{F_1}{A_1} = \frac{F_2}{A_2} \quad \Rightarrow \quad \boxed{F_2 = \frac{A_2}{A_1} F_1} \tag{2.3}$$

With the small effort ($F_1 = m_1 g$), the heavier load ($F_2 = m_2 g$) gets lifted up. Thus, this system is equivalent to a simple lever mechanism, as the force gets amplified.

The *mechanical advantage* is, thus, defined as the ratio of the fall in height of the smaller piston (h_1) to the rise in height of the larger piston (h_2) as the volumes of fluid displaced in each cylinder are equal and is given by

$$\text{Mechanical advantage} = \frac{h_1}{h_2} = \frac{A_2}{A_1} \tag{2.4}$$

where A_1 and A_2 are the cross-sectional areas of pistons 1 and 2, respectively. The mechanical advantage or the Pascal' law finds application in hydraulic jack, hydraulic cranes, hydraulic brakes, dead weight pressure testers, etc.

Example 2.1 A schematic diagram of a hydraulic braking system is shown in Fig. 2.4. If the driver applies a force of 100 N, compute the force F available at the brakes. Take specific gravity of the fluid to be 0.8.

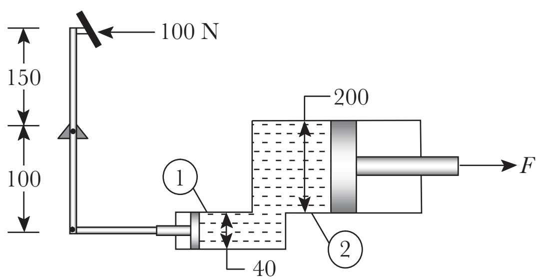

Fig. 2.4

Solution: The force available at the small piston can be calculated by taking moments about the hinge in the vertical lever as shown in the following equation.

$$F_1 = \frac{100 \times 0.15}{0.1} \quad \Rightarrow \quad F_1 = 150 \text{ N}$$

From Pascal's law,

$$\frac{F}{A_2} = \frac{F_1}{A_1} \quad \Rightarrow \quad F = \frac{A_2}{A_1} \times F_1$$

$$\Rightarrow \quad F = \frac{200^2}{40^2} \times 150 \quad \Rightarrow \quad F = 3.75 \text{ kN}$$

2.3 PRESSURE VARIATION WITH DEPTH

If a fluid is at rest, the pressure is not same as one moves deeper into it. The pressure increases linearly with depth, as more fluid rests on the deeper fluid layers. At the free surface, the only pressure is the atmospheric pressure. While going deeper into the fluid, the pressure due to increasing fluid weight keeps on

adding to the atmospheric pressure. Consider an infinitesimal rectangular fluid element of dimensions dx and dy in x and y directions, respectively, in the bulk of the fluid. Let the upper edge of the element experience pressure p whereas pressure at the lower edge is $p + dp$. The pressure at the right and left edges will cancel out each other. At the free liquid surface, the pressure is atmospheric (i.e., gauge pressure is zero) (refer to Section 2.4.1 for details).

Under equilibrium conditions

$$\sum F_z = 0 \quad \Rightarrow \quad pdx - (p + dp)dx + dm \times g = 0$$

$$\Rightarrow \quad pdx - (p + dp)dx + \rho(dxdz \times 1)g = 0$$

$$\Rightarrow \quad dp = \rho g dz \quad \Rightarrow \quad p = \rho gz + C$$

At $\quad z = 0,\ p = 0 \quad \Rightarrow \quad C = 0$

Hence, $$\boxed{p = \rho gz} \tag{2.5}$$

The pressure in this expression is termed as *hydrostatic pressure* (*hydro* means water and *static* means motionless). It can be seen from Eq. (2.5) that the hydrostatic pressure is directly proportional to the fluid density and the depth. At a given depth, higher the fluid density higher will be the hydrostatic pressure. This is the reason why mercury is used in manometers for the measurement of high pressures. The pressure profile, shown in Fig. 2.5, is linear. The pressure indicated in the profile is the gauge pressure (explained in the subsequent section). The hydrostatic pressure is constant at a given depth in a horizontal plane and is independent of the shape of the container (Fig. 2.6). It must be noted that the pressure acts always perpendicular to the surface, as shown by arrows in the figure. The hydrostatic pressure at points A, B, C,…, and J will

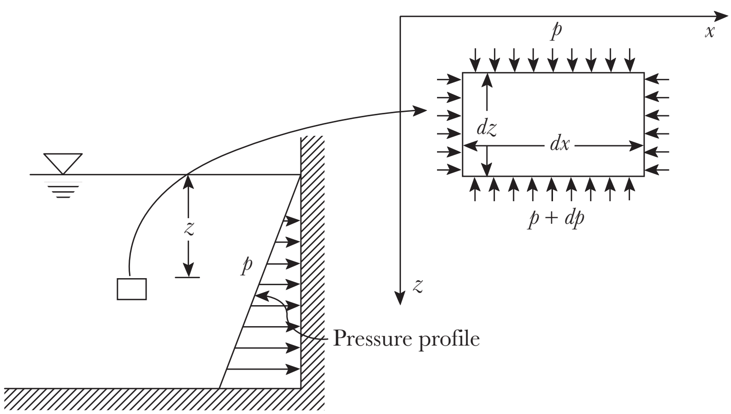

Fig. 2.5 Pressure variation with depth

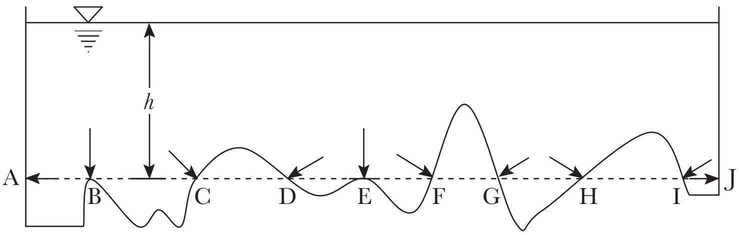

Fig. 2.6 Constant pressure at a given depth

be the same (i.e., ρgh) as all these points lie on the same horizontal plane at a depth of h from the free surface.

$$p_A = p_B = p_C = p_D = p_E = p_F = p_G = p_H = p_I = p_J = \rho gh \tag{2.6}$$

Example 2.2 A 4 m deep tank of uniform cross-section is completely filled with water and oil (SG = 0.9) in equal volumes. Determine the pressure at the interface of the two fluids and at the bottom of the tank. Draw the pressure profile along the depth. Take p_{atm} = 101.325 kPa.

Solution: Since the specific gravity of oil is lower than that of water, it will occupy the upper portion of the tank as shown in Fig. 2.7. In addition, since the volumes of the two fluids are same, each fluid will occupy half of the total volume of the tank (as it is completely filled). Pressure at the interface of the two fluids is only due to oil, that is,

$$p_{\text{interface}} = p_{\text{atm}} + \rho_o g h_o \quad \Rightarrow \quad p_{\text{interface}} = (101.325 + 0.9 \times 9.81 \times 2) \times 10^3$$

$$\Rightarrow \quad p_{\text{interface}} = 119 \text{ kPa}$$

Pressure at the bottom of the tank is

$$p_{\text{bottom}} = p_{\text{atm}} + \rho_o g h_o + \rho_w g h_w$$

$$p_{\text{bottom}} = (101.325 + 0.9 \times 9.81 \times 2 + 9.81 \times 2) \times 10^3 \quad \Rightarrow \quad p_{\text{bottom}} = 138.6 \text{ kPa}$$

The pressure profile is shown in Fig. 2.7.

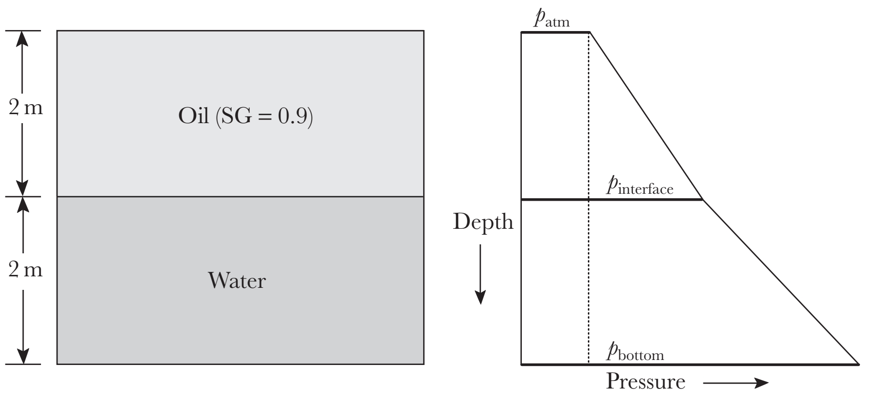

Fig. 2.7

2.4 MEASUREMENT OF PRESSURE

A number of instruments are commercially available to measure pressure. The most common of them are bourdon tube pressure gauge and manometers. Other pressure-measuring instruments are pressure transducers and piezoelectric sensors. Before the description of pressure gauges and manometers, it is important to understand the concept of gauge, vacuum, and absolute pressure.

2.4.1 Gauge, Vacuum, and Absolute Pressure

The *absolute pressure* (p_{abs}) is the actual pressure at a point. The pressure above the atmospheric pressure is called *gauge pressure* (p_g) and the pressure below the atmospheric pressure is termed as *vacuum pressure* (p_v). The gauge pressure, as the name suggests, is measured by a pressure-measuring gauge. Similarly, for the measurement of vacuum pressure, vacuum gauges are available. A compound gauge measures both positive (gauge) and negative (vacuum) pressures. Such instruments always indicate zero corresponding to the atmospheric pressure. Figure 2.8 shows the difference between absolute, gauge, and vacuum pressures. If p_g, p_v, and p_{abs} represent gauge, vacuum, and absolute pressures, respectively, the following relations can be derived:

$$p_{abs} = p_{atm} + p_g \tag{2.7a}$$

$$p_{abs} = p_{atm} - p_v \tag{2.7b}$$

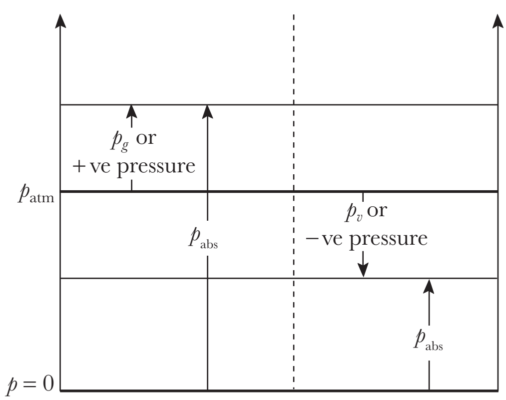

Fig. 2.8 Relation between gauge, vacuum, and absolute pressures

2.4.2 Bourdon Tube Pressure Gauge

The outside and inside views of bourdon tube pressure gauge are shown in Fig. 2.9. A pressure gauge measures the positive pressure (above atmospheric pressure), a vacuum gauge measures the negative pressure (below atmospheric

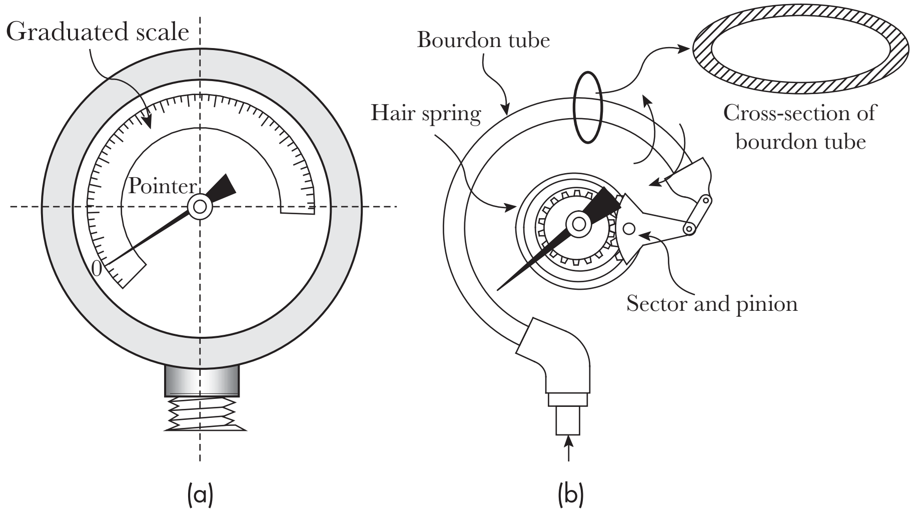

Fig. 2.9 Bourdon tube pressure gauge (a) Outside view (b) Inside view

pressure), and a compound gauge can measure both. Figure 2.9 shows a compound gauge, where the pointer reads zero against atmospheric pressure. For positive pressure, the pointer moves in a clockwise direction and for negative pressure measurement, it moves in a counterclockwise direction. It has a copper tube of elliptical cross-section, known as Bourdon tube, which is open at one end and closed at the other. The closed end is attached with the sector and pinion to drive the pointer, and the open end is connected to the system to measure its pressure. The closed end will swing outwards when connected to the system maintained at a pressure above the atmospheric pressure, whereas it will swing inwards if connected to a system maintained at a pressure lower than the atmospheric pressure. The movement of the closed end is transmitted to the sector and pinion by means of a link. The pinion drives the pointer and its deflection is calibrated in terms of applied pressure. A graduated scale is placed on the dial to enable the pressure gauge reading. A hair spring is connected to the pointer to avoid *hysteresis*.

In instrumentation, *hysteresis* is the condition when an instrument gives different readings for the same value of measured quantity during the increasing and decreasing modes of operation.

2.4.3 Bellows Type Pressure Gauge

Bellows type pressure gauge, shown in Fig. 2.10, is similar to Bourdon tube pressure gauge with a difference that instead of an elliptical Bourdon tube, bellows and spring are used to transmit the pressure signal to the sector and pinion arrangement. Bellows is a convoluted unit that expands and contracts

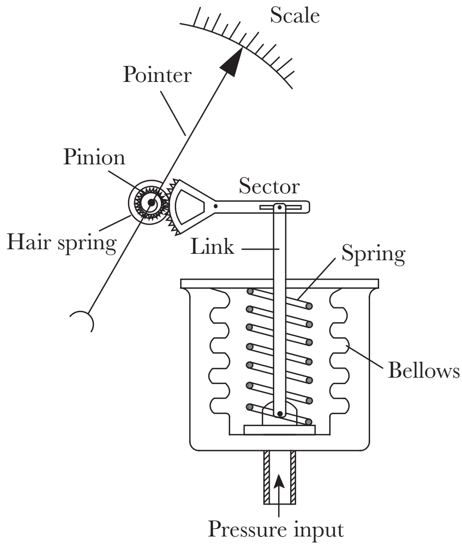

Fig. 2.10 Bellows type pressure gauge

on the application of pressure. It is made up of a mix metal such as brass or copper–beryllium, which is soft and has a higher strength. In fact, the purpose of providing a spring is to prevent full contraction or expansion of bellows, thus prolonging its life. The pinion drives the pointer and its deflection is calibrated in terms of applied pressure. A graduated scale is placed on the dial to enable the pressure gauge reading. They are suitable for low and medium pressure measurement.

2.4.4 Dead Weight Pressure Tester

The pressure gauges or transducers are calibrated with the help of *dead weight pressure gauge tester*, shown in Fig. 2.11. It works on Pascal's law. It consists of an oil reservoir, the mounting for the pressure gauge to be calibrated, and a floating pan for placing standard weights. The oil is filled in the tester through

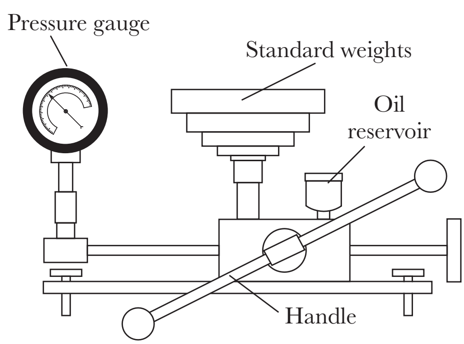

Fig. 2.11 Dead weight pressure gauge tester

the oil reservoir/cup. The pressure gauge is mounted and the standard weights corresponding to the desired calibration pressure are placed on the pan. The handle that is meant for pressurizing the oil is rotated slowly. With the rotation of handle, the rise in pressure is reflected on the pressure gauge. A point is reached when the standard weight gets lifted up to a designated height. At this point, the indicated reading of the gauge and the corresponding weight on the pan should be equal. Any deviation in the pressure gauge reading from the corresponding standard weight will be due to an error in the pressure-measuring device. The procedure is repeated for other calibration pressures, and a plot between the indicated and actual pressure is drawn. This plot is also known as a *calibration curve*.

2.4.5 Manometers

A manometer is the simplest of pressure-measuring devices. It employs a liquid column in a glass tube and a graduated scale to measure the difference in pressure as shown in Fig. 2.12. The liquid inside the manometer glass tube is known as the manometric fluid. The procedure for calculating the pressure difference has been mentioned later in the description of Fig. 2.15.

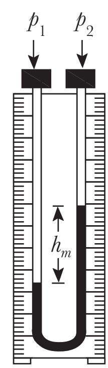

Fig. 2.12 Manometer

The pressure of liquid flowing through a pipe can be measured by drilling a hole on the pipe's wall and fixing a glass tube along with a graduated scale on the hole. The rise in water level in the glass tube can be expressed in terms of pressure as shown in Fig. 2.13. This simple arrangement of measuring pressure of fluid in a pipe is known as a *piezometer* (Fig. 2.13a). For this arrangement, the pressure inside the pipe must be greater than the atmospheric pressure. However, a piezometer can also be used to measure small negative pressure by providing a bend as shown in Fig. 2.13(b).

To measure the pressure of a greater magnitude (positive or negative), the manometric fluid of higher specific gravity is employed in addition to the working fluid. A piezometer, on the other hand, does not require a manometric fluid, the working fluid (the fluid whose pressure is to be measured) in itself acts as the manometric fluid. A higher specific gravity fluid like mercury is used in a U-tube manometer to measure pressure of higher magnitudes. Figure 2.13(c) shows one such arrangement. It should be remembered at this stage that the manometric fluid and working fluid must be immiscible. Single-column manometers, shown in Figs 2.13(a) and (b), are used to measure the gauge pressure at a point in a pipe or a pressurized tank. Such manometers suffer a major drawback that they can be used only for the measurement of pressure

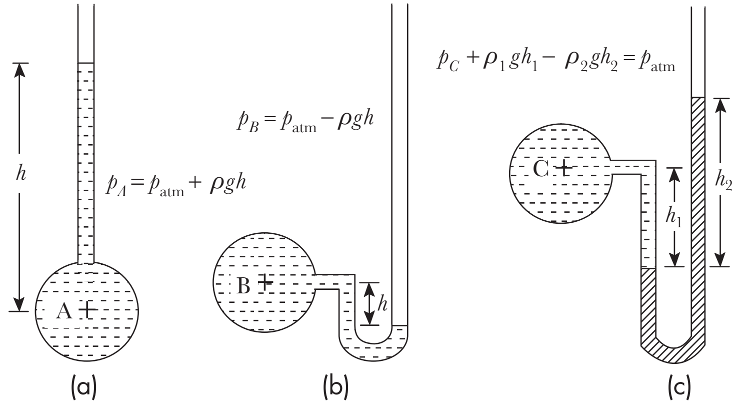

Fig. 2.13 Single-column manometers (a) For positive (b) For small negative (c) For large pressure measurement

of some specific non-volatile liquids. Moreover, if the pressure is high, a very long tube will be required, which is impractical.

NOTE

The manometric height is a function of the pressure difference and specific gravity of the manometric fluid. Higher the specific gravity, smaller will be the manometric height and vice versa for a given pressure difference. The selection of a manometric fluid must be done carefully on the basis of the range of the pressure difference to be measured.

If a manometer is used to measure the pressure difference at two different points, it is termed as a *differential manometer*. Depending upon the specific gravity of the manometric fluid, differential manometers will have different orientations as shown in Fig. 2.14. When the specific gravity of the manometric fluid is greater than that of the working fluid, a differential manometer in an upright position is employed (Fig. 2.14a), whereas if the specific gravity of the manometric fluid is lower than that of the working fluid, a differential manometer in an inverted position is employed (Fig. 2.14b).

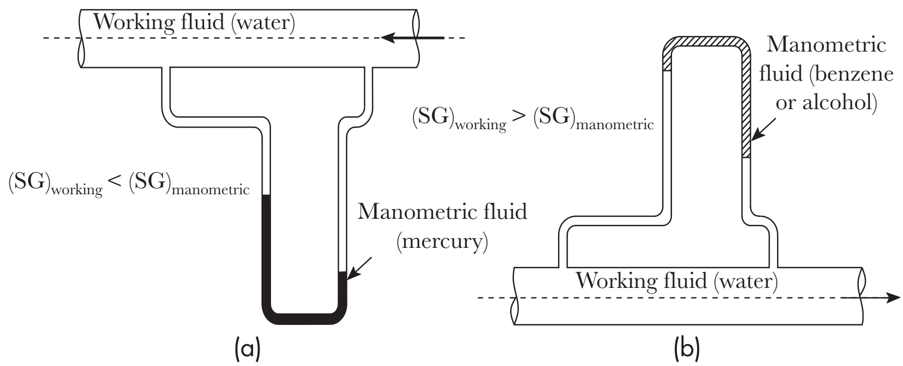

Fig. 2.14 Differential manometer in (a) Upright position (b) Inverted position

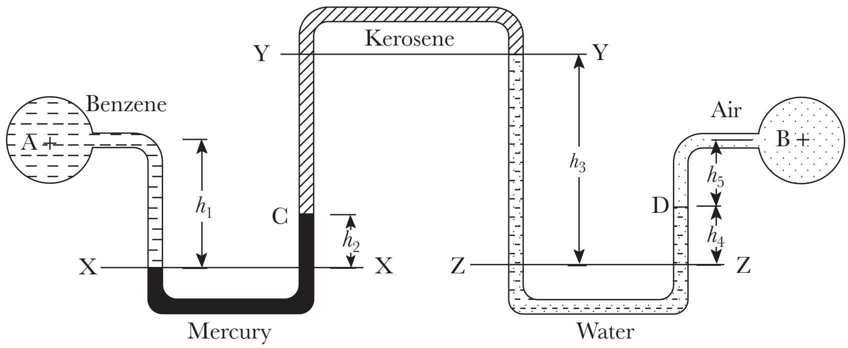

Fig. 2.15 Pressure determination using a manometer

Figure 2.15 shows the step-by-step procedure of determining the pressure difference using a manometer with more than one manometric fluid. In the figure, a manometer is placed to measure the pressure difference between points A and B.

1. Start from A where the pressure is p_A
2. The plane X–X lies below point A, therefore the pressure at X–X plane will be more than that at A and is equal to $p_A + \rho_{\text{benzene}} g h_1$
3. The point C lies above X–X plane, the pressure at C will be less than that at X–X and is therefore equal to $p_A + \rho_{\text{benzene}} g h_1 - \rho_{\text{mercury}} g h_2$
4. The Y–Y plane lies above point C and hence will have lower pressure and it is equal to $p_A + \rho_{\text{benzene}} g h_1 - \rho_{\text{mercury}} g h_2 - \rho_{\text{kerosene}} g(h_3 - h_2)$
5. The Z–Z plane lies below the Y–Y plane and hence will have higher pressure and the pressure at Z–Z plane is equal to $p_A + \rho_{\text{benzene}} g h_1 - \rho_{\text{mercury}} g h_2 - \rho_{\text{kerosene}} g(h_3 - h_2) + \rho_{\text{water}} g h_3$
6. The point D lies above the Z–Z plane and, therefore, the pressure at D is equal to $p_A + \rho_{\text{benzene}} g h_1 - \rho_{\text{mercury}} g h_2 - \rho_{\text{kerosene}} g(h_3 - h_2) + \rho_{\text{water}} g h_3 - \rho_{\text{water}} g h_4$
7. Lastly, the pressure at point B will be less than that at point D and it is equal to $p_A + \rho_{\text{benzene}} g h_1 - \rho_{\text{mercury}} g h_2 - \rho_{\text{kerosene}} g(h_3 - h_2) + \rho_{\text{water}} g h_3 - \rho_{\text{water}} g h_4 - \rho_{\text{air}} g h_5$

Finally, the expression for pressure at B can be written as

$$p_B = p_A + \rho_{\text{benzene}} g h_1 - \rho_{\text{mercury}} g h_2 - \rho_{\text{kerosene}} g(h_3 - h_2)$$
$$+\rho_{\text{water}} g(h_3 - h_4) - \rho_{\text{air}} g h_5 \tag{2.8}$$

Inclined Tube Manometer

To measure small positive pressures, one of the limbs of the differential manometer is inclined at an angle θ. Small values of pressure cause a small change in the height h of manometric fluid in the vertical limb. Tilting of the

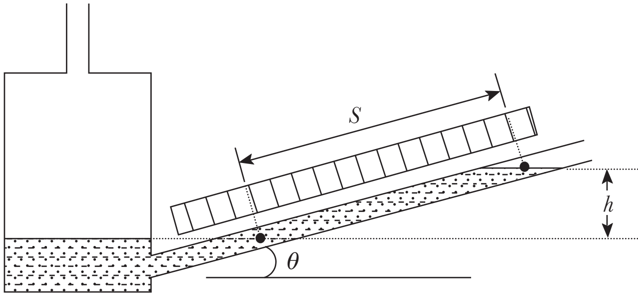

Fig. 2.16 Inclined tube manometer

limb causes this small change in vertical height to elongate, that is, $S = h/\sin\theta$. Hence, the inclined tube arrangement improves readability for small values of pressure and such a manometer is known as an *inclined tube manometer* (Fig. 2.16). The pressure difference measured from an inclined manometer is given by

$$\Delta p = \rho g S \sin\theta \tag{2.9}$$

Micromanometer

Another manometer that is used to measure extremely small pressure differences is *micromanometer*, shown in Fig. 2.17. It uses two manometric fluids of different specific gravities and two identical reservoirs or wells. Their purpose is to get

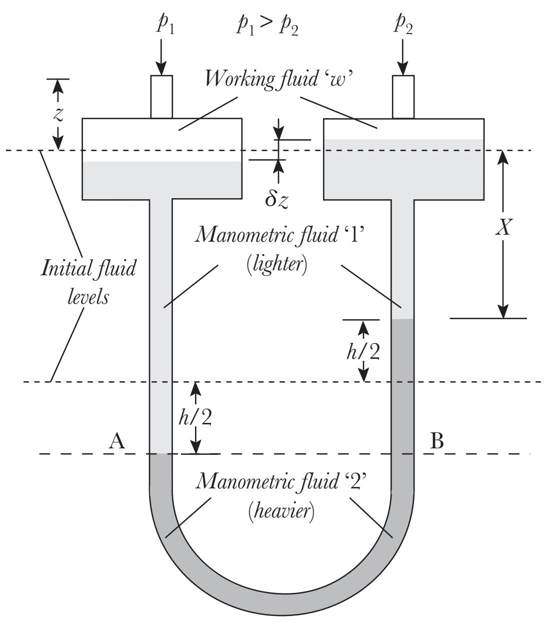

Fig. 2.17 Micromanometer

an elongated column for a small pressure difference. The two fluids in the manometer adjust themselves according to their specific weights, that is, the fluid having higher specific weight will occupy the lower portion of the manometer. Use of a high specific weight fluid ensures the compactness of a manometer, whereas lighter fluid elongates the column height for higher accuracy. As soon as the reservoirs are connected to the points whose pressure difference is to be measured, there is a slight fall in the fluid level inside the reservoir connected to higher pressure point and a corresponding rise in fluid level in the reservoir connected to the lower pressure point. In accordance to the fluid continuity, the fluid volume displaced in the reservoir must be equal to the fluid volume displaced in the tube below it. Since the area of reservoir A is very large compared to that of tube a, the fluid displacement in the tube will be large, that is,

$$\rho_1 A \frac{\delta z}{2} = \rho_1 a \frac{h}{2} \tag{2.10}$$

The displaced fluid pushes the heavier fluid down in one limb, which in turn pushes the lighter fluid up in the other limb to produce a magnified difference between the meniscus levels in the two limbs.

The hydrostatic pressure balance at section AB is

$$p_1 + \rho_w g\left(z + \frac{\delta z}{2}\right) + \rho_1 g\left(X + h - \frac{\delta z}{2}\right)$$

$$= p_2 + \rho_w g\left(z - \frac{\delta z}{2}\right) + \rho_1 g\left(X + \frac{\delta z}{2}\right) + \rho_2 gh \tag{2.11}$$

$$p_1 - p_2 = -\rho_w g\delta z + \rho_1 g(-h + \delta z) + \rho_2 gh \tag{2.12}$$

From Eq. (2.10),

$$p_1 - p_2 = -\rho_w gh\frac{a}{A} - \rho_1 gh\left(1 - \frac{a}{A}\right) + \rho_2 gh \tag{2.13}$$

Since $\frac{a}{A} \approx 0$, the pressure difference approximately equals to

$$\boxed{p_1 - p_2 \approx (\rho_2 - \rho_1)gh} \tag{2.14}$$

Advantages and disadvantages of manometers In general, manometers offer the following advantages over other pressure-measuring devices:

1. They are simple in construction and are inexpensive.
2. Given the low cost, they are highly accurate.
3. They do not have moving parts, thus, they do not require service or maintenance.
4. Unlike other pressure-measuring devices, they do not require calibration.

Manometers also have the following limitations:

1. They cannot be employed for high pressure measurement or measurement of large pressure differences.
2. The glass tube diameter should be large enough to avoid errors due to capillary effect.
3. Their response is slow; thus, they are not suitable for transient applications.
4. The lines connecting a manometer with the system whose pressure is to be measured must be free from air bubbles.

Example 2.3 Compute the pressure difference between points A and B in the manometers shown in Fig. 2.18. All dimensions are in mm.

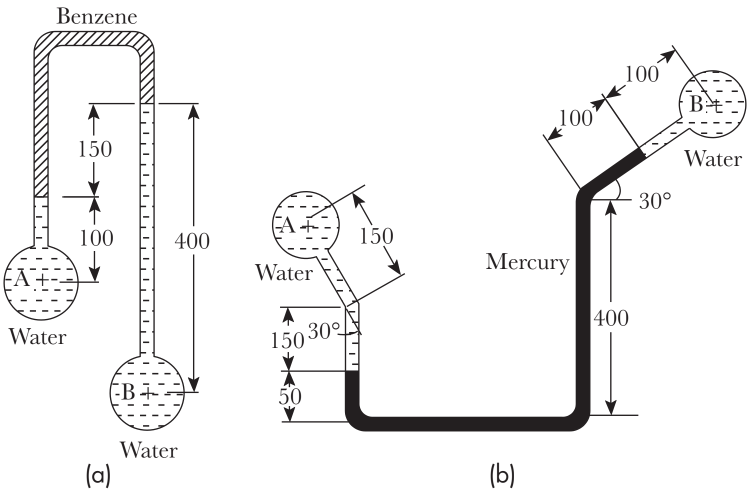

Fig. 2.18

Given data: The densities of the fluids shown in Fig. 2.18, in kg/m³, are

$$\rho_{\text{benzene}} = 880;\ \rho_{\text{water}} = 1000;\ \rho_{\text{mercury}} = 13{,}600$$

Solution: Consider the manometer shown in Fig. 2.18(a)

$$p_A - \rho_{\text{water}} g(0.1) - \rho_{\text{benzene}} g(0.15) + \rho_{\text{water}} g(0.4) = p_B$$

$$p_B - p_A = 1000 \times 9.81 \times 0.3 - 880 \times 9.81 \times 0.15$$

$$\Rightarrow \quad p_B - p_A = 1.648 \text{ kPa}$$

Let us now consider the manometer shown in Fig. 2.18(b)

$$p_A + \rho_{\text{water}} g(0.15 \sin 60° + 0.15) - \rho_{\text{mercury}} g[(0.4 - 0.05) + 0.1 \times \sin 30°]$$
$$- \rho_{\text{water}} g(0.1 \times \sin 30°) = p_B$$

$$p_A - p_B = - 1000 \times 9.81 \times (0.13 + 0.15) + 13,600 \times 9.81 \times (0.35 + 0.05)$$
$$+ 1000 \times 9.81 \times 0.05$$

$$\Rightarrow \quad p_A - p_B = 51.11 \text{ kPa}$$

Example 2.4 Compute the height of water in the arrangement shown in Fig. 2.19.

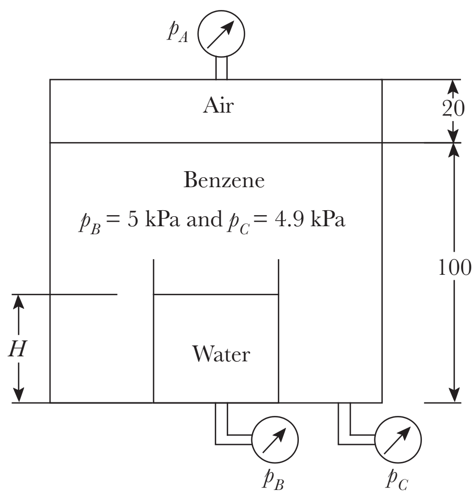

Fig. 2.19

Given data: The densities of the fluids shown in Fig. 2.16, in kg/m^3, are

$$\rho_{\text{benzene}} = 880; \quad \rho_{\text{water}} = 1000; \quad \rho_{\text{air}} = 1.2$$

Solution: The reading in pressure gauge A can be determined in the following way:

$$p_A + \rho_{\text{air}} g h_{\text{air}} + \rho_{\text{benzene}} g h_{\text{benzene}} = p_C$$

$$p_A = 4.9 \times 10^3 - 1.2 \times 9.81 \times 0.02 - 880 \times 9.81 \times 0.1 \quad \Rightarrow \quad p_A = 4.036 \text{ kPa}$$

To find out the height of water H, apply the hydrostatics between gauge A and gauge B:

$$p_A + \rho_{\text{air}} g h_{\text{air}} + \rho_{\text{benzene}} g(h_{\text{benzene}} - H) + \rho_{\text{water}} g H = p_B$$

$$1.2 \times 9.81 \times 0.02 + 880 \times 9.81 \times (0.1 - H) + 1000 \times 9.81 \times H = (5 - 4.036) \times 10^3$$

$$\Rightarrow \quad H = 85.3 \text{ mm}$$

Example 2.5 An inclined manometer with water as the manometric fluid, shown in Fig. 2.20, made up of a glass tube having uniform cross-sectional area of 50 mm^2 is attached to an air conditioning duct. Compute the pressure inside the duct, if the deflection in the inclined limb of the manometer is 100 mm. If 8000 mm^3 of oil of specific gravity 0.9 is added into the manometer through the open end of the inclined tube, find the new deflection in the inclined limb. Take reservoir area as 200 mm^2.

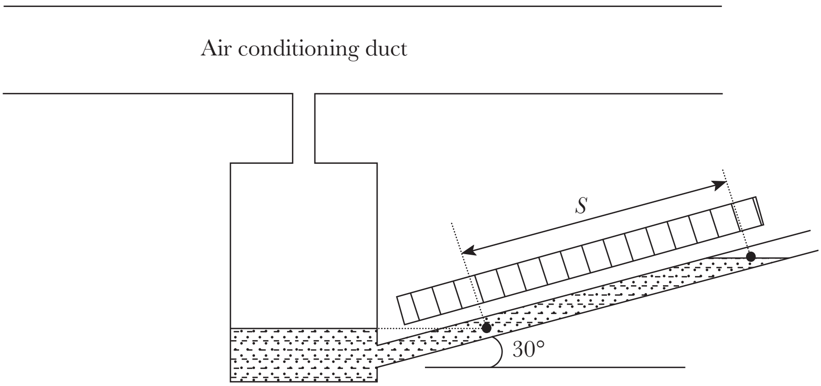

Fig. 2.20

Solution: Since the inclined tube of the manometer is open to the atmosphere, the pressure difference is

$$p - p_{atm} = \rho_w g S \sin\theta$$

$$p - p_{atm} = 1000 \times 9.81 \times 0.1 \times \sin 30° \quad \Rightarrow \quad p - p_{atm} = 490.5\,\text{Pa}$$

After the addition of oil in the inclined limb shown in Fig. 2.21, the length occupied by the oil in the inclined tube is computed in the following manner:

$$S_1 + S_2 = \frac{8000}{50} \quad \Rightarrow \quad S_1 + S_2 = 160\text{ mm} \tag{1}$$

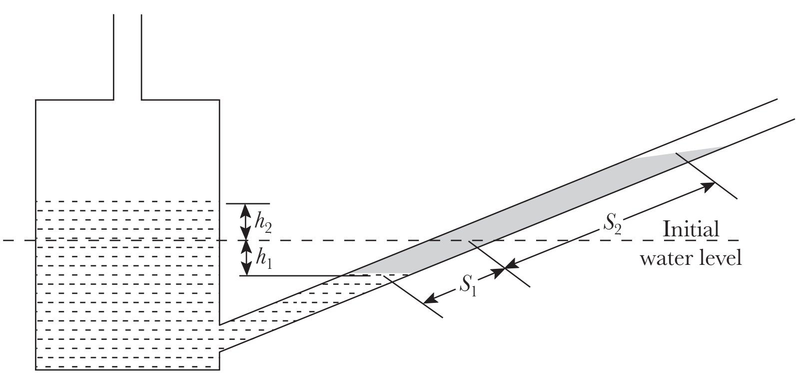

Fig. 2.21

Applying the manometric equation on the inclined manometer (ignoring the pressure exerted by air column) (see Fig. 2.19)

$$p + \rho_w g(h_1 + h_2) = \rho_o g(S_1 + S_2)\sin\theta + p_{\text{atm}}$$

$$h_1 + h_2 = \frac{\rho_o g(S_1 + S_2)\sin\theta - (p - p_{\text{atm}})}{\rho_w g}$$

$$\Rightarrow \quad h_1 + h_2 = \frac{900 \times 9.81 \times 0.16 \sin 30° - 490.5}{1000 \times 9.81} \quad \Rightarrow \quad h_1 + h_2 = 22 \text{ mm} \qquad (2)$$

Applying continuity,

$$(S_1 + S_2) \times A_{\text{tube}} = S_2 \times A_{\text{tube}} + h_2 \times A_{\text{reservoir}} \quad \Rightarrow \quad S_1 = 4h_2 \qquad (3)$$

In addition, $$h_1 = S_1 \sin 30° \quad \Rightarrow \quad S_1 = 2h_1 \qquad (4)$$

From Eqs (1) to (4)

$$h_1 = 14.66 \text{ mm}; \quad h_2 = 7.33 \text{ mm}; \quad S_1 = 29.32 \text{ mm}; \quad S_2 = 130.7 \text{ mm}$$

2.4.6 Barometer

The pressure sensors (pressure gauges and manometers) described in the previous two sections measure only gauge pressure. They give atmospheric pressure reading as zero. To know the actual pressure, the local atmospheric pressure needs to be added to the indicated pressure sensor reading. Barometers are the devices particularly designed to measure the local atmospheric pressure. The most commonly used barometer is *mercury barometer*.

A simple mercury barometer, shown in Fig. 2.22, consists of a mercury reservoir and a sufficiently long glass tube. The glass tube completely filled with mercury is made upside down such that the open end gets submerged in the reservoir. The vertical mercury column starts receding due to its own weight, creating vacuum at the top of the tube, until it gets balanced by the local atmospheric pressure acting on the exposed surface of mercury in the reservoir. A graduated scale is placed along the vertical mercury column to measure its height. The height of the mercury column is the measure of the local atmospheric pressure. The standard atmospheric (at sea level) pressure is 760 mm of Hg. The atmospheric pressure decreases with the altitude.

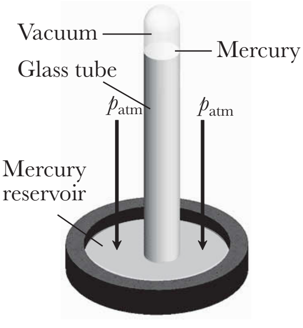

Fig. 2.22 Mercury barometer

Example 2.6 A test tube filled with mercury is inverted and placed into a beaker containing mercury as shown in Fig. 2.23. Determine the inside pressure at the middle and top end of the test tube, if the local atmospheric pressure is 100 kPa.

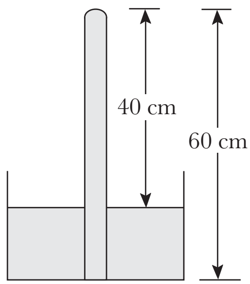

Fig. 2.23

Solution: Let p_t be the pressure at the top end, p_b the pressure at the bottom end, and p_c the pressure at the middle of the test tube.

Pressure at the bottom end of the test tube is given by

$$p_b = p_t + \rho_m g (h_m)_{\text{test tube}} \tag{1}$$

In addition, the pressure at the bottom with respect to the free surface of mercury in the beaker is

$$p_b = p_{\text{atm}} + \rho_m g (h_m)_{\text{beaker}} \tag{2}$$

From Eqs (1) and (2), pressure at the top end of the test tube is

$$p_t = p_{\text{atm}} + \rho_m g [(h_m)_{\text{beaker}} - (h_m)_{\text{test tube}}] \tag{3}$$

$$p_t = 100 \times 10^3 - 13.6 \times 10^3 \times 9.81 \times 0.4 \quad \Rightarrow \quad p_t = 46.6 \text{ kPa}$$

Pressure at the middle of test tube is greater than the pressure at the top end and is obtained as

$$p_c = p_t + \rho_m g (h_m)_{\text{test tube}}/2 \tag{4}$$

$$p_c = 46.6 \times 10^3 + 13.6 \times 10^3 \times 9.81 \times 0.3 \quad \Rightarrow \quad p_c = 86.62 \text{ kPa}$$

2.5 SUBMERGED SURFACES

When a surface is submerged in a stagnant fluid, it experiences a force known as *hydrostatic pressure force*, which depends upon its position from the free surface (or depth) and the orientation and shape of the surface. Such an analysis is important in designing the gates of hydraulic structures such as dams. Gates are employed in hydraulic structures to serve the following purposes:

1. Flood control
2. Flow regulation in water bodies
3. Navigation of boats in canals
4. Cleaning of water reservoirs, etc.

Table 2.2 shows the various classifications of gates.

Table 2.2 Classifications of gates

Basis	Types	Description
Purpose	Service gates	Used for the continuous regulation of flow or water level, e.g., spillways, bottom outlet gates, lock gates
	Emergency gates	To completely shut/open the flow of water in case of emergency, e.g., intake gates, draft tubes gates
	Maintenance gates	To empty the canal or flow conduit for the maintenance, e.g., stoplog
Motion	Translation gates	Can be either sliding or rolling, e.g., stoplog, caterpillar, slide, etc.
	Rotation gates	Turns around a fixed axis called hinged axis, e.g., flap, miter, segment, drum, etc.
	Translo-rotation gates	Performs a combined motion of rotation and translation, e.g., roller gate (only gate that undergoes translo-rotation movement)
Head	Low head gates	$H \leq 15\,\text{m}$
	Medium head gates	$15\,\text{m} \leq H \leq 30\,\text{m}$
	High head gates	$H > 30\,\text{m}$

In order to design a gate, the first step is to compute the hydrostatic pressure force on either side of the gate (if both sides are exposed to the fluid). The maximum value of hydrostatic pressure force corresponds to the condition when the gate is fully closed and is subjected to the highest possible head.

In the present analysis, the submerged surfaces (*plane* or *curved*) in general are analysed based on the assumption that the surface or plane is thin and has zero weight. It should be remembered that while designing the actual gates for any hydraulic structure, their weights are also taken into consideration.

2.5.1 Submerged Plane Surface

For the sake of better understanding, the analyses for plane surfaces will be presented for horizontal, vertical, and inclined surfaces separately. In fact, horizontal and vertical orientations are special cases of inclined plane.

Horizontal plane When a plane is horizontal, all the points on the surface of the plane will be equidistant from the free surface. Figure 2.24 shows a

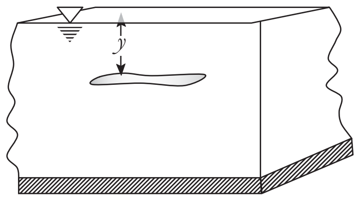

Fig. 2.24 Hydrostatic force on horizontal plane

horizontal plane at a depth of y from the free surface. Hence, the plane will experience the hydrostatic pressure force equal to

$$F = \rho g y A \tag{2.15}$$

Vertical plane Consider a vertical plane of any arbitrary shape submerged in a pool of liquid with its top edge at a depth of y_t as shown in Fig. 2.25. The point on the surface where the resultant hydrostatic pressure force acts is known as the *centre of pressure*. The centre of pressure is abbreviated as CP and is denoted by P in the figure. The point on the surface where the weight of the body is supposed to be concentrated is known as the *centre of gravity*. The centre of gravity is abbreviated as CG and is denoted by G in the figure. It has been shown in Section 2.3 that the hydrostatic pressure increases linearly with depth, which means that the top edge will experience less pressure than the bottom edge. This means that the CP will always lie below the CG.

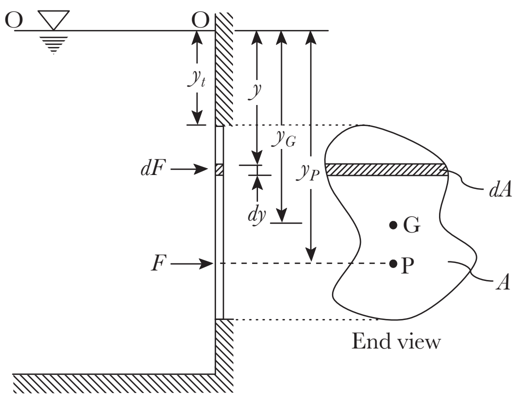

Fig. 2.25 Hydrostatic force on vertical plane

Let us consider an infinitesimal element of thickness dy at a depth of y from the free surface (O–O). The hydrostatic force dF acting on the element is given by

$$dF = pdA = \rho g y dA \tag{2.16}$$

where p is the hydrostatic pressure acting on the element.

The resultant hydrostatic pressure force, F, acting on the plane will be the area integral of the right-hand side of Eq. (2.16), that is,

$$F = \rho g \int_A y dA \tag{2.17}$$

where $\int y dA$ is termed as *first area moment of inertia* and is equivalent to the product of total the area of the plane and the position of CG from the free liquid surface, that is,

$$y_G A = \int_A y dA \tag{2.18}$$

The position of CG from the free surface, y_G is given by the following equation:

$$\boxed{y_G = \frac{1}{A}\int_A y dA} \tag{2.19}$$

From Eqs (2.17) and (2.18), the resultant force is

$$\boxed{F = \rho g y_G A} \tag{2.20}$$

In a similar fashion, the position of CP, y_P, can be evaluated:

$$y_P F = \int y dF \tag{2.21}$$

$$y_P \rho g y_G A = \rho g \int_A y^2 dA \tag{2.22}$$

$$y_P = \frac{\int_A y^2 dA}{y_G A} \tag{2.23}$$

The integral $\int_A y^2 dA$ represents the *second area moment of inertia* about the free surface O–O, that is,

$$I_o = \int_A y^2 dA \tag{2.24}$$

From parallel axis theorem,

$$I_o = I_G + A y_G^2 \tag{2.25}$$

Using Eqs (2.24) and (2.25), Eq. (2.23) reduces to

$$y_P = y_G + \frac{I_G}{y_G A} \tag{2.26}$$

Inclined plane It is the most generalized case of plane surfaces submerged in a pool of liquid. In Fig. 2.26, the plane is inclined at an angle θ with the free surface. The procedure for determining the hydrostatic pressure force on an inclined plane is similar to that of the vertical plane.

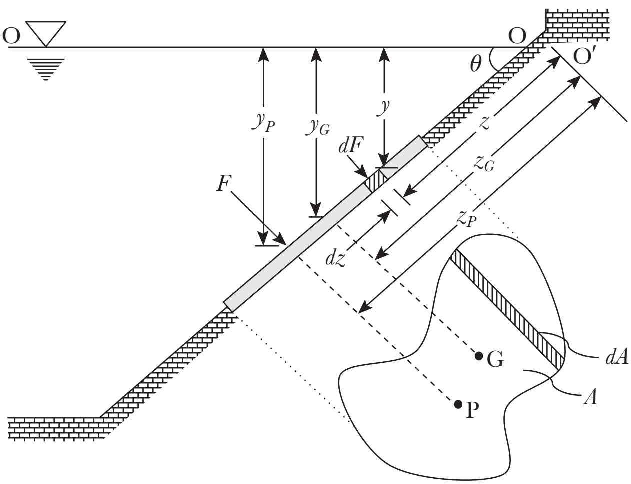

Fig. 2.26 Hydrostatic force on inclined plane

Let us consider an infinitesimal element of thickness dy at a depth of y from the free surface (O–O). The hydrostatic force dF acting on the element is given by

$$dF = pdA = \rho gydA \tag{2.27}$$

In addition, from Fig. 2.22,

$$y = z\sin\theta; \quad y_G = z_G \sin\theta; \quad y_P = z_P \sin\theta$$

Equation (2.27) reduces to

$$dF = \rho gz \sin\theta \, dA \tag{2.28}$$

The resultant hydrostatic pressure force, F, acting on the plane will be the area integral of the right-hand side of Eq. (2.28), that is,

$$F = \rho g \sin\theta \int_A z dA \tag{2.29}$$

It has been seen earlier (i.e., Eq. 2.18) that

$$\int_A z dA = z_G A \tag{2.30}$$

Therefore, the resultant force is

$$\boxed{F = \rho g \sin\theta \, z_G A = \rho g y_G A} \tag{2.31}$$

On the same lines, the position of CP can also be evaluated, that is,

$$z_P F = \int z dF \tag{2.32}$$

$$z_P \rho g z_G \sin\theta \, A = \rho g \int_A z^2 \sin\theta \, dA \tag{2.33}$$

$$z_P = \frac{\int_A z^2 dA}{z_G A} = \frac{I'_o}{z_G A} \tag{2.34}$$

From parallel axis theorem,

$$I_{o'} = I_G + z_G^2 A \tag{2.35}$$

Thus, Eq. (2.34) reduces to

$$\boxed{z_P = z_G + \frac{I_G}{z_G A}} \tag{2.36}$$

or $$\frac{y_P}{\sin\theta} = \frac{y_G}{\sin\theta} + \frac{I_G}{\frac{y_G}{\sin\theta} A}$$

Hence, the position of CP is equal to

$$\boxed{y_P = y_G + \frac{I_G \sin^2\theta}{y_G A}} \tag{2.37}$$

If $\theta = 0°$, the surface becomes horizontal and, therefore, $y_p = y_G$

If $\theta = 90°$, the surface becomes vertical and, therefore, $y_P = y_G + \dfrac{I_G}{y_G A}$

The area, position of CG, and area moment of inertia of some common geometrical shapes are shown in Table 2.3. This table will be useful in solving problems based on hydrostatics.

Table 2.3 Area, position of CG, and area moment of inertia about CG for different shapes

Shape	Area (A)	Position of CG (y_G)	Area moment of inertia (I_G)
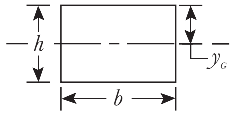	bh	$\frac{h}{2}$	$\frac{bh^3}{12}$
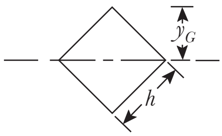	h^2	$\frac{h}{\sqrt{2}}$	$\frac{h^4}{12}$
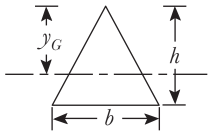	$\frac{bh}{2}$	$\frac{2}{3}h$	$\frac{bh^3}{36}$
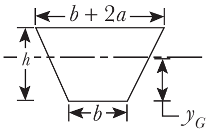	$(2b+a)\frac{h}{2}$	$\frac{h}{3}\left(\frac{3b+2a}{2b+a}\right)$	$\frac{h^3}{36}\left(\frac{6b^2+6ba+a^2}{2b+a}\right)$
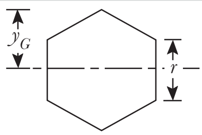	$\frac{3\sqrt{3}}{2}r^2$	r	$\frac{5\sqrt{3}}{16}r^4$
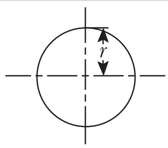	$\frac{\pi}{4}d^2$ or πr^2	r	$\frac{\pi}{64}d^4$ or $\frac{\pi}{4}r^4$
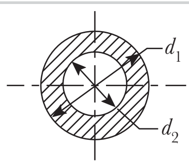	$\frac{\pi}{4}\left(d_1^2-d_2^2\right)$	$\frac{d_1}{2}$	$\frac{\pi}{64}\left(d_1^4-d_2^4\right)$
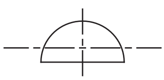	$\frac{\pi r^2}{2}$	$\frac{4r}{3\pi}$	$\left(\frac{\pi}{8}-\frac{8}{9\pi}\right)r^4$
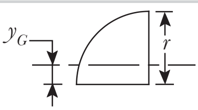	$\frac{\pi r^2}{4}$	$\frac{4r}{3\pi}$	$0.055r^4$
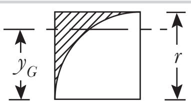	$r^2\left(1-\frac{\pi}{4}\right)$	$0.7766r$	$0.0075r^4$

Example 2.7 Calculate the position of CG and CP for a rectangular plane of width b and depth d. In addition, calculate the magnitude of area moment of inertia about its CG.

Solution: To find out the positions of CP and CG, choose an infinitesimal horizontal rectangular strip of thickness dy at a depth of y from the x-axis, shown in Fig. 2.27.

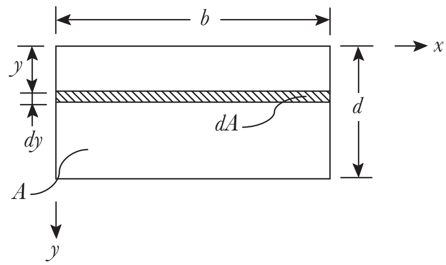

Fig. 2.27

Area of the plane:

$$A = \int_A dA = \iint dxdy = \int_0^d \int_0^b dxdy = bd$$

Centre of gravity:

$$y_G = \frac{1}{A}\int_A ydA = \frac{1}{A}\iint ydxdy = \frac{1}{A}\int_0^d \int_0^b ydxdy$$

$$y_G = \frac{b}{A}\int_0^d ydy = \frac{1}{d}\frac{d^2}{2} = \frac{d}{2}$$

$$\Rightarrow \quad y_G = \frac{d}{2}$$

Area moment of inertia:

The area of moment of inertia about x-axis

$$I_o = \int_A y^2 dA = \int_0^d \int_0^b y^2 dxdy \quad \Rightarrow \quad I_o = b\int_0^d y^2 dy \quad \Rightarrow \quad I_o = b\frac{d^3}{3}$$

The area moment of inertia about its CG,

$$I_G = I_o - Ay_G^2 \quad \Rightarrow \quad I_G = \frac{bd^3}{3} - bd \times \left(\frac{d}{2}\right)^2$$

$$\Rightarrow \quad I_G = \frac{bd^3}{12}$$

Centre of pressure:

The CP can be computed either by

$$y_P = \frac{I_o}{y_G A} = \frac{bd^3/3}{d/2 \times bd} = \frac{2}{3}d$$

or
$$y_P = y_G + \frac{I_G}{y_G A} = \frac{d}{2} + \frac{bd^3/12}{d/2 \times bd} = \frac{2}{3}d$$

$$\Rightarrow \quad y_P = \frac{2}{3}d$$

This also shows that CP lies below CG.

Example 2.8 Compute the hydrostatic pressure force and the position of CP for the gates shown in Fig. 2.28.

Solution: Consider Fig. 2.28(a), the hydrostatic pressure force can be evaluated by finding out the position of CG for the parabolic gate.

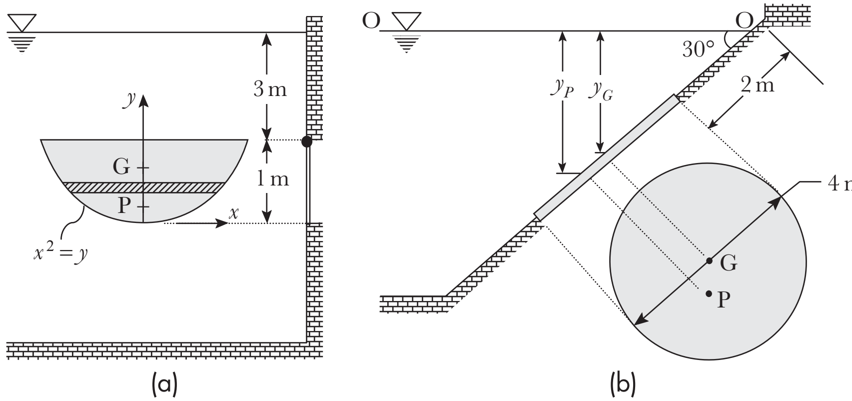

Fig. 2.28

Area of the parabolic gate:

$$A = \int_0^1 \int_{-\sqrt{y}}^{\sqrt{y}} dxdy \quad \Rightarrow \quad A = 2\int_0^1 \sqrt{y}dy \quad \Rightarrow \quad A = 2\left|\frac{y^{3/2}}{3/2}\right|_0^1$$

$$\Rightarrow \quad A = \frac{4}{3}\,\text{m}^2$$

Gate's centre of gravity:

$$y_G = \frac{1}{A}\int_A ydA \quad \Rightarrow \quad y_G = \frac{1}{A}\int_0^1 \int_{-\sqrt{y}}^{\sqrt{y}} ydxdy \quad \Rightarrow \quad y_G = \frac{3}{2}\int_0^1 y\sqrt{y}dy$$

$$\Rightarrow \quad y_G = \frac{3}{2}\left|\frac{y^{5/2}}{5/2}\right|_0^1 \quad \Rightarrow \quad y_G = \frac{3}{5}\,\text{m}$$

The position of CG from the free surface is, therefore, given by

$$Y_G = 4 - \frac{3}{5} = 3.4 \text{ m}$$

Hydrostatic pressure force:

$$F = \rho g Y_G A \quad \Rightarrow \quad F = 1000 \times 9.81 \times 3.4 \times 4/3 = 44.472 \text{ kN}$$

Centre of pressure:

$$y_P = y_G + \frac{I_G}{y_G A}$$

where, $I_G = I_{xx} - Ay_G^2$

The area moment of inertia about x-axis

$$I_{xx} = \int_A y^2 dA \quad \Rightarrow \quad I_{xx} = \int_0^1 \int_{-\sqrt{y}}^{\sqrt{y}} y^2 dxdy \quad \Rightarrow \quad I_{xx} = 2\int_0^1 y^2 \sqrt{y} dy$$

$$I_{xx} = 2\left|\frac{y^{7/2}}{7/2}\right|_0^1 \quad \Rightarrow \quad I_{xx} = \frac{4}{7} \text{ m}^4$$

Therefore, the area moment of inertia about the line passing through the CG parallel to x-axis

$$I_G = I_{xx} - Ay_G^2 \quad \Rightarrow \quad I_G = \frac{4}{7} - \frac{4}{3} \times \left(\frac{3}{5}\right)^2 \quad \Rightarrow \quad I_G = 0.09143 \text{ m}^4$$

The position of CP,

$$y_P = 0.6 + \frac{0.09143}{0.6 \times 4/3} = 0.7143 \text{ m}$$

The position of CP from the free surface is, therefore, given by

$$Y_P = 4 - 0.7143 = 3.2857 \text{ m}$$

Now consider Fig. 2.28(b) in which a circular gate is inclined at an angle of $30°$. The position of CG from the free surface is

$$y_G = 4 \sin 30° = 2 \text{ m}$$

The magnitude of hydrostatic force acting on the gate is

$$F = \rho g y_G A \quad \Rightarrow \quad F = 1000 \times 9.81 \times 2 \times \pi \times 2^2 = 246.55 \text{ kN}$$

The position of CP

$$y_P = y_G + \frac{I_G}{y_G A} \quad \Rightarrow \quad y_P = y_G + \frac{\pi D^4/64}{y_G \times \pi D^2/4}$$

$$\Rightarrow \quad y_P = 2 + \frac{4^2}{2 \times 16} = 2.5 \text{ m}$$

2.5.2 Submerged Curved Surface

In this section, the hydrostatic pressure force on a curved surface submerged in a pool of liquid will be determined. The surface may be exposed to the liquid either from the top or from the bottom. Unlike the vertical plane surface, here the direction of the hydrostatic pressure changes along the curved surface. In Fig. 2.29, the curved surface is exposed to the liquid from the top. For the sake of convenience, the resultant hydrostatic pressure force, F, is resolved into the horizontal and vertical components, F_H and F_V, respectively.

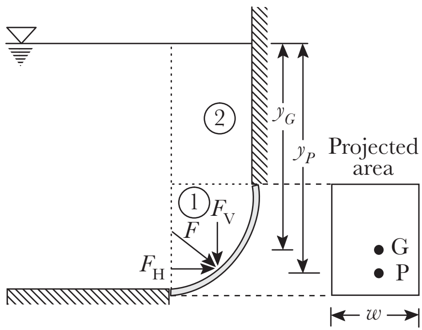

Fig. 2.29 Curved surface exposed to liquid from the top

The horizontal component of force is the hydrostatic pressure force acting on the projected plane, that is,

$$F_H = \rho g y_G A_p \tag{2.38}$$

where A_p is the area of the projected plane of the curved surface, given by

$$A_P = h \times w \tag{2.39}$$

where h = height of the curved surface and w = width of the plane (into the paper).

Figure 2.30 shows the lines of action of horizontal and vertical forces. The line of action of horizontal forces passes through the CP of the projected plane

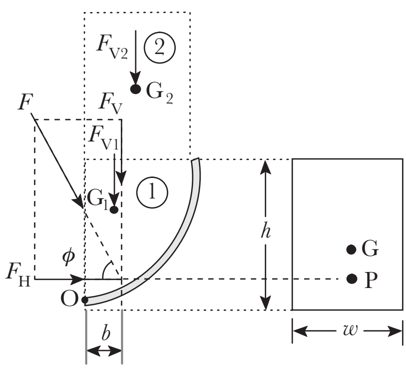

Fig. 2.30 Lines of action of horizontal and vertical components of forces

for regions 1 and 2. The vertical component of force is the weight of the liquid vertically above the curved surface, that is,

$$F_V = \rho \forall g = \rho \forall_1 g + \rho \forall_2 g = F_{V1} + F_{V2} \tag{2.40}$$

where $\forall$ is the volume of liquid above the curved surface given by

$$\forall = \forall_1 + \forall_2 = (A_1 + A_2) \times w \tag{2.41}$$

where A_1 and A_2 are the areas of regions 1 and 2 above the curved surface, and F_{V1} and F_{V2} are the weight of liquid in the regions 1 and 2, respectively.

The line action of vertical force F_V or its distance from the vertical line passing through point O, that is, x, can be evaluated from the following equation:

$$x = \frac{x_1 F_{V1} + x_2 F_{V2}}{F_V} \tag{2.42}$$

where x_1 and x_2 are distances of CG of regions 1 and 2 above the curved surface from the vertical line passing through O.

The magnitude of resultant force F on the curved surface is

$$F = \sqrt{F_H^2 + F_V^2} \tag{2.43}$$

The direction or line of action of the resultant force F on the curved surface is

$$\phi = \tan^{-1}\left(\frac{F_V}{F_H}\right) \tag{2.44}$$

Let us now consider a curved plane exposed to a liquid from the bottom (see Fig. 2.31). The analysis remains similar to the aforementioned discussion. The vertical component of force F_V will act in the upwards direction while the horizontal force F_H will act along the line passing through the CP in the leftward direction. The magnitude of the horizontal force will be same as given by Eq. (2.38). In order to calculate the magnitude of the upward vertical force, it is assumed that an imaginary liquid of same specific gravity occupies the

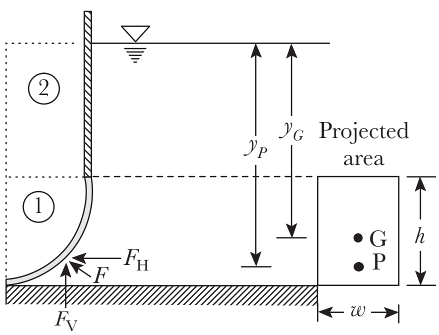

Fig. 2.31 Curved surface exposed to liquid from the bottom

space above the curved surface. The weight of the imaginary liquid above the curved surface will give the magnitude of the vertical component of hydrostatic force. In the present case, the free surface of the imaginary liquid will be at the same height as that of the free surface of actual liquid in the reservoir.

Example 2.9 Derive the expression of force F required to keep the parabolic gate, shown in Fig. 2.32, in the upright position.

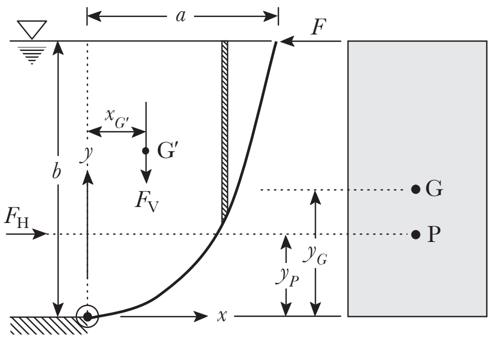

Fig. 2.32

Solution:

Equation of gate's parabolic profile:

Let the equation be

$$x^2 = ky$$

The point of application of the force F is (a, b), which lies on the parabola. Thus, this point must satisfy the equation of a parabola. In doing so, the constant k is evaluated:

$$k = a^2/b$$

Thus, the equation is $x^2 = a^2y/b$

The area of the parabolic region is calculated by choosing an infinitesimal vertical rectangular strip of thickness dx at a distance of x from the y-axis. The lower end of the strip lies on the parabolic gate ($y = bx^2/a^2$) while the upper end lies on the line parallel to the x-axis ($y = b$).

Area of the parabolic region:

$$A = \int_0^a \int_{bx^2/a^2}^b dydx = \frac{4ab}{3}$$

CG for the parabolic region:

$$x_{G'} = \frac{1}{A}\int_A xdA \;\Rightarrow\; x_{G'} = \frac{1}{A}\int_0^a \int_{bx^2/a^2}^b xdxdy \;\Rightarrow\; x_{G'} = \frac{3a}{16}$$

Calculation of forces:

The horizontal component of the hydrostatic force is calculated as

$$F_H = \rho g y_G A_p$$

where $y_G = \frac{b}{2}$, $y_p = \frac{b}{3}$, and $A_p = bw$ for the projected plane

$$F_H = \frac{\rho g b^2 w}{2}$$

The vertical component of the hydrostatic force is given by

$$F_V = \rho \forall g \quad \Rightarrow \quad F_V = \rho g(Aw) \quad \Rightarrow \quad F_V = \frac{4abw\rho g}{3}$$

The force, *F*, can be determined by taking moments about the hinge, that is,

$$F \times a = F_H \times y_P + F_v \times x_{G'}$$

$$F = \rho g w \frac{b^3/6 + a^2 b/4}{a}$$

$$\Rightarrow \quad F = \rho g w \left(\frac{2b^3 + 3a^2 b}{12a} \right)$$

Example 2.10 Compute the magnitude and direction of the hydrostatic pressure force on the arrangements shown in Fig. 2.33. The width in each case may be assumed unity.

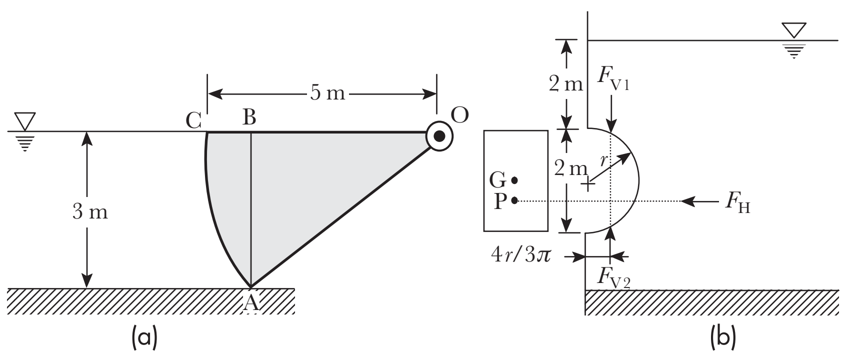

Fig. 2.33

Solution: To compute the hydrostatic force on the gate, shown in Fig. 2.33(a), the horizontal and vertical forces are to be evaluated. The horizontal component is easier to determine as the projected area for any curved surface is a rectangle. The CG and CP from the free surface for the projected plane are

$$y_G = \frac{3}{2}\,\text{m} \quad \text{and} \quad y_P = \frac{2}{3} \times 3\,\text{m} = 2\,\text{m}$$

The horizontal component of hydrostatic pressure force is

$$F_H = \rho g y_G A_p \quad \Rightarrow \quad F_H = 1000\times 9.81\times 1.5\times(3\times 1) = 44.145\ \text{kN}(\rightarrow)$$

The vertical component of hydrostatic pressure force is equal to the weight of the imaginary liquid (same as in the reservoir) in the region enclosed in ABC.

$$F_V = \rho g \forall_{ABC}$$

The volume of the region ABC is equal to the area of region ABC times the width of the gate (which is unity)

$$\forall_{ABC} = A_{ABC}\times 1 = ar(OAC) - ar(\Delta OAB)$$

The angle subtended at O is calculated as

$$\sin\theta = \frac{3}{5} \quad \Rightarrow \quad \theta = 36.87^\circ$$

The area of the gate

$$ar(OAC) = \frac{36.87}{360}\times\pi\times 5^2 = 8.044\ \text{m}^2$$

The area of ΔOAB

$$ar(\Delta OAB) = \frac{1}{2}\times 3\times 5 = 7.5\ \text{m}^2$$

The vertical component of force is, therefore

$$F_V = 1000\times 9.81\times(8.044 - 7.5) = 5.33\ \text{kN}\ (\uparrow)$$

Thus, the magnitude of resultant hydrostatic pressure force is

$$F = \sqrt{F_H^2 + F_V^2} \quad \Rightarrow \quad F = \sqrt{44.145^2 + 5.33^2} \quad \Rightarrow \quad F = 44.44\ \text{kN}$$

and its direction is

$$\phi = \tan^{-1}(F_V/F_H) \quad \Rightarrow \quad \phi = \tan^{-1}(5.33/44.145) \quad \Rightarrow \quad \phi = 6.88^\circ$$

Now consider the semi-circular contour in the tank, shown in Fig. 2.33(b). The CG and CP from the free surface for the projected plane are

$$y_G = 3\ \text{m} \quad \text{and} \quad y_P = 2 + \frac{2}{3}\times 2 = \frac{10}{3}\ \text{m}$$

The horizontal component of hydrostatic pressure force is

$$F_H = \rho g y_G A_p \quad \Rightarrow \quad F_H = 1000\times 9.81\times 3\times(2\times 1) = 58.86\ \text{kN}\ (\leftarrow)$$

The net vertical force is equal to the difference in the upward vertical force at the bottom of contour and the downward vertical force at the top of contour.

$$F_V = F_{V2} - F_{V1} \quad \Rightarrow \quad F_V = \rho g(\forall_2 - \forall_1) \quad \Rightarrow \quad F_V = \rho g \forall_{\text{semicircle}}$$

$$\Rightarrow \quad F_V = 1000 \times 9.81 \times \left(\frac{\pi \times 1^2}{2} \times 1\right) \quad \Rightarrow \quad F_V = 15.4 \text{ kN}(\uparrow)$$

Thus, the magnitude of resultant hydrostatic pressure force is

$$F = \sqrt{F_H^2 + F_V^2} \quad \Rightarrow \quad F = \sqrt{58.86^2 + 15.4^2} \quad \Rightarrow \quad F = 60.84 \text{ kN}$$

and its direction is

$$\phi = \tan^{-1}(F_V/F_H) \quad \Rightarrow \quad \phi = \tan^{-1}(15.4/58.86) \quad \Rightarrow \quad \phi = 14.66°$$

2.6 BUOYANCY AND STABILITY

When a body is submerged in a fluid partially or fully, it experiences an upward force known as *buoyant force* and the phenomenon is known as *buoyancy*. The magnitude of this force is determined from the famous *Archimedes' principle*, which states that a body is buoyed upon by a force equal to the weight of fluid it displaces, when it is submerged in it partially or wholly. To prove this principle, consider an infinitesimal prism running through the body submerged in the pool of liquid as shown in Fig. 2.34. The cross-sectional area of the prism is dA. The

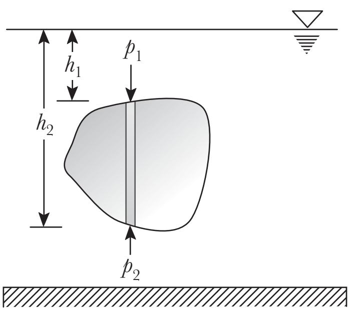

Fig. 2.34 Buoyant force computation

horizontal pressure forces will cancel out each other. The buoyant force acting on the elemental prism is the difference of hydrostatic forces acting across it:

$$dF_B = (p_2 - p_1)dA$$

$$dF_B = (\rho g h_2 - \rho g h_1)dA$$

$$dF_B = \rho g(h_2 - h_1)dA = \rho g d\forall$$

On integration,

$$F_B = \rho g \forall \tag{2.45}$$

The right-hand side of Eq. (2.45) represents the weight of the fluid displaced. Since buoyant force is a function of fluid density, a higher density fluid will exert more buoyant force than lower density fluids. This is the reason why a diver experiences more upward thrust in sea water. *Stability* is defined as the tendency of a body to regain its original position after it is given a small tilt. The stability criterion of fully submerged bodies differs from that of floating bodies.

2.6.1 Stability of Submerged Bodies

The stability of submerged bodies depends upon the relative positions of CG and centre of buoyancy. The relative position of these centres decides whether a body is in stable, unstable, or neutral equilibrium. The examples, in Fig. 2.35, demonstrate different equilibriums. Figure 2.35(a) depicts a test tube fitted with a cork. The cork, being heavier, makes the CG to shift towards it. The centre of buoyancy, on the other hand, is the geometric centre of the assembly through which the buoyant force will act. The magnitude of the buoyant force is negligibly small in comparison to the weight of the tube–cork assembly as the surrounding fluid is air. The slight tilt will cause the heavier part to occupy the lowermost position and an overturning couple will cause it to topple and the equilibrium is termed as an *unstable equilibrium*. The same tube–cork assembly becomes *stable* if it is made upside down (Fig. 2.35b) as the restoring moment acts on it after the tilt. Therefore, it can be concluded that the body is stable if the CG lies below the centre of buoyancy.

Now consider the sphere submerged in a pool of liquid, in this case the centre of buoyancy and CG are coincident. Such a condition is possible when the specific weight of the liquid is equal to the specific weight of the body (i.e., the densities of the liquid and the body must be comparable). In such a case, the slight rotation will cause the sphere to assume a new equilibrium position and the equilibrium is, thus, termed as *neutral equilibrium* (Fig. 2.35c). In such

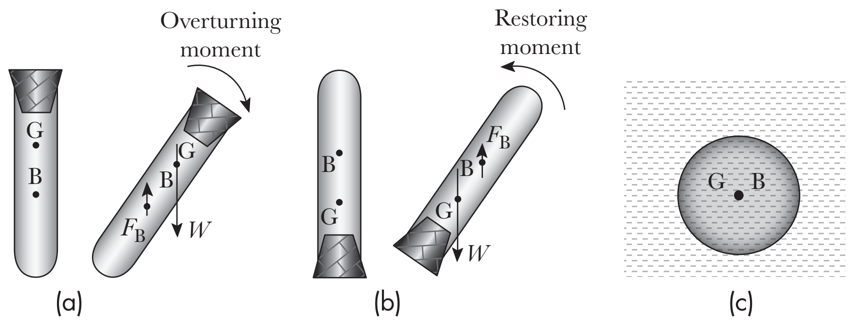

Fig. 2.35 Submerged bodies (a) Unstable (b) Stable (c) Neutral equilibria

a scenario, the body is neither unstable nor stable, that is, after an initial disturbance, the body will not have a tendency to return to its original position. Nonetheless, the body becomes stable at the new position itself.

Example 2.11 A steel ball of radius 1 cm is hanging inside the water tank by means of a string attached to a hollow plastic ball having radius 3 cm weighing 10 g floating at the free surface, as shown in Fig. 2.36. Determine the tension in the string and volume of the plastic ball submerged in water. Take density of the steel ball to be 7850 kg/m^3.

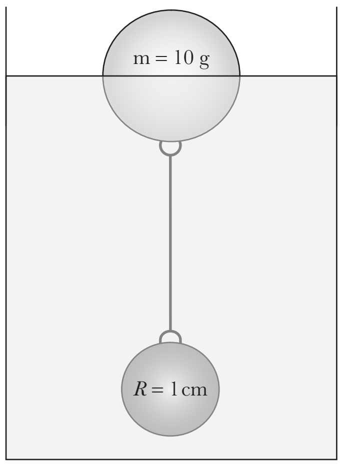

Fig. 2.36

Solution: The free body diagrams for each ball are shown in Fig. 2.37. The forces which act on each ball are weight W, buoyant force F_B, and tension T.

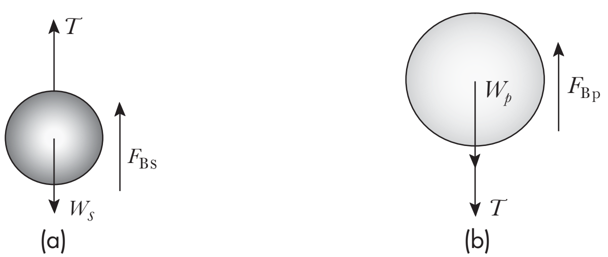

Fig. 2.37 Free body diagrams (a) Steel ball (b) Plastic ball

Applying force balance on each ball,

Steel ball:

$$T + F_{Bs} = W_s$$

$$T + \rho_f \forall_s g = \rho_s \forall_s g$$

$$T = (\rho_s - \rho_f)\forall_s g \quad \Rightarrow \quad T = (7850 - 1000) \times \left(\frac{4}{3}\right)\pi(0.01)^3 \times 9.81$$

$$\Rightarrow \quad T = 0.281\ \text{N}$$

Plastic ball:

$$T + W_p = F_{\mathrm{Bp}}$$

$$T + mg = \rho_f (\forall_p)_{\mathrm{sub}}\, g$$

The submerged volume of plastic ball

$$(\forall_p)_{\mathrm{sub}} = \frac{T + mg}{\rho_f g} \Rightarrow (\forall_p)_{\mathrm{sub}} = \frac{0.281 + 0.01 \times 9.81}{1000 \times 9.81} \Rightarrow (\forall_p)_{\mathrm{sub}} = 38.6\,\mathrm{cm}^3$$

Volume fraction of the plastic ball submerged in water

$$\frac{(\forall_p)_{\mathrm{sub}}}{\forall_p} = \frac{38.6}{\left(\frac{4}{3}\right) \times \pi \times (3)^3} = \frac{38.6}{113.09} \Rightarrow \frac{(\forall_p)_{\mathrm{sub}}}{\forall_p} = 34.13\%$$

2.6.2 Stability of Floating Bodies

The stability of floating bodies does not depend upon the relative positions of the centres of buoyancy and gravity only. The body remains in a stable equilibrium even if the centre of buoyancy lies above the CG. In fact, there exists another point known as the *metacentre*, whose position with respect to the CG is of importance. Figure 2.38 shows the stable and unstable equilibrium conditions for a floating body.

In case of floating bodies, shown in Fig. 2.38, the centre of buoyancy lies below the CG, the reason being the displaced liquid volume is lesser than the total volume of the body. In fact, it is equal to the fraction of the body volume that is inside the liquid. The tilting will cause the centre of buoyancy to shift in the direction of the tilt as the volume of the liquid displaced is more on that side. The vertical line passing through the shifted centre of buoyancy (B′) and

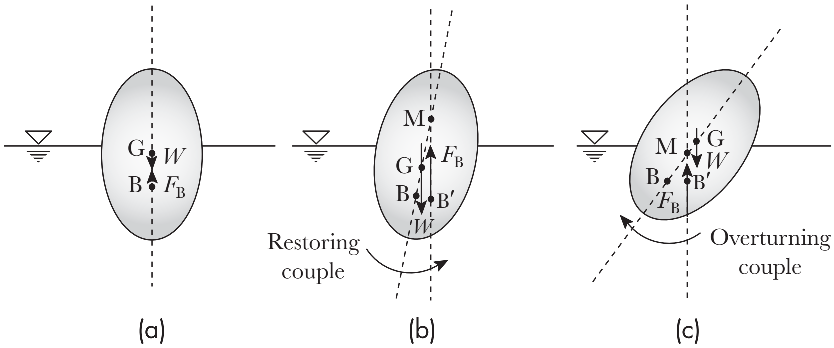

Fig. 2.38 Stable and unstable equilibrium for a floating body (a) Untilted (b) Stable (c) Unstable

the line passing through points G and B will intersect at a point M, known as the *metacentre*. It is defined as the point of intersection of the normal axis of floating body and the line action of buoyancy force when it is tilted. The distance between the CG and the metacentre is known as the *metacentric height* (MG). From Archimedes' principle, the weight of liquid displaced, that is, buoyant force is equal to the weight of the body. This means that on slight tilting, the weight of the body and the buoyant force form a couple. In Fig. 2.38(b), the couple formed is a restoring couple as it will try to restore the body back to an untilted position. The floating body is said to be in the state of stable equilibrium. An increase in the tilt will cause metacentre M to move towards G. Further tilting will cause it to move beyond G. In such a case, the couple formed is an overturning couple as it will topple the body and the body is said to be in unstable equilibrium as shown in Fig. 2.38(c).

It can be concluded that a floating body is stable if the metacentre (M) lies above the CG (or metacentric height must be positive MG > 0) and for instability, M must lie below G (or metacentric height must be negative MG < 0).

To derive the expression for metacentric height, let us consider a boat shown in Fig. 2.39. As the boat is tilted towards the right, it will displace more water towards the right and hence, the centre of buoyancy gets shifted towards the right. The wedge-shaped shaded region shows the excess volume displaced on the right side and a region equal in area on the left moves out of the water during the tilt. This means that there is an increase in the buoyant force on the right side of the boat and there is a reduction in the buoyant force by the same amount on the left side, say dF_B. The small buoyant force dF_B will act through the CGs of the shaded regions as shown in the Fig 2.39(b).

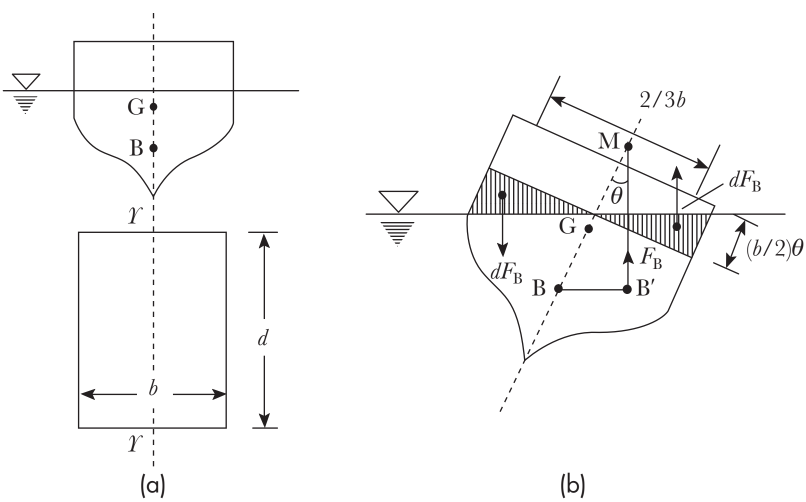

Fig. 2.39 Determination of metacentric height

Therefore, under equilibrium conditions, the restoring moment due to shift in the centre of buoyancy is equal to the couple formed by the force dF_B on each wedge (shaded region).

$$F_B \times BB' = dF_B \times \frac{2}{3}b$$

where b is the width of the boat.

$$\rho g \forall \times BB' = \rho g \forall_w \times \frac{2}{3}b$$

$$\rho g \forall \times MB \sin\theta = \rho g\left(\frac{1}{2}\frac{b}{2}\frac{b}{2}\theta \times d\right)\times \frac{2}{3}b$$

When θ is small, $\sin\theta \approx \theta$

$$\forall \times MB = \frac{db^3}{12} = I_{Y-Y}$$

$$\boxed{MB = \frac{I_{Y-Y}}{\forall}} \qquad (2.46)$$

The metacentric height is, therefore, given by

$$\boxed{MG = \frac{I_{Y-Y}}{\forall} - GB} \qquad (2.47)$$

where $\forall$ is the submerged volume and I_{Y-Y} is the area moment of inertia of the projected plane about $Y-Y$ axis.

Example 2.12 A solid cylinder is 200 mm in diameter and 400 mm high has its base made of 25 mm thick material of specific gravity 4 as shown in Fig. 2.40. The specific gravity of other part of cylinder is 0.8. Find out if it is stable in water.

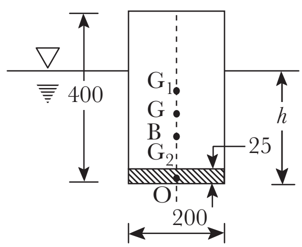

Fig. 2.40

Solution: From Archimedes' principle, the weight of liquid displaced is equal to the weight of the body,

$$\rho_w g\left(\frac{\pi}{4}D^2 h\right) = \rho_m g\left(\frac{\pi}{4}D^2 h_m\right) + \rho_{\text{cyl}} g\left(\frac{\pi}{4}D^2 h_{\text{cyl}}\right)$$

$$\Rightarrow \quad h = 5\times 25 + 0.8\times 375 \quad \Rightarrow \quad h = 312.5\,\text{mm}$$

The position of CG is determined in the following way:

$$W_{\text{total}} \times OG = W_{\text{metal}} \times OG_2 + W_{\text{cyl}} \times OG_1$$

$$\Rightarrow \quad OG = \frac{5\times 25\times 12.5 + 0.8\times 375\times(25+375/2)}{5\times 25 + 0.8\times 375} = 153.67\,\text{mm}$$

The metacentric height can be determined as

$$MG = \frac{I}{\forall} - BG \quad \Rightarrow \quad MG = \frac{\pi D^4/64}{\pi D^2 h/4} - \left(OG - \frac{h}{2}\right)$$

$$\Rightarrow \quad MG = \frac{200^2}{16 \times 312.5} - (153.67 - 156.25) = 10.58\,\text{mm}$$

Since MG is positive, so this is the case of stable equilibrium.

Example 2.13 A 100 kN pontoon (a flat-bottomed boat) of 4 m × 6 m × 0.8 m is to be used to transport a 200 kN cylindrical drum of 2 m in diameter through a river as shown in Fig. 2.41. Check whether the arrangement would be feasible.

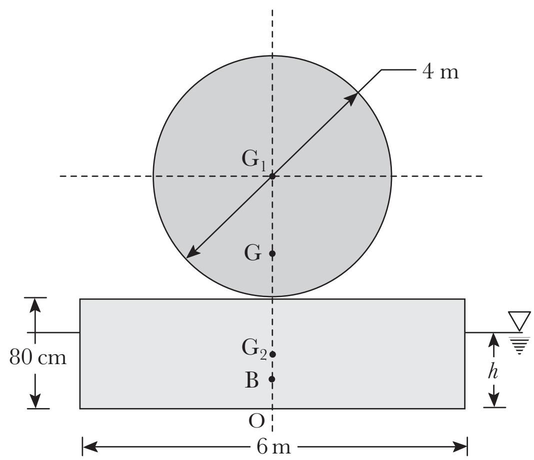

Fig. 2.41

Solution: From Archimedes' principle, the weight of liquid displaced is equal to the total weight,

$$1000 \times 9.81 \times (4 \times 6 \times h) = 300 \times 10^3$$

$$\Rightarrow \quad h = 1.27\ \text{m}$$

The pontoon will be fully submerged. Hence, the given pontoon will not be feasible for transporting the given drum. To check further, the metacentric height is calculated to find out its stability.

The position of CG is determined in the following way:

$$W_{\text{total}} \times OG = W_{\text{pontoon}} \times OG_2 + W_{\text{drum}} \times OG_1$$

$$\Rightarrow \quad OG = \frac{100 \times 0.4 + 200 \times (0.8 + 1)}{300} = 1.33\,\text{m}$$

The metacentric height can be determined as

$$\text{MG} = \frac{I}{\forall} - BG \quad \Rightarrow \quad \text{MG} = \frac{6 \times 4^3}{6 \times 4 \times 0.637} - \left(1.33 - \frac{1.27}{2}\right)$$

$$\Rightarrow \quad \text{MG} = 24.42 \text{ m}$$

Since MG is positive, the arrangement is stable but not feasible as the river water reaches the drum.

2.7 FLUID IN A RIGID BODY MOTION

Under certain circumstances fluids behave like a rigid body, which means they do not deform under the action of forces. As there is no deformation of the fluid, there cannot be any shear stress and the only stress, in such a situation, is the pressure. The following cases will be discussed under this section:

1. Fluid in a tank that is accelerating linearly
2. Fluid in a tank that is rotating about its axis at a uniform angular velocity

The fluid in a uniformly accelerating tank behaves like a rigid mass with each fluid particle having the same acceleration. In addition, the fluid in a tank rotating at a constant angular velocity shows a similar behaviour with each fluid particle rotating at the same angular speed.

First, a generalized equation will be derived for fluid in rigid body motion and later on it will be applied to analyse these two cases.

Consider an infinitesimal three-dimensional rectangular fluid element of dimensions *dx, dy,* and *dz* in *x*-, *y*-, and *z*-directions, respectively. In addition to its weight, it is acted upon by pressures p_x and p_{x+dx} in the *x*-direction, p_y and p_{y+dy} in the *y*-direction, and p_z and p_{z+dz} in the *z*-direction as shown in Fig. 2.42.

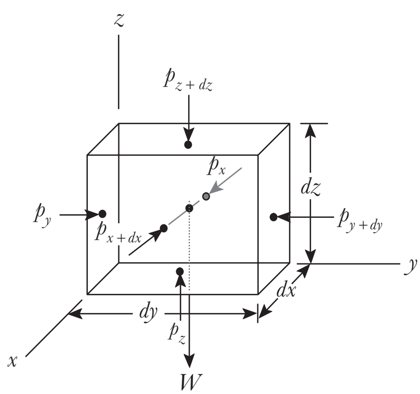

Fig. 2.42 Forces on a fluid element

Applying Newton's second law of motion,

$$\left.\begin{aligned}\sum F_x &= ma_x\\ \sum F_y &= ma_y\\ \sum F_z &= ma_z\end{aligned}\right\} \tag{2.48}$$

where m is the mass of the fluid element given by

$$m = \rho d\forall = \rho\, dxdydz \tag{2.49}$$

and, a_x, a_y, and a_z are the components of acceleration in x-, y-, and z-directions, respectively. In addition, from Pascal's law, pressures $p_x = p_y = p_z = p$

For *x-direction:*

$$\sum F_x = ma_x \quad \Rightarrow \quad (p_x - p_{x+dx})dydz = \rho\, dxdydz\, a_x \tag{2.50}$$

From Taylor's series expansion,

$$p_{x+dx} = p + \frac{\partial p}{\partial x}dx \tag{2.51}$$

In Eq. (2.51), the higher-order terms have been ignored as dx is very small. Equation (2.50), therefore, reduces to

$$-\frac{\partial p}{\partial x} = \rho a_x \tag{2.52}$$

Similarly, for *y-direction*,

$$-\frac{\partial p}{\partial y} = \rho a_y \tag{2.53}$$

For *z-direction*, the weight also acts on the element in addition to pressure

$$(p_z - p_{z+dz})dxdy - W = \rho\, dxdydz\, a_z \tag{2.54}$$

$$(p_z - p_{z+dz})dxdy - \rho\, dxdydz\, g = \rho\, dxdydz\, a_z \tag{2.55}$$

$$-\frac{\partial p}{\partial z} - \rho g = \rho a_z \tag{2.56}$$

In vector form,

$$-\frac{\partial p}{\partial x}\hat{i} - \frac{\partial p}{\partial y}\hat{j} - \left(\frac{\partial p}{\partial z} + \rho g\right)\hat{k} = \rho\left(a_x\hat{i} + a_y\hat{j} + a_z\hat{k}\right) \tag{2.57}$$

$$-\vec{\nabla}p + \rho\vec{g} = \rho\vec{a} \tag{2.58}$$

$$\vec{a} = -\frac{\vec{\nabla}p}{\rho} + \vec{g} \tag{2.59}$$

where $\vec{g} = -g\hat{k}$

Equation (2.59) is the basic equation for fluids in a rigid body motion.

2.7.1 Fluid in an Accelerating Tank

The fluid in a tank moving at uniform acceleration a is shown in Fig. 2.43. The fluid inside the tank will climb up on the rear wall and its surface takes a slanting shape. This happens because of inertia when the fluid does not catch up with the accelerating vehicle on which it is kept. The rise of liquid level on the rear wall is the same as the fall in it on the front wall. In this case,

$$a_x = a \quad \text{and} \quad a_y = a_z = 0$$

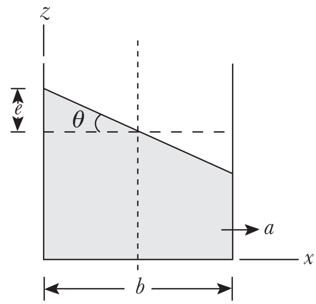

Fig. 2.43 Fluid in accelerating tank

Equations (2.52) and (2.56) are

$$\frac{\partial p}{\partial x} = -\rho a$$

$$\frac{\partial p}{\partial z} = -\rho g$$

Equation (2.53) yields

$$\frac{\partial p}{\partial y} = 0 \text{ which means } p \neq p(y)\text{, that is, } p = p(x, z)$$

Mathematically, $dp = \dfrac{\partial p}{\partial x} dx + \dfrac{\partial p}{\partial z} dz$

$$dp = -adx - gdz$$

At the liquid surface, $p = p_{atm}$ = constant, that is, $dp = 0$

$$-\frac{dz}{dx} = \frac{a}{g} = \tan\theta$$

In addition, $\tan\theta = \dfrac{e}{b/2}$

$$\boxed{e = \frac{ba}{2g}} \tag{2.60}$$

It can be concluded that e will be more if b is more or a is more. Further, it may be concluded that in order to avoid spilling of liquid from the tank, it should be oriented in such a way that the shortest side is aligned in the direction of motion.

Example 2.14 A completely filled petrol tanker, shown in Fig. 2.44, accelerates at $3\,\text{m/s}^2$. If the minimum pressure inside the cylindrical petrol tank is 110 kPa, find out the maximum pressure and its location in the tank. The specific gravity of petrol may be taken as 0.765.

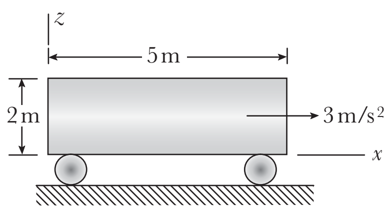

Fig. 2.44

Solution: The vector form of Euler's equation is

$$\vec{a} = -\frac{\vec{\nabla} p}{\rho} + \vec{g}$$

The x- and z-directions Euler's equations, respectively, are

$$\frac{\partial p}{\partial x} = -\rho a \tag{1}$$

$$\frac{\partial p}{\partial z} = -\rho g \tag{2}$$

Integrating Eq. (1),

$$p = -\rho a x + f(z) + \text{C}_1 \tag{3}$$

Differentiating Eq. (3) with respect to z

$$\frac{\partial p}{\partial z} = 0 + f'(z) + 0 \tag{4}$$

From Eqs (2) and (4),

$$f'(z) = -\rho g \tag{5}$$

Integrating Eq. (5),

$$f(z) = -\rho g z + \text{C}_2 \tag{6}$$

Substituting Eq. (6) in Eq. (3),

$$p = -\rho a x - \rho g z + \text{C} \tag{7}$$

where constant C is the sum of constants C_1 and C_2.

The pressure will be minimum at the front top edge where $x = 5$ and $z = 2$ and maximum at the rear bottom edge of the tank where $x = 0$ and $z = 0$.

The constant C can be evaluated by applying boundary condition ($p = p_{min}$ at $x = 5$ and $z = 2$) to Eq. (7), that is,

$$1{,}10{,}000 = -765 \times 3 \times 5 - 765 \times 9.81 \times 2 + C$$

$$\Rightarrow \quad C = 136484.3$$

The maximum pressure is obtained as mentioned here by substituting $x = 0$ and $z = 0$ in Eq. (7)

$$p_{max} = -\rho a(0) - \rho g(0) + C$$

$$\Rightarrow \quad p_{max} = 136.484\,\text{kPa}$$

2.7.2 Fluid in a Rotating Cylindrical Tank

The fluid in a tank rotating at a uniform angular velocity ω is shown in Fig. 2.45. The surface of the water will take the shape of a paraboloid or a *forced vortex*. If the cylindrical tank is open from the top, the liquid may spill out at a particular angular velocity. To find out the height of the parabola, an approach similar to the previous case of accelerating tank has also been followed in the present case. Since the problem involves a cylindrical vessel, the cylindrical coordinates system (r, θ, z) will be taken into consideration; $a_r = -\omega^2 r$ (centripetal acceleration) and $a_\theta = a_z = 0$. The pressure gradients in r, θ, z directions are

$$\frac{1}{\rho}\frac{\partial p}{\partial r} = -a_r = \omega^2 r$$

$$\frac{1}{\rho}\frac{\partial p}{\partial z} = -g$$

$$\frac{\partial p}{\partial \theta} = 0 \text{ which means } p \neq p(\theta)\text{, that is, } p = p(r, z)$$

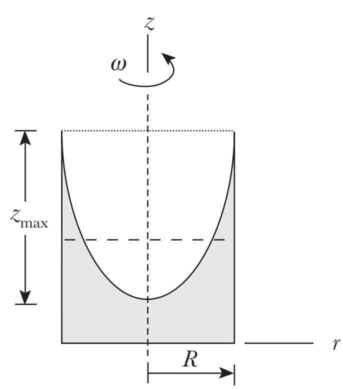

Fig. 2.45 Fluid in rotating tank

Mathematically, $dp = \frac{\partial p}{\partial r}dr + \frac{\partial p}{\partial z}dz$

$$dp = \rho\omega^2 r dr - \rho g dz$$

At the liquid surface, $p = p_{atm}$ = constant, that is, $dp = 0$.

At $r = R$, $z = z_{max}$

$$z_{max} = \frac{\omega^2 R^2}{2g} \tag{2.61}$$

The volume of the paraboloid is given by

$$\forall_{paraboloid} = \frac{1}{2} \times A \times z_{max} \tag{2.62}$$

where A is the area of cross-section of the pipe.

Example 2.15 A 200 mm diameter and 500 mm high open cylindrical drum is filled with water up to the brim. Determine the height of water when the drum is rotated at (a) 200 rpm, (b) 400 rpm, and then brought to rest.

Solution: The depth of parboloid form at 200 rpm is given by

$$z_{max} = \frac{\omega^2 R^2}{2g} \Rightarrow z_{max} = \frac{\left(\frac{2\pi \times 200}{60}\right)^2 \times 0.1^2}{2 \times 9.81} \Rightarrow z_{max} = 0.224\,\text{m}$$

Figure 2.46(a) has been drawn for the case when the drum is rotated at 200 rpm.

Volume of water left inside the drum = volume of the drum − volume of the paraboloid,

$$\forall_{left\text{-}out} = \forall_{drum} - \forall_{paraboloid}$$

that is, $A \times h = A \times H - \frac{1}{2} \times A \times z_{max} \Rightarrow h = 0.5 - 0.224/2 \Rightarrow h = 0.388\,\text{m}$

Now consider the case when the vessel rotates at 400 rpm, the depth of paraboloid formed is given by

$$z_{max} = \frac{\omega^2 R^2}{2g} \Rightarrow z_{max} = \frac{\left(\frac{2\pi \times 400}{60}\right)^2 \times 0.1^2}{2 \times 9.81} \Rightarrow z_{max} = 0.894\,\text{m}$$

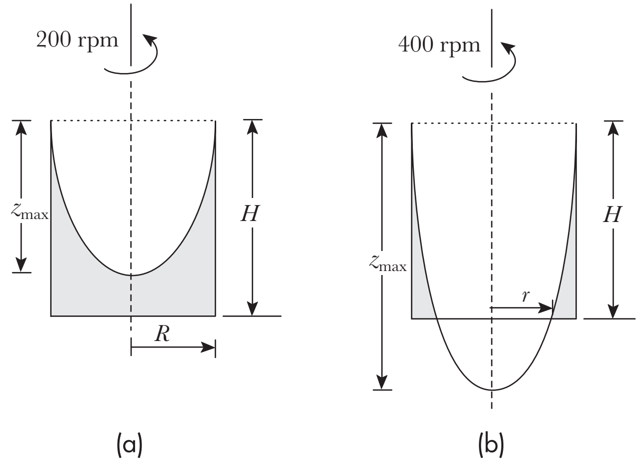

Fig. 2.46

In this case, the depth of the paroboloid exceeds the height of drum, which is shown in Fig. 2.46(b). The volume of water left inside the drum can be found out in the following manner:

$$\forall_{\text{left-out}} = \forall_{\text{drum}} - (\forall_{\text{big paraboloid}} - \forall_{\text{small paraboloid}})$$

$$A \times h = A \times H - \left(\frac{1}{2} \times A \times z_{\max} - \frac{1}{2} \times A_r \times (z_{\max} - H)\right)$$

The height of left-out water remaining in the tank

$$\Rightarrow \quad h = H - \left(\frac{1}{2} z_{\max} - \frac{1}{2} \times \frac{A_r}{A} \times (z_{\max} - H)\right)$$

$$\Rightarrow \quad h = H - \left(\frac{1}{2} z_{\max} - \frac{1}{2} \times \frac{r^2}{R^2} \times (z_{\max} - H)\right) \tag{1}$$

The depths for big and small paraboloids can be written as $z_{\max} = \dfrac{\omega^2 R^2}{2g}$ and $z_{\max} - H = \dfrac{\omega^2 r^2}{2g}$. Since the rotational speed is same for both the parboloids, r can be evaluated as

$$\frac{2g(z_{\max} - H)}{r^2} = \frac{2g z_{\max}}{R^2} = \omega^2 \quad \Rightarrow \quad \frac{r^2}{R^2} = 1 - \frac{H}{z_{\max}} \tag{2}$$

Substituting Eq. (2) in Eq. (1),

$$h = H - \frac{1}{2}\left(z_{\max} - \frac{(z_{\max} - H)^2}{z_{\max}} \right)$$

$$h = 0.5 - \frac{1}{2}\left(0.894 - \frac{(0.894 - 0.5)^2}{0.894} \right) \Rightarrow h = 0.140\,\text{m}$$

Example 2.16 A closed cylindrical vessel of 200 mm in diameter and 400 mm high is completely filled with water. The vessel is rotated at 1000 rpm about its axis. Determine the force at the top and bottom lids of the vessel.

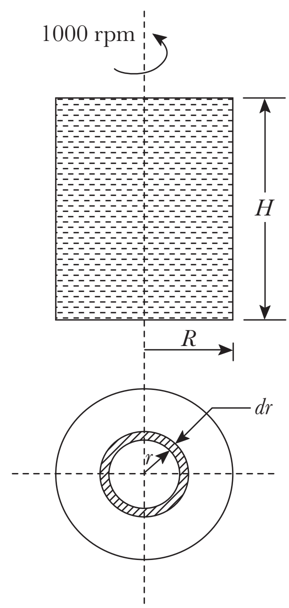

Fig. 2.47

Solution: The force on the top lid is given by considering an elemental ring of thickness dr at a radius r from the axis as shown in Fig. 2.47. The force on the top lid is, thus, given by

$$F_{\text{top}} = \int_0^R p 2\pi r dr$$

where pressure p can be evaluated as

$$p = \rho g z \quad \Rightarrow \quad p = \rho g \frac{\omega^2 r^2}{2g}$$

The expression of force at top reduces to

$$F_{\text{top}} = \pi\rho \int_0^R \omega^2 r^3 dr$$

$$F_{\text{top}} = 1000\pi \left(\frac{2\pi \times 1000}{60} \right)^2 \times \frac{0.1^4}{4} \quad \Rightarrow \quad F_{\text{top}} = 861.3\text{ N}$$

The force at the bottom lid is

$$F_{\text{bottom}} = F_{\text{top}} + \rho g H A_{\text{lid}} \quad \Rightarrow \quad F_{\text{bottom}} = 861.3 + 1000 \times 9.81 \times 0.4 \times \pi \times 0.1^2$$

$$\Rightarrow \quad F_{\text{bottom}} = 984.57\,\text{N}$$

POINTS TO REMEMBER

- According to Pascal's law, the static fluid exerts the same pressure at a point in all the directions.
- Hydrostatic pressure increases linearly with depth and always acts perpendicular to the container surface.
- The hydrostatic pressure force always acts through a point known as the centre of pressure (CP). CP always lies below the CG of a given submerged plane. It is due to the fact that the hydrostatic pressure force increases linearly with the depth. Had it been constant, the two points would have been coincident.
- For submerged curved planes, the hydrostatic pressure force has two components. The vertical component of the force is equal to the weight of fluid vertically above it, if the curved plane is exposed to the fluid from the top. In case if the plane is exposed to the fluid from the bottom, the vertical component will act in the upward direction and is equal to the weight of the imaginary fluid of the same density vertically above it. The horizontal force is equal to the hydrostatic pressure force acting on the projected area of the curved plane.
- For submerged bodies, the stability criterion is that the centre of buoyancy must lie above the CG. For floating bodies, the metacentre must lie above the CG.
- According to Archimedes' principle, the buoyant force acting on a body, partially or fully submerged in a fluid, is always equal to the weight of the volume of fluid it displaces.
- Sometimes, fluids also behave like a rigid body. A fluid in an accelerating tank and fluid in a rotating tank are two such situations.

SUGGESTED READINGS

Cengel, Y., J.M. Cimbala, *Fluid Mechanics—Fundamentals and Applications*, Tata McGraw-Hill Education, New Delhi, 2010.

Fox, R.W., A.T. McDonald, *Introduction to Fluid Mechanics*, 5th Ed., John Wiley & Sons, New Delhi, 2004.

Streeter, V.L., E.B. Wylie, and K.W. Bedford, *Fluid Mechanics*, 9th Ed., Tata McGraw-Hill Education, New Delhi, 2010.

White, F.M., *Fluid Mechanics*, 6th Ed., Tata McGraw-Hill Education, New Delhi, 2008.

MULTIPLE-CHOICE QUESTIONS

2.1 The standard atmospheric pressure (at sea level) is not equal to

(a) 760 mm Hg
(b) 10.3 m of H_2O
(c) 18.2 m of benzene
(d) 101.325 kPa

2.2 A metal in a fluid of the same specific gravity will
(a) float over the surface
(b) be partly immersed
(c) be fully immersed with the top surface touching the free surface of the fluid
(d) sink

2.3 If the magnitude of air pressure to be measured at a point is low, which manometric fluid would be preferred?
(a) Mercury
(b) Water
(c) Brine
(d) Alcohol

2.4 A piece of metal of specific gravity 7 floats in mercury. What fraction of volume is under mercury?
(a) Less than 0.5
(b) More than 0.5
(c) Equal to 0.5
(d) None of these

2.5 A gas at a pressure of 225 torr exerts a force of ____________ kN on an area of $2.0\,m^2$.
(a) 15
(b) 50
(c) 60
(d) 70

2.6 Vacuum pressure at any point is the pressure
(a) above atmospheric pressure
(b) below atmospheric pressure
(c) equal to atmospheric pressure
(d) equal to absolute zero pressure

2.7 A body weighs 1 kg in air, 0.8 kg in water, and 0.6 kg in oil. The specific gravity of oil is
(a) 1
(b) 1.5
(c) 2
(d) 2.5

2.8 Increase in pressure at the outer edge of a drum of radius R due to rotation at ω rad/s, full of liquid of density ρ will be
(a) $\rho\omega^2R^2/2$
(b) $\rho\omega^2R^2$
(c) $2\rho\omega^2R^2$
(d) $\rho\omega^2R$

2.9 A floating body will be under stable equilibrium if
(a) the metacentre lies above the CG
(b) the metacentre lies below the CG
(c) the metacentre lies between the CG and centre of buoyancy
(d) the metacentre lies below the centre of buoyancy

2.10 A submerged body will be under stable equilibrium if
(a) the CG lies below the centre of buoyancy
(b) the CG lies above the centre of buoyancy
(c) the CG coincides with the centre of buoyancy
(d) the metacentre lies below the centre of buoyancy

2.11 Buoyant force depends upon the
(a) mass of displaced liquid
(b) surface tension
(c) position of the CP
(d) viscosity of liquid

2.12 A floating body will oscillate about its ____________ if given a slight displacement.
(a) CG
(b) Centre of buoyancy
(c) CP
(d) Metacentre

2.13 It is easier to swim in sea compared to river because
(a) sea water has higher density
(b) sea has larger volume
(c) waves and tides aid in swimming
(d) all of these

2.14 A floating ice cube in a glass slowly melts, the level of water in the glass will
(a) rise
(b) fall
(c) remain constant
(d) first rise and then fall

2.15 A truck is carrying a tank that is partially filled with water. On the application of brakes, the water level will
(a) rise on the front wall
(b) rise on the back wall
(c) remain constant
(d) none of these

2.16 When a water-filled cylindrical tank is rotated about its axis, the water level rise along the wall is ________________ the level fall at the axis of rotation with respect to the initial water level when the tank is stationary.
(a) greater than
(b) lesser than
(c) same as
(d) independent of

2.17 The distance between the CG and CP of a rectangular plane of width (d) and length (b) is
(a) $d/3$
(b) $d/2$
(c) $2d/3$
(d) $d/6$

2.18 The vertical component of hydrostatic pressure force on a curved surface exposed to the liquid from the bottom is equal to the weight of the
(a) same liquid vertically above it
(b) imaginary liquid of the same density vertically above it
(c) pressure force acting along the surface
(d) none of these

2.19 The horizontal component of the hydrostatic pressure force acting on a curved surface is equal to the product of specific weight area and position of CG of ____________ from the free surface
(a) bottom
(b) top
(c) the projected plane
(d) the lateral plane

2.20 An opening in the hydraulic structure used to regulate flow is known as
(a) orifice
(b) venturi
(c) gate
(d) guide

REVIEW QUESTIONS

2.1 Differentiate between *stress* and *pressure*.
2.2 Explain why a dam has a trapezoidal section with its base thicker than the top.
2.3 What are the drawbacks of a piezometer?
2.4 How would you calibrate a pressure sensor?
2.5 What are the instruments and techniques available to detect small pressure differences?
2.6 How do you justify the selection of a manometric fluid for a given application?
2.7 What is buoyancy? State the Archimedes' principle.

2.8 It has been observed that during boiling of water in a kettle, the vapour bubbles appear on the heated surface. They grow in size and detach from the surface and rise to reach the free surface. Why do the bubbles detach from the heated surface after attaining a particular size? Explain the phenomenon taking into account buoyancy and surface tension.

2.9 How would you know whether a floating body is in stable, unstable, or neutral equilibria? How is it different from stable equilibrium of submerged bodies?

2.10 Which edge of the rectangular tank placed on a uniformly accelerating truck would experience maximum pressure and why?

UNSOLVED PROBLEMS

2.1 Find out the pressure difference between points A and B for the manometers shown in Fig. 2.48.

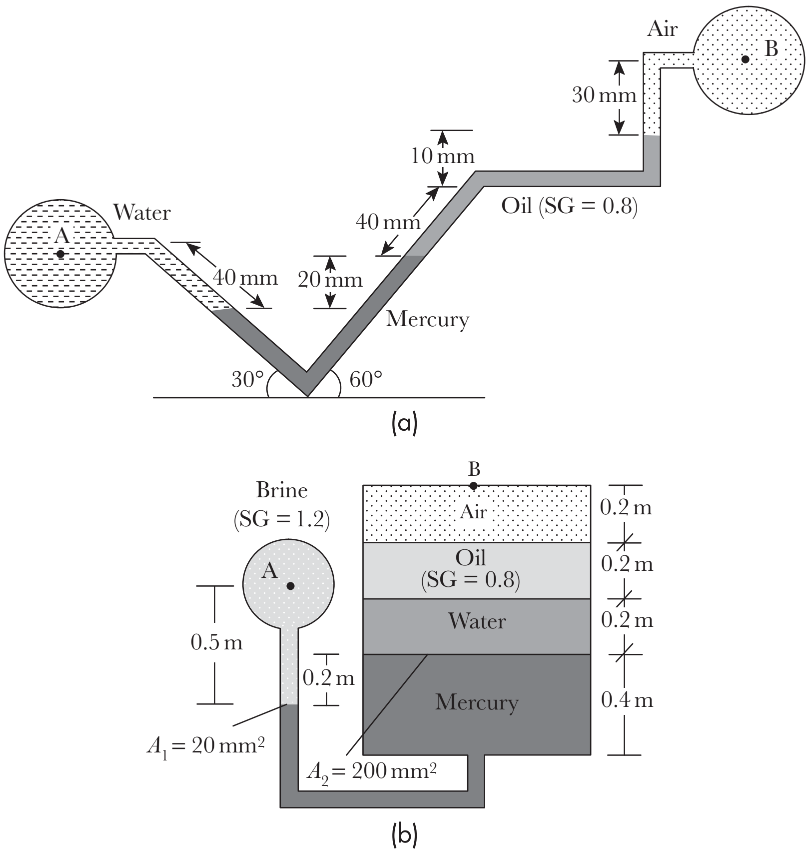

Fig. 2.48

[Ans: (a) 2.8226 kPa (b) 24.331 kPa]

2.2 Determine the absolute pressure of air flowing in a circular duct using an inclined tube manometer, as shown in Fig. 2.49. The barometer reading is 740 mm Hg.

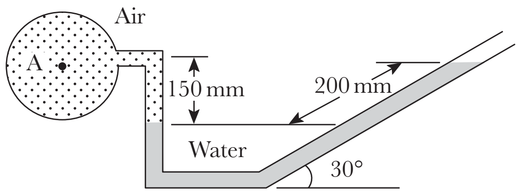

Fig. 2.49

[Ans: 102.304 kPa]

2.3 The water reservoir has an L-shaped gate, as shown in Fig. 2.50. The rise in water level above the hinge would ultimately cause the gate to open. Find the minimum height of water above the hinge that would cause the gate to open. Take the width of the gate as 5 m.

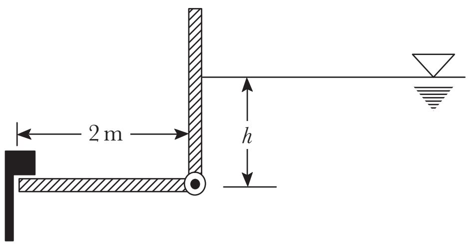

Fig. 2.50

[Ans: 2 m]

2.4 Determine the magnitude of force F required to keep the gate, shown in Fig. 2.51, in position.

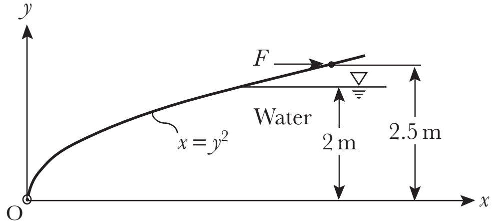

Fig. 2.51

[Ans: 5232 N per unit width]

2.5 Find the net horizontal/vertical forces on the gate/bulge/dam shown in Fig. 2.52. The width of the gate/bulge/dam (into the paper) may be taken as unity in all the cases:

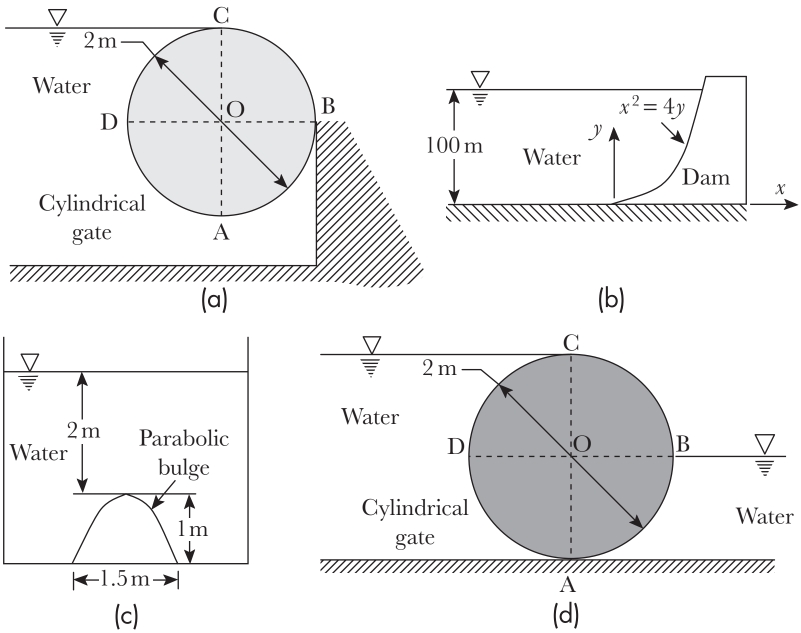

Fig. 2.52

[Ans: (a) $F_H = 4.905$ kN, $F_V = 32.924.3$ kN (b) $F_H = 49.05$ MN, $F_V = 13.08$ MN, (c) $F_H = 0$ N, $F_V = 19.62$ kN (d) $F_H = 14.715$ kN, $F_V = 23.114$ kN]

2.6 Check whether the floating objects having specific gravity 0.8 shown in Fig. 2.53 are stable or not.

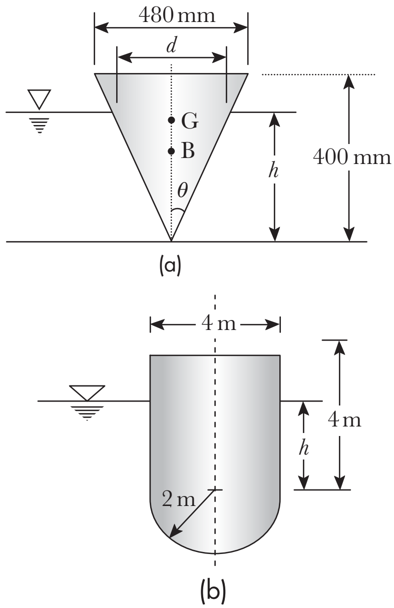

Fig. 2.53

[Ans: (a) MG = 0.07855, stable (b) MG = −0.3041, unstable]

2.7 An open tank, shown in Fig. 2.54, having dimensions 4 m × 3 m × 2 m contains water to a height of 1.0 m. If the tank is moving on a horizontal path at a constant acceleration of 2 m/s², check whether water stays in the tank or it will spill out. In addition, find out the pressure at the bottom of the tank front and rear edges of the tank. Determine the magnitude of acceleration at which the water starts spilling.

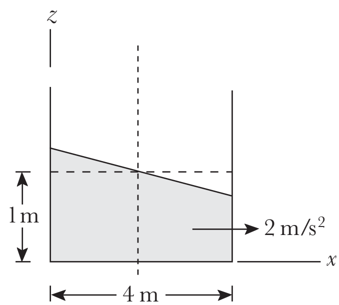

Fig. 2.54

[Ans: No spillage, 5.193 kPa (front), 14.426 kPa (rear), 4.905 m/s²]

2.8 An open cylindrical tank of 1 m × 2 m × 1.5 m high is filled with water up to a height of 1.4 m, as shown in Fig. 2.55. The tank is towed on a truck that accelerates at 5 m/s². Find out whether the water spills out of the tank or not. If yes, also determine the volume of water spilled out of the tank.

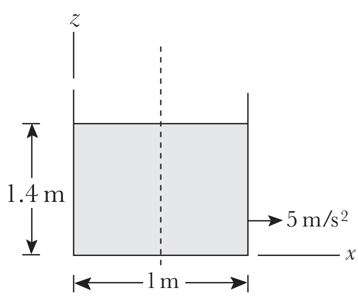

Fig. 2.55

[Ans: 0.04704 m³]

2.9 A 1 m diameter and 2 m high sealed cylindrical tank completely filled with petrol (SG = 0.765) is rotated about its axis at 100 rpm. Determine the difference in pressure between the centre of the top and bottom lids.

[Ans: 11.788 kN]

2.10 A 0.5 m diameter and 1 m high open cylindrical container having water up to a height of 0.2 m is rotating about its axis. Determine the speed at which the paraboloid formed touches the bottom of the tank.

[Ans: 107 rpm]

2.11 Determine the value of h for the arrangement shown in Fig. 2.56. Take $y_1 = 10$ cm and $y_2 = 1$ cm.

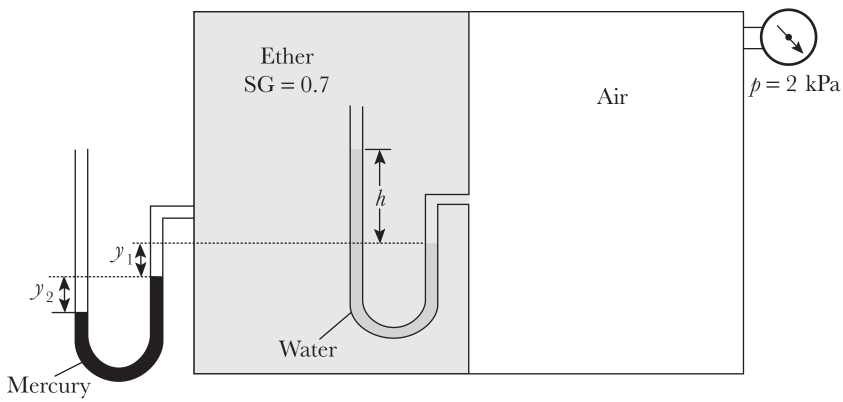

Fig. 2.56

[Ans: 1.366 m]

2.12 Derive the expression for the position of CG and area moment of inertia about the axis passing through CG for the shapes (shaded region) shown in the Fig. 2.57.

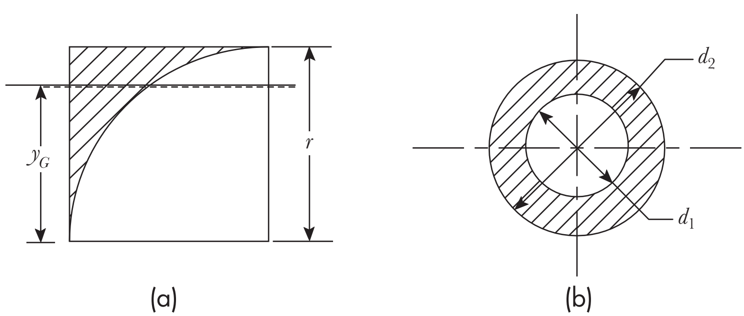

Fig. 2.57

2.13 Figure 2.58 shows a spherical ball of diameter 15 cm tied to the base of a tank filled with water by means of a string. If the mass of the ball is 0.5 kg, determine the tension in the string.

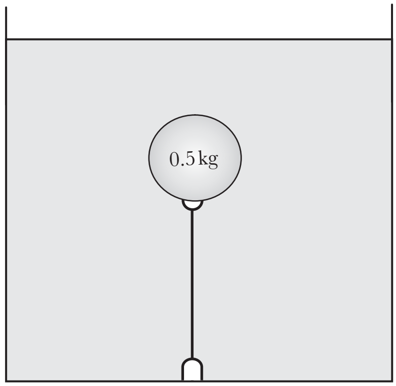

Fig. 2.58

[Ans: 12.43 N]

2.14. Determine the density of the solid block floating at the interface of oil (SG = 0.8) and water as shown in Fig. 2.59, if the fraction of volume of the solid block in water is 0.7.

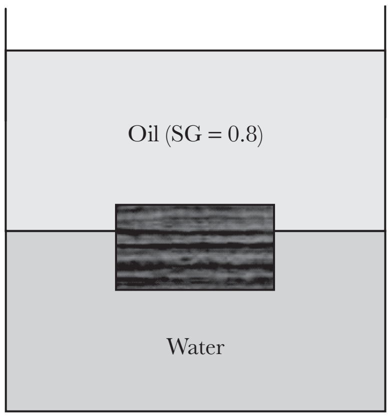

Fig. 2.59

[Ans: 940 kg/m^3]

2.15. A spherical tank of diameter 3 m is quarter filled with water. Determine the inclination of the free surface if it accelerates at 15 m/s^2. In addition, find out the maximum pressure and its location.

[Ans: 56.81°, 9.604 kPa]

Answers to Multiple-choice Questions

2.1 (c)	2.2 (c)	2.3 (d)	2.4 (b)	2.5 (c)
2.6 (b)	2.7 (c)	2.8 (a)	2.9 (a)	2.10 (a)
2.11 (a)	2.12 (d)	2.13 (a)	2.14 (c)	2.15 (a)
2.16 (c)	2.17 (d)	2.18 (b)	2.19 (c)	2.20 (c)

DESIGN OF EXPERIMENTS

Experiment 2.1 Determination of the Centre of Pressure

Objective

To determine the centre of pressure (CP) experimentally

Theory

When a body is submerged in a liquid, it experiences a hydrostatic pressure force that increases linearly as one goes deeper into the liquid. The point on the surface where the resultant hydrostatic pressure force acts is known as the *centre of pressure* (P). The point on the surface where the weight of the body is supposed to be concentrated is known as the *centre of gravity* (CG). The CP always lies below the CG as the hydrostatic pressure increases linearly with depth. It has been shown already that the hydrostatic pressure increases linearly with the depth, which means that the top edge will experience less pressure than the bottom edge. The general expression for the resultant hydrostatic force on a body whose CG lies at a depth of y_G from the free surface is given by

$$F = \rho g y_G A \tag{E2.1}$$

For rectangular section,

$$F_R = \rho g \frac{bd^2}{2} \tag{E2.2}$$

The position of the CP from the free surface is given by

$$y_P = y_G + \frac{I_G}{y_G A} \tag{E2.3}$$

For a rectangular section, theoretically it has been found to be

$$y_P = \frac{2}{3} d \tag{E2.4}$$

Experimental Set-up

A schematic diagram of the experimental set-up is shown in Fig. E2.1. It consists of a beam supported on the knife edge or hinge on the top of a tank. A quadrant clamped to the beam hangs inside the tank. The counterweight is moved back and forth to keep the beam in a horizontal position and to balance the load of quadrant. The water level in the tank is measured with the help of a level indicator attached to one of its side walls. With rise in water level in the tank, the quadrant starts sinking and also starts experiencing a resultant hydrostatic force, which is balanced by applying known weights in the loading pan so that the beam remains horizontal.

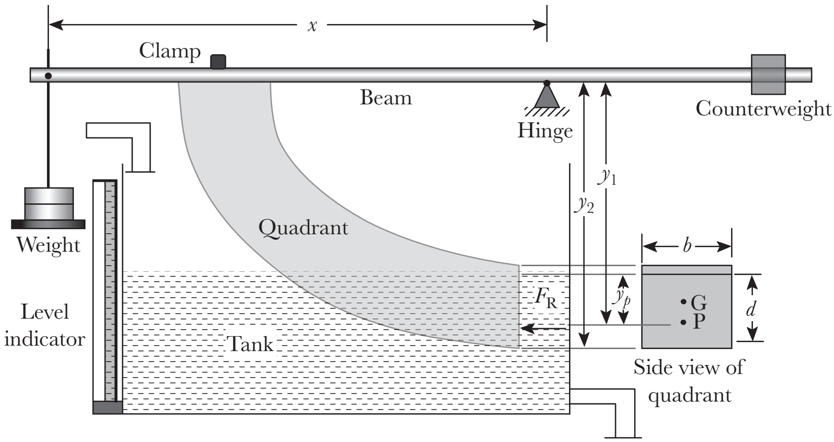

Fig. E2.1 Experimental set-up

The moment of the applied weights balances the moment due to resultant hydrostatic force acting on the quadrant about the hinge, that is,

$$W \times x = F_R \times y_1 \quad \Rightarrow \quad y_1 = \frac{W \times x}{F_R} \tag{E2.5}$$

The experimental value of CP is

$$y_{P,\,\exp} = y_1 - (y_2 - d) \tag{E2.6}$$

Procedure

1. Fix the quadrant on the beam and make it horizontal using a counterweight. Measure x and y_2.
2. Fill the tank till a portion of the quadrant is submerged and note the level indicator's reading.
3. Apply weight on the weighing pan so that the beam becomes horizontal and note down the magnitude of the applied weight.
4. Repeat the experiment for different level of water.

Results and Discussion

1. Draw and discuss the plot y_P versus d.
2. Carry out uncertainty analysis.
3. Point out the sources of error.

Conclusions

Draw conclusions on the results obtained.

Observation Table

Reading no.	Water level reading (m)	Submerged portion, d(m)	Applied load W (N)	$F_R = \rho g \frac{bd^2}{2}$ (N)	$y_1 = \frac{W \times x}{F_R}$ (m)	$y_{P,\exp} = y_1 - (y_2 - d)$ (m)	$y_{P,\text{th}} = \frac{2}{3}d$ (m)	% error = $\frac{\lvert y_{\exp} - y_{\text{th}} \rvert}{y_{\text{th}}}$
1.								
2.								
3.								
…								

Experiment 2.2 Determination of Metacentric Height

Objective

To determine the metacentric height experimentally

Theory

As per Archimedes' principle, a body when immersed into a liquid partially or wholly displaces the liquid equal to its weight. A floating body is said to be stable if after giving a tilt, it comes back to its initial position. Otherwise it is unstable. In technical terms, a floating body is stable if the metacentre (M) lies above its CG. The centre of buoyancy (B) is the CG of the submerged portion of the body or displaced liquid. The metacentric height is given by

$$\mathrm{MG} = \frac{I_{\gamma-\gamma}}{\forall} - GB \tag{E2.7}$$

where, $\forall$ is the submerged volume, $I_{\gamma\text{-}\gamma}$ is the moment of inertia of the projected area of submerged portion of the body.

If MG > 0, the floating body is stable.

If MG < 0, the floating body is unstable.

If MG = 0, the floating body is in neutral equilibrium

Experimental Set-up

The schematic diagram for the experimental set-up is shown in Fig. E2.2. It consists of a body (model), floating in a tank filled with water, having two sliding masses, one in horizontal and the other in vertical direction. The sliding mass in vertical direction (m_v) changes the position of CG whereas sliding mass in horizontal direction (m_h) changes

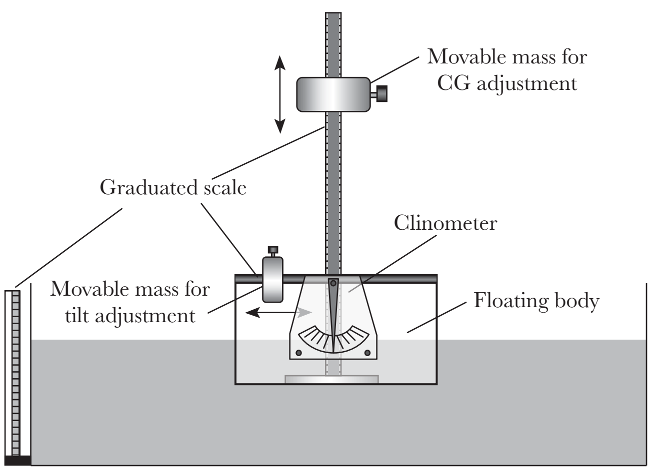

Fig. E2.2 Set-up for metacentric height measurement

the angle of tilt (θ). The title angle is measured using a clinometer. The metacentric height can be obtained experimentally by

$$MG = \frac{W_m x}{W \tan\theta} \tag{E2.8}$$

where W_m is the weight of movable mass m_h, and W is the weight of the model or floating body.

Procedure

1. Note the level of water in the tank.
2. Place the model and again note down the level of water in the tank.
3. Set the movable mass (m_v) at a position (say G_1) and note down the value from the scale.
4. Slide the movable mass (m_h) to a given position x and note the corresponding tilt angle reading from the clinometer. Repeat this step for different positions of m_h.
5. Repeat step 4 for different positions of m_v.

Observation Table

Area of tank, A = ______________________ m^2
Initial water level in the tank without the model, y_1 = ______________ m
Final water level with model, y_2 = ______________________ m
Weight of the model $W = \rho_w A(y_2 - y_1)$ = ____________________ N
Weight of the movable mass for tilt adjustment, $W_m = m_h \times g$ = __________ N

Position of m_v (m)	**Position of m_h from buoyancy axis x (m)**	**Tilt angle θ (°C)**	**Experimental metacentric height $MG = \frac{W_m x}{W \tan\theta}$ (m)**	**Theoretical metacentric height $MG = \frac{I_{Y-Y}}{\forall} - GB$ (m)**	**% error = $\frac{\lvert MG_{exp} - MG_{th} \rvert}{MG_{th}} \times 100$**
G_1					
G_2					
…					

Results and Discussion

Draw MG versus x/θ and discuss the nature.

Conclusions

Draw conclusions on the results obtained.

CHAPTER

3 Fluid Kinematics

LEARNING OBJECTIVES

After studying this chapter, the reader will be able to:

- Develop an understanding about the different types of fluid motion, their salient features, and visualization
- Understand the concept of stream function and velocity potential function, and their use in describing the basic potential flows
- Use different basic potential flows to analyse some of the common flow problems
- Design simple experiments for the flow visualization

Kinematics deals with the motion of a body without considering the forces that cause the motion. Fluid kinematics deals with the motion of fluids where the fluid motion is described by two different approaches—Lagrangian approach and Eulerian approach. The chapter covers in detail various features of fluid motion—translation, rotation, and deformation. Flow visualization is an important aspect of understanding various fluid flow phenomena, and it is best described by the flow lines, namely, streamline, streakline, pathline, and timeline. The concept of streamlines gives rise to an important parameter known as stream function, which forms the basis of potential flow theory. Although potential flow is the study of the irrotational flow of ideal fluids over solid bodies, the analysis is extremely important in approximating the outcome of real fluid flow problems. A detailed coverage of basic and the resultant potential flows is also included in this chapter.

The potential flow theory finds application in high Reynolds number external flows where the viscous effects are negligibly small.

3.1 LAGRANGIAN AND EULERIAN APPROACHES

There are two ways in which fluid motion can be described, namely, the *Lagrangian approach* and the *Eulerian approach*. According to the Lagrangian approach, the individual fluid particles are tracked, and the fluid motion is defined by means

of their positions and velocity vectors. This approach, of course, is in contrast with the continuum concept, discussed earlier in Chapter 1. Consequently, the frame of reference moves with the particle in this case.

The velocity, pressure, density, etc., of a particle can be expressed as a function of time, that is,

$$\left.\begin{aligned} V_p &= V_p(t) \\ p_p &= p_p(t) \\ \rho_p &= \rho_p(t) \\ &\cdots \end{aligned}\right\} \tag{3.1}$$

where p in the subscript represents particle.

Lagrangian approach is easier to comprehend but difficult to apply, as tracking individual particles in the fluid bulk is difficult and tedious unless the particles to be tracked are small in number. The applicability of this methodology is limited to the cases where the gases are less dense and hence, the tracking of the individual particles is not a problem. Therefore, the problems involving rarefied gas dynamics, the entry of meteors, or the re-entry of space shuttle in the upper atmosphere (has very low density) are generally analysed using this methodology.

Compared to Lagrangian approach, Eulerian approach is easier to apply. In this approach, a control volume fixed in space is defined through which the fluid flows. The field variables are defined within the given control volume as a function of space and time coordinates. For example, pressure, velocity, and acceleration fields can be represented as:

$$\left.\begin{aligned} p &= p(x, y, z, t) \\ \vec{V} &= \vec{V}(x, y, z, t) \\ \vec{a} &= \vec{a}(x, y, z, t) \end{aligned}\right\} \tag{3.2}$$

Together they define a *flow field*. In this case, the frame of reference is fixed.

As velocity vector $\vec{V}$ is a function of four variables x, y, z, and t, the small change in $\vec{V}$ can be expressed as

$$d\vec{V} = \frac{\partial \vec{V}}{\partial x}dx + \frac{\partial \vec{V}}{\partial y}dy + \frac{\partial \vec{V}}{\partial z}dz + \frac{\partial \vec{V}}{\partial t}dt \tag{3.3}$$

Dividing throughout by dt,

$$\frac{d\vec{V}}{dt} = \frac{\partial \vec{V}}{\partial x}\frac{dx}{dt} + \frac{\partial \vec{V}}{\partial y}\frac{dy}{dt} + \frac{\partial \vec{V}}{\partial z}\frac{dz}{dt} + \frac{\partial \vec{V}}{\partial t} \tag{3.4}$$

In addition, velocity vector $\vec{V}$ can be written in terms of x, y, and z components, that is, u, v, and w

$$\vec{V} = u\hat{i} + v\hat{j} + w\hat{k} \tag{3.5}$$

where $u = \frac{dx}{dt}, v = \frac{dy}{dt},$ and $w = \frac{dz}{dt}$

Hence, Eq. (3.4) can be expressed as

$$\frac{d\vec{V}}{dt} = \frac{\partial \vec{V}}{\partial t} + u\frac{\partial \vec{V}}{\partial x} + v\frac{\partial \vec{V}}{\partial y} + w\frac{\partial \vec{V}}{\partial z} \tag{3.6}$$

$$\frac{d\vec{V}}{dt} = \frac{\partial \vec{V}}{\partial t} + (\vec{V}.\vec{\nabla})\vec{V} \tag{3.7}$$

$$\frac{d\vec{V}}{dt} = \left(\frac{\partial}{\partial t} + \vec{V}.\vec{\nabla}\right)\vec{V} \tag{3.8}$$

The total derivative '*d/dt*' is represented by the symbol '*D/Dt*', and is given a special name *material derivative*. The material derivative is a *Lagrangian* concept but it works in *Eulerian* frame of reference. The following equation shows the *Lagrangian* derivative of the *Eulerian* quantity:

$$\vec{a} = \underbrace{\frac{D\vec{V}}{Dt}}_{\substack{\text{Total or Lagrangian}\\ \text{acceleration}}} = \underbrace{\frac{\partial \vec{V}}{\partial t}}_{\substack{\text{Local or Eulerian}\\ \text{acceleration}}} + \underbrace{\vec{V}.\vec{\nabla}\vec{V}}_{\substack{\text{Convective}\\ \text{acceleration}}} \tag{3.9}$$

Since the quantity $\vec{V}$ is defined within the control volume, it's a *Eulerian* quantity. The material derivative is *Lagrangian* as it is with respect to time only. The name *material acceleration* might have been given to describe the acceleration of any material, whether it is a solid or fluid. The matter or material has two forms, namely solid and fluid. The convective term is associated to fluids only. Therefore, to generalize the acceleration for any material (solid or fluid), the term *material acceleration* might have been coined. The material acceleration, shown in Eq. (3.9), comes out to be the sum of *local* and *convective* accelerations.

NOTE

In uniform flow, the fluid properties do not vary from point to point at any instant of time, that is, there will be no spatial variation of fluid properties $(\partial/\partial x_i \equiv 0)$. *In non-uniform flows, there is a spatial variation. In steady flow, the fluid properties do not vary with time, that is,* $\partial/\partial t \equiv 0$. *However, there may be spatial variation of fluid properties in steady flows. The flow is unsteady if the properties change with respect to time.*

Based on the definitions of various flows (refer the Note), the following can be deduced for material acceleration:

1. Material acceleration is zero for steady and uniform flows.
2. It is equal to convective acceleration for steady and non-uniform flows.
3. It is equal to local acceleration for uniform and unsteady flows.

The material acceleration in component form in rectangular, cylindrical, and spherical coordinate systems is given as follows:

1. In rectangular coordinate system

$$\left.\begin{aligned} a_x &= \frac{\partial u}{\partial t} + u\frac{\partial u}{\partial x} + v\frac{\partial u}{\partial y} + w\frac{\partial u}{\partial z} \\ a_y &= \frac{\partial v}{\partial t} + u\frac{\partial v}{\partial x} + v\frac{\partial v}{\partial y} + w\frac{\partial v}{\partial z} \\ a_z &= \frac{\partial w}{\partial t} + u\frac{\partial w}{\partial x} + v\frac{\partial w}{\partial y} + w\frac{\partial w}{\partial z} \end{aligned}\right\} \tag{3.10}$$

2. In cylindrical coordinate system

$$\left.\begin{aligned} a_r &= \frac{\partial v_r}{\partial t} + v_r\frac{\partial v_r}{\partial r} + \frac{v_\theta}{r}\frac{\partial v_r}{\partial \theta} + v_z\frac{\partial v_r}{\partial z} - \frac{v_\theta^2}{r} \\ a_\theta &= \frac{\partial v_\theta}{\partial t} + v_r\frac{\partial v_\theta}{\partial r} + \frac{v_\theta}{r}\frac{\partial v_\theta}{\partial \theta} + v_z\frac{\partial v_\theta}{\partial z} + \frac{v_r v_\theta}{r} \\ a_z &= \frac{\partial v_z}{\partial t} + v_r\frac{\partial v_z}{\partial r} + \frac{v_\theta}{r}\frac{\partial v_z}{\partial \theta} + v_z\frac{\partial v_z}{\partial z} \end{aligned}\right\} \tag{3.11}$$

3. In spherical coordinate system

$$\left.\begin{aligned} a_r &= \frac{\partial v_r}{\partial t} + v_r\frac{\partial v_r}{\partial r} + \frac{v_\phi}{r}\frac{\partial v_r}{\partial \phi} + \frac{v_\theta}{r\sin\phi}\frac{\partial v_r}{\partial \theta} - \frac{v_\phi^2 + v_\theta^2}{r} \\ a_\phi &= \frac{\partial v_\phi}{\partial t} + v_r\frac{\partial v_\phi}{\partial r} + \frac{v_\phi}{r}\frac{\partial v_\phi}{\partial \phi} + \frac{v_\theta}{r\sin\phi}\frac{\partial v_\phi}{\partial \theta} - \frac{v_r v_\phi}{r} - \frac{v_\theta^2\cot\phi}{r} \\ a_\theta &= \frac{\partial v_\theta}{\partial t} + v_r\frac{\partial v_\theta}{\partial r} + \frac{v_\phi}{r}\frac{\partial v_\theta}{\partial \phi} + \frac{v_\theta}{r\sin\phi}\frac{\partial v_\theta}{\partial \theta} + \frac{v_\theta v_r}{r} + \frac{v_\theta v_\phi\cot\phi}{r} \end{aligned}\right\} \tag{3.12}$$

Example 3.1 A 2D velocity field is represented by $\vec{V} = 3y^2\hat{i} + 2x\hat{j}$. Compute at point (2, 3) the (a) velocity, (b) local acceleration, (c) convective acceleration, and (d) total acceleration.

Solution:

The magnitude of velocity is given as

$$V = \sqrt{u^2 + v^2} \quad \Rightarrow \quad V = \sqrt{(3y^2)^2 + (2x)^2}$$

$$\Rightarrow \quad V = \sqrt{9 \times 3^4 + 4 \times 2^2} \quad \Rightarrow \quad V = 27.3 \text{ units}$$

The local acceleration is given as

$$\frac{\partial V}{\partial t} = 0$$

The convective acceleration is given as

$$\vec{a} = (\vec{V}.\nabla)\vec{V}$$

x-component is given as

$$a_x = u\frac{\partial u}{\partial x} + v\frac{\partial u}{\partial y} \quad \Rightarrow \quad a_x = 3y^2 \times 0 + 2x \times 6y \quad \Rightarrow \quad a_x = 12xy$$

y-component is given as

$$a_y = u\frac{\partial v}{\partial x} + v\frac{\partial v}{\partial y} \quad \Rightarrow \quad a_y = 3y^2 \times 2 + 2x \times 0 \quad \Rightarrow \quad a_y = 6y^2$$

The magnitude of convective acceleration is

$$\Rightarrow \quad a = \sqrt{a_x^2 + a_y^2} \quad \Rightarrow \quad a = \sqrt{144x^2y^2 + 36y^4}$$

$$\Rightarrow \quad a = \sqrt{144 \times 2^2 \times 3^2 + 36 \times 3^4} \quad \Rightarrow \quad a = 90 \text{ units}$$

The total acceleration will be same as the convective acceleration.

3.2 FLOW LINES

The visual examination of flow is termed as *flow visualization*. For a better understanding of any fluid flow phenomenon, the flow domain is best described by imaginary lines known as *flow lines*, namely, streamline, streakline, pathline, and timeline. Each type of flow line has its own relevance and importance in comprehending fluid flow behaviour. The concept of each flow line is described in Sections 3.2.1–3.2.4.

3.2.1 Streamline

Streamline is a curve that is tangential to the velocity vector. In other words, a tangent at any point on the streamline gives the direction of flow. The streamlines never intersect, and there can be no flow across them.

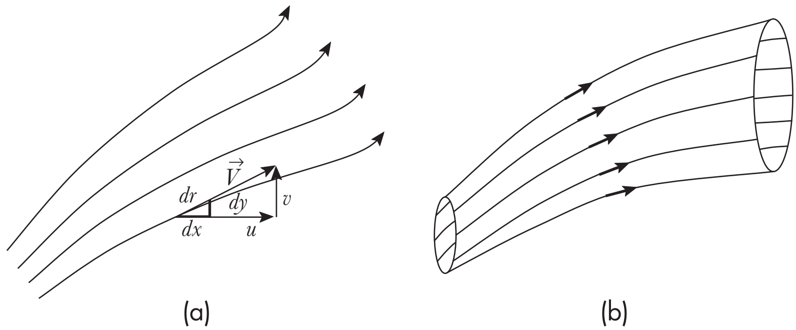

Fig. 3.1 (a) Streamlines (b) Stream tube

Figure 3.1(a) shows a velocity vector and the small element of length *dr* on the streamline, such that the displacement vector for the infinitesimal element is given by

$$d\vec{r} = dx\hat{i} + dy\hat{j} \tag{3.13}$$

The velocity vector in terms of *x* and *y* components is given as

$$\vec{V} = u\hat{i} + v\hat{j} \tag{3.14}$$

The two triangles formed by the velocity components and the displacement components are similar, therefore

$$\frac{dr}{V} = \frac{dx}{u} = \frac{dy}{v} \tag{3.15}$$

Equation (3.15) represents the *equation of streamline* for 2D flow.

Stream tube is a tubular region surrounded by streamlines, as shown in Fig. 3.1(b). Since there can be no flow across the streamlines, the boundary of stream tube behaves like a frictionless solid boundary. A stream tube is termed as *stream filament* if its cross-sectional area is infinitesimally small. If the flow is unsteady, the shape of the stream tube and its position will keep on changing with time. Nevertheless, for steady flow the stream tube will act like an actual tube with fluid flowing through it. Its position and shape will remain unchanged with time.

3.2.2 Pathline

Pathline is a Lagrangian concept in which the motion of the individual fluid particles is tracked. *Pathline* is defined as the actual path traced by a fluid particle. The concept of pathline is used in *particle image velocimetry* (*PIV*) systems, shown in Fig. 3.2.

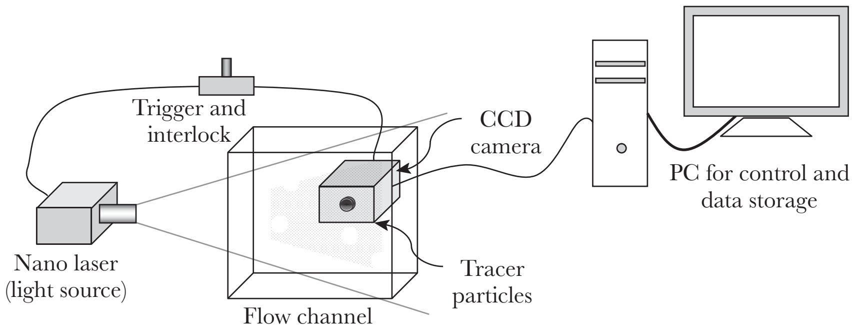

Fig. 3.2 PIV system

The tracer particles are added into the flow stream and they are illuminated by a light source. The camera captures the position of tracer particles in the time interval $t = t_i$ to $t = t_f$. The tracer particle can, thus, be located from the following equation:

$$\vec{x} = \vec{x}_i + \int_{t_i}^{t_f} \vec{V} dt \tag{3.16}$$

In differential form, the pathline for 3D flow is represented by the following:

$$\frac{dx}{dt} = u; \quad \frac{dy}{dt} = v; \quad \frac{dz}{dt} = w \tag{3.17}$$

3.2.3 Streakline

A *streakline* is the instantaneous locus of all the fluid particles that have passed through a fixed point. Figure 3.3 is drawn to illustrate the concept of pathlines and streaklines. The particles emerge from the origin (fixed point), and each particle has its own trajectory referred to as pathline. Streakline is obtained by joining the instantaneous positions of different particles that have passed through the fixed point (in this case origin O). The dashed lines shown in the figure are the streaklines at different instants.

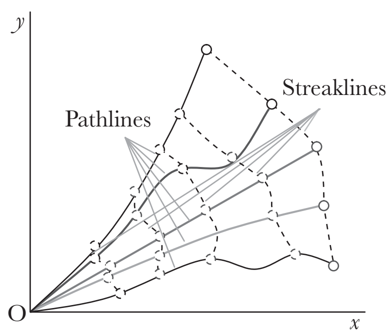

Fig. 3.3 Pathline and streakline

One can visualize a *streakline* by injecting a dye in the liquid flowing in a transparent pipe or injecting smoke in a wind tunnel. The point of injection of the dye is the fixed point through which all the dyed fluid particles passed. Line obtained by joining all such particles at a given instant is the streakline. In fact, the *Reynolds experiment*, shown in Fig. 3.4, makes use of this concept in identifying whether the flow is laminar or turbulent. If *streakline* appears like a continuous thread throughout the length of the pipe, the flow is termed as laminar. On the other hand, if the flow is turbulent, there will not be a continuous well-defined *streakline*. In turbulent flow, the thread breaks down and the dye disperses all across the tube cross section.

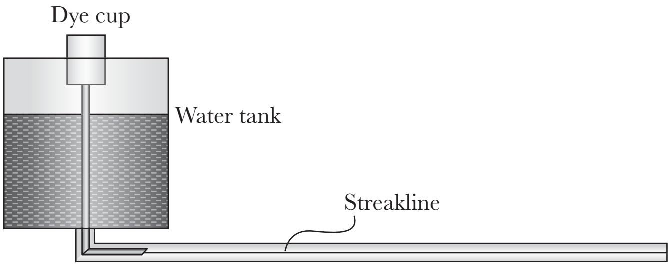

Fig. 3.4 Reynolds experiment

The equation of streakline can be obtained by using the pathline equation to find out the particles that have passed through a predefined point (x_0, y_0) for different values of $\tau < t$ (see Example 3.2).

3.2.4 Timeline

Timeline is the curve formed by joining the locations of different fluid particles at any instant of time. Figure 3.5 shows the *timeline* of a set of fluid particles at different time instants. These lines are helpful to ascertain whether the flow is uniform or not.

Although both streakline and timeline are the locus of different fluid particles at a given instant, the only difference is that for streakline all the particles should have passed through the same fixed point whereas for timeline it is not a precondition.

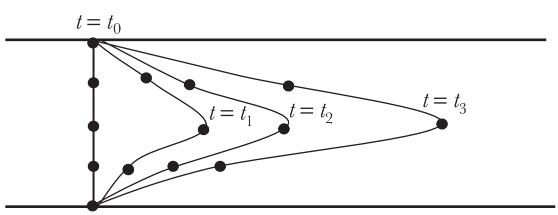

Fig. 3.5 Timelines at different time instants

NOTE

In a steady flow, the streamlines, pathlines, and streaklines are identical, whereas in case of unsteady or transient flow, the streamline pattern evolves with time; pathlines and streaklines are generated during the course of time.

Example 3.2 If the velocity distribution for a 2D ideal flow is given by

$$u = \frac{x}{2+t}; \quad v = \frac{y}{1+3t}$$

Obtain the equation of (a) the streamlines, (b) the pathlines, and (c) the streaklines that pass through point (1, 2) at $t = 0$.

Solution:

Streamline From the equation of streamline:

$$\frac{dx}{u} = \frac{dy}{v} = ds \text{ (say)}$$

Substituting u and v in this equation and simplifying we get

$$\frac{dx}{x} = \frac{ds}{2+t} \quad \text{and} \quad \frac{dy}{y} = \frac{ds}{1+3t}$$

Integrating these equations (note that t is independent of s) we get

$$x = C_1 \exp\left(\frac{s}{2+t}\right) \quad \text{and} \quad y = C_2 \exp\left(\frac{s}{1+3t}\right)$$

These equations represent family of curves for different values of s.

At time $t = 0$, taking $s = 0$ for the streamline passing through point (1, 2). The substitution gives the value of constants as $C_1 = 1$ and $C_2 = 2$. The equation of streamline passing through point (1, 2) is

$$x = \exp\left(\frac{s}{2+t}\right) \quad \text{and} \quad y = 2 \exp\left(\frac{s}{1+3t}\right)$$

Eliminating s, the final equation of streamline is

$$y = 2x^{\left(\frac{2+t}{1+3t}\right)}$$

The streamlines represented by this equation are shown in Fig. 3.6.

Pathline From the equation of pathline:

$$\frac{dx}{dt} = u = \frac{x}{2+t}; \quad \frac{dy}{dt} = v = \frac{y}{1+3t}$$

On separating the variables,

$$\frac{dx}{x} = \frac{dt}{2+t}; \quad \frac{dy}{y} = \frac{dt}{1+3t}$$

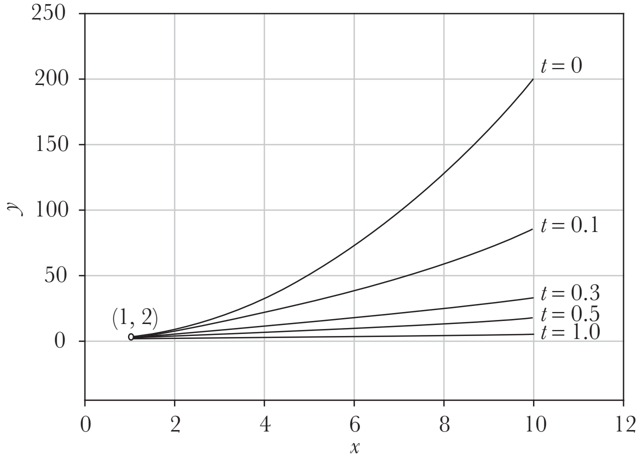

Fig. 3.6 Streamlines

On integration,

$$x = C_1(2+t); \quad y = C_2(1+3t)^{1/3} \tag{1}$$

To evaluate the constants applying the initial condition, that is, at $t = 0$, $x = 1$ and $y = 2$, $C_1 = 1/2$ and $C_2 = 2$.

Eliminating t after substituting the constants in Eq. (1), the final equation of pathline becomes:

$$y = 2(6x-5)^{1/3}$$

The pathline represented by this equation is shown in Fig. 3.7.

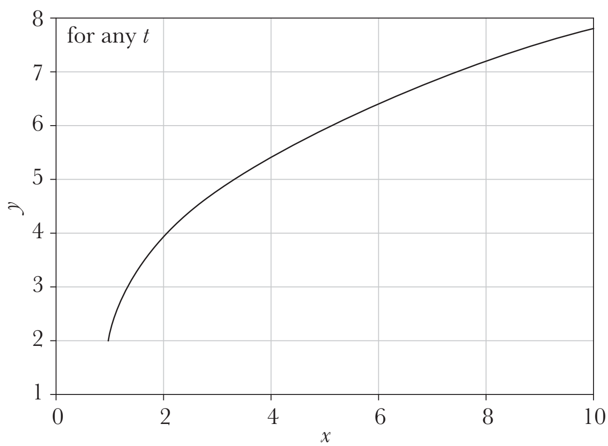

Fig. 3.7 Pathline

Streakline To find the streakline, the general parametric equation of pathline, that is, Eq. (1) is used to find out the particles that have passed through the point (1, 2) for all $\tau < t$.

For $t = \tau$, $x = 1$, and $y = 2$, that is,

$$1 = C_1(2+\tau); \quad 2 = C_2(1+3\tau)^{1/3}$$

The values of constants are

$$C_1 = 1/(2+\tau); \quad C_2 = 2/(1+3\tau)^{1/3}$$

Substituting the constants in Eq. (1):

$$x = \frac{2+t}{2+\tau}; \quad y = 2\left(\frac{1+3t}{1+3\tau}\right)^{1/3}$$

Eliminating τ, the final equation of streakline is

$$y = 2\left(\frac{(1+3t)x}{6+3t-5x}\right)^{1/3}$$

The streaklines represented by this equation are shown in Fig. 3.8.

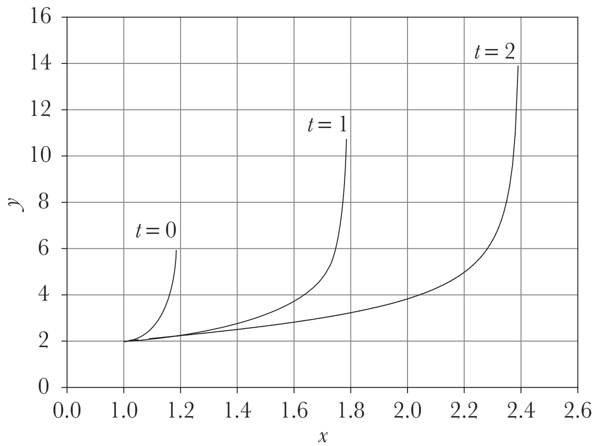

Fig. 3.8 Streaklines

Example 3.3 For the 2D inviscid flow through a duct shown in Fig. 3.9, find out the equation of the streamline passing through the point (0, 0.6). The flow may be assumed to be uniform at the entrance of the duct.

Solution:

The ratio of discharge (per unit duct depth) between the streamlines passing through (0, 3) and (0, 0.6), and the streamlines passing through (0, 3) and (0, 0) is

$$\frac{q'}{q} = \frac{3-0.6}{3-0} = 0.8 \tag{1}$$

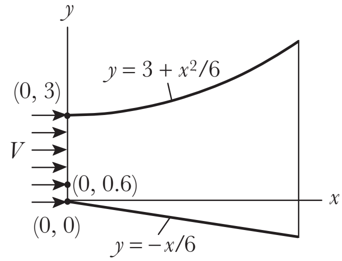

Fig. 3.9

Let the stream line passing through (0, 0.6) be represented by $f(x, y)$. Equation (1) is equal to the difference between the respective stream functions.

$$\frac{q'}{q} = \frac{\psi|_{(0,3)} - \psi|_{(0,0.6)}}{\psi|_{(0,3)} - \psi|_{(0,0)}}$$

$$\frac{q'}{q} = \frac{(y - x^2/6 - 3) - f(x, y)}{(y - x^2/6 - 3) - (y + x/6)} \tag{2}$$

From Eqs (1) and (2),

$$f(x, y) = y - \frac{x^2}{30} + \frac{2}{15}x - 3/5$$

$$f(0, 0.6) = y - \frac{x^2}{30} + \frac{2}{15}x - 3/5 = 0$$

Therefore, the equation of streamline $\psi|_{(0,0.6)}$ is given by

$$y = \frac{x^2}{30} - \frac{2}{15}x + \frac{3}{5}$$

3.3 FEATURES OF FLUID MOTION

In *solid mechanics*, the motion of solid objects is described by *translation* and/or *rotation*. The fluid motion, on the other hand, is characterized by *translation*, *rotation*, and *deformation rate*. Solids do undergo deformation as discussed in Section 1.1 of Chapter 1. It is the rate of deformation that differentiates fluids from solids. To understand these features, the following three cases have been analysed:

Case I—Translation Consider an infinitesimal rectangular fluid element of dimensions dx and dy in x- and y-directions, respectively, shown in Fig. 3.10. The figure shows the element's position at time $t = 0$ and its position at $t = \delta t$. The element is placed in a flow field, represented by the following constant velocity components:

$$\left.\begin{aligned} u &= C_1 \\ v &= C_2 \end{aligned}\right\} \tag{3.18}$$

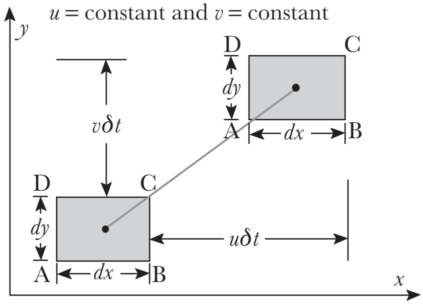

Fig. 3.10 Pure translation

As the fluid element moves with a constant velocity, there will neither be any change in the physical dimensions of the element nor in the included angle (angle between the adjacent sides). Thus, the flow field will be completely uniform in such a case.

Case II—Translation and linear deformation If the element is placed in a flow field, where the velocity components are the function of their respective coordinates, such that

$$\left.\begin{aligned} u &= u(x) \\ v &= v(y) \end{aligned}\right\} \tag{3.19}$$

In such a case, the element will undergo translation and deformation simultaneously (Fig. 3.11). The magnitude of deformation in the x- and y-directions is proportional to the velocity components in those directions. It is interesting to note that there is no change in the included angles, that is, there will be no angular deformation. The rate of linear deformation is termed as *linear strain rate*. Linear strain rates in x- and y-directions are given by

$$\dot{\varepsilon}_x = \frac{\partial u}{\partial x}\, dx/dx \;\Rightarrow\; \boxed{\dot{\varepsilon}_x = \frac{\partial u}{\partial x}} \tag{3.20}$$

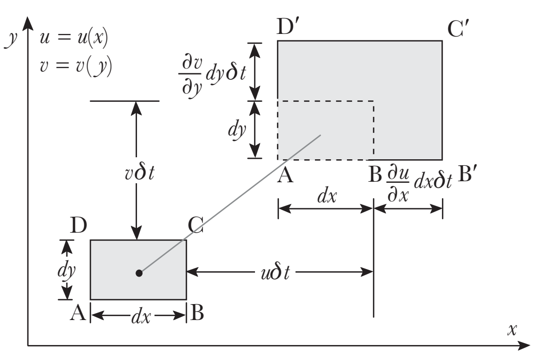

Fig. 3.11 Translation and linear deformation

Similarly,

$$\dot{\varepsilon}_y = \frac{\partial v}{\partial y}dy/dy = \frac{\partial v}{\partial y} \quad \Rightarrow \quad \boxed{\dot{\varepsilon}_y = \frac{\partial v}{\partial y}} \tag{3.21}$$

Case-III—Translation, angular deformation, and rotation A fluid element will exhibit translation, angular deformation, and rotation when both the velocity components are the function of both x and y (Fig. 3.12).

$$\left.\begin{array}{l} u = u(x, y) \\ v = v(x, y) \end{array}\right\} \tag{3.22}$$

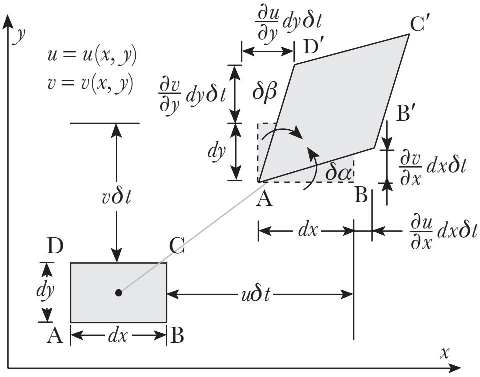

Fig. 3.12 Translation, angular deformation, and rotation

In this case, the element will undergo a continuous change in linear as well as in angular dimensions. The linear strain rate is given by Eqs (3.20) and (3.21). The angular strain rate is given by

$$\dot{\gamma}_{xy} = \frac{1}{2}\left(\frac{\delta\alpha}{\delta t} + \frac{\delta\beta}{\delta t}\right) \quad \Rightarrow \quad \dot{\gamma}_{xy} = \frac{1}{2}\left(\frac{\frac{\partial v}{\partial x}dx\delta t/dx}{\delta t} + \frac{\frac{\partial u}{\partial y}dy\delta t/dy}{\delta t}\right) \tag{3.23}$$

$$\boxed{\dot{\gamma}_{xy} = \frac{1}{2}\left(\frac{\partial v}{\partial x} + \frac{\partial u}{\partial y}\right)} \tag{3.24}$$

The rate with which B moves to B′ with respect to A, that is, $\delta\alpha/\delta t$, and D to D′ with respect to A, that is, $\delta\beta/\delta t$ can be treated as rotation. If the counter clockwise direction is taken as positive, the rate of rotation or angular velocity is given by

$$\omega_z = \frac{1}{2}\left(\frac{\delta\alpha}{\delta t} - \frac{\delta\beta}{\delta t}\right) \tag{3.25}$$

$$\Rightarrow \quad \omega_z = \frac{1}{2}\left(\frac{\partial v}{\partial x} - \frac{\partial u}{\partial y}\right) \tag{3.26}$$

Special cases

1. Pure rotation without deformation is obtained when $\dot{\gamma}_{xy} = 0$

$$\frac{\partial v}{\partial x} = -\frac{\partial u}{\partial y} \quad \Rightarrow \quad \omega_z = 2\frac{\partial v}{\partial x} = -2\frac{\partial u}{\partial y}$$

2. Deformation without rotation is obtained when $\omega_z = 0$

$$\frac{\partial v}{\partial x} = \frac{\partial u}{\partial y} \quad \Rightarrow \quad \dot{\gamma}_{xy} = 2\frac{\partial v}{\partial x} = 2\frac{\partial u}{\partial y}$$

For 3D flow,

$$\left.\begin{aligned} \omega_x &= \frac{1}{2}\left(\frac{\partial w}{\partial y} - \frac{\partial v}{\partial z}\right) \\ \omega_y &= \frac{1}{2}\left(\frac{\partial u}{\partial z} - \frac{\partial w}{\partial x}\right) \\ \omega_z &= \frac{1}{2}\left(\frac{\partial v}{\partial x} - \frac{\partial u}{\partial y}\right) \end{aligned}\right\} \tag{3.27}$$

In vector form, the angular velocity is

$$\vec{\omega} = \frac{1}{2}\vec{\nabla} \times \vec{V} \tag{3.28}$$

The rotational motion of fluid element is also defined by the terms *vorticity* and *circulation*. *Vorticity* is defined as the *curl* of velocity vector, which is equal to twice the angular velocity, that is,

$$\vec{\Omega} = \vec{\nabla} \times \vec{V} = 2\vec{\omega} \tag{3.29}$$

Circulation is defined as the *line integral* of the tangential component of the fluid velocity around a closed loop C.

$$\Gamma = \oint_C \vec{V}.d\vec{s} \tag{3.30}$$

where $d\vec{s}$ is an element on the closed loop C, as shown in Fig. 3.13.

From the *Stokes' theorem*, line integral of velocity vector $\vec{V}$ around a closed loop is equal to the flux of curl $\vec{V}$ through any surface A bounded by a closed loop, that is,

$$\int_C \vec{V}.d\vec{s} = \int_A (\vec{\nabla} \times \vec{V}).d\vec{A} \tag{3.31}$$

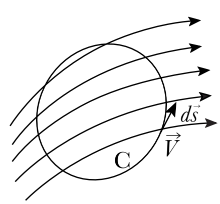

Fig. 3.13 Circulation around closed loop

From Eqs (3.29), (3.30), and (3.31), the *circulation* and *vorticity* can be related as

$$\Gamma = \int_A \vec{\Omega}.d\vec{A} \tag{3.32}$$

Example 3.4 If the velocity field is defined by

$$\vec{V} = (-3x + 5y)\hat{i} + (x^2 + 3y)\hat{j}$$

Determine the circulation around a path enclosed by $x_1 = 1$, $x_2 = 3$, $y_1 = 0$, and $y_2 = 2$ (Fig. 3.14).

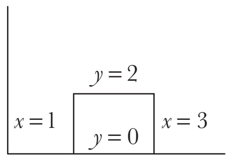

Fig. 3.14

Solution: The circulation, by definition, is

$$\Gamma = \oint_C \vec{V}.d\vec{s} \quad \Rightarrow \quad \Gamma = \oint_C [(-3x + 5y)\hat{i} + (x^2 + 3y)\hat{j}].[dx\hat{i} + dy\hat{j}]$$

or $$\Gamma = \int_1^3 (-3x + 5y)\,dx + \int_0^2 (x^2 + 3y)\,dy + \int_3^1 (-3x + 5y)\,dx + \int_2^0 (x^2 + 3y)\,dy$$

or $$\Gamma = \left| -3\frac{x^2}{2} + 5xy \right|_{x=1}^{x=3} + \left| x^2 y + 3\frac{y^2}{2} \right|_{y=0}^{y=2} + \left| -3\frac{x^2}{2} + 5xy \right|_{x=3}^{x=1} + \left| x^2 y + 3\frac{y^2}{2} \right|_{y=2}^{y=0}$$

$$\Gamma = \left\{ \left(-3\times\frac{3^2}{2} + 5\times 3\times 0 \right) - \left(-3\times\frac{1^2}{2} + 5\times 1\times 0 \right) \right\}$$

$$+ \left\{ \left(3^2\times 2 + 3\times\frac{2^2}{2} \right) - \left(3^2\times 0 + 3\times\frac{0^2}{2} \right) \right\}$$

$$+ \left\{ \left(-3\times\frac{1^2}{2} + 5\times 3\times 2 \right) - \left(-3\times\frac{3^2}{2} + 5\times 3\times 2 \right) \right\}$$

$$+ \left\{ \left(1^2\times 0 + 3\times\frac{0^2}{2} \right) - \left(1^2\times 2 + 3\times\frac{2^2}{2} \right) \right\}$$

$$\Gamma = \left\{ \left(-\frac{27}{2} \right) - \left(-\frac{3}{2} \right) \right\} + \{24 - 0\} + \left\{ \left(\frac{57}{2} \right) - \left(\frac{33}{2} \right) \right\} + \{0 - 8\} = 16\,\text{units}$$

3.4 CONDITION FOR THE EXISTENCE OF FLOW

The laws of the universe must not be violated by a material body, whether it is solid or fluid. A fluid must obey the mass conservation principle or *the continuity equation*. Like energy conservation principle, the mass conservation

principle states that the total mass of a system remains constant. Thus, the flow field represented by the velocity vector $\vec{V} = u\hat{i} + v\hat{j} + w\hat{k}$ must obey the mass conservation principle. The *continuity equation* in differential form will be derived in Chapter 4.

In vector form,

$$\frac{\partial \rho}{\partial t} + \vec{\nabla}.\rho\vec{V} = 0 \tag{3.33}$$

For the incompressible fluid (ρ = constant), the *continuity equation* in rectangular and cylindrical system, respectively, is given as

$$\frac{\partial u}{\partial x} + \frac{\partial v}{\partial y} + \frac{\partial w}{\partial z} = 0 \quad \text{(rectangular)} \tag{3.34a}$$

$$\frac{\partial v_r}{\partial r} + \frac{v_r}{r} + \frac{1}{r}\frac{\partial v_\theta}{\partial \theta} + \frac{\partial v_z}{\partial z} = 0 \quad \text{(cylindrical)} \tag{3.34b}$$

or

$$\dot{\varepsilon}_x + \dot{\varepsilon}_y + \dot{\varepsilon}_z = 0 \tag{3.35}$$

NOTE

It should be noted that the flow will exist if and only if the components of the velocity vector $\vec{V}$ satisfy the continuity equation. In other words, for the existence of a flow field, the continuity equation must be satisfied.

Example 3.5 A 2D incompressible flow in polar coordinates is given by

$$v_r = a(b - c/r^2)\cos\theta \quad \text{and} \quad v_\theta = -a(b + c/r^2)\sin\theta$$

State whether the flow exists.

Solution: Applying the continuity equation in polar form on the given velocity field to check whether the flow exists or not,

$$\frac{\partial v_r}{\partial r} + \frac{v_r}{r} + \frac{1}{r}\frac{\partial v_\theta}{\partial \theta} = 0$$

$$\text{LHS} = \frac{\partial v_r}{\partial r} + \frac{v_r}{r} + \frac{1}{r}\frac{\partial v_\theta}{\partial \theta}$$

$$= \frac{\partial}{\partial r}[a(b - c/r^2)\cos\theta] + \frac{a(b - c/r^2)\cos\theta}{r} + \frac{1}{r}\frac{\partial}{\partial \theta}[-a(b + c/r^2)\sin\theta]$$

$$= a(2c/r^3)\cos\theta + \frac{a(b - c/r^2)\cos\theta}{r} - \frac{1}{r}a(b + c/r^2)\cos\theta$$

$$= 0 = \text{RHS}$$

The given radial and circumferential velocity components satisfy the continuity equation. Hence, the flow represented by them will exist.

3.5 STREAM FUNCTION AND VELOCITY POTENTIAL FUNCTION

The concepts of stream function and the velocity potential function were proposed by *Joseph Louis Lagrange*. The *stream function* is the direct result of continuity equation. The stream function (ψ) is defined for 2D incompressible flow in the following manner:

$$\boxed{\left.\begin{aligned} u &= \frac{\partial \psi}{\partial y} \\ v &= -\frac{\partial \psi}{\partial x} \end{aligned}\right\}} \tag{3.36}$$

such that it satisfies the continuity equation for 2D flow

$$\frac{\partial u}{\partial x} + \frac{\partial v}{\partial y} = 0 \quad \Rightarrow \quad \frac{\partial^2 \psi}{\partial x \partial y} - \frac{\partial^2 \psi}{\partial y \partial x} = 0 \tag{3.37}$$

This means that the stream function is defined only for 2D flows.

In case of irrotational flow,

$$\omega_z = \frac{1}{2}\left(\frac{\partial v}{\partial x} - \frac{\partial u}{\partial y}\right) = 0 \tag{3.38}$$

or
$$\frac{\partial v}{\partial x} - \frac{\partial u}{\partial y} = 0 \tag{3.39}$$

$$\Rightarrow \quad \boxed{\frac{\partial^2 \psi}{\partial x^2} + \frac{\partial^2 \psi}{\partial y^2} = 0} \quad \Rightarrow \quad \boxed{\nabla^2 \psi = 0} \tag{3.40}$$

Equation (3.40) is known as *Laplace equation*. As stream function (ψ) is defined for 2D flow only, thus

$$\psi = \psi(x, y) \tag{3.41}$$

Mathematically, the small change in stream function can be written as

$$d\psi = \frac{\partial \psi}{\partial x} dx + \frac{\partial \psi}{\partial y} dy \tag{3.42}$$

For constant ψ, the left hand side of the Eq. (3.42) becomes zero and using Eq. (3.36), Eq. (3.42) reduces to

$$0 = -vdx + udy \tag{3.43}$$

$$\Rightarrow \quad \boxed{\frac{dx}{u} = \frac{dy}{v}} \tag{3.44}$$

Equation (3.44) is the *equation of streamline*. Hence, it can be concluded that line of constant stream function represents a *streamline*. Perhaps, the stream function got its name because of this. In other words, the change in stream function ψ

along a streamline is zero. The difference between the two stream functions represents the discharge (volume flow rate) per unit depth (in z-direction) between them.

$$d\psi = -vdx + udy = \vec{V}.d\vec{A} = \vec{V}.(d\vec{r} \times 1) = dQ \tag{3.45}$$

Unlike, stream function, *velocity potential function* is defined for 3D flows in the following manner:

$$\left. u = \frac{\partial \phi}{\partial x}; \quad v = \frac{\partial \phi}{\partial y}; \quad w = \frac{\partial \phi}{\partial z} \right\} \tag{3.46}$$

such that it satisfies the *condition of irrotationality* in 2D flows:

$$\omega_z = 0 \quad \Rightarrow \quad \frac{\partial v}{\partial x} - \frac{\partial u}{\partial y} = 0 \quad \Rightarrow \quad \frac{\partial^2 \phi}{\partial x \partial y} - \frac{\partial^2 \phi}{\partial y \partial x} = 0 \tag{3.47}$$

Physically, the velocity potential function is the potential responsible for flow in a particular direction. The flow always takes place from a higher potential region to a lower potential region. This potential may be due to pressure, gravity, etc.

Like stream function, it also satisfies *Laplace equation*, that is,

$$\frac{\partial u}{\partial x} + \frac{\partial v}{\partial y} = 0 \quad \Rightarrow \quad \frac{\partial^2 \phi}{\partial x^2} + \frac{\partial^2 \phi}{\partial y^2} = 0 \quad \Rightarrow \quad \nabla^2 \phi = 0 \tag{3.48}$$

The lines of constant potential function are known as *equipotential lines*. For 2D flow,

$$\phi = \phi(x, y) \tag{3.49}$$

Mathematically, the small change in stream function can be written as

$$d\phi = \frac{\partial \phi}{\partial x} dx + \frac{\partial \phi}{\partial y} dy \tag{3.50}$$

For an equipotential line, ϕ is constant, the left-hand side of Eq. (3.50) will be zero. Using Eq. (3.46), Eq. (3.50) becomes

$$0 = udx + vdy \tag{3.51}$$

Hence, the slope of an equipotential line is

$$\left(\frac{dy}{dx} \right)_{\phi = \text{constant}} = -\frac{u}{v} \tag{3.52}$$

In addition, the slope of streamline from Eq. (3.44) is

$$\left(\frac{dy}{dx} \right)_{\psi = \text{constant}} = \frac{v}{u} \tag{3.53}$$

The product of the slopes of equipotential and streamline gives '-1', which means the two lines are orthogonal (perpendicular to each other). Together they

form a *flow net*, as shown in Fig. 3.15. If $\phi_1 > \phi_2 > \phi_3 > \phi_4$, then the flow will occur from left to right. Flow nets facilitate the simple graphical solutions for 2D irrotational, inviscid, and incompressible flow problems. More specifically, using a flow net, one can find out the discharge between two streamlines, pressure, and velocity distribution, etc. Flow nets are useful in (a) designing of the seepage and upward pressure below the hydraulic structure and (b) streamlining the outlets of flow conduits, etc. The flow net analysis also has some limitations—its application should be avoided in the regions near the solid boundary as viscous effects are predominant there.

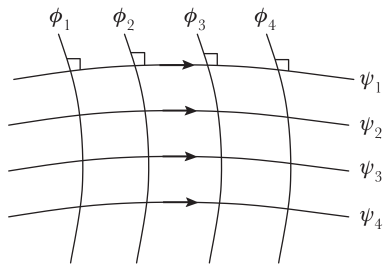

Fig. 3.15 Flow net

From Eqs (3.36) and (3.46) we get,

$$\left.\begin{aligned} u &= \frac{\partial \psi}{\partial y} = \frac{\partial \phi}{\partial x} \\ v &= -\frac{\partial \psi}{\partial x} = \frac{\partial \phi}{\partial y} \end{aligned}\right\} \tag{3.54}$$

In polar form, the stream function and the velocity potential function is defined by the following equation:

$$\left.\begin{aligned} v_r &= \frac{\partial \phi}{\partial r} = \frac{1}{r}\frac{\partial \psi}{\partial \theta} \\ v_\theta &= \frac{1}{r}\frac{\partial \phi}{\partial \theta} = -\frac{\partial \psi}{\partial r} \end{aligned}\right\} \tag{3.55}$$

Equations (3.54) and (3.55) are known as *Cauchy–Riemann* (C–R) equations.

Example 3.6 The inviscid, steady, and incompressible 2D flows are given by

(a) $\phi = x^3 - 3xy^2$

(b) $\psi = x^2 - 2xy - y^2$

In each case, find the components of velocity in x- and y-directions.

Solution:

(a) The given velocity potential function is

$$\phi = x^3 - 3xy^2$$

For the possibility of the flow, the given velocity function must satisfy Laplace equation:

$$\frac{\partial^2 \phi}{\partial x^2} + \frac{\partial^2 \phi}{\partial y^2} = 0$$

Therefore, $\dfrac{\partial \phi}{\partial x} = 3x^2 - 3y^2 \quad \Rightarrow \quad \dfrac{\partial^2 \phi}{\partial x^2} = 6x$ and

$$\frac{\partial \phi}{\partial y} = -6xy \quad \Rightarrow \quad \frac{\partial^2 \phi}{\partial y^2} = -6x \quad \Rightarrow \quad \frac{\partial^2 \phi}{\partial x^2} + \frac{\partial^2 \phi}{\partial y^2} = 6x - 6x = 0$$

Thus, the Laplace equation is satisfied, ϕ represents a possible case of flow.

The velocity components in x- and y-directions, respectively, are given by

$$u = \frac{\partial \phi}{\partial x} \quad \text{and} \quad v = \frac{\partial \phi}{\partial y}$$

The velocity component in x-direction is $u = \dfrac{\partial \phi}{\partial x} = 3(x^2 - y^2)$ and the velocity component in y-direction is $v = \dfrac{\partial \phi}{\partial y} = -6xy$.

(b) The given stream function $\psi = x^2 - 2xy - y^2$ will represent an irrotational flow, if it satisfies the Laplace equation:

$$\frac{\partial^2 \psi}{\partial x^2} + \frac{\partial^2 \psi}{\partial y^2} = 0$$

Therefore, $\dfrac{\partial \psi}{\partial x} = 2x - 2y \quad \Rightarrow \quad \dfrac{\partial^2 \psi}{\partial x^2} = 2$

and $\dfrac{\partial \psi}{\partial y} = -2x - 2y \quad \Rightarrow \quad \dfrac{\partial^2 \psi}{\partial y^2} = -2$

$$\Rightarrow \quad \frac{\partial^2 \psi}{\partial x^2} + \frac{\partial^2 \psi}{\partial y^2} = 2 - 2 = 0$$

Thus, the Laplace equation is satisfied, ψ represents an irrotational flow.

The velocity components in x- and y-directions, respectively, are given by

$$u = \frac{\partial \psi}{\partial y} \quad \text{and} \quad v = -\frac{\partial \psi}{\partial x}$$

The velocity component in x-direction is $u = \dfrac{\partial \psi}{\partial y} = 2x - 2y$ and the velocity component in y-direction is $v = -\dfrac{\partial \psi}{\partial x} = -2x - 2y$.

Example 3.7 A velocity potential function for 2D flow is given by

$$\phi = y^2 - x^2 + Axy$$

Compute the value of the constant A when the discharge between the streamlines passing through the points (1, 3) and (1, 6) is 21 units.

Solution: The velocity components in x- and y-directions, respectively, is given by

$$u = \frac{\partial \phi}{\partial x} = \frac{\partial \psi}{\partial y} \quad \text{and} \quad v = \frac{\partial \phi}{\partial y} = -\frac{\partial \psi}{\partial x}$$

The x-direction velocity component is

$$u = \frac{\partial \phi}{\partial x} \quad \Rightarrow \quad u = -2x + Ay$$

The y-direction velocity component is

$$v = \frac{\partial \phi}{\partial y} \quad \Rightarrow \quad v = 2y + Ax$$

The stream function can be obtained by integrating either u with respect to y or v with respect to x:

$$\psi = A\frac{y^2}{2} + f(x) + C_1$$

Differentiating the stream function with respect to x, we get

$$\frac{\partial \psi}{\partial x} = f'(x) = -v$$

or $$f'(x) = -2y - Ax$$

Integrating with respect to x,

$$f(x) = -2xy - Ax^2/2 + C_2$$

The stream function is, thus, given by

$$\psi = A\frac{(y^2 - x^2)}{2} - 2xy + C_1 + C_2$$

or $$\psi = A\frac{(y^2 - x^2)}{2} - 2xy + C$$

The streamlines passing through the points (1, 3) and (1, 6) are obtained as

$$\psi\big|_{(1,3)} = A\frac{(3^2 - 1^2)}{2} - 2(1)(3) + C \quad \Rightarrow \quad \psi\big|_{(1,3)} = 4A - 6 + C$$

$$\psi\big|_{(1,6)} = A\frac{(6^2 - 1^2)}{2} - 2(1)(6) + C \quad \Rightarrow \quad \psi\big|_{(1,6)} = 17.5A - 12 + C$$

The discharge between the streamlines is equal to the difference of stream functions

$$\psi|_{(1,6)} - \psi|_{(1,3)} = q$$

$$13.5A - 6 = 12 \quad \Rightarrow \quad A = 18/13.5 \quad \Rightarrow \quad A = 4/3$$

Example 3.8 Draw the flow net for inviscid, steady, and incompressible 2D flow represented by $\phi = x^2 - y^2$.

Solution:

The given velocity potential function is

$$\phi = x^2 - y^2$$

For the possibility of the flow, the given velocity function must satisfy Laplace equation:

$$\frac{\partial^2\phi}{\partial x^2} + \frac{\partial^2\phi}{\partial y^2} = 0$$

Therefore, $\dfrac{\partial\phi}{\partial x} = 2x \quad \Rightarrow \quad \dfrac{\partial^2\phi}{\partial x^2} = 2$

and $\dfrac{\partial\phi}{\partial y} = -2y \quad \Rightarrow \quad \dfrac{\partial^2\phi}{\partial y^2} = -2 \quad \Rightarrow \quad \dfrac{\partial^2\phi}{\partial x^2} + \dfrac{\partial^2\phi}{\partial y^2} = 2 - 2 = 0$

Thus, the Laplace equation is satisfied, ϕ represents a possible case of flow.

Using C–R equations to find out the expression for stream function,

$$\frac{\partial\psi}{\partial y} = \frac{\partial\phi}{\partial x} \quad \Rightarrow \quad \frac{\partial\psi}{\partial y} = 2x \quad \Rightarrow \quad \psi = 2xy + f(x) + C_1 \quad -\frac{\partial\psi}{\partial x} = \frac{\partial\phi}{\partial y}$$

$$\Rightarrow \quad -\frac{\partial}{\partial x}(2xy + f(x) + C_1) = -2y \quad \Rightarrow \quad -2y - f'(x) = -2y$$

$$\Rightarrow \quad f'(x) = 0 \quad \Rightarrow \quad f(x) = C_2$$

Hence, $\psi = 2xy + C_2 + C_1 \quad \Rightarrow \quad \psi = 2xy + C$

Flow net, shown in Fig. 3.16, is obtained by plotting the equations of stream function and velocity potential function: xy = constant (rectangular hyperbola) and $x^2 - y^2$ = constant (hyperbola).

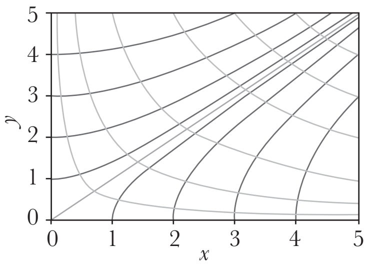

Fig. 3.16

3.6 POTENTIAL FLOW

The velocity potential functions are defined for all types of irrotational flows, such flows are termed as *potential flows*. The potential flow theory is used to describe the variety of irrotational incompressible and inviscid fluid flows, that is, flow of irrotational ideal fluids. This theory disregards the existence of viscous stresses in the flow, as the ideal fluid has zero viscosity. Although potential flow is the study of the flow of ideal fluids over solid bodies, the analysis is extremely important in approximating the outcome of real fluid flow problems. The complex variables that are used to describe the potential flows of various types are given by

$$\left.\begin{aligned} z &= x + iy = r(\cos\theta + i\sin\theta) = re^{i\theta} \\ w &= \phi + i\psi \end{aligned}\right\} \tag{3.56}$$

where z represents the point having rectangular coordinates (x, y) or polar coordinates (r, θ) in Argand plane (Fig. 3.17), and the complex variable w is known as *complex potential*. Since, both stream function and velocity potential function satisfy the C–R equations, complex potential w is a function of 'z', which represents a 2D flow.

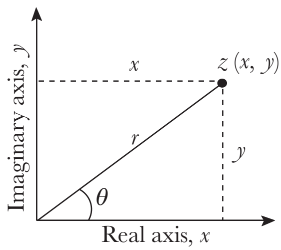

Fig. 3.17 Argand plane

$$w(z) = \phi + i\psi \tag{3.57}$$

The derivative of w (z) with respect to z is known as *complex velocity* and is given by

$$\frac{dw}{dz} = \lim_{\delta z \to 0} \frac{\delta w}{\delta z} \tag{3.58}$$

For the sake of convenience, one may take δz parallel to x-axis as the derivative is independent of the orientation of δz.

$$\frac{dw}{dz} = \lim_{\delta x \to 0} \frac{\delta w}{\delta x} = \frac{\partial w}{\partial x} \tag{3.59}$$

$$\Rightarrow \quad \frac{dw}{dz} = u - iv \tag{3.60}$$

The potential flows comprise elementary flows (also known as basic flows) and different combinations of the elementary flows. The common elementary flows are uniform flow, source and sink flow, and vortex flow.

NOTE

It should be noted that for ideal fluid (incompressible and inviscid) flow, the viscous effects are disregarded everywhere in the flow field including the region near solid boundary. That is, a no-slip condition (at the solid boundary the fluid velocity is equal to the velocity of the solid boundary, which is zero if the solid

body is stationary) does not hold good for the flow of ideal fluids over a solid body. In case of flow of ideal fluids over a solid body, the velocity is tangential at every point on the solid surface/boundary and there is no component of flow velocity normal to the surface. This condition is known as flow-tangency condition.

3.6.1 Uniform Flow

Consider uniform flow having magnitude of velocity U at an angle α (with the x-axis), as shown in Fig. 3.18. The complex velocity potential for uniform flow is given by

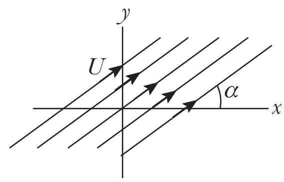

Fig. 3.18 Uniform flow

$$w = Uze^{-i\alpha} \tag{3.61}$$

$$\Rightarrow \quad \frac{dw}{dz} = U(\cos\alpha - i\sin\alpha) = u - iv \tag{3.62}$$

The velocity components are obtained by comparing the real and imaginary terms of complex velocity, that is,

$$\Rightarrow \quad \boxed{\begin{aligned} u &= U\cos\alpha \\ v &= U\sin\alpha \end{aligned}} \tag{3.63}$$

3.6.2 Source and Sink Flows

A flow is said to be a *source flow*, if the streamlines are emanating from a point radially outward whereas in a *sink flow*, the streamlines converge radially into a point. In such flows the velocity varies inversely with the distance from the point. The source flow is represented by the complex potential,

$$w(z) = \frac{m}{2\pi}\ln z \tag{3.64}$$

where m represents the source strength. Expressing the complex number z in terms of polar coordinates,

$$w = \frac{m}{2\pi}\ln(re^{i\theta}) \tag{3.65}$$

$$w = \frac{m}{2\pi}\ln r + i\frac{m}{2\pi}\theta = \phi + i\psi \tag{3.66}$$

The velocity potential function is obtained by comparing the real terms of the complex potential in Eq. (3.66).

$$\boxed{\phi = \frac{m}{2\pi}\ln r} \tag{3.67}$$

Equation (3.67) in rectangular form is obtained by substituting $r = \sqrt{x^2 + y^2}$.

$$\boxed{x^2 + y^2 = \exp\left(\frac{4\pi\phi}{m}\right)} \tag{3.68}$$

The equipotential lines for source flow represent concentric circles having their centres at the origin and radii $r = \sqrt{\exp(4\pi\phi/m)}$.

On comparing imaginary terms of complex potential in Eq. (3.66), the stream function is

$$\psi = \frac{m}{2\pi}\theta \tag{3.69}$$

Equation (3.69) is rewritten in rectangular form by substituting $\theta = \tan^{-1}(y/x)$.

$$y = \tan\left(\frac{2\pi\psi}{m}\right)x \tag{3.70}$$

The streamlines for the source flow are represented by a family of straight lines passing through the origin having slopes given by $\tan(2\pi\psi/m)$.

The sink flow is represented by the same complex potential, that is, Eq. (3.64), with a minus sign. In Fig. 3.19, the stream and velocity potential functions are plotted in the Argand plane. From Eq. (3.68), velocity potential function

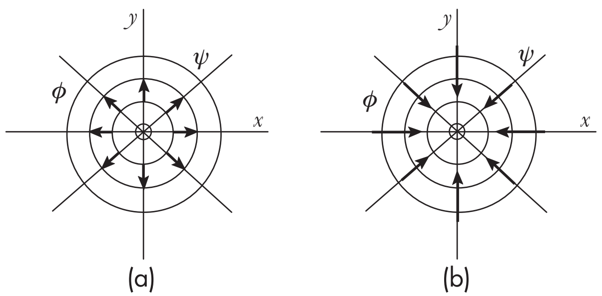

Fig. 3.19 (a) Source flow (b) Sink flow

represents concentric circles having centre at the origin for different radii r whereas stream function represents straight lines passing through the origin. From the figure, it is clear that the flow is directed radially outwards for the source and it is inwards in case of sink. The component of velocities in r and θ directions can be found as

$$\begin{aligned} v_r &= \frac{\partial\phi}{\partial r} = \frac{m}{2\pi r} \\ v_\theta &= \frac{1}{r}\frac{\partial\phi}{\partial\theta} = 0 \end{aligned} \tag{3.71}$$

It can be concluded from Eq. (3.71) that only radial component of velocity exists in source/sink flows.

3.6.3 Vortex Flow

If the fluid particles move in circular paths about a point, the flow is known as *free (irrotational) vortex flow*. Unlike source/sink flow, only the tangential velocity component exists in free vortex flows. The tangential velocity components vary with the distance from the centre in such a way that circulation remains constant. The complex potential for free vortex flow is given by

$$w(z) = -i\frac{\Gamma}{2\pi}\ln z = -i\frac{\Gamma}{2\pi}(\ln r + i\theta) \tag{3.72}$$

where Γ is *circulation* in the counter clockwise direction. The velocity potential and stream functions for irrotational vortex flow are obtained by comparing the real and imaginary terms of complex potential.

$$\begin{aligned} \phi &= \frac{\Gamma}{2\pi}\theta \\ \psi &= -\frac{\Gamma}{2\pi}\ln r \end{aligned} \tag{3.73}$$

The shapes of equipotential lines and streamlines are determined in a similar way as explained in Section 3.6.2 and are shown in Fig. 3.20.

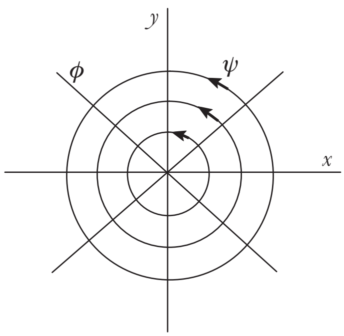

Fig. 3.20 Vortex flow

Streamlines

$$x^2 + y^2 = \exp\left(-\frac{4\pi\psi}{\Gamma}\right)$$

This expression represents a family of concentric circles with centre (0, 0) and magnitude of radius $\sqrt{\exp(-4\pi\psi/\Gamma)}$, which varies with stream function ψ.

Equipotential lines

$$y = \tan\left(\frac{2\pi\phi}{\Gamma}\right)x$$

This expression represents a family of straight lines passing through (0, 0) and magnitude of slope is $\tan(2\pi\phi/\Gamma)$, which varies with velocity potential function ϕ.

The components of velocity in radial and circumferential directions are obtained as

$$v_r = \frac{\partial \phi}{\partial r} = 0$$
$$v_\theta = \frac{1}{r}\frac{\partial \phi}{\partial \theta} = \frac{\Gamma}{2\pi r} \qquad (3.74)$$

NOTE

Free vortex flow is always an irrotational flow. A question that haunts our mind is that how can a flow undergoing circular path be termed as irrotational? The answer lies in the fact that irrotational flow has nothing to do with the path, but behaviour of the fluid element. Actually, at element level the flow remains irrotational (fluid elements do not undergo rotation while translating in circular path).

Example 3.9 Find the resultant velocity induced at point P in Fig. 3.21 by the uniform stream, line source, line sink, and line vortex.

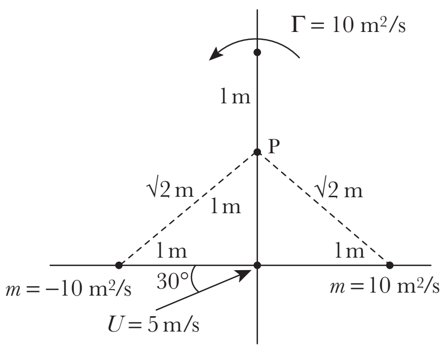

Fig. 3.21

Solution: The velocity induced at point P due to

(a) Source of $m = 10$ m²/s

$$V = \frac{m}{2\pi r} = \frac{10}{2\pi(\sqrt{2})} = 1.125\,\text{m/s}$$

The direction is towards point P along the dashed line:

(b) Sink of $m = -10\,\text{m}^2/\text{s}$

Since, sink is of the same strength and is placed symmetrically about y-axis, the magnitude of velocity induced at P will be the same, that is, $V = 1.125$ m/s but the direction is away from point P.

(c) Uniform flow with $U = 5$ m/s

The velocity induced at point P is same as that of uniform flow, that is, $V = 5$ m/s and at the same angle of 30°.

(d) Vortex flow with $\Gamma = 10\,\mathrm{m^2/s}$

$$V = \frac{\Gamma}{2\pi r} = \frac{10}{2\pi(1)} = 1.591\,\mathrm{m/s}$$

The direction of velocity induced at point P is along the positive x-direction.

The velocity vectors at point P are shown in Fig. 3.22.

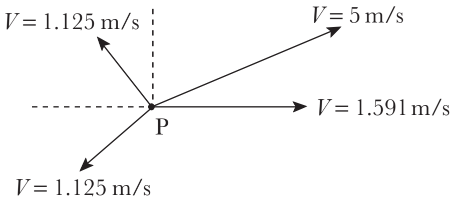

Fig. 3.22

The horizontal component of resultant velocity vector is given by

$$V_H = 1.591 + 5\cos 30° - 1.125\cos 45° - 1.125\cos 45° = 4.33\ \mathrm{m/s}$$

The vertical component of resultant velocity vector is given by

$$V_V = 5\sin 30° + 1.125\sin 45° - 1.125\sin 45° = 2.5\ \mathrm{m/s}$$

The magnitude of the resultant velocity vector,

$$V_P = \sqrt{V_H^2 + V_V^2} = \sqrt{4.33^2 + 2.5^2} = 5\ \mathrm{m/s}$$

The direction of the resultant velocity vector:

$$\theta_P = \tan^{-1}\left(\frac{V_V}{V_H}\right) = \tan^{-1}\left(\frac{2.5}{4.33}\right) = 30°$$

3.6.4 Doublet—Combination of Source and Sink of Equal Strengths

A *doublet* (also known as *hydrodynamic dipole*) is formed when source and sink of equal strengths approach each other. Let the doublet be formed by placing the source at $x = -a$ and sink at $x = a$ such that their strengths increase with the gap between them approaching zero, as shown in Fig. 3.23(a). The complex potential for the resultant flow is

$$w(z) = \lim_{a\to 0}\left[\frac{m}{2\pi}\ln(z+a) - \frac{m}{2\pi}\ln(z-a)\right] \tag{3.75}$$

$$w(z) = \lim_{a\to 0}\left[\frac{m}{2\pi}\ln\left(\frac{z+a}{z-a}\right)\right] = \lim_{a\to 0}\left[\frac{m}{2\pi}\ln\left(\frac{1+a/z}{1-a/z}\right)\right] \tag{3.76}$$

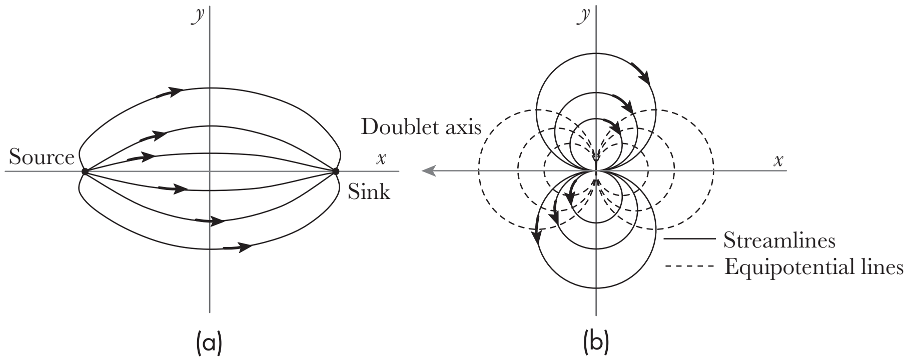

Fig. 3.23 (a) Source and sink (b) Doublet

The expansion of $\ln(1+x) = x - \frac{x^2}{2} + \frac{x^2}{3} - \frac{x^4}{4} + \ldots$ and $\ln(1-x) = -x - \frac{x^2}{2} - \frac{x^2}{3} - \frac{x^4}{4} - \ldots$

Therefore, the expansion of $\ln\left(\frac{1+x}{1-x}\right)$ is obtained by subtracting $\ln(1-x)$ from $\ln(1+x)$

$$\ln\left(\frac{1+x}{1-x}\right) = 2x\left(1 + \frac{x^2}{3} + \frac{x^4}{5} + \ldots\right) \tag{3.77}$$

Here $x = a/z$, Eq. (3.76) can be written as

$$w(z) = \lim_{a\to 0}\left[\frac{m}{2\pi} \times 2\frac{a}{z}\left(1 + \frac{a^2}{3z^2} + \frac{a^4}{5z^4} + \ldots\right)\right] \tag{3.78}$$

$$w(z) = \lim_{a\to 0}\left(\frac{m}{\pi}\frac{a}{z}\right) = \frac{\mu}{z} \tag{3.79}$$

where $\mu = \lim\limits_{a\to 0}\frac{ma}{\pi}$ is known as doublet strength.

The complex potential for doublet is given by

$$w(z) = \frac{\mu}{r}e^{-i\theta} = \frac{\mu}{r}(\cos\theta - i\sin\theta) = \phi + i\psi \tag{3.80}$$

$$\Rightarrow \quad \begin{aligned} \phi &= \frac{\mu}{r}\cos\theta = \frac{\mu x}{x^2 + y^2} \\ \psi &= -\frac{\mu}{r}\sin\theta = -\frac{\mu y}{x^2 + y^2} \end{aligned} \tag{3.81}$$

The equation of streamlines for doublet can be obtained as

$$x^2 + y^2 + \frac{\mu y}{\psi} = 0 \tag{3.82}$$

Equation (3.82) represents the equation of a circle whose *centre* $\equiv (0, -\mu/2\psi)$ and *radius* $= \mu/2\psi$, as shown in Fig. 3.23(b).

Example 3.10 A pair of source and sink having strength of 6 m²/s and 18 m²/s are located at the points (–2, 0) and (3, 0), respectively. Determine the velocity and stream function at points (2, 2) lying on the resultant flow net.

Solution: The complex velocity potential for the resultant flow (source and sink) is given by

$$w(z) = \frac{m_1}{2\pi}\ln(z+a) - \frac{m_2}{2\pi}\ln(z-b)$$

where

$$m_1 = 6\ \text{m}^2/\text{s}; \quad m_2 = 18\ \text{m}^2/\text{s}; \quad a = -2; \quad b = 3$$

Rewriting complex velocity potential function as

$$w(z) = \frac{m_1}{2\pi}\ln\left(r_1 e^{i\theta_1}\right) - \frac{m_2}{2\pi}\ln\left(r_2 e^{i\theta_2}\right)$$

or $$w(z) = \frac{m_1}{2\pi}(\ln r_1 + i\theta_1) - \frac{m_2}{2\pi}(\ln r_2 + i\theta_2)$$

Separating real and imaginary parts,

$$w(z) = \frac{m_1}{2\pi}(\ln r_1) - \frac{m_2}{2\pi}(\ln r_2) + i\left(\frac{m_1\theta_1}{2\pi} - \frac{m_2\theta_2}{2\pi}\right) = \phi + i\psi$$

Equating real and imaginary parts,

$$\phi = \frac{m_1}{2\pi}(\ln r_1) - \frac{m_2}{2\pi}(\ln r_2)$$

$$\psi = \frac{m_1\theta_1}{2\pi} - \frac{m_2\theta_2}{2\pi}$$

where $r_1 = \sqrt{(x+a)^2 + y^2}$; $r_2 = \sqrt{(x-b)^2 + y^2}$; $\theta_1 = \tan^{-1}\left(\frac{y}{x+a}\right)$; $\theta_2 = \tan^{-1}\left(\frac{y}{x-b}\right)$

The value of stream function at the point P(2, 2) is

$$\psi\big|_{(2,2)} = \frac{6\times\tan^{-1}\left(\frac{2}{2+2}\right)}{2\pi} - \frac{18\times\tan^{-1}\left(\frac{2}{2-3}\right)}{2\pi} \Rightarrow \psi\big|_{(2,2)} = 3.614$$

The velocity component in x- and y-directions is

$$u = \frac{\partial\psi}{\partial y} \quad\Rightarrow\quad u = \frac{m_1}{2\pi}\left(\frac{x+a}{(x+a)^2 + y^2}\right) - \frac{m_2}{2\pi}\left(\frac{x-b}{(x-b)^2 + y^2}\right)$$

$$\Rightarrow \quad u\big|_{(2,2)} = 12/5\pi$$

$$v = -\frac{\partial\psi}{\partial x} \quad\Rightarrow\quad v = \frac{m_1}{2\pi}\left(\frac{y}{(x+a)^2 + y^2}\right) - \frac{m_2}{2\pi}\left(\frac{y}{(x-b)^2 + y^2}\right)$$

$$\Rightarrow \quad v\big|_{(2,2)} = -33/10\pi$$

Therefore, the resultant velocity at point P(2, 2) is

$$V = \sqrt{u^2 + v^2} \quad\Rightarrow\quad V_{(2,2)} = 1.3\ \text{units}$$

Example 3.11 The velocity at a point P(0.5, 1) lying on one of the streamlines of a doublet flow net is 2 m/s. Calculate the strength of doublet and value of stream function at the point P.

Solution: The doublet flow is represented by the following velocity potential and stream functions: $\phi = \dfrac{\mu x}{x^2 + y^2}$ and $\psi = -\dfrac{\mu y}{x^2 + y^2}$.

The velocity component in x- and y-directions is

$$u = \frac{\partial \psi}{\partial y} \quad \Rightarrow \quad u = -\mu\left(\frac{x^2 - y^2}{(x^2 + y^2)^2}\right)$$

$$v = -\frac{\partial \psi}{\partial x} \quad \Rightarrow \quad v = -\mu\left(\frac{2xy}{(x^2 + y^2)^2}\right)$$

The resultant velocity is

$$V = \sqrt{u^2 + v^2} \quad \Rightarrow \quad V = \frac{\mu}{x^2 + y^2}$$

Therefore, the resultant velocity at point P(0.5, 1) is

$$V = \frac{\mu}{0.5^2 + 1^2} = 2$$

The strength of doublet is

$$\mu = 2.5\,\text{m}^3/\text{s}$$

3.6.5 Flow Over a Blunt Body—Combination of Uniform Flow and Source Flow

A blunt body is formed as a result of the combination of uniform flow and source flow, as shown in Fig. 3.24. The body is termed as blunt due to the round shape of its nose.

In the figure, S is the stagnation point (the point of maximum pressure and zero velocity) and O is the origin. The source is placed at the origin.

The velocity potential function for the half blunt body is given by

$$w(z) = Uz + \frac{m}{2\pi}\ln z \tag{3.83}$$

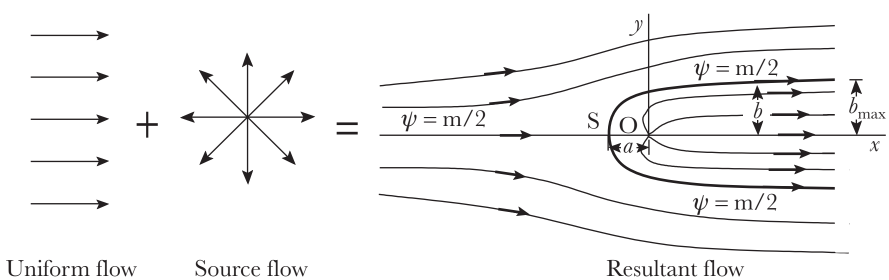

Fig. 3.24 Superposition of uniform and source flows

$$w(z) = Ur(\cos\theta + i\sin\theta) + \frac{m}{2\pi}(\ln r + i\theta) \quad (3.84)$$

Therefore, the velocity potential and stream functions components are given as

$$\begin{aligned} \phi &= Ur\cos\theta + \frac{m}{2\pi}\ln r \\ \psi &= Ur\sin\theta + \frac{m}{2\pi}\theta \end{aligned} \quad (3.85)$$

The complex velocity is given by

$$\frac{dw}{dz} = U + \frac{m}{2\pi z} \quad (3.86)$$

Stagnation Point

At the stagnation point S, the velocity must be zero. The coordinates of stagnation point are $(-a, 0)$. Substituting $z = -a$ in Eq. (3.86), we get

$$U - \frac{m}{2\pi a} = 0 \quad \Rightarrow \quad \boxed{a = \frac{m}{2\pi U}} \quad (3.87)$$

Streamline Passing Through Stagnation Point

The equation of streamline passing through the stagnation point (where $r = a$ and $\theta = \pi$) is

$$\psi_S = Ur\sin\theta + \frac{m}{2\pi}\theta \quad \Rightarrow \quad \boxed{\psi_S = \frac{m}{2}} \quad (3.88)$$

This streamline also represents the shape of the body, as shown in Fig. 3.25.

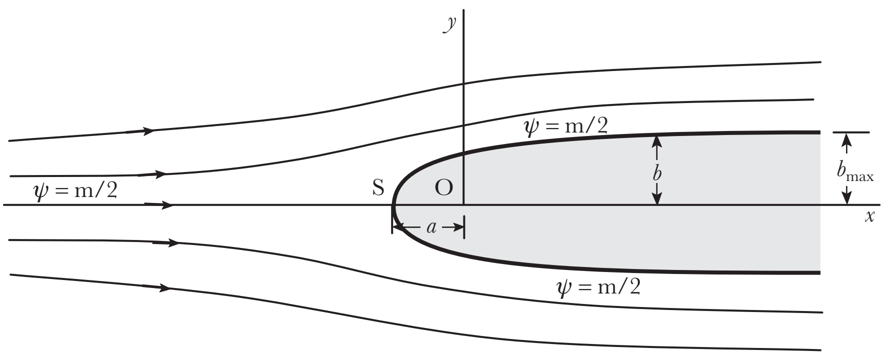

Fig. 3.25 Flow over blunt body

Half-width

The half-width ($b = r\sin\theta$) of blunt body can be found out from the stream function in Eq. (3.85), where $\psi = \psi_S$:

$$\psi_S = Ub + \frac{m}{2\pi}\theta \quad \Rightarrow \quad \frac{m}{2} = Ub + \frac{m}{2\pi}\theta \quad \Rightarrow \quad \boxed{b = \frac{m}{2\pi U}(\pi - \theta)} \tag{3.89}$$

Therefore, half-width of blunt body becomes maximum if $\theta \to 0$:

$$\boxed{b_{\max} = \frac{m}{2U}} \tag{3.90}$$

Coefficient of Pressure

The pressure distribution can be found out by applying Bernoulli's equation on the surface of blunt body and at the upstream side of it (along the streamline, $\psi = m/2$).

$$p + \frac{1}{2}\rho V^2 = p_\infty + \frac{1}{2}\rho U^2 \tag{3.91}$$

In terms of *coefficient of pressure*, C_p is

$$\boxed{C_p = \frac{p - p_\infty}{\rho U^2/2} = 1 - \frac{V^2}{U^2}} \tag{3.92}$$

Figure 3.26 shows the variation of pressure along the surface of the blunt body. The pressure is maximum at the stagnation point S and it keeps on decreasing until a point E is reached, where pressure at the surface equals the free stream pressure, p_∞ (same as upstream pressure). Beyond point E on the surface, the pressure remains less than the upstream pressure. This peculiar way of showing variation of pressure on the surface is done to see how the body reacts to pressure changes. To elaborate it further between the points S and E, the body experiences a *push* whereas beyond E along the surface, it experiences a *pull*.

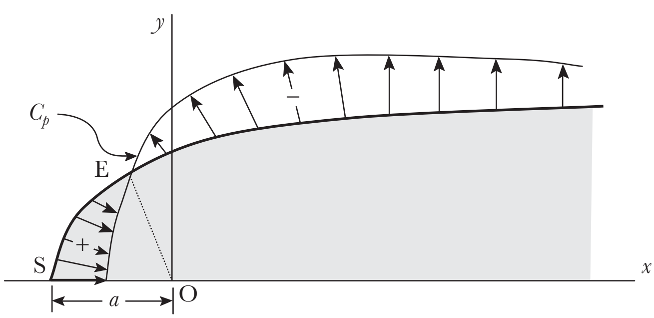

Fig. 3.26 Pressure distribution over blunt body

Example 3.12 Determine the velocity and coefficient of pressure at $\theta = 30°$ (clockwise) from stagnation point on the surface of a blunt body having maximum half-width of 100 mm. The body is placed in the uniform air stream of velocity 10 m/s.

Solution: At the surface radial velocity component will be zero, the tangential component is obtained by

$$v_\theta = -\frac{\partial\psi}{\partial r} = -\frac{\partial}{\partial r}\left(Ur\sin\theta + \frac{m}{2\pi}\theta\right)$$

$$v_\theta = -U\sin\theta \quad \Rightarrow \quad v_\theta = -10\times\sin(-30°) \quad \Rightarrow \quad v_\theta = 5\text{ m/s}$$

The coefficient of pressure is

$$C_p = 1 - \frac{V^2}{U^2} \quad \Rightarrow \quad C_p = 1 - \frac{5^2}{10^2} \quad \Rightarrow \quad C_p = 0.75$$

3.6.6 Flow Past Circular Cylinder—Combination of Uniform Flow and Doublet

The resultant of superposition of uniform flow and doublet is equivalent to the flow past a right circular cylinder of radius R, as shown in Figs 3.27 and 3.28.

If cylinder radius is R, the complex potential for circular cylinder is given by

$$w(z) = Uz + \frac{\mu}{z} \tag{3.93}$$

The complex velocity is given by

$$\frac{dw}{dz} = U - \frac{\mu}{z^2} \tag{3.94}$$

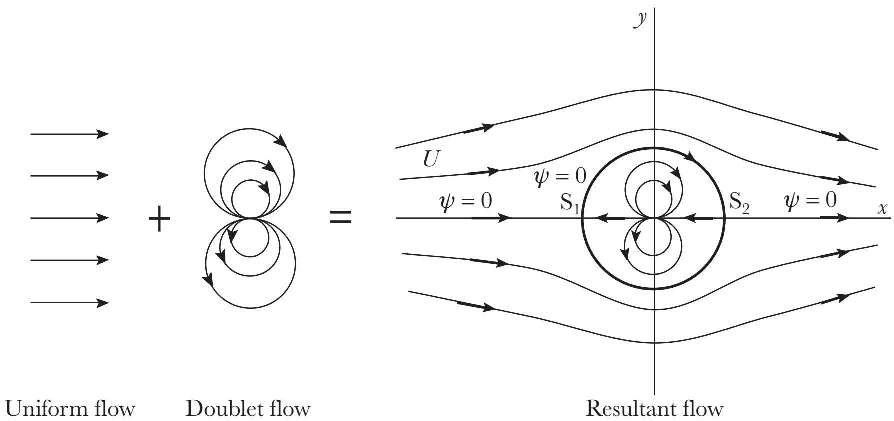

Fig. 3.27 Superposition of uniform and doublet flows

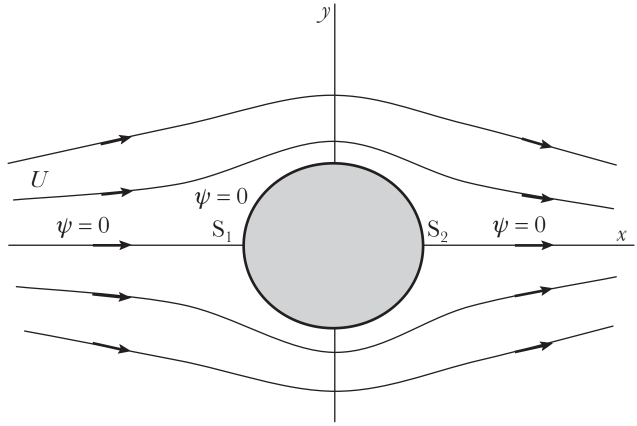

Fig. 3.28 Circular cylinder

Stagnation Points

There will be two stagnation points in this case, $S_1(R, \pi)$ and $S_2(R, 0)$. At stagnation points, the velocity is zero, that is, at $z = R$, $dw/dz = 0$, Eq. (3.94) gives

$$R^2 = \frac{\mu}{U} \tag{3.95}$$

Equation (3.93) can now be written as

$$w(z) = U\left(z + \frac{R^2}{z}\right) = U\left[r(\cos\theta + i\sin\theta) + \frac{R^2}{r}(\cos\theta - i\sin\theta)\right] \tag{3.96}$$

The velocity potential and stream functions are

$$\begin{aligned} \phi &= U\cos\theta\left(r + \frac{R^2}{r}\right) \\ \psi &= U\sin\theta\left(r - \frac{R^2}{r}\right) \end{aligned} \tag{3.97}$$

The velocity components are

$$\begin{aligned} v_r &= \frac{\partial \phi}{\partial r} = U\cos\theta\left(1 - \frac{R^2}{r^2}\right) \\ v_\theta &= \frac{1}{r}\frac{\partial \phi}{\partial \theta} = -U\sin\theta\left(1 + \frac{R^2}{r^2}\right) \end{aligned} \tag{3.98}$$

The magnitude of velocity at the surface of the cylinder is given by

$$V = v_\theta\big|_{r=R} = 2U\sin\theta \tag{3.99}$$

Coefficient of Pressure

The maximum velocity achieved at the top and bottom of the cylinder is $2U$ as the area of flow is minimum, that is, at $(R, \pi/2)$ and $(R, -\pi/2)$, in accordance with the continuity equation. The pressure at these points will be minimum as per the Bernoulli's principle. The pressure distribution at the surface of the cylinder is given by

$$C_p = \frac{p - p_\infty}{\rho U^2/2} = 1 - \frac{V^2}{U^2} = 1 - 4\sin^2\theta \tag{3.100}$$

The variation of pressure coefficient along the surface of the cylinder is shown in Fig. 3.29. At the stagnation points, the value of pressure coefficient is maximum as the pressure is maximum. Accordingly, the pressure coefficient is least on the top and bottom of the cylinder. This distribution, however, is valid only for the flow of ideal fluids. In fact, in case of the flow of real fluids, there is only one stagnation point at the upstream side. Due to flow separation a low pressure *wake* is formed in the downstream side of the cylinder. This inconsistency in the flow of ideal and real fluids is known as *d' Alembert's paradox*. This paradox will be explained in detail in Chapter 5.

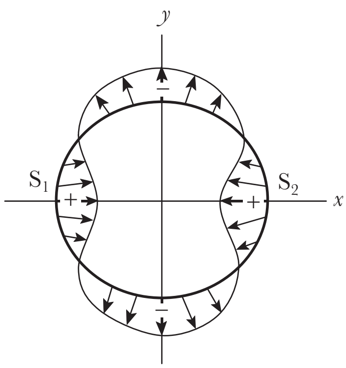

Fig. 3.29 Pressure distribution around cylinder

Example 3.13 Determine the velocity and pressure at $\theta = 45°$ on the surface of a circular cylinder of radius 100 mm, when it is placed in the uniform air stream having velocity of 10 m/s. Take free stream pressure as 100 kPa and air density as 1.12 kg/m^3.

Solution: Since the point at which the pressure and the velocity is to be determined lies on the surface, the radial velocity component will be zero. The tangential velocity component is

$$v_\theta = -U\sin\theta\left(1+\frac{R^2}{r^2}\right) \Rightarrow v_\theta = -10\sin 45°\left(1+\frac{R^2}{R^2}\right) \Rightarrow v_\theta = -14.14\,\text{m/s}$$

The coefficient pressure is given by

$$C_p = \frac{p - p_\infty}{\rho U^2/2} = 1 - 4\sin^2\theta \quad \Rightarrow \quad C_p = 1 - 4\sin^2 45° \quad \Rightarrow \quad C_p = -1$$

The pressure at the given point is given as

$$\frac{p - p_\infty}{\rho U^2/2} = -1 \quad \Rightarrow \quad p = 100\times 10^3 - 1\times 1.12\times 100/2 \quad \Rightarrow \quad p = 99.944\,\text{kPa}$$

3.6.7 Rotating Circular Cylinder—Combination of Uniform, Doublet, and Vortex Flows

The flow past a circular cylinder without circulation has already been discussed in the Section 3.6.6. The flow over rotating cylinder can be obtained by superimposing vortex flow, on the combination of uniform and doublet flows. The complex potential function for circular cylinder with clockwise circulation is given by

$$w(z) = U\left(z + \frac{R^2}{z}\right) + i\frac{\Gamma}{2\pi}\ln\left(\frac{z}{R}\right) \tag{3.101}$$

$$w = U\left[r(\cos\theta + i\sin\theta) + \frac{R^2}{r}(\cos\theta - i\sin\theta)\right] + i\frac{\Gamma}{2\pi}\left(\ln\frac{r}{R} + i\theta\right) \tag{3.102}$$

The velocity potential and stream functions are

$$\begin{aligned} \phi &= U\cos\theta\left(r + \frac{R^2}{r}\right) - \frac{\Gamma}{2\pi}\theta \\ \psi &= U\sin\theta\left(r - \frac{R^2}{r}\right) + \frac{\Gamma}{2\pi}\ln\left(\frac{r}{R}\right) \end{aligned} \tag{3.103}$$

The tangential component of velocity is

$$v_\theta = \frac{1}{r}\frac{\partial\phi}{\partial\theta} = -U\sin\theta\left(1 + \frac{R^2}{r^2}\right) - \frac{\Gamma}{2\pi r} \tag{3.104}$$

At the surface of the cylinder, only tangential velocity exists and is given by

$$v_\theta\big|_{r=R} = -2U\sin\theta - \frac{\Gamma}{2\pi R} \tag{3.105}$$

To find out stagnation point, the velocity is equated to zero:

$$\sin\theta = -\frac{\Gamma}{4\pi RU} \tag{3.106}$$

Three cases arise:

1. If $\Gamma < 4\pi RU$, the two values of θ will satisfy Eq. (3.106). This means that there will be two stagnation points on the surface of the cylinder, shown in Fig. 3.30(a).
2. If $\Gamma = 4\pi RU$, $\theta = -\pi/2$ and there will be single stagnation point at the bottom of cylinder, shown in Fig. 3.30(b).
3. If $\Gamma > 4\pi RU$, the stagnation point lies outside the cylinder surface, shown in Fig. 3.30(c). To find out the position of stagnation point substitute $\theta = -\pi/2$ in Eq. (3.104) and r is given by

$$r = \frac{1}{4\pi U}\left[\Gamma \pm \sqrt{\Gamma^2 - (4\pi RU)^2}\right] \tag{3.107}$$

One root lies outside the cylinder while other will lie inside the cylinder.

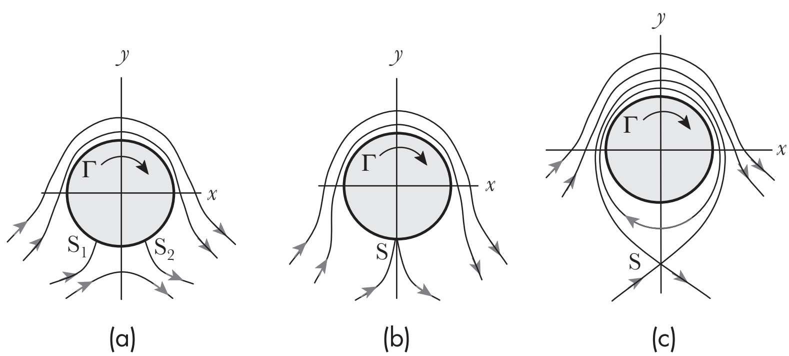

Fig. 3.30 Rotating cylinder (a) $\Gamma < 4\pi RU$ (b) $\Gamma = 4\pi RU$ (c) $\Gamma > 4\pi RU$

The pressure distribution on the rotating cylinder can be obtained by applying *Bernoulli's equation*:

$$p + \frac{1}{2}\rho V^2 = p_\infty + \frac{1}{2}\rho U^2 \tag{3.108}$$

Using Eq. (3.105), the pressure at the surface is

$$p|_{r=R} = p_\infty + \frac{1}{2}\rho\left[U^2 - \left(-2U\sin\theta - \frac{\Gamma}{2\pi R}\right)^2\right] \tag{3.109}$$

The flow is symmetric about y-axis, this means there would not be any component of pressure force on the rotating cylinder in x-direction (known as *drag*). The only component of pressure force is in y-direction, and is termed as *lift*, and is given by

$$L = -\int_0^{2\pi} p|_{r=R} \sin\theta R d\theta = \rho U \Gamma \tag{3.110}$$

The lateral force experienced by rotating bodies is known as *Magnus effect*. Magnus effect can be observed in the deviation of trajectories of the spinning balls in table tennis, cricket, football, etc. The concept of lift and drag has been elaborated in Chapter 5.

Example 3.14 If the cylinder in Example 3.13 is rotating in the direction of flow at vortex strength of $10\,\text{m}^2/\text{s}$. Calculate the velocity at $\theta = 45°$ at the surface of the cylinder. Determine the stagnation points and calculate the lift on the rotating cylinder.

Solution: Since the point at which the pressure and the velocity is to be determined lies on the surface, the radial velocity component will be zero. The tangential velocity component for rotating cylinder is given by

$$v_\theta|_{r=R} = -2U\sin\theta - \frac{\Gamma}{2\pi R} \quad \Rightarrow \quad v_\theta|_{r=R} = -2\times 10\times \sin 45° - \frac{10}{2\pi\times 0.1}$$

$$\Rightarrow \quad v_\theta = -30.057\,\text{m/s}$$

Since, $\Gamma < 4\pi RU$, there will be two stagnation points lying on cylinder surface and they are determined by

$$\sin\theta = -\frac{\Gamma}{4\pi RU} \quad \Rightarrow \quad \sin\theta = -\frac{10}{4\pi\times 0.1\times 10} = -0.796 \quad \Rightarrow \quad \theta = 307.3°,\ 232.7°$$

Lift on the cylinder is given by

$$L = \rho U\Gamma \quad \Rightarrow \quad L = 1.12\times 10\times 10 \quad \Rightarrow \quad L = 112\,\text{N}$$

POINTS TO REMEMBER

- Fluid motion can be explained in two ways—Lagrangian and Eulerian approaches. The Lagrangian approach disregards the concept of fluid as continuum, and is based on the motion of individual fluid particles. Thus, this approach is limited to the condition where the particles are small in number. Eulerian approach is more common as it uses the control volume concept to analyse any flow problem with the assumption of fluid being continuum.
- The flow can be described by means of some conventional imaginary flow lines such as *streamline*, *pathline*, *streakline*, and *timeline*. *Streamline* is tangential to the direction of flowing stream, *pathline* is path traced by an individual fluid particle, *streakline* is the line obtained by joining the current location of all the fluid particles that have passed through a fixed point in space, and *timeline* is the line obtained by joining the location of different fluid particles at a given instance of time.
- In a steady flow, the streamlines, pathlines, and streaklines are identical whereas in case of unsteady or transient flow, the streamline pattern evolves with time; pathlines and streaklines are generated during the course of time.
- For the existence of a flow field, the continuity equation must be satisfied.
- The concepts of stream and velocity potential functions emerge from the mass conservation principle and the condition of irrotationality, respectively.
- The discharge per unit width between any two streamlines is constant and is equal to the difference of their stream functions.
- The potential flow theory is used to describe the variety of flow of ideal fluids. The velocity potential functions are defined for all types of irrotational flows, such flows are termed as *potential flows*. The uniform flow, source and sink flows, and vortex flows are termed as elementary flows. The superposition of these flows results in interesting physical flow problems.

SUGGESTED READINGS

Anderson, J.D., *Fundamentals of Aerodynamics*, 5th Ed., McGraw-Hill Education, New Delhi, 2013.

Cimbala, J.M., Y.A. Cengel, *Essentials of Fluid Mechanics—Fundamentals and Applications*, McGraw-Hill Education, New Delhi, 2013.

Kundu, P.K., I.M. Cohen, *Fluid Mechanics*, 4th Ed., Elsevier, New Delhi, 2008.

White, F.M., *Fluid Mechanics*, 6th Ed., Tata-McGraw Hill, New Delhi, 2008.

MULTIPLE-CHOICE QUESTIONS

3.1 The direction of fluid velocity vector is
(a) along the streamline
(b) tangent to the streamline
(c) along the pathline
(d) tangent to the pathline

3.2 The pathlines, streaklines, and streamlines are identical for
(a) uniform flow
(b) steady flow
(c) unsteady flow
(d) they cannot be identical, as they represent different parameters

3.3 If both local and convective accelerations exist for a flow then it is a
(a) steady uniform flow
(b) steady non-uniform flow
(c) unsteady uniform flow
(d) unsteady non-uniform flow

3.4 Which of the following is not true about streamline?
(a) It is an imaginary line
(b) It represents equal velocity in flow
(c) The tangent to it at any point represents the direction of the instantaneous velocity
(d) Is fixed in space in steady flow

3.5 Streamlines and equipotential lines
(a) intersect
(b) are always orthogonal
(c) are parallel
(d) none of these

3.6 Circulation per unit area is
(a) vorticity
(b) lift
(c) drag
(d) none of these

3.7 The point in a flow field where velocity is zero is called the
(a) centre of pressure
(b) centre gravity
(c) metacentre
(d) stagnation point

3.8 Flow past a rotating circular cylinder can be simulated by superposition of uniform flow and
(a) a doublet
(b) a vortex
(c) a doublet and a vortex
(d) a source and a vortex

3.9 The phenomenon of generation of lift by a rotating object placed in a stream is known as
(a) scale effect
(b) magnus effect
(c) buoyancy effect
(d) coanda effect

3.10 If velocity vector is $\vec{V} = x\hat{i} - y\hat{j}$, then equation of the streamline passing through the point (1, 1) is
(a) $xy = 1$
(b) $x = y$
(c) $x/y = 1$
(d) $x - y = 1$

3.11 The velocity potential function for a line sink is proportional to
(a) r
(b) $1/r$
(c) $1/r^2$
(d) $\ln(r)$

3.12 For a 2D flow, the stream function is $\psi = 4x^3y$. The velocity at a point (−1, 1) is
(a) 10.65 units
(b) 11.65 units
(c) 12.65 units
(d) 13.65 units

3.13 $\Delta\psi$ represents the
(a) area between the streamlines
(b) discharge per unit depth between the streamlines
(c) pressure difference between the streamlines
(d) volume of flow between the streamlines

3.14 If $\nabla^2\psi \neq 0$, then the flow is
(a) rotational
(b) irrotational
(c) steady
(d) not possible

3.15 Which of the following stream functions represent irrotational flow?
(a) $\psi = 5x^2y^2$
(b) $\psi = 5x^2y$
(c) $\psi = 5xy^2$
(d) $\psi = 5xy$

3.16 If ω_x represents the angular velocity of fluid about x-axis, the vorticity along x-axis is
(a) $\omega_x/2$
(b) $2\omega_x$
(c) 0
(d) ω_x^2

3.17 The stream function for a flow is $\psi = (x^2 - y^2)/2$, the corresponding velocity potential function
(a) $\phi = x^2y$
(b) $\phi = -xy^2$
(c) $\varphi = -xy$
(d) $\phi = (x^2 + y^2)/2$

3.18 Find out the stagnation point in the flow field represented by the velocity potential function $\phi = 6x - 3\ln(x^2 + y^2)$
(a) (0, 0)
(b) (1, 0)
(c) (0, 1)
(d) (1, 1)

3.19 In an idealized 2D flow, which of the following combinations does not exist?
(a) $u = x^2 + y^2$ and $v = x^2 - y^2$
(b) $u = x + y$ and $v = x - y$
(c) $u = 2xy$ and $v = x^2 - y^2$
(d) $u = x^3y$ and $v = -3x^2y^2/2$

3.20 Which of the following is a C–R equation?
(a) $\dfrac{\partial\varphi}{\partial r} = \dfrac{1}{r}\dfrac{\partial\psi}{\partial\theta};\ \dfrac{1}{r}\dfrac{\partial\varphi}{\partial\theta} = -\dfrac{\partial\psi}{\partial r}$
(b) $\dfrac{\partial\phi}{\partial r} = \dfrac{\partial\psi}{\partial\theta};\ \dfrac{\partial\phi}{\partial\theta} = -\dfrac{\partial\psi}{\partial r}$
(c) $\dfrac{\partial\phi}{\partial r} = -\dfrac{1}{r}\dfrac{\partial\psi}{\partial\theta};\ \dfrac{1}{r}\dfrac{\partial\phi}{\partial\theta} = \dfrac{\partial\psi}{\partial r}$
(d) $\dfrac{1}{r}\dfrac{\partial\phi}{\partial r} = \dfrac{\partial\psi}{\partial\theta};\ \dfrac{\partial\phi}{\partial\theta} = -\dfrac{1}{r}\dfrac{\partial\psi}{\partial r}$

REVIEW QUESTIONS

3.1 Distinguish between the following:
(a) Lagrangian and Eulerian approaches in fluid motion
(b) streakline and timeline
(c) streamline and pathline
(d) stream function and velocity potential function
(e) rotational and irrotational flow
(f) no-slip condition and flow-tangency condition

3.2 Discuss the features of fluid motion, namely translation, deformation, and rotation.

3.3 Describe the utility of flow nets. In addition discuss their limitations.
3.4 Why is it not recommended to use flow net analysis near the solid boundary?
3.5 Why is the free vortex flow termed as irrotational?
3.6 No fluid is an ideal fluid. Then why is there a need to study potential flow theory as its applications are limited to the flow of ideal fluids only?
3.7 What is coefficient of pressure? Discuss its importance in potential flow theory.
3.8 Show that the difference between the stream functions representing two streamlines in a 2D flow field is equal to the discharge between them.
3.9 Prove that the equipotential lines are always perpendicular to the streamlines.
3.10 What is Magnus effect? Explain with the help of real life examples.

UNSOLVED PROBLEMS

3.1 For the following flow fields, determine whether the flow exists or not:

(a) $\vec{V} = ke^x\hat{i} - ke^x y\hat{j}$

(b) $\vec{V} = -kx/y\hat{i} + k\ln(x^2y)\hat{j}$

[Ans: (a) flow exists (b) flow exists]

3.2 Calculate the value of y-components of velocity for the existence of flow if x-components of velocity are:

$u = k\cos xy$ and $u = k\ln(x/y)$

$$\left[\textbf{Ans: (a) } v = -\frac{ky\cos xy}{x} + \frac{k\sin xy}{x^2} + f(x) + c \quad \textbf{(b) } v = -\frac{ky}{x} + f(x) + c\right]$$

3.3 Determine linear and angular strain rates for the following flow fields:

(a) $\vec{V} = y^3\hat{i} + 2x\hat{j}$

(b) $\vec{V} = x^2yz\hat{i} - y^2z^3\hat{j} + yz^2\left(\frac{z^2}{2} - x\right)\hat{k}$

In addition find angular velocity in each case.

$$\left[\textbf{Ans: (a) } \dot{\varepsilon}_x = \dot{\varepsilon}_y = 0,\ \dot{\gamma}_{xy} = \frac{1}{2}(2+3y^2),\ \omega_z = \frac{1}{2}(2-3y^2)\right.$$

$$\textbf{(b) } \dot{\varepsilon}_x = 2xyz,\ \dot{\varepsilon}_y = -2yz^3,\ \dot{\varepsilon}_z = 2yz^3 - 2xyz,$$

$$\dot{\gamma}_{xy} = \frac{1}{2}(x^2z),\ \dot{\gamma}_{yz} = \frac{1}{2}\left(\frac{z^4}{2} - z^2x - 3y^2z^2\right),\ \dot{\gamma}_{zx} = \frac{1}{2}(x^2y - yz^2)$$

$$\left.\omega_z = -\frac{1}{2}(x^2z),\ \omega_x = \frac{1}{2}\left(\frac{z^4}{2} - z^2x + 3y^2z^2\right),\ \omega_y = \frac{1}{2}(x^2y + yz^2)\right]$$

3.4 Consider a steady, incompressible, 2D velocity field for motion parallel to the x-axis with constant shear. The shear rate is $du/dy = Ay$. Obtain an expression for the velocity field $\vec{V}$. Calculate the rate of rotation. Evaluate the stream function for this flow field.

$$\left[\textbf{Ans: } \vec{V} = \left(\frac{Ay^2}{2} + B\right)\hat{i},\ \omega_z = -\frac{Ay}{2},\ \psi = -\frac{Ay^3}{6} + By + C\right]$$

3.5 If the velocity field is defined by $\vec{V} = -2xy\hat{i} + y^2\hat{j}$, determine the circulation around a path enclosed by the coordinates (1, 1), (4, 1), (4, 4), and (1, 4).

[Ans: 45 units]

3.6 A steady, incompressible, inviscid 2D velocity field is given by

$$\vec{V} = (2x + 3y - 5)\hat{i} + (x - y - 2)\hat{j}$$

Determine the convective, local, and total acceleration at the point (1, 2).

[Ans: $a_x = -9$ units, $a_y = 13$ units]

3.7 A steady, incompressible, inviscid 2D velocity field is given by

$$\vec{V} = \left(\frac{x^3}{3} + ay\right)\hat{i} - (8x^2 - by)\hat{j}$$

For what value of x and y, the field will represent irrotational flow if $b - a = 64$?

[Ans: $x = 8$, y (any value)]

3.8 If the velocity distribution for a 2D ideal flow is given by

$$u = \frac{x}{(1+t)^2}; \quad v = \frac{y}{1+2t}$$

Obtain the equation of:

(a) the streamlines
(b) the pathlines
(c) the streaklines that pass through point (1, 1) at $t = 0$.

$$\left[\textbf{Ans: (a) } y = x^{\frac{(1+t)^2}{1+2t}} \quad \textbf{(b) } y = \left[\frac{1+\ln(x)}{1-\ln(x)}\right]^{1/2} \quad \textbf{(c) } y = \left[\frac{(1+2t)\{1+(1+2t)\ln(x)\}}{1+2t-\ln(x)}\right]^{1/2}\right]$$

3.9 A velocity field is given by $\vec{V} = Axy\hat{i} - \frac{1}{2}Ay^2\hat{j}$. Is this a possible case of incompressible flow? If yes, obtain the stream function and find the value of constant A for which the flow rate between the streamlines passing through the points (3, 3) and (3, 4) is 18 units.

$$\left[\textbf{Ans: } \psi = \frac{Axy^2}{2} + C,\ A = \frac{12}{7}\right]$$

3.10 The stream function for a steady, incompressible, 2D flow in polar coordinates is $\psi = Ar^{1/3}\cos(\theta/3)$.

(a) Sketch the streamlines.
(b) Find the v_r and v_θ at points P (0, 0) and Q (−1, 1).

(c) Find the volumetric flow rate across any line joining the points P and Q. Consider only the region $0 \le \theta \le 3\pi/2$.

[Ans: (b) At point P $v_r = v_\theta = 0$, at point Q $v_r = v_\theta = -0.187A$, (c) $0.7937A$ units]

3.11 For a 2D flow, the velocity potential function is given by $\phi = x^2 - y^2$, find the velocity at points (2, 2) and (2, 4). In addition, determine the flow rate between the streamlines passing through these points.

[Ans: $4\sqrt{2}$ units, $4\sqrt{5}$ units, 8 units]

3.12 The stream function of a 2D incompressible and inviscid flow is represented by $\psi = \pi xy$. Locate the point where the velocity vector has a magnitude of 22 units and find the angle it makes with x-axis, if the velocity along y-axis is $\sqrt{3}$ times the velocity along x-axis.

[Ans: $P(11/\pi, 11\sqrt{3}/\pi)$, 60°]

3.13 A uniform flow with a velocity of 3 m/s is superimposed on the plane source of strength 20 m²/s. The velocity at a point P located at a distance of 0.6 m from the source in the resultant flow field is 5.967 m/s. Determine the stream function at the point P.

[Ans: 6.32 units]

3.14 A circular cylinder 3 cm in diameter is placed in a stream of gas $(\rho = 1.661\,\text{kg/m}^3)$ having uniform velocity of 6 m/s. For what value of circulation Γ, cylinder will have a single stagnation point on its surface. In addition, estimate the lift experienced by the cylinder. If with same velocity, stream of another gas having density twice of the given gas is passed over the same circulating cylinder, find the position of stagnation point.

[Ans: 11.3 m²/s, 112.6 N per m of cylinder length]

3.15 Find the resultant velocity induced at point P in Fig. 3.31 by the uniform stream, line source, line sink, and line vortex.

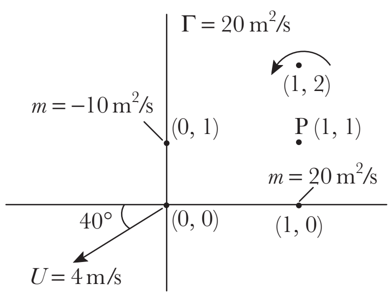

Fig. 3.31

[Ans: 1.819 m/s, 19.89°]

3.16 Analyse the flow past Rankine oval shown in Fig. 3.32, formed as a result of superposition of uniform flow, source and sink flow of equal strengths.

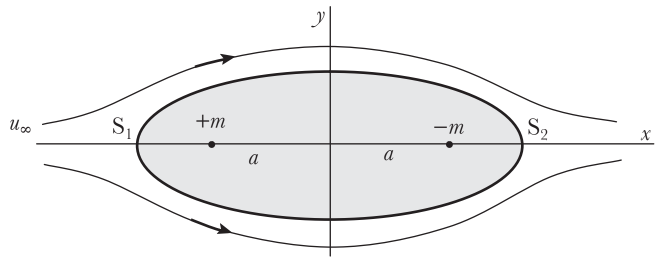

Fig. 3.32 Rankine oval

Answers to Multiple-choice Questions

3.1 (b)	3.2 (b)	3.3 (d)	3.4 (b)	3.5 (b)
3.6 (a)	3.7 (d)	3.8 (a)	3.9 (b)	3.10 (a)
3.11 (d)	3.12 (c)	3.13 (b)	3.14 (a)	3.15 (d)
3.16 (b)	3.17 (c)	3.18 (b)	3.19 (a)	3.20 (a)

DESIGN OF EXPERIMENTS

Experiment 3.1 Reynolds Experiment

Objective

To identify the laminar, transition, and turbulent flow regimes in pipe flow using Reynolds experiment.

Theory

Osborne Reynolds (1842–1912 AD), an Anglo Irish physicist, proposed an extremely useful non-dimensional number, which was named after him as *Reynolds number* (Re), for the flow classification as laminar or turbulent. Flow is termed as laminar if it is highly ordered such that the flow is conceived as the movement of one lamina (layer) over another. Turbulent flow, on the other hand, is highly chaotic. Reynolds number is defined as the ratio of inertia force to the viscous force in a flowing fluid. For the flow through pipe, the Reynolds number is calculated using the following equation

$$\mathrm{Re} = \frac{\rho V D}{\mu} \tag{E3.1}$$

where, V is the average flow velocity in the pipe cross section, D is the pipe diameter, ρ is the density, and μ is the dynamic viscosity.

On the basis of experimental results, *Osborne Reynolds* classified the flow regimes for different Reynolds number ranges as:

Laminar	$\mathrm{Re} < 2300$
Transition	$2300 < \mathrm{Re} < 4000$
Turbulent	$\mathrm{Re} > 4000$

The value of critical Reynolds number for the flow through pipe is usually taken as 2300.

Experimental Set-up

A schematic diagram of the experimental set-up, consisting of a glass tube, dye cup and injector assembly, supply tank, and flow measuring tank, is shown in Fig. E3.1. A pump is used to fill the supply tank connected to the glass tube from its bottom edge. The flow through the glass tube is controlled by a flow control valve fixed at its outlet. The control valve regulates the flow velocity inside the glass tube, thereby attaining a given Reynolds number. The dye is allowed to enter the glass tube through a needle injector by opening the dye control valve, as shown in the figure. The flow measuring tank measures the volume flow rate through the glass tube. The rise in the water level for a given time interval determines the volume flow rate. The average velocity inside the glass tube is calculated by dividing the volume flow rate with the cross-sectional area of glass tube.

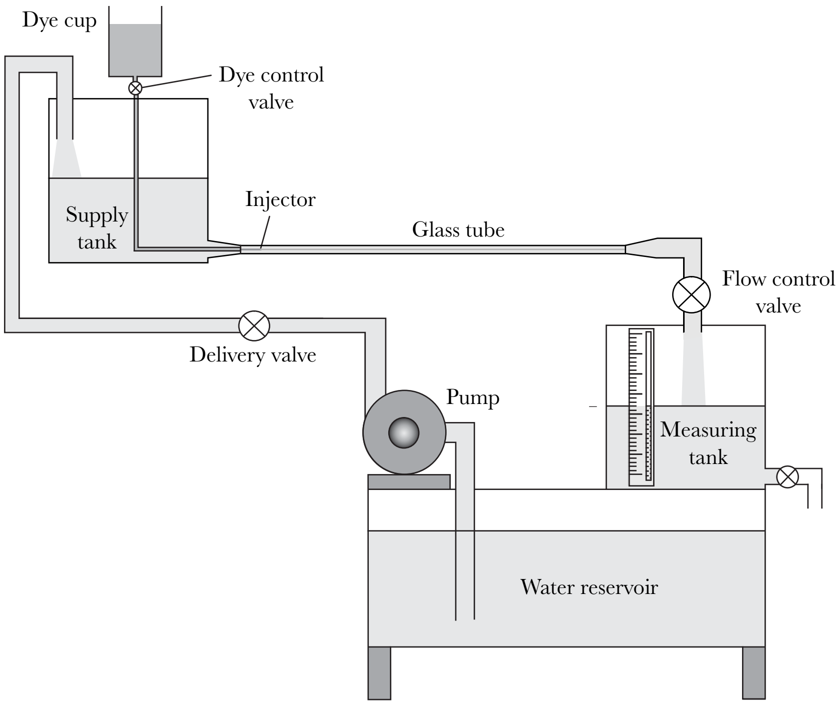

Fig. E3.1 Experimental set-up

Procedure

1. Run the pump to fill the supply tank.
2. Open the flow control valve slightly and allow the flow to become steady.
3. Adjust the flow of dye so that fine coloured thread is observed.
4. Note down the flow pattern observed.
5. Measure the volume flow rate using the measuring tank. Determine the flow velocity and the corresponding Reynolds number.
6. Repeat the experiment by gradually increasing the flow rate.
7. If the dye exhibits a continuous straight line flow pattern throughout the glass tube, the flow is termed as laminar flow. If the dye thread does not remain straight all along the tube, the flow is said to be in transition from laminar to turbulent regime. In turbulent regime, the dye thread, as soon as it leaves the injector needle, starts undulating and is dispersed in water, as shown in Fig. E3.2.

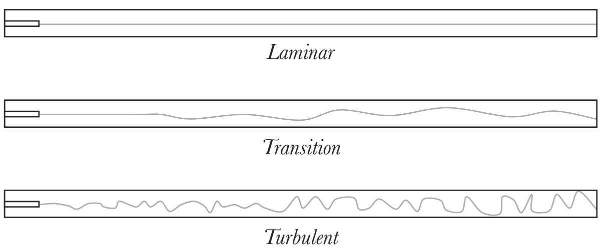

Fig. E3.2 Flow patterns

Observation Table

S. no.	Rise in water level, h (m)	Time taken to rise in water level, t (s)	Volume flow rate $Q = Ah/t$ (m^3/s)	Flow velocity inside the tube $V = Q/A_{glass}$ (m/s)	Reynolds number Re = $\rho VD/\mu$	Flow pattern/ regime (laminar/ transition/ turbulent)
1.						
2.						
3.						
…						

Sample Calculations

From the property table of water, corresponding to water temperature, select the value of dynamic viscosity μ and density ρ.

The discharge through the glass tube is measured using the measuring tank having cross-sectional area A and is given by

$$Q = Ah/t$$

The average flow velocity inside the glass tube is obtained by dividing the discharge by its cross-sectional area, A_{glass} as

$$V = Q/A_{glass}$$

Compute Reynolds number using Eq. (E3.1).

Results and Discussion

1. Determine the critical Reynolds number from your experimental visual observation and compare it with the established value of critical Reynolds number for pipe flow, that is, 2300.
2. Calculate the percentage error and discuss the reasons for deviation.

Conclusions

Draw conclusions on the results obtained.

Experiment 3.2 Flow Visualization Using Particle Image Velocimetry

Objective

To analyse the flow patterns across a vertical plate using particle image velocimetry technique.

Theory

The particle image velocimetry (PIV) system has already been explained in Fig. 3.2. It consists of a laser source for illuminating the tracer particles mixed in the flow stream. Tracer particles are of the order of 50 microns and specific gravity close

to that of working fluid. It also consists of a camera synchronized with the pulses of the laser source in order to capture the position of different tracer particles with respect to time. Such systems are useful in visualizing the flow patterns over/across any geometry.

Experimental Set-up

The schematic diagram of the experimental set-up, shown in Fig. E3.3, consists of PIV system having a test section of required geometry over which the flow visualization is to be done. The water mixed with tracer particles is pumped into the test section from

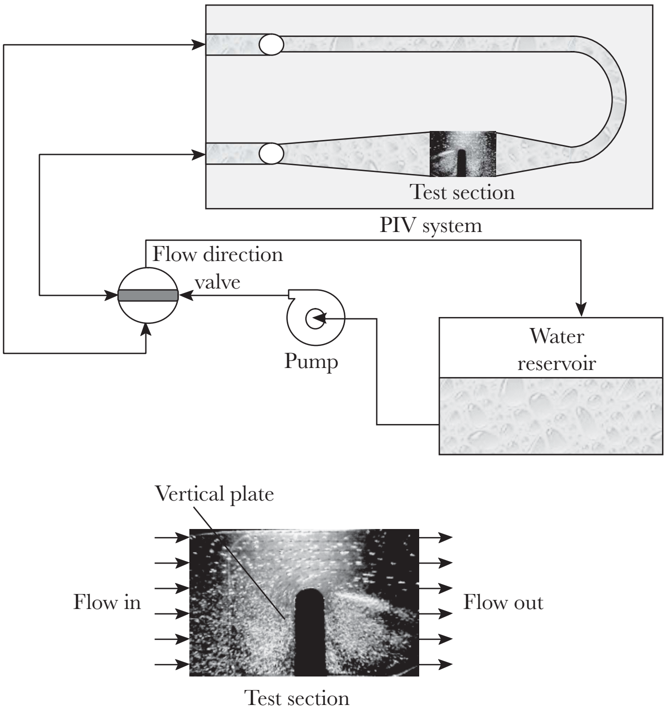

Fig. E3.3 Schematic diagram of the experimental set-up
Courtesy: ePIV™ Interactive Flow Studies

the reservoir at a controlled rate. The flow direction valve is used to reverse the flow direction in the test section. The camera in the PIV system captures the position of illuminated tracer particles over the test section and velocity vector plot for each tracer particles is generated. Thus, the flow pattern is visualized.

Procedure

1. Choose an appropriate geometry (here in the present case it is vertical plate) and clamp it in the test section.
2. Start the pump and set a particular flow rate.

3. Follow the instruction of the available PIV system to capture the tracer particle position.
4. Observe the flow patterns inside the wake of the geometry.
5. Repeat the experiment for different Reynolds number.

Results and Discussion

Discuss the effect of Re on the flow patterns over the given geometry.

Conclusions

Draw conclusions on the results obtained.

CHAPTER

4 Conservation Equations

LEARNING OBJECTIVES

After studying this chapter, the reader will be able to:

- Employ Reynolds transport theorem for deriving the conservation equations for control volume
- Understand the integral and differential approaches for deriving the conservation equations in a clear-cut way
- Apply conservation equations for obtaining analytical solutions for simple flow problems
- Design simple experiments to verify the theoretically derived conservation equations

The laws of conservation of mass, momentum, and energy are helpful in developing the governing equations for any fluid flow problem. The mass conservation principle is also known as continuity equation. The momentum conservation is Newton's second law of motion. The energy conservation principle is the first law of thermodynamics, which is useful in cases where the fluid flow is accompanied with heat transfer.

In this chapter, the conservation equations for mass, momentum, and energy are derived in two ways: (a) integral approach using Reynolds transport theorem and (b) differential approach. The integral approach is useful for understanding the overall flow behaviour in a flow field. It does not give a detailed idea of flow at a point or infinitesimal level in the flow field, which differential approach provides.

The governing equations developed in this chapter form the backbone of the design of any fluid flow system, and thus, have enormous applications.

4.1 INTEGRAL APPROACH

The laws of conservation of mass, momentum, and energy for the fixed mass of fluid in a system are quite understandable and a background for these laws has already been built through the school level courses in physics. However, when it comes to fluid mechanics, the aforementioned laws are essentially the same, but they are applied differently as the same mass of fluid does not remain in the system. In Chapter 1, the concept of different systems has already

been introduced, for example, a *system* is one in which the fluid mass is fixed whereas in *control volume* the fluid mass can enter and leave. In fluid mechanics, we mostly deal with the flow systems in which the mass can enter and leave. Thus, control volume approach is generally applied in such systems. In order to apply the conservation laws on control volume, the fluid properties that will be required must be independent of the mass. Such properties are known as *intensive properties*.

4.1.1 Reynolds Transport Theorem

The Reynolds transport theorem is a tool that relates a change in the extensive property in a system to the change in the corresponding intensive property for the control volume.

If N is the extensive property and η is the corresponding intensive property such that

$$\eta = \frac{dN}{dm} \tag{4.1}$$

Intensive property is also defined as the extensive property per unit mass given by Eq. (4.1). The expression for the Reynolds transport theorem is

$$\frac{dN_s}{dt} = \frac{\partial}{\partial t}\int_{\text{CV}} \eta\rho d\forall + \int_{\text{CS}} \eta\rho\vec{V}.d\vec{A} \tag{4.2}$$

The term on the left-hand side (LHS) of Eq. (4.2) represents the change in the extensive property of a system (subscripts s is used for system and CV for control volume). On the right-hand side (RHS), the first term represents the change in the extensive property inside the control volume whereas the second term represents the change in the extensive property due to the net efflux of fluid through the control surface.

To prove this theorem, let us consider a system and control volume of same size placed in a flow field represented by velocity vector $\vec{V} = u\hat{i} + v\hat{j} + w\hat{k}$. Figure 4.1 shows the positions of system and control volume at time $t = t_0$ and time $t = t_0 + \Delta t$. The control volume is fixed in space whereas the system will move with the flow field. The system does not allow mass to enter or leave through its boundary. In other words, a system will have the same fluid particles at any time. As a matter of convenience, the system boundary is represented by a solid line and the control surface by a dashed (porous) line to complement their definitions.

At time $t = t_0$, both system and control volume are overlapping. Further, at time $t = t_0 + \Delta t$, the system gets displaced by $\vec{V}\Delta t$. At this time, together system and control volume can be thought to have three different regions, viz. A, C, and B; C is the region common to both system and control volume.

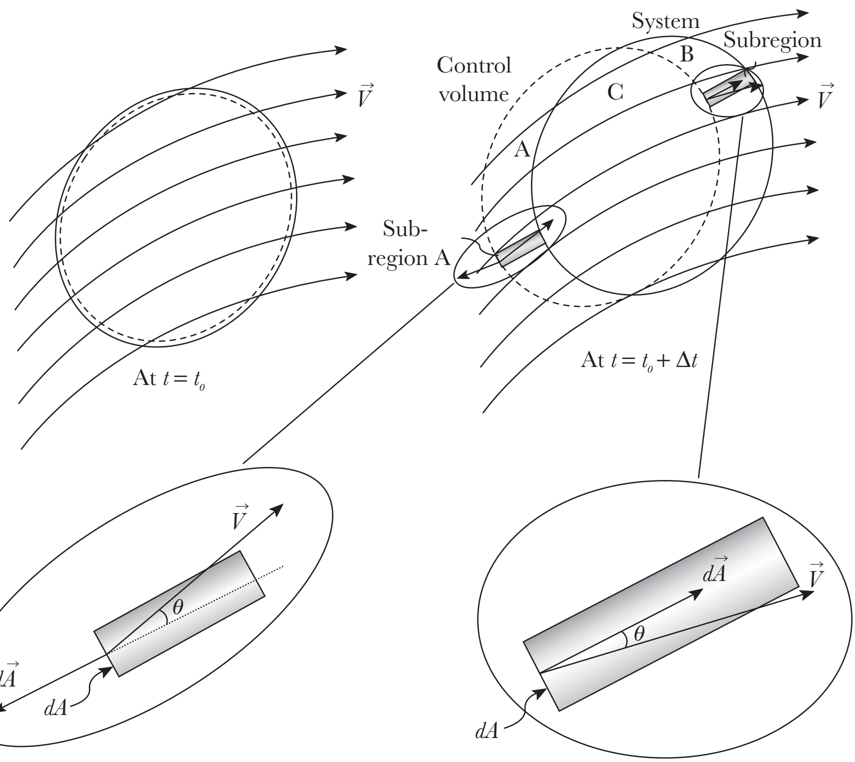

Fig. 4.1 System and control volume at different times

From the first principle, the LHS of Eq. (4.2) can be written as

$$\frac{d\mathcal{N}_s}{dt} = \lim_{\Delta t \to 0} \frac{\mathcal{N}_s|_{t_0+\Delta t} - \mathcal{N}_s|_{t_0}}{\Delta t} \tag{4.3}$$

However, $\mathcal{N}_s = \mathcal{N}_C + \mathcal{N}_B$ at time $t = t_0 + \Delta t$ and $\mathcal{N}_s = \mathcal{N}_{\text{CV}}$ at time $t = t_0$,

$$\frac{d\mathcal{N}_s}{dt} = \lim_{\Delta t \to 0} \frac{(\mathcal{N}_C + \mathcal{N}_B)|_{t_0+\Delta t} - \mathcal{N}_{\text{CV}}|_{t_0}}{\Delta t} \tag{4.4}$$

In addition, $\mathcal{N}_C = \mathcal{N}_{\text{CV}} + \mathcal{N}_A$,

$$\frac{d\mathcal{N}_s}{dt} = \lim_{\Delta t \to 0} \frac{(\mathcal{N}_{\text{CV}} - \mathcal{N}_A + \mathcal{N}_B)|_{t_0+\Delta t} - \mathcal{N}_{\text{CV}}|_{t_0}}{\Delta t} \tag{4.5}$$

Rearranging different terms in Eq. (4.5)

$$\frac{d\mathcal{N}_s}{dt} = \underbrace{\lim_{\Delta t \to 0} \frac{(\mathcal{N}_{\text{CV}}|_{t_0+\Delta t} - \mathcal{N}_{\text{CV}}|_{t_0})}{\Delta t}}_{\text{I-term}} + \underbrace{\lim_{\Delta t \to 0} \frac{\mathcal{N}_B|_{t_0+\Delta t}}{\Delta t}}_{\text{II-term}} - \underbrace{\lim_{\Delta t \to 0} \frac{\mathcal{N}_A|_{t_0+\Delta t}}{\Delta t}}_{\text{III-term}} \tag{4.6}$$

I-Term $$\lim_{\Delta t \to 0} \frac{(\mathcal{N}_{CV}|_{t_0+\Delta t} - \mathcal{N}_{CV}|_{t_0})}{\Delta t} = \frac{\partial}{\partial t}(\mathcal{N}_{CV}) \tag{4.7}$$

The extensive property can be expressed in terms of intensive property for control volume in the following manner: $\mathcal{N}_{CV} = \int_{CV} \eta\rho d\forall$

$$\lim_{\Delta t \to 0} \frac{(\mathcal{N}_{CV}|_{t_0+\Delta t} - \mathcal{N}_{CV}|_{t_0})}{\Delta t} = \frac{\partial}{\partial t} \int_{CV} \eta\rho d\forall \tag{4.8}$$

II-Term $$\lim_{\Delta t \to 0} \frac{\mathcal{N}_B|_{t_0+\Delta t}}{\Delta t} = \lim_{\Delta t \to 0} \frac{\int_{CS-B} \eta\rho(\Delta s \cos\theta dA)}{\Delta t} \tag{4.9}$$

where Δs is the length of the streamline intercepted in the sub-region B. Therefore the length of the element in sub-region B is $\Delta s \cos\theta$ and the volume of the element is $\Delta s \cos\theta dA$.

In addition, $$V = \frac{ds}{dt} = \lim_{\Delta t \to 0}\left(\frac{\Delta s}{\Delta t}\right) \tag{4.10}$$

$$\lim_{\Delta t \to 0} \frac{\mathcal{N}_B|_{t_0+\Delta t}}{\Delta t} = \int_{CS-B} \eta\rho V \cos\theta dA = \int_{CS-B} \eta\rho \vec{V}.d\vec{A} \tag{4.11}$$

In a similar fashion

III-Term $$\lim_{\Delta t \to 0} \frac{\mathcal{N}_A|_{t_0+\Delta t}}{\Delta t} = \int_{CS-A} \eta\rho V \cos(180-\theta) dA = -\int_{CS-A} \eta\rho \vec{V}.d\vec{A} \tag{4.12}$$

It must be noted that area $d\vec{A}$ is a vector quantity whose direction is vertically outward, as shown in Fig. 4.1. This area is the elemental area on the control surface of the control volume intercepted by the sub-region or the cross-sectional of the elemental sub-region. It must also be noted that the length of the intercepted streamline segment will be the same in the two sub-regions A and B as the system, as a whole, is displaced by an amount $\vec{V}\Delta t$. Equation (4.6) is written as follows

$$\frac{dN_s}{dt} = \frac{\partial}{\partial t}\int_{CV} \eta\rho d\forall + \int_{CS-B} \eta\rho\vec{V}.d\vec{A} + \int_{CS-A} \eta\rho\vec{V}.d\vec{A} \tag{4.13}$$

Together regions A and B represent the entire control surface of the control volume,

$$\frac{dN_s}{dt} = \frac{\partial}{\partial t}\int_{CV} \eta\rho d\forall + \int_{CS} \eta\rho\vec{V}.d\vec{A} \tag{4.14}$$

In the subsequent sections, the conservation equations for mass, momentum, and energy have been developed for system as well as for control volume, using the *Reynolds transport equation* (RTE), that is, Eq. (4.14).

NOTE

It should be noted that the RTE in Eq. (4.14) has been developed for a fixed control volume. The RTE can also be obtained for a moving control volume with the fluid velocity being replaced by the fluid velocity relative to the control volume.

4.1.2 Mass Conservation Principle

The mass conservation law for a system state that the total mass of the system remains constant, that is, there will be no change in mass of the system with time. Mathematically,

$$\frac{dm}{dt} = 0 \tag{4.15}$$

Using Reynolds transport theorem, the mass conservation principle for control volume can be obtained by substituting $N = m$ and $\eta = 1$, from Eq. (4.1).

$$\frac{dm}{dt} = \frac{\partial}{\partial t}\int_{\text{CV}} 1.\rho d\forall + \int_{\text{CS}} 1.\rho \vec{V}.d\vec{A} \tag{4.16}$$

Therefore, the mass conservation equation or *continuity equation* in integral form is given by

$$\frac{\partial}{\partial t}\int_{\text{CV}} \rho d\forall + \int_{\text{CS}} \rho \vec{V}.d\vec{A} = 0 \tag{4.17}$$

For steady flow, Eq. (4.17) reduces to

$$\int_{\text{CS}} \rho \vec{V}.d\vec{A} = 0 \tag{4.18}$$

For incompressible flow the density ρ is constant

$$\rho \int_{\text{CS}} \vec{V}.d\vec{A} = 0 \tag{4.19}$$

For the flow through a closed conduit of an arbitrary cross-section having area A, the angle between the velocity and area vectors is zero. Hence,

$$\rho \int_{\text{CS}} V dA \cos 0 = 0 \quad \Rightarrow \quad \rho A V = \text{const} \tag{4.20}$$

This equation is the *integral form of the continuity equation.*

Example 4.1 A hemispherical tank of diameter 1 m is connected to a pipe of 10 cm in diameter as shown in Fig. 4.2. Initially if the water height inside the tank is 10 cm, calculate the time required to fill the rest of the tank.

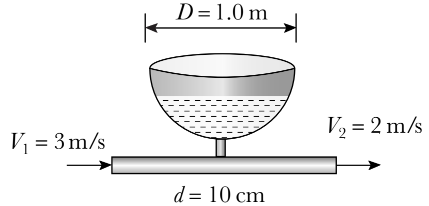

Fig. 4.2

Solution: Applying continuity equation on the system shown in Fig. 4.2,

$$A_1V_1 = A_2V_2 + \dot{Q}_T$$

where $\dot{Q}_T$ is the volume flow rate of water into the tank.

$$\dot{Q}_T = A(V_1 - V_2) \quad \Rightarrow \quad \dot{Q}_T = \frac{\pi}{4}d^2(V_1 - V_2)$$

$$\dot{Q}_T = \frac{\pi}{4} \times 0.1^2 \times (3-2) \quad \Rightarrow \quad \dot{Q}_T = 0.00785\,\text{m}^3/\text{s}$$

The initial volume of water inside the tank,

$$\forall_0 = \frac{1}{3}\pi h^2(3R - h)$$

where R is the radius of hemispherical tank and h is the initial water height inside the tank.

Unfilled tank volume = total tank volume – initial volume of water

$$\forall = \frac{2}{3}\pi R^3 - \frac{1}{3}\pi h^2(3R - h)$$

$$\forall = \frac{2}{3}\pi \times 0.5^3 - \frac{1}{3}\pi \times 0.1^2(3 \times 0.5 - 0.1)$$

$$\forall = 0.247\,\text{m}^3$$

Time required to fill the tank

$$t = \frac{\forall}{\dot{Q}_T} \quad \Rightarrow \quad t = \frac{0.247}{0.00785} \quad \Rightarrow \quad t = 31.5\,\text{s}$$

4.1.3 Linear Momentum Conservation Principle

The momentum conservation principle is the *Newton's second law of motion*, which states that the rate of change of momentum of a body is directly proportional to the force applied on it. Fluid is also a material body and the laws of motion

are valid on fluids as well. The momentum conservation principle for a system is given by

$$\vec{F} = \frac{d\vec{P}}{dt} \tag{4.21}$$

where $\vec{P} = m\vec{V}$ represents momentum and $\vec{F}$ represents force.

Using Reynolds transport theorem, the momentum conservation principle for control volume can be obtained by substituting $\mathcal{N} = \vec{P}$ and $\eta = \vec{V}$, from Eq. (4.1).

$$\frac{d\vec{P}}{dt} = \frac{\partial}{\partial t}\int_{\text{CV}} \vec{V}\rho d\forall + \int_{\text{CS}} \vec{V}\rho\vec{V}.d\vec{A} \tag{4.22}$$

or

$$\vec{F} = \frac{\partial}{\partial t}\int_{\text{CV}} \vec{V}\rho d\forall + \int_{\text{CS}} \vec{V}\rho\vec{V}.d\vec{A} \tag{4.23}$$

The force vector on LHS of Eq. (4.23) is the summation of all the forces acting on the control volume.

$$\sum \vec{F}_{\text{CV}} = \frac{\partial}{\partial t}\int_{\text{CV}} \vec{V}\rho d\forall + \int_{\text{CS}} \vec{V}\rho\vec{V}.d\vec{A} \tag{4.24}$$

Considering the RHS of Eq. 4.24

$$\text{RHS} = \frac{\partial}{\partial t}\int_{\text{CV}} \vec{V}\rho d\forall + \int_{\text{CS}} \vec{V}\rho\vec{V}.d\vec{A}$$

$$= \int_{\text{CV}} \frac{\partial}{\partial t}(\rho\vec{V})d\forall + \int_{\text{CS}} \vec{V}\rho\vec{V}.d\vec{A}$$

From divergence theorem, the surface integral can be transformed to the volume integral

$$\int_{\text{CS}} \vec{V}\rho\vec{V}.d\vec{A} = \int_{\text{CV}} \vec{V}(\vec{\nabla}.\rho\vec{V}).d\forall \tag{4.25}$$

$$\text{RHS} = \int_{\text{CV}} \frac{\partial}{\partial t}(\rho\vec{V})d\forall + \int_{\text{CV}} \vec{V}(\vec{\nabla}.\rho\vec{V})d\forall$$

$$= \int_{\text{CV}} \left(\frac{\partial}{\partial t}(\rho\vec{V}) + \vec{V}(\vec{\nabla}.\rho\vec{V})\right)d\forall \tag{4.26}$$

In addition, $\vec{V}(\vec{\nabla}.\rho\vec{V}) = (\vec{V}.\vec{\nabla})\rho\vec{V}$, therefore

$$\text{RHS} = \int_{\text{CV}} \left[\frac{D(\rho\vec{V})}{Dt}\right]d\forall \tag{4.27}$$

Considering the LHS of Eq. (4.23), that is, the forces acting on the control volume

$$\vec{F} = \vec{F}_S + \vec{F}_B \tag{4.28}$$

The force that can act on a fluid element may be either the surface force or a body force. The surface forces are forces due to viscous stress and pressure whereas gravitational force (body weight) comes under the category of body forces. Figure 4.3 shows the stress and pressure at a point. However, for the sake of better understanding the point has been shown by means of an infinitesimal cubical fluid element. From the *Pascal's law*, the pressure at a point is equal in all directions.

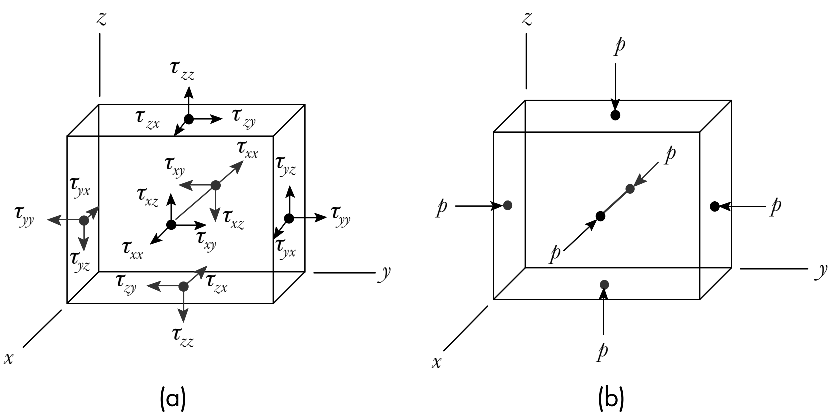

Fig. 4.3 Surface stress (a) Shear stress (b) Pressure

The viscous stress components shown in Fig. 4.3 can be evaluated from the *generalized Hooke's law*, which states that stress is directly proportional to strain rate. Mathematically, this law is expressed as

$$\tau_{ij} = \mu \dot{\varepsilon}_{ij} \tag{4.29}$$

The strain rate in the Eq. (4.29) is given by

$$\dot{\varepsilon}_{ij} = \frac{1}{2}\left(\frac{\partial v_j}{\partial x_i} + \frac{\partial v_i}{\partial x_j}\right) \tag{4.30}$$

In fact, Eqs (4.29) and (4.30) have been derived in Section 3.3 of Chapter 3.

The *viscous stress tensor* can be expressed as

$$\tau_{ij} = \begin{bmatrix} \tau_{xx} & \tau_{xy} & \tau_{zx} \\ \tau_{yx} & \tau_{yy} & \tau_{zy} \\ \tau_{xz} & \tau_{yz} & \tau_{zz} \end{bmatrix} \tag{4.31}$$

For isotropic fluid, $\tau_{ij} = \tau_{ji}$.

The pressure is scalar; to make it tensor it is multiplied with unit matrix known as *Kronecker delta*, δ_{ij}:

$$\delta_{ij} = \begin{bmatrix} 1 & 0 & 0 \\ 0 & 1 & 0 \\ 0 & 0 & 1 \end{bmatrix} \tag{4.32}$$

The *generalized stress tensor* includes pressure, isotropic, and non-isotropic viscous stress components:

$$\sigma_{ij} = -p\delta_{ij} + 2\mu\left(\dot{\varepsilon}_{ij} - \frac{1}{3}\dot{\varepsilon}_{ii}\delta_{ij}\right) \tag{4.33}$$

In tensor form,

$$\sigma_{ij} = \begin{bmatrix} -p + \frac{4}{3}\mu\dot{\varepsilon}_{xx} & 2\mu\dot{\varepsilon}_{xy} & 2\mu\dot{\varepsilon}_{xz} \\ 2\mu\dot{\varepsilon}_{yx} & -p + \frac{4}{3}\mu\dot{\varepsilon}_{yy} & 2\mu\dot{\varepsilon}_{yz} \\ 2\mu\dot{\varepsilon}_{zx} & 2\mu\dot{\varepsilon}_{zy} & -p + \frac{4}{3}\mu\dot{\varepsilon}_{zz} \end{bmatrix} \tag{4.34}$$

Therefore, the surface force can be evaluated as the integral of the dot product of generalized stress tensor and the area dA:

$$\vec{F}_S = \int_{CS} \sigma_{ij}.d\vec{A} \tag{4.35}$$

From divergence theorem, Eq. (4.35) can be written as

$$\vec{F}_S = \int_{CV} (\vec{\nabla}.\sigma_{ij})d\forall \tag{4.36}$$

The body force is the weight of the infinitesimal fluid element shown in Fig. 4.3 and is, thus, given by

$$\vec{F}_B = \int_{CV} (\rho\vec{g})d\forall \tag{4.37}$$

The LHS and RHS of Eq. (4.23) have been evaluated and the momentum principle for a control volume is reduced to

$$\int_{CV}\left[\frac{D(\rho\vec{V})}{Dt}\right]d\forall = \int_{CV}(\rho\vec{g})d\forall + \int_{CV}(\vec{\nabla}.\sigma_{ij})d\forall \tag{4.38}$$

Bringing all the terms to the LHS

$$\int_{CV}\left[\frac{D(\rho\vec{V})}{Dt} - \rho\vec{g} - \vec{\nabla}.\sigma_{ij}\right]d\forall = 0 \tag{4.39}$$

Since $d\forall$ is non-zero, the integrant will be zero to satisfy Eq. 4.39.

$$\frac{D(\rho\vec{V})}{Dt} = \rho\vec{g} + \vec{\nabla}.\sigma_{ij} \tag{4.40}$$

This equation is known as *Cauchy's equation*. For incompressible fluids this equation takes the following form:

$$\frac{D\vec{V}}{Dt} = \vec{g} + \frac{1}{\rho}\vec{\nabla}.\sigma_{ij} \tag{4.41}$$

Momentum Equation

For steady flow processes, the first term on the RHS of Eq. (4.24) vanishes and it reduces to

$$\sum \vec{F}_{\text{CV}} = \int_{\text{CS}} \vec{V}\rho\vec{V}.d\vec{A} \tag{4.42}$$

In component form,

$$\sum F_x = \int_{\text{CS}} \rho V_x \vec{V}.d\vec{A} \tag{4.43a}$$

$$\sum F_y = \int_{\text{CS}} \rho V_y \vec{V}.d\vec{A} \tag{4.43b}$$

If the flow at inlet (denoted by subscript 1) and exit (denoted by subscript 2) of a control volume is uniform, the integral on the RHS reduces to multiplications. The force exerted on the flow passage is thus obtained by

$$F = \rho_2 A_2 V_2^2 - \rho_1 A_1 V_1^2 \tag{4.44}$$

Equation (4.44) is a well-known *momentum equation*. This equation is a useful tool to determine the force exerted by a flowing fluid on a pipe bend, impact of jet on moving blades of a turbine, thrust in jet propulsion system, etc. The impact of fluid jet on moving turbine blades has been discussed in detail in Chapter 9.

Alternately, the momentum equation can also be derived in the following manner:

Consider a mass of fluid ABCD at time $t = 0$ in a stream tube shown in Fig. 4.4. After a small time interval $t = \delta t$, the mass of fluid moves to A′B′C′D′.

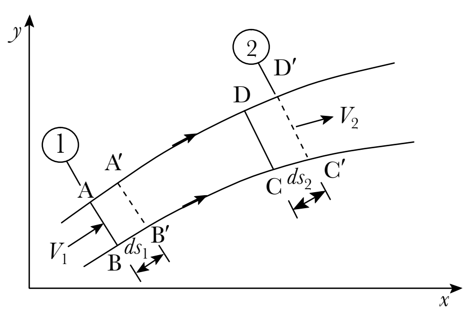

Fig. 4.4 Fluid in a stream tube

Since there can be no flow across the streamline, the stream tube surface will behave like a solid surface.

From mass conservation,

$$m_{ABCD} = m_{A'B'C'D'} \tag{4.45}$$

Region A′B′CD is common to both positions of fluid mass at $t = 0$ and $t = \delta t$

$$m_{ABB'A'} + \cancel{m_{A'B'CD}} = \cancel{m_{A'B'CD}} + m_{DCC'D'} \tag{4.46}$$

$$\rho_1 A_1 ds_1 = \rho_2 A_2 ds_2 \tag{4.47}$$

Momentum of fluid mass in ABB′A′ $= \rho_1 A_1 ds_1 \times V_1 = \rho_1 A_1 V_1 \delta t \times V_1$

Momentum of fluid mass in DCC′D′ $= \rho_2 A_2 ds_2 \times V_2 = \rho_2 A_2 V_2 \delta t \times V_2$

Therefore, the rate of change of momentum $= \rho_2 A_2 V_2^2 - \rho_1 A_1 V_1^2$

As per *Newton's second law of motion*, the rate of change in momentum is equal to the force, that is,

$$F = \rho_2 A_2 V_2^2 - \rho_1 A_1 V_1^2 \tag{4.44}$$

This is the force exerted by the bend on the fluid. From *Newton's third law of motion*, the force exerted by the fluid on the bend will be equal and opposite to the force exerted by the bend on the fluid, that is,

$$R = \rho_1 A_1 V_1^2 - \rho_2 A_2 V_2^2 \tag{4.48}$$

If the flow is taking place in a closed conduit, the pressure forces have to be taken into consideration. In such a case, the force exerted by the fluid on the bend is given by

$$R = (p_1 A_1 + \rho_1 A_1 V_1^2) - (p_2 A_2 + \rho_2 A_2 V_2^2) \tag{4.49}$$

Example 4.2 In Fig. 4.5, water enters a bend of diameter 30 cm fitted with nozzle of diameter 15 cm at the end at a pressure 15 kPa (gauge). The discharge through the bend is 90 L/s. Determine the horizontal component of force acting at the inlet.

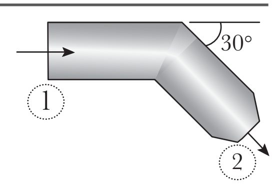

Fig. 4.5

Solution: From continuity equation,

$$Q = A_1 V_1 = A_2 V_2$$

The velocities at sections 1 and 2,

$$V_1 = \frac{Q}{A_1} = \frac{4Q}{\pi d_1^2} \Rightarrow V_1 = \frac{4 \times 0.09}{\pi (0.3)^2} \Rightarrow V_1 = 1.27\,\text{m/s}$$

$$V_2 = \frac{Q}{A_2} = \frac{4Q}{\pi d_2^2} \Rightarrow V_2 = \frac{4 \times 0.09}{\pi (0.15)^2} \Rightarrow V_2 = 5.09\,\text{m/s}$$

Applying momentum equation in the horizontal direction

$$\sum F_x = \int_{A_2} V_{x_2}\, d\dot{m}_2 - \int_{A_1} V_{x_1}\, d\dot{m}_1 = p_1 A_1 - R_x$$

$$p_1 A_1 - R_x = \rho A_2 V_2 (V_2 \cos 30°) - \rho A_1 V_1 (V_1)$$

$$R_x = p_1 A_1 - \rho Q (V_2 \cos 30° - V_1)$$

$$R_x = 15 \times 10^3 \times \frac{\pi \times 0.3^2}{4} - 1000 \times 90 \times 10^{-3} \times (5.09 \times \cos 30 - 1.27)$$

$$\Rightarrow \quad R_x = 777.9\,\text{N}$$

Example 4.3 A 150 mm diameter pipe is split into two pipes of 75 mm diameter each, as shown in Fig. 4.6. Each pipe discharges water into atmosphere at a velocity of 8 m/s. If the junction is in horizontal plane and the friction is negligible, calculate the magnitude and direction of the resultant force.

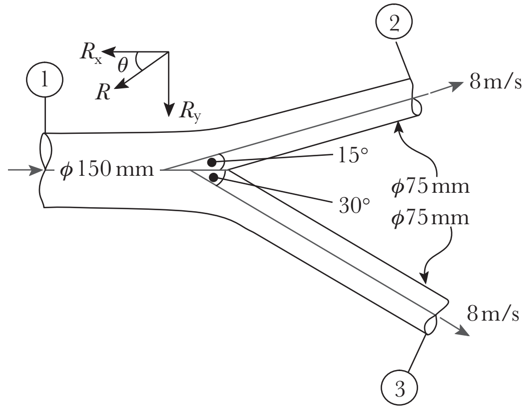

Fig. 4.6

Solution: The pressure at section 1 is calculated by applying Bernoulli's equation between sections 1 and 2:

$$\frac{p_1}{\rho g} + \frac{V_1^2}{2g} + z_1 = \frac{p_2}{\rho g} + \frac{V_2^2}{2g} + z_2$$

The pressure at section 2 is atmospheric pressure. Therefore, the gauge pressure at section 2 is zero. In addition, since the junction is lying on the horizontal plane, the potential (datum) head will be the same throughout. Hence, the pressure at section 1 is

$$\frac{p_1}{\rho g} = \frac{V_2^2}{2g} - \frac{V_1^2}{2g}$$

From continuity equation

$$A_1V_1 = A_2V_2 + A_3V_3 \quad \Rightarrow \quad V_1 = \frac{D_2^2}{D_1^2}(V_2 + V_3)$$

$$\Rightarrow \quad V_1 = \frac{75^2}{150^2}(8+8) \quad \Rightarrow \quad V_1 = 4\,\text{m/s}$$

The pressure at section 1 is

$$p_1 = \frac{\rho}{2}\left(V_2^2 - V_1^2\right) \quad \Rightarrow \quad p_1 = \frac{1000}{2}(64-16) = 24\,\text{kPa}$$

Applying momentum equation in x-direction

$$p_1A_1 - R_x = \dot{m}_2V_2\cos 15° + \dot{m}_3V_3\cos 30° - \dot{m}_1V_1$$

$$R_x = p_1A_1 - (\dot{m}_2V_2\cos 15° + \dot{m}_3V_3\cos 30° - \dot{m}_1V_1)$$

where $\quad \dot{m} = \rho Q$

$$R_x = p_1A_1 - \rho(Q_2V_2\cos 15° + Q_3V_3\cos 30° - Q_1V_1)$$

$$R_x = 24\times 10^3 \times \frac{\pi}{4}\times 0.15^2$$

$$-1000\left[\frac{\pi}{4}\times 0.075^2\times 8^2(\cos 15° + \cos 30°) - \frac{\pi}{4}\times 0.15^2\times 4^2\right]$$

$$\Rightarrow \quad R_x = 188.9\,\text{N}$$

Applying momentum equation in y-direction

$$-R_y = \dot{m}_2V_2\sin 15° - \dot{m}_3V_3\sin 30°$$

$$R_y = \rho(Q_3V_3\sin 30° - Q_2V_2\sin 15°)$$

$$R_x = 1000\times\frac{\pi}{4}\times 0.075^2\times 8^2(-\sin 15° + \sin 30°)$$

$$\Rightarrow \quad R_y = 68.2\,\text{N}$$

The magnitude of resultant force is given by

$$R = \sqrt{R_x^2 + R_y^2} \quad \Rightarrow \quad R = 200.8\,\text{N}$$

The direction of resultant force is

$$\theta = \tan^{-1}\left(\frac{R_y}{R_x}\right) \quad \Rightarrow \quad \theta = 19.85°$$

Example 4.4 Determine the magnitude of horizontal and vertical forces required to keep the box stationary, as show in Fig. 4.7. Assume no mass accumulation inside the box.

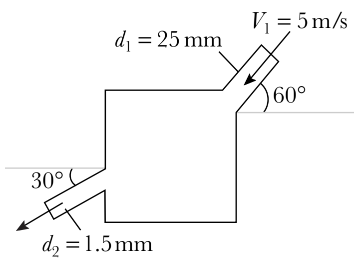

Fig. 4.7

Solution: The discharge throughout the system remains constant as there is no mass accumulation. The discharge and the velocity at port 2 can, thus, be obtained by applying the continuity equation

$$Q = A_1V_1 = A_2V_2$$

$$Q = \frac{\pi}{4}d_1^2V_1 \quad \Rightarrow \quad Q = \frac{\pi}{4}\times 0.025^2 \times 5$$

$$\Rightarrow \quad Q = 2.454\times 10^{-3}\ \text{m}^3/\text{s}$$

$$V_2 = \frac{A_1}{A_2}V_1 \quad \Rightarrow \quad V_2 = \left(\frac{25}{12.5}\right)^2 \times 5 \quad \Rightarrow \quad V_2 = 20\,\text{m/s}$$

Applying momentum equation in horizontal direction

$$\sum F_x = \int_{A_2} V_{x_{\text{out}1}}\,d\dot{m}_{\text{out}} - \int_{A_1} V_{x_{\text{in}}}\,d\dot{m}_{\text{in}} = R_x$$

$$R_x = \rho A_2V_2(-V_2\cos\theta_2) - \rho A_1V_1(-V_1\cos\theta_1)$$

$$R_x = \rho Q(-V_2\cos\theta_2 + V_1\cos\theta_1)$$

$$R_x = 1000\times 2.454\times 10^{-3}\times(-20\cos 30 + 5\cos 60)$$

$$\Rightarrow \quad R_x = -36.37\,\text{N} \quad \Rightarrow \quad R_x = 36.37\,\text{N towards left}$$

Applying momentum equation in vertical direction

$$\sum F_y = \int_{A_2} V_{y_{\text{out}1}}\, d\dot{m}_{\text{out}} - \int_{A_1} V_{y_{\text{in}}}\, d\dot{m}_{\text{in}} = R_y$$

$$R_y = \rho A_2 V_2 (-V_2 \sin\theta_2) - \rho A_1 V_1 (-V_1 \sin\theta_1)$$

$$R_x = \rho Q(-V_2 \sin\theta_2 + V_1 \sin\theta_1)$$

$$R_x = 1000 \times 2.454 \times 10^{-3} \times (-20 \sin 30 + 5 \sin 60)$$

$$\Rightarrow \quad R_x = -13.91\,\text{N} \quad \Rightarrow \quad R_x = 13.91\,\text{N in downward direction}$$

Example 4.5 A jet of water issued from 10 mm diameter nozzle fitted at the end of pipe strikes the centre of a vertical circular plate of 100 mm diameter (Fig. 4.8). The 2 kN force required for moving the plate against the jet with a constant speed of 1 m/s. Determine the pressure in the pipe of 20 mm diameter.

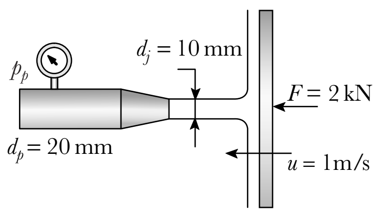

Fig. 4.8

Solution: The relative velocity of jet striking the plate is equal to the sum of jet velocity and the plate velocity (the direction of plate velocity is opposite to the jet velocity)

$$V_R = V_j + u \tag{1}$$

The discharge approaching the plate

$$Q_R = A_j V_R = \left(\frac{\pi}{4} d_j^2\right) V_R$$

Reaction of plate in x-direction is same as the force required to move the plate against the jet, which can be obtained by applying momentum equation in x-direction

$$R_x = F = \rho Q_R V_R \quad \text{or} \quad F = \rho A_j V_R^2$$

$$2000 = 1000 \times \left(\frac{\pi}{4} \times 0.01^2\right) \times V_R^2$$

$$\Rightarrow \quad V_R = 159.6\,\text{m/s}$$

The jet velocity is obtained from Eq. (1)

$$\Rightarrow \quad V_j = 159.6 - 1 = 158.6\,\text{m/s}$$

The flow velocity inside the pipe is obtained by applying the continuity equation

$$Q = A_p V_p = A_j V_j \quad \Rightarrow \quad V_p = \frac{A_j}{A_p} V_j$$

$$\Rightarrow \quad V_p = (10/20)^2 \times 158.6 = 39.7\,\text{m/s}$$

Applying Bernoulli's equation between the pipe and the jet

$$\frac{p_p}{\rho g} + \frac{V_p^2}{2g} + z_p = \frac{p_j}{\rho g} + \frac{V_j^2}{2g} + z_j$$

Since, the datum level is same as the pipe and jet are horizontal, the potential head will be zero. In addition, the atmospheric pressure is acting on the water jet, thus, the gauge pressure acting on the jet is zero. The pressure inside the pipe is obtained by applying the aforementioned constraints on the Bernoulli's equation

$$p_p = \frac{1}{2}\rho\left(V_j^2 - V_p^2\right)$$

$$\Rightarrow \quad p_p = 0.5 \times 1000(158.6^2 - 39.7^2) = 11.79\,\text{MPa (gauge)}$$

4.1.4 Angular Momentum Conservation Principle

The angular momentum conservation principle is analogous to linear momentum conservation principle, where the force is replaced by torque and linear acceleration by angular acceleration. It states that the rate of change of angular momentum of a body is directly proportional to the torque applied on it. Mathematically, the angular momentum conservation equation for a system is represented as

$$\vec{T} = \frac{d\vec{H}}{dt} \tag{4.50}$$

where $\vec{H} = m(\vec{r} \times \vec{V})$ represents angular momentum and $\vec{T}$ represents torque.

Using Reynolds transport theorem, the momentum conservation principle for control volume can be obtained by substituting $N = \vec{H}$ and $\eta = \vec{r} \times \vec{V}$, from Eq. (4.1).

$$\frac{d\vec{H}}{dt} = \frac{\partial}{\partial t}\int_{\text{CV}} (\vec{r} \times \vec{V})\rho d\forall + \int_{\text{CS}} (\vec{r} \times \vec{V})\rho \vec{V}.d\vec{A} \tag{4.51}$$

or
$$\vec{T} = \frac{\partial}{\partial t}\int_{\text{CV}} (\vec{r} \times \vec{V})\rho d\forall + \int_{\text{CS}} (\vec{r} \times \vec{V})\rho \vec{V}.d\vec{A} \tag{4.52}$$

where the applied torque is the sum of moment of surface force $\vec{F}_s$ exerted, moment due to gravity force (weight) and external torque $\vec{T}_{ext}$, if any. That is,

$$\vec{T} = \vec{r} \times \vec{F}_s + \int_{CV} (\vec{r} \times \vec{g})\rho d\forall + \vec{T}_{ext} \tag{4.53}$$

From Eqs (4.52) and (4.53)

$$\vec{r} \times \vec{F}_s + \int_{CV} (\vec{r} \times \vec{g})\rho d\forall + \vec{T}_{ext} = \frac{\partial}{\partial t}\int_{CV} (\vec{r} \times \vec{V})\rho d\forall + \int_{CS} (\vec{r} \times \vec{V})\rho \vec{V}.d\vec{A} \tag{4.54}$$

This is the general formulation for angular momentum conservation principle for control volume using an integral approach.

Example 4.6 A sprinkler, shown in Fig. 4.9, having radius $R = 200$ mm and area of each nozzle 1 cm^2 which are inclined at angle $\alpha = 30°$. The total discharge entering the sprinkler is $Q = 500$ mL/s. Determine (a) the rotational speed of the sprinkler in absence of restraining torque (b) the restraining torque required to keep it stationary (c) torque associated with the sprinkler rotating at 50 rad/s.

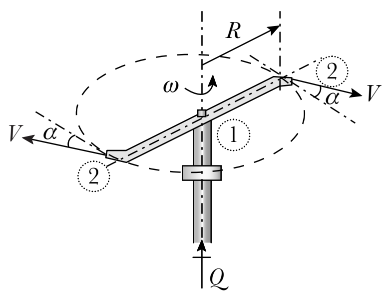

Fig. 4.9

Solution: In a sprinkler, the reaction of jet leaving through the nozzles will cause it to rotate in a direction opposite to that of jet. Assume a control volume in the rotational plane (horizontal X–Y plane) of the sprinkler, thus the torque will be about vertical z-axis. Using angular momentum equation for steady flow

$$\vec{T} = \int_{CS} (\vec{r} \times \vec{V})\rho \vec{V}.d\vec{A}$$

$$T_z = \rho Q\left(r_2 V_2^t \cos\phi_2 - r_1 V_1 \cos\phi_1\right)$$

where subscripts 1 and 2 are assigned for inlet and outlet respectively. ϕ_1 and ϕ_2 are the angles between area and velocity vectors at the inlet outlet, respectively. Since, the fluid is entering the control volume in the z-direction, there will be no initial momentum of fluid in rotational plane, $\phi_1 = 90°$. In addition, $\phi_2 = 0$ and $r_2 = R$. Only tangential component of the absolute jet velocity V will contribute towards the torque whereas radial component will not have any contribution in it.

Angular momentum conservation principle is valid for inertial frame of reference (ground in the present case). The relative tangential velocity with which the fluid jet leaving the sprinkler nozzle is given by

$$V_2^t = V\cos\alpha - \omega R$$

The expression of torque, thus, reduces to

$$T_z = \rho QR(V\cos\alpha - \omega R)$$

(a) Setting $T_z = 0$ in this equation, the rotational speed of the sprinkler is

$$\rho QR(V\cos\alpha - \omega R) = 0$$

$$\omega = \frac{V\cos\alpha}{R}$$

The velocity of jet through the nozzle

$$V = \frac{Q/2}{A} = \frac{0.25\times10^{-3}}{1\times10^{-4}} = 2.5 \text{ m/s}$$

Hence, the rotational speed is

$$\omega = \frac{V\cos\alpha}{R} \quad\Rightarrow\quad \omega = \frac{2.5\cos30°}{0.2} \quad\Rightarrow\quad \omega = 10.82\,\text{rad/s}$$

$$N = \frac{60\omega}{2\pi} \quad\Rightarrow\quad N = \frac{60\times10.82}{2\pi} \quad\Rightarrow\quad \omega = 103\,\text{rpm}$$

(b) To keep the sprinkler stationary, that is, $\omega = 0$, the resisting or restraining torque required

$$T_z = \rho QRV\cos\alpha \quad\Rightarrow\quad T_z = 1000\times0.5\times10^{-3}\times0.2\times2.5\cos30°$$

$$\Rightarrow\quad T_z = 0.216\,\text{Nm}$$

(c) The resisting torque required corresponding to $\omega = 50$ rad/s

$$T_z = \rho QR(V\cos\alpha - \omega R)$$

$$T_z = 1000\times0.5\times10^{-3}\times0.2\times(2.5\cos30° - 50\times0.2) \quad\Rightarrow\quad T_z = -0.783\,\text{Nm}$$

An additional torque is required to rotate the sprinkler at $\omega = 50$ rad/s is 0.783 Nm.

Example 4.7 A lawn sprinkler with unequal arms, shown in Fig. 4.10, discharges water at 1 L/s through its each opening of area 1 cm^2. Determine (a) the rotational speed of the sprinkler in absence of restraining torque (b) the restraining torque required to keep it stationary.

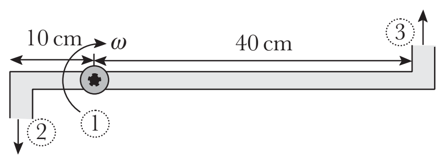

Fig. 4.10

Solution:

Water jet velocity at both nozzle 2 and 3

$$V = \frac{Q}{A} = \frac{1\times10^{-3}}{1\times10^{-4}} = 10\,\text{m/s}$$

Since in a sprinkler, the reaction of jet leaving through the nozzles will cause it to rotate in a direction opposite to that of jet. Assume a control volume in the rotational plane (horizontal X–Y plane) of the sprinkler, thus the torque will be about vertical z-axis. The water is entering the control volume in the z-direction; there will be no initial momentum of fluid in rotational plane. Using angular momentum equation for steady flow

$$\vec{T} = \int_{\text{CS}} (\vec{r}\times\vec{V})\rho\vec{V}.d\vec{A}$$

$$T_z = \rho Q(r_3V_3 + r_2V_2)$$

Angular momentum conservation principle is valid for inertial frame of reference (ground in the present case). The relative tangential velocity with which the fluid jet leaving the sprinkler nozzle is given by

$$V_2 = V - \omega r_2$$

$$V_3 = V - \omega r_3$$

The expression of torque, thus, reduces to

$$T_z = \rho Q\left[r_3(V-\omega r_3) + r_2(V-\omega r_2)\right]$$

(a) In absence of restraining torque setting $T_z = 0$ in this equation, the rotational speed of the sprinkler is given as

$$r_2(V-\omega r_2) + r_3(V-\omega r_3) = 0$$

$$\omega = \frac{V(r_3+r_2)}{r_3^2+r_2^2} \quad\Rightarrow\quad \omega = \frac{10\times(0.4+0.1)}{0.4^2+0.1^2} \quad\Rightarrow\quad \omega = 29.4\,\text{rad/s}$$

Hence, the rotational speed is

$$N = \frac{60\omega}{2\pi} \quad \Rightarrow \quad N = \frac{60 \times 29.4}{2\pi} \quad \Rightarrow \quad N = 280.9\,\text{rpm}$$

(b) The restraining torque required to keep the sprinkler stationary, that is, $\omega = 0$

$$T_z = \rho Q\left[r_2(V - \omega r_2) + r_3(V - \omega r_3)\right] \quad \Rightarrow \quad T_z = \rho QV(r_3 + r_2)$$

$$T_z = 1000 \times 1 \times 10^{-3} \times 10 \times 0.5 \quad \Rightarrow \quad T_z = 5\,\text{Nm}$$

4.1.5 Energy Conservation Principle

Energy conservation principle states that energy can neither be created nor destroyed but it can be transformed from one form to another. The energy conservation principle is the basis of *first law of Thermodynamics*, which states that if heat energy is supplied to a system, a part of it is utilized in doing some useful work (mechanical energy) and the remaining will increase its total energy, that is,

$$\dot{Q} - \dot{W} = \frac{dE}{dt} \tag{4.55}$$

where $\dot{Q}$ and $\dot{W}$ are the rate of heat supplied and the rate of work done, respectively and E is the change in total energy (which is the sum of internal energy, kinetic energy, and potential energy).

Using Reynolds transport theorem, the energy conservation principle for control volume can be obtained by substituting $N = E$ and $\eta = e$, from Eq. (4.2):

$$\frac{dE}{dt} = \frac{\partial}{\partial t}\int_{\text{CV}} e\rho d\forall + \int_{\text{CS}} e\rho \vec{V}.d\vec{A} \tag{4.56}$$

or
$$\dot{Q} - \dot{W} = \frac{\partial}{\partial t}\int_{\text{CV}} e\rho d\forall + \int_{\text{CS}} e\rho \vec{V}.d\vec{A} \tag{4.57}$$

where $\dot{W}$ is the algebraic sum of different types work such as shaft work, work done by shear stress and pressure, and any other work.

$$\dot{W} = \dot{W}_{\text{shaft}} + \dot{W}_{\text{pressure}} + \dot{W}_{\text{shear}} + \ldots \tag{4.58}$$

$\dot{W}_{\text{shaft}}$ is the rate of useful mechanical work, $\dot{W}_{\text{pressure}}$ and $\dot{W}_{\text{shear}}$ is the rate of work done due to pressure and shear stress acting on the control surface.

The work done is the dot product of force applied and the corresponding displacement. Thus, the rate of work done is the dot product of force and velocity. The rate of work done due to pressure and shear stress are given by

$$\dot{W}_{\text{pressure}} = \int_{CS} p d\vec{A}.\vec{V} \Rightarrow \dot{W}_{\text{pressure}} = \int_{CS} p\vec{V}.d\vec{A} \tag{4.59}$$

$$\dot{W}_{\text{shear}} = \int_{CS} \tau d\vec{A}.\vec{V} \Rightarrow \dot{W}_{\text{shear}} = \int_{CS} \tau\vec{V}.d\vec{A} \tag{4.60}$$

The control volume is usually chosen in such a way that the control surface cuts the passage perpendicular to the flow (velocity vector) to make the work done due to shear stress zero.

In addition, the total energy per unit mass as mentioned earlier is the sum of specific internal energy u, potential energy per unit mass and kinetic energy per unit mass, that is,

$$e = u + \frac{V^2}{2} + gz \tag{4.61}$$

Using Eqs (4.58)–(4.61) in Eq. (4.57)

$$\dot{Q} - \dot{W}_{\text{shaft}} - \int_{CS} p\vec{V}.d\vec{A} = \frac{\partial}{\partial t}\int_{CV}\left(u + \frac{V^2}{2} + gz\right)\rho d\forall$$

$$+ \int_{CS}\left(u + \frac{V^2}{2} + gz\right)\rho\vec{V}.d\vec{A} \tag{4.62}$$

On rearranging the terms

$$\dot{Q} - \dot{W}_{\text{shaft}} = \frac{\partial}{\partial t}\int_{CV}\left(u + \frac{V^2}{2} + gz\right)\rho d\forall$$

$$+ \int_{CS}\left(u + pv + \frac{V^2}{2} + gz\right)\rho\vec{V}.d\vec{A} \tag{4.63}$$

where v is the specific volume.

For steady flow processes, first term on the RHS of Eq. (4.63) will vanish. In addition, by definition, enthalpy h is the sum of internal energy and flow work (product of pressure and specific volume). Thus, the first law of thermodynamics for steady flow for a control volume is given by

$$\dot{Q} - \dot{W}_{\text{shaft}} = \int_{CS}\left[h + \frac{V^2}{2} + gz\right]\rho\vec{V}.d\vec{A} \tag{4.64}$$

Example 4.8 A 60 kW air compressor activates the atmospheric air from 300 K, 1 atm, 1 m/s to 600 K, 12 atm and 20 m/s. The compressed air then enters a constant pressure heat exchanger where it is cooled down to 360 K. Determine the heat transfer rate inside the exchanger.

Solution: The energy conservation equation for steady flow for a control volume is given by

$$\dot{Q} - \dot{W}_{\text{shaft}} = \int_{\text{CS}} \left[h + \frac{V^2}{2} + gz \right] \rho \vec{V} . d\vec{A}$$

Considering compressor unit as control volume and applying this equation between 1 and 2 (Fig. 4.11),

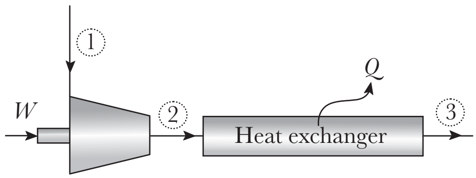

Fig. 4.11

$$\dot{Q} - \dot{W}_{\text{shaft}} = \dot{m} \left[h_2 - h_1 + \frac{V_2^2 - V_1^2}{2} + g(z_2 - z_1) \right]$$

Flow through the compressor is adiabatic $\dot{Q} = 0$ and the difference in datum level between 1 and 2 is negligibly small $z_2 \approx z_2$. This equation reduces to

$$-\dot{W}_{\text{shaft}} = \dot{m} \left[c_p (T_2 - T_1) + \frac{V_2^2 - V_1^2}{2} \right]$$

$$\Rightarrow \quad 60 \times 10^3 = \dot{m} \left[1005 \times (600 - 300) + \frac{20^2 - 1^2}{2} \right] \quad \Rightarrow \quad \dot{m} = 0.199 \, \text{kg/s}$$

Again applying the energy equation between 2 and 3

$$\dot{Q} - \dot{W}_{\text{shaft}} = \dot{m} \left[h_3 - h_2 + \frac{V_3^2 - V_2^2}{2} + g(z_3 - z_2) \right]$$

There is no work done, no change in velocity inside the exchanger no difference in the datum level, that is, $V_2 = V_3$ and $z_2 = z_3$. Hence, this equation reduces to

$$\dot{Q} = \dot{m}(h_3 - h_2) \quad \Rightarrow \quad \dot{Q} = 0.199 \times [1005 \times (360 - 600)] \quad \Rightarrow \quad \dot{Q} = -48 \, \text{kW}$$

4.2 DIFFERENTIAL APPROACH

In this method, an infinitesimal fluid element is chosen and the laws of mass, momentum, and energy conservations are applied to obtain the differential governing equations. An analysis on cubical fluid element has been presented for the development of governing equations in rectangular coordinates. Readers are advised to apply the approach on cylindrical fluid element for the development of governing equations in cylindrical coordinates. However, the final governing equations for cylindrical coordinates have been mentioned at the end of each section.

4.2.1 Mass Conservation—Continuity Equation

To derive the continuity equation, consider an infinitesimal control volume of lengths dx, dy, and dz in x-, y-, and z-directions, respectively in the flow field represented by the velocity vector $\vec{V} = u\hat{i} + v\hat{j} + w\hat{k}$, as shown in Fig. 4.12. According to mass conservation principle, rate of mass of fluid entering the CV = rate of mass of fluid leaving the CV + rate of accumulation of fluid mass inside the CV

$$\dot{m}_x + \dot{m}_y + \dot{m}_z = \dot{m}_{x+dx} + \dot{m}_{y+dy} + \dot{m}_{z+dz} + \frac{\partial m}{\partial t} \tag{4.65}$$

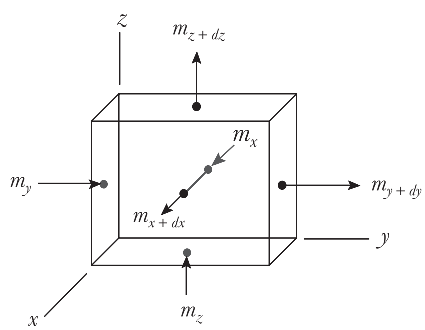

Fig. 4.12 Mass flux through a differential element

From Taylor's series expansion (ignoring higher-order terms as dx, dy, and dz is small)

$$\dot{m}_{x+dx} = \dot{m}_x + \frac{\partial \dot{m}_x}{\partial x}dx; \quad \dot{m}_{y+dy} = \dot{m}_y + \frac{\partial \dot{m}_y}{\partial y}dy; \quad \dot{m}_{z+dz} = \dot{m}_z + \frac{\partial \dot{m}_z}{\partial z}dz \tag{4.66}$$

Equation (4.65) can now be written as

$$\frac{\partial \dot{m}_x}{\partial x}dx + \frac{\partial \dot{m}_y}{\partial y}dy + \frac{\partial \dot{m}_z}{\partial z}dz + \frac{\partial m}{\partial t} = 0 \tag{4.67}$$

The mass flow rate entering control volume in x-, y-, and z-directions

$$\dot{m}_x = \rho u dydz; \quad \dot{m}_y = \rho v dxdz; \quad \dot{m}_z = \rho w dxdy \tag{4.68}$$

The rate of accumulation of fluid mass inside the control volume is

$$\frac{\partial m}{\partial t} = \frac{\partial(\rho \forall)}{\partial t} = \frac{\partial \rho}{\partial t} dxdydz \tag{4.69}$$

Substituting Eqs (4.68) and (4.69) in Eq. (4.67) and on simplification

$$\frac{\partial(\rho u)}{\partial x} + \frac{\partial(\rho v)}{\partial y} + \frac{\partial(\rho w)}{\partial z} + \frac{\partial \rho}{\partial t} = 0 \tag{4.70}$$

Equation (4.70) is known *as continuity equation in differential form.*

In vector form,

$$\frac{\partial \rho}{\partial t} + \vec{\nabla}.\rho\vec{V} = 0 \tag{4.71}$$

For incompressible fluid, (ρ = constant), *the continuity equation* is

$$\frac{\partial u}{\partial x} + \frac{\partial v}{\partial y} + \frac{\partial w}{\partial z} = 0 \tag{4.72}$$

or $\vec{\nabla}.\vec{V} = 0$ (divergence is zero) (4.73)

The continuity equation *in cylindrical coordinates*

$$\frac{\partial \rho}{\partial t} + \frac{1}{r}\frac{\partial(\rho r v_r)}{\partial r} + \frac{1}{r}\frac{\partial(\rho v_\theta)}{\partial \theta} + \frac{\partial(\rho v_z)}{\partial z} = 0 \tag{4.74}$$

4.2.2 Momentum Conservation—Navier–Stokes Equations

To derive the Navier–Stokes equations (N–S equations), consider an infinitesimal control volume of lengths dx, dy, and dz in x-, y-, and z-directions, respectively, as shown in Fig. 4.13. The stress and pressure acting on the differential control volume that cause change in momentum are shown in Figs 4.13(a) and (b). The corresponding change in momentum flux has been shown in Fig. 4.13(c).

According to Newton's second law of motion, the rate of change of momentum of a body is directly proportional to the net force applied on it.

$$\sum \vec{F} = \{\text{Net momentum efflux rate} \\ + \text{Rate of momentum stored inside the CV}\}$$

$$\vec{F}_S + \vec{F}_B = \frac{\partial}{\partial t}\Big\{\Big[(m\vec{V})_{x+dx} - (m\vec{V})_x\Big] + \Big[(m\vec{V})_{y+dy} - (m\vec{V})_y\Big] \\ + \Big[(m\vec{V})_{z+dz} - (m\vec{V})_z\Big] + \frac{\partial(m\vec{V})}{\partial t}dt\Big\} \tag{4.75}$$

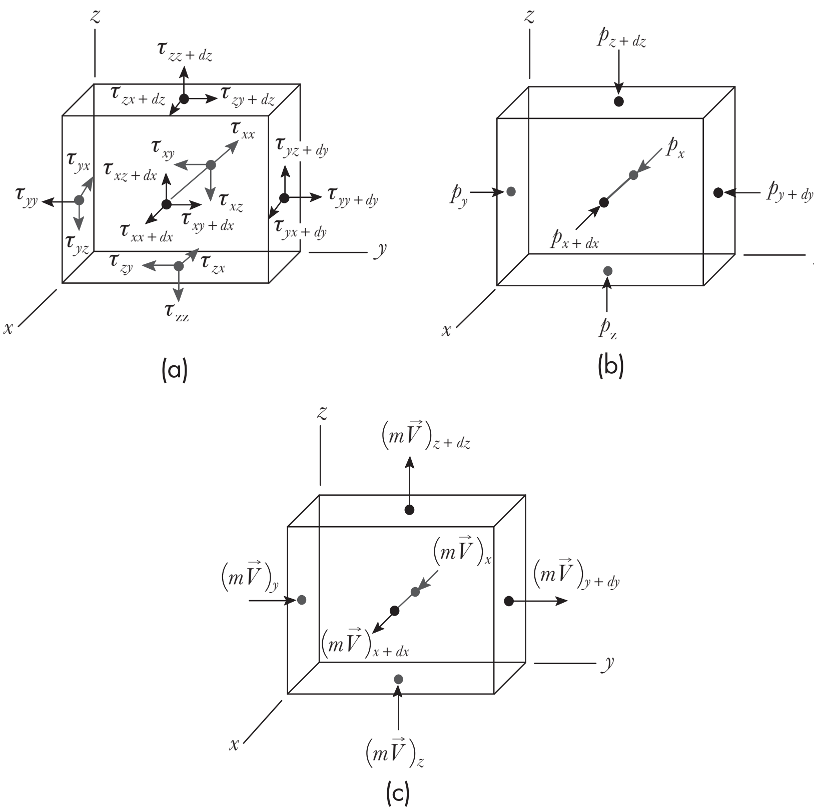

Fig. 4.13 Differential control volume (a) Stresses (b) Pressure (c) Momentum flux

Since Eq. (4.75) is big, the RHS and LHS are simplified separately for the sake of clarity and convenience. The RHS of Eq. (4.75)

$$\text{RHS} = \frac{\partial}{\partial t}\left\{\left[\frac{\partial(m\vec{V})}{\partial x}dx\right] + \left[\frac{\partial(m\vec{V})}{\partial y}dy\right] + \left[\frac{\partial(m\vec{V})}{\partial z}dz\right] + \frac{\partial(m\vec{V})}{\partial t}dt\right\}$$

$$\text{RHS} = \left[\frac{\partial(m\vec{V})}{\partial x}\frac{dx}{dt}\right] + \left[\frac{\partial(m\vec{V})}{\partial y}\frac{dy}{dt}\right] + \left[\frac{\partial(m\vec{V})}{\partial z}\frac{dz}{dt}\right] + \frac{\partial(m\vec{V})}{\partial t}$$

$$\text{RHS} = \left[\frac{\partial(m\vec{V})}{\partial x}u\right] + \left[\frac{\partial(m\vec{V})}{\partial y}v\right] + \left[\frac{\partial(m\vec{V})}{\partial z}w\right] + \frac{\partial(m\vec{V})}{\partial t}$$

Mass of the element is the product of density of the fluid and volume of the fluid element. Here the fluid has been considered incompressible.

$$\text{RHS} = \rho dxdydz\left\{\left[\frac{\partial \vec{V}}{\partial x}u\right]+\left[\frac{\partial \vec{V}}{\partial y}v\right]+\left[\frac{\partial \vec{V}}{\partial z}w\right]+\frac{\partial \vec{V}}{\partial t}\right\}$$

$$\text{RHS} = \rho dxdydz\left\{\left[u\frac{\partial u}{\partial x}+v\frac{\partial u}{\partial y}+w\frac{\partial u}{\partial z}+\frac{\partial u}{\partial t}\right]\hat{i}\right.$$

$$+\left[u\frac{\partial v}{\partial x}+v\frac{\partial v}{\partial y}+w\frac{\partial v}{\partial z}+\frac{\partial v}{\partial t}\right]\hat{j}$$

$$\left.+\left[u\frac{\partial w}{\partial x}+v\frac{\partial w}{\partial y}+w\frac{\partial w}{\partial z}+\frac{\partial w}{\partial t}\right]\hat{k}\right\}$$

Now consider the LHS of Eq. (4.75)

$$\text{LHS} = \vec{F}_S + \vec{F}_B = (\vec{F}_{\text{vis}} + \vec{F}_p) + \vec{F}_{\text{grv}}$$

$$\begin{aligned}\text{LHS} = &\Big[\big((\sigma_{xx+dx}-\sigma_{xx})dydz+(\sigma_{yx+dy}-\sigma_{yx})dzdx\\ &+(\sigma_{zx+dz}-\sigma_{zx})dxdy\big)+\rho g_x dxdydz\Big]\hat{i}\\ &+\Big[\big((\sigma_{xy+dy}-\sigma_{xy})dydz+(\sigma_{yy+dy}-\sigma_{yy})dzdx\\ &+(\sigma_{zy+dy}-\sigma_{zy})dxdy\big)+\rho g_y dxdydz\Big]\hat{j}\\ &+\Big[\big((\sigma_{xz+dz}-\sigma_{xz})dydz+(\sigma_{yz+dz}-\sigma_{yz})dzdx\\ &+(\sigma_{zz+dz}-\sigma_{zz})dxdy\big)+\rho g_z dxdydz\Big]\hat{k}\end{aligned}$$

$$\text{LHS} = \begin{bmatrix}\left(\dfrac{\partial \sigma_{xx}}{\partial x}+\dfrac{\partial \sigma_{yx}}{\partial y}+\dfrac{\partial \sigma_{zx}}{\partial z}+\rho g_x\right)\hat{i}\\ +\left(\dfrac{\partial \sigma_{xy}}{\partial x}+\dfrac{\partial \sigma_{yy}}{\partial y}+\dfrac{\partial \sigma_{zy}}{\partial z}+\rho g_y\right)\hat{j}\\ +\left(\dfrac{\partial \sigma_{xz}}{\partial x}+\dfrac{\partial \sigma_{yz}}{\partial y}+\dfrac{\partial \sigma_{zz}}{\partial z}+\rho g_z\right)\hat{k}\end{bmatrix}dxdydz$$

Equating LHS and RHS of Eq. (4.75)

$$\rho\left\{\begin{array}{l}\left[u\dfrac{\partial u}{\partial x}+v\dfrac{\partial u}{\partial y}+w\dfrac{\partial u}{\partial z}+\dfrac{\partial u}{\partial t}\right]\hat{i}\\+\left[u\dfrac{\partial v}{\partial x}+v\dfrac{\partial v}{\partial y}+w\dfrac{\partial v}{\partial z}+\dfrac{\partial v}{\partial t}\right]\hat{j}\\+\left[u\dfrac{\partial w}{\partial x}+v\dfrac{\partial w}{\partial y}+w\dfrac{\partial w}{\partial z}+\dfrac{\partial w}{\partial t}\right]\hat{k}\end{array}\right\}dxdydz$$

$$=\left[\begin{array}{l}\left(\dfrac{\partial\sigma_{xx}}{\partial x}+\dfrac{\partial\sigma_{yx}}{\partial y}+\dfrac{\partial\sigma_{zx}}{\partial z}+\rho g_x\right)\hat{i}\\+\left(\dfrac{\partial\sigma_{xy}}{\partial x}+\dfrac{\partial\sigma_{yy}}{\partial y}+\dfrac{\partial\sigma_{zy}}{\partial z}+\rho g_y\right)\hat{j}\\+\left(\dfrac{\partial\sigma_{xz}}{\partial x}+\dfrac{\partial\sigma_{yz}}{\partial y}+\dfrac{\partial\sigma_{zz}}{\partial z}+\rho g_z\right)\hat{k}\end{array}\right]dxdydz \tag{4.76}$$

In component form:

For *x-direction*

$$u\frac{\partial u}{\partial x}+v\frac{\partial u}{\partial y}+w\frac{\partial u}{\partial z}+\frac{\partial u}{\partial t}=g_x+\frac{1}{\rho}\left[\frac{\partial\sigma_{xx}}{\partial x}+\frac{\partial\sigma_{yx}}{\partial y}+\frac{\partial\sigma_{zx}}{\partial z}\right] \tag{4.77}$$

$$u\frac{\partial u}{\partial x}+v\frac{\partial u}{\partial y}+w\frac{\partial u}{\partial z}+\frac{\partial u}{\partial t}$$

$$=g_x+\frac{1}{\rho}\left[\frac{\partial}{\partial x}\left(-p+\frac{4}{3}\mu\frac{\partial u}{\partial x}\right)+\mu\frac{\partial}{\partial y}\left(\frac{\partial v}{\partial x}+\frac{\partial u}{\partial y}\right)+\mu\frac{\partial}{\partial z}\left(\frac{\partial w}{\partial x}+\frac{\partial u}{\partial z}\right)\right] \tag{4.78}$$

Using Eqs (4.29) and (4.30), Eq. (4.78) reduces to

$$u\frac{\partial u}{\partial x}+v\frac{\partial u}{\partial y}+w\frac{\partial u}{\partial z}+\frac{\partial u}{\partial t}$$

$$=g_x-\frac{1}{\rho}\frac{\partial p}{\partial x}+\frac{\mu}{\rho}\left(\frac{\partial^2 u}{\partial x^2}+\frac{\partial^2 u}{\partial y^2}+\frac{\partial^2 u}{\partial z^2}\right)+\frac{1}{3}\frac{\mu}{\rho}\frac{\partial}{\partial x}\left(\frac{\partial u}{\partial x}+\frac{\partial v}{\partial y}+\frac{\partial w}{\partial z}\right) \tag{4.79a}$$

Similarly, for *y-direction*

$$u\frac{\partial v}{\partial x}+v\frac{\partial v}{\partial y}+w\frac{\partial v}{\partial z}+\frac{\partial v}{\partial t}$$

$$=g_y-\frac{1}{\rho}\frac{\partial p}{\partial y}+\frac{\mu}{\rho}\left(\frac{\partial^2 v}{\partial x^2}+\frac{\partial^2 v}{\partial y^2}+\frac{\partial^2 v}{\partial z^2}\right)+\frac{1}{3}\frac{\mu}{\rho}\frac{\partial}{\partial y}\left(\frac{\partial u}{\partial x}+\frac{\partial v}{\partial y}+\frac{\partial w}{\partial z}\right) \quad (4.79b)$$

For *z-direction*

$$u\frac{\partial w}{\partial x}+v\frac{\partial w}{\partial y}+w\frac{\partial w}{\partial z}+\frac{\partial w}{\partial t}$$

$$=g_z-\frac{1}{\rho}\frac{\partial p}{\partial z}+\frac{\mu}{\rho}\left(\frac{\partial^2 w}{\partial x^2}+\frac{\partial^2 w}{\partial y^2}+\frac{\partial^2 w}{\partial z^2}\right)+\frac{1}{3}\frac{\mu}{\rho}\frac{\partial}{\partial z}\left(\frac{\partial u}{\partial x}+\frac{\partial v}{\partial y}+\frac{\partial w}{\partial z}\right) \quad (4.79c)$$

Rewriting Eqs (4.79a–c) in vector form,

$$\boxed{\frac{D\vec{V}}{Dt}=\vec{g}-\frac{\vec{\nabla}p}{\rho}+\upsilon\nabla^2\vec{V}+\frac{1}{3}\upsilon\vec{\nabla}(\vec{\nabla}.\vec{V})} \quad (4.80)$$

This equation is the most general and most useful equation in fluid mechanics and is popularly known as *Navier–Stokes equation* (*N–S equation*).

For *incompressible viscous flows* $(\vec{\nabla}.\vec{V}=0)$, the last term on the RHS of the N–S equation vanishes and it reduces to

$$\boxed{\frac{D\vec{V}}{Dt}=\vec{g}-\frac{\vec{\nabla}p}{\rho}+\upsilon\nabla^2\vec{V}} \quad (4.81)$$

Following are the *N–S equations* for incompressible flow *in rectangular coordinates:*

For *x-direction*

$$u\frac{\partial u}{\partial x}+v\frac{\partial u}{\partial y}+w\frac{\partial u}{\partial z}+\frac{\partial u}{\partial t}=g_x-\frac{1}{\rho}\frac{\partial p}{\partial x}+\upsilon\left(\frac{\partial^2 u}{\partial x^2}+\frac{\partial^2 u}{\partial y^2}+\frac{\partial^2 u}{\partial z^2}\right) \quad (4.82a)$$

For *y-direction*

$$u\frac{\partial v}{\partial x}+v\frac{\partial v}{\partial y}+w\frac{\partial v}{\partial z}+\frac{\partial v}{\partial t}=g_y-\frac{1}{\rho}\frac{\partial p}{\partial y}+\upsilon\left(\frac{\partial^2 v}{\partial x^2}+\frac{\partial^2 v}{\partial y^2}+\frac{\partial^2 v}{\partial z^2}\right) \quad (4.82b)$$

For *z-direction*

$$u\frac{\partial w}{\partial x}+v\frac{\partial w}{\partial y}+w\frac{\partial w}{\partial z}+\frac{\partial w}{\partial t}=g_z-\frac{1}{\rho}\frac{\partial p}{\partial z}+\upsilon\left(\frac{\partial^2 w}{\partial x^2}+\frac{\partial^2 w}{\partial y^2}+\frac{\partial^2 w}{\partial z^2}\right)\qquad(4.82c)$$

Following are the *N–S equations for incompressible flow in cylindrical coordinates:*

For *r-direction*

$$v_r\frac{\partial v_r}{\partial r}+\frac{v_\theta}{r}\frac{\partial v_r}{\partial \theta}-\frac{v_\theta^2}{r}+v_z\frac{\partial v_r}{\partial z}+\frac{\partial v_r}{\partial t}$$

$$=g_r-\frac{1}{\rho}\frac{\partial p}{\partial r}+\upsilon\left[\frac{1}{r}\frac{\partial}{\partial r}\left(r\frac{\partial v_r}{\partial r}\right)-\frac{v_r}{r^2}+\frac{1}{r^2}\frac{\partial^2 v_r}{\partial \theta^2}-\frac{2}{r^2}\frac{\partial v_\theta}{\partial \theta}+\frac{\partial^2 v_r}{\partial z^2}\right]\qquad(4.83a)$$

For *θ-direction*

$$v_r\frac{\partial v_\theta}{\partial r}+\frac{v_\theta}{r}\frac{\partial v_\theta}{\partial \theta}-\frac{v_r v_\theta}{r}+v_z\frac{\partial v_\theta}{\partial z}+\frac{\partial v_\theta}{\partial t}$$

$$=g_\theta-\frac{1}{\rho}\frac{\partial p}{r\partial \theta}+\upsilon\left[\frac{1}{r}\frac{\partial}{\partial r}\left(r\frac{\partial v_\theta}{\partial r}\right)-\frac{v_\theta}{r^2}+\frac{1}{r^2}\frac{\partial^2 v_\theta}{\partial \theta^2}+\frac{2}{r^2}\frac{\partial v_r}{\partial \theta}+\frac{\partial^2 v_\theta}{\partial z^2}\right]\qquad(4.83b)$$

For *z-direction*

$$v_r\frac{\partial v_z}{\partial r}+\frac{v_\theta}{r}\frac{\partial v_z}{\partial \theta}+v_z\frac{\partial v_z}{\partial z}+\frac{\partial v_z}{\partial t}$$

$$=g_z-\frac{1}{\rho}\frac{\partial p}{\partial z}+\upsilon\left[\frac{1}{r}\frac{\partial}{\partial r}\left(r\frac{\partial v_z}{\partial r}\right)+\frac{1}{r^2}\frac{\partial^2 v_z}{\partial \theta^2}+\frac{\partial^2 v_z}{\partial z^2}\right]\qquad(4.83c)$$

For *inviscid flow and incompressible flow*

For inviscid flow ($\upsilon = 0$) and incompressible flow ($\vec{\nabla}.\vec{V}=0$), the N–S equation reduces to

$$\boxed{\frac{D\vec{V}}{Dt}=\vec{g}-\frac{\vec{\nabla}p}{\rho}}\qquad(4.84)$$

This equation is known as *Euler's equation.*

For one-dimensional ($u = v = 0$, $w = V$), steady flow ($\partial/\partial t \equiv 0$), the z-direction Euler's equation can be written as

$$V\frac{dV}{dz} = -g - \frac{1}{\rho}\frac{dp}{dz} \tag{4.85}$$

as $g_z = -g$ and flow is one-dimensional $\partial/\partial z \equiv d/dz$. Rearranging and then integrating Eq. (4.85)

$$\frac{p}{\rho} + \frac{V^2}{2} + gz = C \tag{4.86}$$

This equation is well-known in fluid mechanics and is known as *Bernoulli's equation*. The Bernoulli's principle, named after the Dutch–Swiss mathematician *Daniel Bernoulli* (1700–1782 AD) is an approximate but extremely useful relation between pressure energy, kinetic energy, and potential energy. The approximation is that this principle is applicable for inviscid and incompressible flow (ideal flow). Despite of the approximation, the Bernoulli's equation is used in many practical applications. This equation is extensively used for designing pipelines, irrigation channels, flow measuring devices such as constriction meters and pitot-tube, etc.

Differential Approach for Derivation of Bernoulli's Equation

This section describes a differential approach to derive the Bernoulli's equation.

The Bernoulli's equation is derived assuming that the flow is steady, incompressible, and frictionless (inviscid) with no external work and heat transfer. In addition, it is applicable along the streamline.

Consider an infinitesimal fluid element of length ds and cross-sectional area A, along the streamline, as shown in Fig. 4.14. Applying Newton's second law of motion in tangential direction (i.e., s-direction),

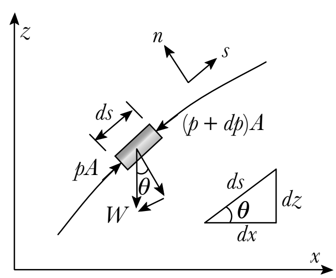

Fig. 4.14 Element along streamline

$$\boxed{\sum F_s = ma_s} \tag{4.87}$$

Pressure force   Gravitational force   Viscous force $\rightarrow 0$ Inertia force

$$pA - (p + dp)A - W\sin\theta = ma_s \tag{4.88}$$

The velocity can be expressed as a function of distance along the streamline and time

$$V = V(s,\ t) \tag{4.89}$$

Mathematically, small change in velocity can be expressed as

$$dV = \frac{\partial V}{\partial s}ds + \frac{\partial V}{\partial t}dt \tag{4.90}$$

Therefore, acceleration is expressed as

$$a_s = \frac{dV}{dt} = \frac{\partial V}{\partial s}\frac{ds}{dt} + \frac{\partial V}{\partial t} \tag{4.91}$$

Since the flow is steady, that is, $\partial/\partial t \equiv 0$

$$a_s = \frac{dV}{dt} = V\frac{\partial V}{\partial s} \tag{4.92}$$

Substituting a_s and $W = mg = (\rho A ds)g$ in Eq. (4.88),

$$\frac{dp}{\rho} + VdV + gds\sin\theta = 0 \tag{4.93}$$

In addition, $ds\sin\theta = dz$

$$\frac{dp}{\rho} + VdV + gdz = 0 \tag{4.94}$$

On integration

$$\boxed{\underbrace{\frac{p}{\rho}}_{\text{Flow energy/work}} + \underbrace{\frac{V^2}{2}}_{\text{Kinetic energy}} + \underbrace{gz}_{\text{Potential energy}} = \mathrm{C}} \tag{4.95a}$$

$$\underbrace{p}_{\substack{\text{Static}\\\text{pressure}}} + \underbrace{\rho\frac{V^2}{2}}_{\substack{\text{Dynamic}\\\text{pressure}}} + \underbrace{\rho g z}_{\substack{\text{Hydrostatic}\\\text{pressure}}} = \mathrm{C} \tag{4.95b}$$

$$\underbrace{\frac{p}{\rho g}}_{\substack{\text{Pressure}\\\text{head}}} + \underbrace{\frac{V^2}{2g}}_{\substack{\text{Velocity}\\\text{head}}} + \underbrace{z}_{\substack{\text{Potential}\\\text{head}}} = \mathrm{C} \tag{4.95c}$$

The value of constant C is different for different streamlines. Equations (4.95a–c) are different forms of *Bernoulli's equation.*

Other Forms of Bernoulli's Equation

In this section, some other forms of *Bernoulli's equation* are discussed:

1. As a matter of fact, work transfer devices such as turbine, pump, or compressor break the streamlines. Thus, Bernoulli's equation cannot be applied on a system, where the work is either done by it or the work is done on it. However, the equation can be modified to incorporate the work done by applying the energy balance at the two sections, shown in Fig. 4.15. If w is the work done by an external agency per unit mass flow rate, the modified Bernoulli's equation is

$$\frac{p_1}{\rho} + \frac{V_1^2}{2} + gz_1 + w = \frac{p_2}{\rho} + \frac{V_2^2}{2} + gz_2 \tag{4.96}$$

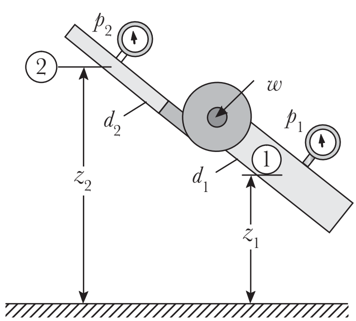

Fig. 4.15 Energy balance

2. In fluid mechanics, the analysis of system and the surroundings is done with the assumption that both the system and its surroundings are maintained at the same temperature. The heat transfer causes the change in temperature, which in turn changes the fluid properties. Hence, the Bernoulli's equation

cannot be applied on the flow systems undergoing heat exchange process. For such cases, steady flow energy equation, described in Section 4.1.5, is employed.

3. The Bernoulli's equation can be modified to incorporate friction losses associated with viscous (real) flows in a closed conduit:

$$\frac{p_1}{\rho}+\frac{V_1^2}{2}+gz_1=\frac{p_2}{\rho}+\frac{V_2^2}{2}+gz_2+h_f \tag{4.97}$$

where h_f is the head loss due to friction.

Example 4.9 Water flows through a pipe of 100 mm diameter at a pressure of 150 kPa. If the pipe is 10 m above the ground and the total head is 50 m, compute the discharge.

Solution: Applying energy conservation principle,

$$\frac{p}{\rho g}+\frac{V^2}{2g}+z=H$$

$$\frac{150\times10^3}{1000\times9.81}+\frac{V^2}{2\times9.81}+10=50 \quad\Rightarrow\quad V=\sqrt{19.62\times(50-10-15.29)}$$

$$\Rightarrow\quad V=22\,\text{m/s}$$

The discharge is the product of cross-sectional area and flow velocity

$$Q=AV=\frac{\pi}{4}D^2\times V \quad\Rightarrow\quad Q=\frac{\pi}{4}\times0.1^2\times22 \quad\Rightarrow\quad Q=0.173\,\text{m}^3/\text{s}$$

Example 4.10 A pump in a supply line increases the pressure of water from 150 kPa to 450 kPa, as shown in Fig. 4.16. The discharge through the pump is 900 L/min. Calculate the power delivered to water by the pump. Neglect the losses due to friction.

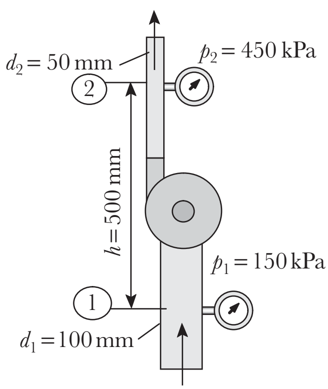

Fig. 4.16

Solution: Applying energy balance between sections 1 and 2,

$$\frac{p_1}{\rho}+\frac{V_1^2}{2}+gz_1+w=\frac{p_2}{\rho}+\frac{V_2^2}{2}+gz_2 \tag{1}$$

From continuity equation,

$$Q = A_1V_1 = A_2V_2$$

The velocities at sections 1 and 2,

$$V_1=\frac{Q}{A_1}=\frac{4Q}{\pi d_1^2} \quad \Rightarrow \quad V_1=\frac{4(0.9/60)}{\pi(0.1)^2}$$

$$\Rightarrow \quad V_1 = 1.91\,\text{m/s}$$

$$V_2=\frac{Q}{A_2}=\frac{4Q}{\pi d_2^2} \quad \Rightarrow \quad V_2=\frac{4(0.9/60)}{\pi(0.05)^2}$$

$$\Rightarrow \quad V_2 = 7.64\,\text{m/s}$$

Rewriting Eq. (1) to find out the pump work

$$w=\frac{p_2-p_1}{\rho}+\frac{V_2^2-V_1^2}{2}+gh$$

$$\Rightarrow \quad w=\frac{(450-150)\times 1000}{1000}+\frac{7.64^2-1.91^2}{2}+9.81\times 0.5$$

$$\Rightarrow \quad w = 332.27\ \text{J/kg}$$

The power delivered to the water

$$P=\rho Q w$$

$$\Rightarrow \quad P = 1000\times(0.9/60)\times 332.27$$

$$\Rightarrow \quad P = 4.984\,\text{kW}$$

4.3 STEADY INCOMPRESSIBLE VISCOUS FLOWS

This section deals with the analytical solution of simple steady incompressible viscous flows. A general procedure to solve a flow problem involves the following steps:

1. Obtaining the governing equation for the flow problem based on
   (a) Mass conservation, that is, continuity equation
   (b) Momentum conservation, that is, N–S equation

2. Identifying the boundary and initial conditions
3. Solution
   (a) Analytical (exact solution)
   (b) Numerical (approximate solution), for example, computational fluid dynamics (CFD) analysis using any of the following methods: (a) finite difference method (FDM), (b) finite volume method (FVM), and (c) finite element method (FEM).

The analytical solution is possible for only simple and small number of problems. For complex flow problems, the CFD techniques are used. In the subsequent section, the analytical solutions of simpler cases of incompressible viscous flows are presented.

4.3.1 Flow Between Infinite Parallel Plates

Figure 4.17 shows the two infinite parallel plates through which the fluid flows. The gap between the plates is '$2a$'. The flow is

1. one dimensional$\rightarrow$ $v = w = 0$
2. steady$\rightarrow$ $\partial/\partial t \equiv 0$
3. incompressible$\rightarrow$ $\rho =$ constant or $\vec{\nabla}.\vec{V} = 0$

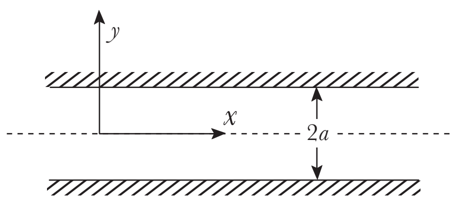

Fig. 4.17 Infinite parallel plates flow domain

Governing Equation

The *continuity equation* for incompressible flow in differential form is

$$\frac{\partial u}{\partial x} + \cancelto{0}{\frac{\partial v}{\partial y}} + \cancelto{0}{\frac{\partial w}{\partial y}} = 0 \quad \Rightarrow \quad \frac{\partial u}{\partial x} = 0 \quad \Rightarrow \quad u \neq u(x) \quad \Rightarrow \quad u = u(y, z, t)$$

In addition, the flow is steady, u will be independent of time t. Since, plates dimensions are infinite in z-direction (into the paper), hence at any z, the velocity profile between the plates will be identical, which means, u is also independent of z. Hence, the velocity u is a function of y only.

$$\boxed{u = u(y)} \quad \Rightarrow \quad \boxed{\frac{\partial u}{\partial y} = \frac{du}{dy}} \quad \Rightarrow \quad \boxed{\frac{\partial^2 u}{\partial y^2} = \frac{d^2 u}{dy^2}} \tag{4.98}$$

Following is the *N–S equation* for incompressible flow:

$$\frac{D\vec{V}}{Dt} = \vec{g} - \frac{\vec{\nabla} p}{\rho} + \upsilon \nabla^2 \vec{V} + \frac{1}{3}\upsilon \vec{\nabla}(\cancelto{0}{\vec{\nabla}.\vec{V}}) \tag{4.99}$$

x-direction N–S equation

$$\cancelto{0}{u\frac{\partial u}{\partial x}} + \cancelto{0}{v\frac{\partial u}{\partial y}} + \cancelto{0}{w\frac{\partial u}{\partial z}} + \cancelto{0}{\frac{\partial u}{\partial t}} = \cancelto{0}{g_x} - \frac{1}{\rho}\frac{\partial p}{\partial x} + \upsilon\left(\cancelto{0}{\frac{\partial^2 u}{\partial x^2}} + \frac{\partial^2 u}{\partial y^2} + \cancelto{0}{\frac{\partial^2 u}{\partial z^2}}\right) \tag{4.100}$$

$$\Rightarrow \quad \boxed{\frac{\partial^2 u}{\partial y^2} = \frac{1}{\mu}\frac{\partial p}{\partial x}} \tag{4.101}$$

y-direction N–S equation

$$\cancelto{0}{u\frac{\partial v}{\partial x}} + \cancelto{0}{v\frac{\partial v}{\partial y}} + \cancelto{0}{w\frac{\partial v}{\partial z}} + \cancelto{0}{\frac{\partial v}{\partial t}} = \cancelto{0}{g_y} - \frac{1}{\rho}\frac{\partial p}{\partial y} + \cancelto{0}{\upsilon\left(\cancelto{0}{\frac{\partial^2 v}{\partial x^2}} + \cancelto{0}{\frac{\partial^2 v}{\partial y^2}} + \cancelto{0}{\frac{\partial^2 v}{\partial z^2}}\right)} \tag{4.102}$$

The gravity term is zero in y-direction due to the flow is taking place between the *horizontal* plates.

$$\Rightarrow \quad \frac{\partial p}{\partial y} = 0 \quad \Rightarrow \quad p \neq p(y) \tag{4.103}$$

Similarly, *z-direction N–S equation* will yield similar result for pressure gradient in that direction

$$\Rightarrow \quad \frac{\partial p}{\partial z} = 0 \quad \Rightarrow \quad p \neq p(z) \tag{4.104}$$

From Eqs (4.103) and (4.104), p is a function of x only.

$$\Rightarrow \quad p = p(x) \quad \text{that is,} \quad \boxed{\frac{\partial p}{\partial x} = \frac{dp}{dx}} \tag{4.105}$$

Therefore Eq. (4.101) can be written as

$$\boxed{\frac{d^2 u}{dy^2} = \frac{1}{\mu}\frac{dp}{dx}} \tag{4.106}$$

This equation is the *governing equation* for the flow between two parallel plates. The pressure gradient is taken constant as the flow area between the plates is constant.

Boundary Conditions

From no-slip condition, the velocities at the plates surfaces

$$\left.\begin{aligned} u &= 0 \quad \text{at} \quad y = a \\ u &= 0 \quad \text{at} \quad y = -a \end{aligned}\right\} \tag{4.107}$$

Analytical Solution

Integrating the governing equation twice, that is, Eq. (4.106),

$$u = \frac{1}{2\mu}\frac{dp}{dx}y^2 + C_1 y + C_2 \tag{4.108}$$

where C_1 and C_2 are constants of integration. Applying boundary conditions on Eq. (4.108) to obtain these constants

$$\left.\begin{aligned} C_1 &= 0 \\ C_2 &= \frac{1}{2\mu}\frac{dp}{dx}a^2 \end{aligned}\right\} \tag{4.109}$$

The solution is, thus, given by

$$u = -\frac{1}{2\mu}\frac{dp}{dx}(a^2 - y^2) \tag{4.110}$$

The solution represents a parabola and this velocity distribution is plotted between plates in Fig. 4.18.

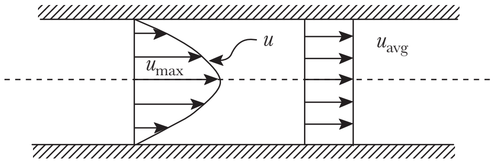

Fig. 4.18 Velocity distribution

Maximum Velocity

The maximum velocity is obtained by differentiating u with respect to y

$$\frac{du}{dy} = 0 \quad \Rightarrow \quad y = 0 \tag{4.111}$$

The velocity is maximum at the centre line ($y = 0$)

$$u_{max} = -\frac{1}{2\mu}\frac{dp}{dx}a^2 \tag{4.112}$$

Average Velocity

The maximum velocity u_{max} cannot be the true representative of the flow as the flow velocity is not the same throughout the cross section; it varies from 0 at plate surfaces and reaches the maximum at the centre line. The average velocity, shown in Fig. 4.18, will truly represent the flow. Mathematically, it is calculated as

$$u_{avg} = \int_{-a}^{a} u dy \Big/ \int_{-a}^{a} dy = -\frac{1}{3\mu}\frac{dp}{dx}a^2 \tag{4.113}$$

or $$\boxed{u_{avg} = \frac{2}{3}u_{max}} \tag{4.114}$$

Wall Shear Stress

The shear stress can be calculated from *Newton's law of viscosity*

$$\tau = \mu\frac{du}{dy} = \frac{dp}{dx}y \tag{4.115}$$

This shows that the shear stress varies linearly with y, as shown in Fig. 4.19. Shear stress is maximum at the plate surfaces and zero at the centre line.

$$\tau_w = a\frac{dp}{dx} \tag{4.116}$$

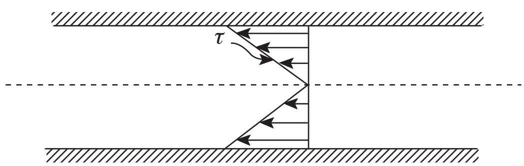

Fig. 4.19 Shear stress distribution

Friction Factor

The coefficient of skin friction is defined as the ratio of wall shear stress to the dynamic pressure and is given by

$$C_f = \frac{\tau_w}{\left(1/2\rho u_{avg}^2\right)} \tag{4.117}$$

$$C_f = \frac{\tau_w}{\left(1/2\rho u_{avg}^2\right)} = \frac{6\mu}{a\rho u_{avg}} \tag{4.118}$$

$$C_f = \frac{12}{\rho u_{\text{avg}}(2a)/\mu} = \frac{12}{\text{Re}} \tag{4.119}$$

Darcy's friction factor is defined as

$$f = 4C_f \tag{4.120}$$

$$\Rightarrow \quad \boxed{f = \frac{48}{\text{Re}}} \tag{4.121}$$

where Re is the Reynolds number

Example 4.11 Oil having dynamic viscosity of 200 cP flows between the two parallel infinite fixed plates 20 mm apart. If the magnitude of pressure gradient in the flow of direction is 1.0 kPa/m. Determine the discharge and wall shear stress.

Solution: The velocity distribution for the flow between two parallel stationary plates is given by

$$u = -\frac{1}{2\mu}\frac{dp}{dx}(a^2 - y^2)$$

Here $\mu = 0.2$ Pa-s; $a = 0.01$ m; $dp/dx = -1000$ Pa/m (negative sign indicates the favourable pressure gradient or pressure gradient in the direction of flow)

Discharge is given by

$$Q = \int_{-a}^{a} u(bdy)$$

where b is the width of the plates. The discharge per unit width

$$q = Q/b = \int_{-a}^{a} udy \quad \Rightarrow \quad q = -\frac{1}{2\mu}\frac{dp}{dx}\int_{-a}^{a}(a^2 - y^2)dy$$

$$\Rightarrow \quad q = -\frac{1}{\mu}\frac{dp}{dx}\int_{0}^{a}(a^2 - y^2)dy \quad \Rightarrow \quad q = -\frac{1}{\mu}\frac{dp}{dx}\left(a^2y - \frac{y^3}{3}\right)_0^a$$

$$\Rightarrow \quad q = -\frac{2}{3}\frac{a^3}{\mu}\frac{dp}{dx} \quad \Rightarrow \quad q = \frac{2}{3}\times\frac{0.01^3}{0.2}\times 1000 \quad \Rightarrow \quad q = 3.33\,\text{L/s} - \text{m}$$

Wall shear stress is given by

$$\tau = \mu\left.\frac{du}{dy}\right|_{y=-a} \quad \Rightarrow \quad \tau = \mu\left\{\frac{d}{dy}\left[-\frac{1}{2\mu}\frac{dp}{dx}(a^2 - y^2)\right]\right\}_{y=-a}$$

$$\Rightarrow \quad \tau = -a\frac{dp}{dx} \quad \Rightarrow \quad \tau = -0.01\times -1000 \quad \Rightarrow \quad \tau = 10\,\text{Pa}$$

4.3.2 Couette Flow

Couette flow is one dimensional incompressible viscous flow in which the upper plate moves with a velocity U and the bottom plate is stationary (Fig. 4.20). The governing equation remains the same in this case as well.

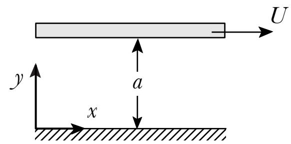

Fig. 4.20 Couette flow

Governing Equation

$$\frac{d^2u}{dy^2} = \frac{1}{\mu}\frac{dp}{dx} \tag{4.106}$$

Boundary Conditions

From no-slip condition, the fluid velocity is same as the plate velocity

$$\left.\begin{aligned} u &= 0 \quad \text{at} \quad y = 0 \\ u &= U \quad \text{at} \quad y = a \end{aligned}\right\} \tag{4.122}$$

Analytical Solution

Integrating twice the governing equation, that is, Eq. (4.106),

$$u = \frac{1}{2\mu}\frac{dp}{dx}y^2 + C_1 y + C_2 \tag{4.123}$$

where C_1 and C_2 are constants of integration. Applying boundary conditions on Eq. (4.123) to obtain these constants

$$\left.\begin{aligned} C_1 &= \frac{1}{a}\left(U - \frac{1}{2\mu}\frac{dp}{dx}a^2\right) \\ C_2 &= 0 \end{aligned}\right\} \tag{4.124}$$

The solution is, thus, given by

$$u = \frac{1}{2\mu}\frac{dp}{dx}y^2 + \frac{y}{a}\left(U - \frac{1}{2\mu}\frac{dp}{dx}a^2\right) \tag{4.125}$$

$$\frac{u}{U} = \frac{1}{2\mu U}\frac{dp}{dx}y^2 + \frac{y}{a}\left(1 - \frac{1}{2\mu U}\frac{dp}{dx}a^2\right) \tag{4.126}$$

$$\frac{u}{U} = \left(\frac{y}{a}\right) - \frac{a^2}{2\mu U}\frac{dp}{dx}\left(\frac{y}{a}\right)\left(1 - \frac{y}{a}\right) \tag{4.127}$$

Substituting $-\dfrac{a^2}{2\mu U}\dfrac{dp}{dx}=k,$ Eq. (4.127) reduces to

$$\frac{u}{U}=(k+1)\left(\frac{y}{a}\right)-k\left(\frac{y}{a}\right)^2 \tag{4.128}$$

Special Cases

(a) For $k=0 \quad \Rightarrow \quad \dfrac{u}{U}=\dfrac{y}{a}$

u/U varies linearly with y/a

(b) For $k=-1 \quad \Rightarrow \quad \dfrac{u}{U}=\left(\dfrac{y}{a}\right)^2$

Parabola with vertex at (0, 0)

(c) For $k=+1 \quad \Rightarrow \quad \dfrac{u}{U}=2\left(\dfrac{y}{a}\right)-\left(\dfrac{y}{a}\right)^2 \quad \Rightarrow \quad \dfrac{u}{U}-1=-\left(\dfrac{y}{a}-1\right)^2$

Parabola with vertex at (1, 1)

The velocity profiles for different values of k have been drawn in Fig. 4.21. For the three aforementioned cases, the explanation is given in Table 4.1.

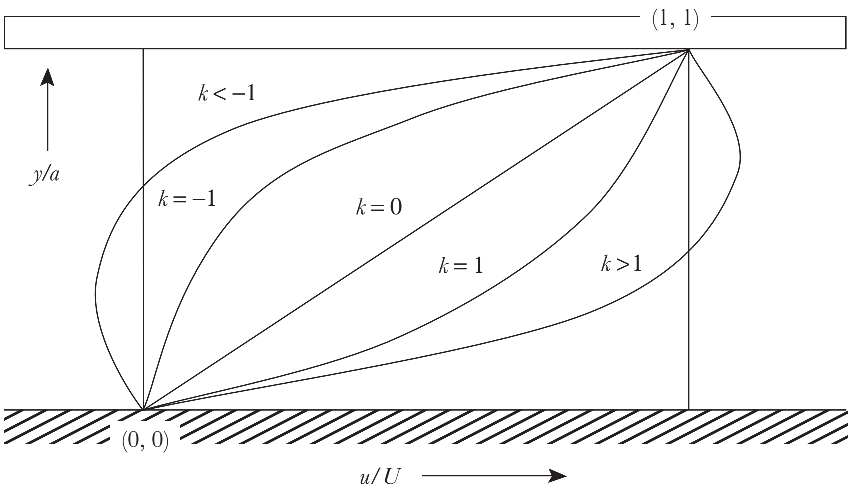

Fig. 4.21 Velocity profiles for different k's

Table 4.1 Velocity profiles for different pressure gradients

Cases	**Velocity profile**	**Description**
$k = 0$ i.e., $\frac{dp}{dx} = 0$	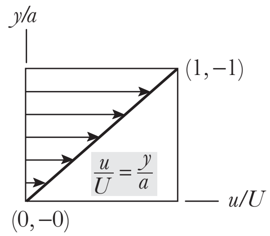	In the absence of pressure gradient, the fluid between the plates is stationary until the upper plate is moved with a velocity, U. There won't be any slip (or any relative motion) between the plate surface and the contacting fluid. The velocity varies linearly between the two plates.
$k = -1$ i.e., $\frac{dp}{dx} > 0$	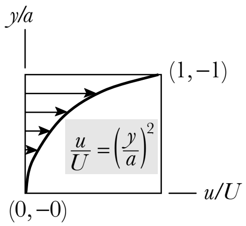	In the presence of adverse pressure gradient ($dp/dx > 0$), pressure increases in the flow of direction, thus it acts as a barrier to the flow. As such, the velocities at different y's between the plates reduce as compared to the case when there was no pressure gradient. The velocity profile for this case is a parabola with vertex (0, 0) and axis as the x-axis.
Large negative values of k i.e., $\frac{dp}{dx} >> 0$	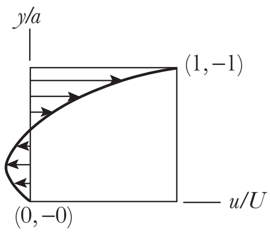	In the presence of very strong adverse pressure gradient $dp/dx >> 0$, the flow velocities near the stationary plate are extremely low. The inertia force is not strong enough to counter the strong pressure force. This leads to the flow of reversal near the surface of stationary plate. However, the behaviour remains parabolic. There will be plane in between the plates where the flow velocity is zero.
$k = 1$ i.e., $\frac{dp}{dx} < 0$	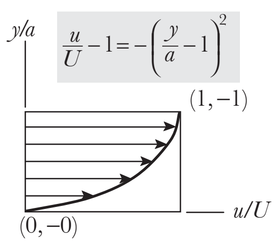	In the presence of favourable pressure gradient $dp/dx > 0$, pressure falls in the flow of direction, thus it will aid flow. As such, the velocities at different y's between the plates increase as compared to the case when there was no pressure gradient. The velocity profile for this case is a parabola with vertex (1, 1) and $y = a$ is the axis.
Large positive values of k i.e., $\frac{dp}{dx} << 0$	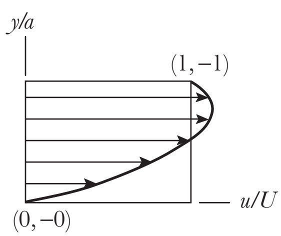	In the presence of very strong favourable pressure gradient $dp/dx << 0$, the velocity somewhere in between the plate will go beyond the magnitude of the plate velocity. The plane of maximum velocity will move towards the stationary plate with further increase in the pressure gradient, depending upon the value of k. However, the velocity profile remains parabolic with vertex shifting downwards and rightwards with the increase in pressure gradient.

Example 4.12 Two infinite parallel plates, shown in Fig. 4.22, are 20 mm apart. The upper plate is moving at a speed of 5 m/s while the lower plate is stationary. The fluid between them is water at 20°C (viscosity of 1002 μPa-s and density 998.2 kg/m^3). Assuming the pressure to be constant, calculate the shear stress at the walls of two plates.

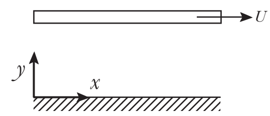

Fig. 4.22

Solution: It's Couette flow problem in which the pressure is constant and as such there won't be any pressure gradient. The velocity profile will be linear, that is, the velocity varies linearly from 0 m/s at the wall of stationary plate to 5 m/s at the wall of moving plate.

Governing equation:

$$\frac{\partial^2 u}{\partial y^2} = 0$$

Boundary conditions are derived from the no-slip conditions

$$\text{At} \quad y = 0 \qquad u = 0;$$
$$\text{At} \quad y = 0.02\,\text{m} \qquad u = 5\,\text{m/s}$$

General solution:

Integrating the governing equation twice

$$u = c_1 y + c_2$$

The constants c_1 and c_2 can be evaluated by substituting the boundary conditions in the general solution.

$$c_2 = 0$$
$$c_1 = \frac{5}{0.02} = 250$$

The velocity profile is linear and is given by

$$u = 250y$$

The shear stress is given by Newton's law of viscosity

$$\tau = \mu \frac{du}{dy} \quad \text{where} \quad \frac{du}{dy} = 250$$

Thus, the value of shear stress will be same throughout the gap between the plates

$$\tau = 1002 \times 10^{-6} \times 250$$
$$\Rightarrow \quad \tau = 0.2505\,\text{Pa}$$

4.3.3 Fully Developed Laminar Flow Through Circular Pipe (Hagen–Poiseuille Flow)

The *Hagen–Poisueille flow*, named after German physicist *Gotthilf Heinrich Ludwig Hagen* (1797–1884 AD) and French physician and physiologist *Jean Louis Marie Poiseuille* (1797–1869 AD), is the fully developed viscous flow through a circular pipe. Developing and fully developed flow is explained in Chapter 6.

The governing equation for this flow problem is obtained either from the N–S equations in cylindrical coordinates or the equation is derived by applying force balance on an infinitesimal element. The second approach is used here.

Consider an infinitesimal hollow cylindrical axisymmetric element of length dz, internal radius r, and thickness dr inside the circular pipe of radius R, shown in Fig. 4.23.

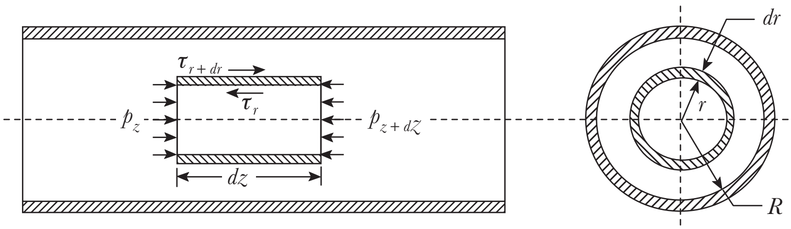

Fig. 4.23 Forces on hollow cylindrical element

Under equilibrium conditions

$$\sum F_z = 0 \tag{4.129}$$

$$\Rightarrow \quad (p_z - p_{z+dz})2\pi r dr + \left[\tau_{r+dr}\, 2\pi(r+dr)dz - \tau_r\, 2\pi r dz\right] = 0 \tag{4.130}$$

From Taylor series expansion (ignoring higher order terms)

$$\left.\begin{aligned} p_{z+dz} &= p_z + \frac{\partial p_z}{\partial z}dz \\ \tau_{r+dr} &= \tau_r + \frac{\partial \tau_r}{\partial r}dr \end{aligned}\right\} \tag{4.131}$$

If $p_z = p$ and $\tau_r = \tau$, Eq. (4.130) can be written as

$$-\frac{\partial p}{\partial z}2\pi r dr dz + \tau \times 2\pi dr dz + \frac{\partial \tau}{\partial r}2\pi r dr dz = 0 \tag{4.132}$$

In Eq. (4.132), the term containing $dr^2 dz$ (being small) is ignored. Since, $p = p(z)$ and $\tau = \tau(r)$, Eq. (4.132) can be written as

$$\boxed{\frac{1}{r}\frac{d(r\tau)}{dr} = \frac{dp}{dz}} \tag{4.133}$$

However, $\tau = \mu \dfrac{du}{dr}$ (from Newton's law of viscosity)

$$\boxed{\frac{d}{dr}\left(r\frac{du}{dr}\right) = \frac{r}{\mu}\frac{dp}{dz}} \tag{4.134}$$

This is the governing equation for the flow under investigation. Integrating Eq. (4.134)

$$r\frac{du}{dr}=\frac{r^2}{2\mu}\frac{dp}{dz}+C_1 \tag{4.135}$$

Again integrating

$$u=\frac{r^2}{4\mu}\frac{dp}{dz}+C_1\ln r+C_2 \tag{4.136}$$

The boundary condition from no-slip condition is

$$u=0 \quad \text{at} \quad r=R \tag{4.137}$$

The solution from Eq. (4.136) will not be finite for $r = 0$. In order to have the finite value of the velocity at $r=0$, C_1 has to be made zero, that is, setting $C_1=0$.

Using boundary condition shown in Eq. (4.137), Eq. (4.136) yields

$$C_2=-\frac{R^2}{4\mu}\frac{dp}{dz} \tag{4.138}$$

Therefore, the solution is

$$u=-\frac{R^2}{4\mu}\frac{dp}{dz}\left(1-\frac{r^2}{R^2}\right) \tag{4.139}$$

This equation represents a parabola. The solution is plotted within the pipe in Fig. 4.24.

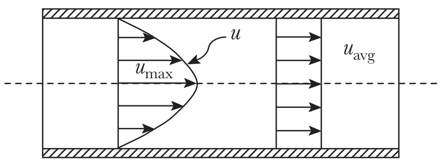

Fig. 4.24 Velocity distribution in a pipe

Maximum Velocity

The maximum velocity is obtained by differentiating u with respect to r

$$\frac{du}{dr}=0 \quad \Rightarrow \quad r=0 \tag{4.140}$$

The velocity is maximum at the axis of the pipe ($r = 0$)

$$u_{max}=-\frac{R^2}{4\mu}\frac{dp}{dz} \tag{4.141}$$

Dividing Eq. (4.139) by Eq. (4.141)

$$\frac{u}{u_{max}}=1-\frac{r^2}{R^2} \tag{4.142}$$

Average Velocity

It is computed as

$$u_{avg} = \int_0^R u 2\pi r dr \Big/ \int_0^R 2\pi r dr = u_{max} \frac{\int_0^R \left(1 - \frac{r^2}{R^2}\right) r dr}{\frac{R^2}{2}} \tag{4.143}$$

or $$\boxed{u_{avg} = \frac{1}{2} u_{max}} \tag{4.144}$$

The average velocity has also been shown in Fig. 4.24.

Wall Shear Stress

The shear stress can be calculated from *Newton's law of viscosity*

$$\tau = \mu \frac{du}{dr} = \mu u_{max} \left(-\frac{2r}{R^2}\right) \tag{4.145}$$

This shows the shear stress varies linearly with *r*, as shown in Fig. 4.25. Shear stress is maximum at the wall and zero at the centre line.

$$\tau_w = -\frac{4\mu u_{avg}}{R} \tag{4.146}$$

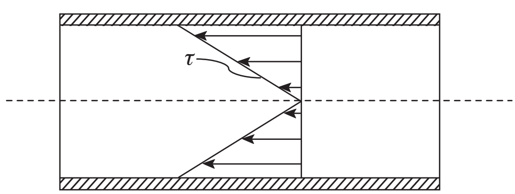

Fig. 4.25 Shear stress distribution in a pipe

Friction Factor

The coefficient of skin friction is defined as the ratio of wall shear stress to the dynamic pressure and is given by

$$C_f = \frac{|\tau_w|}{\left(1/2 \rho u_{avg}^2\right)} = \frac{8\mu}{\rho u_{avg} R} \tag{4.147}$$

$$C_f = \frac{16}{\rho u_{avg} D/\mu} = \frac{16}{\text{Re}} \tag{4.148}$$

Darcy's friction factor is defined as

$$\Rightarrow \quad \boxed{f = 4C_f = \frac{64}{\text{Re}}} \tag{4.149}$$

where Re is the Reynolds number.

Discharge Through Pipe

The discharge through a pipe can be computed in the following way:

$$\boxed{Q = \int_A u\,dA = \int_0^R u 2\pi r\,dr} \tag{4.150}$$

$$\Rightarrow \quad Q = 2\pi u_{\max} \int_0^R \left(1 - \frac{r^2}{R^2}\right) r\,dr \tag{4.151}$$

$$\Rightarrow \quad Q = \frac{\pi R^2 u_{\max}}{2} = \frac{\pi R^2}{2}\left(-\frac{R^2}{4\mu}\frac{dp}{dz}\right) \tag{4.152}$$

Integrating the Eq. (4.152), if the pressure drop is Δp across the pipe length L, the pressure gradient is $-\dfrac{dp}{dz} = \dfrac{\Delta p}{L}$

The discharge through the pipe of length L is, therefore, given by

$$\Rightarrow \quad \boxed{Q = \frac{\pi D^4 \Delta p}{128 \mu L}} \tag{4.153}$$

Example 4.13 The maximum velocity for the viscous flow through a 200 mm diameter pipe is 3 m/s. Determine the average velocity and the radial distance from the pipe axis at which it occurs. In addition, determine the velocity at 25 mm from the pipe wall.

Solution: This is the problem of viscous flow through a circular pipe (Hagen–Poiseuille flow). The velocity profile is given by

$$u = u_{\max}\left(1 - \frac{r^2}{R^2}\right)$$

The average velocity

$$u_{\text{avg}} = \frac{1}{2} u_{\max}$$

$$u_{\text{avg}} = \frac{3}{2} = 1.5\,\text{m/s}$$

Substituting $u = u_{\text{avg}}$ in expression of velocity profile, to get its radial location

$$1 - \frac{r^2}{R^2} = \frac{1}{2} \quad \Rightarrow \quad r = \frac{R}{\sqrt{2}} \quad \Rightarrow \quad r = \frac{100}{\sqrt{2}} = 70.7\,\text{mm}$$

The velocity at 25 mm from the wall (i.e., $r = 75$ mm)

$$u = 3\times\left(1-\frac{75^2}{100^2}\right) \Rightarrow u = 1.31\,\text{m/s}$$

Example 4.14 An oil of viscosity 1.0 P and density 850 kg/m^3 is flowing through a horizontal pipe of diameter 25 mm and length 10 m at a rate of 1000 L/h. Determine the average velocity, Reynolds number, pressure drop, and the power required. Assume the flow to be fully developed flow.

Solution: The average velocity inside the pipe is obtained by dividing the discharge by the cross-sectional of the pipe, that is,

$$V = \frac{Q}{A} \Rightarrow V = \left(\frac{1000\times10^{-3}}{3600}\right)\bigg/\left(\frac{\pi\times0.025^2}{4}\right) \Rightarrow V = 0.566\,\text{m/s}$$

Reynolds number is given by

$$\text{Re} = \frac{\rho V d}{\mu} \Rightarrow \text{Re} = \frac{850\times0.566\times0.025}{0.1} \Rightarrow \text{Re} = 120.3$$

This shows that the flow is laminar as Re is less than the critical value of Reynolds number (2300). The pressure drop can be calculated using the Hagen–Poiseuille equation:

$$\Delta p = \frac{128\mu L}{\pi d^4}Q \Rightarrow \Delta p = \frac{128\times0.1\times10}{\pi\times0.025^4}\times\frac{1}{3600} \Rightarrow \Delta p = 28973.3\,\text{Pa}$$

The power required to maintain the flow is

$$P = Q\,\Delta p \Rightarrow P = 28973.3\times\frac{1}{3600} \Rightarrow P = 8.04\,\text{W}$$

4.4 ENERGY AND MOMENTUM CORRECTION FACTORS

In a flow through a closed conduit or pipe and open channel, the velocity does not remain constant throughout the cross-section. It varies from zero at the solid boundary to maximum at the pipe centreline. The average or mean velocity V is used to represent the flow and for the calculation of other useful parameters such as momentum flux and kinetic energy. The calculation of these parameters using the average velocity is generally less than the actual momentum flux and kinetic energy. Thus, the following correction factors are introduced to account for the loss in energy and momentum:

Energy Correction Factor

$$\alpha = \frac{\text{Actual kinetic energy}}{\text{Average kinetic energy}}$$

$$\alpha = \frac{\int (1/2)(\rho dA u)u^2}{(1/2)(\rho A V)V^2} \Rightarrow \alpha = \frac{1}{AV^3}\int u^3 dA \tag{4.154}$$

Momentum Correction Factor

$$\beta = \frac{\text{Actual momentum flux}}{\text{Average momentum flux}}$$

$$\beta = \frac{\int (\rho dAu)u}{(\rho AV)V} \quad \Rightarrow \quad \boxed{\beta = \frac{1}{AV^2}\int u^2 dA} \tag{4.155}$$

The momentum and energy correction factors are always greater than unity. For steady and uniform flows their values are unity.

Example 4.15 Determine the momentum and energy correction factors for the fully developed laminar flow (Hagen–Poiseuille flow).

Solution: The velocity profile for fully developed laminar flow is given by

$$u = u_{\max}\left(1 - \frac{r^2}{R^2}\right) \quad \Rightarrow \quad u = 2V\left(1 - \frac{r^2}{R^2}\right)$$

where V is the average velocity.

Momentum correction factor, by definition, is

$$\beta = \frac{1}{AV^2}\int u^2 dA \quad \Rightarrow \quad \beta = \frac{1}{\pi R^2 V^2}\int_0^R \left[2V\left(1 - \frac{r^2}{R^2}\right)\right]^2 2\pi r dr$$

$$\Rightarrow \quad \beta = \frac{8}{R^2}\int_0^R r\left(1 - \frac{r^2}{R^2}\right)^2 dr \quad \Rightarrow \quad \beta = \frac{8}{R^2}\int_0^R \left(r + \frac{r^5}{R^4} - 2\frac{r^3}{R^2}\right) dr$$

$$\Rightarrow \quad \beta = \frac{8}{R^2}\left(\frac{R^2}{2} + \frac{R^6}{6R^4} - 2\times\frac{R^4}{4R^2}\right) \quad \Rightarrow \quad \beta = \frac{8}{R^2}\times\frac{R^2}{6} \quad \Rightarrow \quad \beta = \frac{4}{3}$$

Energy correction factor, by definition, is

$$\alpha = \frac{1}{AV^3}\int u^3 dA \quad \Rightarrow \quad \alpha = \frac{1}{\pi R^2 V^3}\int_0^R \left[2V\left(1 - \frac{r^2}{R^2}\right)\right]^3 2\pi r dr$$

$$\Rightarrow \quad \alpha = \frac{16}{R^2}\int_0^R r\left(1 - \frac{r^2}{R^2}\right)^3 dr \quad \Rightarrow \quad \alpha = \frac{16}{R^2}\int_0^R \left(r - \frac{r^7}{R^6} - 3\frac{r^3}{R^2} + 3\frac{r^5}{R^4}\right) dr$$

$$\Rightarrow \quad \alpha = \frac{16}{R^2}\left(\frac{R^2}{2} - \frac{R^8}{8R^6} - 3\frac{R^4}{4R^3} + 3\frac{R^6}{6R^4}\right) \quad \Rightarrow \quad \alpha = \frac{16}{R^2}\times\frac{R^2}{8} \quad \Rightarrow \quad \alpha = 2$$

POINTS TO REMEMBER

- Reynolds transport equation is a tool to convert system analysis to a control volume analysis. It relates the rate of change of an extensive property of a system to the rate of change of the corresponding intensive property in a control volume.
- N–S equations are the most versatile equations in fluid dynamics, and can be used for solving almost all types of flow problems, that is, steady, unsteady, uniform, non-uniform, viscous, non-viscous, incompressible, compressible, one dimensional, and multidimensional.
- The momentum equation is based on Newton's second law of motion and is helpful in determining the forces and reactions in flow systems such as bends, impinging jets, and thrust calculations.
- Bernoulli's equation is a condensed form of N–S equation applicable for steady, incompressible, inviscid, and one-dimensional flow problems. The Bernoulli's equation can be modified to incorporate the work done by applying the energy balance across the external work agency.
- In Couette flow, the incompressible viscous flow between the two parallel plates is studied with one plate moving while the other is made stationary. The pressure gradient affects the magnitude of flow velocities between the two plates. The favourable pressure gradient causes flow velocity to increase whereas the adverse pressure gradient retards the flow.
- In Hagen–Poiseuille flow, the fully developed incompressible viscous flow through circular pipe is studied. The effect of viscous shear is highest near the pipe wall and it diminishes to zero at the centre of the pipe. The average flow velocity in a pipe is half the centre line velocity (maximum velocity).

SUGGESTED READINGS

Borgnakke, C., R.E. Sonntag, *Fundamentals of Thermodynamics*, 7th Ed., John Wiley & Sons, New Delhi, 2009.

Fox, R.W., A.T. McDonald, *Introduction to Fluid Mechanics*, 5th Ed., John Wiley & Sons, New Delhi, 2004.

White, F.M., *Fluid Mechanics*, 6th Ed., Tata McGraw-Hill Education, New Delhi, 2008.

White, F.M., *Viscous Fluid Flow*, 3rd Ed., Tata McGraw-Hill Education, New Delhi, 2011.

MULTIPLE-CHOICE QUESTIONS

4.1 If the velocity of jet striking a stationary flat plate is doubled, the normal force acting on the plate due to the jet impact will

(a) be doubled
(b) be quadrupled
(c) remain unchanged
(d) depend on the viscosity

4.2 For a fully developed laminar flow through a circular pipe, the Darcy's friction factor is

(a) $\frac{16}{Re}$ (c) $\frac{48}{Re}$

(b) $\frac{32}{Re}$ (d) $\frac{64}{Re}$

4.3 Shear stress for a laminar flow through a circular pipe

(a) has parabolic distribution across the section (c) is zero at the centre and increases linearly towards the pipe wall

(b) has linear distribution across the section (d) is zero at the wall and increases linearly to the centre

4.4 If the average velocity is doubled in case of *Hagen–Poiseuille* flow, the ratio of the average velocity to the maximum velocity will be

(a) 2.0 (c) 1.0

(b) 1.5 (d) 0.5

4.5 Euler's equation of motion is based on

(a) conservation of mass (c) Newton's second law of motion

(b) conservation of energy (d) none of these

4.6 The flow between two parallel plates in which one is at rest and the other is moving is called

(a) Hagen–Poiseulle flow (c) Hiemenz flow

(b) Couette flow (d) none of these

4.7 The extensive property that is responsible for the development of N–S equation is

(a) mass (c) energy

(b) momentum (d) none of these

4.8 In a flow through a pipe, the shear stress is maximum at

(a) the centreline (c) the middle of the pipe's surface and the centreline

(b) the pipe's internal surface (d) none of these

4.9 Reynolds transport theorem converts

(a) control volume analysis to system analysis (c) extensive property into intensive property

(b) system analysis to control volume analysis (d) none of these

4.10 For laminar flow, the friction factor for pipes depends on

(a) density (c) velocity

(b) viscosity (d) all of these

4.11 A jet of air (density = 1.2 kg/m^3) with cross-sectional area of 200 cm^2 and velocity 25 m/s strikes the plate normally. What would be the impact of the air?

(a) 10 N (c) 20 N

(b) 15 N (d) 25 N

4.12 The dimension of Darcy friction factor is

(a) M^0LT^{-2} (c) M^0L^0T

(b) $M^0L^0T^{-1}$ (d) $M^0L^0T^0$

4.13 In Couette flow, in absence of any pressure gradient the velocity distribution is
(a) linear (c) elliptic
(b) parabolic (d) hyperbolic

4.14 In Couette flow, the velocity distribution in the presence of favourable pressure gradient is
(a) linear (c) elliptic
(b) parabolic (d) hyperbolic

4.15 The Bernoulli's equation cannot be used for
(a) steady flow (c) one-dimensional flow
(b) incompressible flow (d) non-adiabatic flow

4.16 For the incompressible flow through a frictionless conduit shown in Fig. 4.26, the pressure would be
(a) maximum at section 1 (c) maximum at section 3
(b) maximum at section 2 (d) same throughout

4.17 For the incompressible flow through a closed conduit conduit shown in Fig. 4.26, the velocity would be
(a) minimum at section 1 (c) minimum at section 3
(b) minimum at section 2 (d) same throughout

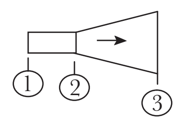

Fig. 4.26

4.18 The linear momentum equation is based on
(a) Newton's law of gravitation (c) Newton's 3rd law of motion
(b) Newton's 2nd law of motion (d) Newton's law of viscosity

4.19 The continuity equation is based on the law of
(a) energy conservation (c) angular momentum conservation
(b) linear momentum conservation (d) mass conservation

4.20 For a fully developed flow through a pipe with Re = 500, the value of skin friction coefficient is
(a) 0.004 (c) 0.016
(b) 0.128 (d) 0.032

REVIEW QUESTIONS

4.1 What is the difference between integral and differential approaches in fluid mechanics?
4.2 What is the need of Reynolds transport theorem?
4.3 What is momentum equation and what are its practical applications?
4.4 Sprinklers are used to water the lawns. What causes the sprinkler to rotate without any external drive? Explain the working principle.
4.5 What do you understand by anisotropy in fluids? Give some examples of anisotropic fluids.
4.6 What are the limitations of Bernoulli's equation?
4.7 Despite the fact that the Bernoulli's equation is applicable only to incompressible and inviscid flows, it has numerous practical applications. Justify the statement.

4.8 Under what conditions does the flow reversal take place near the stationary plate in Couette flow? Explain.
4.9 What is the significance of average fluid velocity in a pipe flow?
4.10 Why does shear stress vanish at the pipe axis?

UNSOLVED PROBLEMS

4.1 Two infinite parallel plates, shown in Fig. 4.27, are 10 mm apart. The upper plate is moving at a speed of 1 m/s while the lower plate is stationary. The fluid between them is water at 20°C (viscosity of 1002 μPa-s and density 998.2 kg/m^3). If the pressure drop between two sections, 50 m apart, is 30 kPa, determine the following:
(a) Velocity profile
(b) Discharge per unit width, and
(c) Shear stress on the walls of both the plates

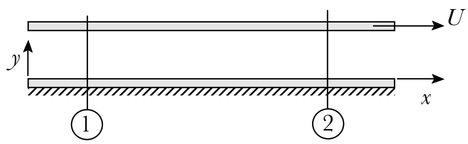

Fig. 4.27

[Ans: (a) $u = -299401.2y^2 + 3094y$ (b) 0.0549 m^2/s (c) 3.1 Pa (bottom), –2.8998 Pa (top)]

4.2 The oil having a viscosity 0.8 Pa-s flows between the two parallel infinite fixed plates. The velocity distribution between the plate is given by

$$u = -\frac{a^2}{2\mu}\frac{dp}{dx}\left[1-\left(\frac{y}{a}\right)^2\right]$$

where $a = 5$ mm, $dp/dx = -1.5$ kPa/m. Calculate the following:
(a) Discharge per unit width
(b) Shear stress at the upper plate

[Ans: (a) 0.03125 m^2/s (b) –1500 Pa]

4.3 An oil (SG = 0.5 and μ = 500 cP) flows through a horizontal circular pipe of 250 mm diameter. If the pressure gradient is –50 Pa/m, find the following:
(a) Discharge of oil through the pipe
(b) Maximum velocity in the pipe
(c) The velocity and shear stress at 25 mm from the pipe wall
(d) The power required to maintain the flow

[Ans: (a) 9.5874 × 10–3 m^3/s (b) 0.39 m/s (c) 0.1404 m/s; –2.496 Pa (d) 0.4794 W/m]

4.4 A tank containing water is placed on a trolley, which is attached to the wall by a cable, as shown in Fig. 4.28. A pipe bend is connected to the tank through which a jet of water is coming out with a velocity of 7.5 m/s. If the diameter of the nozzle is 40 mm, calculate the tension in the cable.

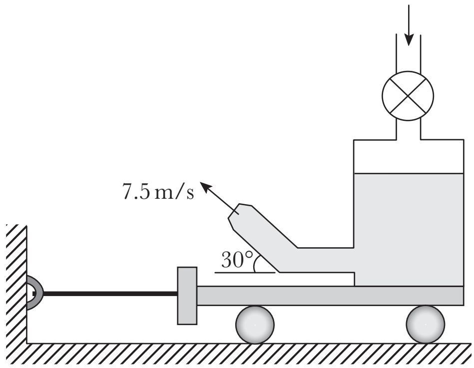

Fig. 4.28

[Ans: 61.215 N]

4.5 The water flows in a 4 m wide canal at a velocity of 5 m/s. A wedge-shaped column bifurcates the stream, as shown in Fig. 4.29. Calculate the force per unit depth exerted by the water stream on the column, if the wedge angle (α) is 30°.

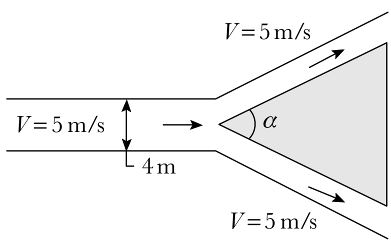

Fig. 4.29

[Ans: 3407.4 N]

4.6 Show that velocity profile for fully developed laminar flow on an inclined plane, shown in Fig. 4.30, is given by

$$u = \rho g \frac{\sin\theta}{\mu}\left(hy - \frac{y^2}{2}\right)$$

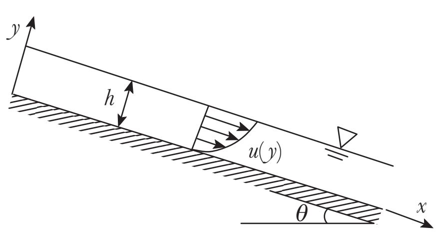

Fig. 4.30

4.7 Find the power required to pump water from one tank to another, as shown in Fig. 4.31. The discharge through the pump is 30 L/s. Neglect all the losses.

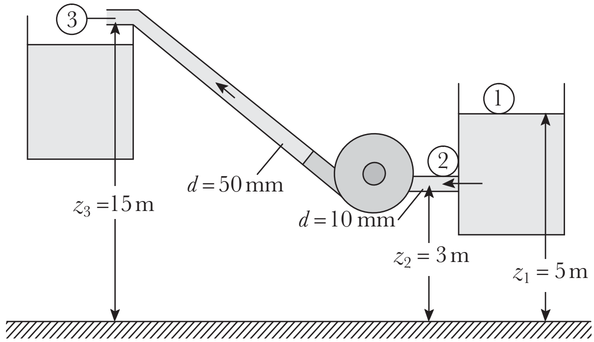

Fig. 4.31

[Ans: 6.445 kW]

4.8 Show that the circumferential velocity for the incompressible viscous flow between two infinitely long concentric cylinders having radii R_1 and R_2 with the inner cylinder rotating at angular velocity ω and outer cylinder being fixed is given by

$$v_\theta = \frac{1}{R_2^2 - R_1^2}\left(\frac{\omega R_1^2 R_2^2}{r} - \omega R_1^2 r\right)$$

4.9 A lawn sprinkler with unequal arms, shown in Fig. 4.32, discharges water at 1 L/s through its each opening of area 1 cm^2. Determine (a) the rotational speed of the sprinkler in absence of restraining torque and (b) the restraining torque required to keep it stationary.

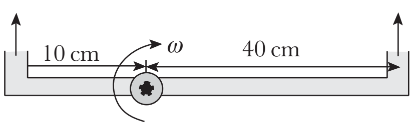

Fig. 4.32

[Ans: (a) 168.5 rpm (b) 3 N-m]

4.10 A lawn sprinkler, shown in Fig. 4.33, supplies water at a total discharge of 1 L/s. The area of each jet is 0.2 cm^2. Determine the resisting torque needed to keep the sprinkler stationary. In addition, determine the angular speed in absence of resisting torque.

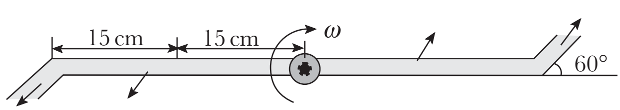

Fig. 4.33

[Ans: 9.7425 N-m, 413.5 rpm]

4.11 A four-arm lawn sprinkler, shown in Fig. 4.34, sprays water at the rate of 2 L/s. The area of each jet is 0.5 cm^2 and each arm length is 20 cm. Determine the angular speed in absence of resisting torque.

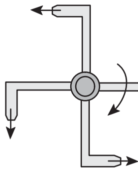

Fig. 4.34

[Ans: 477.5 rpm]

4.12 Air at 200 L/s enters a flat plate solar air heater at 15°C temperature and 100 kPa pressure and leaves it to enter a circular duct of diameter 20 cm at 50°C temperature and 105 kPa pressure. Determine the air velocity inside the duct and the heat transfer rate.

[Ans: 6.37 m/s; 8.446 kW]

4.13 Water flows through a diffuser of length 500 mm has inlet and outlet diameters 200 mm and 400 mm, respectively. The discharge through the diffuser is 25 L/s and the gauge pressure at the inlet is 10 kPa. Determine for vertical as well as horizontal orientation of diffuser (a) velocities at inlet and outlet, (b) pressure at outlet, (c) total force acting on the wall. In addition, compare the results in the two orientations.

[Ans: Horizontal (a) 0.796 m/s, 0.199 m/s (b) 10.297 kPa (c) 965.4 N
Vertical: (a) 0.796 m/s, 0.199 m/s (b) 5.392 kPa (c) 965.4 N]

4.14 Determine the momentum and energy correction factors for the fully developed turbulent flow through pipe of internal radius R having the velocity distribution given by

$$\frac{u}{u_{\max}} = \left(1 - \frac{r}{R}\right)^{1/7}$$

where u is the velocity at any radius r and $u_{\max}$ is the centreline velocity.

[Ans: 1.020408, 1.05838]

4.15 Derive the following expression for discharge through an annulus for a steady laminar flow:

$$Q = \frac{\pi \Delta p}{8\mu L}\left[r_o^4 - r_i^4 - \frac{(r_o^2 - r_i^2)^2}{\ln(r_o/r_i)}\right]$$

where Δp is the pressure drop for a given length L of an annulus having inner and outer radii r_i and r_o, respectively.

Answers to Multiple-choice Questions

4.1 (b)	4.2 (d)	4.3 (c)	4.4 (d)	4.5 (c)
4.6 (b)	4.7 (b)	4.8 (b)	4.9 (b)	4.10 (d)
4.11 (b)	4.12 (d)	4.13 (a)	4.14 (b)	4.15 (d)
4.16 (c)	4.17 (c)	4.18 (b)	4.19 (d)	4.20 (d)

DESIGN OF EXPERIMENTS

Experiment 4.1 Verification of Bernoulli's Equation

Objective

To verify the Bernoulli's equation

Theory

Bernoulli's equation is the energy conservation equation, which means that the total energy of a flow system is constant. The condition for the application of Bernoulli's equation is that the flow should be incompressible, non-viscous, steady, and irrotational. In addition, there should be no heat transfer and work done. The expression of Bernoulli's equation is given as

$$\underbrace{\frac{p}{\rho}}_{\text{Flow energy/ work}} + \underbrace{\frac{V^2}{2}}_{\text{Kinetic energy}} + \underbrace{gz}_{\text{Potential energy}} = C \tag{E4.1}$$

Equation (E4.1) for a flow conduit between any two sections is given by

$$\frac{p_1}{\rho g} + \frac{V_1^2}{2g} + z_1 = \frac{p_2}{\rho g} + \frac{V_2^2}{2g} + z_2$$

or

$$p_1 + \frac{1}{2}\rho V_1^2 + \rho g z_1 = p_2 + \frac{1}{2}\rho V_2^2 + \rho g z_2 \tag{E4.2}$$

where p is the static pressure, V is the flow velocity, and z is the datum head. For horizontal flow the datum head is constant. Equation (E4.2) is valid for ideal fluid flow through a closed conduit. No fluid is an ideal fluid. For the flow of real fluid, the losses due to viscous dissipation are added on the RHS.

$$\frac{p_1}{\rho g} + \frac{V_1^2}{2g} + z_1 = \frac{p_2}{\rho g} + \frac{V_2^2}{2g} + z_2 + h_L \tag{E4.3}$$

Experimental Set-up

A schematic diagram of the experimental set-up is shown in Fig. E4.1. A variable area passage is required to change the velocity as well as pressure. That is why it consists of a divergent-convergent flow passage (venturi), which is installed inside the test section of a wind tunnel. The passage has pressure tappings at its bottom that are connected to an

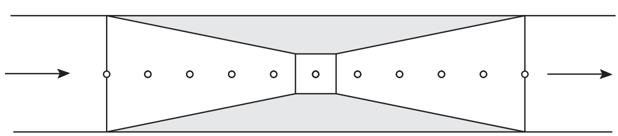

Fig. E4.1 Top view of the test section

appropriate manometer for the measurement of pressure. Since one of the limitations of Bernoulli's equation is that the flow should be incompressible, the velocity inside the test section of the wind tunnel must not surpass the velocity corresponding to Mach number 0.3, up to which the compressibility effects can be ignored (refer Chapter 8 for details).

Procedure

1. Install the venturi inside the test section of the wind tunnel with tappings connected to the bank of manometer tubes.
2. Switch on the fan of the wind tunnel and set a particular velocity inside the test section.
3. Note down the manometer readings and calculate the pressures.
4. Compute the flow velocity at each of the sections where the pressure tap is provided using continuity equation.
5. Add velocity and pressure heads for each section.
6. According to Bernoulli's equation, the total head should remain constant.
7. Repeat the experiment for different flow velocities (or free stream Reynolds number).

Observation Table

(% fan speed) free stream Re	**Tap no.**	$p_s = \rho_m g h_m$ **(Pa)**	$p_d = \frac{1}{2}\rho V^2$ **(Pa)**	$p_t = p_s + p_d$ **(Pa)**	**% loss in energy at each section (tap)** **% loss** $= \frac{\lvert p_{tn} - p_{t1}\rvert}{p_{t1}} \times 100$
Re_1	1.				
	2.				
	3.				
	…				
Re_2	1.				
	2.				
	3.				
	…				
…					

Sample Calculations

If ρ_m and h_m are density and deflection of manometric fluid, the static pressure is computed as

$$p_s = \rho_m g h_m \tag{E4.4}$$

The dynamic pressure in a section where tap is provided is given by

$$p_d = \frac{1}{2}\rho V^2 \tag{E4.5}$$

The velocity at any section can be obtained using continuity equation:

$$V_n = \frac{Q}{A_n} \tag{E4.6}$$

where subscript n is the tap number. The discharge Q is known at the inlet section or it can be calculated by multiplying the free stream velocity at the inlet and cross-sectional area of venturi at the inlet.

The total pressure is the sum of static and dynamic pressure, that is,

$$p_t = p_s + p_d \tag{E4.7}$$

The loss in energy is the difference in energy between any section and the inlet section. It is computed as

$$\%\ \text{loss} = \frac{p_{tn} - p_{t1}}{p_{t1}} \times 100 \tag{E4.8}$$

Results and Discussion

Draw and discuss the following plots:

1. p_s versus x, p_d versus x
2. % loss versus x
3. % loss at the outlet versus Re

Conclusions

Draw conclusions on the results obtained.

Experiment 4.2 Verification of Momentum Equation

Objective

To verify the linear momentum equation using the impact of jet experiment.

Theory

The force generated by impinging jet on a plate can be theoretically evaluated using momentum equation. In the proposed design, a water jet symmetric to the vertical axis of the plate has been considered. Let us assume a control volume over the gliding fluid stream on the plate surface due to jet impingement with subscript 1 for inlet and 2 for the outlet, as shown in Fig. E4.2. From continuity equation (integral form),

$$A_1V_1 = A_2V_2 \tag{E4.9}$$

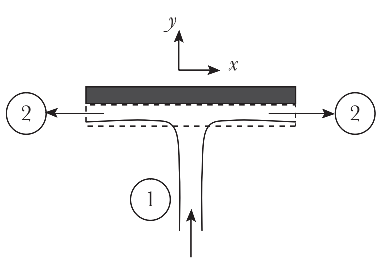

Fig. E4.2

If friction between the plate and fluid surface is ignored, the velocity remains the same. The cross-sectional area of the flow stream at the inlet and outlet will be equal. Applying x-direction momentum equation,

$$\sum F_x = \int_{CS} \rho V_x \vec{V}.d\vec{A} \quad \Rightarrow \quad R_x = \rho V_2 (V_2 A_2) + \rho(-V_2)(V_2 A_2)$$

$$\Rightarrow \quad \boxed{R_x = 0} \tag{E4.10}$$

Applying y-direction momentum equation,

$$\sum F_y = \int_{CS} \rho V_y \vec{V}.d\vec{A} \quad \Rightarrow \quad -R_y = \rho V_1 (V_1 A_1 \cos 180°)$$

$$\Rightarrow \quad \boxed{R_y = \rho A_1 V_1^2} \tag{E4.11}$$

The reaction force on the plate is given by Eq. (E4.11). In order to verify the magnitude of the reaction force, a design of the experimental set-up is proposed in next section.

Experimental Set-up

A schematic diagram of the proposed experimental set-up has been shown in Fig. E4.3. It consists of a nozzle connected to a pump. The pump takes water from the collecting

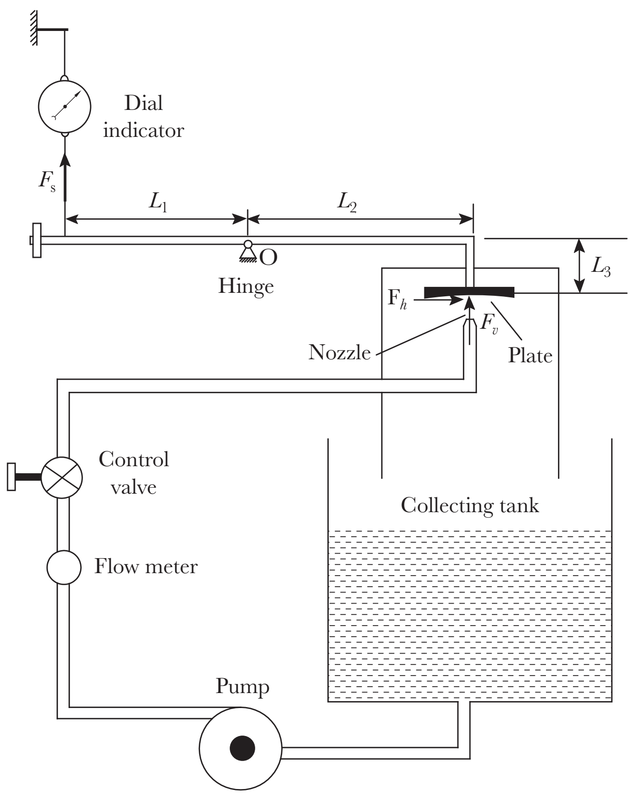

Fig. E4.3 Schematic diagram for the impact of jet experiment

tank and supplies it to the nozzle, through which a jet emerges. The jet impinges on the plate that is connected to a beam hinged at point O. The impact of the jet pushes the plate upwards causing the other end of the beam to move downwards about the hinge. This develops tension in the cord connected to the load sensor having dial indicator. The flow rate is measured using a flow meter installed between the pump and the nozzle. A control valve is also provided to change the velocity of the impinging jet.

The vertical force generated by the jet on the plate can be obtained by applying moments about hinge O.

$$F_s \times L_1 = F_v \times L_2 + F_h \times L_3 \tag{E4.12}$$

Since, there is no horizontal force, $F_h = 0$. The vertical force on the plate, thus, becomes

$$F_v = F_s \times \frac{L_1}{L_2} \tag{E4.13}$$

The magnitude of the force in E4.13 must be equal to the reaction forced obtained theoretically in the previous section.

$$F_v = |R_y| \tag{E4.14}$$

Procedure

1. Measure L_1, L_2, and L_3.
2. Start the pump and set a particular flow rate using the control valve.
3. Note down the reading of force F_s from the dial indicator.
4. Repeat the experiment for different flow rates using control valve.

Observation Table

Reading no.	**Discharge Q (flow meter reading) (m³/s)**	**Jet velocity V_1(m/s)**	**F_s (N)**	**F_v (N)**	**R_y (N)**	**% error = $\frac{\lvert F_v - R_y \rvert}{R_y} \times 100$**
1.						
2.						
3.						
…						

Sample Calculations

The velocity of jet is obtained by dividing the discharge by cross-sectional area of nozzle, that is,

$$V_1 = Q/A_1 \tag{E4.15}$$

The vertical reaction by the plate due to impinging jet is obtained as

$$R_y = \rho A_1 V_1^2 \tag{E4.16}$$

Vertical force exerted by the jet is

$$F_v = F_s \times \frac{L_1}{L_2} \tag{E4.17}$$

The percentage error is the absolute value of the difference in the magnitudes of reaction and vertical force which is obtained as

$$\%\ \text{error} = \frac{|F_v - R_y|}{R_y} \times 100 \tag{E4.18}$$

Results and Discussion

Draw F_v versus V_1 and discuss the nature.

Conclusions

Draw conclusions on the results obtained.

CHAPTER

5 Boundary Layer Flow

LEARNING OBJECTIVES

After studying this chapter, the reader will be able to:
- Understand the concept of boundary layer phenomenon, the governing equations and their possible solutions, boundary layer separation, etc.
- Get a basic understanding of lift and drag
- Infer the techniques for avoiding flow separation, which lead to reduction in drag
- Design simple experiments for the measurement of boundary layer thickness and lift and drag

In previous chapters, the governing equations, based on the laws of mass, momentum, and energy conservation, for incompressible viscous and non-viscous flows have been developed. The analytical solutions of some simple but important flow problems have also been obtained. In this chapter, an important phenomenon related to viscous flow known as *boundary layer flow* has been introduced. The concept of boundary layer and their governing equations for flat as well as curved surfaces have been described. The basic understanding of lift and drag has also been developed.

The boundary layer phenomenon plays a crucial role in fluid-structure interaction problems. It has wide applications in aerodynamic design of vehicles, aircrafts, rockets, missiles, submarines, turbomachinery blades, etc.

5.1 CONCEPT OF BOUNDARY LAYER

The concept of boundary layer was introduced by a German scientist *Ludwig Prandtl* (1875–1953 AD) in 1904. When a solid body moves on a solid surface, there exists a frictional force between them, which tries to act as a barrier to the motion. A similar phenomenon takes place when a fluid flows over a solid surface; the fluid motion near the surface is hindered due to the presence of viscous shear forces. The fluid velocity at the solid surface is zero, which is known as *no slip* condition. Fluid velocity increases with

distance from solid surface and approaches the magnitude of free stream velocity. This variation in velocity is limited in a thin region near the solid surface, known as *boundary layer*.

Figure 5.1 shows the shape of boundary layer formed on an infinitely long flat plate. The plate is kept in a flow stream having free stream velocity u_∞. Due to *no slip* condition, the velocity at the solid surface is zero. The velocity increases from zero at the surface to the free stream velocity at an infinite distance from the plate. In fact, the upper bound for the boundary layer is marked at a distance where the velocity becomes 99% of the free stream velocity.

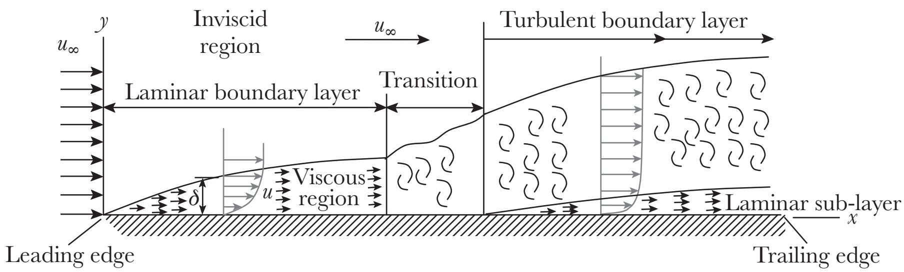

Fig. 5.1 Boundary layer

It is because of the viscous effects that the velocity inside the boundary layer does not remain constant. The viscous effects are related to the velocity variations by the Newton's law of viscosity.

$$\tau = \mu \frac{du}{dy} \tag{5.1}$$

The dynamic viscosity, μ, is constant for the fluid at a given temperature whereas the velocity gradient, du/dy, varies within the boundary layer. This gradient becomes negligibly small as the velocity reaches the free stream velocity, that is, $du/dy \rightarrow 0$ making the flow essentially non-viscous (inviscid) outside the boundary layer region.

It can further be seen in Fig. 5.1, the thickness of the boundary layer increases in the direction of flow, that is, zero at the leading edge and maximum at the trailing edge. In fact, the boundary layer undergoes transition from laminar flow to turbulent flow if the plate is sufficiently long. There are inherent disturbances in the flow, which get amplified due to the weakening of viscous forces in the increasing thickness of boundary layer in the downstream

direction. This transition is quantified by the Reynolds number. For the flow over flat plate it is defined as

$$\mathrm{Re}_x = \frac{u_\infty x}{\upsilon} \tag{5.2}$$

where, x is the distance from the leading edge.

With increase in x, Re_x increases and a point is reached in the downstream direction, where the value of the Reynolds number is equal to the critical Reynolds number, Re_{crit} (Reynolds number at which the flow turns turbulent). To determine whether the boundary layer is laminar or turbulent one has to compute the value of Re_x. If it is less than Re_{crit}, the boundary layer is laminar, otherwise it is turbulent. The value of Re_{crit} for the flow over flat plate has been experimentally established as 5×10^5. It should be noted that there is no abrupt transition from laminar to turbulent flow within the boundary layer. The transition region is of finite length. For the sake of convenience, the transition region is generally clubbed with the turbulent boundary layer region. In the downstream of transition region, the turbulent fluctuations cause the mixing of different fluid layers and as a result boundary layer in the turbulent region further swells. Like laminar boundary layer, the thickness of turbulent boundary layer also increases in the direction of flow. It has been observed that within the turbulent boundary layer, there exists an extremely thin viscous region close to the surface known as viscous (or laminar) sub-layer. In this layer, the viscous effects are even stronger than those of laminar boundary layer. The region is so narrow that the velocity profile may be assumed 'linear'.

5.2 BOUNDARY LAYER THICKNESSES

The thickness of boundary layer is the perpendicular distance from the solid surface where the fluid velocity is 99% of free stream velocity, as given in Eq. (5.3):

$$y = \delta \quad \Leftrightarrow \quad u = 0.99u_\infty \tag{5.3}$$

One of the consequences of boundary layer is flow retardation near the solid surface, which leads to the reduction in mass, momentum, and energy rates. These deficits are quantified by comparing the mass, momentum, and energy rates with the condition when there is no boundary layer (inviscid flow). The deficits in mass, momentum, and energy rates are expressed in terms of displacement, momentum, and energy thicknesses. To find out these thicknesses, an infinitesimal element of thickness dy is considered in the deficit region,

as shown in Fig. 5.2. The mass, momentum, and energy deficits are calculated through the elemental strip and then integrated for the whole region.

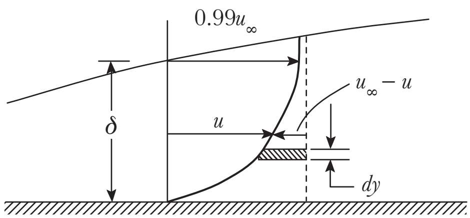

Fig. 5.2 Flow deficit in boundary layer

5.2.1 Displacement Thickness

The mass flow rate within the boundary layer is less than the mass flow rate in the absence of a boundary layer. The mass flow rate is retarded by the amount shown in Eq. (5.4):

$$\delta\dot{m} = \int_0^\infty \rho(u_\infty - u)\,dy \times 1 \tag{5.4}$$

where width is unity in z-direction.

The displacement thickness is the measure of this mass flow rate deficit, and physically can be understood as the distance by which a surface is to be displaced to compensate this deficit in mass flow rate, as shown in Fig. 5.3.

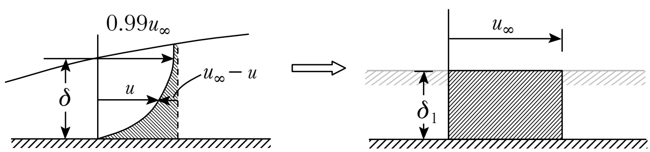

Fig. 5.3 Displacement thickness

If displacement thickness is δ_1, then

$$\rho u_\infty(\delta_1 \times 1) = \int_0^\infty \rho(u_\infty - u)\,dy \times 1 \tag{5.5}$$

Therefore, the displacement thickness is given by

$$\boxed{\delta_1 = \int_0^\infty \left(1 - \frac{u}{u_\infty}\right)dy \approx \int_0^\delta \left(1 - \frac{u}{u_\infty}\right)dy} \tag{5.6}$$

5.2.2 Momentum Thickness

The reduction in momentum flux in the boundary layer region is given by

$$\delta \dot{P} = \int_0^\infty \rho (u_\infty - u) u dy \times 1 \tag{5.7}$$

In the absence of boundary layer, the equivalent momentum flux is

$$\delta \dot{P} = \int_0^\infty \rho (u_\infty - u) u dy \times 1 = \rho u_\infty (\delta_2 \times 1) u_\infty \tag{5.8}$$

where, δ_2 is momentum thickness.

On re-arrangement, the momentum thickness comes out to be

$$\delta_2 = \int_0^\infty \frac{u}{u_\infty}\left(1 - \frac{u}{u_\infty}\right) dy \approx \int_0^\delta \frac{u}{u_\infty}\left(1 - \frac{u}{u_\infty}\right) dy \tag{5.9}$$

Figure 5.4 shows the reduction in momentum flux within the boundary layer. The momentum thickness is thus the measure of the deficit in momentum flux due to the presence of a boundary layer.

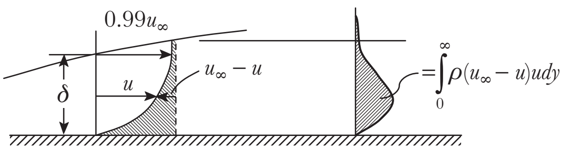

Fig. 5.4 Loss in momentum flux

5.2.3 Energy Thickness

The loss of kinetic energy through the elemental strip, *dy* is shown in Fig. 5.2.

$$\delta \dot{e} = \int_0^\infty \frac{1}{2} \rho \left(u_\infty^2 - u^2\right) u dy \times 1 \tag{5.10}$$

In the absence of a boundary layer, the equivalent loss in kinetic energy is given by

$$\delta \dot{e} = \int_0^\infty \frac{1}{2} \rho \left(u_\infty^2 - u^2\right) u dy \times 1 = \frac{1}{2} \rho u_\infty^2 (\delta_3 \times 1) u_\infty \tag{5.11}$$

where δ_3 is energy thickness.

The energy thickness is, thus, given by

$$\delta_3 = \int_0^\infty \frac{u}{u_\infty}\left(1 - \frac{u^2}{u_\infty^2}\right) dy \approx \int_0^\delta \frac{u}{u_\infty}\left(1 - \frac{u^2}{u_\infty^2}\right) dy \tag{5.12}$$

The energy thickness is, therefore, the measure of the deficit in kinetic energy due to the formation of a boundary layer.

Example 5.1 Find out the values of constants if velocity within the boundary layer is represented by the following functions using the appropriate boundary conditions:

(a) $u = c_1 + c_2 y + c_3 y_2$
(b) $u = c_1 \sin(c_2 y)$

In addition, determine the displacement, momentum, and energy thicknesses in each case.

Solution:

(a) For the velocity profile within the boundary layer given by $u = c_1 + c_2 y + c_3 y^2$, requires the following three boundary conditions for the evaluation of constants c_1, c_2, and c_3:

$$u = 0 \quad \text{at} \quad y = 0$$

$$u = u_\infty \quad \text{at} \quad y = \delta$$

$$\frac{\partial u}{\partial y} = 0 \quad \text{at} \quad y = \delta$$

Applying the boundary conditions (BCs) to the velocity profile expression

$$\text{BC-I:} \quad 0 = c_1 + c_2(0) + c_3(0)^2 \quad \Rightarrow \quad c_1 = 0$$

$$\text{BC-II:} \quad u_\infty = c_2(\delta) + c_3(\delta)^2$$

$$\text{BC-III:} \quad 0 = c_2 + 2c_3\delta \quad \Rightarrow \quad c_2 = -2c_3\delta$$

Substituting c_2 in BC-II to obtain c_3, we get:

$$u_\infty = -2c_3(\delta)^2 + c_3(\delta)^2 \quad \Rightarrow \quad c_3 = -\frac{u_\infty}{\delta^2} \quad \Rightarrow \quad c_2 = \frac{2u_\infty}{\delta}$$

The velocity profile in terms of known constants is

$$\frac{u}{u_\infty} = 2\frac{y}{\delta} - \left(\frac{y}{\delta}\right)^2$$

The displacement thickness is

$$\delta_1 = \int_0^\delta \left(1 - \frac{u}{u_\infty}\right) dy$$

$$\delta_1 = \int_0^\delta \left(1 - 2\frac{y}{\delta} + \frac{y^2}{\delta^2}\right) dy$$

$$\delta_1 = \left[y - \frac{2}{\delta}\left(\frac{y^2}{2}\right) + \frac{1}{\delta^2}\left(\frac{y^3}{3}\right)\right]_0^\delta$$

$$\delta_1 = \delta - \delta + \frac{\delta}{3} \quad \Rightarrow \quad \delta_1 = \frac{\delta}{3}$$

The momentum thickness is

$$\delta_2 = \int_0^\delta \frac{u}{u_\infty}\left(1-\frac{u}{u_\infty}\right)dy$$

$$\delta_2 = \int_0^\delta \left(2\frac{y}{\delta}-\frac{y^2}{\delta^2}\right)\left(1-2\frac{y}{\delta}+\frac{y^2}{\delta^2}\right)dy$$

$$\delta_2 = \int_0^\delta \left(2\frac{y}{\delta}-5\frac{y^2}{\delta^2}+4\frac{y^3}{\delta^3}-\frac{y^4}{\delta^4}\right)dy$$

$$\delta_2 = \left[\frac{2}{\delta}\left(\frac{y^2}{2}\right)-\frac{5}{\delta^2}\left(\frac{y^3}{3}\right)+\frac{4}{\delta^3}\left(\frac{y^4}{4}\right)-\frac{1}{\delta^4}\left(\frac{y^5}{5}\right)\right]_0^\delta$$

$$\delta_2 = \left(1-\frac{5}{3}+1-\frac{1}{5}\right)\delta \quad\Rightarrow\quad \delta_2 = \frac{2}{15}\delta$$

The energy thickness is

$$\delta_3 = \int_0^\delta \frac{u}{u_\infty}\left(1-\frac{u^2}{u_\infty^2}\right)dy$$

$$\delta_3 = \int_0^\delta \left(2\frac{y}{\delta}-\frac{y^2}{\delta^2}\right)\left(1-\left\{2\frac{y}{\delta}-\frac{y^2}{\delta^2}\right\}^2\right)dy$$

Substitute $\frac{y}{\delta}=\eta \quad\rightarrow\quad dy=\delta\, d\eta$

$$\delta_3 = \delta\int_0^1 (2\eta-\eta^2)(1-\{2\eta-\eta^2\}^2)\,d\eta$$

$$\delta_3 = \delta\int_0^1 (2\eta-\eta^2-8\eta^3+12\eta^4-6\eta^5+\eta^6)\,d\eta$$

$$\delta_3 = \delta\left[2\frac{\eta^2}{2}-\frac{\eta^3}{3}-8\frac{\eta^4}{4}+12\frac{\eta^5}{5}-6\frac{\eta^6}{6}+\frac{\eta^7}{7}\right]_0^1$$

$$\delta_3 = \left(1-\frac{1}{3}-2+\frac{12}{5}-1+\frac{1}{7}\right)\delta \quad\Rightarrow\quad \delta_2 = \frac{22}{105}\delta$$

(b) For the velocity profile within the boundary layer given by $u = c_1 \sin(c_2 y)$, requires the following two boundary conditions for the evaluation of constants c_1 and c_2.

$$u = u_\infty \quad \text{at} \quad y=\delta$$

$$\frac{\partial u}{\partial y} = 0 \quad \text{at} \quad y=\delta$$

Applying the BCs to the velocity profile expression, we get

BC-I: $u_\infty = c_1.\sin(c_2.\delta)$

BC-II: $0 = c_1.c_2.\cos(c_2.\delta) \;\Rightarrow\; \cos(c_2\delta)=0 \;\Rightarrow\; c_2 = \frac{n\pi}{2\delta}$ (as $c_1, c_2 \neq 0$)

where, $n = 1$ at $y = \delta$ as shown in Fig. 5.5.

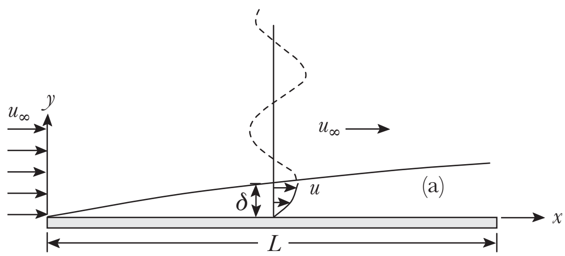

Fig. 5.5 Sinusoidal velocity profile (n = 1)

Substituting c_2 in BC-I to obtain c_1

$$u_\infty = c_1 . \sin\left(\frac{\pi}{2}\right) \quad \Rightarrow \quad c_1 = u_\infty$$

The velocity profile in terms of known constants is

$$\frac{u}{u_\infty} = \sin\left(\frac{\pi}{2}\frac{y}{\delta}\right)$$

The displacement thickness is

$$\delta_1 = \int_0^\delta \left(1 - \frac{u}{u_\infty}\right) dy$$

$$\delta_1 = \int_0^\delta \left[1 - \sin\left(\frac{\pi}{2}.\frac{y}{\delta}\right)\right] dy$$

$$\delta_1 = \left[y + \frac{\cos\left(\frac{\pi}{2}.\frac{y}{\delta}\right)}{\frac{\pi}{2\delta}} \right]_0^\delta$$

$$\delta_1 = (\delta + 0) - \left(0 + \frac{2\delta}{\pi}\right) \quad \Rightarrow \quad \delta_1 = \left(1 - \frac{2}{\pi}\right)\delta = 0.3633\delta$$

The momentum thickness is

$$\delta_2 = \int_0^\delta \frac{u}{u_\infty}\left(1 - \frac{u}{u_\infty}\right) dy$$

$$\delta_2 = \int_0^\delta \sin\left(\frac{\pi}{2}.\frac{y}{\delta}\right)\left[1 - \sin\left(\frac{\pi}{2}.\frac{y}{\delta}\right)\right] dy$$

$$\delta_2 = \int_0^\delta \left[\sin\left(\frac{\pi}{2}.\frac{y}{\delta}\right) - \sin^2\left(\frac{\pi}{2}.\frac{y}{\delta}\right)\right] dy \quad \Rightarrow \quad \delta_2 = 0.1366\delta$$

The energy thickness is

$$\delta_3 = \int_0^\delta \frac{u}{u_\infty}\left(1-\frac{u^2}{u_\infty^2}\right)dy$$

$$\delta_3 = \int_0^\delta \sin\left(\frac{\pi}{2}.\frac{y}{\delta}\right)\left[1-\sin^2\left(\frac{\pi}{2}.\frac{y}{\delta}\right)\right]dy \quad \Rightarrow \quad \delta_3 = 0.2122\delta$$

5.3 BOUNDARY LAYER EQUATIONS

To develop the governing equations for the boundary layer flow over a flat plate shown in Fig. 5.6, the order of magnitude technique has been applied to the *Navier–Stokes* (N–S) equation. According to this technique, the insignificant terms (i.e., the terms with negligible order of magnitude) are dropped and the governing equations are evolved.

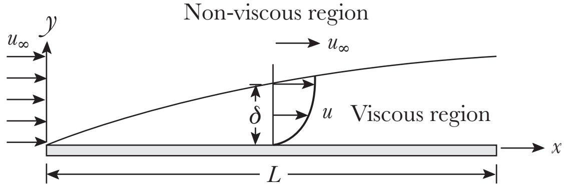

Fig. 5.6 Boundary layer over a flat plate

In this section, the governing equations for the boundary layer flow have been developed for steady and incompressible two-dimensional (2-D) flow.

The *continuity equation* for steady incompressible 2-D flow in differential form is

$$\frac{\partial u}{\partial x}+\frac{\partial v}{\partial y}=0 \quad \text{or} \quad \vec{\nabla}.\vec{V}=0 \tag{5.13}$$

The *N–S equation* for steady incompressible 2-D flow:

$$\frac{D\vec{V}}{Dt}=\vec{g}-\frac{\vec{\nabla}p}{\rho}+\upsilon\nabla^2\vec{V}+\frac{1}{3}\upsilon\vec{\nabla}(\underbrace{\cancel{\vec{\nabla}.\vec{V}}}_{0}) \tag{5.14}$$

x-direction N–S equation:

$$u\frac{\partial u}{\partial x}+v\frac{\partial u}{\partial y}=-\frac{1}{\rho}\frac{\partial p}{\partial x}+\upsilon\left(\frac{\partial^2 u}{\partial x^2}+\frac{\partial^2 u}{\partial y^2}\right) \tag{5.15}$$

y-direction N–S equation:

$$u\frac{\partial v}{\partial x}+v\frac{\partial v}{\partial y}=-\frac{1}{\rho}\frac{\partial p}{\partial y}+\upsilon\left(\frac{\partial^2 v}{\partial x^2}+\frac{\partial^2 v}{\partial y^2}\right) \tag{5.16}$$

Equation (5.16) does not contain gravity term because the flow is taking place in horizontal direction (or the potential head is same all along the *x*-axis).

The first step in the order of magnitude technique is to non-dimensionalize the parameters in the following manner:

$$x_* = \frac{x}{L} \quad y_* = \frac{y}{L} \quad u_* = \frac{u}{u_\infty} \quad v_* = \frac{v}{u_\infty} \quad p_* = \frac{p}{\rho u_\infty^2} \tag{5.17}$$

Rewriting *continuity equation* in non-dimensional form:

$$\frac{\partial(u_* u_\infty)}{\partial(x_* L)} + \frac{\partial(v_* u_\infty)}{\partial(y_* L)} = 0 \quad \Rightarrow \quad \frac{\partial u_*}{\partial x_*} + \frac{\partial v_*}{\partial y_*} = 0 \tag{5.18}$$

Similarly, rewriting *N–S equations* in non-dimensional form:

$$u_* \frac{\partial u_*}{\partial x_*} + v_* \frac{\partial u_*}{\partial y_*} = -\frac{\partial p_*}{\partial x_*} + \frac{1}{\mathrm{Re}}\left(\frac{\partial^2 u_*}{\partial x_*^2} + \frac{\partial^2 u_*}{\partial y_*^2}\right) \tag{5.19}$$

$$u_* \frac{\partial v_*}{\partial x_*} + v_* \frac{\partial v_*}{\partial y_*} = -\frac{\partial p_*}{\partial y_*} + \frac{1}{\mathrm{Re}}\left(\frac{\partial^2 v_*}{\partial x_*^2} + \frac{\partial^2 v_*}{\partial y_*^2}\right) \tag{5.20}$$

As a second step, the order of magnitude for non-dimensional variables is to be computed. The order of magnitude of non-dimensional parameters, as defined in Eq. (5.17), has been shown in Table 5.1.

Table 5.1 Order of parameters

Variable	**Maximum value**	**Non-dimensional variable**	**Order**
u	u_∞	u_*	1
x	L	x_*	1
y	δ	y_*	$\in (= \delta/L) << 1$

For the other unknown terms the order of magnitude is obtained as follows:

Applying the order of magnitude approach to the non-dimensional governing equations:

$$\frac{\partial u_*}{\partial x_*} + \frac{\partial v_*}{\partial y_*} = 0 \quad \Rightarrow \quad \frac{(1)}{(1)} + \frac{v_*}{(\in)} = 0 \quad \Rightarrow \quad \frac{(1)}{(1)} + \frac{v_*}{(\in)} = 0$$

$$\Rightarrow \quad v_* \approx O(\in) \tag{5.21}$$

The order of magnitude for y-direction velocity component, v, is insignificant as compared to x-direction velocity component, u.

Applying the order of magnitude approach to x-direction N–S equations:

$$u_* \frac{\partial u_*}{\partial x_*} + v_* \frac{\partial u_*}{\partial y_*} = -\frac{\partial p_*}{\partial x_*} + \frac{1}{\mathrm{Re}}\left(\frac{\partial^2 u_*}{\partial x_*^2} + \frac{\partial^2 u_*}{\partial y_*^2}\right)$$

$$\Rightarrow \quad (1)\frac{(1)}{(1)} + (\in)\frac{(1)}{(\in)} = -\frac{\partial p_*}{\partial x_*} + \frac{1}{\mathrm{Re}}\left[\frac{(1)}{(1)^2} + \frac{(1)}{(\in)^2}\right] \tag{5.22}$$

Following are the conclusions:

1. $\dfrac{\partial^2 u_*}{\partial y_*^2} >> \dfrac{\partial^2 u_*}{\partial x_*^2}$ and hence $\dfrac{\partial^2 u_*}{\partial x_*^2} + \dfrac{\partial^2 u_*}{\partial y_*^2} \approx \dfrac{\partial^2 u_*}{\partial y_*^2}$
2. The terms in Eq. (5.22) must have the same order on LHS and RHS, that is, $O(1)$. The order of $-\dfrac{\partial p_*}{\partial x_*} \approx O(1)$ and $\dfrac{1}{\mathrm{Re}} \approx O(\in)^2$

Equation (5.19) can be written as

$$u_* \frac{\partial u_*}{\partial x_*} + v_* \frac{\partial u_*}{\partial y_*} = -\frac{\partial p_*}{\partial x_*} + \frac{1}{\mathrm{Re}}\frac{\partial^2 u_*}{\partial y_*^2} \tag{5.23}$$

Application of order of magnitude approach to y-direction N–S equations gives:

$$u_* \frac{\partial v_*}{\partial x_*} + v_* \frac{\partial v_*}{\partial y_*} = -\frac{\partial p_*}{\partial y_*} + \frac{1}{\mathrm{Re}}\left(\frac{\partial^2 v_*}{\partial x_*^2} + \frac{\partial^2 v_*}{\partial y_*^2}\right)$$

$$\Rightarrow \quad (1)\frac{(\in)}{(1)} + (\in)\frac{(\in)}{(\in)} = -\frac{\partial p_*}{\partial y_*} + (\in)^2\left[\frac{(\in)}{(1)^2} + \frac{(\in)}{(\in)^2}\right] \tag{5.24}$$

All the terms in y-direction momentum equation are insignificant as they are of the order of $\in$, which is very small. It can be further concluded that the order of pressure gradient in y-direction is $\in$, that is, $-\dfrac{\partial p_*}{\partial y_*} \approx O(\in)$. This means $\dfrac{\partial p}{\partial y}$ is negligibly small.

$$p \neq p(y) \quad \Rightarrow \quad p = p(x) \quad \Rightarrow \quad \frac{\partial p}{\partial x} = \frac{dp}{dx}$$

Further, as $y \to \delta, u \to u_\infty$, in the inviscid region above the boundary layer, one can apply the Bernoulli's equation comfortably, that is,

$$p + \rho\frac{u_\infty^2}{2} = \text{constant} \quad \Rightarrow \quad -\frac{1}{\rho}\frac{dp}{dx} = u_\infty \frac{du_\infty}{dx} \tag{5.25}$$

For the flow over flat plate, the free stream velocity will be constant throughout the length of the plate. Hence, the pressure gradient in x-direction is zero.

$$\frac{dp}{dx} = 0 \tag{5.26}$$

Equation (5.23) can be reduced to

$$u_* \frac{\partial u_*}{\partial x_*} + v_* \frac{\partial u_*}{\partial y_*} = \frac{1}{\mathrm{Re}} \frac{\partial^2 u_*}{\partial y_*^2} \tag{5.27}$$

The *Prandtl boundary layer* equations for curved as well as flat surfaces are summarized in Table 5.2.

Table 5.2 Prandtl boundary layer equations

Non-dimensional form	**Dimensional form**	**Applicability**
$\frac{\partial u_*}{\partial x_*} + \frac{\partial v_*}{\partial y_*} = 0$	$\frac{\partial u}{\partial x} + \frac{\partial v}{\partial y} = 0$	For both flat and curved surfaces
$u_* \frac{\partial u_*}{\partial x_*} + v_* \frac{\partial u_*}{\partial y_*} = -\frac{dp_*}{dx_*} + \frac{1}{\mathrm{Re}} \frac{\partial^2 u_*}{\partial y_*^2}$	$u \frac{\partial u}{\partial x} + v \frac{\partial u}{\partial y} = -\frac{1}{\rho} \frac{dp}{dx} + \upsilon \frac{\partial^2 u}{\partial y^2}$	For curved surface
$u_* \frac{\partial u_*}{\partial x_*} + v_* \frac{\partial u_*}{\partial y_*} = \frac{1}{\mathrm{Re}} \frac{\partial^2 u_*}{\partial y_*^2}$	$u \frac{\partial u}{\partial x} + v \frac{\partial u}{\partial y} = \upsilon \frac{\partial^2 u}{\partial y^2}$	For flat surface

5.4 NEAR-EXACT SOLUTION—BLASIUS SOLUTION FOR LAMINAR BOUNDARY LAYER FLOW OVER FLAT PLATE

The solutions presented for few viscous flow problems in Section 4.3 of Chapter 4 were obtained analytically and are generally referred to as the exact solutions. These solutions are exact because they have no error. It should be remembered that, it is always desirable to have an analytical or exact solution for a given problem. However, exact solutions are hardly achievable for complex flow problems. In such a scenario, the solution is obtained using the appropriate numerical techniques.

The near-exact solution to the boundary layer equation for the flow over flat plate was given by German fluid dynamics engineer, *Paul Richard Heinrich Blasius* (1883–1970 AD), a doctoral student of *Ludwig Prandtl*. The solution methodology by Blasius involves the conversion of governing boundary layer partial differential equations (PDEs) into the ordinary differential equation (ODE) using certain similarity considerations. The ODE obtained is a third-order non-linear differential equation, which cannot be solved analytically.

Using *Runge–Kutta* order 4 (RK-4) numerical technique, the solution with a high degree of accuracy is obtained. The solution is termed as near-exact solution as the PDEs are first converted to ODEs. Thereby avoiding the loss of accuracy that would have appeared if the PDEs were solved directly using a finite difference scheme (a popular numerical technique discussed in Chapter 1).

Rewriting the governing equations, that is, the boundary layer equations:

Governing Equations

$$\frac{\partial u}{\partial x}+\frac{\partial v}{\partial y}=0 \tag{5.28}$$

$$u\frac{\partial u}{\partial x}+v\frac{\partial u}{\partial y}=\upsilon\frac{\partial^2 u}{\partial y^2} \tag{5.29}$$

Boundary Conditions

From no slip condition, the velocity at the plate surface is zero and at an infinite distance from the plate surface, the velocity is equal to free stream velocity, that is,

$$\left.\begin{array}{lll} u=0 & \text{at} & y=0 \\ u=u_\infty & \text{at} & y=\infty \end{array}\right\} \tag{5.30}$$

Blasius proposed the Prandtl boundary layer equation, given by Eq. (5.29), that is a PDE needs to be converted into an ODE before finding its solution. It will be seen later that the resulting ODE is a third-order, non-linear differential equation, whose analytical solution is not possible. A numerical technique known as RK-4 is used to find out the solution of resulting ODE. The RK-4 method is a well-known numerical method for finding out solution of a non-linear ODE with high degree of accuracy.

The Blasius analysis is based on the idea that the velocity profiles at all locations from the leading edge are similar, as shown in Fig. 5.7. The velocity profiles differ by scaling factors in y and u. These velocity profiles can be made congruent on a coordinate system, which can be non-dimensionalized with respect to the scaling factors (also known as similarity parameters).

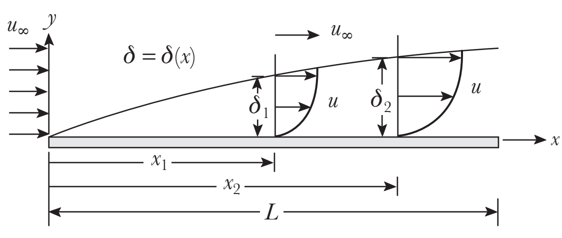

Fig. 5.7 Similarity in velocity profiles at different *x*'s

The similarity parameter or scaling factor in y is defined by

$$\eta = \frac{y}{\delta} \tag{5.31}$$

It can be easily understood that higher the fluid viscosity, thicker is the boundary layer. In addition, higher the free stream velocity, thinner will be the boundary layer. This has the basis from experimental observations. The boundary layer is zero at the leading and maximum at the trailing edge. Therefore, the *Stokes* solution relates the boundary layer thickness with distance from the leading edge, kinematic viscosity, and the free stream velocity, that is,

$$\delta \sim \sqrt{\upsilon x / u_\infty}$$

Therefore, the similarity parameter in y reduces to

$$\eta = y\sqrt{\frac{u_\infty}{\upsilon x}} \tag{5.32}$$

Similarly, the similarity parameter or scaling factor in u is defined by

$$g(\eta) = \frac{u}{u_\infty} \tag{5.33}$$

From the definition of stream function, we get

$$\psi = \int u dy \quad \Rightarrow \quad \psi = \int u_\infty g(\eta)\sqrt{\frac{\upsilon x}{u_\infty}} d\eta \quad \Rightarrow \quad \psi = \sqrt{u_\infty \upsilon x}\int g(\eta) d\eta \tag{5.34}$$

The integral of $g(\eta)$ will be another function of η, that is, $\int g(\eta) d\eta = f(\eta)$

$$\psi = f(\eta)\sqrt{u_\infty \upsilon x} \tag{5.35}$$

Again from the definition of stream function, the velocity component in x-direction is

$$u = \frac{\partial \psi}{\partial y} = \frac{\partial \psi}{\partial \eta}\frac{\partial \eta}{\partial y} \quad \Rightarrow \quad u = \left[\sqrt{u_\infty \upsilon x} f'(\eta)\right]\left(\sqrt{\frac{u_\infty}{\upsilon x}}\right)$$

$$\Rightarrow \quad u = u_\infty f'(\eta) \tag{5.36}$$

$$\frac{\partial u}{\partial x} = u_\infty f''(\eta)\frac{\partial \eta}{\partial x} \quad \Rightarrow \quad \frac{\partial u}{\partial x} = -u_\infty f''(\eta)\frac{\eta}{2x} \tag{5.37}$$

and the velocity component in y-direction is

$$v = -\frac{\partial \psi}{\partial x} \quad \Rightarrow \quad v = -\left(\sqrt{u_\infty \upsilon x}\frac{\partial f}{\partial x} + \frac{1}{2} f\sqrt{\frac{\upsilon u_\infty}{x}}\right)$$

where, $$\frac{\partial f}{\partial x} = \frac{\partial f}{\partial \eta}\frac{\partial \eta}{\partial x} = -f'\frac{\eta}{2x} \Rightarrow v = -\frac{1}{2}\sqrt{\frac{\upsilon u_\infty}{x}}(f - \eta f') \tag{5.38}$$

$$\frac{\partial u}{\partial y} = \frac{\partial}{\partial y}(u_\infty f'(\eta)) \Rightarrow \frac{\partial u}{\partial y} = u_\infty\sqrt{\frac{u_\infty}{\upsilon x}}f''(\eta) \tag{5.39}$$

$$\frac{\partial^2 u}{\partial y^2} = \frac{\partial}{\partial y}\left(u_\infty\sqrt{\frac{u_\infty}{\upsilon x}}f''(\eta)\right) \Rightarrow \frac{\partial^2 u}{\partial y^2} = \frac{u_\infty^2}{\upsilon x}f''' \tag{5.40}$$

Substituting these terms in Eq. (5.29), we get:

$$(u_\infty f')\left(-u_\infty f''\frac{\eta}{2x}\right) + \left(-\frac{1}{2}\sqrt{\frac{\upsilon u_\infty}{x}}(f - \eta f')\right)\left(u_\infty\sqrt{\frac{u_\infty}{\upsilon x}}f''(\eta)\right)$$
$$= \upsilon\frac{u_\infty^2}{\upsilon x}f''' \tag{5.41}$$

On simplification, we get

$$2f''' + ff'' = 0 \tag{5.42}$$

Equation (5.42) is known as *Blasius Equation*. This equation is a non-linear ODE.

The boundary conditions in terms of similarity parameters are given as

$$\left.\begin{array}{lll} u = 0 & \text{at} & y = 0 \\ u = u_\infty & \text{at} & y = \infty \end{array}\right\} \Rightarrow \left.\begin{array}{lll} f' = 0 & \text{at} & \eta = 0 \\ f' = 1 & \text{at} & \eta = \infty \end{array}\right\} \tag{5.43}$$

The analytical solution of *Blasius equation* is not possible. The solution is obtained by RK-4 numerical technique. In fact, this is the reason why the solution is called near-exact solution. For pure numerical solution of the boundary layer equation, a PDE can be solved without converting it to ODE. However, in that case, the accuracy will be less as compared to the present case due to the involvement of more parameters. The results obtained by solving Blasius equation using RK-4 technique are shown in Fig. 5.8 and Table 5.3.

As per the definition, boundary layer thickness is the distance above the plate where the velocity reaches 99% of free stream velocity, for $\eta = 5$, $u/u_\infty = 0.9915$. Therefore, the boundary layer thickness is given by

$$5 = \delta\sqrt{\frac{u_\infty}{\upsilon x}} \Rightarrow \delta = 5\sqrt{\frac{\upsilon x}{u_\infty}} \Rightarrow \delta = \frac{5x}{\sqrt{\mathrm{Re}_x}} \tag{5.44}$$

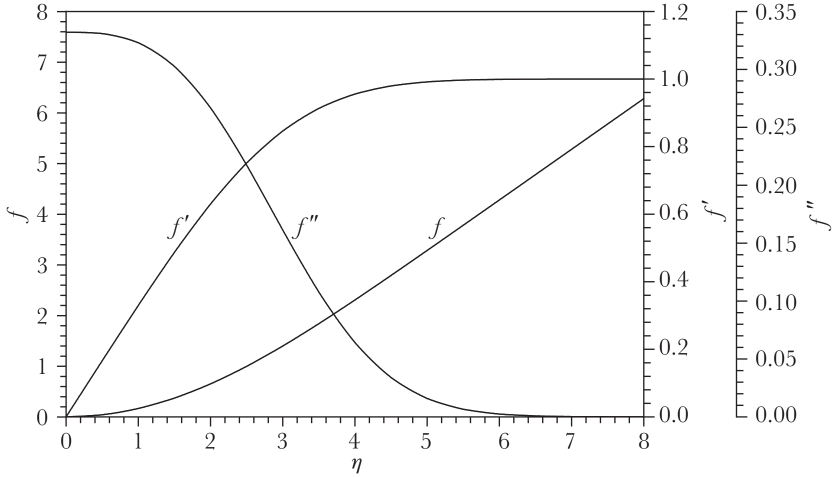

Fig. 5.8 Solution of Blasius equation

Table 5.3 Results of numerical solution

η	f	$f' = \frac{u}{u_\infty}$	f''
0	0	0	0.3321
1	0.1656	0.3298	0.323
2	0.65	0.6298	0.2668
3	1.3968	0.846	0.1614
4	2.3057	0.9555	0.0642
5	3.2833	0.9915	0.0159
6	4.2796	0.999	0.0024
7	5.2792	0.9999	0.0002
8	6.2792	1	0

The local coefficient of skin friction is

$$C_f = \frac{\tau_w}{\left(1/2\rho u_\infty^2\right)} = \frac{\mu\left[\partial u/\partial y\right]_{y=o}}{\left(1/2\rho u_\infty^2\right)} \tag{5.45}$$

$$\Rightarrow \quad C_f = \frac{\mu u_\infty \sqrt{\dfrac{u_\infty}{\upsilon x}} f''(0)}{\left(1/2\rho u_\infty^2\right)} \quad \Rightarrow \quad \boxed{C_{f,x} = \frac{0.664}{\sqrt{\mathrm{Re}_x}}} \tag{5.46}$$

Equation (5.46) is used to calculate the local value of skin friction coefficient at any distance x from the leading edge. The local skin friction coefficient decreases along the plate in the direction of flow. At the leading edge, the local skin friction coefficient is theoretically infinite. For the computation of drag experienced by the plate, an average value of skin friction coefficient is used, which is obtained as

$$\overline{C_f} = \frac{\int_0^L C_{f,x}\,dx}{\int_0^L dx} \Rightarrow \boxed{\overline{C_f} = 2C_f\Big|_{x=L} = \frac{1.328}{\sqrt{\mathrm{Re}_L}}} \tag{5.47}$$

The drag force experienced by the plate is given by

$$D = \tau_w A \Rightarrow \boxed{D = \frac{1}{2}\rho u_\infty^2 \overline{C_f} A} \tag{5.48}$$

where A is the area of plate in contact with the fluid.

Example 5.2 Use numerical solution to determine the velocity components in x- and y-directions for the flow of air at 10 m/s over 2 m long flat plate at $x = 0.4$ m and $\eta = 4$. Take kinematic viscosity of air to be $1.5 \times 10^{-5}\,\mathrm{m^2/s}$.

Solution: The velocity component in x-direction is given by

$$\frac{u}{u_\infty} = f' \Rightarrow u = u_\infty f'(\eta)$$

which can be evaluated directly from Table 5.3.

$$u\big|_{\eta=4} = 10 \times f'(4) \Rightarrow u\big|_{\eta=4} = 10 \times 0.9555 \Rightarrow u\big|_{\eta=4} = 9.555\,\mathrm{m/s}$$

The velocity component in y-direction is given by Eq. (5.38)

$$v = -\frac{1}{2}\sqrt{\frac{\upsilon u_\infty}{x}}(f - \eta f') \Rightarrow v = \frac{1}{2}\sqrt{\frac{\upsilon u_\infty}{x}}(\eta f' - f)$$

Using Table 5.3, we get

$$v\big|_{\eta=4} = \frac{1}{2}\sqrt{\frac{1.5\times 10^{-5}\times 10}{0.5}}(4\times 0.9555 - 2.3057) \Rightarrow v_{\eta=4} = 0.01313\,\mathrm{m/s}$$

Example 5.3 Use numerical solution for the boundary layer flow over flat plate to compute the ratio of displacement thickness to the boundary layer thickness for (a) $\eta = 5$, (b) $\eta = 6$, (c) $\eta \to \infty$.

Solution: The displacement thickness, by definition is

$$\delta_1 = \int_0^\infty \left(1 - \frac{u}{u_\infty}\right) dy$$

Since, $\eta = \dfrac{y}{\delta}$, that is $\eta = y\sqrt{\dfrac{u_\infty}{\upsilon x}} \Rightarrow dy = \sqrt{\dfrac{\upsilon x}{u_\infty}} d\eta$ and $\dfrac{u}{u_\infty} = \dfrac{df}{d\eta} = f'$. The displacement thickness in terms of η is given as

$$\delta_1 = \sqrt{\frac{\upsilon x}{u_\infty}} \int_0^{\eta_{max}} (1 - f')d\eta \tag{1}$$

From Eq. (5.44), we get

$$\sqrt{\frac{\upsilon x}{u_\infty}} = \frac{\delta}{5} \tag{2}$$

From Eqs (1) and (2), the ratio of displacement thickness to boundary layer is given by

$$\frac{\delta_1}{\delta} = \frac{1}{5}\int_0^{\eta_{max}} (1 - f')d\eta \;\Rightarrow\; \frac{\delta_1}{\delta} = \frac{1}{5}(\eta - f)_0^{\eta_{max}} \;\Rightarrow\; \frac{\delta_1}{\delta} = \frac{1}{5}\left(\eta_{max} - f(\eta_{max})\right) \tag{3}$$

Using Table 5.3 and Eq. (3) to compute the required ratio for given η_{max}, we get

(a) $\eta = 5$

$$\left.\frac{\delta_1}{\delta}\right|_{\eta=5} = \frac{1}{5}(5 - 3.2833) \;\Rightarrow\; \left.\frac{\delta_1}{\delta}\right|_{\eta=5} = 0.34334$$

(b) $\eta = 6$

$$\left.\frac{\delta_1}{\delta}\right|_{\eta=6} = \frac{1}{5}(6 - 4.2796) \;\Rightarrow\; \left.\frac{\delta_1}{\delta}\right|_{\eta=6} = 0.344$$

(c) For $\eta \to \infty$, the velocity reaches free stream velocity at $\eta = 8$. Hence, the ratio of displacement thickness to boundary layer thickness will be the same for $\eta \geq 8$:

$$\left.\frac{\delta_1}{\delta}\right|_{\eta\to\infty} = \frac{1}{5}(8 - 6.7292) \;\Rightarrow\; \left.\frac{\delta_1}{\delta}\right|_{\eta=5} = 0.34416$$

It can be concluded that the variation in the ratio of displacement thickness to boundary layer keeps on reducing as η varies from 5 to infinity.

Example 5.4 Use numerical solution to determine the slope of streamline passing through a point at $x = 0.1$ m from the leading edge of the flat plate and the flow velocity is 84.6% of free stream velocity. If the free stream velocity of air is 5 m/s, determine the distance of the point from the plate surface. Take kinematic viscosity of air to be 1.5×10^{-5} m²/s.

Solution:

Given: $\dfrac{u}{u_\infty} = 0.846; \quad x = 0.1\,\text{m}; \quad u_\infty = 5\,\text{m/s}.$

From Table 5.3

$$\text{Corresponding to } \frac{u}{u_\infty} = 0.846 \quad \Rightarrow \quad \eta = 3$$

The distance from the plate surface at which the velocity is 84.6% of free stream velocity can be determined from the following

$$\eta = y\sqrt{\frac{u_\infty}{\upsilon x}} \quad \Rightarrow \quad y = \eta\sqrt{\frac{\upsilon x}{u_\infty}} \quad \Rightarrow \quad y = 3\sqrt{\frac{1.5\times10^{-5}\times0.1}{5}} \quad \Rightarrow \quad y = 1.643\,\text{mm}$$

The velocity component in y-direction is

$$v = \frac{1}{2}\sqrt{\frac{\upsilon u_\infty}{x}}(\eta f' - f) \quad \Rightarrow \quad v = \frac{1}{2}\sqrt{\frac{1.5\times10^{-5}\times5}{0.1}}(3\times0.846-1.3968)$$

$$\Rightarrow \quad v = 0.0156\,\text{m/s}$$

The velocity component in x-direction is

$$\frac{u}{u_\infty} = 0.846 \quad \Rightarrow \quad u = 0.846\times5 \quad \Rightarrow \quad u = 4.23\,\text{m/s}$$

Slope of the streamline passing through (0.1, 0.001643) is

$$\frac{dy}{dx} = \frac{v}{u} \quad \Rightarrow \quad \frac{dy}{dx} = \frac{0.0156}{4.23} \quad \Rightarrow \quad \frac{dy}{dx} = 3.688\times10^{-3}$$

5.5 APPROXIMATE SOLUTION—VON KARMAN MOMENTUM INTEGRAL EQUATION

In Section 5.4, a near-exact solution for the flat plate laminar boundary layer problem has been obtained. Another method for obtaining an approximate solution for the same problem was proposed by Hungarian–American aerospace engineer *Theodore von Karman* (1881–1963 AD), another doctoral student of *Ludwig Prandtl*. In this approach, the differential boundary layer momentum equation is first converted to momentum integral equation. The velocity profile is assumed as some function of y and then boundary layer thickness is calculated by substituting assumed velocity profile expression in the integral momentum equation. The accuracy of this approximate solution is compared with that of Blasius solution (see Fig. 5.9).

The governing equations for boundary layer flow over flat plate are

$$\frac{\partial u}{\partial x} + \frac{\partial v}{\partial y} = 0 \tag{5.49}$$

$$u\frac{\partial u}{\partial x}+v\frac{\partial u}{\partial y}=\upsilon\frac{\partial^2 u}{\partial y^2} \tag{5.50}$$

Integrating within Eq. (5.50) with respect to y within the boundary layer, we get

$$\underbrace{\int_0^\delta u\frac{\partial u}{\partial x}dy}_{\text{I-term}}+\underbrace{\int_0^\delta v\frac{\partial u}{\partial y}dy}_{\text{II-term}}=\underbrace{\int_0^\delta \upsilon\frac{\partial^2 u}{\partial y^2}dy}_{\text{III-term}} \tag{5.51}$$

II-Term

$$\int_0^\delta v\frac{\partial u}{\partial y}dy$$

Consider the following integral:

$$\int_0^\delta \frac{\partial}{\partial y}(vu)dy=\int_0^\delta v\frac{\partial u}{\partial y}dy+\int_0^\delta u\frac{\partial v}{\partial y}dy \tag{5.52}$$

$$[vu]_0^\delta=\int_0^\delta v\frac{\partial u}{\partial y}dy-\int_0^\delta u\frac{\partial u}{\partial x}dy \tag{5.53}$$

In Eq. (5.53) $\frac{\partial v}{\partial y}$ is replaced by $-\frac{\partial u}{\partial x}$ from continuity equation, that is, Eq. (5.49).

Further, from *no slip* condition, the velocities at the surface are zero, that is, at $y = 0$, $u = v = 0$. II-term can be obtained from Eq. (5.53)

$$\int_0^\delta v\frac{\partial u}{\partial y}dy=u_\infty v\big|_{y=\delta}+\int_0^\delta u\frac{\partial u}{\partial x}dy \tag{5.54}$$

To evaluate $v\big|_{y=\delta}$, integrating the continuity equation, the velocity component in y-direction can be expressed as

$$v\big|_{y=\delta}=-\int_0^\delta \frac{\partial u}{\partial x}dy \tag{5.55}$$

Therefore, II-term finally can be written as

$$\int_0^\delta v\frac{\partial u}{\partial y}dy=-u_\infty\int_0^\delta \frac{\partial u}{\partial x}dy+\int_0^\delta u\frac{\partial u}{\partial x}dy \tag{5.56}$$

III-Term

$$\int_0^\delta \upsilon \frac{\partial^2 u}{\partial y^2} dy = \upsilon \int_0^\delta \frac{\partial^2 u}{\partial y^2} dy = \upsilon \left. \frac{\partial u}{\partial y} \right|_{y=0}^{y=\delta} \tag{5.57}$$

At $y = \delta, u \to u_\infty \Rightarrow \left. \dfrac{\partial u}{\partial y} \right|_{y=\delta} = 0$

$$\int_0^\delta \upsilon \frac{\partial^2 u}{\partial y^2} dy = -\upsilon \left. \frac{\partial u}{\partial y} \right|_{y=0} = -\frac{\tau_w}{\rho} \tag{5.58}$$

Substituting II- and III-terms in Eq. (5.51), we get

$$\int_0^\delta u \frac{\partial u}{\partial x} dy - u_\infty \int_0^\delta \frac{\partial u}{\partial x} dy + \int_0^\delta u \frac{\partial u}{\partial x} dy = -\frac{\tau_w}{\rho} \tag{5.59}$$

$$\int_0^\delta \frac{\partial}{\partial x} \left[u(u_\infty - u) \right] dy = \frac{\tau_w}{\rho} \tag{5.60}$$

$$\frac{\partial}{\partial x} \int_0^\delta \left[u(u_\infty - u) \right] dy = \frac{\tau_w}{\rho} \tag{5.61}$$

The integrand will yield a function of δ, which is a function of x alone. The partial derivative can be suitably replaced by the total derivative. Equation (5.61) can be rewritten as

$$\frac{d}{dx} \int_0^\delta \left[u(u_\infty - u) \right] dy = \frac{\tau_w}{\rho} \tag{5.62}$$

Equation (5.62) is known as *von Karman momentum integral equation*. Dividing this equation throughout by u_∞^2, Eq. (5.62) reduces to

$$\frac{d}{dx} \int_0^\delta \left[\frac{u}{u_\infty} \left(1 - \frac{u}{u_\infty} \right) \right] dy = \frac{\tau_w}{\rho u_\infty^2} \tag{5.63}$$

Equation (5.63) can be expressed in terms of momentum thickness and coefficient of skin friction as

$$\frac{d\delta_2}{dx} = \frac{C_f}{2} \tag{5.64}$$

Equations (5.63) and (5.64) are two other forms of *von Karman momentum integral equation*.

To solve Eq. (5.64), the equation of velocity profile within the boundary layer is needed. As such, the velocity inside the boundary layer is assumed as a cubic polynomial in y:

$$u = c_1 + c_2 y + c_3 y^2 + c_4 y^3 \tag{5.65}$$

Equation (5.65) has four constants; to evaluate these constants at least four boundary conditions are required. Following are the four boundary conditions:

$$\left.\begin{aligned} &u = 0 \quad \text{at} \quad y = 0 \\ &u = u_\infty \quad \text{at} \quad y = \delta \\ &\frac{\partial u}{\partial y} = 0 \quad \text{at} \quad y = \delta \\ &\frac{\partial^2 u}{\partial y^2} = 0 \quad \text{at} \quad y = 0 \end{aligned}\right\} \tag{5.66}$$

The fourth boundary condition is derived from the boundary layer equation, that is, Eq. (5.50) itself. Substituting $u = v = 0$ for $y = 0$ in Eq. (5.66). After applying these boundary conditions, the values of constants obtained are as follows:

$$\left.\begin{aligned} &c_1 = 0 \\ &c_2 = \frac{3}{2}\frac{u_\infty}{\delta} \\ &c_3 = 0 \\ &c_4 = -\frac{1}{2}\frac{u_\infty}{\delta^3} \end{aligned}\right\} \tag{5.67}$$

The velocity profile is, therefore, given by

$$\frac{u}{u_\infty} = \frac{3}{2}\frac{y}{\delta} - \frac{1}{2}\left(\frac{y}{\delta}\right)^3 \tag{5.68}$$

Substituting this velocity profile in *von Karman momentum integral equation*, that is, Eq. (5.63), we get

$$\frac{d}{dx}\int_0^\delta \left\{ \frac{3}{2}\frac{y}{\delta} - \frac{1}{2}\left(\frac{y}{\delta}\right)^3 - \left[\frac{3}{2}\frac{y}{\delta} - \frac{1}{2}\left(\frac{y}{\delta}\right)^3\right]^2 \right\} dy = \frac{\tau_w}{\rho u_\infty^2} = \frac{\upsilon}{u_\infty}\left(\frac{3}{2\delta}\right) \tag{5.69}$$

$$\frac{39}{280}\delta\frac{d\delta}{dx} = \frac{\tau_w}{\rho} = \frac{\upsilon}{u_\infty}\left(\frac{3}{2\delta}\right) \tag{5.70}$$

Integrating Eq. (5.70), we get

$$\frac{\delta^2}{2} = \frac{140}{13}\frac{\upsilon x}{u_\infty} + C \tag{5.71}$$

where, C is the constant of integration, which can be evaluated by applying the boundary condition in x at the leading edge of the flat plate, that is, at $x = 0$, $\delta = 0 \Rightarrow C = 0$.

$$\delta = \sqrt{\frac{280}{13}\frac{\upsilon x}{u_\infty}} \quad \Rightarrow \quad \delta = \frac{4.64x}{\sqrt{\mathrm{Re}_x}} \tag{5.72}$$

The skin friction coefficient is

$$C_f = \frac{\tau_w}{\left(1/2\rho u_\infty^2\right)} = \frac{\mu\left[\partial u/\partial y\right]_{y=o}}{\left(1/2\rho u_\infty^2\right)} \tag{5.73}$$

$$C_f = \frac{0.646}{\sqrt{\mathrm{Re}_x}} \tag{5.74}$$

Equations (5.72) and (5.74) are the approximate solutions for the boundary layer flow over the flat plate. The percentage deviation in the boundary layer thickness and local skin friction coefficient are −7.2% and −2.71%, respectively, compared to the Blasius solution. The choice of velocity profile has a bearing on the accuracy of the solution obtained. However, the von Karman approach is easier to apply.

Example 5.5 Plot $\frac{y}{\delta}$ versus $\frac{u}{u_\infty}$ obtained from near-exact solution of Blasius equation and compare with approximate parabolic, cubic, and sinusoidal velocity profiles.

Solution:

Remember: $y = \delta$ at $\eta = 5$ as $u = 0.9915\ u_\infty$. The data in Table 5.3 is used to plot near-exact velocity profile. Similarly, following equations have been used to draw the approximate velocity profiles in Fig. 5.9:

(a) Parabolic: $\frac{u}{u_\infty} = 2\frac{y}{\delta} - \left(\frac{y}{\delta}\right)^2$

(b) Cubic: $\frac{u}{u_\infty} = \frac{3}{2}\frac{y}{\delta} - \frac{1}{2}\left(\frac{y}{\delta}\right)^3$

(c) Sinusoidal: $\frac{u}{u_\infty} = \sin\left(\frac{\pi}{2}\frac{y}{\delta}\right)$

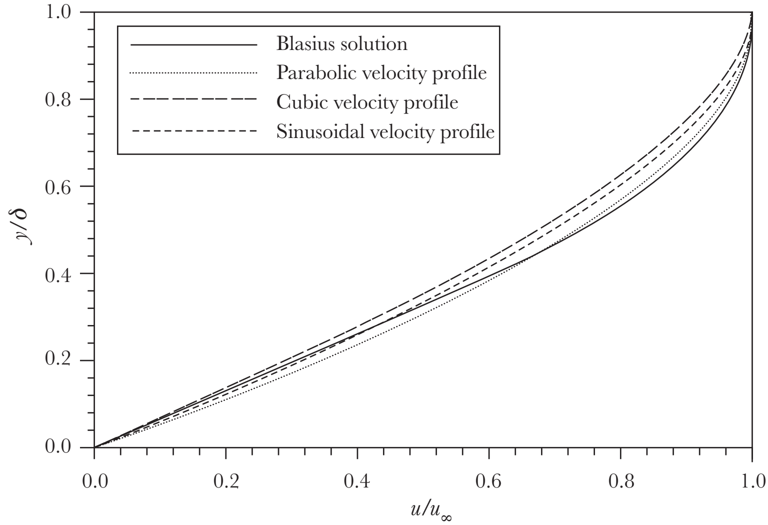

Fig. 5.9

Example 5.6 Determine the boundary layer thickness and local skin friction coefficient for the velocity profiles obtained in Example 5.1.

Solution: The local skin friction coefficient is determined by

$$C_f = \frac{\tau_w}{\left(1/2\rho u_\infty^2\right)} = \frac{\mu\left[\partial u/\partial y\right]_{y=0}}{\left(1/2\rho u_\infty^2\right)}$$

(a) For the velocity profile $\dfrac{u}{u_\infty} = 2\dfrac{y}{\delta} - \left(\dfrac{y}{\delta}\right)^2$

$$\frac{\partial u}{\partial y} = u_\infty\left[\frac{2}{\delta} - \frac{2\,y}{\delta^2}\right] \quad \Rightarrow \quad \left.\frac{\partial u}{\partial y}\right|_{y=0} = \frac{2u_\infty}{\delta}$$

Substituting the velocity profile in *von Karman momentum integral equation*, that is, Eq. (5.62), we get

$$\frac{d}{dx}\int_0^\delta \left\{2\frac{y}{\delta} - \left(\frac{y}{\delta}\right)^2 - \left(2\frac{y}{\delta} - \left(\frac{y}{\delta}\right)^2\right)^2\right\} dy = \frac{\tau_w}{\rho u_\infty^2} = \frac{\mu}{\rho u_\infty}\left(\frac{2}{\delta}\right)$$

Substitute $\dfrac{y}{\delta} = \eta \rightarrow dy = \delta d\eta$ in the aforementioned equation,

$$\frac{d\delta}{dx}\int_0^1 \left[2\eta - \eta^2 - (2\eta - \eta^2)^2\right] d\eta = \frac{2\upsilon}{\delta u_\infty}$$

$$\frac{2}{15}\delta\frac{d\delta}{dx} = \frac{2\upsilon}{u_\infty}$$

Integrating this equation, we get

$$\frac{\delta^2}{2} = 15\frac{\upsilon x}{u_\infty} + \mathrm{C}$$

where, C is the constant of integration, which can be evaluated by applying the boundary condition in x at the leading edge of the flat plate, that is, at $x = 0$, $\delta = 0 \Rightarrow$ C = 0.

$$\delta = \sqrt{30\frac{\upsilon x}{u_\infty}} \quad \Rightarrow \quad \delta = \frac{5.477x}{\sqrt{\mathrm{Re}_x}}$$

The local skin friction coefficient is

$$C_f = \frac{\tau_w}{\left(1/2\rho u_\infty^2\right)} = \frac{\mu\left[\partial u/\partial y\right]_{y=o}}{\left(1/2\rho u_\infty^2\right)}$$

$$C_f = \frac{0.730}{\sqrt{\mathrm{Re}_x}}$$

(b) For the velocity profile $\frac{u}{u_\infty} = \sin\left(\frac{\pi y}{2\delta}\right)$

$$\frac{\partial u}{\partial y} = u_\infty \frac{\pi}{2\delta}\cos\left(\frac{\pi y}{2\delta}\right) \quad \Rightarrow \quad \left.\frac{\partial u}{\partial y}\right|_{y=0} = \frac{\pi u_\infty}{2\delta}$$

Substituting the velocity profile in *von Karman momentum integral equation*, that is, Eq. (5.62), we get

$$\frac{d}{dx}\int_0^\delta \left[\sin\left(\frac{\pi y}{2\delta}\right) - \sin^2\left(\frac{\pi y}{2\delta}\right)\right]dy = \frac{\tau_w}{\rho u_\infty^2} = \frac{\mu}{\rho u_\infty}\left(\frac{\pi}{2\delta}\right)$$

Substitute $\frac{y}{\delta} = \eta \rightarrow dy = \delta d\eta$ in the aforementioned equation

$$\frac{d\delta}{dx}\int_0^1 \left[\sin\left(\frac{\pi\eta}{2}\right) - \sin^2\left(\frac{\pi\eta}{2}\right)\right]d\eta = \frac{\pi\upsilon}{2\delta u_\infty}$$

$$0.1366\delta\frac{d\delta}{dx} = \frac{1.57\upsilon}{u_\infty}$$

Integrating this equation, we get

$$\frac{\delta^2}{2} = 11.5\frac{\upsilon x}{u_\infty} + \mathrm{C}$$

where, C is the constant of integration, which can be evaluated by applying the boundary condition in x at the leading edge of the flat plate, that is, at $x = 0$, $\delta = 0 \Rightarrow$ C = 0.

$$\delta = \sqrt{23\frac{\upsilon x}{u_\infty}} \quad \Rightarrow \quad \delta = \frac{4.796x}{\sqrt{\mathrm{Re}_x}}$$

The local skin friction coefficient is

$$C_f = \frac{\tau_w}{\left(1/2\rho u_\infty^2\right)} = \frac{\mu\left[\partial u/\partial y\right]_{y=0}}{\left(1/2\rho u_\infty^2\right)}$$

$$C_f = \frac{0.655}{\sqrt{\mathrm{Re}_x}}$$

5.6 TURBULENT BOUNDARY LAYER

As soon as the flow turns turbulent on the surface within the boundary layer, an extremely thin viscous region appears at the surface where turbulent fluctuations (disturbances) are damped, shown in Fig. 5.1. This region is called *viscous* (or *laminar*) *sub-layer*. The region is so thin that the velocity profile is assumed linear, as shown in Fig. 5.10.

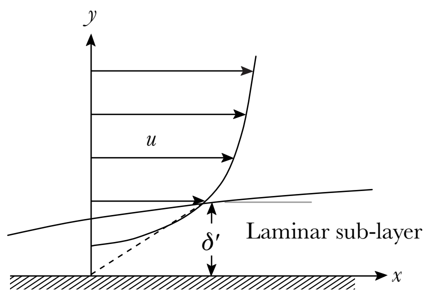

Fig. 5.10 Viscous or laminar sub-layer

$$\left(\frac{\partial u}{\partial y}\right)_{\substack{\text{Viscous}\\\text{sublayer}}} = \text{constant} \tag{5.75}$$

From the experiments, it has been found that the thickness of the viscous sub-layer thickness can be expressed as

$$\delta' = 11.5\upsilon\left(\frac{\tau_w}{\rho}\right)^{-0.5} \tag{5.76}$$

The thickness of the sub-layer depends on the free stream velocity. Higher the free stream velocity, stronger will be the wall shear stress and thinner will be the laminar sub-layer.

For the sake of better understanding, the turbulent boundary layer may be divided into two distinct regions—1 and 2, as shown in Fig. 5.11. Region 1 extends from the surface up to 20% of the total boundary layer thickness and

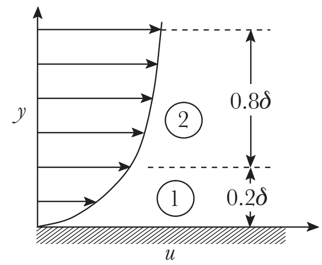

Fig. 5.11 Turbulent boundary layer

remaining is the region 2. Region 1 has the velocity profile represented by viscous sub-layer near the surface, the profile above it, that is, in region 2 may be represented by the power law given by

$$\frac{\overline{u}}{u_\infty} = \left(\frac{y}{\delta}\right)^{\frac{1}{n}} \tag{5.77}$$

To model the turbulent velocity profile, $n = 7$ is usually taken. In fact, this law can be comfortably extended to region 1. Generally, the viscous sub-layer region is very thin, the velocity gradient may be assumed to be infinite. Using Eq. (5.77), the solution to the turbulent boundary layer can be obtained.

Example 5.7 The velocity profile in a turbulent boundary layer is generally 1/7-th of the power law:

$$\frac{u}{u_\infty} = \eta^{1/7} \quad \text{where} \quad \eta = \frac{y}{\delta}$$

Determine the boundary layer thickness and local skin friction coefficient.

Solution: Using von Karman momentum integral equation, we get

$$\frac{d\delta}{dx}\int_0^1 \left[\eta^{1/7}(1-\eta^{1/7})\right]d\eta = \frac{\tau_w}{\rho u_\infty^2}$$

The velocity gradient within the viscous sub-layer is almost infinite; the given profile cannot be used to calculate the wall shear stress. Hence, the shear stress for the flat plate can be obtained from *Laufer's* (1954) analysis for fully developed turbulent flow through pipes,

$$\tau_w = 0.0233\rho u_\infty^2 \left(\frac{\upsilon}{\delta u_\infty}\right)^{1/4}$$

Substituting the shear stress in the momentum integral equation, we get

$$\frac{d\delta}{dx}\int_0^1\left[\eta^{1/7}(1-\eta^{1/7})\right]d\eta = 0.0233\left(\frac{\upsilon}{\delta u_\infty}\right)^{1/4}$$

$$\frac{7}{72}\frac{d\delta}{dx} = 0.0233\left(\frac{\upsilon}{\delta u_\infty}\right)^{1/4}$$

$$\delta^{1/4}\frac{d\delta}{dx} = 0.2397\left(\frac{\upsilon}{u_\infty}\right)^{1/4}$$

Integrating this equation, we get

$$\frac{4}{5}\delta^{5/4} = 0.2397\left(\frac{\upsilon}{u_\infty}\right)^{1/4} x + \mathrm{C}$$

where, C is the constant of integration, which can be evaluated by applying the boundary condition in x at the leading edge of the flat plate, that is, at $x = 0$, $\delta = 0 \Rightarrow \mathrm{C} = 0$.

$$\delta = 0.381\left(\frac{\upsilon}{u_\infty}\right)^{1/5} x^{4/5} \quad \Rightarrow \quad \delta = \frac{0.381x}{\mathrm{Re}_x^{1/5}}$$

The local skin friction coefficient is

$$C_f = \frac{\tau_w}{\left(1/2\rho u_\infty^2\right)}$$

$$C_f = 0.0466\left(\frac{\upsilon}{\delta u_\infty}\right)^{1/4} \quad \Rightarrow \quad C_f = \frac{0.0593}{\mathrm{Re}_x^{1/5}}$$

5.7 BOUNDARY LAYER FLOW OVER CURVED SURFACE

Figure 5.12 shows the boundary layer flow over a curved surface. Unlike flat plate, the free stream velocity does not remain constant above the curved surface and as a result, the pressure gradient (dp/dx) on the curved body

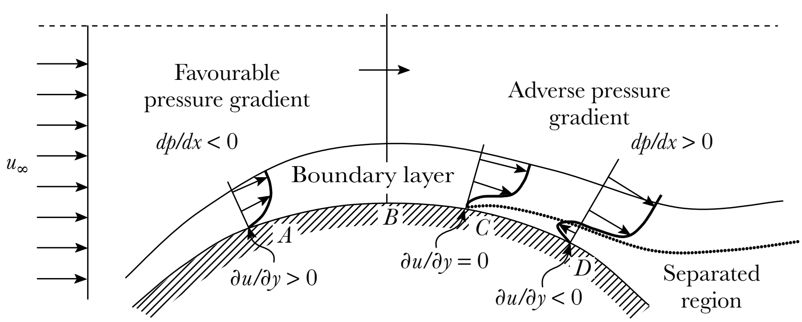

Fig. 5.12 Boundary layer flow over curved surface

is non-zero. On the upstream side of the peak point B on the curved surface, the flow velocity increases owing to the reduction in the area of flow (as per continuity equation). In accordance with Bernoulli's principle, the pressure at the upstream side of point B decreases. In other words, the pressure gradient is negative. Since the fall in pressure is causing an increase in the flow velocity, the *negative* pressure gradient is also termed as *favourable* pressure gradient. Similarly, on the downstream side of peak point B, the area of flow starts increasing in the direction of flow causing the velocity to decrease. The fall in velocity is associated with the rise in pressure in the direction of flow (or pressure gradient is positive).

Since the *positive* pressure gradient is responsible for the retardation of flow, it is also termed as an *adverse* pressure gradient. The magnitude of *adverse* pressure gradient will keep on increasing with the increase in area of flow above the curved surface until a point C on the curved surface is reached, where the flow within the boundary layer gets stopped. At point C, the adverse pressure gradient neutralizes the wall shear, as the velocity gradient at the wall becomes zero. The point C marks the onset of separation of boundary layer and is termed as the *point of separation*. This implies that the condition of boundary layer separation is $\partial u/\partial y\big|_{y=0} = 0$ or $\tau_w = 0$. Beyond point C, the increasing adverse pressure gradient causes the flow within the boundary layer to reverse, as shown at point D in Fig. 5.12.

To demonstrate the effect of pressure gradient on the velocity, its first and second derivatives have been drawn in Fig. 5.12.

Favourable Pressure Gradient ($dp/dx < 0$)

In Fig. 5.13(a), the effect has been shown for favourable pressure gradient, that is, $dp/dx < 0$. The velocity increases parabolically within the boundary layer from zero at the wall to the maximum at the upper edge of the boundary layer. The viscous shear stress is proportional to the first derivative of velocity by Newton's law of viscosity. As a matter of fact, the viscous effects are maximum at the wall and approaches to zero at the upper edge of the boundary layer. Thus, $\partial u/\partial y$ decreases along the y-axis until it approaches zero. The second derivative of velocity can be linked to pressure gradient by substituting no slip condition ($u = v = 0$) in the Prandtl boundary layer equation (dimensional form) for the flow over curved surface in Table 5.2.

$$0 = -\frac{1}{\rho}\frac{dp}{dx} + \upsilon \left.\frac{\partial^2 u}{\partial y^2}\right|_{y=0} \quad \Rightarrow \quad \left.\frac{\partial^2 u}{\partial y^2}\right|_{y=0} = \frac{1}{\mu}\frac{dp}{dx} \tag{5.78}$$

For favourable pressure gradient, that is, $dp/dx < 0$, the second derivative of velocity will be maximum negative at the wall, that is, $\partial^2 u/\partial y^2\big|_{y=0} < 0$.

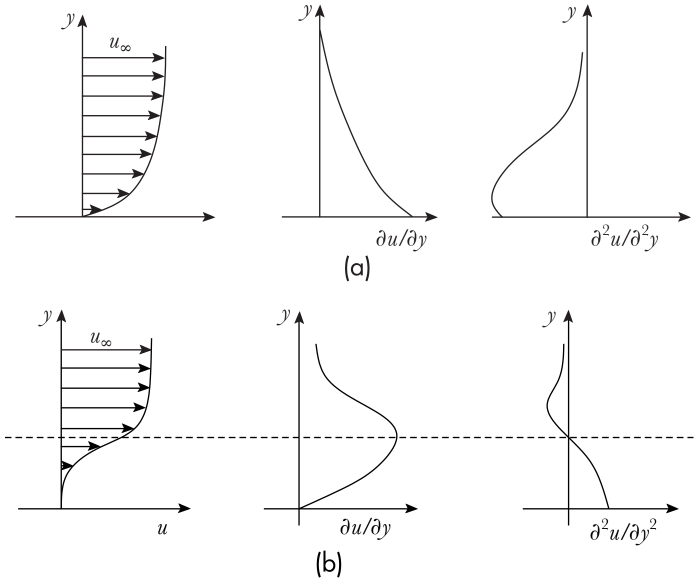

Fig. 5.13 Velocity distribution within the boundary layer (a) Favourable pressure gradient (b) Adverse pressure gradient

Along y-direction, its magnitude reduces and finally approaches zero, that is, $\partial^2 u/\partial^2 y \to 0$.

Adverse Pressure Gradient **(*dp/dx* > 0)**

In Fig. 5.13(b), the effect of adverse pressure gradient, that is, $dp/dx > 0$, on the velocity and its first and second derivatives have been demonstrated. In the presence of adverse pressure gradient, the pressure increases in the direction of flow and thus, it acts as a barrier for the flow. Since the magnitudes of velocities near the wall within boundary layer region are small, the effect of adverse pressure gradient is seen near the wall. The increased pressure in flow direction neutralizes the velocity near the wall and the velocity remains zero up to a little distance from the wall. The velocity beyond this starts increasing and a point is reached when the velocity profile curvature changes its sign, shown by a dashed line in Fig. 5.13(b). This point is known as a *point of inflection* (inflexion). As far as viscous shear stress is concerned, it becomes zero at the wall as the velocity gradient or first derivative of velocity or slope of velocity profile or velocity variation in y-direction at the wall is zero, that is, $\partial u/\partial y = 0$ (a condition of boundary layer separation). The magnitude of shear stress increases along y-direction up to the point of inflexion and beyond that the viscous effects start diminishing until $\partial u/\partial y \to 0$ at the upper edge of the boundary layer. From Eq. (5.78), the adverse pressure

gradient, that is, $dp/dx > 0$ results in $\partial^2 u/\partial y^2\big|_{y=0} > 0$. Near the upper edge of the boundary layer, it has been seen in Fig. 5.12 that $\partial^2 u/\partial y^2\big| < 0$. Thus, it is clear that $\partial^2 u/\partial y^2$ undergoes a change in its sign. This change occurs at the point of inflexion.

The boundary layer equation for the flow over curved surface is given by:

$$u\frac{\partial u}{\partial x} + v\frac{\partial u}{\partial y} = -\frac{1}{\rho}\frac{dp}{dx} + \upsilon\frac{\partial^2 u}{\partial y^2} \tag{5.79}$$

At the edge of the boundary layer, $u \approx u_\infty$ and $\partial u/\partial y = 0 \Rightarrow u \neq u(y) \Rightarrow \partial^2 u/\partial y^2 = 0$, Eq. (5.79) is reduced to

$$u_\infty \frac{du_\infty}{dx} = -\frac{1}{\rho}\frac{dp}{dx} \tag{5.80}$$

From Eqs (5.79) and (5.80), we get

$$u\frac{\partial u}{\partial x} + v\frac{\partial u}{\partial y} = u_\infty\frac{du_\infty}{dx} + \upsilon\frac{\partial^2 u}{\partial y^2} \tag{5.81}$$

At the curved surface, from *no slip* condition $u = v = 0$, Eq. (5.79) reduces to

$$\mu\frac{\partial^2 u}{\partial y^2} = \frac{dp}{dx} \tag{5.82}$$

Integrating Eq. (5.81), we get:

$$\underbrace{\int_0^\delta u\frac{\partial u}{\partial x}dy}_{\text{I-term}} + \underbrace{\int_0^\delta v\frac{\partial u}{\partial y}dy}_{\text{II-term}} = \underbrace{\int_0^\delta u_\infty\frac{du_\infty}{dx}dy}_{\text{III-term}} + \underbrace{\int_0^\delta \upsilon\frac{\partial^2 u}{\partial y^2}dy}_{\text{IV-term}} \tag{5.83}$$

The integral of the third term is not a function of y. The other terms have already been evaluated while deducing the *von Karman* momentum integral equation for the boundary layer flow over flat plate analysis in the Section 5.6.

$$\frac{\tau_w}{\rho} = u_\infty^2\frac{d\delta_2}{dx} + u_\infty\frac{du_\infty}{dx}\delta \tag{5.84}$$

For the flow over curved surface, the free stream velocity does not remain constant as explained before; therefore, Eq. (5.84) takes the following form:

$$\frac{\tau_w}{\rho} = \frac{d\left(u_\infty^2\delta_2\right)}{dx} + u_\infty\frac{du_\infty}{dx}\delta \tag{5.85}$$

Expanding Eq. (5.85), we get:

$$\tau_w = 2u_\infty \rho \delta_2 \frac{du_\infty}{dx} + \rho u_\infty^2 \frac{d\delta_2}{dx} + \rho u_\infty \frac{du_\infty}{dx}\delta \tag{5.86}$$

Multiplying Eq. (5.86) by $\dfrac{2\delta_2}{\mu u_\infty}$, we get

$$\frac{2\delta_2}{\mu u_\infty}\tau_w = \frac{4\delta_2^2}{\upsilon}\frac{du_\infty}{dx} + \frac{2\delta_2 u_\infty}{\upsilon}\frac{d\delta_2}{dx} + \frac{2\delta\delta_2}{\upsilon}\frac{du_\infty}{dx} \tag{5.87}$$

or

$$\frac{2\delta_2}{\mu u_\infty}\tau_w = \frac{4\delta_2^2}{\upsilon}\frac{du_\infty}{dx} + \frac{u_\infty}{\upsilon}\frac{d\delta_2^2}{dx} + \frac{2\delta\delta_2}{\upsilon}\frac{du_\infty}{dx} \tag{5.88}$$

On rearranging, we get

$$\frac{u_\infty}{\upsilon}\frac{d\delta_2^2}{dx} = \frac{2\delta_2}{\mu u_\infty}\tau_w - 2\left(2 + \frac{\delta}{\delta_2}\right)\frac{\delta_2^2}{\upsilon}\frac{du_\infty}{dx} \tag{5.89}$$

The wall shear stress is $\dfrac{\tau_w}{\mu} = \left.\dfrac{\partial u}{\partial y}\right|_{y=0}$ and defining $\dfrac{\delta_2^2}{\upsilon}\dfrac{du_\infty}{dx} = \lambda$, Eq. (5.89) reduces to

$$\frac{u_\infty}{\upsilon}\frac{d\delta_2^2}{dx} = \frac{2\delta_2}{u_\infty}\left.\frac{\partial u}{\partial y}\right|_{y=0} - 2\left(2 + \frac{\delta}{\delta_2}\right)\lambda \tag{5.90}$$

Thwaites proposed an empirical method for laminar boundary layer, which allows Eq. (5.90) to take the following form:

$$\frac{u_\infty}{\upsilon}\frac{d\delta_2^2}{dx} = \mathrm{A} - \mathrm{B}\lambda \tag{5.91}$$

where, A and B are constants whose values were found to be 0.45 and 6, respectively.

$$\frac{u_\infty}{\upsilon}\frac{d\delta_2^2}{dx} + 6\frac{\delta_2^2}{\upsilon}\frac{du_\infty}{dx} = 0.45 \tag{5.92}$$

Multiplying Eq. (5.92) by υu_∞^5

$$u_\infty^6 \frac{d\delta_2^2}{dx} + 6u_\infty^5 \frac{du_\infty}{dx}\delta_2^2 = 0.45\upsilon u_\infty^5 \tag{5.93}$$

Equation (5.93) reduces to the following form

$$\frac{d}{dx}\left(\delta_2^2 u_\infty^6\right) = 0.45\upsilon u_\infty^5 \tag{5.94}$$

Integrating between $x = 0$ and $x = x$, we get

$$\delta_2^2\Big|_{x=0}^{x=x} = \frac{0.45\upsilon}{u_\infty^6}\int_0^x u_\infty^5\,dx \tag{5.95}$$

The momentum thickness at a distance x from the stagnation point of the curved surface is

$$\delta_2^2\Big|_{x=x} = \delta_2^2\Big|_{x=0} + \frac{0.45\upsilon}{u_\infty^6}\int_0^x u_\infty^5\,dx \tag{5.96}$$

The momentum thickness at $x = 0$ (stagnation point) is zero. Therefore, Eq. (5.96) reduces to

$$\delta_2^2\Big|_{x=x} = \frac{0.45\upsilon}{u_\infty^6}\int_0^x u_\infty^5\,dx \tag{5.97}$$

For flat plate, the free stream velocity is constant; the momentum thickness is, thus, given by

$$\delta_2 = \sqrt{\frac{0.45\upsilon x}{u_\infty}} = \frac{0.671x}{\sqrt{\mathrm{Re}_x}} \tag{5.98}$$

For curved surface, the integral on the RHS of Eq. (5.97) can be evaluated numerically for a known value of u_∞. The numerically evaluated value of δ_2 will then help in finding out the wall shear stress from the following empirical relationship:

$$\tau_w = \frac{\mu u_\infty}{\delta_2}(\lambda + 0.082)^{0.62} \tag{5.99}$$

Regardless of the involvement of empirical relations, Thwaites' integral method is still considered the best among different integral boundary layer techniques. At the point of separation, as discussed earlier, the wall shear stress should be zero. From Eq. (5.99), this will happen when $\lambda = -0.082$.

5.8 BOUNDARY LAYER SEPARATION

In Section 5.7, it was seen that the boundary layer does not remain intact in case of fluid flowing over curved bodies. Figure 5.14 shows a comparison of flow over a cylinder for an ideal fluid and that of a real fluid.

For Ideal Fluid

Figure 5.14(a) shows the flow of an ideal fluid over a circular cylinder. When an ideal fluid flows over a curved body (here cylinder) there exists two stagnation points, that is, one on the front (S_1) and another on the rear (S_2). At stagnation

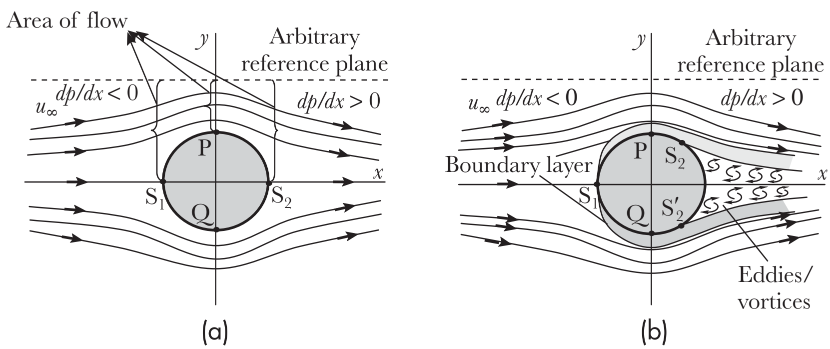

Fig. 5.14 Flow past a cylinder (a) Ideal fluid (b) Real fluid

points, the velocity is zero and the pressure is maximum. The area of flow decreases from maximum at point S_1 to minimum at P or Q from any arbitrary reference plane (shown by dashed line).

The area of flow increases in the same way from point P or Q to stagnation point S_2. From continuity, the velocity will increase from S_1 to P/Q and decrease from P/Q to S_2. In accordance to Bernoulli's principle, the pressure will fall in the front half of the cylinder and the pressure in the rear half of the cylinder rises by an equal amount. Thus, there is a 100% recovery in pressure in the rear half of cylinder. The pressure becomes maximum at point S_2 (same as the pressure at S_1). It should be remembered that there will not be any boundary layer formation when an ideal fluid flows over solid body.

For Real Fluid

Figure 5.14(b) shows the flow of real fluid over the same cylinder for a considerably high free stream Reynolds number. Unlike ideal fluid flow, the flow of real fluid flow will not result in two stagnation points. In fact, there is only one stagnation point at the front, that is, S_1. Due to the formation of boundary layer and its subsequent detachment in the rear half of the cylinder due to the presence of adverse pressure gradient. The recovery of pressure is not 100% in the rear half of the cylinder. The pressure recovery is only partial and takes place only in the regions between point P and point of separation S_2 in the upper half and between point Q and point of separation S'_2 in the lower half of the cylinder. The region between points S_2 and S'_2 is thus a low pressure region known as *wake*. The wake or separated region consists of *eddies* or *vortices*, which are characterized by swirling of fluid and also by the existence of reverse current generated as the fluid flows over an obstacle. Actually, a long chain of vortices known as *von Karman vortex street* is formed in the downstream side of the cylinder. Larger the wake, larger is the pressure difference across the cylinder. If a body is designed in a way that the wake is almost eliminated (i.e., no flow separation), it is

termed as *streamlined body*. The bodies such as cylinder, sphere, or any other body contour where the wake is formed as a result of flow separation are termed as *bluff bodies*. Such bodies are always acted upon by an additional drag due to the difference in pressures across them. This type of drag is known as *pressure* (or *form*) *drag*. The pressure distribution of flow of an ideal and real fluid past a cylinder is shown in Fig. 5.15, (plus sign indicates rise in pressure and minus indicates fall in pressure). The pressure distribution for the flow of an ideal fluid over a cylinder is symmetric (already presented in Chapter 3), whereas the pressure distribution is asymmetric if real fluid flows over a cylinder at relatively higher Reynolds number. Due to the boundary layer separation, a low pressure wake is formed on the downstream side of the cylinder. This inconsistency in the flow of ideal and real fluids is known as *d' Alembert's paradox*.

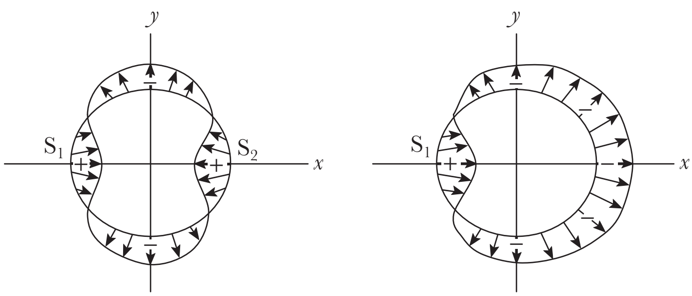

Fig. 5.15 Pressure distribution on cylinder for the flow of (a) Ideal fluid (b) Real fluid

For the flow past a cylinder or sphere, the characteristic dimension used in the computation of Reynolds number is the diameter D, that is,

$$\mathrm{Re} = \frac{u_\infty D}{\upsilon} \tag{5.100}$$

For extremely low velocity flows of real fluids (i.e., Re < 4), the fluid follows the contour of body with no boundary layer separation. The flow pattern would be similar to the one shown in Fig. 5.14(a). The effect of Reynolds number on the flow pattern is shown in Fig. 5.16. With the increase in free stream Re, the adverse pressure gradient created will start increasing. The boundary layer separation takes place. The points of separation move towards the top and bottom of the cylinder. Up to $\mathrm{Re} = 2 \times 10^5$, the boundary layer flow remains laminar and separation occurs at an angle of about 80°. Increasing the Re beyond 2×10^5 would see a transition from laminar to turbulent boundary flow within the boundary layer. The increased inertia causes the flow within the turbulent boundary layer to remain intact with the contour of the cylinder in the downstream side and the separation is delayed. The wake formed is narrower and the separation occurs at an angle of about 140°.

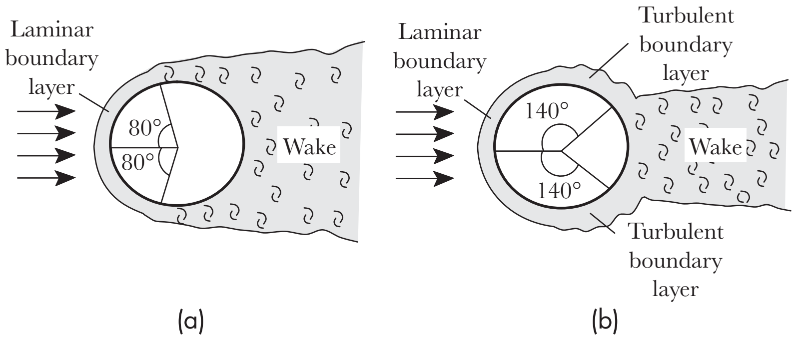

Fig. 5.16 Flow patterns over a circular cylinder (a) Re < 2×10^5 (b) Re > 2×10^5

In some cases, the formation of turbulent boundary is desirable as it helps in the reduction of overall drag. For instance, dimples are provided on the golf ball surface, which make the flow turbulent within the boundary layer. As mentioned earlier, the separation is delayed resulting in a reduced pressure drag. This helps the golf ball to cover longer distances.

It has been observed that the boundary layer separation gives rise to an additional pressure drag. Hence, the separation is not desirable from aerodynamics point of view. Following are the techniques employed to avoid boundary layer separation:

Streamlining Requires the body to be elongated to narrow down the wake region and to minimize the adverse pressure gradient, as shown in Fig. 5.17. It has been observed that the streamlining reduces the drag coefficient by almost 95%.

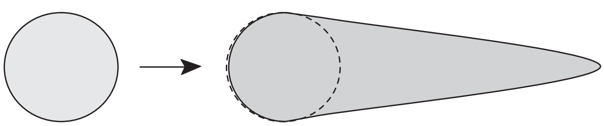

Fig. 5.17 Streamlining of cylindrical body

Fluid injection Requires blowing of the high energy fluid from the surface at the point where separation is expected to occur, as shown in Fig. 5.18. This will increase turbulence which, in turn, would increase skin friction. The magnitude of rise in skin friction drag is negligible in comparison to the reduction in pressure drag.

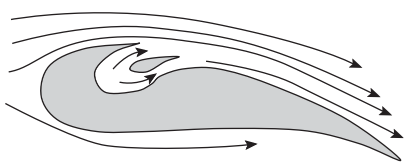

Fig. 5.18 Fluid injection technique

Suction Requires creation of low pressure suction slots on the surface of the body. This will remove low-momentum fluid particles near the surface delaying the transition to turbulent boundary layer formation.

Example 5.8 The velocity distribution in the laminar boundary layer is of the form for the flow over curved surface

$$\frac{u}{u_\infty} = f(\eta) + \lambda g(\eta)$$

where, $\eta = \dfrac{y}{\delta}$; $\lambda = \dfrac{\delta^2}{\nu}\dfrac{du_\infty}{dx}$; $f(\eta) = 2\eta - \eta^2$; $g(\eta) = \dfrac{3}{2}\eta - \dfrac{1}{2}\eta^3$

Determine the value of λ at the point of separation and also find the ratio of displacement to the boundary layer thickness at that point.

Solution: At the point of separation, the velocity gradient at the surface of the body must be zero, that is,

$$\left.\frac{\partial u}{\partial y}\right|_{y=0} = 0 \Rightarrow \left.\frac{\partial u}{\partial y}\right|_{y=0} = u_\infty\left(\frac{2}{\delta} + \frac{3\lambda}{2\delta}\right) = 0 \Rightarrow \lambda = -4/3$$

The displacement thickness is given by

$$\delta_1 = \int_0^\delta \left(1 - \frac{u}{u_\infty}\right) dy$$

$$\delta_1 = \delta \int_0^1 \left(1 - 2\eta + \eta^2 - \lambda\left\{\frac{3}{2}\eta - \frac{1}{2}\eta^3\right\}\right) d\eta$$

$$\delta_1 = \delta \left(\eta - \eta^2 + \frac{\eta^3}{3} - \lambda\left\{\frac{3}{4}\eta^2 - \frac{1}{8}\eta^4\right\}\right)_0^1$$

The ratio of displacement to the boundary layer thickness is

$$\frac{\delta_1}{\delta} = 1 - 1 + \frac{1}{3} - \lambda\left\{\frac{3}{4} - \frac{1}{8}\right\} \Rightarrow \frac{\delta_1}{\delta} = \frac{1}{3} - \frac{5}{8}\lambda$$

Substituting the value of λ, we get

$$\frac{\delta_1}{\delta} = \frac{1}{3} + \frac{5}{6} \Rightarrow \frac{\delta_1}{\delta} = \frac{7}{6}$$

5.9 LIFT AND DRAG

The concept of lift has already been introduced in the last section of Chapter 3, which has dealt with the flow of ideal fluids (potential flow). Figure 5.19 shows the various forces acting on an airfoil making an angle α (known as *angle of attack*) with the uniform flow stream having velocity u_∞. In general, when a fluid flows over a body, it is acted upon by a resultant force R known as *aerodynamic*

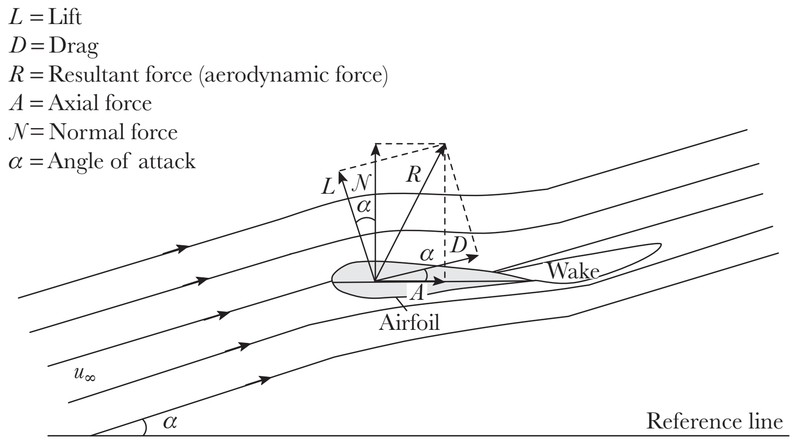

Fig. 5.19 Flow over an airfoil

force whose horizontal component parallel to the flow stream is known as *drag* D, and vertical component perpendicular to the flow stream is known as *lift* L. The component of the aerodynamic force acting along the *chordline* (straight line joining the leading edge and trailing edge) of the airfoil is known as *axial* force A whereas the component of the aerodynamic force perpendicular to the chordline is termed as *normal* force N.

The lift and the drag can be expressed in terms of axial and normal forces, respectively, as

$$\begin{aligned} L &= N\cos\alpha - A\sin\alpha \\ D &= N\sin\alpha + A\cos\alpha \end{aligned} \tag{5.101}$$

It has been seen earlier that the pressure does not remain constant when the flow is taking place over a curved surface. The forces, shown in Fig. 5.19, arise due to the variation of pressure and shear stress along the surface of the airfoil. For the sake of clarity, pressure and shear stress distribution along the surface of an airfoil is shown in Fig. 5.20.

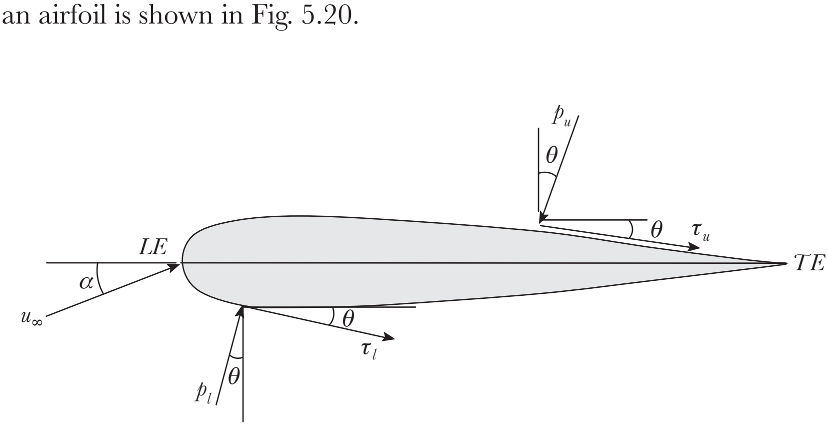

Fig. 5.20 Pressure and shear stress variation along the surface of an airfoil

The following are the normal and axial forces on the upper and lower surfaces of the airfoil:

$$
\begin{aligned}
N &= -\int_{LE}^{TE} (p_u \cos\theta + \tau_u \sin\theta) ds_u + \int_{LE}^{TE} (p_l \cos\theta - \tau_l \sin\theta) ds_l \\
A &= \int_{LE}^{TE} (-p_u \sin\theta + \tau_u \cos\theta) ds_u + \int_{LE}^{TE} (p_l \sin\theta + \tau_l \cos\theta) ds_l
\end{aligned}
\qquad (5.102)
$$

Another practical way to find out lift and drag forces is to express them in terms of free stream velocity, that is,

$$
\begin{aligned}
L &= C_L \left(\frac{1}{2} \rho u_\infty^2 \right) A_p \\
D &= C_D \left(\frac{1}{2} \rho u_\infty^2 \right) A_p
\end{aligned}
\qquad (5.103)
$$

where, C_L and C_D are known as lift and drag coefficients, respectively, and A_p is the projected area. The lift and drag coefficients are determined experimentally using a wind tunnel.

The drag is of two types, namely, *skin friction drag* and *pressure* (or *form*) *drag*. The *skin friction drag* is the drag due to the viscous shear acting on the body within the boundary layer. The procedure has been explained in detail in Section 5.4. The drag force due to skin friction is obtained by multiplying the wall shear stress to the surface area of the body up to the point of boundary layer separation. The *pressure drag*, on the other hand, is the drag induced due to the non-recovery of pressure in the rear side of the bluff body due to the boundary layer separation. This results in a difference of pressure across the body in the direction of flow. For better understanding of these two types of drags, Fig. 5.21 has been drawn. The horizontal thin flat plate will be subjected to only *skin friction drag* (due to the boundary layer formation on either side of the plate) whereas the vertical thin plate will have drag only due to pressure difference, that is, the *pressure drag*, across it. Consequently, an inclined plate will experience both skin friction drag and pressure drag.

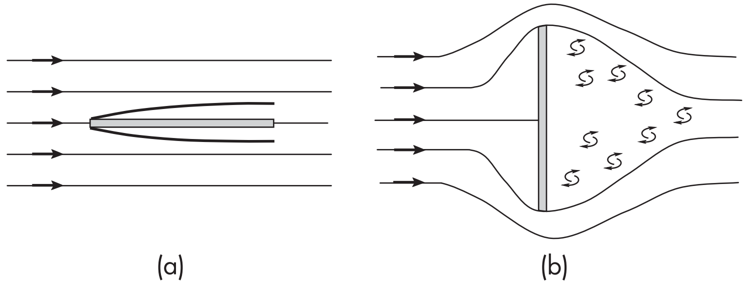

Fig. 5.21 Flow over (a) Horizontal plate (b) Vertical plate

As explained in the previous section, the free stream Reynolds number affects the separation of boundary layer and the subsequent formation of low pressure wake, which is responsible for the drag. The variation of drag coefficient with Reynolds number for the flow over cylinder and sphere is shown in Fig. 5.22.

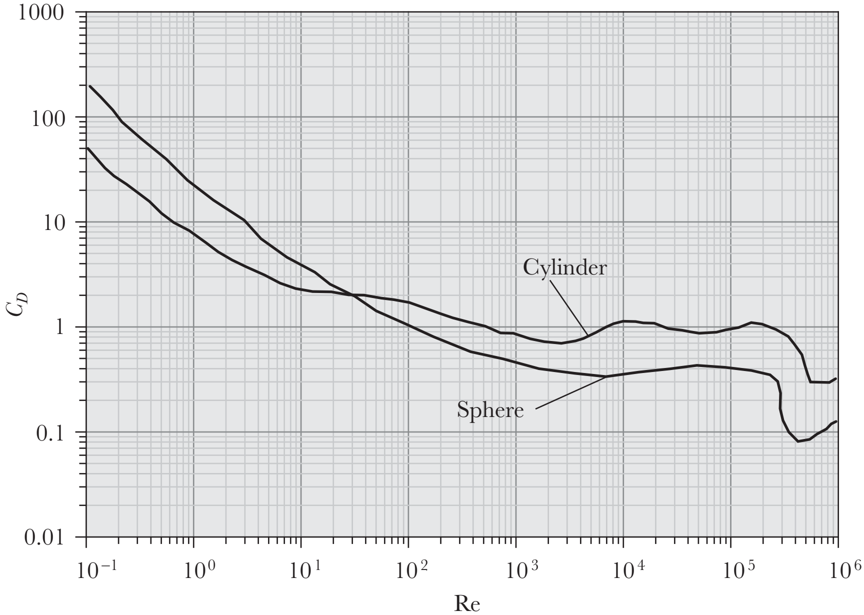

Fig. 5.22 Variation of drag coefficients for the flow over cylinder and sphere

The drag is higher at low Reynolds number due to higher viscous shear and vice versa. With the onset of turbulent boundary layer there is a sharp drop in the drag due to the delay in separation resulting in higher pressure recovery (i.e., low pressure drag).

Unlike the drag coefficient, the lift coefficient is largely independent of Reynolds number. However, both lift and drag coefficients are affected by the angle of attack and this variation has been shown for an airfoil in Fig. 5.23.

The lift coefficient varies linearly with the angle of attack whereas the drag coefficient varies non-linearly with the increase in angle of attack. For angles above 15°, the lift coefficient reaches maximum. The landing and take-off of an airplane is governed by changing the angle of attack of the flaps and slats provided on its wings. An important phenomenon associated with airfoils is *stalling*, which is characterized by a sudden reduction in lift coefficient and large increase in drag as the angle of attack attains a large value. This happens due to the flow separation from the upper surface of the airfoil leading to the formation of large low-pressure wake in the rear portion of the airfoil. It can also be noticed that the lift is positive non-zero at zero angle of attack.

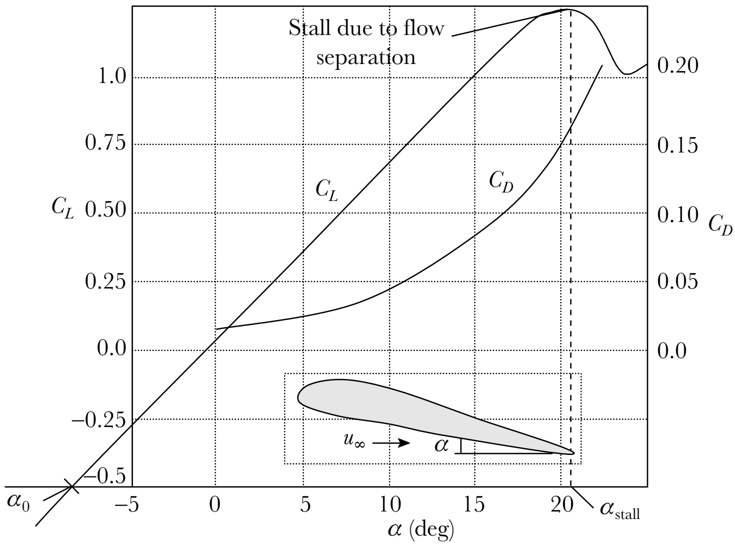

Fig. 5.23 Variation of lift and drag coefficients with angle of attack for an airfoil

In fact, lift becomes zero at some negative angle of attack termed as *zero-lift angle of attack*, α_0. For higher negative angle of attacks, negative lift coefficient is obtained, which is useful during the landing of an aircraft.

Example 5.9 A solar flat plate collector 2 m long and 1 m wide used to heat air is installed at the roof. Find the drag force on the absorber plate if the air is flowing along its length with a velocity of 20 m/s. Take density of air as 1.2 kg/m^3 and its dynamic viscosity as 1.8×10^{-5} kg/m-s.

Solution: The critical Reynolds number for the flow over flat plate is 5×10^5. The critical length of the plate is

$$x_{crit} = \frac{\mu \mathrm{Re}_{crit}}{\rho u_\infty} \Rightarrow x_{crit} = \frac{1.8\times10^{-5}\times5\times10^{5}}{1.2\times20} = 0.375\,\mathrm{m}$$

The flow undergoes transition from laminar to turbulent within the boundary layer at 0.375 m from the leading edge, as shown in Fig. 5.24.

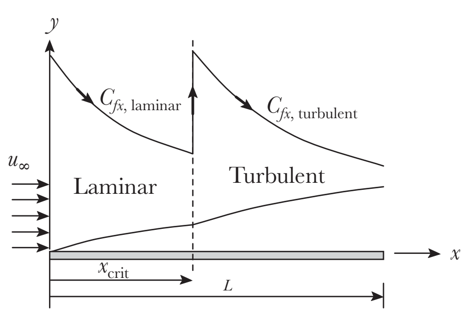

Fig. 5.24

The average friction coefficient on the plate is due to the combined effect of laminar and turbulent flow as

$$\overline{C_f} = \frac{1}{L}\left(\int_0^{x_{\text{crit}}} C_{f,\,\text{lam}}\,dx + \int_{x_{\text{crit}}}^{L} C_{f,\,\text{tur}}\,dx\right)$$

The local skin friction coefficient for laminar boundary layer has been taken from Blasius solution, whereas for turbulent boundary layer the local friction coefficient has been taken from the solution of Example 5.3.

$$\overline{C_f} = \frac{1}{2}\left(\int_0^{0.375} \frac{0.664}{\text{Re}_x^{1/2}}dx + \int_{0.375}^{2} \frac{0.0593}{\text{Re}_x^{1/5}}dx\right)$$

In terms of x:

$$\overline{C_f} = \frac{1}{2}\left(0.664\sqrt{\frac{\mu}{\rho u_\infty}}\int_0^{0.375} x^{-1/2}dx + 0.0593\left(\frac{\mu}{\rho u_\infty}\right)^{1/5}\int_{0.375}^{2} x^{-1/5}\,dx\right)$$

$$\overline{C_f} = \frac{1}{2}\left(\frac{0.664}{1/2}\sqrt{\frac{1.85\times10^{-5}}{1.2\times20}}\sqrt{0.375} + \frac{0.0593}{4/5}\left(\frac{1.85\times10^{-5}}{1.2\times20}\right)^{1/5}(2^{4/5} - 0.375^{4/5})\right)$$

$$\overline{C_f} = \frac{1}{2}(7.14\times10^{-4} + 5.70\times10^{-3}) \Rightarrow \overline{C_f} = 3.21\times10^{-3}$$

The drag force on the absorber plate is

$$D = \overline{C_f}\,A\left(\frac{1}{2}\rho u_\infty^2\right)$$

$$D = 3.21\times10^{-3}(2\times1)\left(\frac{1}{2}\times1.2\times20^2\right) \Rightarrow F_D = 1.541\text{N}$$

Example 5.10 A thin plate having dimensions 1m by 0.5 m is immersed horizontally in a water canal with shorter side aligned in the direction of flow. If the water is flowing at a velocity of 0.5 m/s and the temperature of water is 20°C ($\rho = 998.3$ kg/m^3; $\mu = 1\times10^{-3}$ kg/m-s), determine the total drag experienced by the plate.

Solution: The critical length of the plate is given by

$$x_{\text{crit}} = \frac{\mu \text{Re}_{\text{crit}}}{\rho u_\infty} \Rightarrow x_{\text{crit}} = \frac{1\times10^{-3}\times5\times10^5}{998.3\times0.5} = 1.002\,\text{m}$$

Since $x_{crit} > 0.5$ m, the flow within the boundary layer remains laminar throughout the plate length in the direction of flow. The local skin friction coefficient is evaluated from the Blasius solution. The average value of skin friction coefficient is

$$\overline{C_f} = \frac{1}{L}\int_0^L C_f\,dx \quad \Rightarrow \quad \overline{C_f} = \frac{1}{0.5}\int_0^{0.5}\frac{0.664}{\mathrm{Re}_x^{1/2}}dx$$

$$\overline{C_f} = \frac{0.664}{L}\sqrt{\frac{\mu}{\rho u_\infty}}\int_0^{0.5} x^{-1/2}dx$$

$$\overline{C_f} = 2C_{f,x=L} \quad \Rightarrow \quad \overline{C_f} = 1.328/(\mathrm{Re}_L)$$

$$\overline{C_f} = \frac{1.328}{\sqrt{998.3\times 0.5\times 0.5/0.001}} \quad \Rightarrow \quad \overline{C_f} = 2.658\times 10^{-3}$$

The drag force on either side of the plate is

$$D = \overline{C_f}\,A\left(\frac{1}{2}\rho u_\infty^2\right)$$

The total drag force will be equal to the sum of drag force on top and bottom side of the plate is

$$D_{\text{total}} = 2\times\overline{C_f}\,A\left(\frac{1}{2}\rho u_\infty^2\right)$$

$$D_{\text{total}} = 2.658\times 10^{-3}(0.5\times 1)(998.3\times 0.5^2) \quad \Rightarrow \quad D_{\text{total}} = 0.331\,\text{N}$$

Example 5.11 The cylindrical chimney of a thermal power plant has diameter 5 m and is 20 m tall. Calculate the drag force on it if air is flowing with a velocity of 30 m/s. Take the drag coefficient as 0.8 and the density of air is 1.2 kg/m³.

Solution: The drag force on a cylindrical chimney is given by

$$D = C_D A_p\left(\frac{1}{2}\rho u_\infty^2\right)$$

where, A_p is the project area = height of chimney × diameter

$$D = 0.8\times(20\times 5)\times\left(\frac{1}{2}\times 1.2\times 30^2\right) \quad \Rightarrow \quad D = 43.2\,\text{kN}$$

Example 5.12 Calculate the drag coefficient for a cylinder 100 mm diameter and 200 mm long placed in a uniform flow stream having velocity 1m/s. The axis of cylinder is perpendicular to the flow direction. The drag force acting on the cylinder is measured as 50 N. Take the density of fluid to be 1000 kg/m³. Determine the velocity at the point on the cylinder's surface where the pressure is 200 Pa above the ambience.

Solution: The drag coefficient can be obtained from the expression of drag force as

$$C_D = \frac{D}{A_p\left(\frac{1}{2}\rho u_\infty^2\right)} \Rightarrow C_D = \frac{50}{(0.1\times 0.2)\times(0.5\times 1000\times 1^2)} \Rightarrow C_D = 5$$

$$p - p_\infty = \frac{1}{2}\rho\left(u_\infty^2 - u^2\right)$$

$$200 = \frac{1}{2}\times 1000\times(1^2 - u^2)$$

$$u^2 = 1 - \frac{200\times 2}{1000} \Rightarrow u = 0.774\,\text{m/s}$$

POINTS TO REMEMBER

- The viscous effects are limited only to a small region near the solid surface known as boundary layer. Above the boundary layer, the flow may be treated as inviscid.
- Within the turbulent boundary layer, there is an extremely thin region (viscous or laminar sub-layer) near the solid surface where the viscous effects are tremendously high.
- The boundary layer separation occurs only due to the existence of adverse pressure gradient.
- Since there is no variation in pressure along the solid flat surface, the boundary layer remains intact with the surface. Hence, there is no boundary layer separation.
- In case of curved bodies, the pressure is not fully recovered and the body experiences a drag due to the difference in pressure between its front and rear portions.
- Larger the wake size, larger will be the pressure drop across a non-flat body and higher will be the pressure drag.
- Reynolds number governs the flow separation on curved bodies such as cylinders or spheres.
  - (a) At very low Reynolds number ($Re < 4$), there is no flow separation as the adverse pressure gradient in the rear side is negligibly small due to ultra-low free stream velocity.
  - (b) For $Re < 2 \times 10^5$, the flow separates at an angle of about 80° for flow over a cylinder.
  - (c) For $Re > 2 \times 10^5$, the flow separates at an angle of about 140° for flow over a cylinder.
- Airfoil is said to be stalled when there is a sudden drop in lift coefficient at a large angle of attack.
- Lift is usually non-zero at zero angle of attack for an airfoil.

SUGGESTED READINGS

Anderson, Jr., J.D., *Fundamentals of Aerodynamics*, 5th Ed., McGraw-Hill Education, New Delhi, 2013.

Massey, B., J. Ward-Smith, *Mechanics of Fluids*, 8th Ed., Taylor and Francis, London, 2006.

Schlichting, H., *Boundary Layer Theory*, 8th revised and enlarged edition, Springer, Berlin, 2000.

Shames, I.H., Mechanics of Fluid, 4th Ed., Tata McGraw-Hill Education, New Delhi, 2002.

MULTIPLE-CHOICE QUESTIONS

5.1 The boundary layer thickness for the flow of an ideal fluid over a solid body is
(a) zero
(b) less than that of a real fluid
(c) more than that of a real fluid
(d) depends upon the temperature

5.2 The drag force due to shear stress at the wall is
(a) form drag
(b) skin friction drag
(c) pressure drag
(d) all of these

5.3 For the point of separation
(a) shear stress at wall is maximum
(b) pressure gradient is maximum
(c) shear stress at wall is zero
(d) pressure is zero

5.4 With increase in the angle of attack, the drag coefficient for an airfoil
(a) remains the same
(b) increases linearly
(c) decreases non linearly
(d) none of these

5.5 Which of the following is responsible for pressure drag?
(a) pressure difference across the body
(b) formation of wake
(c) shape of the body
(d) all of these

5.6 For the flow of air ($\upsilon = 15 \times 10^{-6}\,\text{m}^2/\text{s}$) with free stream velocity 18.5 m/s over a thin flat plate, the distance from leading edge where transition zone of boundary layer starts is approximately
(a) 20 cm
(b) 40 cm
(c) 60 cm
(d) none of these

5.7 The boundary layer thickness in turbulent flow over a flat plate varies as
(a) $x^{\frac{1}{7}}$
(b) $x^{\frac{4}{5}}$
(c) $x^{\frac{6}{7}}$
(d) none of these

5.8 The viscous sub-layer exists only in the
(a) laminar boundary layers
(b) transition region of the boundary layer
(c) turbulent boundary layers
(d) separated flow region

5.9 Which of the following is the condition for flow reversal

(a) $\left(\frac{\partial u}{\partial y}\right)_{y=0} = 0$

(b) $\left(\frac{\partial u}{\partial y}\right)_{y=0} > 0$

(c) $\left(\frac{\partial u}{\partial y}\right)_{y=0} < 0$

(d) none of these

5.10 What will happen if an airfoil is stalled?

(a) The engine will stop working

(b) There will be a sudden drop in the flight altitude

(c) There will be a sudden increase in the flight speed

(d) The aircraft wing will break

5.11 The momentum thickness at stagnation point is

(a) zero

(b) maximum

(c) minimum

(d) depends upon the geometry of the object

5.12 In laminar boundary layer on a flat plate, the shear stress

(a) increases with x

(b) decreases with x

(c) does not vary with x

(d) depends on Reynolds number

5.13 Which of the following is *not* a method to control boundary layer separation?

(a) By equipping objects with suction slots

(b) Streamlining the object's geometry

(c) Blowing jets directed into critical areas

(d) By diluting the fluid

5.14 The coefficient of skin friction by Blasius solution for boundary layer flow over flat plate is given as

(a) $C_f = \frac{5x}{\sqrt{\mathrm{Re}_x}}$

(b) $C_f = \frac{0.664}{\sqrt{\mathrm{Re}_x}}$

(c) $C_f = \frac{4.64}{\sqrt{\mathrm{Re}_x}}$

(d) $C_f = \frac{0.646}{\sqrt{\mathrm{Re}_x}}$

5.15 The momentum thickness δ_2 for a flat plate is given by

(a) $\frac{4.64x}{\sqrt{\mathrm{Re}_x}}$

(b) $\frac{4.64}{\sqrt{\mathrm{Re}_x}}$

(c) $\frac{0.671x}{\sqrt{\mathrm{Re}_x}}$

(d) $\frac{0.671}{\sqrt{\mathrm{Re}_x}}$

5.16 The stalling occurs at an angle of about

(a) 10°

(b) 15°

(c) 20°

(d) 25°

5.17 The energy thickness is a quantitative idea of

(a) energy of fluid flowing with high velocity

(b) deficit in kinetic energy due to boundary layer

(c) increase in kinetic energy due to separation

(d) all of these

5.18 The drag on flat plate for a given Reynolds number is maximum, when it is kept
(a) horizontal
(b) inclined at 45°
(c) vertical
(d) independent of orientation

5.19 The zero-lift angle of attack is about
(a) 5°
(b) 2°
(c) –2°
(d) –5°

5.20 The lift-to-drag ratio with angle of attack
(a) remains constant
(b) decreases
(c) increases
(d) increases up to a certain value and then decreases

REVIEW QUESTIONS

5.1 Flow outside the boundary layer is frictionless. Justify the statement.
5.2 Discuss the physical significance of displacement, momentum, and energy thicknesses.
5.3 Why is the Blasius solution for the boundary layer flow over flat plate termed as near-exact solution?
5.4 What are the various methods available for preventing the boundary layer separation?
5.5 Discuss in detail the role of Reynolds number on the flow past circular cylinder.
5.6 Explain the phenomenon of flow separation on a curved body.
5.7 How does the flow of real fluids differ from that of ideal fluids over a solid object?
5.8 Discuss the role of favourable and adverse pressure gradient on the velocity and its first- and second-order derivatives within the boundary layer.
5.9 Explain the concept of lift and drag. What are the factors that influence these forces?
5.10 Define the term stalling for an airfoil. In addition, discuss the effect of angle of attack on the lift and drag.

UNSOLVED PROBLEMS

5.1 Use numerical results of Blasius solution for the flow over a flat plate to derive the following expression for wall shear stress.

$$\tau_w = \sqrt{\mu\rho u_\infty^3}\, f''(0) x^{-1/2}$$

Compute the shear stress at a distance of 0.3 m from the leading edge for the air flowing at a velocity of 2.5 m/s. The density and the kinematic viscosity of air are 1.2 kg/m^3 and 1.6×10^{-5} m^2/s, respectively. In addition calculate the total drag on the plate for L = 1.0 m.

[Ans: 0.0126 N per unit plate width]

5.2 Plot τ/τ_w versus η using the numerical solution of Blasius equation and compare it with that of the approximate solution obtained using cubic velocity profile.

5.3 Use appropriate boundary conditions to evaluate the constants in the boundary layer velocity profile given by

$$u = c_1 + c_2 y + c_3 y^2 + c_4 y^3 + c_5 y^4$$

Determine the displacement, momentum, and energy thicknesses.

[Ans: $3\delta/10$, $37\delta/315$, $2771\delta/15015$]

5.4 Determine the values of local and average skin friction coefficients for the velocity profile mentioned in Problem 5.3.

$$\left[\textbf{Ans: } \delta = 5.8355x\Big/\sqrt{\mathrm{Re}_x},\ C_{fx} = 0.685\Big/\sqrt{\mathrm{Re}_x},\ \bar{C}_f = 1.37\Big/\sqrt{\mathrm{Re}_L}\right]$$

5.5 The velocity profile in a turbulent boundary layer is approximated by (a) 1/6-th power law (b) 1/8-th power law. Derive the expression for boundary layer thickness and the local skin friction coefficient using von Karman momentum integral equation. [*Hint*: Refer Example 5.7]

5.6 Consider a sufficiently long flat plate such that both laminar and turbulent boundary layers appear. Derive the expression for the drag force using skin friction coefficients obtained from Blasius solution for laminar boundary layer and (a) 1/6-th power law (b) 1/8-th power law for turbulent boundary layer.

5.7 The rectangular roof sheet of a kennel has a dimension of 6 m × 2 m. Calculate the drag force on its upper surface if the wind is blowing parallel to its length at 3 m/s. The density and the kinematic viscosity of air are 1.2 kg/m^3 and 1.6×10^{-5} m^2/s, respectively.

[Ans: 0.195 N]

5.8 Calculate the drag coefficient and drag force on a cylindrical shape flag post of the ship having diameter 60 mm and 3 m long exposed to wind velocity of 10 m/s. The density and the kinematic viscosity of air are 1.2 kg/m^3 and 1.6×10^{-5} m^2/s respectively.

[Ans: 10.8 N]

5.9 A submarine is propelling underwater with a velocity of 6 m/s. Discuss the nature of the boundary layer formed at one of its rectangular fins if water flow is along its width of 0.5 m. The density of water is 998 kg/m^3 and the kinematic viscosity is 1×10^{-6} m^2/s.

[Ans: Combined laminar-turbulent boundary layer]

5.10 In a laminar boundary layer, the shear stress distribution is given as $\tau = \tau_o(1 - \eta)$, where $\eta = y/\delta$. Calculate the displacement and momentum thickness of this boundary layer.

[Ans: $\delta_1 = \delta/3$, $\delta_2 = \delta/15$]

Answers to Multiple-choice Questions

5.1 (a)	5.2 (b)	5.3 (c)	5.4 (d)	5.5 (d)
5.6 (b)	5.7 (b)	5.8 (c)	5.9 (c)	5.10 (b)
5.11 (a)	5.12 (b)	5.13 (d)	5.14 (b)	5.15 (c)
5.16 (c)	5.17 (b)	5.18 (c)	5.19 (d)	5.20 (d)

DESIGN OF EXPERIMENTS

Experiment 5.1 Determination of Boundary Layer Thickness

Objective

To measure the boundary layer thickness on smooth and rough flat plates.

Theory

Whenever a flowing fluid interacts with the solid body, a thin viscous region (boundary layer) appears on the surface of the body. The velocity varies from zero at the solid surface due to no slip to the maximum at the edge of the boundary layer. The distance from the solid surface to the point where the velocity reaches 99% of free stream velocity is termed as the boundary layer thickness. In case of flow over a smooth flat plate, the boundary layer thickness is zero at the leading edge and it increases parabolically in the direction of flow. The flow inside the boundary layer remains laminar until the Re_x reaches $\mathrm{Re}_{\mathrm{crit}} = 5 \times 10^5$ and is termed as laminar boundary layer. The laminar boundary layer thickness as proposed by Blasius:

$$\delta_{\mathrm{th}} = \frac{5x}{\sqrt{\mathrm{Re}_x}} \tag{E5.1}$$

where, x is the distance from the leading edge and Re_x is the Reynolds number given by

$$\mathrm{Re}_x = \frac{u_\infty x}{\upsilon} \tag{E5.2}$$

where, u_∞ is the free stream velocity, υ is the kinematic viscosity of the flowing fluid.

For $\mathrm{Re}_x > \mathrm{Re}_{\mathrm{crit}} = 5 \times 10^5$, the flow inside the boundary layer no longer takes place in an orderly layer-wise manner and turns turbulent. The boundary layer is then termed as turbulent boundary layer. Due to turbulence, the mixing of different layer causes the boundary layer thickness to increase. If a rough plate is used, the turbulence occurs at a value of Re_x much lower than the critical Reynolds number for the flow over smooth plate, that is, $\mathrm{Re}_{\mathrm{crit}} = 5 \times 10^5$. The thickness of the boundary layer can be computed from velocity represented by 1/7-th power law:

$$\frac{\bar{u}}{u_\infty} = \left(\frac{y}{\delta}\right)^{\frac{1}{7}} \tag{E5.3}$$

Experimental Set-up

The set-up requires a wind tunnel, the test plates (smooth and rough), and the Pitot tube. A schematic diagram of the experimental set-up is shown in Fig. E5.1. The test plate is placed inside the test section of the wind tunnel. The Pitot tube, fitted with a micrometer, is placed on the surface of the test plate at a given distance from

the leading edge and is slowly moved away from the plate surface in a perpendicular direction, as shown in Fig. E5.1. The flow velocity is measured along the perpendicular direction. The micrometer reading at the point where the velocity reaches 99% free stream velocity is the boundary layer thickness.

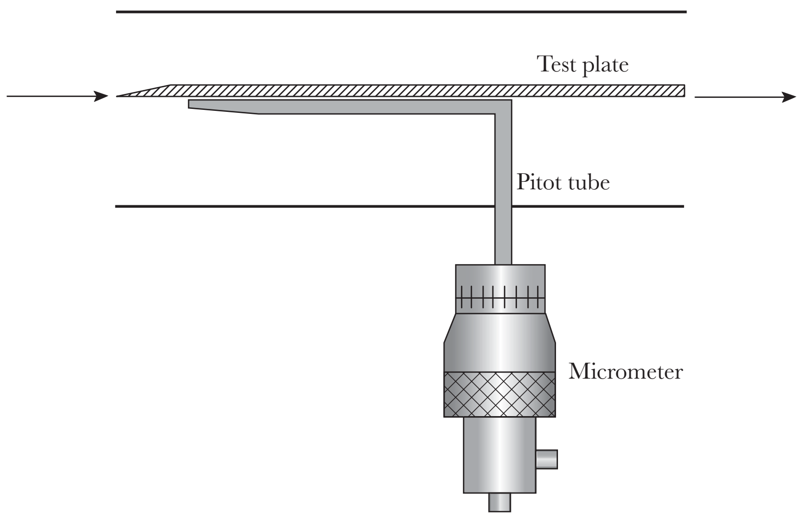

Fig. E5.1 Top view of the test section

Procedure

1. Install the test plate (smooth) inside the test section of the wind tunnel.
2. Place the Pitot tube with its tappings connected to the manometer at the surface of the plate.
3. Switch on the fan of the wind tunnel and set a particular velocity inside the test section.
4. Note down the manometer readings and calculate the velocity.
5. Move the Pitot tube slightly away from the surface with the help of micrometer and note down the corresponding manometer readings
6. Repeat the procedure until a point is reached where the velocity is 99% of test section velocity. Note down micrometer reading corresponding to this point.
7. Repeat the experiment for different flow velocities (or free stream Reynolds number).
8. Repeat the procedure for other test plate (rough).

Observation Table

Distance of tip of the Pitot tube from the leading edge of the test plate,

$x =$ ____________ mm.

Air density, $\rho =$ ______________________ kg/m^3.

Free stream Re (% fan speed)	Micrometer reading (mm)	$p_d - p_s = \rho_m g h_m$ (Pa)	Velocity $\sqrt{\frac{2(p_d - p_s)}{\rho}}$ (m/s)	$\delta_{th} = \frac{5x}{\sqrt{Re_x}}$ (mm)	% error $\% \text{ error} = \frac{\delta_{exp} - \delta_{th}}{\delta_{th}} \times 100$
$u_\infty, 1$					
	…				
	δ_{exp}		$0.99 u_\infty, 1$		
$u_\infty, 2$					
…					

Results and Discussion

1. Draw and discuss the following plot: δ_{exp} versus Re_x for both smooth and rough test plates.
2. Discuss the difference in the results for smooth and rough plates.

Conclusions

Draw conclusions on the results obtained.

Experiment 5.2 Determination of Lift and Drag

Objective

To determine the lift and drag coefficients for a given airfoil.

Theory

Whenever a moving fluid comes in contact with a solid object, it (solid body) experiences an aerodynamic force, the horizontal component of which is termed as drag whereas its vertical component is known as lift. The drag has two components: (a) skin friction drag is due to viscous forces predominating in the boundary layer region (b) pressure drag is due to the difference in pressure across the body (occurs in curved bodies), the boundary layer may not follow the contour and the separation occurs in the presence of adverse pressure gradient. The theoretical drag and lift can be computed using Eq. (5.101).

Experimental Set-up

This experiment also requires a wind tunnel with a given airfoil installed in the test section. The drag D and lift L forces can be measured using load cell fitted to

the airfoil. The lift and drag coefficients can then be determined using following relationships:

$$C_L = L \Big/ \left(\frac{1}{2}\rho u_\infty^2\right) A_p$$
$$C_D = D \Big/ \left(\frac{1}{2}\rho u_\infty^2\right) A_p \qquad \text{(E5.4)}$$

where, A_p is the projected area, which is nothing but the area of rectangle having length equal to the span of airfoil and width is the distance between the projections of leading and trailing edge. Thus, projected area varies with the change in angle of attack.

Procedure

1. Install the given airfoil into the test section of the wind tunnel at a particular angle of attack.
2. Switch on the fan of the wind tunnel and set a particular velocity inside the test section.
3. Note down the load cell readings for horizontal as well as vertical components.
4. Repeat experiment for different angle of attacks.

Observation Table

Free stream velocity u_∞ = ______________________ m/s
Air density, ρ = ________________________ kg/m^3

Angle of attack, α (deg)	**Projected area, A_p (m^2)**	**Load cell readings**		**Coefficients**	
		Lift L (N)	**Drag D (N)**	$C_L = L \Big/ \left(\frac{1}{2}\rho u_\infty^2\right) A_p$	$C_D = D \Big/ \left(\frac{1}{2}\rho u_\infty^2\right) A_p$

Results and Discussion

Draw and discuss the following plots:

1. C_L versus α
2. C_D versus α

Conclusions

Draw conclusions on the results obtained.

CHAPTER

6 Pipe Flow

LEARNING OBJECTIVES

After studying this chapter, the reader will be able to:

- Understand the development of flow in a pipe (laminar or turbulent)
- Calculate the losses and discharge in individual branches of any pipe network
- Comprehend the working principle of different flow-measuring techniques
- Infer the concept of water hammer and slurry flows
- Design simple experiments to calculate losses in a piping system and to measure the flow using constriction meters

In Chapter 5, the boundary layer flow over the solid bodies has been discussed in detail. Such flows are often termed as *external flows*. The viscous flow completely bounded by a solid surface with its cross-section running full is referred as *internal flow*, for example, flow through ducts, pipes, nozzles, diffusers, etc. If the pipe is not running full, that is, the pipe cross-section has a free surface, the flow would be under the influence of gravity and is considered as an *open channel flow* (discussed in next chapter). The internal flows are primarily driven by the pressure difference across the inlet and outlet. Thus, they are also termed as *pressure driven flows*.

This chapter deals with various aspects of internal flows—developing and fully developed laminar and turbulent flows. The understanding of pipe networks has been developed with a focus on evaluation of different types of losses and discharge in each branch. The important flow measurement techniques and their principles have also been included for the sake of completeness. The concepts of siphon, water hammer, and slurry flows have also been introduced.

The internal flows are very common and have many applications ranging from household water distribution network to complex piping network in oil refineries. Hence, the topics covered in this chapter are of immense importance due to their wide range of applications.

6.1 FLOW DEVELOPMENT IN PIPE

At the entrance of the pipe, there is a region where the flow is in the developing stage due to the formation of boundary layer around the pipe's internal periphery, shown in Fig. 6.1. The thickness of boundary layer increases from zero at the edge of pipe entrance until the boundary layer merges itself along the pipe centreline. The velocity varies within the boundary layer region due to viscous effects whereas at the core the velocity remains constant. The distance from pipe entrance to the point where boundary layer merges is known as *entrance length* and the flow within this region is termed as *developing flow*. Beyond the entrance length, the velocity profile attains a well-defined shape and becomes symmetric with maximum velocity at the centreline. The flow beyond the entrance length is termed as *fully developed flow*. On the basis of magnitude of fluid inertia (velocity), the flow is classified as either *laminar* or *turbulent*. The flow inside the pipe

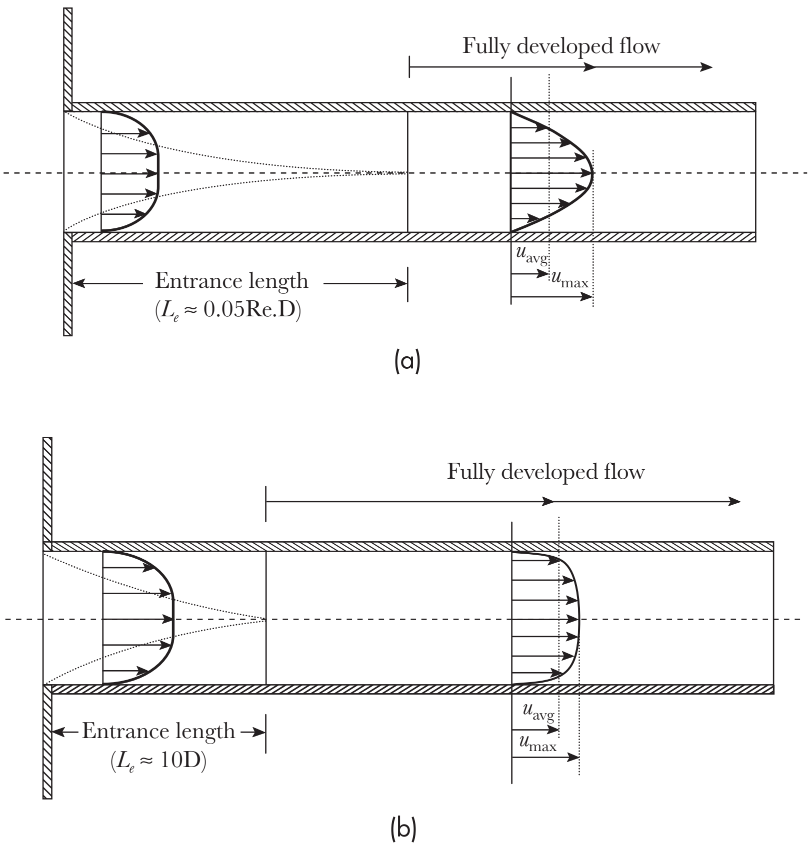

Fig. 6.1 Flow inside a pipe (a) Laminar (b) Turbulent

is *laminar* if the flow velocity is small in magnitude. In this regime, the fluid flows in an orderly manner. The flow occurs in layers or laminae and there is no mixing of layers. The layer farthest from the solid boundary will have the maximum velocity, that is, centreline velocity is maximum in pipes. On the other hand, if the magnitude of flow velocity is very high, the flow is termed as *turbulent flow*. In this regime, the flow inside the pipe is highly chaotic (or disturbed) and as such it is difficult to predict the path of randomly moving fluid particles.

Let us recall the boundary layer description for the flow over flat plate (Chapter 5). It is known that the boundary layer is thicker in turbulent flow region than the boundary layer in laminar flow region. As a result, the entrance length is shorter for turbulent flow through a pipe, shown in Fig. 6.1. The approximate entrance lengths for both laminar and turbulent flows are also mentioned in the figure. It also shows the velocity profiles in the entrance and fully developed regions of a pipe for each type of flow. In laminar flow, the flow gradually develops from the pipe entrance into a fully developed flow with parabolic velocity profile (For details see Section 4.3.3 of Chapter 4), given by

$$\frac{u}{u_{\max}} = 1 - \frac{r^2}{R^2} \tag{4.142}$$

The velocity varies from zero at the wall to the maximum at pipe centreline. Maximum velocity $u_{\max}$ cannot be used to represent the flow through a pipe because it represents the centreline velocity of the pipe only. The *mean* or *average velocity* truly represents the flow inside the pipe as it is the average of all velocities throughout its cross-section and is given by

$$u_{\text{avg}} = \frac{1}{2} u_{\max} \tag{4.144}$$

Shear stress,

$$\tau = \mu \frac{du}{dr} \quad \Rightarrow \quad \tau = \mu u_{\max}\left(-\frac{2r}{R^2}\right) \quad \Rightarrow \quad \tau = -\frac{4\mu u_{\text{avg}} r}{R^2} \tag{4.145}$$

In turbulent flow, the viscous effects are limited to a very thin region near the pipe's internal surface, termed as *viscous sublayer*. The flow remains laminar within this thin layer. Hence, it is also termed as *laminar sublayer*. Across laminar sublayer, there is a sudden rise in velocity. Outside this layer, the flow is turbulent and the velocity variation with respect to time at a point is shown

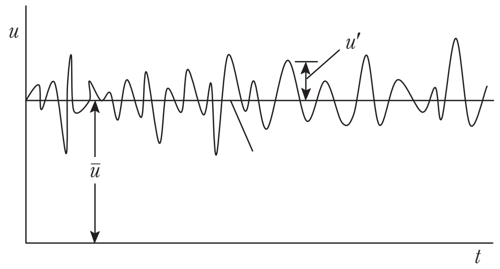

Fig. 6.2 Velocities in a turbulent flow

in Fig. 6.2. Thus, the components of flow velocities in x, y, and z directions can be considered as the sum of time averaged velocity and the fluctuating component in the respective directions, that is,

$$\left.\begin{aligned} u &= \bar{u} + u' \\ v &= \bar{v} + v' \\ w &= \bar{w} + w' \end{aligned}\right\} \tag{6.1}$$

where $\bar{u}$, $\bar{v}$, and $\bar{w}$ are the time-averaged velocity components in x, y, and z directions, respectively, and u', v', and w' are the corresponding fluctuating velocity components.

Flow turbulence causes the formation of *eddies* of different sizes. Eddies are the swirling fluid chunks in a flow stream. These eddies cause rapid mixing of different layers of flow resulting in the time-averaged velocity to become almost constant as depicted by the flatter velocity profile in Fig. 6.1(b). The velocity profile for turbulently boundary layer over a flat plate can be fit into $1/n$ power law, which has already been described in Chapter 5, that is,

$$\frac{\bar{u}}{u_\infty} = \left(\frac{y}{\delta}\right)^{\frac{1}{n}} \tag{5.77}$$

Based on Eq. (5.77), the velocity profile for fully developed turbulent flow in a pipe can simply be represented by

$$\frac{\bar{u}}{u_{\max}} = \left(1 - \frac{r}{R}\right)^{1/n} \tag{6.2}$$

where exponent n can have the values 6, 7, 8, and so on.

A comparison of different turbulent velocity profiles (represented by different values of n) with laminar velocity profile in a pipe is shown in Fig. 6.3. It can be seen that with the increase in n, the viscous region adjacent to wall gets

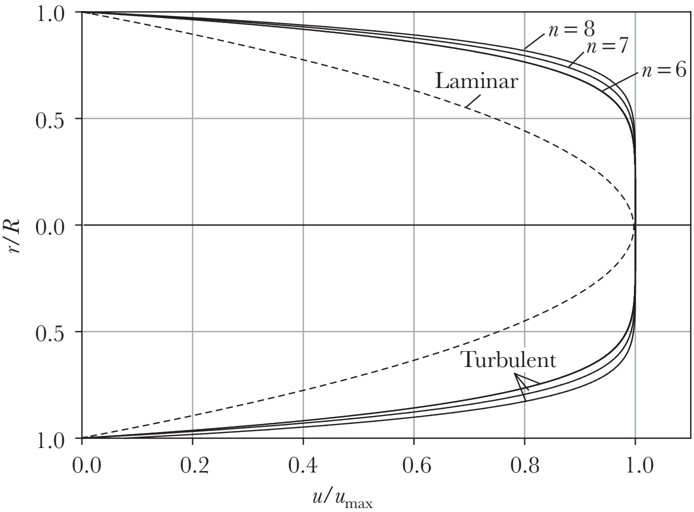

Fig. 6.3 Velocity profiles

narrower. Exponent n = 7 approximates velocity profiles of many practical turbulent pipe flow problems.

It should be remembered that Newton's law of viscosity [i.e., Eq. (4.146)] cannot be applied on the approximate velocity profile represented by Eq. (6.2) for the computation of shear stress in turbulent flow. In turbulent flows, the shear stress increases significantly in comparison to laminar flow due to turbulent fluctuations. It is given by

$$\tau = \mu \frac{d\bar{u}}{dr} - \rho \overline{u'v'} \tag{6.3}$$

The second term on the right hand side of the Eq. 6.3 (i.e., $-\rho\overline{u'v'}$) is known as *Reynolds stress*. It represents the turbulent component of shear stress. It is zero for laminar flow as laminar flow does not have fluctuations in velocity (i.e., $u' = v' = 0$).

Boussinesq proposed the following relation to represent the turbulent component of shear stress (similar to Newton's law of viscosity):

$$-\rho\overline{u'v'} = \eta \frac{d\bar{u}}{dr} \tag{6.4}$$

where, η is the eddy viscosity, which depends not only on the fluid but also on the flow conditions. Eddy viscosity is given by

$$\eta = \rho \ell_m^2 \frac{d\bar{u}}{dr} \tag{6.5}$$

where, ρ is the fluid density and ℓ_m is known as *Prandtl mixing length*, which is defined as the distance travelled by a fluid particle across the flow stream before it loses its momentum and becomes a part of the bulk flow stream.

Reynolds apparatus, discussed in Chapter 3, is used to establish whether the flow is *laminar* or *turbulent* in a pipe by means of flow visualization (see Fig. E3.2). The coloured dye is injected into the water flowing through a transparent pipe. If the dye forms a fine thread all along the pipe length, the flow is laminar. In case of turbulent flow, the dye disperses and gets mixed with the flowing water stream all across the pipe cross-section. The Reynolds experiment is also helpful in predicting the value of *critical Reynolds number*. *Reynolds number* is defined as the ratio of inertia force to the viscous force. Flow is laminar if viscous forces are predominant whereas it is turbulent when inertia forces are large enough to suppress the effect of viscous forces. The critical Reynolds number is the Reynolds number value at which the flow transition from laminar to turbulent takes place. On the basis of experimental results, the following flow regimes occur for different values of Reynolds number, Re:

Laminar	$Re < 2300$
Transition	$2300 < Re < 4000$
Turbulent	$Re > 4000$

The value of critical Reynolds number for the flow through pipe is usually taken as 2300.

On the basis of viscous sublayer thickness, δ' and average internal surface roughness height, e, pipes may be classified as hydraulically smooth pipe or hydraulically rough pipe. More precisely, if the average roughness height exceeds the thickness of viscous sublayer, the pipe is termed as *hydraulically rough*, otherwise it is *hydraulically smooth*. Figure 6.4 shows the hydraulically smooth and rough surfaces.

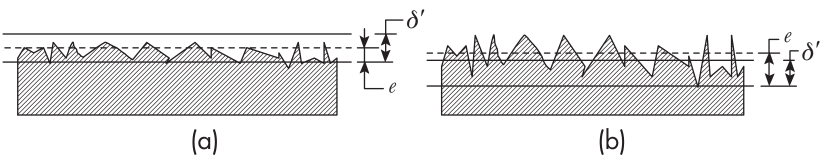

Fig. 6.4 (a) Hydraulically smooth surface (b) Hydraulically rough surface

6.2 LOSSES IN PIPE

When the flow takes place in a closed conduit or pipe, there is a drop in pressure in the direction of flow. This pressure loss in the pipe network is due to various factors, which include friction, geometry, fittings, and so on. The losses in a pipe may be classified into two groups—major losses and minor losses.

The major losses are due to friction whereas the minor losses are due to sudden expansion, sudden contraction, bends, and fittings.

6.2.1 Major Losses

As mentioned in the previous paragraph, the major loss in a pipe is due to friction. The friction is defined either in terms of *skin friction coefficient*, C_f (also known as Fanning's friction factor) or Darcy's friction factor, f. These have been defined earlier also in Chapter 4.

$$f = 4C_f = 4\left(\frac{\tau_w}{\frac{1}{2}\rho V^2}\right) \tag{4.120}$$

where V is the average flow velocity inside the pipe.

Consider an infinitesimal fluid element of length dz within the pipe of diameter D and length L, shown in Fig. 6.5, and applying the momentum conservation equation.

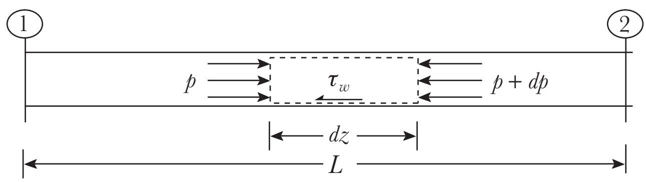

Fig. 6.5 Forces acting on the fluid element inside the pipe

$$pA - (p + dp)A - \tau_w(\pi D)dz = \dot{m}dV \tag{6.6}$$

where A is the area of cross-section of the pipe, that is, $A = \pi D^2/4$.

From the definition of friction factor, the wall shear stress can be expressed in terms of Darcy's friction factor, Eq. (6.6) is then reduced to

$$-dp = \frac{f}{2D}\rho V^2 dz + \rho V dV \tag{6.7}$$

From mass conservation or continuity equation,

$$\rho AV = \text{const} \tag{6.8}$$

The cross-sectional area of the pipe is constant and assuming the density to be constant, the change in velocity will be zero, that is, $dV = 0$.

Therefore, Eq. (6.7) reduces to

$$-dp = \frac{f}{2D}\rho V^2 dz \tag{6.9}$$

Integrating Eq. (6.9) between the sections 1 and 2

$$p_1 - p_2 = f\frac{L}{D}\left(\frac{1}{2}\rho V^2\right) \tag{6.10}$$

Equation (6.10) is known as *Darcy–Weisbach equation*. Another form of this equation is obtained by dividing it by the specific weight of the fluid (ρg),

$$h_f = \frac{\Delta p}{\rho g} = f\frac{L}{D}\frac{V^2}{2g} \Rightarrow h_f = f\frac{L}{D}\frac{Q^2}{A^2 2g} \Rightarrow h_f = \frac{8}{\pi^2 g}\frac{L}{D^5}fQ^2 \tag{6.11}$$

where h_f is the head loss due to friction.

From Eq. (6.11), the head loss due to friction is directly proportional to the pipe length and inversely proportional to the fifth-power of pipe diameter. This means that pressure drop is a very strong function of diameter. Narrow tubes will have higher pressure drop than larger diameter tubes. Due to this reason, the capillary tube is employed as an expansion device in low-capacity refrigeration systems.

For laminar flow in pipe, the friction factor is calculated using the equation derived during analysis of Hagen–Poiseuille flow in Chapter 4, that is,

$$f = \frac{64}{\text{Re}} \tag{4.149}$$

For turbulent flow, the friction factor is evaluated using the friction factor correlations mentioned in Table 6.1 and the Moody chart shown in Fig. 6.6.

Blasius correlation does not take into account the pipe's internal surface roughness and thus, its use is limited to only smooth pipes. The correlations

Table 6.1 Friction factor correlation models for turbulent flow

Researchers	**Friction factor correlations**	**Applicability**
Blasius	$f = \frac{0.316}{\text{Re}^{0.25}}$	Smooth pipes only
Colebrook	$\frac{1}{\sqrt{f}} = 1.14 - 2\log\left(\frac{e}{D} + \frac{9.3}{\text{Re}\sqrt{f}}\right)$	Both smooth and rough pipes
Churchill	$f = 8\left[\left(\frac{8}{\text{Re}}\right)^{12} + \left(\frac{1}{(A+B)^{1.5}}\right)\right]^{\frac{1}{12}}$ where $A = 2.457\ln\left(\frac{1}{(7/\text{Re})^{0.9} + 0.27(e/D)}\right)^{16}$ and $B = \left(\frac{37530}{\text{Re}}\right)^{16}$	Both smooth and rough pipes

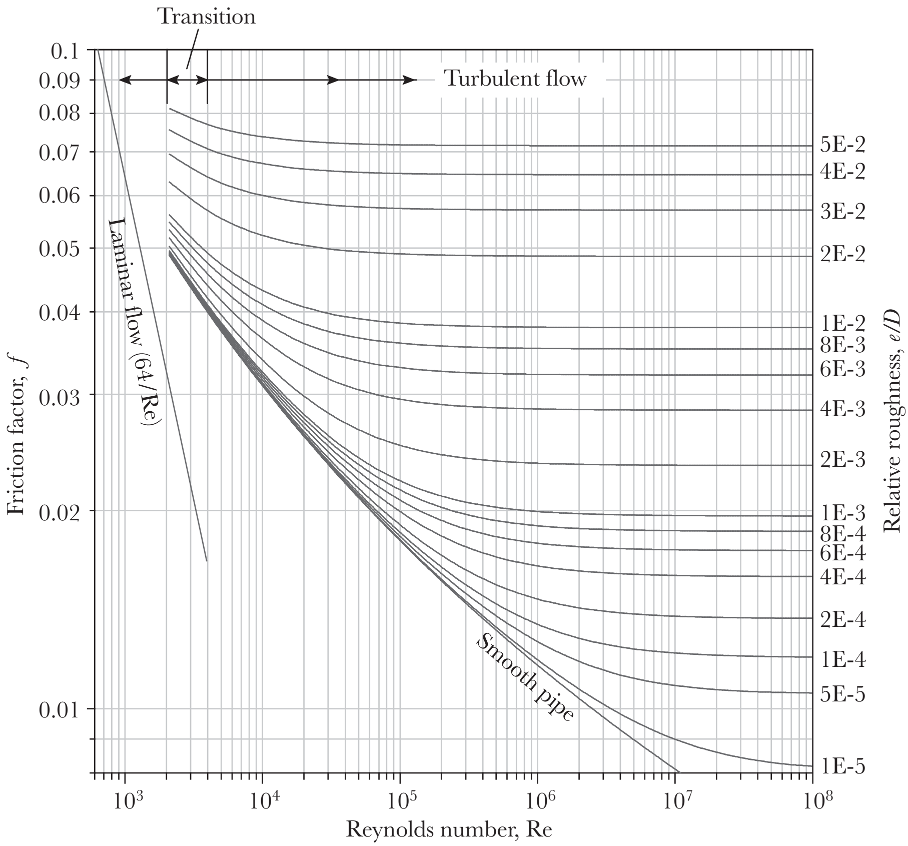

Fig. 6.6 Moody chart

by Colebrook and Churchill predict almost same value of friction factor. They are more versatile than Blasius correlation. These correlations are non-linear equations and their solution requires the knowledge of numerical techniques such as Newton–Raphson method and Bolzano bisection method.

The Moody chart, on the other hand, is simpler to use. It is a plot between the friction factor and the Reynolds number for different values of relative roughness. Both Moody chart and Colebrook equation are accurate within the error band of ±15%. In fact, the chart shown in Fig. 6.4 has been obtained by solving the Colebrook correlation for different Reynolds number and relative roughness values. The correlations mentioned in Table 6.1 and Moody chart can also be used for non-circular pipes by replacing diameter D with hydraulic or equivalent diameter given by

$$D_h = \frac{4A}{P} \tag{6.12}$$

where, A is the area of cross-section and P is the wetted perimeter of the cross-section.

Example 6.1 Determine the pressure loss across the honeycomb structure placed inside the wind tunnel having a square cross-section of side 60 cm, as shown in Fig. 6.7. The honeycomb structure consists of a large number of 15 cm long straws, each having 5 mm diameter. The flow velocity of air at the inlet is 2 m/s. Take viscosity and density of air 0.15 μPa-s and 1.2 kg/m^3, respectively and $f = 0.005$.

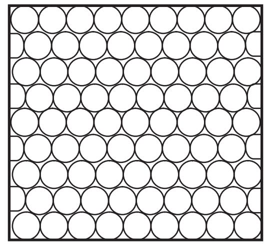

Fig. 6.7

Solution:

Side of wind tunnel, $B = 0.6$ m

Diameter of each straw, $d = 0.005$ m

Air velocity, $V = 2$ m/s

Width of honeycomb structure = length of straw, $L = 0.15$ m

Number of straws in a row/column = $B/d = 0.6/0.005 = 120$

Total number of straws in the honeycomb structure, $n = 120 \times 120 = 14{,}400$

Total pressure drop across the honeycomb structure is equal to pressure drop across each straw

$$\Delta p_f = \rho g h_f \quad \Rightarrow \quad \Delta p_f = f\frac{L}{d}\left(\frac{1}{2}\rho V^2\right) \quad \Rightarrow \quad \Delta p_f = 0.005 \times \frac{0.15}{0.005}\left(\frac{1}{2} \times 1.2 \times 2^2\right)$$

$$\Rightarrow \quad \Delta p_f = 0.36\,\text{Pa}$$

6.2.2 Minor Losses

The minor losses are the pressure losses associated with the following factors:

1. Loss due to sudden expansion
2. Exit loss
3. Loss due sudden contraction
4. Entry loss
5. Loss due to bends, fittings, etc.

Loss Due to Sudden Expansion

The sudden enlargement of a pipe section is shown in Fig. 6.8. As the fluid passes from section 1 and 2, it cannot follow the abrupt change in cross-section and flow

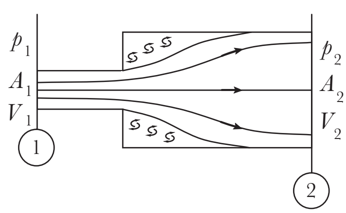

Fig. 6.8 Sudden expansion

separation takes place. The eddies will be formed as such in the separated region and a drop in pressure results. To find out the loss due to sudden expansion, apply momentum conservation equation between sections 1 and 2.

$$p_1A_1 + p'(A_2 - A_1) - p_2A_2 = \dot{m}(V_2 - V_1) \tag{6.13}$$

where p' is the pressure in separated region. Experimentally, it has been confirmed that the pressure in separated region is same as the pressure at section 1, that is, $p' = p_1$.

$$p_1 - p_2 = \frac{\dot{m}}{A_2}(V_2 - V_1) \tag{6.14}$$

From continuity equation,

$$\frac{\dot{m}}{A_2} = \rho V_2 \tag{6.15}$$

Equation (6.13) reduces to

$$p_1 - p_2 = \rho V_2(V_2 - V_1) \tag{6.16}$$

Applying Bernoulli's equation between sections 1 and 2

$$\frac{p_1}{\rho g} + \frac{V_1^2}{2g} + \cancel{z_1} = \frac{p_2}{\rho g} + \frac{V_2^2}{2g} + \cancel{z_2} + h_{Le} \tag{6.17}$$

where h_{Le} is the head loss due to sudden expansion.

The head loss due to friction is ignored as the length of pipe between sections 1 and 2 is very small and also the diameter is large at section 2.

The sudden expansion loss is, therefore, given by

$$h_{Le} = \frac{p_1 - p_2}{\rho g} + \frac{V_1^2 - V_2^2}{2g} \tag{6.18}$$

Substituting Eq. (6.16) in Eq. (6.18),

$$h_{Le} = \frac{V_2(V_2 - V_1)}{g} + \frac{V_1^2 - V_2^2}{2g} \tag{6.19}$$

Therefore, on simplification, the head loss due to sudden expansion is given by

$$\boxed{h_{Le} = \frac{(V_1 - V_2)^2}{2g}} \Rightarrow \boxed{h_{Le} = \frac{V_1^2}{2g}\left(1 - \frac{V_2}{V_1}\right)^2} \tag{6.20}$$

From the continuity equation, $A_1V_1 = A_2V_2$, the head loss due to sudden expansion can be expressed in terms of cross-sectional areas at sections 1 and 2.

$$\boxed{h_{Le} = \frac{V_1^2}{2g}\left(1 - \frac{A_1}{A_2}\right)^2} \quad \text{or} \quad \boxed{h_{Le} = k_e\frac{V_1^2}{2g}} \tag{6.21}$$

where k_e is the *sudden expansion loss factor*, which is given by

$$k_e = \left(1 - \frac{A_1}{A_2}\right)^2 \tag{6.22}$$

Figure 6.9 shows the variation of sudden expansion loss coefficient with the area ratio. It is clear from Eq. (6.22) that there exists a parabolic relation between the k_e and A_1/A_2.

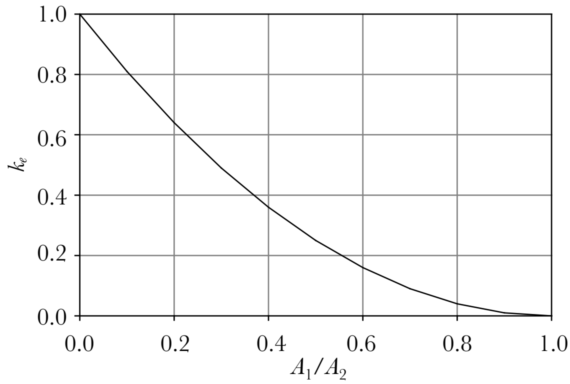

Fig. 6.9 k_e vs A_1/A_2

Example 6.2 In Fig. 6.10, the sudden change in pipe diameter from 20 to 40 cm causes the pressure of water to rise from 150 k to 200 kPa. Compute the discharge.

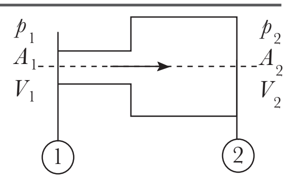

Fig. 6.10

Solution: Applying Bernoulli's equation between section 1 and 2,

$$\frac{p_1}{\rho g} + \frac{V_1^2}{2g} + \cancel{z_1} = \frac{p_2}{\rho g} + \frac{V_2^2}{2g} + \cancel{z_2} + h_{Le}$$

Substituting the loss due to sudden contraction expansion in this equation and rewriting

$$\frac{p_1 - p_2}{\rho g} = \frac{V_2^2 - V_1^2}{2g} + \frac{(V_1 - V_2)^2}{2g}$$

From the continuity equation $Q = A_1V_1 = A_2V_2$ and substituting the velocities in terms of discharge in this equation, we get

$$\frac{p_1 - p_2}{\rho g} = \frac{Q^2}{2g}\left[\left(\frac{1}{A_2^2} - \frac{1}{A_1^2}\right) + \left(\frac{1}{A_1} - \frac{1}{A_2}\right)^2\right] \tag{1}$$

The areas can be computed in following manner:

$$A_1 = \frac{\pi}{4} D_1^2 \quad \Rightarrow \quad A_1 = \frac{\pi}{4}(0.2)^2 \quad \Rightarrow \quad A_1 = 0.03141\ \text{m}^2$$

$$A_2 = \frac{\pi}{4} D_2^2 \quad \Rightarrow \quad A_2 = \frac{\pi}{4}(0.4)^2 \quad \Rightarrow \quad A_2 = 0.12566\ \text{m}^2$$

Substituting the values in Eq. (1) and simplifying

$$190.03Q^2 = 50 \quad \Rightarrow \quad Q = 0.513\ \text{m}^3/\text{s}$$

Exit Loss

The head loss at the pipe exit can be obtained from the expression for the head loss due to sudden expansion, (i.e., Eq. 6.21) making exit area A_2 as infinite.

$$\text{As} \quad A_2 \to \infty \quad \Rightarrow \quad A_1/A_2 \to 0 \quad \Rightarrow \quad k_e \to 1 \ \text{[from Eq. (6.22)]}$$

Thus, the exit loss is given by

$$h_{L,\text{exit}} = \frac{V_1^2}{2g} \tag{6.23}$$

Loss Due to Sudden Contraction

In a sudden contraction, shown in Fig. 6.11, the stream lines converge to form least cross-sectional area of flow immediately after the plane of sudden contraction. The area corresponding to the least flow cross-section is known *vena-contracta*. The loss due to sudden contraction is in fact the loss due to sudden expansion between *vena-contracta* and section 2. Since, the separated region is small as it is taking place in a smaller pipe, it is expected that the loss due to sudden contraction would be smaller than that of the sudden expansion for the same pipe assembly. Using the expression of head loss due to sudden expansion, the head loss due to sudden contraction is given by

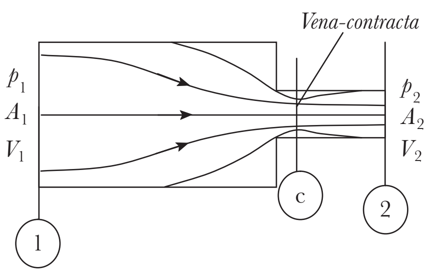

Fig. 6.11 Sudden contraction

$$h_{Lc} = \frac{(V_c - V_2)^2}{2g} \quad \Rightarrow \quad h_{Lc} = \frac{V_2^2}{2g}\left(\frac{V_c}{V_2} - 1\right)^2 \tag{6.24}$$

From the continuity equation, $A_c V_c = A_2 V_2$, the head loss due to sudden contraction can be expressed in terms of cross-sectional areas at sections *c* and 2.

$$h_{Lc} = \frac{V_2^2}{2g}\left(\frac{A_2}{A_c} - 1\right)^2 \tag{6.25}$$

where the ratio of cross-sectional area at *vena-contracta* to pipe's cross-sectional area is known as *contraction coefficient*, C_c, that is, A_c/A_2

$$\boxed{h_{Lc} = \frac{V_2^2}{2g}\left(\frac{1}{C_c} - 1\right)^2} \quad \Rightarrow \quad \boxed{h_{Lc} = k_c \frac{V_2^2}{2g}} \tag{6.26}$$

where k_c is the *sudden contraction loss factor*, which is given by

$$\boxed{k_c = \left(\frac{1}{C_c} - 1\right)^2} \tag{6.27}$$

However, from the expression for head loss due to sudden contraction, it seems as if the contraction loss is independent of the cross-sectional area of larger pipe, A_1. The amount of contraction of streamlines to form *vena-contracta* is strongly dependent upon the ratio of areas A_2/A_1, shown in Fig. 6.12. The smaller the ratio A_2/A_1, higher is the value of sudden contraction loss factor.

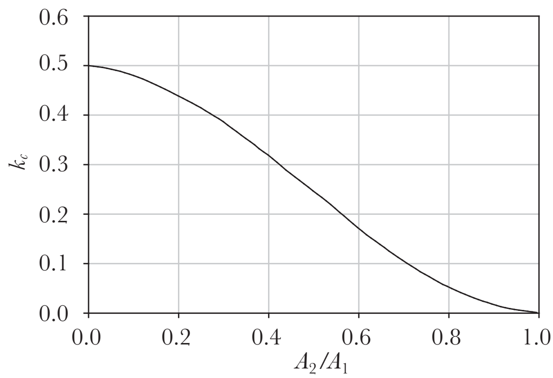

Fig. 6.12 k_c vs A_2/A_1

Example 6.3 In Fig. 6.13, the sudden change in pipe diameter from 40 cm to 20 cm causes the pressure of water to drop from 200 kPa to 150 kPa. Compute the discharge if contraction coefficient is 0.6.

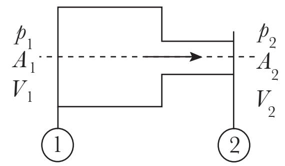

Fig. 6.13

Solution: Applying Bernoulli equation between section 1 and 2,

$$\frac{p_1}{\rho g}+\frac{V_1^2}{2g}+\cancel{z_1}=\frac{p_2}{\rho g}+\frac{V_2^2}{2g}+\cancel{z_2}+h_{Lc}$$

Substituting the loss due to sudden contraction in terms of contraction coefficient in this equation and rewriting it we get

$$\frac{p_1-p_2}{\rho g}=\frac{V_2^2-V_1^2}{2g}+\frac{V_2^2}{2g}\left(\frac{1}{C_c}-1\right)^2$$

From the continuity equation $Q = A_1V_1 = A_2V_2$ and substituting the velocities in terms of discharge in this equation, we get

$$\frac{p_1-p_2}{\rho g}=\frac{Q^2}{2g}\left[\left(\frac{1}{A_2^2}-\frac{1}{A_1^2}\right)+\frac{1}{A_2^2}\left(\frac{1}{C_c}-1\right)^2\right] \tag{1}$$

The areas can be computed in following manner:

$$A_1=\frac{\pi}{4}D_1^2 \quad\Rightarrow\quad A_1=\frac{\pi}{4}(0.4)^2 \quad\Rightarrow\quad A_1=0.12566\,\text{m}^2$$

$$A_2=\frac{\pi}{4}D_2^2 \quad\Rightarrow\quad A_2=\frac{\pi}{4}(0.2)^2 \quad\Rightarrow\quad A_2=0.03141\,\text{m}^2$$

Substituting the values in Eq. (1)

$$\frac{200-150}{1000}=\frac{Q^2}{2}\left[\left(\frac{1}{0.03141^2}-\frac{1}{0.12566^2}\right)+\frac{1}{0.03141^2}\left(\frac{1}{0.6}-1\right)^2\right]$$

$$700.38Q^2 = 50 \quad\Rightarrow\quad Q = 0.267\,\text{m}^3/\text{s}$$

Entry Loss

The entrance loss factor can be obtained from Fig. 6.12. The ratio of A_2/A_1 for entrance is taken zero as area at the inlet section A_1 is infinite. The corresponding k_c value is 0.5. Thus, the head loss at the pipe entry is given by

$$h_{L,\text{entry}}=0.5\frac{V_2^2}{2g} \tag{6.28}$$

Losses in Pipe Fittings

Fittings are employed in a pipe network to connect pipes of different shapes and sizes. For example, straight, elbow (bend), tee, connectors, couplings, etc. Some fittings also serve special purpose of measuring and controlling the flow in a pipeline such as valves, orifices, and nozzles. Figure 6.14 shows different types of fittings.

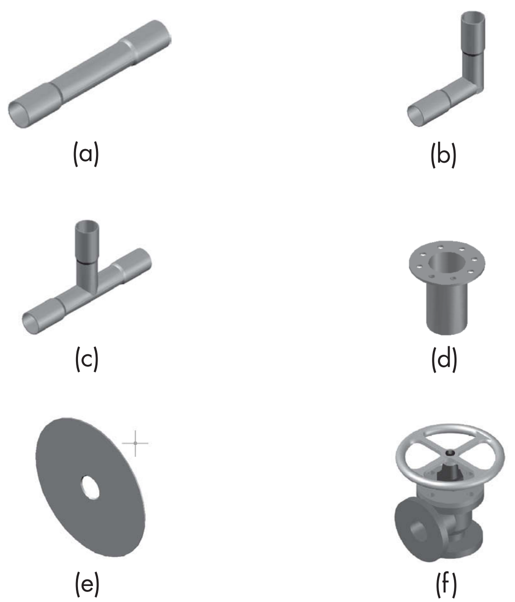

Fig. 6.14 Various types of fittings (a) Straight connector (b) Elbow connector (c) Tee connector (d) Flange (e) Orifice plate (f) Stop valve

The losses across the valves and fittings can be computed in terms of equivalent friction pressure loss in a pipe of given length L and diameter D, that is,

$$h_L = k\frac{V^2}{2g} \tag{6.29}$$

where resistance coefficient k is given by

$$k = f\frac{L_e}{D} \tag{6.30}$$

where L_e is the equivalent length of pipe having same resistance as that of the fitting/valve, D is the pipe diameter, and f is the friction is friction factor. The L_e/D ratio is assigned a particular value to a particular type of fitting.

Example 6.4 Water flows at a rate of 170 L/s through a bend meter, shown in Fig. 6.15. The diameter of bend is 150 mm and pressure drop across it is 300 mm of Hg. Determine the resistance coefficient of the bend.

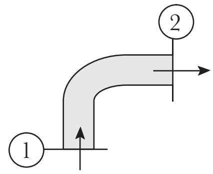

Fig. 6.15

Solution:

Given data:

$Q = 170$ L/s $= 0.17$ m³/s

$$p_1 - p_2 = 0.3 \times 13.6 \times 10^3 \times 9.81 = 40024.8\,\text{Pa},$$

$D = 150\,\text{mm} = 0.15\,\text{m}$

$$A = \frac{\pi}{4}D^2 \quad \Rightarrow \quad A = \frac{\pi}{4}(0.15)^2 \quad \Rightarrow \quad A = 0.01767\,\text{m}^2$$

The head loss across the bend

$$h_L = \frac{p_1 - p_2}{\rho g} \quad \Rightarrow \quad h_L = \frac{40024.8}{1000 \times 9.81} \quad \Rightarrow \quad h_L = 4.08\,\text{m}$$

The head loss across a fitting can always be expressed in terms of resistance coefficient and velocity head.

$$h_L = k\frac{V^2}{2g} \quad \Rightarrow \quad h_L = k\frac{(Q/A)^2}{2g}$$

Therefore, the resistance coefficient for the bend

$$k = \frac{2gh_L}{(Q/A)^2} \quad \Rightarrow \quad k = \frac{2 \times 9.81 \times 4.08}{(0.17/0.01767)^2} \quad \Rightarrow \quad k = 0.865$$

6.3 PIPE NETWORKS

The pipe network problems can be solved easily by drawing an analogy from electrical circuitry. Figure 6.16 shows a simple pipe network consisting of two tanks connected by a pipe of length L and diameter D. The difference in water level in two tanks is ΔH and discharge through the pipe is Q.

Applying Bernoulli's equation between sections 1 and 2

$$\frac{p_1}{\rho g} + \frac{V_1^2}{2g} + (z_1 + H_1) = \frac{p_2}{\rho g} + \frac{V_2^2}{2g} + (z_2 + H_2) + h_{L,\text{entry}} + h_f + h_{L,\text{exit}} \qquad (6.31)$$

The velocity of free surface of water in the two tanks will be small as the cross-sectional areas of the two tanks are large as compared to the pipe cross-sectional

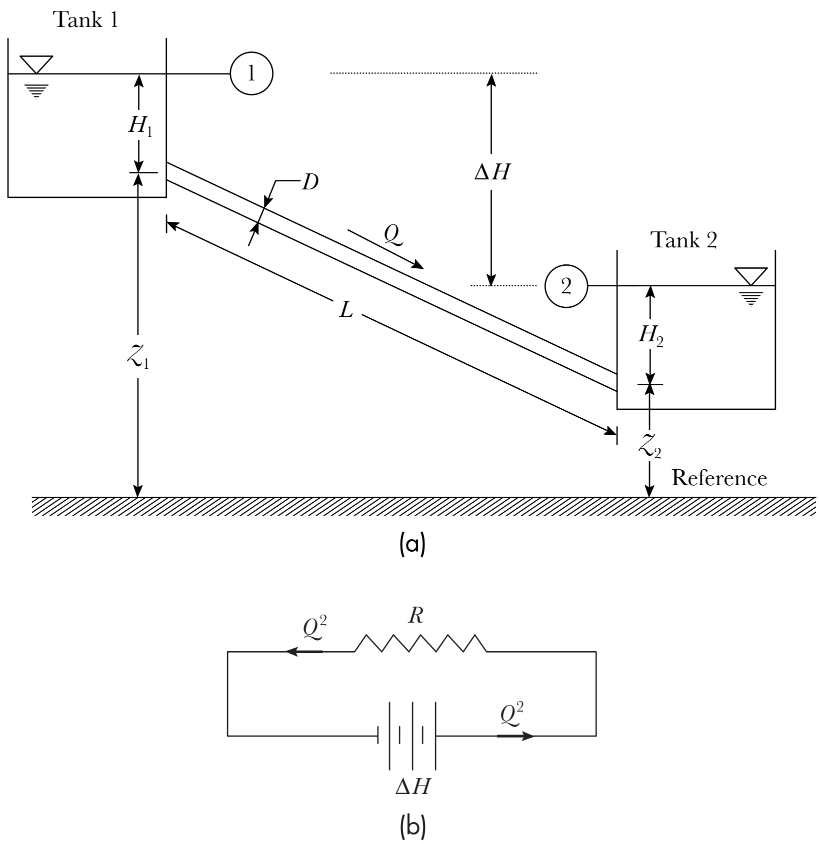

Fig. 6.16 Pipe network (a) Schematic diagram (b) Equivalent electric circuit

area, that is, $V_1 = V_2 = 0$. Further, the pressure at the free surface is same, that is, $p_1 = p_2 = p_{\text{atm.}}$

$$\Delta H = h_{L,\text{entry}} + h_f + h_{L,\text{exit}} \tag{6.32}$$

$$\Delta H = \left(0.5 + f\frac{L}{D} + 1\right)\frac{V^2}{2g} \tag{6.33}$$

The average velocity V inside the pipe can be expressed in terms of discharge per unit pipe's cross-sectional area

$$\Delta H = \left(1.5 + f\frac{L}{D}\right)\frac{Q^2}{A^2 2g} \tag{6.34}$$

$$\Delta H = \left[\frac{8}{\pi^2 D^4 g}\left(1.5 + f\frac{L}{D}\right)\right]Q^2 \tag{6.35}$$

The quantity in the bracket is a constant quantity and is termed *pipe resistance*.

$$\Delta H = RQ^2 \tag{6.36}$$

Equation (6.36) is analogous to the Ohm's law, where the difference in levels of two tanks ΔH is analogous to the potential difference and Q^2 is analogous to current. This equation is also known as *friction equation*.

6.3.1 Pipes in Series

The pipes of different diameters and lengths when joined together coaxially, are said to be connected in series. One such assembly is shown in Fig. 6.17(a), where three pipes are connected in series. The total head H at a point in a pipe network is the algebraic sum of pressure, velocity and potential heads, which is constant as per Bernoulli's equation, that is,

$$H = \frac{p}{\rho g} + \frac{V^2}{2g} + z \tag{6.37}$$

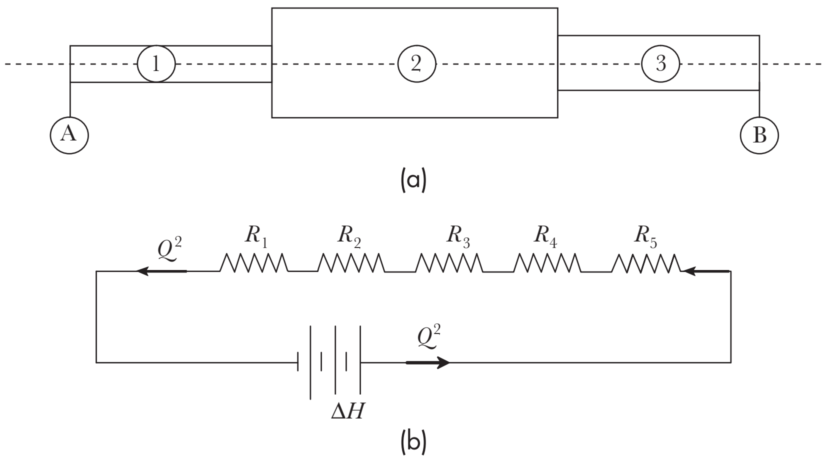

Fig. 6.17 (a) Assembly of pipes in series (b) Equivalent electrical circuit

If H_A and H_B are the total heads at sections A and B, respectively, their difference is equal to the total losses between them in the pipe network.

$$H_A - H_B = h_L \tag{6.38}$$

where h_L is the total loss, which includes all the minor and major losses in the network.

The total head loss

$$h_L = h_{f1} + h_{L,e(1\to2)} + h_{f2} + h_{L,c(2\to3)} + h_{f3} \tag{6.39}$$

Where, $h_f = f\dfrac{L}{D}\dfrac{V^2}{2g} \Rightarrow h_f = \dfrac{8}{\pi^2 g} f \dfrac{L}{D^5}Q^2$

$$h_{L,e(1\to2)} = \frac{(V_1 - V_2)^2}{2g} \Rightarrow h_{L,e(1\to2)} = \frac{8}{\pi^2 D_1^4 g}\left(1 - \frac{D_1^2}{D_2^2}\right)^2 Q^2$$

$$h_{L,\,c(2\to3)} = k\frac{V_3^2}{2g} \Rightarrow h_{L,\,c(2\to3)} = \frac{8}{\pi^2 D_3^4 g}kQ^2$$

$$h_L = \frac{8}{\pi^2 g}\left(f_1\frac{L_1}{D_1^5} + f_2\frac{L_2}{D_2^5} + f_3\frac{L_3}{D_3^5} + \frac{1}{D_1^4}\left(1 - \frac{D_1^2}{D_2^2}\right)^2 + \frac{k}{D_3^4}\right)Q^2 \tag{6.40}$$

Equation (6.40) can be written in terms of resistances and the same is shown in Fig. 6.17(b).

$$\Delta H = (R_1 + R_2 + R_3 + R_4 + R_5)Q^2 \tag{6.41}$$

Therefore, the equivalent resistance is given by

$$R = R_1 + R_2 + R_3 + R_4 + R_5 \tag{6.42}$$

This shows that three pipes connected in series is analogous to an electrical circuit with five resistances connected in series, out of which three resistances are due to friction losses and the other two resistances due to sudden expansion and sudden contraction, respectively.

Example 6.5 Two water tanks are connected by three pipes in series of diameter 100 mm, 150 mm, and 200 mm respectively. Each pipe has a length of 100 m. If the difference in the water levels of the two tanks is 50 m, compute the discharge through them. Find out the percentage error in discharge if minor losses are ignored. Assume friction factor $f = 0.03$.

Solution: The total head losses in a pipe are equal to the available head. Let us consider all the major and minor losses to determine the discharge through the pipes.

$$0.5\frac{V_1^2}{2g} + f\frac{L_1}{D_1}\frac{V_1^2}{2g} + \frac{(V_1 - V_2)^2}{2g} + f\frac{L_2}{D_2}\frac{V_2^2}{2g} + \frac{(V_2 - V_3)^2}{2g} + f\frac{L_3}{D_3}\frac{V_3^2}{2g} + \frac{V_3^2}{2g} = 50$$

$$\frac{16Q^2}{2g\pi^2}\left(\frac{0.5}{D_1^4}+f\frac{L_1}{D_1^5}+\left(\frac{1}{D_1^2}-\frac{1}{D_2^2}\right)^2+f\frac{L_2}{D_2^5}+\left(\frac{1}{D_2^2}-\frac{1}{D_3^2}\right)^2+f\frac{L_3}{D_3^5}+\frac{1}{D_3^4}\right)=50$$

$$\frac{16Q^2}{2g\pi^2}\left(\frac{0.5}{0.1^4}+0.03\times\frac{100}{0.1^5}+\left(\frac{1}{0.1^2}-\frac{1}{0.15^2}\right)^2+0.03\times\frac{100}{0.15^5}\right.$$

$$\left.+\left(\frac{1}{0.15^2}-\frac{1}{0.2^2}\right)^2+0.03\times\frac{100}{0.2^5}+\frac{1}{0.2^4}\right)=50$$

$$\frac{16Q^2}{2g\pi^2}(5000+300000+3086.4+39506.2+378.1+9375+625)=50$$

$$29578Q^2=50 \quad\Rightarrow\quad Q=0.04111\,\text{m}^3/\text{s}$$

Ignoring minor losses, the discharge may be computed in the following manner:

$$f\frac{L_1}{D_1}\frac{V_1^2}{2g}+f\frac{L_2}{D_2}\frac{V_2^2}{2g}+f\frac{L_3}{D_3}\frac{V_3^2}{2g}=50$$

$$\frac{16Q^2}{2g\pi^2}(300000+39506.2+9375)=50$$

$$28827Q^2=50 \quad\Rightarrow\quad Q=0.04165\,\text{m}^3/\text{s}$$

The percentage error due to non-consideration of minor losses,

$$\text{error }(\%)=\frac{0.04165-0.04111}{0.04111}\times 100 \quad\Rightarrow\quad \text{error }(\%)=1.31$$

NOTES

(a) *Increasing the diameter from 100 to 200 mm causes the reduction in friction head loss tremendously, that is, from 3,00,000 to 9375 m.*

(b) *Non-consideration of minor losses results in slight overestimation in discharge by 1.31%.*

6.3.2 Pipes in Parallel

Figure 6.18 shows three pipes connected in parallel. Each pipe in the circuit will be operated under the same potential difference between points A and B. In this case, as per the continuity equation total discharge will be divided among three pipes, that is,

$$Q=Q_1+Q_2+Q_3 \tag{6.43}$$

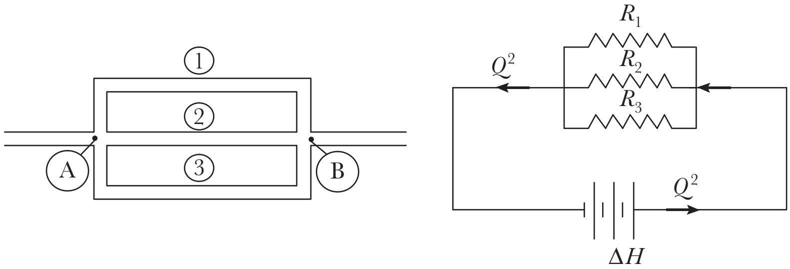

Fig. 6.18 Assembly of (a) Pipes in parallel (b) Equivalent electrical circuit

The application of Bernoulli's equation between points A and B gives the following:

For pipe 1: $$H_A - H_B = \frac{8}{\pi^2 g} f_1 \frac{L_1}{D_1^5} Q_1^2 \Rightarrow H_A - H_B = R_1 Q_1^2 \tag{6.44}$$

For pipe 2: $$H_A - H_B = \frac{8}{\pi^2 g} f_2 \frac{L_2}{D_2^5} Q_2^2 \Rightarrow H_A - H_B = R_2 Q_2^2 \tag{6.45}$$

For pipe 3: $$H_A - H_B = \frac{8}{\pi^2 g} f_3 \frac{L_3}{D_3^5} Q_3^2 \Rightarrow H_A - H_B = R_3 Q_3^2 \tag{6.46}$$

The bend losses have been ignored in Eqs (6.44) and (6.46) for pipes 1 and 3.

If the parallel pipe circuit is to be replaced by an equivalent pipe, then using Eqs (6.44–6.46) in the continuity equation:

$$\sqrt{\frac{H_A - H_B}{R}} = \sqrt{\frac{H_A - H_B}{R_1}} + \sqrt{\frac{H_A - H_B}{R_2}} + \sqrt{\frac{H_A - H_B}{R_3}} \tag{6.47}$$

The equivalent resistance is

$$\boxed{\frac{1}{\sqrt{R}} = \frac{1}{\sqrt{R_1}} + \frac{1}{\sqrt{R_2}} + \frac{1}{\sqrt{R_3}}} \tag{6.48}$$

Example 6.6 A 15 m long and 100 mm diameter pipe is connected to a 10 m long and 150 mm diameter pipe in parallel as shown in Fig. 6.19. A valve is fixed on larger diameter pipe and is adjusted to equalize the discharge in two pipes. Determine valve loss coefficient, if all other minor losses are ignored. Assume friction factor $f = 0.01$.

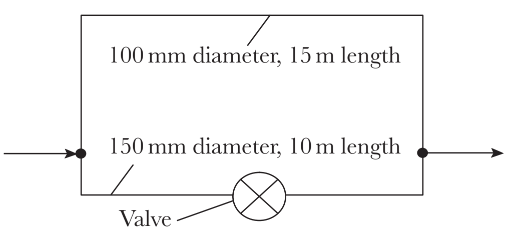

Fig. 6.19

Solution: The head loss due to valve fitting is given by

$$h_{Lv} = k_v \frac{V^2}{2g}$$

where k_v is the valve loss coefficient.

For the pipes connected in parallel, the head losses in each pipe must be same.

$$f\frac{L_1}{D_1}\frac{V_1^2}{2g} = f\frac{L_2}{D_2}\frac{V_2^2}{2g} + k_v\frac{V_2^2}{2g} \tag{1}$$

It is given that discharge is same in each pipe, that is, $Q = A_1V_1 = A_2V_2$. Equation (1) can be written as

$$\frac{16\cancel{Q^2}}{\cancel{\pi^2}\,2g} f\frac{L_1}{D_1^5} = \frac{16\cancel{Q^2}}{\cancel{\pi^2}\,2g}\left(f\frac{L_2}{D_2^5} + k_v\frac{1}{D_2^4}\right)$$

$$k_v = D_2^4 f\left(\frac{L_1}{D_1^5} - \frac{L_2}{D_2^5}\right)$$

$$k_v = 0.01 \times 0.15^4\left(\frac{15}{0.1^5} - \frac{10}{0.15^5}\right) \Rightarrow k_v = 7.49$$

6.3.3 Hardy Cross Method

This method was proposed by Hardy Cross, a Professor of Structural Engineering at the University of Illinois at Urbana-Champaign in 1936. The Hardy Cross method is an iterative technique for determining discharges in individual pipes of a pipe network if the input and output discharge of the pipe network (Fig. 6.20) are known. The following steps are involved in the method:

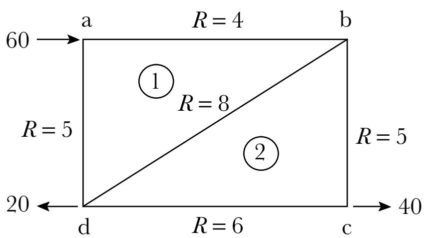

Fig. 6.20 Pipe network

1. Usually, the resistance R is known for individual pipes in a network. The discharge in each pipe is assumed.
2. The algebraic sum of discharges at any junction must be zero, that is, continuity equation must be satisfied at each junction, which is analogous to Kirchhoff's current law (KCL)

$$\boxed{\sum Q = 0} \tag{6.49}$$

3. The algebraic sum of heads (potential, i.e., RQ^2) must be zero in a loop (hydraulic circuit), which is analogous to Kirchhoff's voltage law (KVL)

$$\sum R|Q|Q = 0 \tag{6.50}$$

The absolute value of Q has been used to take into account the direction of flow in an individual pipe in the network. As per the friction equation $\sum RQ^2$ will never be zero.

4. Friction equation must be satisfied for each pipe.
5. The value of head at any point in the network will be unique.

If Q_o is the corrected discharge in a pipe and Q is the assumed discharge, the error in discharge dQ is then defined as

$$Q = Q_o + dQ \tag{6.51}$$

From the friction equation, let us assume

$$H = R|Q|Q \tag{6.52}$$

and $$H' = R|Q_o|Q_o \tag{6.53}$$

From the KVL,

$$\sum H = e \tag{6.54}$$

and $$\sum H' = 0 \tag{6.55}$$

Subtracting Eq. (6.55) from Eq. (6.54)

$$\sum (H - H') = e \tag{6.56}$$

or $$\sum dH = e \tag{6.57}$$

Differentiating Eq. (6.52)

$$\sum dH = \sum 2R|Q|dQ \tag{6.58}$$

From Eqs (6.57) and (6.58),

$$dQ = \frac{e}{\sum 2R|Q|} \tag{6.59}$$

Finally from Eqs (6.52) and (6.59), the error in discharge is given by

$$dQ = \frac{\sum R|Q|Q}{\sum 2R|Q|} \tag{6.60}$$

Equation (6.60) is used to find out the corrected discharge at the beginning of each iteration. Hardy Cross method has been demonstrated for the simple pipe network in following example.

Example 6.7 Determine the discharge in each branch of the pipe network shown in Fig. 6.21.

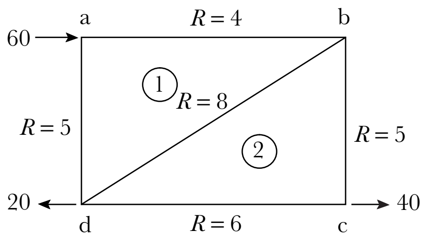

Fig. 6.21 Pipe network

Solution: To solve the pipe networking problem, the first step is to assume the discharge in each branch in such a way that KCL (or continuity) holds good at each junction.

Initialization

$$Q_{ab} = 40$$
$$Q_{ad} = 20$$
$$Q_{bd} = 15$$
$$Q_{bc} = 25$$
$$Q_{cd} = 15$$

Iteration 1

Loop 1			Loop 2		
Pipe	$R\lvert Q\rvert Q$	$2R\lvert Q\rvert$	**Pipe**	$R\lvert Q\rvert Q$	$2R\lvert Q\rvert$
ab	4×40^2	$2 \times 4 \times 40$	bc	5×25^2	$2 \times 5 \times 25$
bd	8×15^2	$2 \times 8 \times 15$	cd	-6×15^2	$2 \times 6 \times 15$
da	-5×20^2	$2 \times 5 \times 20$	db	-8×15^2	$2 \times 8 \times 15$
	$\Sigma = 620$	$\Sigma = 760$		$\Sigma = -25$	$\Sigma = 670$
$dQ = 6200/760 = 8.1579$			$dQ = -25/670 = -0.0373$		

The following points are to be remembered before going to the next iteration:

1. To obtain the corrected values of discharge in each branch for the next iteration, the error in discharge dQ is *subtracted* from the discharge in previous iteration while moving *in the direction of flow* in a loop whereas dQ is *added* to the discharge in previous iteration while moving *against the flow* in a loop.
2. In the common branch, net error is to be used for the calculation of discharge.

On the basis of these points, the corrected values of discharge in each branch of the pipe network for the next iteration are computed as under:

$$Q_{ab} = 40 - 8.1579 = 31.8421$$
$$Q_{ad} = 20 + 8.1579 = 28.1579$$

$$Q_{bd} = 15 - [8.1579 - (-0.0373)] = 6.8048$$
$$Q_{bc} = 25 - (-0.0373) = 25.0373$$
$$Q_{cd} = 15 + (-0.0373) = 14.9627$$

Iteration 2

Loop 1			Loop 2		
Pipe	$R\|Q\|Q$	$2R\|Q\|$	**Pipe**	$R\|Q\|Q$	$2R\|Q\|$
ab	4×31.8421^2	$2 \times 4 \times 31.8421$	bc	5×25.0373^2	$2 \times 5 \times 25.0373$
bd	8×6.8048^2	$2 \times 8 \times 6.8048$	cd	-6×14.9627^2	$2 \times 6 \times 14.9627$
da	-5×28.1579^2	$2 \times 5 \times 28.1579$	db	-8×6.8048^2	$2 \times 8 \times 6.8048$
	$\sum = 461.78$	$\sum = 645.19$		$\sum = 1420.59$	$\sum = 538.80$
$dQ = 461.78/645.19 = 0.7157$			$dQ = 1420.59/538.8 = 2.6366$		

Corrected values for next iteration are

$$Q_{ab} = 31.8421 - 0.7157 = 31.1264$$
$$Q_{ad} = 28.1579 + 0.7157 = 28.8736$$
$$Q_{bd} = 6.8048 - (0.7157 - 2.6366) = 8.7257$$
$$Q_{bc} = 25.0373 - 2.6366 = 22.4007$$
$$Q_{cd} = 14.9627 + 2.6366 = 17.5993$$

A computer code has been developed to compute the final values of discharge with the acceptable error in the discharge $e = 1 \times 10^{-6}$ (the convergence criteria). The results of the program are shown in given table.

Iterations	Q_{ab}	Q_{ad}	Q_{bd}	Q_{bc}	Q_{cd}
1.	40.000000	20.000000	15.000000	25.000000	15.000000
2.	31.842105	28.157895	6.804792	25.037313	14.962687
3.	31.126373	28.873627	8.725653	22.400720	17.599280
4.	30.659753	29.340247	8.331156	22.328597	17.671403
5.	30.643240	29.356760	8.427007	22.216233	17.783767
6.	30.620893	29.379107	8.408369	22.212525	17.787475
7.	30.620147	29.379853	8.412903	22.207244	17.792756
8.	30.619092	29.380908	8.412023	22.207069	17.792931
9.	30.619057	29.380943	8.412237	22.206820	17.793180
10.	30.619007	29.380993	8.412196	22.206811	17.793189
11.	30.619006	29.380994	8.412206	22.206800	17.793200
12.	30.619003	29.380997	8.412204	22.206799	17.793201

6.3.4 Branching Pipes

In a pipe network, a junction is formed when three or more pipe branches are joined at a point. This type of network is usually seen in water distribution system in a locality. Figure 6.22 shows a three-reservoir system, which is the simplest of all branching pipe networks. Each reservoir is located at a different elevation. The objective is to determine the magnitude and direction of flow in each pipe. As discussed earlier, the flow through a pipe is analogous to the electrical current flowing through a wire following Ohm's law where Q^2 is equivalent to current and ΔH to potential difference. The pipe resistance is equal to the major frictional pressure loss obtained from Darcy–Weisbach equation.

$$\boxed{\Delta H = RQ^2} \quad \text{where} \quad R = \frac{8fL}{\pi^2 D^5 g} \tag{6.61}$$

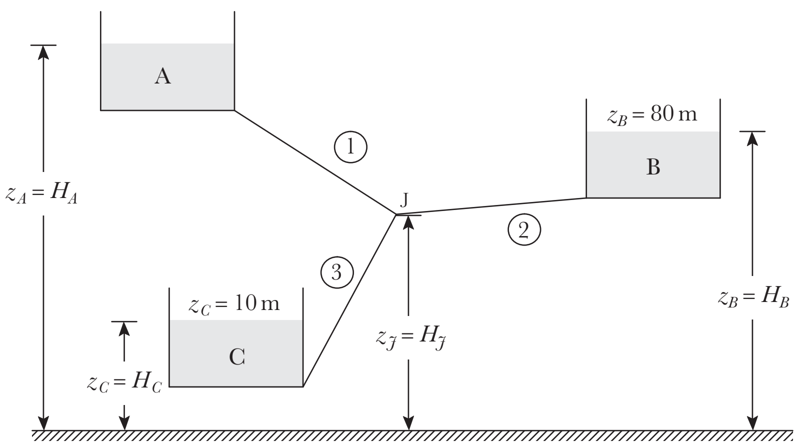

Fig. 6.22 Three reservoir system

At the junction, the KCL must be satisfied, that is, the flow into the junction must be equal to the flow out of the junction. The following methodology is adopted to deal with pipe branching problem shown in Fig. 6.22.

Let us first define the ratios: $\phi = \dfrac{H_A - H_B}{H_B - H_C}$ and $\gamma = \dfrac{R_1}{R_3}$

1. If $\phi > \gamma$, the junction will lie above the free surface of tank B, that is, $H_J > H_B$ and the flow will take place from tank A into the other two tanks, that is, $Q_1 = Q_2 + Q_3$
2. If $\phi < \gamma$, the junction will lie below the free surface of tank B, that is, $H_J < H_B$ and the flow will take place from tank A and tank B into tank C, that is, $Q_1 + Q_2 = Q_3$

The aforementioned method is applicable to three-reservoir systems only.

Example 6.8 Determine the discharge in each branch of the pipe network shown in Fig. 6.23. Assume same friction factor $f = 0.03$ in each pipe.

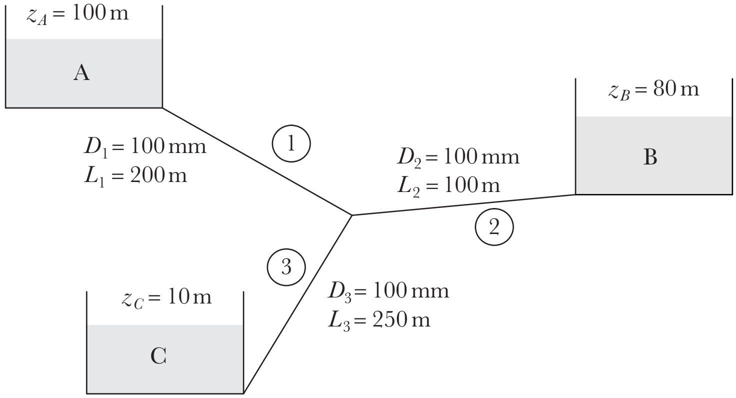

Fig. 6.23

Solution: Let us first check the position of junction with respect to free surface of tank B. Calculating

$$\phi = \frac{H_A - H_B}{H_B - H_C} \Rightarrow \phi = \frac{100-80}{80-10} \Rightarrow \phi = 0.286$$

$$\gamma = \frac{R_1}{R_3} \Rightarrow \gamma = \frac{8f_1L_1}{\pi^2 D_1^5 g} \Bigg/ \frac{8f_3L_3}{\pi^2 D_3^5 g} \Rightarrow \gamma = \frac{L_1}{L_3} \Rightarrow \gamma = 0.8$$

Since $\phi < \gamma$, $Q_1 + Q_2 = Q_3$ (continuity)

Since the diameters of all the three pipes are same, this equation reduces to

$$V_1 + V_2 = V_3 \qquad (1)$$

Applying Bernoulli's equation between the free surfaces of tank A and tank C

$$\underbrace{\cancel{\frac{p_A}{\rho g}}}_{0} + \underbrace{\cancel{\frac{V_A^2}{2g}}}_{0} + z_A = \underbrace{\cancel{\frac{p_C}{\rho g}}}_{0} + \underbrace{\cancel{\frac{V_C^2}{2g}}}_{0} + z_c + f_1 \frac{L_1}{D_1}\frac{V_1^2}{2g} + f_3 \frac{L_3}{D_3}\frac{V_3^2}{2g}$$

$$z_A - z_C = f_1 \frac{L_1}{D_1}\frac{V_1^2}{2g} + f_3 \frac{L_3}{D_3}\frac{V_3^2}{2g}$$

$$0.03 \times \frac{200}{0.1} \times \frac{V_1^2}{2 \times 9.81} + 0.03 \times \frac{250}{0.1} \times \frac{V_3^2}{2 \times 9.81} = 90$$

$$4V_1^2 + 5V_3^2 = 117.72 \qquad (2)$$

Again applying Bernoulli's equation between the free surfaces of tank B and tank C

$$\underbrace{\cancel{\frac{p_B}{\rho g}}}_{0} + \underbrace{\cancel{\frac{V_B^2}{2g}}}_{0} + z_B = \underbrace{\cancel{\frac{p_C}{\rho g}}}_{0} + \underbrace{\cancel{\frac{V_C^2}{2g}}}_{0} + z_c + f_2 \frac{L_2}{D_2}\frac{V_2^2}{2g} + f_3 \frac{L_3}{D_3}\frac{V_3^2}{2g}$$

$$z_B - z_C = f_2 \frac{L_2}{D_2}\frac{V_2^2}{2g} + f_3 \frac{L_3}{D_3}\frac{V_3^2}{2g}$$

$$0.03 \times \frac{100}{0.1} \times \frac{V_2^2}{2 \times 9.81} + 0.03 \times \frac{250}{0.1} \times \frac{V_3^2}{2 \times 9.81} = 70$$

$$2V_2^2 + 5V_3^2 = 91.56 \tag{3}$$

Eliminating V_3 by subtracting Eq. (3) from Eq. (2),

$$2V_1^2 - V_2^2 = 13.08 \quad \Rightarrow \quad V_2 = \sqrt{2V_1^2 - 13.08} \tag{4}$$

Substituting V_3 in Eq. (2) from Eq. (1),

$$4V_1^2 + 5(V_1 + V_2)^2 = 117.72 \tag{5}$$

From Eqs (4) and (5)

$$4V_1^2 + 5\left(V_1 + \sqrt{2V_1^2 - 13.08}\right)^2 = 117.72$$

$$\Rightarrow \quad 161V_1^4 - 5650.56V_1^2 + 33532.93 = 0$$

$$\Rightarrow \quad V_1^2 = 27.53 \quad \text{or} \quad V_1^2 = 7.56$$

$$\Rightarrow \quad V_1 = 5.24\,\text{m/s} \quad \text{or} \quad V_1 = 2.75\,\text{m/s} \;\; \text{(negative values are discarded)}$$

If $V_1 = 5.24\,\text{m/s}$ is extraneous root, which results in violation of continuity, then the correct root is $V_1 = 2.75\,\text{m/s}$. The other two velocities are found out using Eqs (2) and (1) as $V_3 = 9.35\,\text{m/s}$ and $V_2 = 6.60\,\text{m/s}$.

Therefore, the discharge in each pipe is obtained by multiplying the respective velocities with the pipe cross-sectional area ($0.007854\,\text{m}^2$).

$$Q_1 = 0.0216\,\text{m}^3/\text{s}$$

$$Q_2 = 0.0519\,\text{m}^3/\text{s}$$

$$Q_3 = 0.0734\,\text{m}^3/\text{s}$$

6.4 HYDRAULIC AND ENERGY GRADE LINES

The concept of *hydraulic grade line* (HGL) and *energy grade line* (EGL) or *total energy line* (TEL) is employed for graphical representation of mechanical energy level at any point in a pipe network. The EGL represents the summation of pressure head ($p/\rho g$), velocity head ($V^2/\rho g$) and datum head (z) at a point whereas HGL is the summation of pressure and datum head only. Thus, the vertical distance between the EGL and HGL represents the velocity or dynamic head. Figure 6.24 shows two tanks connected by three pipes in series. The EGL represents the change in total energy along the length of the pipe and the HGL represents the changes in the sum of pressure and datum (which is decreasing in the direction of flow in the present case) along the length of the pipe. The pressure due to friction varies linearly along the length of pipe [as per Darcy–Weisbach Eq. (6.10)].

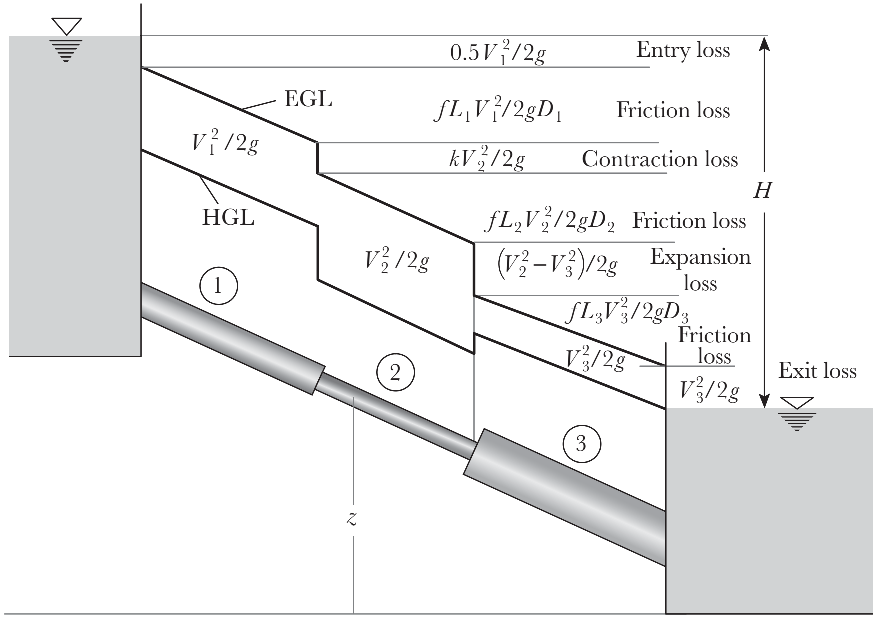

Fig. 6.24 Demonstration of HGL and EGL

From Eq. (6.11), the frictional pressure drop is inversely proportional to fifth power of pipe diameter. Thus, the pressure drop due to friction is more in smaller diameter pipe compared to larger diameter pipe of same length. The slope of the frictional pressure drop line will be more in smaller diameter pipe (not visible in Fig. 6.24). In addition to it, the slope of EGL or HGL will also be influenced by the datum or potential head.

In the present case, datum head is decreasing at a constant rate in the flow direction. At the joints, loss due to sudden contraction (between 1 and 2)/ expansion (between 2 and 3) causes the pressure to drop instantly. It should be noted that reduction in pipe diameter causes the velocity to increase and pressure to decrease. Similarly, an increase in pipe diameter causes the velocity to decrease and pressure to increase. This is in accordance to the Bernoulli's principle. The sudden jump and sudden fall in the HGL is due to this effect. The available head H (difference in the water level in two tanks) must be equal to the sum of all the losses, as shown in Fig. 6.24.

Example 6.9 Determine the discharge of water through the horizontal pipe connected to a tank, shown in Fig. 6.25. The friction factor is 0.04 and contraction coefficient is 0.62. Draw the HGL and EGL.

Solution: The datum head is constant throughout as the pipe is horizontal, hence there won't be any effect of datum head.

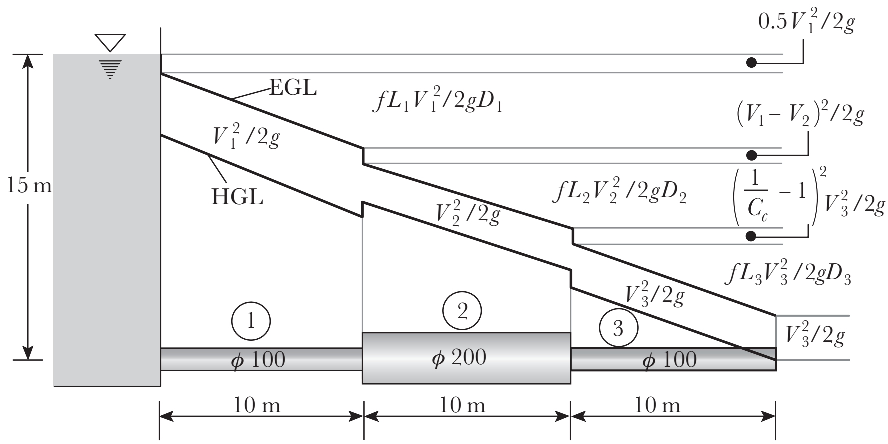

Fig. 6.25

The available head must be equal to the total losses in a pipe network, that is,

$$15 = 0.5\frac{V_1^2}{2g} + f\frac{L_1}{D_1}\frac{V_1^2}{2g} + \frac{(V_1 - V_2)^2}{2g} + f\frac{L_2}{D_2}\frac{V_2^2}{2g} + \left(\frac{1}{C_c} - 1\right)^2\frac{V_3^2}{2g} + f\frac{L_3}{D_3}\frac{V_3^2}{2g} + \frac{V_3^2}{2g}$$

$$15 = \frac{16Q^2}{2g\pi^2}\left(\frac{0.5}{D_1^4} + f\frac{L_1}{D_1^5} + \left(\frac{1}{D_1^2} - \frac{1}{D_2^2}\right)^2 + f\frac{L_2}{D_2^5} + \left(\frac{1}{C_c} - 1\right)^2\frac{1}{D_3^4} + f\frac{L_3}{D_3^5} + \frac{1}{D_3^4}\right)$$

$$15 = \frac{16Q^2}{2\times 9.81\times \pi^2}(5000 + 40000 + 5625 + 1250 + 3756.50 + 40000 + 10000)$$

$$Q^2 = 1.7186\times 10^{-3} \quad \Rightarrow \quad Q = 41.456\times 10^{-3}\ \text{m}^3\text{/s}$$

From continuity, $Q = A_1V_1 = A_2V_2 = A_3V_3$.

The flow velocity in each pipe is

$$V_1 = Q/A_1 \quad \Rightarrow \quad V_1 = \frac{4\times 0.041456}{\pi(0.1)^2} \quad \Rightarrow \quad V_1 = 5.278\,\text{m/s}$$

$$V_2 = Q/A_2 \quad \Rightarrow \quad V_2 = \frac{4\times 0.041456}{\pi(0.2)^2} \quad \Rightarrow \quad V_2 = 1.32\,\text{m/s}$$

$$V_3 = Q/A_3 \quad \Rightarrow \quad V_3 = \frac{4\times 0.041456}{\pi(0.1)^2} \quad \Rightarrow \quad V_3 = 5.278\,\text{m/s}$$

Head loss	Formula	Value (m)
Entry loss	$0.5\frac{V_1^2}{2g}$	0.71
Friction loss in pipe 1	$f\frac{L_1}{D_1}\frac{V_1^2}{2g}$	5.68
Sudden expansion loss	$\frac{(V_1-V_2)^2}{2g}$	0.798
Friction loss in pipe 2	$f\frac{L_2}{D_2}\frac{V_2^2}{2g}$	0.178
Sudden contraction loss	$\left(\frac{1}{C_c}-1\right)^2\frac{V_3^2}{2g}$	0.53
Friction loss in pipe 3	$f\frac{L_3}{D_3}\frac{V_3^2}{2g}$	5.68
Exit loss	$\frac{V_3^2}{2g}$	1.42
Total head loss (m)		14.996* (~15)

* Total head loss is equal to the available head

On the basis of this table, the EGL and HGL have been drawn in Fig. 6.25.

6.5 POWER TRANSMISSION THROUGH PIPES

Pipes are used to transfer a given fluid from one point to another at a required flow rate. In the process, hydraulic power also gets transmitted. The hydraulic power transmitted through a pipe depends upon the density of the fluid, the discharge and the total head available at the inlet and exit of the pipe. Figure 6.26 shows a pipe connected to a tank having fluid of density ρ and head H at the pipe inlet.

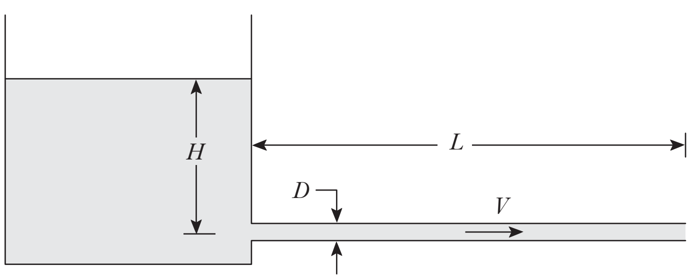

Fig. 6.26 Hydraulic power transmission

If the discharge through the pipe is Q, the hydraulic power available at the inlet is given by

$$P_i = \rho Q g H \tag{6.62}$$

If the head loss due to friction is h_f, the net head available at the pipe outlet is $H - h_f$. The corresponding hydraulic power available at the pipe outlet (power transmitted) is

$$P_o = \rho Q g(H - h_f) \tag{6.63}$$

The transmission efficiency of the pipe is the ratio of power transmitted to the power available at pipe inlet, that is,

$$\eta_t = \frac{P_o}{P_i} \Rightarrow \eta_t = \frac{\rho Q g(H - h_f)}{\rho Q g H} \Rightarrow \eta_t = \frac{H - h_f}{H} \tag{6.64}$$

Using Darcy–Weisbach equation, that is, $h_f = f\frac{L}{D}\frac{V^2}{2g}$ and continuity equation $Q = AV$, the power transmitted is expressed as

$$P_o = \rho g A V\left(H - f\frac{L}{D}\frac{V^2}{2g}\right) \tag{6.65}$$

The *condition for maximum power transmission* can be obtained by differentiating Eq. (6.65) with respect to V and equating it to zero:

$$\frac{dP_o}{dV} = 0 \Rightarrow \rho g A\frac{d}{dV}\left\{V\left(H - f\frac{L}{D}\frac{V^2}{2g}\right)\right\} = 0 \tag{6.66}$$

$$H - 3\left(f\frac{L}{D}\frac{V^2}{2g}\right) = 0 \Rightarrow h_f = \frac{H}{3} \tag{6.67}$$

Thus, the maximum transmission efficiency for a pipeline is

$$\eta_{t,\,\max} = \frac{H - H/3}{H} \Rightarrow \eta_{t,\,\max} = \frac{2}{3} \tag{6.68}$$

From the aforementioned analysis, it is clear that the transmission power is maximum when the head loss due to friction is one-third of the power available at the pipe inlet.

Example 6.10 A 5 km long water pipeline is used to transmit 200 kW of hydraulic power. If the pressure at the inlet is 6 MPa and the pressure drop across the pipe length is 2 MPa. Determine the pipe diameter and its transmission efficiency. Take the friction factor $f = 0.04$.

Solution: Transmission efficiency is given by

$$\eta_t = \frac{P_o}{P_i} \Rightarrow \eta_t = \frac{\rho Q g(H - h_f)}{\rho Q g H} \Rightarrow \eta_t = \frac{H - h_f}{H}$$

The head at the inlet is

$$H = \frac{p_{\text{in}}}{\rho g} \Rightarrow H = \frac{6\times 10^6}{1000\times 9.81} \Rightarrow H = 611.6\,\text{m}$$

The head loss due to pressure loss divided by specific weight of the flowing fluid

$$h_f = \frac{\Delta p_f}{\rho g} \Rightarrow h_f = \frac{2\times 10^6}{1000\times 9.81} \Rightarrow h_f = 203.9\,\text{m}$$

The power at the outlet of the pipe, that is, transmitted power is

$$P_o = \rho Q g(H - h_f)$$

$$\Rightarrow 200\times 10^3 = 1000\times 9.81(611.6 - 203.9)Q$$

$$\Rightarrow Q = 0.05\,\text{m}^3/\text{s}$$

The diameter of the pipe can be obtained from the Darcy–Weisbach equation:

$$f\frac{L}{D}\frac{V^2}{2g} = h_f \Rightarrow \frac{16}{\pi^2} f \frac{L}{2gD^5} Q^2 = h_f \Rightarrow D^5 = \frac{16}{\pi^2} f \frac{L}{2gh_f} Q^2$$

$$\Rightarrow D^5 = \frac{16}{\pi^2}\times 0.04\times \frac{5000}{2\times 9.81\times 203.9}\times 0.05^2 \Rightarrow D = 0.1825\,\text{m}$$

Therefore, the transmission efficiency is

$$\eta_t = \frac{611.6 - 203.9}{611.6} \Rightarrow \eta_t = 0.66$$

6.6 FLOW MEASUREMENT IN PIPES

In this section, various flow measuring devices and techniques have been discussed. They are categorized in following manner:

1. Constriction meters
2. Pitot-static tube
3. Rotameter
4. Hot-wire anemometer
5. Coriolis mass flow meter

6.6.1 Constriction Meters

Constriction meters are the most commonly employed flow measuring devices in internal flow systems. The pressure drop is created by constricting

(or contracting) the flow passage and the resulting drop in pressure is measured using a manometer. This pressure drop is proportional to the discharge through the flow passage. The following are the three types of constriction meters:

1. Venturimeter
2. Orificemeter
3. Flow nozzle

Venturimeter

The *venturimeter* consists of two conical sections, one convergent and another divergent, and a small cylindrical section (also known as throat) in between, as shown in Fig. 6.27. In the converging section, the fluid velocity increases and pressure decreases (in accordance with the Bernoulli's Equation). The velocity becomes maximum at the throat and consequently, the pressure reaches minimum. Thus, in convergent section, the pressure gradient along the convergent section is negative and is *favourable* for the flow. This is evident from the increase in velocity. In the throat, as the area of cross-section is constant, both velocity and pressure will remain unchanged. That is, the pressure gradient is zero along the throat section. In divergent section, the increasing cross-sectional area causes the velocity to decrease and pressure to increase. Thus, the pressure gradient along

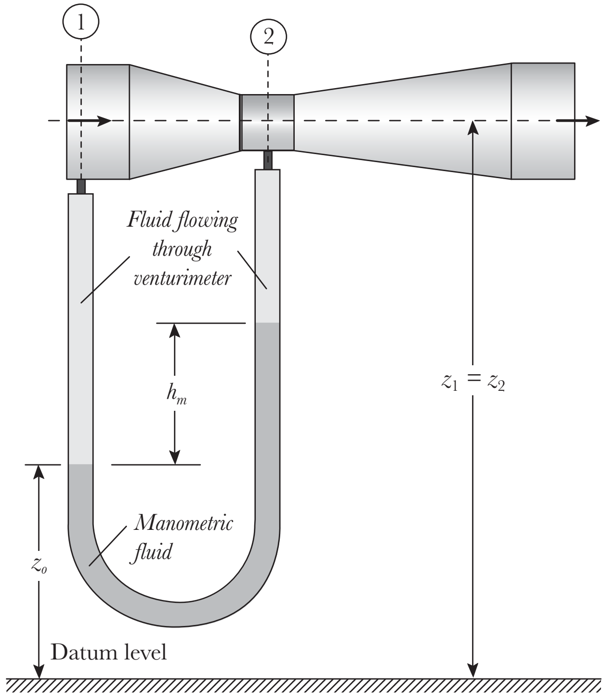

Fig. 6.27 Venturimeter–manometer assembly

the divergent section is positive and *adverse* to the flow, which is obvious from the reduction in velocity. As the pressure difference is maximum between the inlet to convergent section and the throat, the pressure taps are provided at these two points (labelled as 1 and 2 respectively). This difference in pressure can be measured using the mercury filled U-tube manometer as shown in Fig. 6.27. To derive the equation for determining the discharge through the venturimeter, the Bernoulli's equation is applied between sections 1 and 2:

$$\frac{p_1}{\rho g} + \frac{V_1^2}{2g} + \cancel{z_1} = \frac{p_2}{\rho g} + \frac{V_2^2}{2g} + \cancel{z_2} \tag{6.69}$$

$$\frac{p_1 - p_2}{\rho g} = \frac{V_2^2 - V_1^2}{2g} \tag{6.70}$$

The pressure difference between sections 1 and 2 is measured using a manometer. The mano-meter equation is given as

$$p_1 + \rho g(\cancel{z_1} - \cancel{z_o}) - \rho_m g h_m - \rho g(\cancel{z_2} - \cancel{z_o} - h_m) = p_2 \tag{6.71}$$

On simplification,

$$\frac{p_1 - p_2}{\rho g} = \left(\frac{\rho_m}{\rho} - 1\right) h_m \tag{6.72}$$

From Eqs (6.71) and (6.72)

$$\frac{V_2^2 - V_1^2}{2g} = \left(\frac{\rho_m}{\rho} - 1\right) h_m \tag{6.73}$$

Rearranging

$$\frac{V_2^2}{2g}\left(1 - \frac{V_1^2}{V_2^2}\right) = \left(\frac{\rho_m}{\rho} - 1\right) h_m \tag{6.74}$$

Applying continuity equation $(A_1V_1 = A_2V_2)$

$$\frac{V_2^2}{2g}\left(1 - \frac{A_2^2}{A_1^2}\right) = \left(\frac{\rho_m}{\rho} - 1\right) h_m \tag{6.75}$$

The flow velocity at section 2

$$V_2 = \frac{A_1}{\sqrt{A_1^2 - A_2^2}} \sqrt{2gh_m\left(\frac{\rho_m}{\rho} - 1\right)} \tag{6.76}$$

The theoretical discharge through the venturimeter (i.e., the product of area and velocity)

$$Q_{\text{th}} = A_2V_2 = \frac{A_1A_2}{\sqrt{A_1^2 - A_2^2}} \sqrt{2gh_m\left(\frac{\rho_m}{\rho} - 1\right)} \tag{6.77}$$

where A_1 and A_2 are the areas of cross-section of the pipe and the throat, respectively; ρ and ρ_m are the densities of the flowing fluid and the manometric fluid, respectively; and h_m is the height of the manometric liquid column.

From the definition of discharge coefficient, C_d, the actual discharge is given by

$$Q_{\text{act}} = C_d Q_{\text{th}} \quad \Rightarrow \quad Q_{\text{act}} = \frac{C_d A_1 A_2}{\sqrt{A_1^2 - A_2^2}} \sqrt{2gh_m\left(\frac{\rho_m}{\rho} - 1\right)} \tag{6.78}$$

It is important to note that the divergent section of the venturimeter is always kept longer than the convergent section or the angle of divergent section is kept low to facilitate gradual increase in pressure in the direction of flow. This makes *adverse pressure gradient* in the diverging section small resulting in deterrence to *boundary layer separation*. Eddies formed due to separation, if any, are limited to a very thin region near the wall and thus, the corresponding losses are small [Fig. 6.28(a)]. This is the reason why the value of C_d for venturimeter is high (0.95 to 0.98).

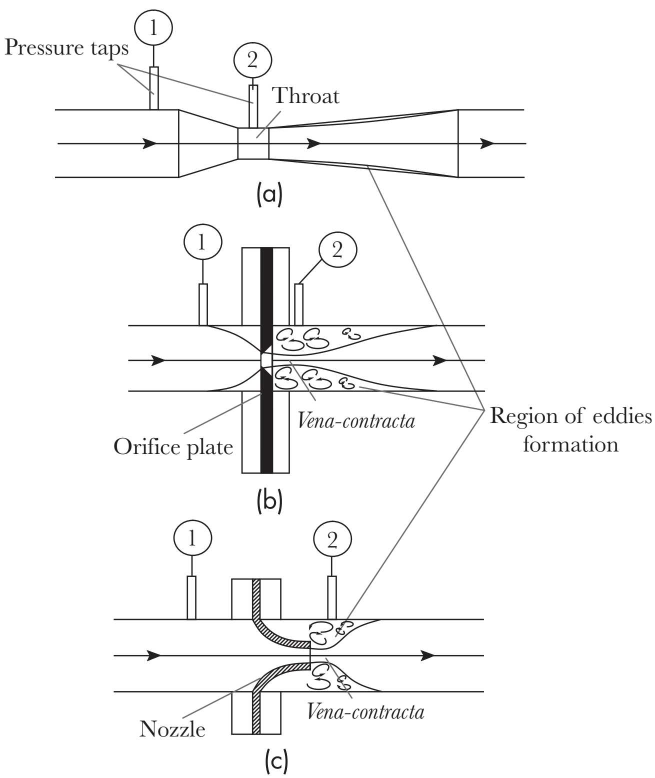

Fig. 6.28 Constriction meters (a) Venturimeter (b) Orificemeter (c) Flow nozzle

Orificemeter

The *orificemeter* is a circular metal plate having a tapered hole at the centre, such that the sharp edge of the hole faces the upstream side, as shown in Fig. 6.28(b). Unlike venturimeter, here the change in cross-section is abrupt, due to which the pressure drops suddenly. The streamline while passing through the orifice converges further in the downstream direction and the *vena-contracta* is formed a little distance away from the orifice. The pressure tap is drilled approximately where the *vena-contracta* has formed. The drop in pressure is measured using a differential U-tube manometer. In the downstream side of the orifice plate, there is a sudden rise in pressure due to abrupt increase in flow area. The sudden pressure rise causes the flow to separate and eddies to form all around the pipe periphery in the downstream of orifice plate until the flow reattaches to the pipe surface. Consequently, the magnitude of losses is large compared to that in venturimeter.

For deriving the discharge equation for an orificemeter, a procedure similar to that of venturimeter is followed. The only difference in this case is that the Bernoulli's equation is applied between section 1 and *vena-contracta*. The resulting discharge equation for an orificemeter is given as

$$Q_{\text{act}} = \frac{C_d A_1 A_o}{\sqrt{A_1^2 - C_c^2 A_o^2}} \sqrt{2 g h_m \left(\frac{\rho_m}{\rho} - 1 \right)} \tag{6.79}$$

where, A_o is the cross-sectional area of the orifice and C_c (already defined in Section 6.2.2) is the contraction coefficient ($=A_c/A_o$)

The value of contraction coefficient is always less than 1 as the area at the *vena-contracta* is smaller than the area A_o of the orifice.

For a sharp-edged or ideal circular orifice: $C_c = \pi/(\pi + 2) = 0.611$

For an orifice that resembles a short tube: $C_c = 1$

Since the separated region is large in case of orificemeter, the value of discharge coefficient will be less compared to that of venturimeter. Its value ranges from 0.6 to 0.65. The orificemeters are usually used to measure the gas flow with water as the manometeric fluid. The ratio of water density to gas density is large as compared to 1, the discharge equation thus reduces to

$$Q_{\text{act}} = \frac{C_d A_1 A_2}{\sqrt{A_1^2 - A_2^2}} \sqrt{2 g h_m \frac{\rho_m}{\rho}} \tag{6.80}$$

Flow Nozzle

In the *flow nozzle* or *nozzle meter*, shown in Fig. 6.28(c), the shape of the obstruction is that of a nozzle. The separation region will not be as large as it

was seen in case of orificemeter. The discharge equation will be same as that of orificemeter. However, the value of discharge coefficient lies in between 0.7 and 0.9.

These constriction meters are widely used in industrial applications and scientific laboratories to measure the flow of various liquids and gases in pipes, ducts, closed conduits, etc.

Example 6.11 Find the diameter of the throat of a venturimeter required to be installed in a 40 mm diameter water pipeline. The maximum deflection (200 mm of Hg) in the limbs of the differential mercury manometer is reached at a discharge of 2.0 L/s. The discharge coefficient for the venturimeter may be assumed 0.98.

Solution:

Given data: $D_1 = 0.04$ m, $C_d = 0.98$, $Q = 0.002$ m^3/s, $h_m = 0.2$ m

The pipe cross-sectional area

$$A_1 = \frac{\pi}{4} D_1^2 \quad \Rightarrow \quad A_1 = \frac{\pi}{4}(0.04)^2 \quad \Rightarrow \quad A_1 = 1.2566 \times 10^{-3}\,\text{m}^2$$

The actual discharge from a venturimeter is calculated using equation:

$$Q = \frac{C_d A_1 A_2}{\sqrt{A_1^2 - A_2^2}} \sqrt{2 g h_m \left(\frac{\rho_m}{\rho} - 1\right)}$$

$$2 \times 10^{-3} = \frac{0.98 \times 1.2566 \times 10^{-3} A_2}{\sqrt{(1.2566 \times 10^{-3})^2 - A_2^2}} \sqrt{2 \times 9.81 \times 0.2 \times (13.6 - 1)}$$

$$\frac{1.579 \times 10^{-6} - A_2^2}{A_2^2} = 18.745 \quad \Rightarrow \quad A_2 = \sqrt{\frac{1.579 \times 10^{-6}}{19.745}}$$

$$\Rightarrow \quad A_2 = 2.828 \times 10^{-4}\,\text{m}^2$$

The diameter of the venturimeter throat

$$D_2 = \sqrt{\frac{4}{\pi} \times 2.828 \times 10^{-4}} \quad \Rightarrow \quad D_2 = 19\,\text{mm}$$

6.6.2 Pitot-static Tube

It has already been discussed in Chapter 2 that pressure of a non-volatile liquid flowing through a pipe can be measured using *piezometer*, which is a glass tube fixed on the pipe wall through a tap. The rise in liquid level inside the glass tube is equal to the *hydrostatic pressure* at that location. The measured pressure is static pressure as velocity at the pipe's internal surface is zero because of *no slip*. If a bent tube as shown in Fig. 6.29(a) is fixed inside the pipe with its opening facing

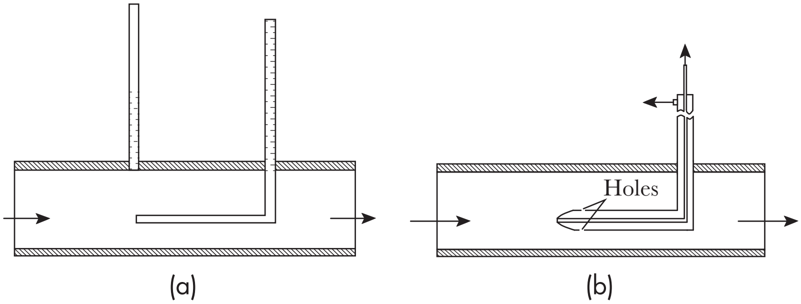

Fig. 6.29 Stagnation and static pressures measurement using (a) Piezometers (b) Pitot-static tube

the incoming fluid stream, it can be used to measure the stagnation pressure as well. It is obvious that the level rise in the bent tube is more compared to the level in vertical tube. This is due to the conversion of kinetic energy of the fluid stream into pressure energy in the horizontal arm of the bent tube. This concept forms the basis for the design of pitot-static tube. It consists of two concentric tubes as shown in Fig. 6.29(b). The outer tube has holes on the periphery at a small distance from the tip. The fluid at the surface of the outer tube is essentially static due to *no slip* condition and hence the pressure inside it is the static pressure. The inner tube is used to measure the stagnation pressure. The flow in the inner tube is brought to rest with no heat transfer (adiabatic) to the fluid in the outer tube since temperature is same throughout. By definition, the stagnation pressure is the pressure of fluid when it is brought to rest through a reversible adiabatic process (isentropic or constant entropy process)

$$p_o = p + \frac{1}{2}\rho V^2 \tag{6.81}$$

where, p_o is the stagnation pressure, p is the static pressure, ρ is the fluid density, and V is the average flow velocity. It can be seen from Eq. (6.81) that the stagnation pressure is equal to the sum of static pressure and dynamic pressure.

The difference in stagnation pressure and the static pressure is measured with the help of manometer. The flow velocity inside the pipe is, thus, measured from Eq. (6.81):

$$V = \sqrt{\frac{2(p_o - p)}{\rho}} \tag{6.82}$$

Compared to piezometric arrangement, pitot tube can be used for the measurement of pressure of any type of fluid (volatile or non-volatile). Unlike

constriction meters, pitot-static tube can be employed to measure the flow rate of internal as well as external flows.

Example 6.12 A Pitot tube is installed on an aircraft to measure its relative velocity with respect to the wind. If the plane cruising at a speed of 600 km/h encounters the wind speed of 45 km/h, find out the differential pressure reading the instrument will register.

Solution:

Given data: $V_a = 600\,\text{km/h} \Rightarrow V_a = \dfrac{600\times1000}{3600} \Rightarrow V_a = 166.7\,\text{m/s}$

$$V_w = 45\,\text{km/h} \Rightarrow V_w = \frac{45\times1000}{3600} \Rightarrow V_w = 12.5\,\text{m/s}$$

The relative velocity of air craft with respect to wind

$$V_{aw} = 166.7 + 12.5 \Rightarrow V_{aw} = 179.2\ \text{m/s}$$

Using Eq. (6.67), the pressure registered by the Pitot tube

$$\Delta p = \frac{1}{2}\rho V_{aw}^2 \Rightarrow \Delta p = \frac{1}{2}\times1.2\times179.2^2 \Rightarrow \Delta p = 19.268\,\text{kPa}$$

6.6.3 Rotameter

Another flow measuring device for internal flows is rotameter. It consists of a tapered glass tube with a metallic float (also known as rota) inside. The rotameter is always connected vertically in flow circuit with fluid flowing upwards. The float will be acted upon by buoyancy and drag (both viscous and pressure) in the flow direction and weight in opposite to the flow direction, that is, downwards. The float will become stationary when the upward and downwards forces balance each other. This balancing is self-maintaining because of varying flow area (annular area between float and the tube) in the direction of flow. The downward acting force is equal to the difference of weight and the buoyancy force, that is,

$$(\rho_m - \rho_f)\forall g,$$

where, ρ_m is the metallic float density, ρ_f is the fluid density, and $\forall$ is volume of the metallic float. Since this downward force is constant for a given fluid, the upward force, which is due to pressure drop across the float (Δp) must be constant. The pressure drop, from the *Darcy–Weisbach equation*, is a function of the square of the discharge for a given flow area. To keep the pressure drop constant for different flow rates, the flow area must be varied accordingly. This is why a tapered tube is used in a rotameter. The position of the float corresponds to a particular discharge reading on the scale fixed adjacent to it, as shown in Fig. 6.30.

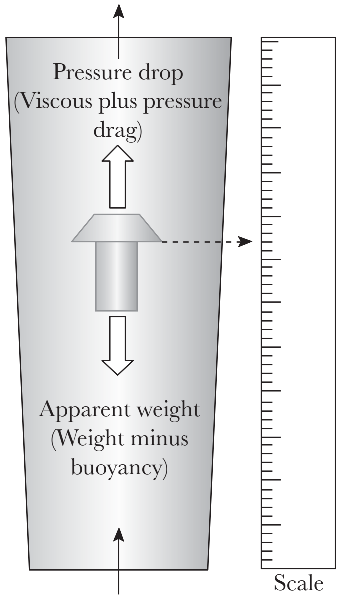

Fig. 6.30 Rotameter

6.6.4 Hot-wire Anemometer

The *hot-wire anemometer* is used to measure not only the velocity of air but also that of other fluids. It consists of a probe, shown in Fig. 6.31, having two prongs with a filament of metal having a high *temperature coefficient of electrical resistance* (the property by virtue of which the electrical resistance of the material changes with temperature). Usually, the wire or filament is made up of platinum or tungsten. Typical dimension of the filament is about 1mm long and 5 microns in diameter. The wire is electrically heated and it is placed in stream of the fluid whose velocity is to be measured. The wire gets cooled as the fluid flows over it and accordingly there is a change in electrical resistance. The variation in electrical resistance is measured by sensing the voltage drop

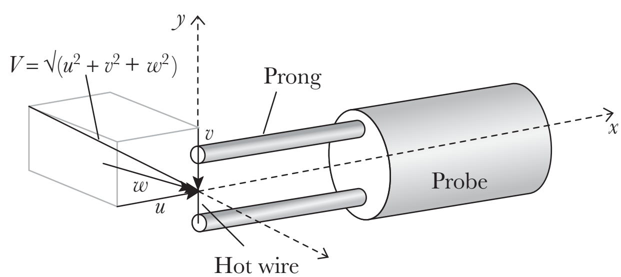

Fig. 6.31 Hot-wire anemometer

variation across the filament. The drop in voltage is calibrated with the known velocity of the fluid.

The hot-wire anemometers have some limitations such as there exists non-linear characteristics between velocity and temperature drop due to complex nature of heat transfer between the wire and the fluid. It should be ensured that the main flow is directed across the length of the filament while measuring the flow velocity.

6.6.5 Coriolis Flow Meter

The *Coriolis flow meter* consists of two parallel non-straight tubes enclosed in a casing, as shown in Fig. 6.32(a). It works on *Coriolis effect*, which is a deflection of moving objects when they are observed in a rotating frame of reference. Such deflections (or twisting) are observed when the fluid passes through a non-straight tube (curved tube). In Coriolis flow meter, the oscillations are induced in both the tubes by some external means generating a sinusoidal wave. The displacement sensors are placed between the tubes near the inlet and outlet sections to measure the displacements. When there is no flow through the tubes,

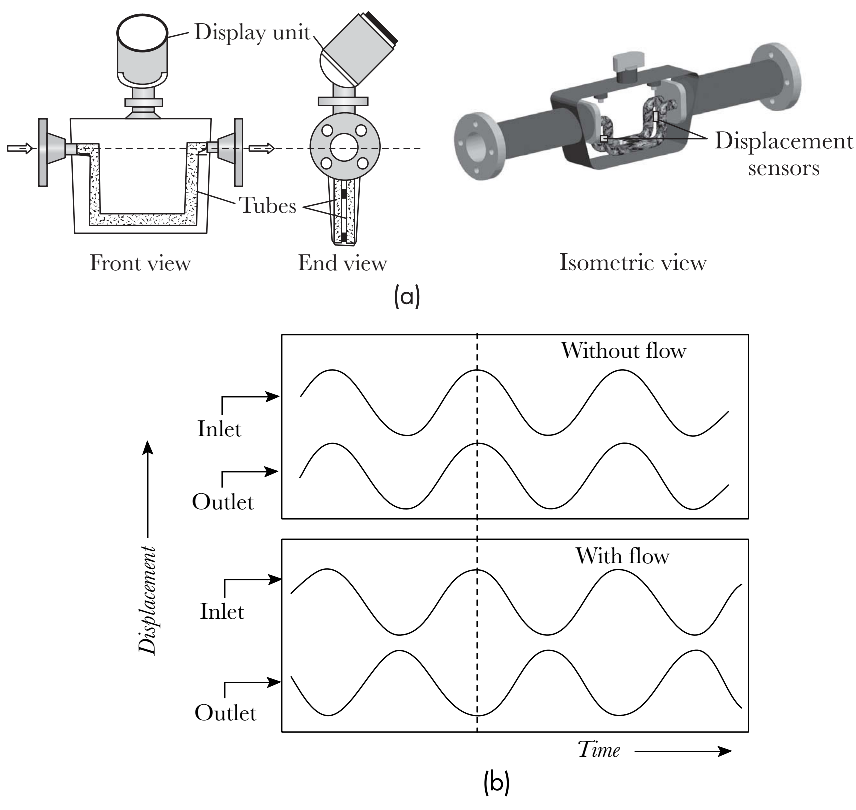

Fig. 6.32 Coriolis flowmeter (a) Schematic diagram (b) Displacement data plot

both tubes oscillate in-phase. However, the tubes oscillate out of phase due to twist induced by Coriolis effect of the flowing fluid. The displacement data from the sensors indicates the phase shift, as shown in Fig. 6.32(b). The phase shift is directly proportional to the mass flow rate of the fluid passing through them.

6.7 ORIFICE AND MOUTHPIECE

An *orifice* is a small opening provided at the bottom or lower part of the sidewall of a tank to measure the flow. Orifices are classified on the basis of the following:

1. Shape of cross-section—*triangular*, *rectangular,* and *circular*
2. Size of the opening—*small* and *large*
3. Shape of the edge—*sharp* and *round* (Fig. 6.33)

The ratios of different parameters that are required to design and calibrate an orifice are termed as *hydraulic coefficients*. The following are the different types of hydraulic coefficients:

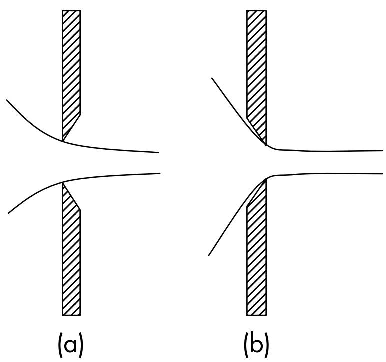

Fig. 6.33 Orifice (a) Sharp-edged (b) Round-edged

Contraction coefficient It is defined as the ratio of cross-sectional area of the jet at *vena-contracta* (A_c) to the cross-sectional area of the orifice (A_o).

$$\boxed{C_c = \frac{A_c}{A_o}} \tag{6.83}$$

The value of contraction coefficient for a sharp-edged orifice is 0.611 and that of rounded edge is 1.0.

Velocity coefficient It is defined as the ratio of jet velocity at *vena-contracta* (V_c) to the theoretical velocity of the jet (V_{th}).

$$\boxed{C_v = \frac{V_c}{V_{\text{th}}}} \Rightarrow C_v = \frac{V_c}{\sqrt{2gH}} \tag{6.84}$$

where H is the head at the centreline of the orifice.

Discharge coefficient It is defined as the ratio of actual discharge (Q_a) to the theoretical discharge (Q_{th}).

$$C_d = \frac{Q_a}{Q_{th}} \tag{6.85}$$

The theoretical discharge through the orifice is the product of its cross-sectional area and the theoretical velocity, whereas actual discharge is the product of jet velocity and its cross-sectional area at *vena-contracta*. Rewriting Eq. (6.85)

$$C_d = \frac{A_c V_c}{A_o V_{th}} \quad \Rightarrow \quad C_d = C_c \times C_v \tag{6.86}$$

Thus, the discharge coefficient is the product of contraction coefficient and velocity coefficient.

Mouthpieces, on the other hand, are the hollow objects that are fixed to the opening (mouth) provided on the lower sidewall/bottom of the tank. Thus, a mouthpiece may be thought as an orifice with a protruded tube. The mouthpieces can be classified on the basis of the following

1. Location—*internal* [Fig. 6.34(a)] and *external* [Fig. 6.34(b)]
2. Shape—*cylindrical* [Figs 6.34(a) and (b)], *convergent* [Fig. 6.34(c)], and *convergent–divergent* [Fig. 6.34(d)]

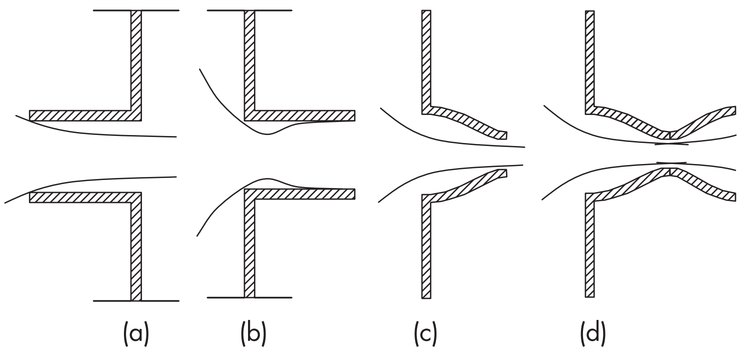

Fig. 6.34 Mouthpiece (a) Internal (b) External (c) Convergent (d) Convergent–divergent

Time Required for Emptying a Tank

The jet of fluid issued from the orifice has a parabolic trajectory due to the gravitational pull, as shown in Fig. 6.35. The equation of trajectory can be obtained using equations of motion:

$$\left.\begin{aligned} x &= V t \\ y &= \frac{1}{2} g t^2 \end{aligned}\right\} \quad \Rightarrow \quad x^2 = V^2 \left(\frac{2y}{g} \right) \tag{6.87}$$

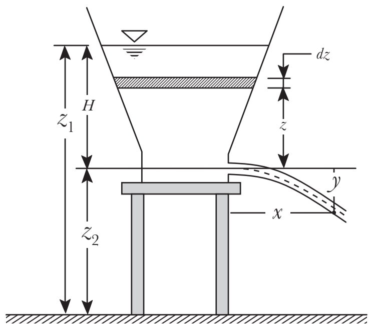

Fig. 6.35 Schematic diagram of emptying tank

In addition, $V = C_v\sqrt{2gH}$

$$C_v = \frac{x}{\sqrt{4yH}} \Rightarrow x^2 = 4ay \quad \text{where} \quad a = C_v^2 H \tag{6.88}$$

which is the standard equation of parabola. The time required for emptying a water tank of any arbitrary shape can be obtained in following manner:

Consider an infinitesimal fluid elemental strip of thickness dz at a distance z from the orifice centreline where the cross-sectional area of the tank is A. The fluid is being drained in small time dt through an orifice of cross-sectional area A_o. As per continuity, the reduction in volume of water level inside the tank must be equal to the volume of water drained out, that is,

$$-Adz = Q_a dt \Rightarrow -Adz = C_d A_o\sqrt{2gz}dt \Rightarrow dt = \frac{-Adz}{C_d A_o\sqrt{2gz}} \tag{6.89}$$

Integrating Eq. (6.89) to obtain the time required for emptying the tank from z_1 to z_2

$$t = \frac{1}{C_d A_o\sqrt{2g}}\int_{z_2}^{z_1}\frac{Adz}{\sqrt{z}} \tag{6.90}$$

In the present case, A is changing with respect to z; hence, A is a function of z.

Example 6.13 Determine the time required for emptying a cylindrical water tank of 5 m diameter through an orifice of diameter 200 mm placed at the bottom of the tank. The initial head available above the orifice is 4 m. Take discharge coefficient 0.6.

Solution: $H = 4\,\text{m}$; $d_o = 0.2\,\text{m}$; $C_d = 0.6$; $D = 5\,\text{m}$

Cross-section area of the tank

$$A = \frac{\pi}{4}D^2 \Rightarrow A = \frac{\pi}{4}\times 5^2 \Rightarrow A = 19.634\,\text{m}^2$$

Cross-section area of the orifice

$$A = \frac{\pi}{4}D^2 \Rightarrow A = \frac{\pi}{4}\times 0.2^2 \Rightarrow A = 0.03142\,\text{m}^2$$

The time required for emptying the tank from $z_1 = H$ to $z_2 = 0$

$$t = \frac{1}{C_d A_o \sqrt{2g}} \int_{z=0}^{z=4} \frac{A dz}{\sqrt{z}} \quad \Rightarrow \quad t = \frac{19.634}{0.6 \times 0.03142\sqrt{2 \times 9.81}} \left(2\sqrt{z}\right)_{z=0}^{z=4}$$

$$\Rightarrow \quad t = 940.5\,\text{s} \quad \Rightarrow \quad t = 15.675\,\text{min}$$

6.8 HYDRAULIC SIPHON

The hydraulic siphon is a pipe that is used for drawing the fluid out of a tank. The siphonic action, shown in Fig. 6.36, takes place in accordance to the Bernoulli's principle by keeping one end of the pipe inside the tank while other end is left in the atmosphere. The suction is created at this end, the flow establishes in pipe until the tank gets emptied or the end touches the free liquid surface.

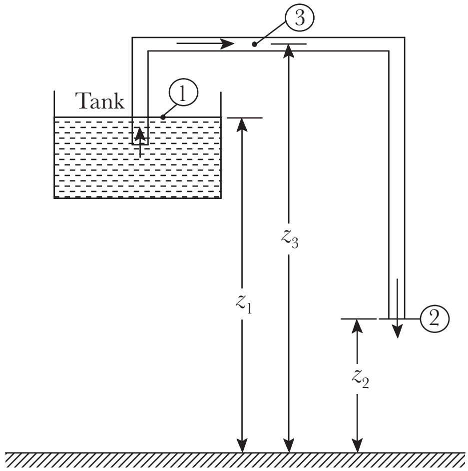

Fig. 6.36 Hydraulic siphon

Applying Bernoulli's equation between sections 1 and 2 (ignoring friction losses),

$$\cancel{\frac{p_1}{\rho g}} + \cancelto{0}{\frac{V_1^2}{2g}} + z_1 = \cancel{\frac{p_2}{\rho g}} + \frac{V_2^2}{2g} + z_2 \tag{6.91}$$

The velocity at section 1 can be ignored due to the fact that tank area is large in comparison to the cross-sectional area of the pipe. In addition, the pressure at the two sections is same and is equal to the atmospheric pressure. The fluid velocity inside the pipe from Eq. (6.91) is

$$V_2 = \sqrt{2g(z_1 - z_2)} \tag{6.92}$$

Again applying Bernoulli's equation between sections 1 and 3 (ignoring friction losses),

$$\frac{p_1}{\rho g} + \cancelto{0}{\frac{V_1^2}{2g}} + z_1 = \frac{p_3}{\rho g} + \frac{V_3^2}{2g} + z_3 \tag{6.93}$$

Where $V_3 = V_2$ and $p_1 = p_{atm}$

The pressure inside the pipe at point 3 is, thus, given by

$$p_3 = p_{atm} - \rho g\left(\frac{V_2^2}{2g} + (z_3 - z_1)\right) \tag{6.94}$$

This shows that the pressure inside the pipe at section 3 is less than the atmospheric pressure. This vacuum in the pipe is responsible for the suction of liquid from the tank.

Example 6.14 Determine the discharge through the siphon of diameter 25 mm as shown in Fig. 6.37. In addition, calculate the minimum pressure inside the siphon.

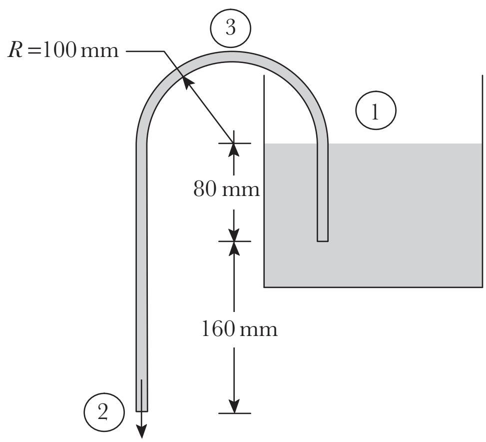

Fig. 6.37

Solution: The fluid velocity inside the siphon is

$$V = \sqrt{2g(z_1 - z_2)}$$

$$\Rightarrow \quad V = \sqrt{2 \times 9.81 \times 0.24} \quad \Rightarrow \quad V = 2.17\,\text{m/s}$$

Discharge through the siphon

$$Q = AV \quad \Rightarrow \quad Q = \frac{\pi}{4} \times 0.025^2 \times 2.17 \quad \Rightarrow \quad Q = 1.0652\,\text{L/s}$$

The pressure inside the siphon at point 3, which is the point of minimum pressure

$$p_{min} = p_{atm} - \rho g\left(\frac{V^2}{2g} + (z_3 - z_1)\right)$$

$$\Rightarrow \quad p_{min} = 101325 - 1000 \times 9.81 \times \left(\frac{2.17^2}{2 \times 9.81} + 0.1\right) \quad \Rightarrow \quad p_{min} = 97989.55\,\text{Pa}$$

6.9 WATER HAMMER

Water hammer, also known as *hydraulic shock*, is the sudden and transient increase in pressure due to an abrupt change in fluid velocity in pipe systems. This is the reason that water hammer is also referred to as pressure transients sometimes. Sudden change in flow velocity is a typical characteristic of almost all the flow systems occurring due to pump start-up, pump stop, or valve opening and closure. Due to the inertia of the fluid, the flow velocity of the liquid column as a whole is no longer capable of adjusting to the new situation. Hence, the fluid is deformed and this deformation is accompanied with pressure transients inducing pressure energy shock waves within the system. The pressure waves move back and forth until the waves get dissipated due to friction losses. Since, velocity of pressure wave is equal to sound velocity, a '*boom*' like sound is created on its collision while it moves back and forth. As neither the water nor the pipe will compress to absorb this shock wave; these pressure waves damage the pipelines, fittings, valves, etc. It is worth mentioning here that only rapid changes in flow velocity will produce this effect and causes degradation in every part of the piping system. Following are the typical events that induce large pressure changes:

Pump start-up It generates high pressures due to collapse of empty space that exists downstream.

Pump shut down or power failure It causes a pressure upsurge on the suction side while a pressure downsurge on the discharge side. The major problem is due to downsurge as often the pressure reaches to vapour pressure, resulting in vapour column separation.

Valve opening and closure Opening and closing of valve is the fundamental operation required for the safety of any pipeline system. Closing a valve installed in downstream end of a pipeline creates a pressure wave that moves toward the reservoir then again towards the valve. Closing a valve in less time than it takes for the pressure surge to travel to the end of the pipeline and back is called *sudden valve closure*. Sudden valve closure will change the flow velocity rapidly and may result in a pressure surge. The pressure surge due to opening of valve is usually not as severe as pressure surge due to sudden valve closure. For example, the sudden closure of water supply from the dam to the inlet of a hydraulic turbine causes a surge in pressure, that is, water hammer, inside the *penstock* (a pipe that connects hydraulic turbine inlet to the dam) and a surge tank is provided to annul the impact of water hammer on the penstock.

The pressure change in a fluid induced due to an abrupt change in flow velocity is calculated using the *Joukowsky equation* given as

$$\Delta p = \rho \times a \times \Delta V \tag{6.95}$$

Where, Δp is the pressure change (N/m^2)

ρ is the density of fluid (kg/m^3)

a is the pressure wave velocity through the fluid (m/s)

ΔV is change in flow velocity (m/s)

It is evident from Eq. (6.95) that larger the magnitude of the velocity change, greater will be the change in pressure. Although it may appear from the Eq. (6.95) that the mass of the fluid inside the flow system has no effect but ultimately it is detrimental as the force experienced by the pipeline components is proportional to it (force experienced is proportional to the area of pipeline which decides mass of fluid contained within). This dependence also explains that the pressure surges occurring in domestic piping systems with their small diameters and lengths are usually negligible. The factors that affect the magnitudes or impact of water hammer phenomenon are pipeline material and its dimensions, pump's moment of inertia, filling around the pipeline, etc. It should be noted that *Joukowsky equation* is only applicable for the time period in which velocity change ΔV is taking place. In addition to this, time period must be equal or shorter than the reflection time t_r of the piping system. The reflection time is given by

$$t_r = \frac{2L}{a} \tag{6.96}$$

where, L is length of pipeline through which pressure wave travelling and a is the sound speed.

6.9.1 Methods to Control Water Hammer

Water hammer can have severe degrading effects on the fluid flow system and it is essential to take this phenomenon under consideration while designing in order to avoid potentially devastating consequences such as instant pipe failure, weakening of pipe sections, damage to components and equipment, fatigue and external wear, risks to personnel, etc. A number of equipment and methods are available to mitigate the effects of water hammer, as shown in Table 6.2. Any protection method is employed after careful consideration of various issues such as the number of pumps in operation, conditions during normal stop and power failure, risk of buckling, fatigue, and clogging. It is critical to have a thorough understanding of the effect that any particular method will have on the flow system. Improper selection of protection method may do more damage than protection. For example, oversizing the surge relief valve or improper selection of the vacuum breaker-air relief valve can increase the severity of water hammer dangerously.

Table 6.2 Methods to control water hammer

Types of method	Protection equipment		Features	Pros	Cons
Active → Only protects during normal pump stops → Dependent upon power supply	Variable frequency drives (VFD)		Match the current frequency with pump to control impeller speed	Fast and easy to handle	Expensive and power needed
	Soft starters		Reduce current during pump start-up	Economical alternative of VFD	No care for power trip, ramp down time is limited
	Slow-closing valves		Gradually decrease the flow before the shutting off the pump	Cheaper	Time consuming, not suitable for emergency cases
Passive → Even protects during pump or power failure → Not dependent upon power supply	Air chambers	Standard	Filled with liquid and compressed air	Reliable, maintenance-free, no need of power	Air recharge needed periodically, valve slamming, large chamber is expensive
		bladder	contains a bladder with compressed air inside		
	Surge towers		Acts as buffer zone or reservoir which absorbs pressure shock either by taking or supplying water to pipeline	Reliable, maintenance-free, no need of power	Tower height must be higher than the total dynamic head
	Release valves		Installed at locations where sub-pressure occurs, permit to enter air if pressure inside pipe falls below a set value	Economical	Clogging and the chance of water columns separation

Example 6.15 Water is flowing through a pipeline of diameter 2 m with a velocity of 3 m/s. A gate valve mounted in the downstream side at distance of 9000 m from the inlet is closed in 6 s. Determine the pressure surge and force exerted on the gate if the pressure wave velocity is 1500 m/s.

Solution:

Given data:

$D = 2\,\text{m}$, $\Delta v = 3\,\text{m/s}$, $a = 1500\,\text{m/s}$, $L = 9000\,\text{m}$.

Since, $6\text{s} < t_r = 12\,\text{s}$, the *Joukowsky equation* can be applied.

$$\Delta p_{\text{jou}} = \rho \times a \times \Delta v \quad \Rightarrow \quad \Delta p = 1000 \times 1500 \times 3$$
$$\Rightarrow \quad \Delta p = 45 \times 10^5 \text{ N/m}^2 = 45 \text{ bar}$$

Area of the pipeline $= \dfrac{\pi}{4} \times d^2 = \dfrac{\pi}{4} \times 2^2 = 3.141 \text{ m}^2$.

Force on the gate $= \Delta p \times A = 45 \times 10^5 \times 3.141 = 14.13$ MN.

6.10 SLURRY FLOW

The slurry is formed by mixing fine solid particles into a liquid. The slurry flow or liquid–solid flow is very important from civil engineering perspective as sediments/solid particles get transported from one place to another in a canal or river or through a sewage line. Slurry flows also find applications in the emerging area of *nanofluids*. The suspended solid particles are dispersed in the carrier fluid and are driven with the flowing fluid by the action of drag force and pressure force acting on them. The flow of the phases is synchronized to avoid settling down or deposition of the solid particles. Such flows are characterized by the two Reynolds Numbers, namely *pipe Reynolds number* (Re) and *particle Reynolds number* (Re_s). The pipe Reynolds number characterizes the total mixture flow in a pipe whereas particle Reynolds number describes the liquid–solid flow behaviour. The patterns and regimes depend upon the shape, size, and distribution of the grains (solid particles). More precisely,

1. For $Re_s < 10^{-6}$, the very fine solid particles are evenly dispersed and remain suspended without any external agitation. The particles exhibit Brownian motion and the flow regime is known as *colloidal dispersions*.
2. For $10^{-6} < Re_s < 10^{-1}$, the fine solid particles are held in suspension homogeneously requiring little external agitation. This regime is termed as *homogeneous flow* regime having low liquid (carrier fluid) velocity. [see Fig. 6.38(a)]
3. For $0.1 < Re_s < 2$, more external agitation is required to hold the solid particles under suspension allowing small amount of segregation in horizontal pipes. This regime is termed as *pseudo-homogeneous flow* regime.
4. For $Re_s > 2$, the segregation is more causing the flow to be more heterogeneous. This regime is termed *heterogeneous flow* regime [see Fig. 6.38(b)].

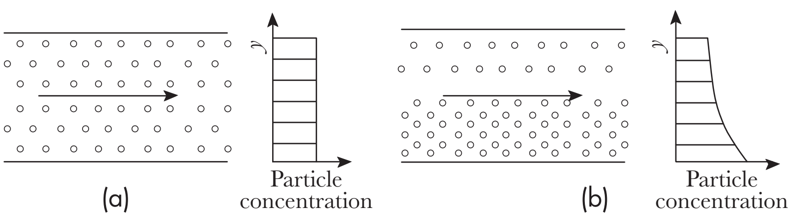

Fig. 6.38 Slurry flow (a) Homogeneous (b) Heterogeneous

In homogeneous flow, the particle concentration remains the same throughout the channel depth/pipe diameter whereas in heterogeneous flow the concentration of solid particles increases in the downward direction (particles settling due to gravity).

POINTS TO REMEMBER

- Flow in a pipe has two distinct regions, namely, developing region near the pipe entrance and the fully developed region beyond that. The viscous effects are limited near the pipe wall in developing region whereas the flow becomes viscous across the entire cross-section in the fully developed region. Thus, the friction factor is constant in fully developed region.
- A pipe is said to be hydraulically smooth if the average roughness height is less than the viscous sublayer thickness else the pipe is hydraulically rough.
- The flow through the pipe is subjected to both major and minor losses. The major losses are due to friction whereas the minor losses are due to sudden expansion, sudden contraction, bends, fittings, valves, etc.
- For laminar flow, the friction factor is the function of Reynolds number alone. However, the friction factor is a function of Reynolds number as well as relative roughness of the pipe in turbulent flow.
- For non-circular ducts, the Reynolds number is determined using the concept of hydraulic diameter, which is defined as the ratio of four times area of duct cross-section to the wetted perimeter of the duct cross-section.
- Pipe network problems are solved using Hardy Cross method, which draws the analogy from electrical circuitry. Accordingly, the Kirchhoff's current and voltage laws are applied. In pipe flow, the current is analogous to the square of the discharge and the voltage drop is analogous to pressure drop.
- Fluid flow in a pipe can be measured in a variety of ways, which include the instruments such as constriction meters, rotameters, Coriolis flow meter, pitot tube, and hotwire anemometer.
- Mouthpieces and orifices are used to measure the flow rate from a tank. The two are essentially the same but slightly differ in their construction. The mouthpieces are orifices with protruded tubes.
- The phenomenon of sudden and transient increase in pressure due to an abrupt change in fluid velocity in pipe systems is known as water hammer. This happens due to the conversion of kinetic energy into elastic energy. The possible scenarios in which it may occur are pump start-up, pump stop, or valve opening and closure. The pressure wave generated is strong enough to inflict severe damage on the piping system.
- Slurry flow is classified into three types—homogeneous, pseudo-homogeneous, and heterogeneous depending upon the size and distribution of solid particles in the carrier fluid.

SUGGESTED READINGS

Cimbala, J.M., Y.A. Cengel, *Essentials of Fluid Mechanics-Fundamentals and Applications*, McGraw-Hill Education, New Delhi, 2013.

Durand, R., *Basic Relationships of the Transportation of Solids in Pipes-Experimental Research*, Proceedings Minnesota International Hydraulics Division, ASCE, pp. 89–103, 1953.

Munson, B.R., D.F. Young, T.H. Okiishi, *Fundamentals of Fluid Mechanics*, 5th Ed., John Wiley & Sons, 2007.

Rathakrishnan, E., *Instrumentation, Measurements and Experiments in Fluids*, Special Indian edition, CRC Press (Taylor and Francis Group), New Delhi, 2009.

MULTIPLE-CHOICE QUESTIONS

6.1 For the flow of fluid through a square duct of length L and cross-sectional area a^2, having velocity V, the Reynolds number is computed as

(a) $\text{Re} = \rho VL/\mu$
(b) $\text{Re} = \rho Va/\mu$
(c) $\text{Re} = \rho V(\sqrt{2}a)/\mu$
(d) $\text{Re} = \rho Va/(\sqrt{2}\mu)$

6.2 The pipe is treated as rough if the

(a) average surface roughness height is greater than boundary layer thickness
(b) average surface roughness height is less than boundary layer thickness
(c) average surface roughness height is greater than viscous sublayer thickness
(d) average surface roughness height is less than viscous sublayer thickness

6.3 Principle on which Pitot tube works is

(a) forcing the liquid to flow through an obstruction
(b) converting kinetic energy into potential energy
(c) converting kinetic energy into pressure energy
(d) None of these

6.4 In which flow regime, the shear stress is greater?

(a) Laminar
(b) Transition
(c) Turbulent
(d) None of these

6.5 The pressure of fluid while flowing through an orifice plate

(a) increases
(b) decreases
(c) remains the same
(d) fluctuates continuously

6.6 Hot-wire anemometer works on the principle of the probe's

(a) electrical resistance that is proportional to fluid velocity
(b) electrical resistance that is proportional to its temperature
(c) thermal resistance that is proportional to fluid velocity
(d) thermal resistance that is proportional to its temperature

6.7 Hot-wire sensors should have

(a) a high temperature coefficient of resistance
(b) a low temperature coefficient of resistance
(c) be independent of temperature coefficient of resistance
(d) none of these

6.8 The gauge pressure at a point where HGL passes through the centreline of the pipe is
(a) maximum
(b) minimum
(c) zero
(d) not defined

6.9 Water is flowing downhill through from a pipe of larger diameter to smaller diameter. The discharge in smaller pipe will be__________ that of larger pipe.
(a) greater than
(b) the same as
(c) less than
(d) none of these

6.10 A water jet discharging from a 20 mm diameter orifice has 18 mm diameter at its *vena-contracta*, then its coefficient of contraction will be
(a) 0.90
(b) 0.81
(c) 0.01
(d) 1.11

6.11 A tapered tube is used in rotameter
(a) to make it suitable for high-flow measurement
(b) to maintain pressure drop constant for different flow rates
(c) to make reading scale more visible
(d) none of these

6.12 If external turbulence is not required to keep the solid particles concentration uniform throughout the fluid, then this flow regime is called
(a) homogenous
(b) pseudo-homogenous
(c) colloidal dispersions
(d) heterogeneous

6.13 If for a given flow the venturimeter is inclined, then its reading on manometric scale will be
(a) less
(b) more
(c) same
(d) erroneous

6.14 If the pipe diameter is large, which instrument would be suitable for flow measurement?
(a) Venturimeter
(b) Coriolis flow meter
(c) Pitot tube
(d) All of these

6.15 The discharge coefficient of an orificemeter of diameter d installed in a pipe of diameter D is a function of
(a) d/D only
(b) Re only
(c) both
(d) none of these

6.16 Which pipe has higher transmission efficiency?
(a) smaller diameter smooth pipe
(b) larger diameter smooth pipe
(c) smaller diameter rough pipe
(d) larger diameter rough pipe

6.17 Which of the following criteria need to be fulfilled for making two different pipe systems equivalent?
(a) same length and diameter
(b) same pressure loss and discharge
(c) same discharge and length
(d) same velocity and diameter

6.18 The head loss in an orifice ($C_v = 0.98$) under the head of 1m is
(a) 2 cm
(b) 3 cm
(c) 4 cm
(d) 5 cm

6.19 Three pipes of same length and diameters D, $2D$, and $D/2$ are connected in series, what is the nearest value of diameter of equivalent pipe?

(a) $D_e = D/3$
(b) $D_e = D/2$
(c) $D_e = 2D/3$
(d) $D_e = 3D/4$

6.20 The equivalent diameter D_e for the n pipes of same diameter D connected in parallel is

(a) $D_e = nD$
(b) $D_e = n^{2/5}D$
(c) $D_e = n^{1/2}D$
(d) $D_e = D/n^{2/5}$

REVIEW QUESTIONS

6.1 Differentiate between the following
(a) Laminar and turbulent flow in pipes
(b) Hydraulically smooth and rough surfaces
(c) Laminar sublayer and laminar boundary layer
(d) Particle Reynolds number and flow Reynolds number
(e) EGL and HGL
(f) Orifice and mouthpiece

6.2 Why are friction losses considered major losses in a pipe network?

6.3 What makes a copper capillary tube to be used as an expansion device in low-capacity refrigeration systems? Explain.

6.4 Why is the divergent section longer than the convergent section in a venturimeter? What would happen if the device is fitted in the reversed manner?

6.5 'Among all the constriction meters, the venturimeter has the highest discharge coefficient.' Justify the statement.

6.6 Why is the glass tube in a rotameter tapered?

6.7 How would you draw an electrical analogy for the flow through pipe? Discuss Hardy Cross method.

6.8 What is a hydraulic siphon? On what principle does it work?

6.9 What do you understand by water hammer? Discuss the methods to prevent water hammer.

6.10 Write a short note on the classification of slurry flows.

UNSOLVED PROBLEMS

6.1 The diameter of a water pipe line has a sudden expansion from 250 to 500 mm causes the pressure head rise by 100 mm of water. Calculate the discharge.

[Ans: 0.1123 m³/s]

6.2 Petrol ($\upsilon = 3.0$ centistokes) at 20°C is being siphoned from a petrol tank of a motor bike through a hose of 10 mm diameter and 2 m long. Determine the discharge of petrol siphoned out. Take friction factor $f = 0.03$. Ignore minor losses.

[Ans: 0.1315 L/s]

6.3 Compute the diameter of the 3 km pipeline for which the transmission efficiency is 60%. The pressure at the inlet is 5 MPa. In addition, determine the power transmitted if the discharge is 5 m³/s. Take friction factor $f = 0.02$.

[Ans: 15 MW]

6.4 In a three-reservoir system, determine the discharge in each branch of the pipe network. Following are the details of the pipe network:

Pipe	**#1**	**#2**	**#3**
Diameter, mm	100	120	140
Length, m	350	400	200
Elevation of corresponding tank, m	200	150	50

Assume same friction factor $f = 0.03$ in each pipe.

[Ans: $Q_1 = 0.0345\ m^3/s$; $Q_2 = 0.0366\ m^3/s$; $Q_1 = 0.0711\ m^3/s$]

6.5 Determine the discharge of water through the pipe, shown in Fig. 6.39. If friction factor is 0.04 and contraction coefficient is 0.62, draw the HGL and EGL

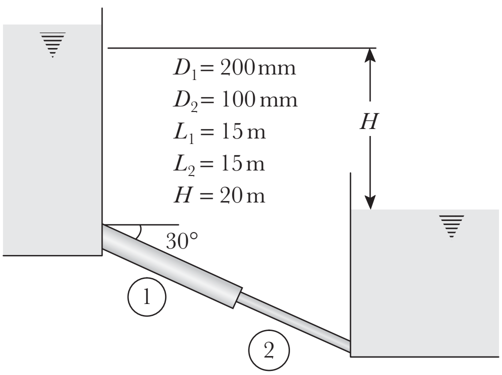

Fig. 6.39

[Ans: $Q = 0.05646\ m^3/s$]

6.6 Determine discharge in each branch of the pipe network shown in Fig. 6.40.

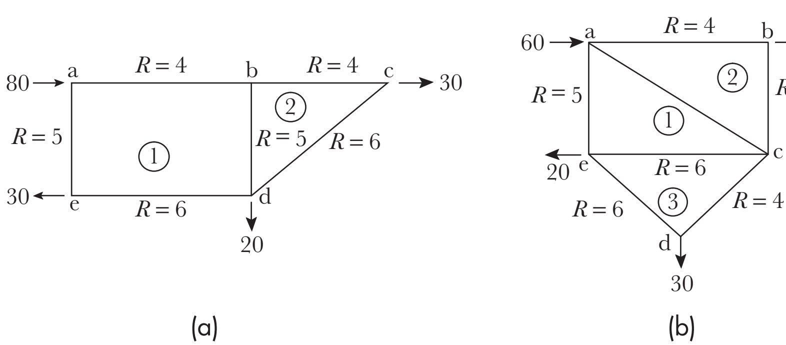

Fig. 6.40

[Refer Example 6.7]

6.7 Find the discharge in each pipe shown in Fig. 6.41. The head available at A is 20 m of water and the friction factor for each pipe may be taken 0.03.

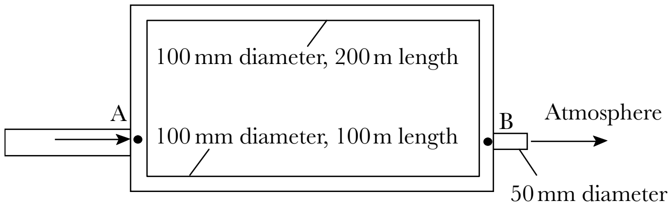

Fig. 6.41

[Ans: Q_1 = 0.01397 m³/s; Q_2 = 0.01976 m³/s]

6.8 Two identical cylindrical water tanks of diameter 1 m each are connected by a horizontal pipe of diameter 100 mm and length 5 m, as shown in Fig. 6.42. Determine the rate of change of water level in tanks, when the initial difference in the water levels is 4 m. Take $f = 0.02$.

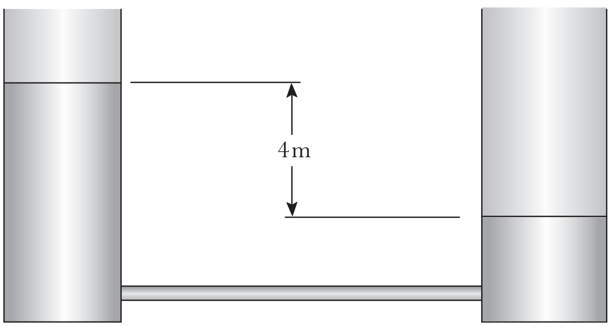

Fig. 6.42

[Ans: 5.6 cm/s]

6.9 The two identical orifices are aligned on the side wall of a water tank as shown in Fig. 6.43. Determine the distance (x) of the point of intersection of the jets issued from the orifices, if the velocity coefficient of each orifice is 0.98 and heads above the orifices are $H_1 = 0.5$ m and $H_2 = 1.5$ m.

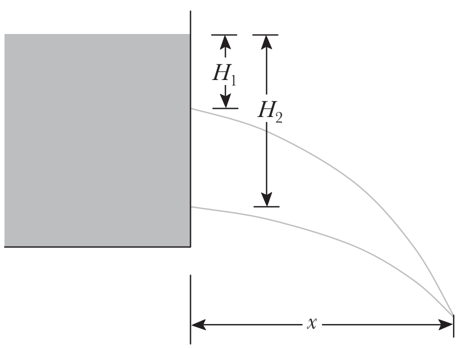

Fig. 6.43

[Ans: x = 1.697 m]

6.10 Determine the air pressure required above the water column to cause the jet to rise 10 m above the nozzle, as shown in Fig. 6.44.

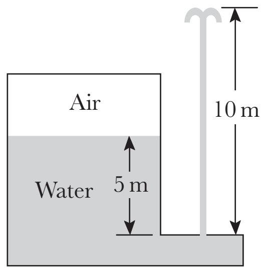

Fig. 6.44

[Ans: 48.95 kPa]

6.11 A venturimeter, shown in Fig. 6.45, having throat of 25 mm diameter, is fitted in a water pipeline of 50 mm diameter inclined at an angle of 45°. Calculate (a) the discharge in the pipe if discharge coefficient is 0.98 and (b) the pressure at the throat if inlet gauge pressure is 100 kPa.

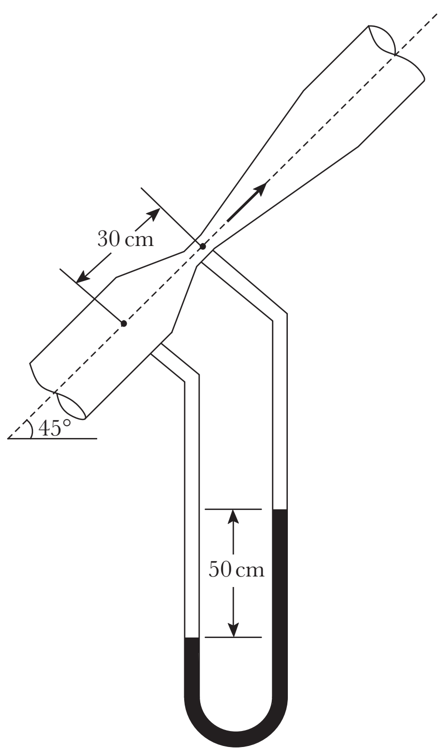

Fig. 6.45

[Ans: (a) 5.5237 L/s (b) 36.115 kPa]

6.12 A Pitot tube fabricated in the lab is to be calibrated using a pressurized air chamber fitted with an orifice ($C_v = 0.98$). The gauge pressure inside the chamber is 200 Pa. The Pitot tube is placed at the *vena-contracta* and its manometer shows 25 mm deflection. If the manometric fluid has specific gravity of 0.9, determine the instrumentation coefficient (C) of the Pitot tube. [*Hint*: $V = C\sqrt{2(p_o - p)/\rho}$]

[Ans: 0.932]

6.13 Prove that the nozzle diameter corresponding to maximum power transmission for the system shown in Fig. 6.46 is given by

$$d = \left(\frac{D^5}{2fL}\right)^{1/4}$$

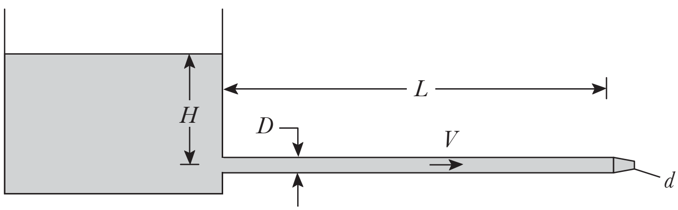

Fig. 6.46

6.14 A 500 m pipeline of diameter 15 cm connects the two tanks having difference of 15 m in their water levels, as shown in Fig. 6.47. Determine the discharge through the pipe. In order to increase the discharge by 25%, another pipeline is connected from the middle of the original pipeline. Determine its diameter, if friction factor is 0.01. Neglect minor losses.

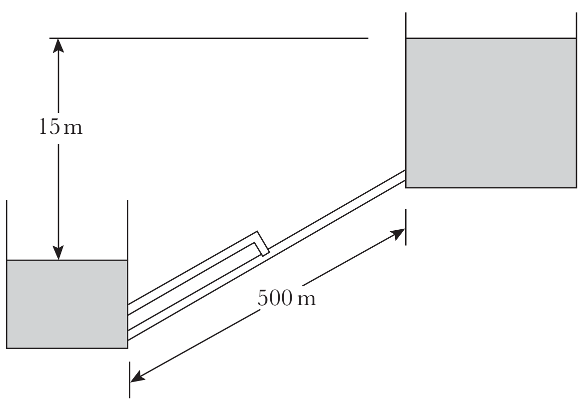

Fig. 6.47

[Ans: 0.143 m]

6.15 A flow nozzle, shown in Fig. 6.48, having diameter d_2 is fitted in a pipe of diameter d_1. Show that the pressure loss coefficient is given by

$$C_l = \frac{p_1 - p_3}{p_1 - p_2} = \frac{1-(d_2/d_1)^2}{1+(d_2/d_1)^2}$$

Trace the graph C_l versus d_2/d_1.

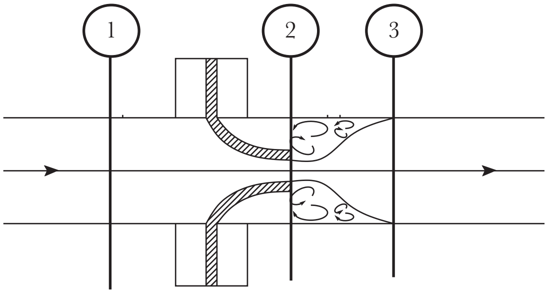

Fig. 6.48

Answers to Multiple-choice Questions

6.1 (b)	6.2 (c)	6.3 (c)	6.4 (c)	6.5 (b)
6.6 (b)	6.7 (a)	6.8 (c)	6.9 (b)	6.10 (b)
6.11 (b)	6.12 (c)	6.13 (c)	6.14 (c)	6.15 (c)
6.16 (b)	6.17 (b)	6.18 (c)	6.19 (b)	6.20 (b)

DESIGN OF EXPERIMENTS

Experiment 6.1 Determination of Major and Minor Losses in a Given Pipe Network

Objective

1. To experimentally determine the friction factor f of a circular pipe in fully developed region of flow and to compare it with the friction factor obtained from Moody diagram and standard Colebrook equation.
2. To determine the head loss in each pipe connected in parallel and the pipes connected in series.

Theory

A pipe is a closed conduit, generally of circular cross-section, used to carry water or any other fluid from one location to another. When the pipe is running full, the flow is considered as 'pressure driven', otherwise, the flow is gravity driven and the pipe behaves as an open channel (pressure is atmospheric). While designing any pipeline system, the designer has to take into account the losses (major and minor) in the pipeline system. The major losses in a pipe are due to friction, given by Darcy–Weisbach equation:

$$h_f = f\frac{L}{D}\frac{V^2}{2g} \tag{E6.1}$$

Friction factor for fully developed laminar flow:

$$f = \frac{64}{\text{Re}} \tag{E6.2}$$

Friction factor for fully developed turbulent flow: Colebrook's equation

$$\frac{1}{\sqrt{f}} = 1.14 - 2\log\left(\frac{e}{D} + \frac{9.3}{\text{Re}\sqrt{f}}\right) \tag{E6.3}$$

Table E6.1 Typical roughness values

Material	**Absolute roughness (e) (micron)**
Galvanized iron	152
Riveted steel	915–9150
Concrete	305–3050
Stainless steel/carbon steel	45
PVC	1.5
Glass tube	1.5

The minor losses in a piping system are due to the following factors:

1. Sudden expansion
2. Sudden contraction
3. Entrance loss
4. Exit loss
5. Bend loss
6. Losses due to fittings

When two pipes are joined in parallel, the discharge in the main pipe is equal to the sum of discharges through the parallel pipes,

$$Q = Q_1 + Q_2 \tag{E6.4}$$

As the pressure heads at the ends of the pipe cannot be different, as they are to merge in single pipe, the head loss in each branch of pipe must be the same

$$h_f = \frac{f_1 L_1}{D_1}\frac{V_1^2}{2g} = \frac{f_2 L_2}{D_2}\frac{V_2^2}{2g} \tag{E6.5}$$

Experimental Set-up

The experimental set-up, shown in Fig. E6.1, can be used to determine the major and minor losses in a pipe network. The network shown in the arrangement can be

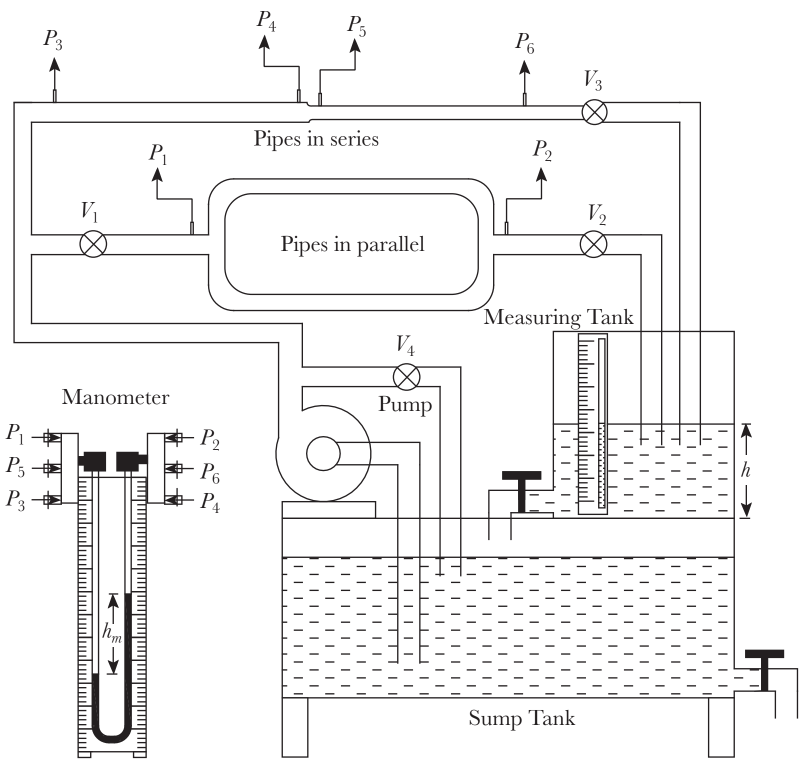

Fig. E6.1 Schematic diagram for the losses in pipe apparatus

conveniently used to determine (a) friction factors for individual pipes (b) the major losses in pipes connected in parallel or series (c) minor losses due to sudden contraction between pipes.

Procedure

1. First open the bypass valve (V_4) and close all other valves and all the manometer tappings.
2. Now start the motor.
3. First take the discharge through pipes connected in series by opening valve (V_3) with valve (V_1) being closed and open the manometer tappings of the pipes connected in series. Then take the following readings:
   (a) Manometer readings
   (b) Time required for 100 mm rise in water level in the measuring tank
4. Take 4/5 readings by repeating the aforementioned procedure for different discharges by adjusting bypass valve (V_4) at different positions.
5. For the pipes connected in parallel, open valves (V_1 and V_2) (V_3 to be closed), the manometer readings are noted against each discharge settings.
6. From the known friction factors obtained before, find the head loss in each pipe.
7. The indicated pressure drop must match the calculated sum of pressure drops in each pipe.

Observation Table

1. Measuring tank cross-sectional area, A ____________ m^2
2. Test pipes (ID) (in series) D_1 = ____ mm, D_2 = ___ mm
   L_1 = ____ mm, L_2 = ___ mm
3. Test pipes (in parallel) D = ____ mm, L = ____ mm
   (with bends)
   Inter-tap spacing = ____ mm

Results and Discussions

A comparison of the friction factors obtained experimentally with those obtained from Moody's chart and Colebrook's equation is to be done. The reasons of deviation from the standard values are to be discussed in detail.

1. Graphs to be plotted:
   (a) f versus Re
   (b) $\log(f)$ versus $\log(\text{Re})$ to calculate the constants K and n in $f = \text{K}(\text{Re})^{\text{n}}$
   (c) $\log(h_f)$ versus $\log(\text{Re})$
2. Discuss the nature of the curves and the possible reasons of deviation from the standard values

Conclusions

Draw conclusions on the results obtained.

Observation Table 1: Friction factor determination

S. no.	Manometer readings			h_f $\frac{\rho_m h_m}{\rho}$	Level rise in tank, h (cm)	Time required for rise in level, t (s)	Actual discharge $Q_{act} = Ah/t$ (m^3/s)	Flow velocity in pipe 1 $V_1 = Q_{act}/A_1$	Flow velocity in pipe 2 $V_2 = Q_{act}/A_2$	Re_1 $\frac{\rho V_1 D_1}{\mu}$	Re_2 $\frac{\rho V_2 D_2}{\mu}$	f_1	f_2
	x_1 (cm)	x_2 (cm)	$h_m = x_2 - x_1$ (m)										
1.													
2.													
3.													
…													

Observation Table 2: Head loss in parallel pipes

S. no.	Manometer readings			Pressure drop $\rho_m g h_m$	Level rise in tank, h (cm)	Time required for rise in level, t(s)	Actual discharge $Q_{act} = Ah/t$ (m^3/s)	Head loss in pipes 1 and 2 h_f(m)	Equivalent pressure drop $\rho g h_f$	Percentage error
	x_1 (cm)	x_2 (cm)	$h_m = x_2 - x_1$ (m)							
1.										
2.										
3.										
….										

Experiment 6.2 Determination of Discharge Coefficient of Different Constriction Meters

Objective

To determine the coefficient of discharge of the venturimeter and orificemeter.

Theory

The constriction meters are the most commonly used flow measuring devices in pipe networks. The pressure drop is created by constricting the flow passage and the drop in pressure is measured by a differential manometer. There are three types of constriction meters, namely, venturimeter, orificemeter, and flow nozzle or nozzlemeter.

The theoretical discharge through any constriction meter is obtained by this equation:

$$Q_{\text{act}} = \frac{C_d A_1 A_2}{\sqrt{A_1^2 - A_2^2}} \sqrt{2gh_m\left(\frac{\rho_m}{\rho} - 1\right)} \tag{E6.6}$$

where

A_1 and A_2 are the areas of cross-section of the pipe and the throat, respectively.
ρ and ρ_m are the densities of the flowing fluid and the manometric fluid, respectively.
h_m is the height of the manometric liquid
C_d is the discharge coefficient

As discussed earlier, the separation region is more in orifice in comparison to venturi owing to the sudden change in cross-section. Consequently, the losses are significantly larger in orificemeter than those in venturimeter. Thus, the value of discharge coefficient for orificemeter is quite low compared to a venturimeter. The typical values of discharge coefficients lie in the range of 0.6–0.65 for orificemeter and 0.95–0.98 for venturimeter.

Experimental Set-up

A schematic diagram of the experimental set-up has been shown in Fig. E6.2.

The discharge coefficient is the ratio of actual discharge to theoretical discharge, that is,

$$C_d = Q_{\text{act}}/Q_{\text{th}} \tag{E6.7}$$

The actual discharge is calculated by dividing the rise in volume of the water level ($A \times h$) in the measuring tank by the time t required to reach that rise in water level.

$$Q_{\text{act}} = Ah/t \tag{E6.8}$$

Procedure

1. First open the bypass valve (V_3) and start the motor.
2. Take the discharge through venturimeter by opening valve (V_1) with orifice valve (V_2) being closed and the manometer tappings of the venturimeter open (only). Then take the following readings:
   (a) Manometer readings
   (b) Time required for 100 mm rise in water level in the measuring tank

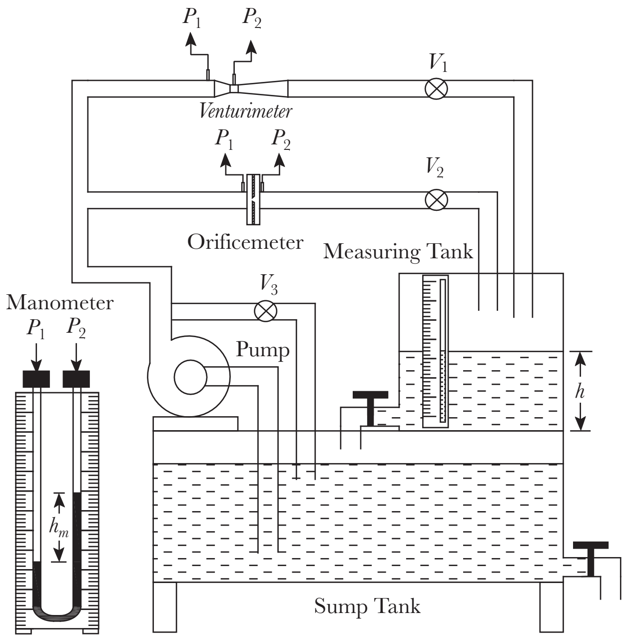

Fig. E6.2 Schematic diagram for the combined Venturimeter-Orificemeter apparatus

3. Take 6/7 readings by repeating the aforementioned procedure for different discharges by adjusting bypass valve (V_3) at different positions.
4. Similar procedure is adopted for orificemeter by opening the valve (V_2) and manometer tappings of the orificemeter. The valve (V_1) and the manometer tappings of the venturimeter are kept closed while the discharge is taking through the Orificemeter.

Observation Table

1. Cross-sectional area of measuring tank A _______________ m^2
2. Pipe diameter _______________ mm
3. Venturimeter throat diameter _______________ mm
4. Orifice diameter _______________ mm

Results and Discussions

Determine the values of C_d for all the set of readings for both venturimeter and the orificemeter:

1. Plot: (a) C_d versus Re (b) C_d versus h_m (c) Q_{act} versus h_m (d) log(Q_{act}) versus log(h_m) to calculate the constants 'K' and 'n' in the $Q_{act} = K(h_m)^n$
2. Discuss the nature of the curves and the reasons of deviation from the standard values

Conclusions

Draw conclusions on the results obtained.

Observation Table 1: Venturimeter

S. no.	Manometer readings			Theoretical discharge Q_{th} (m^3/s)	Level rise in measuring tank, h (cm)	Time required for rise in level, t (sec)	Actual discharge $Q_{act} = Ah/t$	Discharge coefficient $C_d = Q_{act}/Q_{th}$	$Re = \frac{\rho VD}{\mu}$
	x_1 (cm)	x_2 (cm)	$h_m = x_2 - x_1$ (m)						
1.									
2.									
3.									
…									

Observation Table 2: Orificemeter

S. no.	Manometer readings			Theoretical discharge Q_{th} (m^3/s)	Level rise in measuring tank, h (cm)	Time required for rise in level, t (sec)	Actual discharge $Q_{act} = Ah/t$	Discharge coefficient $C_d = Q_{act}/Q_{th}$	$Re = \frac{\rho VD}{\mu}$
	x_1 (cm)	x_2 (cm)	$h_m = x_2 - x_1$ (m)						
1.									
2.									
3.									
…									

CHAPTER 7

Open Channel Flow

LEARNING OBJECTIVES

After studying this chapter, the reader will be able to:

- Understand the characteristics of different open-channel flows
- Derive the governing equations for steady uniform and varied flows
- Comprehend the working principle of different flow-measuring techniques in an open-channel flow
- Design simple experiments to measure the flow in open channels

Unlike pipe flow, where the flow is pressure driven, the open-channel flow or free-surface flow is *gravity driven* as the pressure on the free surface is same (i.e., atmospheric pressure) everywhere. The flow takes place in an open channel under the influence of gravity acting on the fluid mass due to the provision of slope at the channel bed. Moreover, the flow within the pipe or closed conduit is also treated as open-channel flow when it is not running full, as only atmospheric pressure acts everywhere on the free surface. In an open channel, the flow is bounded by solid surface from the bottom and sides while the top surface is open to the atmosphere. The open-channel flow is generally turbulent in nature with negligible surface tension at the free surface.

This chapter deals with different types of steady open-channel flows, namely, uniform flow, gradually varied flow, and rapidly varied flow. Their characteristics and analyses have been presented. The flow measurement in open channels using different types of weirs and venturi flumes has also been discussed in detail.

The irrigation canals, river flow, flow in drains, and underground sewer lines are few of the practical applications of open-channel flow.

7.1 CLASSIFICATION OF OPEN-CHANNEL FLOW

The open-channel flow is broadly classified as *steady* flow and *unsteady* flow as shown in Fig. 7.1. In *steady flow*, the depth of flow at a section is constant with respect to time, whereas in an *unsteady flow*, the depth of flow at a section does

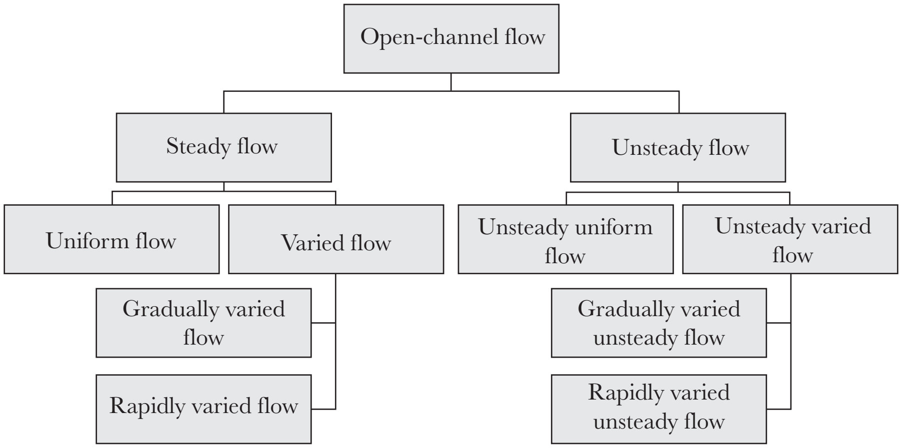

Fig. 7.1 General classification of open-channel flow

not remain constant with respect to time. Most of the flows encountered in an open channel are steady in nature. Thus, their understanding is of great importance. *Steady flows* are further divided into *uniform* and *varied* or *non-uniform flows*. In *steady uniform flow*, conditions do not vary from one section to another and such a flow occurs in channels having a constant cross-section and channel-bed slope. The *steady varied flow* occurs inside the channels where the cross-section does not remain the same. Generally, the change in cross-section occurs near the entry and exit of the channel due to the change in depth. If the depth changes abruptly in a short distance along the channel length, the flow is termed as *rapidly varied flow* (RVF), whereas if the change of depth occurs gradually over a comparatively long distance, the flow is termed as *gradually varied flow* (GVF).

The *unsteady flow* is also classified in a similar manner. In the *unsteady uniform flow*, the depth of flow varies with time and the variation in depth is the same from section to section along the channel. This type of flow is rarely seen. If the depth of flow varies along the channel length as well as with respect to time, the flow is termed as *unsteady varied flow*. Like *steady varied flow*, the unsteady varied flow is also classified as gradually varied unsteady flow and rapidly varied unsteady flow. The various types of flows are illustrated in Fig. 7.2.

7.1.1 Classification on the Basis of Reynolds Number

The Reynolds number for the flow in an open channel is computed in the following manner:

$$\mathrm{Re} = \frac{\rho V m}{\mu} \tag{7.1}$$

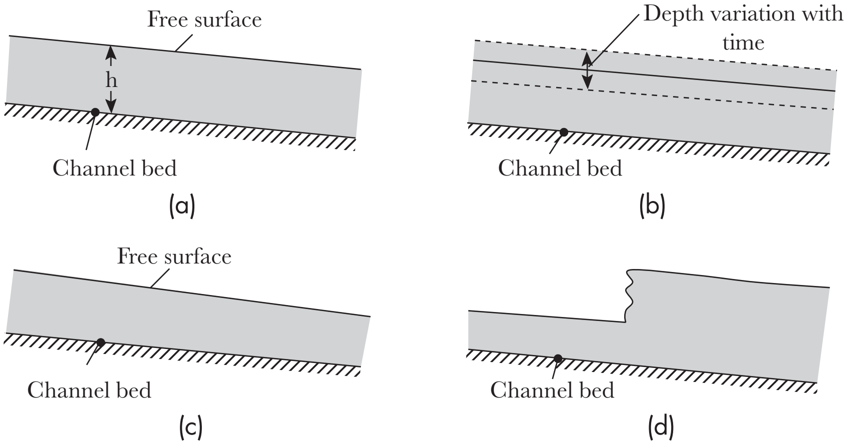

Fig. 7.2 Various types of flows (a) Steady uniform flow (b) Unsteady uniform flow (c) Gradually varied flow (d) Rapidly varied flow

where, V is the mean velocity, ρ is the fluid density, μ is the dynamic viscosity, and m is the *hydraulic mean depth* defined as the ratio of area of channel cross-section to its wetted perimeter, that is,

$$m = \frac{A}{P} = \frac{D_h}{4} \tag{7.2}$$

On the basis of Reynolds number, the open-channel flow is classified as follows:

Laminar flow	Re < 500
Transition flow	500 < Re < 2000
Turbulent flow	Re > 2000

The flow is mostly turbulent in open channels except for the cases where the fluid kinematic viscosity is very high, the mean fluid velocity is low, and the hydraulic mean depth is low.

7.1.2 Classification on the Basis of Froude Number

The free surface of the fluid in an open channel may have a flat or wavy configuration depending upon the channel parameters and fluid velocity. The dimensionless number that relates fluid flow with the wave motion is termed as *Froude number*, which is defined as the square root of the ratio of inertia force to gravity force.

$$Fr = \sqrt{\frac{\text{Inertia force}}{\text{Gravity force}}} \Rightarrow Fr = \frac{V}{\sqrt{\ell g}} \tag{7.3}$$

where ℓ is the characteristic length of the flow. On the basis of Froude number, the open channel is classified as

Subcritical flow (tranquil flow)	$Fr < 1$
Critical flow	$Fr = 1$
Supercritical flow (shooting flow)	$Fr > 1$

To understand this effect of Froude number, Fig. 7.3 showing a wave having velocity c is drawn.

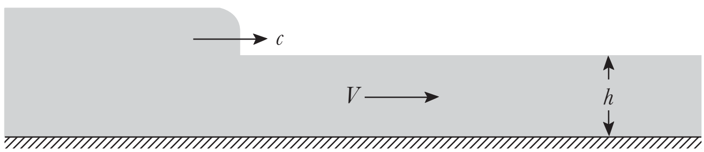

Fig. 7.3 Single wave propagating in the channel

The wave speed can be calculated as

$$c = \sqrt{gh} \tag{7.4}$$

Therefore, Froude number can also be defined as the ratio of fluid velocity to the wave velocity, that is,

$$\boxed{Fr = \frac{V}{c}} \tag{7.5}$$

If $V < c$ ($Fr < 1$), the wave will propagate in the upstream direction with the velocity $c - V$ relative to a stationary observer. This type of flow is termed as *subcritical* or *tranquil flow*. If $V = c$ ($Fr = 1$), the wave will appear stationary to the observer and the flow is termed as *critical flow*. If $V > c$ ($Fr > 1$), the wave appears to propagate in the downstream direction with the velocity $V - c$, and the flow is termed as *supercritical flow*.

7.1.3 Classification on the Basis of Specific Energy

In pipe flow, the pressure energy, kinetic energy, and potential energy are taken into consideration at a section. Since pressure energy is constant everywhere at the free surface in an open-channel flow, only the kinetic and potential energy are considered at a section. However, the pressure energy inside the fluid can be related to hydrostatic pressure, which is the product of specific weight and the depth h from the free surface at a section. The total head or total energy

per unit specific weight above the channel bed is termed as *specific energy*, given by the following equation:

$$E = V^2/2g + h \tag{7.6}$$

This means that for the uniform flow, in which there is no variation in depth along the channel length, specific energy remains constant throughout the channel. For non-uniform or varied flow, if depth changes along the channel length, the specific energy varies accordingly.

7.2 UNIFORM FLOW

The channels that are designed to carry a fluid from one point to another at a constant depth throughout its length are said to have a uniform flow, that is, $dz/dx = 0$. Such flows are common in irrigation canals, roadside drains, etc. In this section, the velocity distribution across the channel depth is described, Chezy and Manning equations are derived, and it is shown that the head loss due to friction for a uniform flow is equal to the difference in datum heads.

7.2.1 Velocity Distribution

The velocity at the channel walls is zero due to no-slip, and its magnitude increases with the distance from the surface of the wall. The velocity variation is within the channel at a section. The constant velocity contours for a rectangular open channel and circular pipe not running full are shown in Fig. 7.4. The velocity contours are symmetric in both the channels about the centre line. As a matter of fact, the lines of low velocity will occupy the regions near the solid walls due to higher shear stresses, whereas the lines of higher velocity will be at a place where the effect of shear stress is low. The diminishing shear stress from the wall towards the free surface causes the fluid velocity to increase. The closed velocity contours below the free surface at the centre line are the zones of highest velocity in the channel section.

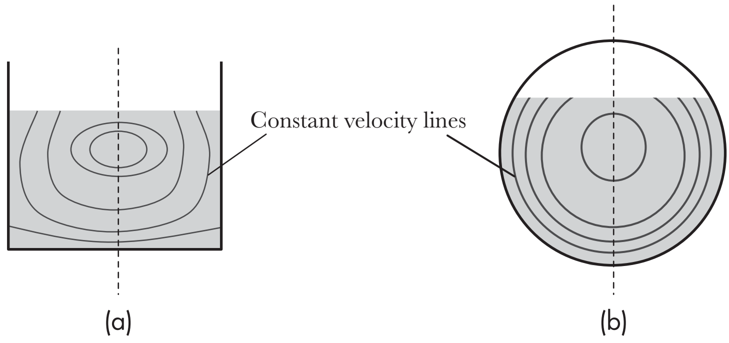

Fig. 7.4 Velocity distribution in (a) Rectangular channel (b) Pipe not running full

To present the variation of velocity along the depth at the centre line of a channel, Fig. 7.5 is drawn. The maximum fluid velocity is attained somewhere below the free surface as the air causes resistance at the interface of air and the flowing fluid, thereby reducing the velocity as shown in Fig. 7.5. Hence, the velocity distribution in an open channel along the depth is not uniform and that is why mean velocity is chosen for the analysis of flow. The *mean fluid velocity* is the average of all the velocities from bed to free surface at a section. In the next section, Chezy and Manning equations are derived to determine the mean fluid velocity in an open channel.

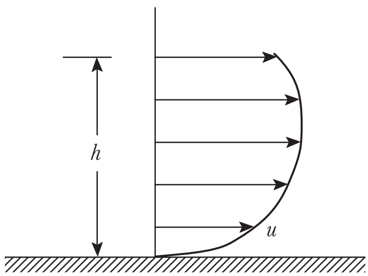

Fig. 7.5 Velocity variation along the depth

7.2.2 Chezy and Manning Equations

In uniform flow, the slope of channel bed is equal to the slope of energy grade line (EGL). The hydraulic grade line (HGL) however, coincides with the free surface of the flow stream. Figure 7.6 shows two different views of an open channel having width b and depth h. The channel bed is always provided with a small bed slope i. The specific energy in case of uniform flow is constant, as flow depth is constant throughout the channel length.

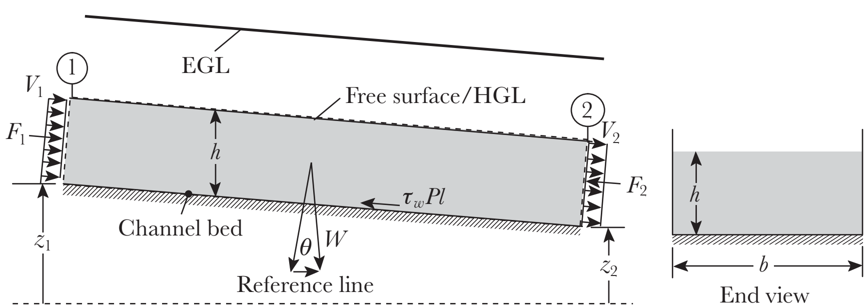

Fig. 7.6 Uniform flow in open channel

Consider a control volume in the open channel between sections 1 and 2 shown by means of dashed lines in Fig. 7.6.

Applying momentum conservation principle on the control volume

$$F_1 - F_2 - \tau_w Pl + W\sin\theta = \rho Q(V_2 - V_1) \tag{7.7}$$

where, l is the channel length between sections 1 and 2, W is the weight of fluid inside the control volume, and P is the wetted perimeter (the part of periphery of channel cross-section wetted by the flowing liquid). Since the channel has a uniform cross-section, from continuity equation

$$Q = A_1V_1 = A_2V_2 \quad \Rightarrow \quad V_1 = V_2 \tag{7.8}$$

In addition, the hydrostatic pressure forces at channel bed on either side of the control volume are same, as the depth of flow is same throughout.

$$F_1 = F_2 = \rho gh A \tag{7.9}$$

From Eqs (7.8) and (7.9), Eq. (7.7) reduces to

$$\tau_w = \frac{W\sin\theta}{Pl} \tag{7.10}$$

Since the channel slope is small, $i = \tan\theta \approx \theta \approx \sin\theta$, Eq. (7.10) can be written as

$$\tau_w = \frac{W \times i}{Pl} \quad \Rightarrow \quad \tau_w = \frac{\rho l A g \times i}{Pl} \quad \Rightarrow \quad \tau_w = \rho g m i \tag{7.11}$$

In addition, we know from the definition of skin friction coefficient that

$$\tau_w = C_f \frac{1}{2}\rho V^2 \tag{7.12}$$

where C_f is the skin friction coefficient.

From Eqs (7.11) and (7.12), the mean flow velocity is obtained as

$$V = \sqrt{\frac{2g}{C_f} mi} \tag{7.13}$$

Defining the *Chezy constant* $\mathrm{C} = \sqrt{2g/C_f} = \sqrt{8g/f}$. Equation (7.13) reduces to

$$\boxed{V = \mathrm{C}\sqrt{mi}} \tag{7.14}$$

Equation (7.14) is the well-known equation termed as *Chezy formula*.

The Chezy constant C is a function of Darcy friction factor f, which has already been related to Reynolds number and wall's relative roughness for turbulent flow using Colebrook correlation presented in Chapter 6. For the open-channel flow, the same correlation can be used by replacing pipe diameter

D (or hydraulic diameter for non-circular pipe) by $4m$, that is,

$$\frac{1}{\sqrt{f}} = 1.14 - 2\log\left(\frac{e}{4m} + \frac{9.3}{\mathrm{Re}\sqrt{f}}\right) \tag{7.15}$$

In terms of Chezy constant,

$$\mathrm{C} = 5.05 - 2\log\left(\frac{e}{4m} + \frac{41.2\mathrm{C}}{\mathrm{Re}}\right) \tag{7.16}$$

Equation (7.16) is a non-linear equation that can be solved using Newton–Raphson technique.

Robert Manning (1816–1897AD) proposed the following simple formula (also known as *Manning equation*) based on his own experimental investigations to determine the mean velocity:

$$V = (1/n)m^{2/3}i^{1/2} \tag{7.17}$$

where n is the *Manning resistance coefficient.*

On comparing Eqs (7.14) and (7.17), the Manning coefficient can be related to Chezy constant and friction factor as

$$n = \frac{m^{1/6}}{\mathrm{C}} \Rightarrow n = \sqrt{\frac{f}{8g}}m^{1/6} \tag{7.18}$$

In Eq. (7.18), Manning coefficient is proportional to the square root of friction factor, which means that Manning resistance coefficient is a measure of channel roughness just like friction factor, which is a measure of pipe roughness. Thus, rougher the channel, higher will be the value of Manning coefficient. Unlike friction factor, the Manning coefficient is not a dimensionless quantity; it has an SI unit of $s/m^{1/3}$. The Manning coefficient gives a better physical interpretation of channel conditions compared to Chezy constant. That is why, Manning equation is more popular than Chezy equation.

7.2.3 Head Loss Due to Friction

Applying the continuity equation between sections 1 and 2 in Fig. 7.6.

$$Q = b_1 h_1 V_1 = b_2 h_2 V_2 \tag{7.19}$$

The values of discharge per unit width at the two sections are

$$\left.\begin{aligned} q_1 &= Q/b_1 = h_1 V_1 \\ q_2 &= Q/b_2 = h_2 V_2 \end{aligned}\right\} \tag{7.20}$$

Applying momentum equation (Newton's second law of motion) between sections 1 and 2.

$$\rho g(A_1 y_{G1} - A_2 y_{G2}) = \rho Q(V_2 - V_1) \tag{7.21}$$

where y_{G1} and y_{G2} are the positions of centre of gravity of the two sections from the free surface.

The total head, H, at any section and at depth of 'y' from the free surface can be obtained by applying Bernoulli's equation

$$H = p/\rho g + V^2/2g + (z + h - y) \tag{7.22}$$

where p is the hydrostatic pressure at a depth of x, that is, $p/\rho g = y$. The total head at any point is; therefore, equal to

$$H = V^2/2g + z + h \tag{7.23}$$

Applying Bernoulli's equation between sections 1 and 2 yields

$$V_1^2/2g + z_1 + h_1 = V_2^2/2g + z_2 + h_2 + h_f \tag{7.24}$$

where h_f is the total head loss, z_1 and z_2 are the datum heads of the channel bed at sections 1 and 2, respectively.

For the flow to be uniform, the total head loss must be equal to the total reduction in potential energy (channel slope must be equal to the slope of EGL), that is,

$$h_f = z_1 - z_2 \tag{7.25}$$

From Eqs (7.7) and (7.8)

$$V_1^2/2g + h_1 = V_2^2/2g + h_2 \tag{7.26}$$

It can be seen that the Bernoulli's equation for an open-channel flow considering friction reduces to Bernoulli's equation for the frictionless flow in a horizontal pipe or channel. This has a physical significance, that is, the loss in fluid's potential energy, as it flows down on the channel's slope, is balanced by the head loss due to friction.

Example 7.1 The velocity at a point 0.5 m deep in the uniform flow through a wide rectangular channel is measured using tube shown in Fig. 7.7. If the rise in water level inside the tube above the free surface is 0.4 m, compute the Manning coefficient. Take bed slope as 1 in 500.

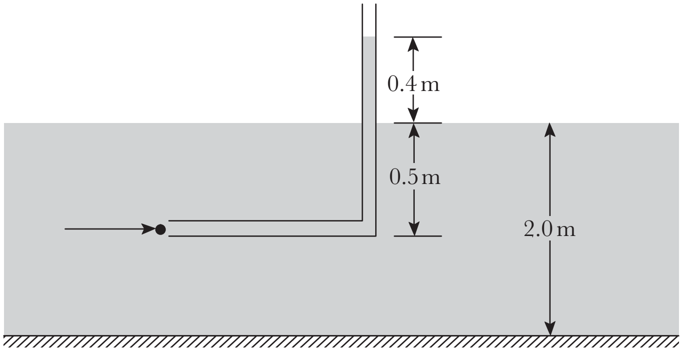

Fig. 7.7

Solution: It is given in the problem that the rectangular channel is wide ($b >> h$). The hydraulic radius or mean depth reduces to the depth of the flow, that is,

$$m = \frac{A}{P} \quad \Rightarrow \quad m = \frac{bh}{b+2h} \quad \Rightarrow \quad m \approx \frac{bh}{b} \quad \Rightarrow \quad m \approx h$$

The static pressure at the tip of the tube (from hydrostatics)

$$p_s = p_{\text{atm}} + \rho g(0.5)$$

The stagnation pressure at the tip of the tube (from hydrostatics)

$$p_o = p_{\text{atm}} + \rho g(0.5) + \rho g(0.4)$$

The dynamic pressure is the difference of stagnation and static pressure

$$p_d = p_o - p_s \quad \Rightarrow \quad \frac{1}{2}\rho V^2 = \rho g(0.4)$$

Thus, the velocity at the tip of the tube is

$$\frac{1}{2}\rho V^2 = \rho g(0.4) \quad \Rightarrow \quad V = \sqrt{2\times 9.81\times 0.4} \quad \Rightarrow \quad V = 2.8\,\text{m/s}$$

Let us assume that the velocity at the tip is equal to the mean fluid velocity inside the channel. Using Manning equation

$$V = (1/n)m^{2/3}i^{1/2} \quad \Rightarrow \quad n = (1/2.8)\times 2^{2/3}\times(1/500)^{1/2} \quad \Rightarrow \quad n = 0.0253$$

Example 7.2 Compute the mean velocity and discharge for a uniform flow through a trapezoidal channel having bed width of 5 m, flow depth of 3 m, channel-bed slope 1/3000 and side wall inclination of 45°. Take Manning's coefficient = 0.02.

Solution: The area of flow $A = \frac{1}{2}(b_1 + b_2)d$

where b_1 is the bottom width and d is the flow depth. From the geometry, the top width

$$b_2 = b_1 + 2d$$

Therefore, flow area is

$$A = (b_1 + d)d \quad \Rightarrow \quad A = (5+3)\times 3 \quad \Rightarrow \quad A = 24\,\text{m}^2$$

Wetted perimeter

$$P = b_1 + 2d/\sin 45° \quad \Rightarrow \quad P = 5 + 2\sqrt{2}\times 3 \quad \Rightarrow \quad A = 13.485\,\text{m}$$

Using Manning formula, the mean velocity is

$$V = (1/n)(A/P)^{2/3} i^{1/2} \quad \Rightarrow \quad V = \frac{1}{0.02}\times\left(\frac{24}{13.485}\right)^{2/3}\left(\frac{1}{3000}\right)^{1/2} \quad \Rightarrow \quad V = 1.34\,\text{m/s}$$

Hence, the discharge is

$$Q = AV \quad \Rightarrow \quad Q = 24 \times 1.34 \quad \Rightarrow \quad Q = 32.16\,\text{m}^3\text{/s}$$

Example 7.3 In a sewer line of circular cross-section of diameter 1.5 m shown in Fig. 7.8, the sewage water is flowing at a rate of 10 L/s. Determine the depth of flow inside the pipe. Take Manning's coefficient = 0.012 and bed slope 0.001.

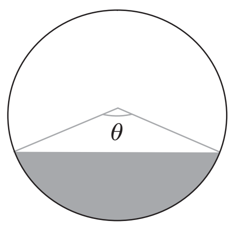

Fig. 7.8

Solution: From Manning's equation, the mean fluid velocity is given by

$$V = (1/n)(m)^{2/3} i^{1/2}$$

The discharge is given by

$$Q = AV \quad \Rightarrow \quad Q = \frac{A}{n}(m)^{2/3} i^{1/2} \tag{1}$$

From the geometry, the area of flow is obtained by subtracting the area of triangle from the sector

$$A = \frac{\theta}{360}\left(\frac{\pi D^2}{4}\right) - \frac{1}{2}\times 2\left(\frac{D}{2}\sin\frac{\theta}{2}\right)\times\frac{D}{2}\cos\frac{\theta}{2} \quad \Rightarrow \quad A = \frac{D^2}{8}(\theta - \sin\theta)$$

Wetted perimeter

$$P = \frac{\theta}{360}\pi D \quad \Rightarrow \quad P = D\frac{\theta}{2}$$

The subtended angle can be computed using Eq. (1):

$$Q = \frac{A}{n}\left(\frac{A}{P}\right)^{2/3} i^{1/2}$$

$$Q = \frac{D^2}{8n}(\theta - \sin\theta)\left(\frac{D(\theta - \sin\theta)}{4\theta}\right)^{2/3} i^{1/2}$$

$$Q = \frac{D^{8/3}}{2^{13/3}}\frac{(\theta - \sin\theta)^{5/3}}{\theta^{2/3}}\frac{i^{1/2}}{n}$$

$$0.01 = \frac{1.5^{8/3}}{2^{13/3}}\frac{(\theta - \sin\theta)^{5/3}}{\theta^{2/3}}\frac{0.001^{1/2}}{0.012}$$

$$(\theta - \sin\theta)^5 - 1.7466\theta^2 = 0$$

This equation is non-linear, which can be solved using Newton–Raphson method.

$$\theta = 2.3041\,\text{rad} \quad \Rightarrow \quad \theta = 132°$$

Depth of flow

$$h = \frac{D}{2} - \frac{D}{2}\cos\frac{\theta}{2} \quad \Rightarrow \quad h = \frac{1.5}{2} - \frac{1.5}{2}\cos\frac{132}{2} \quad \Rightarrow \quad h = 0.386\,\text{m}$$

7.3 OPTIMUM HYDRAULIC CROSS-SECTION

An open channel can have a rectangular, trapezoidal, triangular, and semi-circular cross-section. The optimum channel cross-section in each category would be the one that gives either maximum mass flow rate for a given area or minimum area for a given flow rate. The analysis for a trapezoidal cross-section, shown in Fig. 7.9, has been presented here. Using Chezy formula, the discharge through a channel can be expressed as

$$Q = AC\sqrt{(A/P)i} \tag{7.27}$$

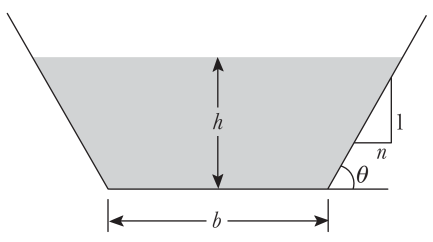

Fig. 7.9 Optimum cross-section

It can be seen from Eq. (7.27) that for a given channel-bed slope i and cross-sectional area A, the discharge Q is maximum if wetted perimeter P is minimum. The trapezoidal channels are optimized for maximum discharge by determining the optimum slope of side walls as follows:

In Eq. (7.27), A, C, and i are constant while h is an independent parameter; the discharge can be maximized if

$$\frac{dQ}{dh}=0 \quad \Rightarrow \quad \frac{dP}{dh}=0 \tag{7.28}$$

The area of trapezoidal section in terms of base width b and depth h is given by

$$A=\frac{1}{2}h\left[b+(h+2nd)\right] \quad \Rightarrow \quad A=h(b+nh) \tag{7.29}$$

The wetted perimeter of the trapezoidal section

$$P=b+2h\sqrt{n^2+1} \tag{7.30}$$

Expressing b in terms of A using Eq. (7.29) and substituting in Eq. (7.30) to obtain

$$P=A/h-nh+2h\sqrt{n^2+1} \tag{7.31}$$

The condition for maximum discharge can be obtained by substituting Eq. (7.31) in Eq. (7.28)

$$\frac{d}{dh}\left(A/h-nh+2h\sqrt{n^2+1}\right)=0 \tag{7.32}$$

or

$$-A/h^2-n+2\sqrt{n^2+1}=0 \tag{7.33}$$

$$\Rightarrow \quad A=h^2\left(n-2\sqrt{n^2+1}\right) \tag{7.34}$$

Therefore, for maximum discharge the base width is obtained by substituting A from Eq. (7.29) in Eq. (7.34)

$$\boxed{b=2h\left(\sqrt{n^2+1}-n\right)} \tag{7.35}$$

The wetted perimeter reduces to

$$P=2h\left(\sqrt{n^2+1}-n\right)+2h\sqrt{n^2+1} \tag{7.36}$$

For maximum efficiency, Eq. (7.36) is differentiated with respect to n and is equated to zero

$$\frac{dP}{dn}=0 \quad \Rightarrow \quad \frac{2n}{\sqrt{n^2+1}}-1=0 \tag{7.37}$$

Squaring and simplifying

$$\boxed{n=1/\sqrt{3}} \tag{7.38}$$

The slope of the channel side walls for maximum efficiency is

$$\tan\theta = \frac{1}{n} = \sqrt{3} \quad \Rightarrow \quad \boxed{\theta = 60^\circ} \tag{7.39}$$

Similarly, for other cross-sections, the best hydraulic cross-section can be found out.

Example 7.4 Calculate the optimum hydraulic cross-section for the rectangular channel of width b and depth h as shown in Fig. 7.10.

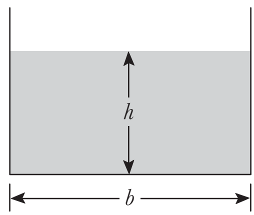

Fig. 7.10

Solution: The optimum hydraulic section for trapezoidal cross-section was obtained using Chezy formula. The discharge through the channel can also be determined by Manning formula. Let us now use the Manning formula for obtaining the optimum rectangular cross-section.

$$Q = \frac{1}{n} A m^{2/3} i^{1/2} \quad \Rightarrow \quad Q = \frac{1}{n} A \left(\frac{A}{P}\right)^{2/3} i^{1/2} \tag{1}$$

The wetted perimeter for rectangular channel, $P = b + 2h$.

The cross-sectional area for rectangular channel, $A = bh$.

Rewriting Eq. (1)

$$Q = \frac{1}{n} A \left(\frac{A}{b+2h}\right)^{2/3} i^{1/2} \quad \Rightarrow \quad Q = \frac{1}{n} A \left(\frac{Ah}{bh+2h^2}\right)^{2/3} i^{1/2}$$

$$\Rightarrow \quad \frac{Qn}{i^{1/2}} = A\left(\frac{Ah}{A+2h^2}\right)^{2/3} \quad \Rightarrow \quad \left(\frac{Qn}{i^{1/2}}\right)^{3/2} = \frac{A^{3/2} Ah}{A+2h^2}$$

or $$\mathrm{K}(A+2h^2) = A^{5/2} h \tag{2}$$

where constant $\mathrm{K} = \left(\dfrac{Qn}{i^{1/2}}\right)^{3/2}$

Differentiating Eq. (2) with respect to h

$$\mathrm{K}\left(\frac{dA}{dh} + 4h\right) = \frac{5}{2} A^{3/2} h \frac{dA}{dh} + A^{5/2} \tag{3}$$

For minimum A, $dA/dh = 0$ and using Eqs (2) and (3) reduces to

$$4h\mathrm{K} = A^{5/2} \quad \Rightarrow \quad 4h \frac{A^{5/2} h}{A+2h^2} = A^{5/2} \quad \Rightarrow \quad 4h^2 = A + 2h^2$$

$$A = 2h^2 \quad \Rightarrow \quad bh = 2h^2 \quad \Rightarrow \quad h = b/2$$

For best performance, the flow depth should be half of the channel width.

Example 7.5 Calculate the dimensions of the most efficient section of the (a) rectangular channel (b) triangular channel (c) trapezoidal channel (d) semi-circular channel for the discharge of $15\,\mathrm{m^3/s}$ at the flow velocity of $2\,\mathrm{m/s}$.

Solution: The area of flow $A = Q/V \;\Rightarrow\; A = 15/2 = 7.5\,\text{m}^2$

Channel shape	**Area (m^2)**	**Depth, h (m)**	**Free surface width (m)**	**Bed width (m)**
Rectangular	$A = 2h^2$	1.936	$b_1 = 2h$ 3.872	$b_2 = 2h$ 3.872
Triangular	$A = h^2$	2.739	$b_1 = 2h$ 5.477	0
Trapezoidal	$A = \sqrt{3}h^2$	2.080	$b_1 = 4h/\sqrt{3}$ 4.804	$b_2 = 2h/\sqrt{3}$ 2.402
Semi-circular	$A = \pi h^2/2$	2.185	$b_1 = 2h$ 4.370	NA

NOTE

The most efficient hydraulic sections have already been obtained for trapezoidal and rectangular channels. For other two channels, solve Problem 7.1 of Unsolved Problems.

7.4 NON-UNIFORM OR VARIED FLOW

A non-uniform flow is characterized by the depth variation along the channel length, that is, $dz/dx \neq 0$. The variation of depth is caused by the change in channel geometry or sudden change in channel slope or by some obstruction in the flow of passage. In addition, the sediment deposition at the channel bed locally changes the flow depth and roughness properties. Unlike uniform flow, the slopes of EGL and the channel bed are not same as shown in Fig. 7.11. In addition, the specific energy in non-uniform flow does not remain constant throughout. Consider a GVF through a rectangular channel of width b.

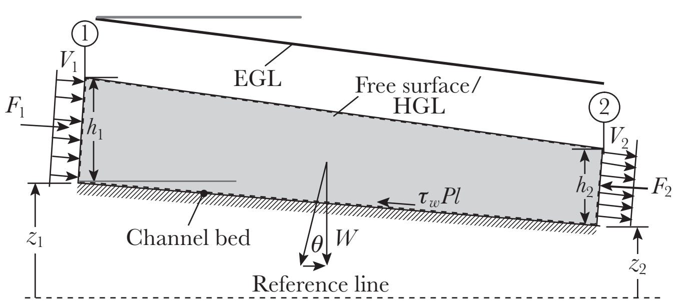

Fig. 7.11 Gradually varied flow

If Q is the discharge with flow depth h changing in the flow of direction, the mean velocity in terms of discharge is

$$V = \frac{Q}{A} = \frac{Q}{bh} = \frac{q}{h} \tag{7.40}$$

where q is the discharge per unit channel width.

Substituting Eq. (7.40) in Eq. (7.6), the specific energy is expressed as

$$E = q^2/2gh^2 + h \tag{7.41}$$

As per Eq. (7.41), for a constant value of specific energy E at a section, either the depth h is large and the discharge per unit width q is small or the depth is small and the discharge per unit width is large.

Multiplying throughout by h^2

$$h^3 - Eh^2 + q^2/2g = 0 \tag{7.42}$$

Equation (7.42) is a cubic polynomial in h with E and q as other two variables. All these three quantities can vary but the two cases of particular interest are (a) E is constant whereas h and q vary (b) q is constant whereas h and E vary. Equation (7.42) has three roots, out of which two are positive and one negative.

The negative depth has no meaning and hence the negative root of the equation is discarded. Equation (7.42) has been plotted for the aforementioned two cases in Fig. 7.12.

The *critical depth* (h_c) can be obtained by differentiating Eq. (7.41) and equating to zero, that is,

$$\frac{dE}{dh} = 0 \quad \Rightarrow \quad h_c = (q^2/g)^{1/3} \tag{7.43}$$

where h_c is the critical depth of flow.

Substituting $q^2 = gh_c^3$ in Eq. (7.41), the critical depth in terms of specific energy is given by

$$h_c = \frac{2}{3}E_{\min} \tag{7.44}$$

Out of the two positive roots (h_1 and h_2) of Eq. (7.42), one is greater than critical depth h_c and the other is lesser than the critical depth h_c. These two values of depths, h_1 and h_2, are known as *alternate depths*. The two branches of the positive roots meet at a particular value of discharge known as *critical* or *maximum discharge per unit width* ($q_{\max}$).

The critical velocity can be computed corresponding to critical depth using Eqs (7.40) and (7.43)

$$V_c = \sqrt{gh_c} \tag{7.45}$$

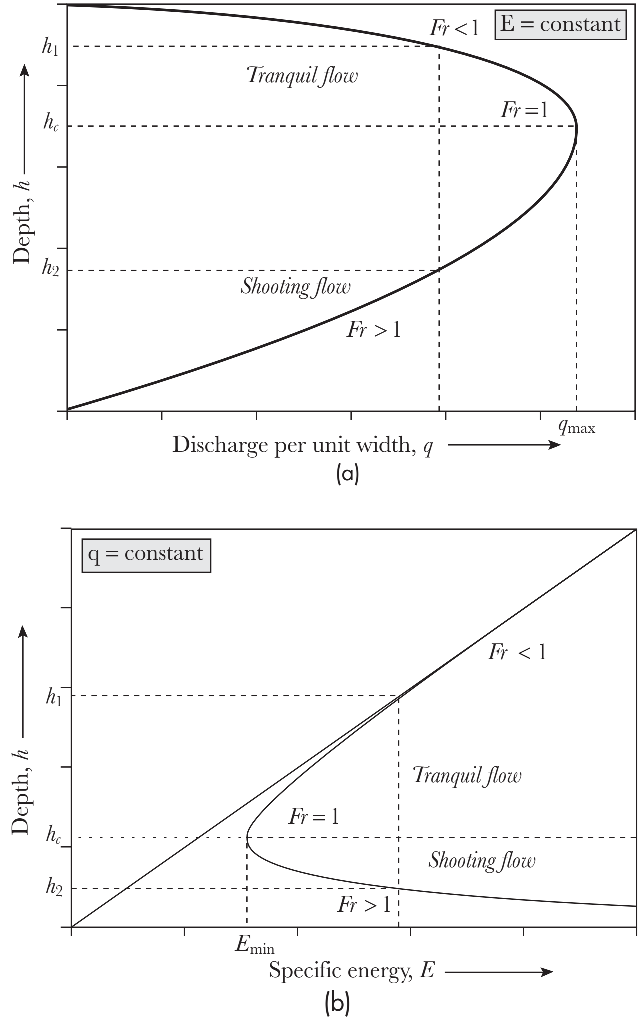

Fig. 7.12 Varied flow with (a) Constant specific energy (b) Constant discharge per unit width

Froude number can also be defined as the ratio of fluid velocity to the critical velocity, that is,

$$Fr = V/V_c \tag{7.46}$$

The classification of varied or non-uniform flow on the basis of Froude number has already been mentioned in the beginning of this chapter as *subcritical flow* ($Fr < 1$), *critical flow* ($Fr = 1$), and *supercritical flow* ($Fr > 1$).

The critical velocity obtained from Eq. (7.45) corresponds to the velocity of propagation of a small-surface wave (disturbance) in shallow liquid as discussed in Section 7.1.2. When the flow velocity is less than the critical velocity, it is

possible for the disturbance to move in both upstream and downstream directions. In this case, the fluid behaviour in upstream gets influenced by the downstream conditions. On the other hand, if the flow velocity is greater than critical velocity, the disturbance seems to move upstream and the behaviour of the fluid is not influenced by downstream conditions. The upper branch of the curve in Fig. 7.12 represents *slow* or *tranquil* or *subcritical* flow, whereas the lower branch corresponds to *rapid* or *shooting* or *supercritical* flow. For subcritical flow, the depth is greater than the critical depth, whereas for supercritical flow, the depth is less than the critical depth.

Example 7.6 For the critical flow conditions, show that the discharge Q through a circular pipe of diameter D running half-full is given by

$$Q = \frac{\pi}{8}\sqrt{\frac{g\pi D^5}{8}}$$

Solution: The specific energy is the sum of velocity head and flow depth, that is,

$$E = \frac{V^2}{2g} + h \quad \Rightarrow \quad E = \frac{Q^2}{2gA^2} + h \tag{1}$$

E is minimum at critical depth for a given discharge. Differentiating Eq. (1) with respect to h and setting it equal to zero

$$\frac{dE}{dh} = -\frac{Q^2}{gA^3}\frac{dA}{dh} + 1 = 0$$

$$\Rightarrow \quad \frac{Q^2}{g} = \frac{A^3}{dA/dh}$$

For any arbitrary channel cross-section, this equation may be generalized for the discharge at critical depth as

$$\frac{Q^2}{g} = \frac{A_c^3}{b_c} \tag{2}$$

where A_c is the cross-sectional area and b_c is the width of the free surface at the critical section.

Using this relation for calculating the discharge through a circular pipe running half-full, the area of flow and free-surface width are

$$A_c = \frac{\pi}{8}D^2 \quad \text{and} \quad b_c = D$$

Therefore, the discharge using Eq. (2) is calculated as

$$Q = \frac{\pi}{8}\sqrt{\frac{g\pi D^5}{8}}$$

Example 7.7 Determine the discharge per unit width, critical depth, and specific energy if the alternate depths for a rectangular channel are 0.5 m and 1 m.

Solution: The specific energy is equal for alternate depths for a given discharge. The specific energy in terms of discharge per unit width and flow depth is given by

$$E = \frac{q^2}{2gh_1^2} + h_1 = \frac{q^2}{2gh_2^2} + h_2$$

$$\Rightarrow \quad \frac{q^2}{2g}\left(\frac{1}{h_1^2} - \frac{1}{h_2^2}\right) = h_2 - h_1 \quad \Rightarrow \quad \frac{q^2}{2g} = \frac{h_1^2 h_2^2}{h_1 + h_2}$$

$$\Rightarrow \quad q = \sqrt{\frac{2g}{h_1 + h_2} h_1 h_2} \quad \Rightarrow \quad q = \sqrt{\frac{2\times 9.81}{1+0.5}\times 1\times 0.5} \quad \Rightarrow \quad q = 1.8083\ \mathrm{m^2/s}$$

The specific energy is

$$E = \frac{q^2}{2gh_1^2} + h_1 \quad \Rightarrow \quad E = \frac{1.8083^2}{2\times 9.81\times 1^2} + 1 \quad \Rightarrow \quad E = 1.167\,\mathrm{m}$$

For a rectangular channel, the critical depth is

$$h_c = \left(\frac{q^2}{g}\right)^{1/3} \quad \Rightarrow \quad h_c = \left(\frac{1.8083^2}{9.81}\right)^{1/3} \quad \Rightarrow \quad h_c = 0.693\,\mathrm{m}$$

7.4.1 Gradually Varied Flow

Consider a GVF through a rectangular channel of width b as shown in Fig. 7.11. If U is the total energy of fluid at any section, then

$$U = z + h + \frac{V^2}{2g} \tag{7.47}$$

Differentiating Eq. (7.47) with respect to flow direction x

$$\frac{dU}{dx} = \frac{dz}{dx} + \frac{dh}{dx} + \frac{V}{g}\frac{dV}{dx} \tag{7.48}$$

Let the slope of EGL be i_e, then Eq. 7.48 can be rewritten as

$$i_e = i + \frac{dh}{dx} + \frac{V}{g}\frac{dV}{dx} \tag{7.49}$$

From Eq. (7.40),

$$V = \frac{q}{h} \quad \Rightarrow \quad \frac{dV}{dx} = -\frac{q}{h^2}\frac{dh}{dx} \quad \Rightarrow \quad \frac{dV}{dx} = -\frac{V}{h}\frac{dh}{dx} \tag{7.50}$$

Equation (7.49) can be written as

$$i_e = i + \frac{dh}{dx} - \frac{V^2}{gh}\frac{dh}{dx} \tag{7.51}$$

From Eqs (7.4) and (7.5)

$$i_e = i + \frac{dh}{dx} - Fr^2 \frac{dh}{dx} \tag{7.52}$$

Rewriting Eq. (7.52)

$$\boxed{\frac{dh}{dx} = \frac{i_e - i}{1 - Fr^2}} \tag{7.53}$$

Hence, the variation in flow depth with flow direction is given by Eq. (7.53), which is nothing but the slope of free surface. On the basis of free-surface slope, GVF can be classified into the following three categories:

1. $dh/dx < 0$, flow depth decreases in the flow direction and is termed as *drop-down curve*
2. $dh/dx = 0$, flow depth is constant and the flow is termed as *uniform depth flow*
3. $dh/dx > 0$, flow depth increases in the flow direction and is termed as *backwater curve*

In GVF, the variation in flow depth is gradual over a length of channel, that is, $dh/dx << 1$. This may occur due to the following (a) the channel slope is not uniform (constant) (b) change in cross-section in flow direction (c) obstruction in the flow path. If channel-bed slope and slope of EGL are not equal, the flow depth will change along the channel.

The shape of free-surface profile depends upon the channel-bed slope and the Froude number. The channel-bed slopes are of three types: (a) *mild slope* is the one at which the flow through it remains subcritical (b) *critical slope* is the slope at which the flow is critical (c) *steep slope* is the slope at which the flow is supercritical.

Figure 7.13 has been drawn to show the effect of channel-bed slope and Froude number on free-surface profiles. Two situations are shown in Fig. 7.13(a) where the channel has a mild slope having subcritical flow at the upstream. In the first case, flow emerges out of the channel and gets accelerated as soon as it reaches its dead end. In the second case, sluice gate causes the flow to be slowed down at the upstream side, whereas flow becomes supercritical in the downstream side.

In Fig. 7.13(b), with critical bed slope, the flow remains critical as the free surface coincides with the critical depth line except in the zone on either side of sluice gate. On the upstream side, flow slows down to become subcritical due to presence of sluice gate, whereas on the downstream side, flow turns supercritical until it slows down to become critical again.

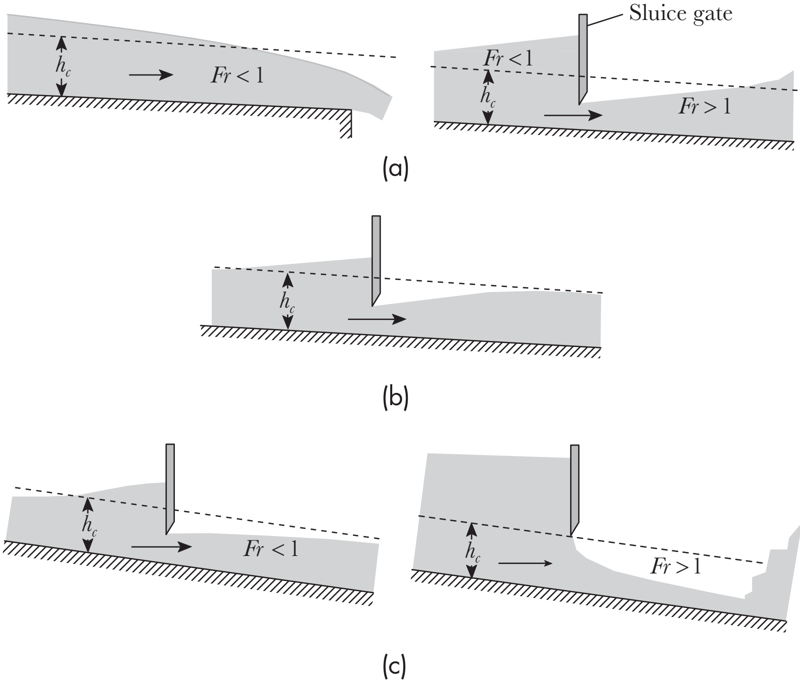

Fig. 7.13 Free surface profiles for different channel-bed slope and Froude number (a) Mild slope ($i<i_c$) (b) Critical slope ($i=i_c$) (c) Steep slope ($i>i_c$)

Figure 7.13(c) shows two cases for the channel having a slope greater than the critical slope. Different free-surface profile shapes are obtained depending upon the upstream conditions of the sluice gate.

Example 7.8 Water is flowing at a depth of 1.5 m through a 4 m wide rectangular channel having a bed slope of 0.002. Determine whether the channel is mild, steep, or critical. Take Manning coefficient as 0.015.

Solution: Area of flow $A = bh \Rightarrow A = 1.5\times 4 = 6\,\text{m}^2$

Wetted perimeter, $P = b + 2h \Rightarrow P = 4 + 2\times 1.5 = 7\,\text{m}$

Using Manning's equation to compute discharge

$$Q = \frac{1}{n} Am^{2/3} i^{1/2} \Rightarrow Q = \frac{1}{0.015}\times 6\times\left(\frac{6}{7}\right)^{2/3}\times(0.002)^{1/2} \Rightarrow Q = 16.14\,\text{m}^3/\text{s}$$

Critical depth is given by

$$\frac{Q^2}{g} = \frac{A_c^3}{b_c} \Rightarrow \frac{Q^2}{g} = h_c A_c^2 \Rightarrow h_c = \frac{16.14^2}{9.81\times 6^2} \Rightarrow h_c = 0.738\,\text{m}$$

Since the critical depth is less than the flow depth, that is, $h_c < h$ the flow will remain subcritical. Hence, the channel slope is considered mild.

7.4.2 Rapidly Varied Flow

The rapidly varied flow (RVF) is characterized by the sudden variation in depth in a relatively shorter distance such that $dh/dx \sim 1$. Whenever there is a sudden drop in flow depth (depth falls below the critical depth), the RVF is termed as *hydraulic drop*, shown in Fig. 7.14(a). Similarly, if there is a sudden rise in flow depth (depth rises above the critical depth), the RVF is termed as *hydraulic jump*, shown in Fig. 7.14(b). In hydraulic drop, the flow transition from subcritical to supercritical state takes place, whereas the flow transforms from supercritical to subcritical state in case of hydraulic jump.

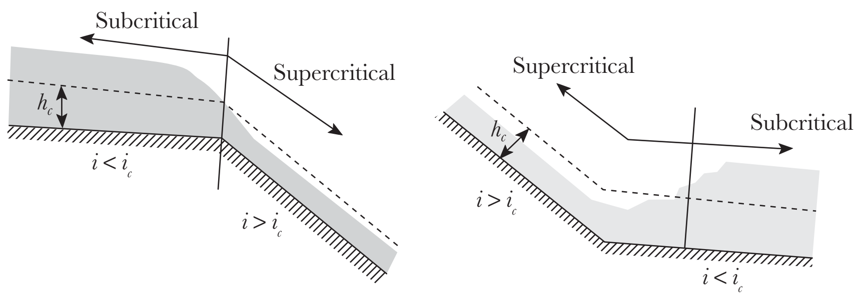

Fig. 7.14 Rapidly varied flow (a) Hydraulic drop (b) Hydraulic jump

7.5 HYDRAULIC JUMP

Hydraulic jump is an RVF where the flow depth increases suddenly while the flow transformation from supercritical to subcritical state takes place. The hydraulic jump takes place through a very short channel length, and thus may be treated as a stepped discontinuity in an open-channel flow such that $dh/dx \to \infty$ for the purpose of analysis.

The wall shear stress may conveniently be neglected as the area occupied by the stepped discontinuity is very small. Since hydraulic jump marks the sudden transition from supercritical to subcritical flow, there is loss of head h_L due to violent turbulent mixing and energy dissipation.

Consider a control volume encompassing the hydraulic jump in a horizontal rectangular channel having a constant width b as shown in Fig. 7.15.

Applying momentum conservation principle on the control volume

$$F_1 - F_2 = \rho Q(V_2 - V_1) \tag{7.54}$$

where F_1 and F_2 are the hydrostatic pressure forces acting on the centre of pressures at sections 1 and 2, respectively and they are given by

$$F_1 = \rho g y_{G1} A_1; \quad F_2 = \rho g y_{G2} A_2 \tag{7.55}$$

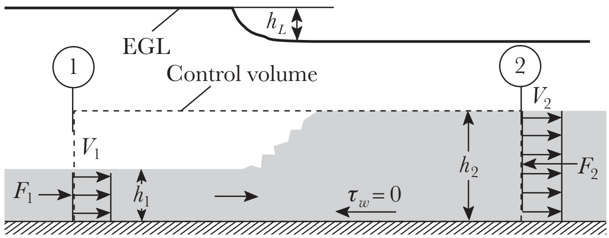

Fig. 7.15 Hydraulic jump

where A_1 and A_2 are the flow areas having a rectangular geometry at sections 1 and 2, respectively.

$$A_1 = bh_1; \quad A_2 = bh_2 \tag{7.56}$$

y_{G1} and y_{G2} are the position of CGs for the area of flow at sections 1 and 2, respectively.

$$y_{G1} = h_1/2; \quad y_{G2} = h_2/2 \tag{7.57}$$

Using Eq. (7.56) and Eq. (7.57), Eq. (7.55) is written as

$$F_1 = \frac{\rho g b h_1^2}{2}; \quad F_2 = \frac{\rho g b h_2^2}{2} \tag{7.58}$$

Since the channel has a uniform cross-section, from continuity equation

$$Q = A_1 V_1 = A_2 V_2 \quad \Rightarrow \quad Q = bh_1 V_1 = bh_2 V_2 \tag{7.59}$$

Substituting Eqs (7.58) and (7.59) in Eq. (7.54)

$$\frac{\rho g b h_1^2}{2} - \frac{\rho g b h_2^2}{2} = \frac{\rho Q^2}{b}\left(\frac{1}{h_2} - \frac{1}{h_1}\right) \tag{7.60}$$

or $$\frac{h_1^2 - h_2^2}{2} = \frac{V_1^2 h_1}{g h_2}(h_1 - h_2) \quad \Rightarrow \quad \frac{h_1 + h_2}{2} = \frac{V_1^2 h_1}{g h_2} \tag{7.61}$$

or $$\frac{h_1 + h_2}{2} = \frac{Fr_1^2 h_1^2}{h_2} \quad \Rightarrow \quad \left(\frac{h_2}{h_1}\right)^2 + \left(\frac{h_2}{h_1}\right) - 2Fr_1^2 = 0 \tag{7.62}$$

Equation (7.62) is quadratic in h_2/h_1, and its solution is given by

$$\frac{h_2}{h_1} = \frac{1}{2}\left(-1 \pm \sqrt{1 + 8Fr_1^2}\right) \tag{7.63}$$

Ignoring the negative root,

$$\frac{h_2}{h_1} = \frac{1}{2}\left(-1 + \sqrt{1 + 8Fr_1^2}\right) \tag{7.64}$$

Now, applying Bernoulli's equation between sections 1 and 2,

$$V_1^2/2g + h_1 = V_2^2/2g + h_2 + h_L \tag{7.65}$$

In dimensionless form, Eq. (7.65) can be written as

$$\frac{h_L}{h_1} = 1 - \frac{h_2}{h_1} + \left(\frac{V_1^2 - V_2^2}{2gh_1}\right) \tag{7.66}$$

$$\frac{h_L}{h_1} = 1 - \frac{h_2}{h_1} + \frac{Fr_1^2}{2}\left[1 - \left(\frac{h_1}{h_2}\right)^2\right] \tag{7.67}$$

The depth ratio across the hydraulic jump, h_2/h_1 as well as the head loss, h_L/h_1 across the hydraulic jump are functions of upstream Froude number. Equations (7.64) and (7.67) are plotted in Fig. 7.16.

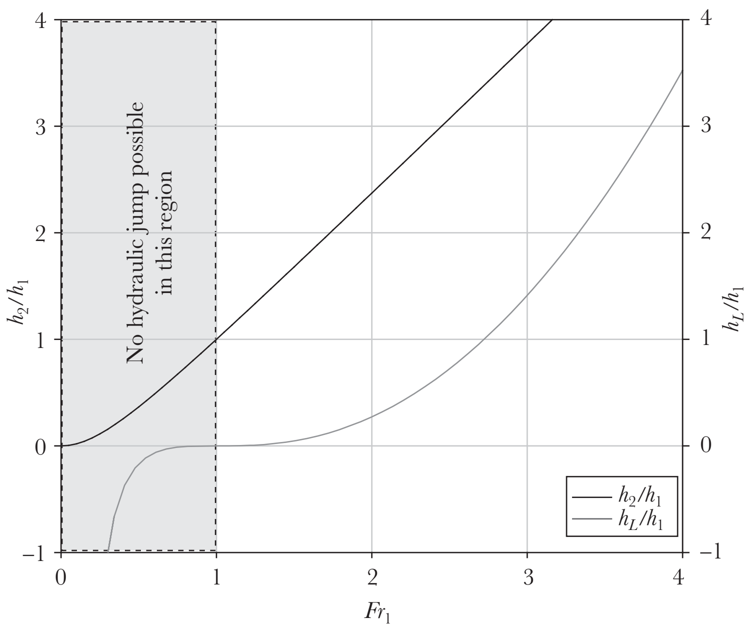

Fig. 7.16 Variation of depth ratio and ratio of head loss to upstream depth with upstream Froude number

It is clear from the figure that both depth ratio and head loss increase as upstream Froude number increases from unity onwards. Higher upstream Froude number results in higher jump and corresponding losses. For an

upstream Froude number having a value below 1, hydraulic jump cannot occur as the flow has to be supercritical on the upstream side for the occurrence of hydraulic jump. Table 7.1 shows different types of hydraulic jumps for different upstream Froude numbers in a rectangular channel.

Table 7.1 Classification of hydraulic jumps

Froude number	**Type of jump**	**Description**	**Profile**
1–1.7	Undular jump (standing wave)	• Surface undulations are formed, which diminish in size gradually • Fraction of energy dissipated is less than 5 per cent • $h_2/h_1 < 2$	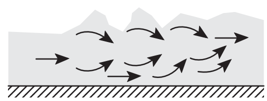
1.7–2.5	Weak jump	• Smooth rise in surface with small rollers • Fraction of energy dissipated is between 5 and 15 per cent • $2 < h_2/h_1 < 3$	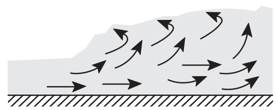
2.5–4.5	Oscillating jump	• Pulsations cause large irregular waves (damaging mostly) and must be avoided • Fraction of energy dissipated is between 15 and 45 per cent • $3 < h_2/h_1 < 5.5$	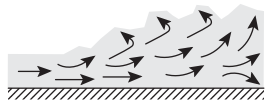
4.5–9.0	Steady jump	• Stable and unaffected by downstream conditions (recommended for design) • Fraction of energy dissipated is between 45 and 70 per cent • $5.5 < h_2/h_1 < 12$	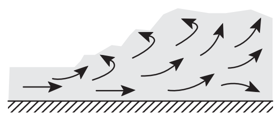
> 9.0	Strong jump	• Rough, intermittent, and often uneconomical • Fraction of energy dissipated is between 70 and 85 per cent • $h_2/h_1 > 12.0$	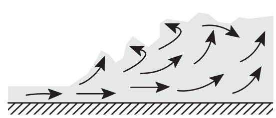

Source: US Department of the Interior, Bureau of Reclamation.

Example 7.9 The velocity and flow depth before the hydraulic jump for the water flowing in a rectangular channel are 8.0 m/s and 0.6 m, respectively. Determine flow depth and Froude number after the jump, head loss, and the power lost during the jump.

Solution: Froude number before the hydraulic jump

$$Fr_1 = \frac{V_1}{\sqrt{gh_1}} \quad \Rightarrow \quad Fr_1 = \frac{8}{\sqrt{9.81 \times 0.6}} \quad \Rightarrow \quad Fr_1 = 3.29 \qquad \text{(flow is supercritical)}$$

The ratio of depths across the jump

$$\frac{h_2}{h_1} = \frac{1}{2}\left(-1+\sqrt{1+8Fr_1^2}\right) \quad \Rightarrow \quad \frac{h_2}{0.6} = \frac{1}{2}\left(-1+\sqrt{1+8\times 3.29^2}\right) \quad \Rightarrow \quad h_2 = 2.5\,\text{m}$$

The velocity after the jump can be obtained from continuity equation

$$V_2 = \frac{h_1}{h_2}V_1 \quad \Rightarrow \quad V_2 = \frac{0.6}{2.5}\times 8 \quad \Rightarrow \quad V_2 = 1.92\ \text{m/s}$$

Froude number after the hydraulic jump

$$Fr_2 = \frac{V_2}{\sqrt{gh_2}} \quad \Rightarrow \quad Fr_2 = \frac{1.92}{\sqrt{9.81\times 2.5}} \quad \Rightarrow \quad Fr_2 = 0.388 \qquad \text{(flow is subcritical)}$$

The head loss during the jump

$$\frac{h_L}{h_1} = 1 - \frac{h_2}{h_1} + \frac{Fr_1^2}{2}\left[1-\left(\frac{h_1}{h_2}\right)^2\right] \quad \Rightarrow \quad \frac{h_L}{0.6} = 1 - \frac{2.5}{0.6} + \frac{3.29^2}{2}\left[1-\left(\frac{0.6}{2.5}\right)^2\right]$$

$$\Rightarrow \quad h_L = 1.16\,\text{m}$$

Alternatively, head loss can also be calculated as the difference of specific energy before and after the jump

$$h_L = h_1 - h_2 + \frac{V_1^2 - V_2^2}{2g} \quad \Rightarrow \quad h_L = 0.6 - 2.5 + \frac{8^2 - 1.92^2}{2\times 9.81} \quad \Rightarrow \quad h_L = 1.17\,\text{m}$$

Power dissipated per unit width

$$P = \rho q g h_L \quad \Rightarrow \quad P = 1000\times(0.6\times 8)\times 9.81\times 1.17 \quad \Rightarrow \quad P = 55.092\,\text{kW/m}$$

Example 7.10 A hydraulic jump occurs at the base of spillway of a dam having upstream and downstream depths of 1 m and 5 m, respectively as shown in Fig. 7.17. Determine the discharge per unit width of spillway. Find out head above the spillway if discharge coefficient is 0.7. In addition, find the head loss and power dissipated.

Solution: The ratio of depths across the jump

$$\frac{h_2}{h_1} = \frac{1}{2}\left(-1+\sqrt{1+8Fr_1^2}\right) \quad \Rightarrow \quad \frac{5}{1} = \frac{1}{2}\left(-1+\sqrt{1+8\times Fr_1^2}\right) \quad \Rightarrow \quad Fr_1 = 3.873$$

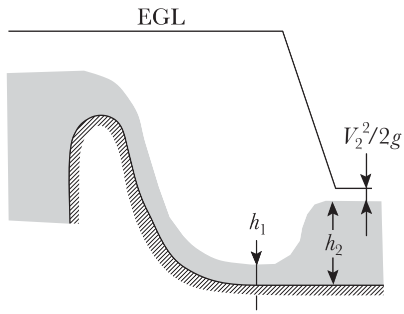

Fig. 7.17

The velocity before the jump can be obtained from

$$V_1 = Fr_1\sqrt{gh_1} \quad \Rightarrow \quad V_1 = 3.87\times\sqrt{9.81\times 1} \quad \Rightarrow \quad V_1 = 12.12\,\text{m/s}$$

Discharge per unit width of the spillway

$$q = \frac{Q}{b_1} = V_1 h_1 \quad \Rightarrow \quad q = 12.12\times 1 \quad \Rightarrow \quad q = 12.12\,\text{m}^2\text{/s}$$

Discharge per unit width of the spillway is also given by (see the derivation of discharge through a rectangular weir in the next section)

$$q = \frac{2}{3}C_d\sqrt{2g}h^{3/2} \quad \Rightarrow \quad 12.12 = \frac{2}{3}\times 0.7\sqrt{2\times 9.81}h^{3/2} \quad \Rightarrow \quad h = 3.25\,\text{m}$$

The head loss is given by

$$\frac{h_L}{h_1} = 1-\frac{h_2}{h_1}+\frac{Fr_1^2}{2}\left[1-\left(\frac{h_1}{h_2}\right)^2\right] \Rightarrow \frac{h_L}{1} = 1-\frac{5}{1}+\frac{3.873^2}{2}\left[1-\left(\frac{1}{5}\right)^2\right] \Rightarrow h_L = 3.2\,\text{m}$$

Power dissipated per unit width

$$P = \rho q g h_L \quad \Rightarrow \quad P = 1000\times 12.12\times 9.81\times 3.2 \quad \Rightarrow \quad P = 38.047\,\text{kW/m}$$

7.6 FLOW MEASUREMENT IN OPEN CHANNELS

The tranquil flow in a channel can be made critical by either raising the channel bed suddenly by providing a hump or by constricting the width of the channel. These two ways are employed to measure the flow in open channels. In *weirs or notches*, raising the channel bed (providing hump) forms the basis of flow measurement, whereas in *venturi flume*, contracting the channel width forms the basis for the same.

7.6.1 Notches and Weirs

Notches or weirs are placed inside the channel to constrict the flow passage by raising the height of the channel for the measurement of flow. The upper surface of the notch or weir over which the liquid flows is termed as *crest* (also known as *sill*).

The crest may have a sharp or a broad edge. The liquid sheet leaving the notch is termed as *nappe*. Notches are made up of metals and are used in small channels, whereas weirs are made of concrete or masonry and are employed in large-scale installations. The following is the classification of notches and weirs on the basis of shapes: rectangular, triangular, trapezoidal, and stepped.

Rectangular Notch or Weir

The analysis of rectangular weir is based on the assumption that the velocity varies uniformly across the depth above its crest, and the pressure under the nappe in the immediate downstream of the crest is atmospheric. However, in actual practice, the pressure under the nappe falls below the atmospheric pressure causing the reattachment of nappe to the crest. As a result, the actual discharge through the notch increases due to low-pressure suction under the nappe shown in Fig. 7.18. In order to avoid the formation of a low-pressure region, the notches are usually *ventilated* with the help of tubes to allow the atmospheric air to fill the low-pressure region.

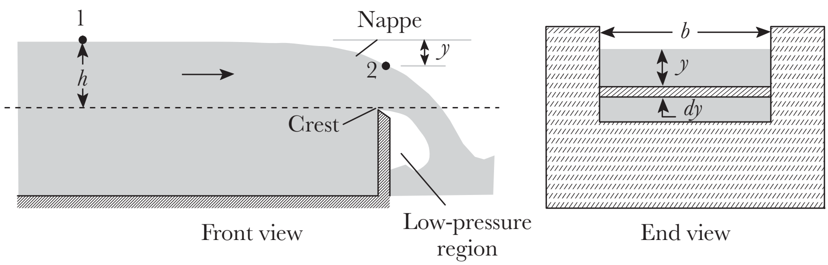

Fig. 7.18 Rectangular weir

Consider an infinitesimal strip of thickness dy at a depth of y in a rectangular weir of width b having a liquid of height h flowing above it as shown in Fig. 7.18.

Velocity of approach, that is, the velocity with which the liquid approaches the notch can be obtained by applying Bernoulli's equation between 1 and 2.

$$0 + h = V_2^2/2g + (h - y) \tag{7.68}$$

$$V = \sqrt{2gy} \tag{7.69}$$

Discharge of liquid through the strip is

$$dQ = bdy\sqrt{2gy} \tag{7.70}$$

Theoretical discharge through the weir is obtained by integrating the liquid height above the weight crest.

$$Q_{\text{th}} = \sqrt{2g}b\int_0^h y^{1/2}dy \quad \Rightarrow \quad Q_{\text{th}} = \frac{2}{3}\sqrt{2g}bh^{3/2} \tag{7.71}$$

The actual discharge through the rectangular weir is given by

$$Q_{\text{act}} = \frac{2}{3} C_d \sqrt{2g} b h^{3/2} \tag{7.72}$$

Equation (7.72) is valid for *suppressed weir* in which the width of the weir crest is same as the channel width. For a rectangular weir having crest width smaller than channel width (shown in Fig. 7.19), the effect of end contraction has to be taken into consideration. The following are the two empirical formulae for unsuppressed weirs:

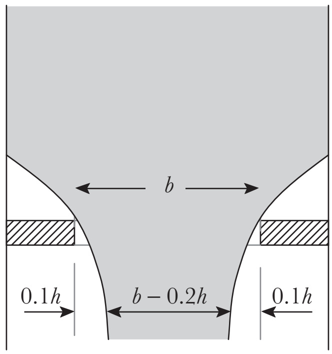

Fig. 7.19 End effects

Francis formula On the basis of exhaustive experimental test runs, Francis established that the width of the flowing sheet above the weir crest gets reduced by $0.1h$ on either side as shown in Fig. 7.14. The actual discharge is thus reduced and is given by

$$Q_{\text{act}} = \frac{2}{3} C_d \sqrt{2g} (b - 0.2h) h^{3/2} \tag{7.73}$$

Bazin formula Bazin also conducted a number of experiments to come up with the following empirical correlation for the discharge over *unsupressed* weir:

$$Q_{\text{act}} = mb\sqrt{2g} h^{3/2} \tag{7.74}$$

where

$$m = 0.405 + \frac{0.003}{h} \tag{7.75}$$

The discharge through the rectangular notch is directly proportional to 3/2-th power of liquid height above the crest, that is,

$$Q = C_1 h^{3/2} \tag{7.76}$$

The error in discharge is obtained by taking log and then differentiating

$$\frac{dQ}{Q} = \frac{3}{2}\frac{dh}{h} \tag{7.77}$$

This means that the error in measurement of discharge through a rectangular weir is 1.5 times the error in measurement of height.

Stepped Notch or Weir

The stepped weir is the combination of rectangular weirs. Figure 7.20 shows a three-step weir having widths b_1, b_2, and b_3 and respective liquid heights above each weir are h_1, h_2, and h_3.

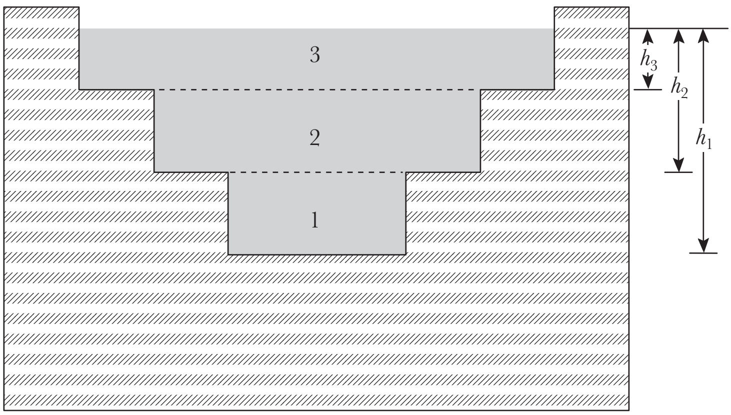

Fig. 7.20 Stepped weir

The discharge through the stepped weir is obtained by adding the individual weir discharges.

$$Q = Q_1 + Q_2 + Q_3 \tag{7.78}$$

$$Q = \frac{2}{3}C_d\sqrt{2g}b_1\left(h_1^{3/2} - h_2^{3/2}\right) + \frac{2}{3}C_d\sqrt{2g}b_2\left(h_2^{3/2} - h_3^{3/2}\right) + \frac{2}{3}C_d\sqrt{2g}b_3h_3^{3/2} \tag{7.79}$$

Triangular Notch or Weir

In triangular notches, there is no need for ventilation as there will be no place for the formation of a low-pressure region. Consider an infinitesimal strip of thickness dy at a depth of y in a triangular weir, shown in Fig. 7.21, having a liquid height of h flowing above it.

Velocity of approach, that is, the velocity with which the liquid approaches the notch

$$V = \sqrt{2gy} \tag{7.80}$$

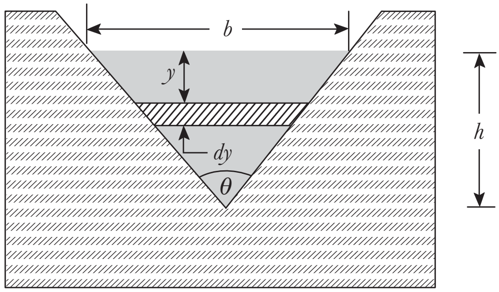

Fig. 7.21 Triangular weir

Discharge of liquid through the strip is

$$dQ = bdy\sqrt{2gy} \quad \Rightarrow \quad dQ = (h-y)\tan(\theta/2)dy\sqrt{2gy} \tag{7.81}$$

Theoretical discharge through the weir is obtained by integrating the liquid height above the weight crest.

$$Q_{\text{th}} = \sqrt{2g}\int_0^h (h-y)\,y^{1/2}dy \quad \Rightarrow \quad Q_{\text{th}} = \frac{8}{15}\sqrt{2g}\,\tan\frac{\theta}{2}h^{5/2} \tag{7.82}$$

The actual discharge through the rectangular weir is given by

$$Q_{\text{act}} = \frac{8}{15}C_d\sqrt{2g}\,\tan\frac{\theta}{2}h^{5/2} \tag{7.83}$$

The discharge through the rectangular notch is directly proportional to 5/2-th power of liquid height above the crest, that is,

$$Q = C_1 h^{5/2} \tag{7.84}$$

The error in discharge is obtained by taking log and then differentiating

$$\frac{dQ}{Q} = \frac{5}{2}\frac{dh}{h} \tag{7.85}$$

This means that the error in measurement of discharge through a triangular weir is 2.5 times the error in measurement of height.

Trapezoidal Notch or Weir

The trapezoidal weir is the combination of rectangular and triangular weirs as shown in Fig. 7.22. Thus, the discharge through a trapezoidal weir is equal to the sum of discharges through the rectangular and triangular weirs.

$$Q = Q_{\text{rect}} + Q_{\text{tri}} \tag{7.86}$$

$$Q = \frac{2}{3}C_{d1}\sqrt{2g}bh^{3/2} + \frac{8}{15}C_{d2}\sqrt{2g}\,\tan\frac{\theta}{2}h^{5/2} \tag{7.87}$$

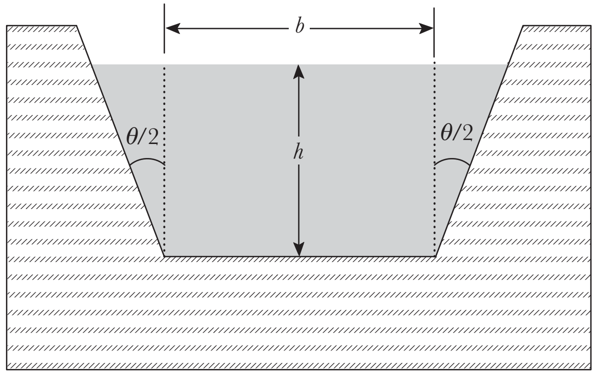

Fig. 7.22 Trapezoidal weir

A trapezoidal weir with side wall slope of 1 horizontal to 4 vertical, that is, $\tan\frac{\theta}{2} = \frac{1}{4}$ is known as *Cippoletti weir*.

Example 7.11 A sharp crested 1 m high rectangular weir is used to measure discharge through a horizontal channel 5 m wide. Determine the discharge if the flow depth in the upstream is 2.0 m. Take $C_d = 0.7$.

Solution: The head above the weir, $h = 2 - 1 = 1$ m.
If the weir is unsuppressed, the discharge is given by

$$Q_{\text{act}} = \frac{2}{3} C_d \sqrt{2g}\, b h^{3/2} \Rightarrow Q_{\text{act}} = \frac{2}{3} \times 0.7 \times \sqrt{2 \times 9.81} \times 5 \times (1)^{3/2}$$

$$\Rightarrow Q_{\text{act}} = 10.33\,\text{m}^3/\text{s}$$

If the weir is suppressed, the discharge is given by Francis formula:

$$Q_{\text{act}} = \frac{2}{3} C_d \sqrt{2g}\,(b - 0.2h) h^{3/2} \quad \Rightarrow \quad Q_{\text{act}} = \frac{2}{3} \times 0.7 \times \sqrt{2 \times 9.81} \times (5 - 0.2 \times 1)(1)^{3/2}$$

$$\Rightarrow \quad Q_{\text{act}} = 9.92\,\text{m}^3/\text{s}$$

Example 7.12 Determine the discharge through a stepped notch shown in Fig. 7.23 if the discharge coefficient of each section is 0.65.

Solution: Discharge through the stepped notch is the summation of discharges through individual rectangular sections, that is,

$$Q = \frac{2}{3} C_d \sqrt{2g} \left[b_1 (h_1^{3/2} - h_2^{3/2}) + b_2 (h_2^{3/2} - h_3^{3/2}) + b_3 h_3^{3/2} \right]$$

$$Q = \frac{2}{3} \times 0.65 \times \sqrt{2 \times 9.81} \left[0.5(1.5^{3/2} - 1^{3/2}) + 1.0 \times (1^{3/2} - 0.5^{3/2}) + 1.5 \times 0.5^{3/2} \right]$$

$$Q = 0.2339\,\text{m}^3/\text{s}$$

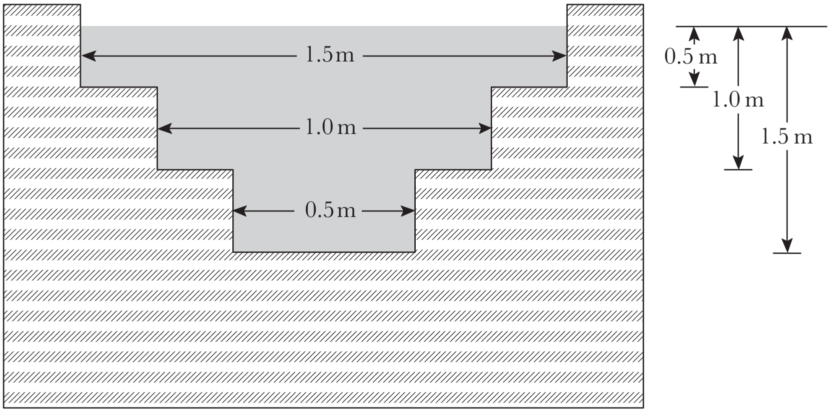

Fig. 7.23

Example 7.13 A discharge of $0.5\,m^3/s$ is to be measured using a rectangular notch having 2m width. What would be the head over the crest? If the graduated scale used to measure the head has the least count of 1mm, calculate the uncertainty in the measured discharge if the discharge coefficient is 0.6.

Solution: Discharge through a rectangular notch is given by

$$Q = \frac{2}{3} C_d b \sqrt{2g} h^{3/2} \tag{1}$$

$$0.5 = \frac{2}{3} \times 0.6 \times 2 \times \sqrt{2 \times 9.81} \times h^{3/2} \quad \Rightarrow \quad h = 0.271\,\text{m}$$

From Eq. (1), it is clear that the discharge is the function of head only, that is,

$$Q = Kh^{3/2} \tag{2}$$

Taking log and differentiating Eq. (2)

$$\frac{dQ}{Q} = \frac{3}{2}\frac{dh}{h} \tag{3}$$

In Eq. (3), dh is the uncertainty in h, which is equal to the least count of the measuring scale, that is, $dh = 1\,\text{mm} = 0.001\,\text{m}$. The uncertainty in discharge dQ can be obtained from Eq. (3).

$$dQ = \frac{3}{2}\frac{dh}{h} Q \quad \Rightarrow \quad dQ = \frac{3}{2} \times \frac{0.001}{0.271} \times 0.5 \quad \Rightarrow \quad dQ = 2.76\,\text{L/s}$$

7.6.2 Venturi Flume

A venturi flume is used for higher discharge measurement in open channels. It has a constriction having a convergent section followed by a divergent section and has a close resemblance with venturimeter used in pipe flow measurement.

The channel side walls are projected to form a venturi causing the cross-section to reduce. This reduction in cross-section ensures the occurrence of critical depth at the throat. Thus, the hydraulic jump occurs at the downstream of the venturi flume. Due to this, these flumes are also known as standing wave flumes. They differ from weirs, as in weirs the critical depth is achieved by providing vertical constriction. Thus, the head loss is less in venturi flume compared to weirs. Absence of vertical constriction leaves no scope for sediments to deposit in dead zone on the upstream side of the crest.

Consider a venturi flume, shown in Fig. 7.24, having throat width b_2, fitted in a channel of width b_1. The venturi flumes are designed to attain critical conditions at the throat. Thus, maximum discharge is attained at the throat.

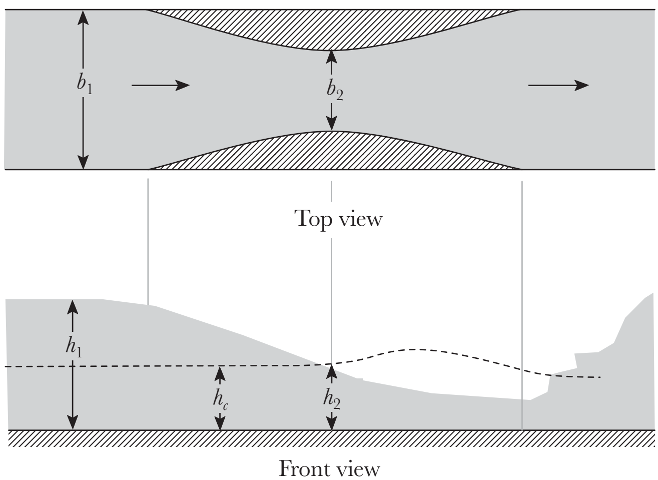

Fig. 7.24 Venturi flume

The discharge is given by

$$Q = b_2 h_2 \sqrt{g h_2} \tag{7.88}$$

From Eq. (7.88), it seems that the discharge can easily be found out if b_2 and h_2 are known. The width at the throat for a given venturi flume is known. The value of h_2 and its exact location in the venturi flume is not easy to determine. Applying Bernoulli's equation between sections 1 and 2 (neglecting losses)

$$\frac{V_1^2}{2g} + h_1 = \frac{V_2^2}{2g} + h_2 \quad \Rightarrow \quad \frac{V_1^2}{2g} + h_1 = \frac{V_2^2}{2g} + h_2 = \frac{g h_2}{2g} + h_2$$

$$\Rightarrow \quad \boxed{\frac{V_1^2}{2g} + h_1 = \frac{3}{2} h_2} \tag{7.89}$$

In addition, the velocity can be expressed in terms of discharge.

$$V_1 = \frac{Q}{b_1 h_1} \quad \Rightarrow \quad V_1 = \frac{b_2 h_2 V_2}{b_1 h_1} \quad \Rightarrow \quad V_1 = \frac{b_2 h_2 \sqrt{g h_2}}{b_1 h_1} \tag{7.90}$$

Substituting Eq. (7.90) in Eq. (7.89).

$$\frac{1}{2g} \times \frac{b_2^2 h_2^2 (g h_2)}{b_1^2 h_1^2} + h_1 = \frac{3}{2} h_2 \quad \Rightarrow \quad \left(\frac{h_1}{h_2}\right)^3 - \frac{3}{2}\left(\frac{h_1}{h_2}\right)^2 + \frac{1}{2}\left(\frac{b_2}{b_1}\right)^2 = 0 \tag{7.91}$$

Substituting $h_1/h_2 = r$ and $b_2/b_1 = \sin\theta$, Eq. (7.91) reduces to

$$r^3 - \frac{3}{2} r^2 + \frac{1}{2}\sin^2\theta = 0 \tag{7.92}$$

The relevant root of Eq. (7.92) is

$$r = \frac{1}{2} + \cos\left(\frac{3}{2}\theta\right) \tag{7.93}$$

If $b_1 >> b_2 \quad \Rightarrow \quad \sin\theta \approx 0 \quad \Rightarrow \quad \theta \approx 0$, the depth ratio becomes

$$r = \frac{3}{2} \tag{7.94}$$

The discharge through the venturi flume can be obtained.

$$Q = b_2 h_2 \sqrt{g h_2} \quad \Rightarrow \quad Q = \left(\frac{2}{3}\right)^{3/2} b_2 \sqrt{g} h_1^{3/2} \tag{7.95}$$

In case of venturi flume, the head losses are very low. The discharge coefficient has a very high value lying between 0.95–0.99. This is why Eq. (7.95) does not contain C_d. Equation (7.95) has been derived for the case when the downstream level is not high enough. In such cases, the rapid flow continues with the continuous fall in level and flume is said to be under *free discharge*.

The following conditions may arise if the flow depth in downstream of venturi flume is increased:

1. If the condition on the downstream is subcritical or flow depth is high in downstream, the flow has to transform from rapid to tranquil while undergoing hydraulic jump. The position of jump will depend upon the flow depth in downstream of the flume. As a limiting case, the jump shrinks to zero height, which means that the jump occurs at the throat itself.
2. If the flow depth in downstream is raised further (about 1.8 times of upstream depth), then the critical velocity is not attained at the throat and the flume is said to be *drowned*. Nevertheless, it must be remembered that flumes are generally designed to run under *free discharge* for all operating conditions.

In venturi flumes, the channel base is flat; only sidewalls are constricted to change the flow depth. However, in modern flumes, like *Parshall flume*, the bed has a hump in addition to the sidewall contraction. The rise in portion of bed (hump) allows the flumes to run under free discharge even at a higher downstream flow depth. This also eliminates the use of extremely small throat, thus, reducing the energy dissipation head loss at higher flow rates.

Example 7.14 A rectangular channel 4 m wide carries water at a depth of 2 m as shown in Fig. 7.25. To estimate the discharge, the channel width is reduced to 3 m and bed is raised by 0.2 m in downstream. Determine the discharge if water level in the contracted section gets dropped by 0.1m.

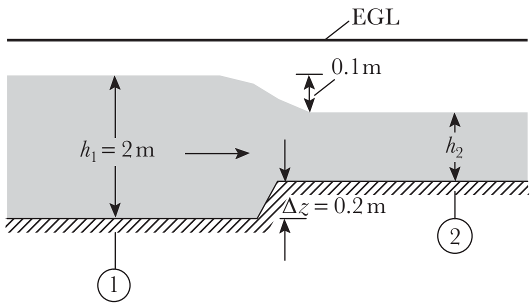

Fig. 7.25

Solution: Applying Bernoulli's equation between sections 1 and 2

$$\frac{V_1^2}{2g} + h_1 = \frac{V_2^2}{2g} + h_2 + \Delta z \tag{1}$$

Assuming no loss of energy between 1 and 2

$$\Rightarrow \quad \frac{V_1^2}{2g} + 0.1 = \frac{V_2^2}{2g} \tag{2}$$

Rewriting Eq. (1) and substituting the value from Eq. (2)

$$h_2 = \frac{V_1^2}{2g} - \frac{V_2^2}{2g} + h_1 - \Delta z$$

$$\Rightarrow \quad h_2 = -.01 + 2 - 0.2 \quad \Rightarrow \quad h_2 = 1.73\,\text{m}$$

In addition, from Eq. (2)

$$\frac{V_2^2}{2g} - \frac{V_1^2}{2g} = 0.1 \quad \Rightarrow \quad \frac{Q^2}{2g}\left[\frac{1}{A_2^2} - \frac{1}{A_2^2}\right] = 0.1$$

$$\Rightarrow \quad \frac{Q^2}{2g}\left[\frac{1}{(3\times 1.73)^2} - \frac{1}{(4\times 2)^2}\right] = 0.1 \quad \Rightarrow \quad Q = 9.552\,\text{m}^3/\text{s}$$

POINTS TO REMEMBER

- Flow through an open channel is gravity-driven flow as the free surface is acted upon by atmospheric pressure everywhere, which means a slope has to be provided at the channel bed for the flow to take place. In addition, if the pipe is not running full (e.g., flow in sewer lines), the flow is treated as an open-channel flow.
- The open-channel flow is broadly classified as steady flow and unsteady flow. In steady flow, the flow depth at a section in a channel does not vary with respect to time, whereas in case of unsteady flow, it varies. Mostly, the flow problems are steady in nature.
- In steady uniform flow, depth of flow is constant throughout the channel length and as such the channel-bed slope is equal to the slope of EGL, whereas in steady non-uniform (varied) flow, the flow depth does not remain constant and consequently, the slope of EGL is not same as that of the channel bed.
- In GVF, the free-surface slope is directly proportional to the difference between EGL slope and channel-bed slope and inversely proportional to $(1 - Fr^2)$. On the basis of this, the channel-bed slope is of three types: (a) *mild slope* is the one at which the uniform flow through it remains subcritical (b) *critical slope* is the slope at which the uniform flow is critical (c) *steep slope* is the slope at which the uniform flow is supercritical.
- For hydraulic jump to take place, the flow at the upstream must be supercritical ($Fr > 1$). Higher the Fr, greater will be the jump height and higher will be the losses due to energy dissipation. On the basis of Froude number range, the hydraulic jumps for a rectangular channel are classified as undular, weak, oscillating, steady, and strong jumps.
- Critical depth in a channel can be achieved by reducing the channel cross-section, which can be done either by raising the portion of channel bed or by contracting the channel side walls. These two principles form the basis of flow measurement in open channel. Raising a portion of channel bed is the methodology used in devices like *notches* and *weirs*, while contracting the channel side walls is the basis for flow measurement by *venturi flumes*.
- The weirs/notches are classified mainly on the basis of shape of the cross-section—rectangular, triangular, trapezoidal, etc. Notches are made up of metals and are employed in small channels, whereas weirs are made up of concrete/masonry and are employed in large installations.
- Flumes are generally designed to run under *free discharge* (i.e., no jump in downstream) for all operating conditions.

SUGGESTED READINGS

Chow, V.T., *Open-Channel Hydraulics*, McGraw-Hill Book Company, New York, 1959.

Kanakatti, S., *Flow in Open Channels*, 3rd Ed., Tata McGraw-Hill Education Pvt. Ltd., New Delhi, 2009.

Massey, B., *Mechanics of Fluids*, 8th Ed., Taylor and Francis, Noida, 2010.

Munson, B.R., D.F. Young, and T.H. Okiishi, *Fundamentals of Fluid Mechanics*, 5th Ed., John Wiley and Sons, New Delhi, 2007.

MULTIPLE-CHOICE QUESTIONS

7.1 In an open-channel flow, the specific energy is defined as
- (a) the total energy per unit volume
- (b) the total energy per unit mass
- (c) the total energy per unit specific weight
- (d) the total energy with respect to the channel bottom as reference

7.2 Hydraulic jump occurs when the
- (a) channel bed is smooth
- (b) flow changes from subcritical to subcritical
- (c) flow changes from supercritical to subcritical
- (d) slope of bed changes from steep to mild

7.3 Hydraulic mean depth for a circular pipe of diameter d running full is
- (a) d
- (b) $d/2$
- (c) $d/4$
- (d) $0.29d$

7.4 Froude number may be used for the calculation of
- (a) hydraulic waves and jumps in open-channel flow
- (b) major losses in pipe flow
- (c) major losses in open-channel flow
- (d) slope of flow

7.5 A triangular channel will be hydraulic efficient if the vertex angle at the bottom of its bed is
- (a) 30°
- (b) 45°
- (c) 60°
- (d) 90°

7.6 Which of the following is the most efficient channel section?
- (a) Triangular
- (b) Rectangular
- (c) Circular
- (d) Trapezoidal

7.7 For Froude number less than 1, the disturbances can propagate in
- (a) upstream only
- (b) downstream only
- (c) upstream as well as downstream
- (d) none of these

7.8 If upstream level is not affected by downstream conditions, then the flow is called
- (a) subcritical
- (b) supercritical
- (c) critical
- (d) uniform

7.9 Critical depth for a flow rate of $5\,m^2/s$ per unit width in an open rectangular channel is
(a) 1.357m (c) 2.50m
(b) 1.640m (d) none of these

7.10 The nature of flow for a discharge of $2.5\,m^3/s$ through a rectangular open channel of bottom width 1m and depth 5m is
(a) critical (c) subcritical
(b) supercritical (d) depends upon the nature of fluid

7.11 For a rectangular weir, the discharge varies with the head to the power
(a) 2/3 (c) 1/2
(b) 3/4 (d) 3/2

7.12 The hydraulic radius for an open rectangular channel 2m wide laid on 2° bed slope with 0.5m flow depth is
(a) 0.20m (c) 0.48m
(b) 0.33m (d) 0.75m

7.13 Shooting flow can never take place
(a) in a horizontal channel (c) in a steep slope channel
(b) in a mild slope channel (d) directly after the hydraulic jump

7.14 The alternate depths for an open rectangular channel are 0.5m and 1m. The specific energy head is
(a) 1/6m (c) 7/6m
(b) 5/6m (d) 1m

7.15 The alternate depths for an open rectangular channel are 0.5m and 1m. The critical depth is
(a) 0.593m (c) 0.893m
(b) 0.693m (d) 0.993m

7.16 The critical depth is the flow depth at which
(a) the discharge is minimum for a fixed potential energy (c) the discharge is minimum for a fixed specific energy
(b) the discharge is maximum for a fixed kinetic energy (d) the discharge is maximum for a fixed specific energy

7.17 In an open rectangular channel flow the Froude number is Fr_o at a depth of h_o, then h_c/h_o is
(a) $Fr_o^{1/2}$ (c) Fr_o^{2}
(b) $Fr_o^{1/3}$ (d) Fr_o^{3}

7.18 The instrument that may be used for measuring discharge through channel is
(a) venturi flume (c) current meter
(b) rotameter (d) flow nozzle

7.19 The weir is used to measure
(a) discharge through a small channel (c) velocity through a small channel
(b) discharge through a large channel (d) discharge through a small pipe

7.20 The value of angle for which the discharge is maximum over a triangular weir is
(a) 45° (c) 90°
(b) 60° (d) 120°

REVIEW QUESTIONS

7.1 Differentiate between the following:
   (a) Open-channel flow and pipe flow
   (c) Subcritical flow and supercritical flow
   (b) Uniform flow and varied flow
   (d) Weir and notch

7.2 'Pipe not running full is essentially an open-channel flow.' Justify the statement.

7.3 What is the physical significance of Froude number?

7.4 What is the significance of specific energy in an open-channel flow?

7.5 Write a short note on hydraulic jump and its classification.

7.6 Prove that the occurrence of hydraulic jump in a channel is impossible if the Froude number at inlet is less than unity.

7.7 What is the role of end contraction on the performance of a weir?

7.8 What do you understand by ventilation of notch? In which type of notch it is not needed?

7.9 What is the working principle of venturi flume? Discuss its merits and demerits over weir.

7.10 What is the advantage of providing a hump in a venturi flume?

UNSOLVED PROBLEMS

7.1 Show that the optimum hydraulic cross-section corresponds to
   (a) included angle $\theta = 90^\circ$ for a triangular channel
   (b) flow depth equal to radius for a semi-circular channel
   [*Hint*: Refer Example 7.4]

7.2 Show that the average wall shear stress in an open channel is given by

$$\tau_w = \frac{\rho g n^2 V^2}{m^{1/3}}$$

where symbols have their usual meanings.

7.3 Determine the critical depth for a triangular channel having an included angle 60° and the discharge through it is 2.0 m³/s.

[Ans: 1.196 m]

7.4 Calculate the discharge through a circular channel of diameter 2.0 m running critically at half-full.

[Ans: 4.36 m³/s]

7.5 Determine the discharge through a circular drainage pipe of diameter 1.0 m with a flow depth of 0.75 m. Take the slope of drainage pipe and Manning coefficient as 0.001 and 0.012, respectively.

[Ans: 0.749 m³/s]

7.6 For the pipe of diameter D not running full, determine the depth corresponding to maximum discharge using

(a) Manning equation and

(b) using Chezy equation for a given bed slope. Discuss the variation in results.

[Ans: (a) 0.938*D* (b) 0.9496*D*]

7.7 The discharge per unit width through a rectangular channel is 4 m^2/s with a depth of 2 m. Compute

(a) minimum rise in the channel bed for the attainment of critical conditions and

(b) corresponding fall in water level.

[Ans: (a) 0.4382 m (b) 0.3846 m]

7.8 A rectangular channel 4 m wide carries water at a discharge of 10 m^3/s at a depth of 2 m as shown in Fig. 7.25. Determine the height by which the bed should be raised to make the flow critical at the section where the channel width is reduced to 3 m.

[Ans: 0.5157 m]

7.9 Water is flowing at 0.1 m^3/s through a 90° triangular channel with a bed slope of 0.001. Determine whether the channel is mild, steep, or critical. Take Manning coefficient as 0.015.

[Ans: Mild slope]

7.10 The velocity and flow depth after the hydraulic jump in a rectangular channel are 1.0 m/s and 2.0 m, respectively. Determine flow depth before the jump and the head loss.

[Ans: 0.186 m, 4.027 m]

7.11 The discharge of water is measured with a sharp crested triangular weir as shown in Fig. 7.26. Determine the discharge through the weir if $C_d = 0.65$.

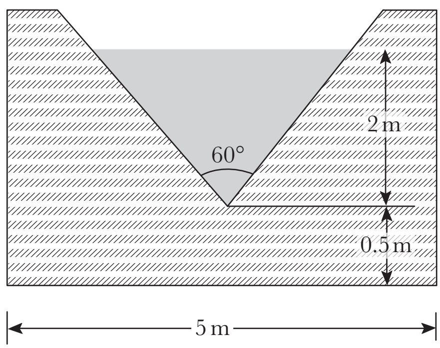

Fig. 7.26

[Ans: 5.015 m^3/s]

7.12 A wide rectangular channel has 2 m^2/s discharge per unit width and Manning coefficient of 0.02. If there is a sudden change in the channel slope from 0.001 to 0.01, what kind of transition in gradually varied flow will be observed?

[Ans: Mild to steep slope]

7.13 In a 4 m wide rectangular channel, the discharge of the GVF is 12 m³/s. Compute the slope of EGL between two sections 500 m apart and having depths of 1.5 m and 1.0 m, respectively. Take Manning's coefficient = 0.02.

[Ans: 2.69 × 10^{-3}]

7.14 Derive the following expression of discharge for the hydraulic jump taking place in a triangular channel having included angle θ with h_1 and h_2 as the conjugate heights:

$$\frac{Q^2}{g} = \frac{1}{3}\left[\frac{\left(h_2^3 - h_1^3\right)h_2^2 h_1^2}{\left(h_2^2 - h_1^2\right)}\right]\tan^2\left(\frac{\theta}{2}\right)$$

7.15 A hydraulic jump is formed in a laboratory experiment in downstream of sluice gate installed in a horizontal rectangular channel. If the depth of flow and specific energy before the jump are 0.3 m and 5 m, respectively, determine the depth of flow after the jump and energy lost.

[Ans: 2.23 m, 2.648 m]

Answers to Multiple-choice Questions

7.1 (d)	7.2 (c)	7.3 (c)	7.4 (a)	7.5 (d)
7.6 (d)	7.7 (c)	7.8 (c)	7.9 (a)	7.10 (b)
7.11 (d)	7.12 (b)	7.13 (a)	7.14 (c)	7.15 (b)
7.16 (d)	7.17 (c)	7.18 (a)	7.19 (b)	7.20 (c)

DESIGN OF EXPERIMENTS

Experiment 7.1 Determination of Discharge Coefficient of a Given Notch

Objective

To determine the discharge coefficient of a triangular/rectangular notch.

Experimental Set-up

Notches and weirs, as shown in Fig. E7.1, are used to measure the flow of water in an open channel. A notch is made up of a metallic plate and is placed at the end of a small channel, whereas a weir is a concrete or masonry structure in an open channel, over which the liquid flow takes place. Another difference between a notch and weir is that a notch has a small size whereas a weir is of a larger size. The sheet of water flowing through a notch or weir is known as nappe.

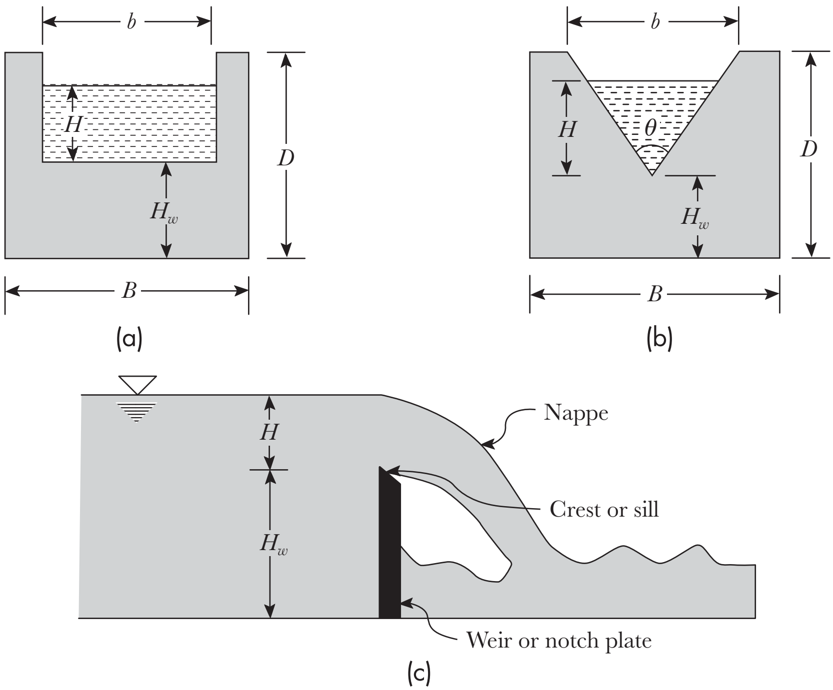

Fig. E7.1 Notches (a) Rectangular (b) Triangular (c) Side view

The bottom edge of a notch or a top edge of a weir over which the water flows is called crest or sill. A rectangular notch is called a suppressed notch if its crest length is equal to the width of the channel. However, if the width is shorter than the channel width, the effect of end contraction is considered. On the basis of experiments, Francis established that each end contraction reduces the effective length of the crest of weir by $0.1 \times H$ ('b' becomes '$b - 0.2 \times H$'). Thus, the actual discharge through the unsuppressed weirs decreases.

The theoretical discharge through the rectangular and triangular notches is given

Notch	Suppressed notch	Notch not suppressed
Rectangular notch	$Q_{\text{th}} = \frac{2}{3} b\sqrt{2g}H^{3/2}$	$Q_{\text{th}} = \frac{2}{3}(b-0.2H)\sqrt{2g}H^{3/2}$
Triangular notch	$Q_{\text{th}} = \frac{8}{15}\sqrt{2g}\tan\left(\frac{\theta}{2}\right)H^{5/2}$	NA

A schematic diagram of the experimental set-up has been shown in Fig. E7.2.

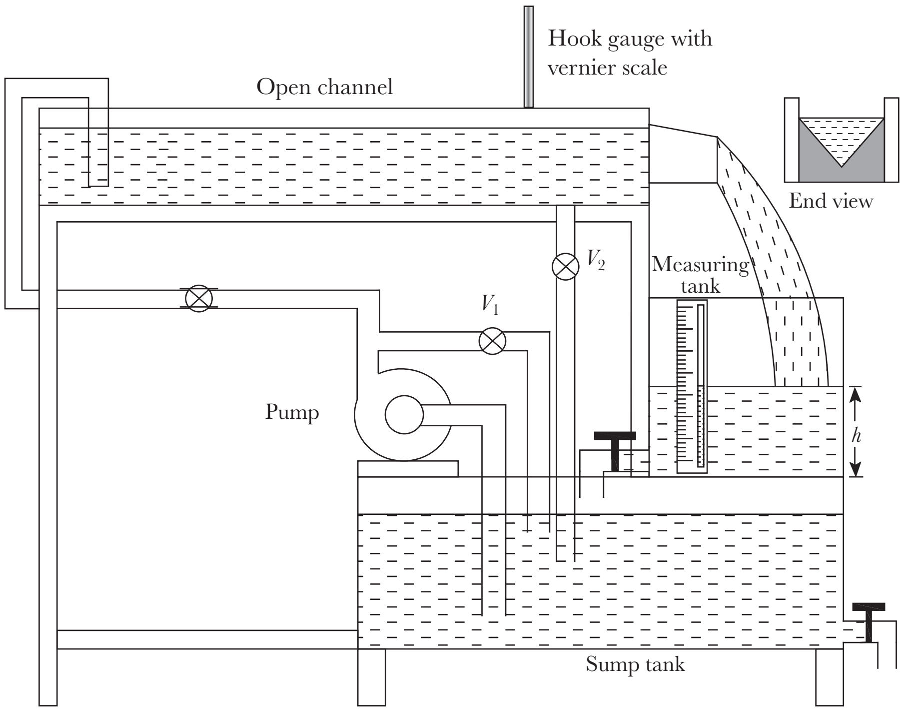

Fig. E7.2 Schematic diagram for the notch apparatus

Procedure

1. First, open the bypass valve (V_1) and close all other valves.
2. Start the motor and close the valve (V_1) until the water level reaches crest (weir) height. Take the initial reading using Hook's gauge.
3. Again open the valve (V_1) and adjust a discharge in the channel by adjusting the valve (V_2). Note down the following:
   (a) Final Hook's gauge reading when the hook (needle) touches the free stream surface
   (b) Time required for a 100 mm rise in water level in the measuring tank

4. Take 4/5 readings by repeating the aforementioned procedure for different discharges by adjusting the valves (V_1 and V_2) at different positions.
5. Stop the motor and open the valve (V_2) to drain out the remaining water out of the channel.

Observation Table

1. Measuring tank dimensions ____ mm ×____ mm × ____ mm
2. Channel dimensions ____ mm ×____ mm × ____ mm
3. Rectangular notch dimensions ($b \times d$) ____ mm × ____ mm
4. Triangular notch dimensions (90° notch angle) ____ mm × ____ mm
5. Triangular notch dimensions (60° notch angle) ____ mm × ____ mm

S. no.	Hook gauge readings			Theoretical discharge Q_{th} (m³/s)	Level rise in measuring tank, h(cm)	Time required for rise in level, t(sec)	Actual discharge $Q_{act} = Ah/t$	Discharge coefficient $C_d = Q_{act}/Q_{th}$
	x_1 (cm)	x_2 (cm)	$H = x_2 - x_1$ (cm)					
1.								
2.								
3.								
…								

Results and Discussions

1. Graphs to be plotted:
   (a) C_d versus H
   (b) Q_{act} versus H
   (c) $\log(Q_{act})$ versus $\log(H)$ to calculate the constants 'K' and 'n' in $Q_{act} = K(H)^n$
2. Discuss the nature of the curves and the reasons of deviation from the standard values

Conclusions

Draw conclusions on the results obtained.

Experiment 7.2 Calibration of Venturi Flume

Objective

To calibrate the given venturi flume.

Experimental Set-up

Venturi flume is a convergent–divergent passage constructed in a rectangular channel to measure its discharge. The experimental set-up shown in Fig. E7.3 consists of a rectangular

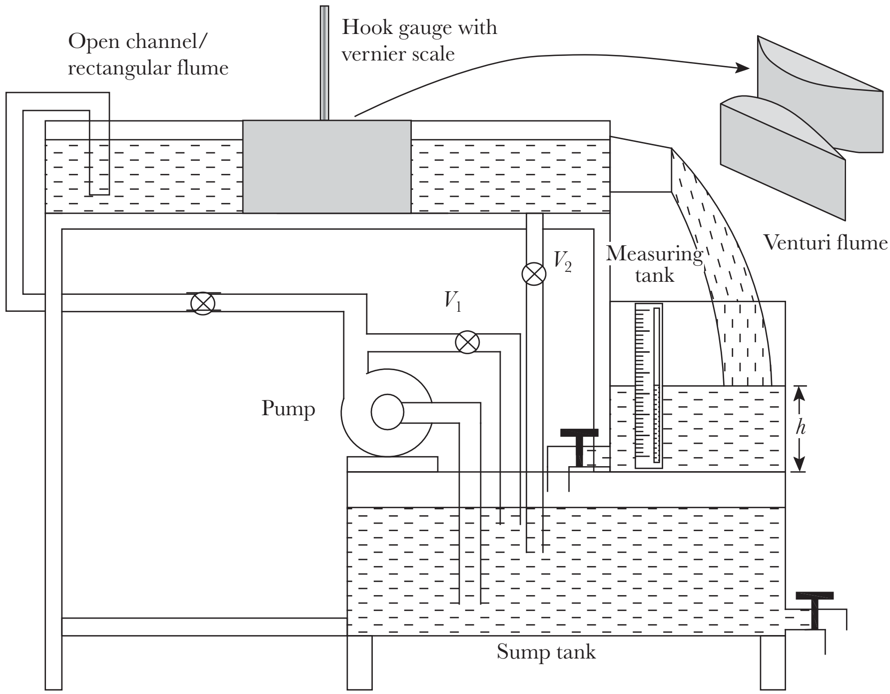

Fig. E7.3 Schematic diagram for the venturi flume apparatus

channel fitted with venturi flume to be calibrated with an arrangement to measure the water level at any section inside the flume, for example, Hook gauge fitted with vernier.

The discharge through the venturi flume can be obtained by

$$Q_{\text{th}} = \left(\frac{2}{3}\right)^{3/2} b_2 \sqrt{g} h_1^{3/2} \tag{E7.1}$$

where h_1 is the depth of flow at the venturi flume inlet and b_2 is the width at the throat.

The actual discharge is measured using the volume of water collected in measuring tank and the time required for water collection.

$$Q_{\text{act}} = \frac{Ah}{t} \tag{E7.2}$$

where A is the measuring tank's cross-sectional area and h is the rise in water level inside the measuring tank in time t.

Procedure

1. First open the bypass valve (V_1) and close all other valves.
2. Start the motor and close the valve (V_1) until the water level reaches crest (weir) height. Take the initial reading using Hook's gauge.

3. Again open the valve (V_1) and adjust a discharge in the channel by adjusting the valve (V_2). Note down the following:
   (a) Final Hook's gauge reading when the hook (needle) touches the free stream surface
   (b) Time required for 100 mm rise in water level in measuring tank
4. Take 4/5 readings by repeating the aforementioned procedure for different discharges by adjusting valves (V_1 and V_2) at different positions.
5. Stop the motor and open the valve (V_2) to drain out the remaining water out of the channel.

Observation Table

1. Measuring tank dimensions ____ mm × ____ mm ×____ mm
2. Channel dimensions ____ mm × ____ mm × ____ mm
3. Venturi flume width at the throat (b_2) ________________________ mm

S. no.	Hook gauge readings at venturi flume inlet h_1(m)	Theoretical discharge Q_{th} (m³/s)	Level rise in measuring tank, h(cm)	Time required for rise in level, t(sec)	Actual discharge $Q_{act} = Ah/t$	% error = $(1 - Q_{th}/Q_{act}) \times 100$
1.						
2.						
3.						
…						

Results and Discussions

1. Graphs to be plotted:
   (a) Q_{act} versus h_1
   (b) $\log(Q_{act})$ versus $\log(h_1)$ to calculate the constants 'K' and 'n' in $Q_{act} = K(h_1)^n$
2. Discuss the nature of the curves and the reasons of deviation from the standard values

Conclusions

Draw conclusions on the results obtained.

CHAPTER

8

Compressible Flow

LEARNING OBJECTIVES

After studying this chapter, the reader will be able to:

- Differentiate between compressible and incompressible flows
- Develop the governing equations for isentropic flow through variable area ducts (nozzles/diffusers), adiabatic flow through a constant area friction duct (Fanno flow), and non-adiabatic flow through a constant area frictionless duct (Rayleigh flow)
- Understand the phenomena of choking and shocks in the aforementioned cases
- Design simple experiments to investigate different compressible flow aspects

This chapter presents the fundamentals of compressible fluid flow. The general perception about compressible flow is that it is the flow of compressible fluids (i.e., gases). Nevertheless, this perception is not always correct; it may be true to some extent. Even the flow of compressible fluids may conveniently be treated as incompressible flow as long as the fluid velocity is less than thirty percent of sound velocity in that fluid (briefly introduced in Section 1.5.3). Moreover, it is not just the consideration of compressibility effects that differentiates it from incompressible flow, rather the existence of phenomena such as *choking* and *shock* makes the compressible flow peculiar. Compressible flows are always characterized by change in fluid density, which happens due to the change in pressure and/or temperature. Therefore, the knowledge of thermodynamics is a prerequisite to understand the compressible flow phenomenon.

This chapter revolves around reversible adiabatic (isentropic) flow through variable area ducts (nozzles and diffusers) and adiabatic flow with irreversibilities through constant area ducts. The irreversibilities in compressible flows are due to one or all of the following—friction, heat transfer, and shocks. The adiabatic flow through a constant area frictional duct is known as Fanno flow. The flow accompanied with heat transfer in a constant area frictionless duct is known as Rayleigh flow. The adiabatic flow through variable area ducts, Fanno and Rayleigh flows (flows through constant area ducts) are characterized by the phenomenon of *choking*,

which is referred to the situation where conditions at duct outlet do not have a bearing on the flow characteristics. The *shock*, in itself, is irreversibility and is considered to take place adiabatically through constant area. The governing equations are obtained by applying the laws of conservation of mass, momentum, and energy for each category. Keeping in view the importance of airfoils, a section dedicated to the compressible flow over airfoils has also been included.

The phenomenon of compressible flow has tremendous applications in the design of high-speed aircrafts, missiles, and rockets and design of turbo-machinery components.

8.1 REVIEW OF THERMODYNAMICS

An obvious question that may come into the mind of readers is that why there is a need to learn thermodynamics in order to understand the compressible flow phenomena. Conversely, the knowledge of thermodynamics is not required to comprehend the incompressible fluid flow behaviour. The reason is simple as compressible flows are variable density flows that occur due to change in pressure and/or temperature. The pressure, temperature, and specific volume (reciprocal of density) are the fluid properties known as thermodynamic state variables (explained in the next paragraph). These variables have greater dependence over one another for compressible fluids such as gases or vapours. Any change in pressure has hardly any bearing on the density of liquids. To substantiate this, Table 8.1 has been drawn, which shows the variation in density with pressure for air (compressible fluid) and water (incompressible fluid) at a temperature of 25°C. Increasing the pressure from 0.1 to 10 MPa causes almost 100 times increase in density of air; whereas, for the same change in pressure, the increase in density of water is negligibly small. Thus, the liquids are considered as practically incompressible.

Table 8.1 Density variation with pressure

Fluid	**Temperature (°C)**	**Pressure (MPa)**	**Density (kg/m³)**	**Change in density (%)**
Air	25	0.1	1.1685	9981.3
		10	117.80	
Water	25	0.1	997.05	0.446
		10	1001.5	

The small change in pressure changes the density of compressible fluids significantly, thereby changing its thermodynamic state, and that is the reason for thermodynamics being a prerequisite for the understanding

of compressible flow. In this section, a summary of thermodynamics fundamentals has been presented.

8.1.1 Thermodynamic State Variables

Let us consider a system that is not undergoing any change. One can measure or calculate all its properties at this point of time. This set of properties describes the *state* of the system. In other words, at a given state, all the properties of a system have fixed values. It has been established that not all properties are needed to fix the state of a system. The state can be fixed by fixing only a few properties. For example, only one property is needed to fix the state of a pure substance when it is saturated; otherwise at least two properties are needed to fix the state of a pure substance if it is not saturated. A minimum number of parameters are required to define the state of a system. Any relation in these parameters is known as *equation of state*. For example,

$$f(p,\forall,T)=0 \tag{8.1}$$

where $p,\forall,$ and T represent pressure, volume, and temperature, respectively.

A *process* is said to be done if a system undergoes a change in state. In a *cyclic process* both the initial and final states are same. A process is said to be *reversible* if the system and its surroundings can be restored to its initial state.

A constant temperature process is known as *isothermal process*. A constant volume process is *isochoric*, a constant pressure is *isobaric*, constant enthalpy process is *isenthalpic*, and constant entropy process is *isentropic*. In an *adiabatic process*, there is no heat transfer between the system and its surroundings. In addition, if the adiabatic process is reversible as well then it is termed as *reversible adiabatic* process, which is same as *isentropic process*. Table 8.2 shows the different processes and the corresponding relationships.

Table 8.2 Thermodynamic processes

Process	**Relation**
Isothermal	$dT=0$
Isochoric	$d\forall=0$
Isobaric	$dp=0$
Isenthalpic	$dh=0$
Adiabatic	$\delta Q=0$
Isentropic or reversible adiabatic	$ds=0;\delta Q=0$

Ideal Gas

A gas that obeys Boyle's and Charles' laws is termed as *ideal gas*. The following are the expressions for these laws:

$$\text{Boyle's law:} \quad (p\forall)_T = \text{constant} \tag{8.2}$$

$$\text{Charles' law:} \quad \left(\frac{\forall}{T}\right)_p = \text{constant} \tag{8.3}$$

$$\text{Gay-Lussac's law:} \quad \left(\frac{p}{T}\right)_\forall = \text{constant} \tag{8.4}$$

From Eqs (8.2), (8.3), and (8.4),

$$\frac{p\forall}{T} = \text{constant} \tag{8.5}$$

or

$$p\forall = m\mathrm{R}T \quad \text{or} \quad p\forall = n\mathrm{R}_o T \tag{8.6}$$

Equation (8.6) is known as *ideal gas law* or *ideal gas equation* where, m is the mass of gas, n is the number of moles in a given mass of gas, R is the specific gas constant $(\mathrm{R}=\mathrm{R}_o/M_w)$, and R_o is the universal gas constant, which is equal to 8.314 kJ/kmol-K, and M_w is the molecular mass of the gas. In terms of density or specific volume, Eq. (8.6) can be rewritten as

$$p = \rho\mathrm{R}T \quad \text{or} \quad pv = \mathrm{R}T \tag{8.7}$$

where, v is the specific volume of the gas.

The gas that follows the ideal gas law is known as *ideal gas*. A *perfect gas* is an ideal gas, which has constant specific heats at all temperatures. A *semi-perfect gas* is one that has specific heats as a function of temperature. Specific heats have been defined later in this section. A *real gas* follows the following relationship:

$$pv = z\mathrm{R}T \tag{8.8}$$

where z is known as the *compressibility factor*, a useful thermodynamic parameter for modifying the ideal gas law to account for the real gas behaviour. The air behaviour can be approximated as an ideal gas within broad range of temperature and pressure with reasonable accuracy.

Equilibrium implies a state of balance within the system. In other words, there exists no gradient within it, that is, temperature gradient, velocity gradient, concentration gradient, etc., are absent for the system in equilibrium. If temperature of the system is same throughout, it is said to be in *thermal equilibrium*. For *mechanical equilibrium*, the forces within the system must be balanced (net force within it is zero). *Chemical equilibrium* is the uniformity of concentration

or chemical composition everywhere in the system. *Thermodynamic equilibrium* is achieved only when the system is in thermal, mechanical, and chemical equilibria.

8.1.2 Laws of Thermodynamics

There are four laws of thermodynamics, namely, zeroth, first, second, and third. The zeroth law forms the basis of temperature measurement (thermometry). The first law is the energy conservation principle and its consequence is the property known as *internal energy*. It says that heat and work are interchangeable. However, it does not tell how much heat can be converted into work. The second law establishes that not all the heat energy will be converted into work. Some heat has to be rejected to the sink (unavailable energy). Its consequence is a property known as *entropy*, which is also an index of unavailable energy. Third law of thermodynamics gives the reference datum for entropy. It says that entropy of a perfect crystal is zero at absolute zero temperature.

Zeroth Law of Thermodynamics

It states that

> *In a system of three bodies, if body A is in thermal equilibrium with body B, and body B is in thermal equilibrium with body C, then all the three bodies will be in thermal equilibrium with each other.*

First Law of Thermodynamics—Energy Conservation Principle

The first law of thermodynamics is the principle of energy conservation, which can be stated in the following way:

> *Energy can neither be created nor destroyed but it can be transformed from one form to another.*

The first law of thermodynamics for cyclic process, closed system, and control volume is as follows:

1. For cyclic process

In a cyclic process, the initial state and final state of a system is same, that is, the system returns to its initial state after going through a series of processes. The heat is either absorbed or released in various processes of a thermodynamic cycle. In addition, the work is either done by the system or done on the system in different processes of the cycle. The net heat supplied is equal to net work done in a cycle, that is,

$$\oint \delta Q = \oint \delta W \quad \Rightarrow \quad \oint (\delta Q - \delta W) = 0 \tag{8.9}$$

Consider state points 1 and 2 connected by paths A, B, and C as shown in Fig. 8.1. To reach state point 2 from state point 1, there are two paths A and B, and to return to state point 1, path C is followed.

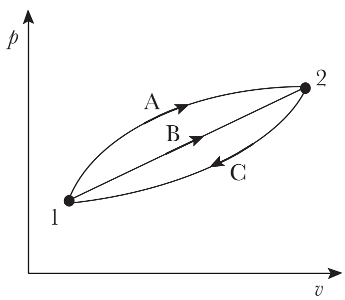

Fig. 8.1 Cyclic process

Applying the first law of thermodynamics on cycle 1–A–2–C–1

$$\oint(\delta Q - \delta W) = \int_{1A}^{2}(\delta Q - \delta W) + \int_{2C}^{1}(\delta Q - \delta W) \tag{8.10}$$

Again applying the first law of thermodynamics on cycle 1–B–2–C–1

$$\oint(\delta Q - \delta W) = \int_{1B}^{2}(\delta Q - \delta W) + \int_{2C}^{1}(\delta Q - \delta W) \tag{8.11}$$

From Eqs (8.10) and (8.11)

$$\int_{1A}^{2}(\delta Q - \delta W) = \int_{1B}^{2}(\delta Q - \delta W) \tag{8.12}$$

The quantity $(\delta Q - \delta W)$ is independent of path; and hence, it is a property known as *energy*, given by

$$dE = \delta Q - \delta W \tag{8.13}$$

2. For a closed system undergoing a process

In a closed system, only energy interactions between the system and its surroundings are permissible, whereas, mass cannot enter or leave the system. Such a system is also known as *non-flow system*. The total energy of the system is the sum of its internal energy, kinetic energy, and potential energy.

$$dE = \underbrace{dU}_{\substack{\text{Internal}\\\text{energy}}} + \underbrace{mVdV}_{\substack{\text{Kinetic}\\\text{energy}}} + \underbrace{mgdz}_{\substack{\text{Potential}\\\text{energy}}} \tag{8.14}$$

Ignoring the effects of potential and kinetic energies and using Eq. (8.13), Eq. (8.14) reduces to

$$\delta Q = dU + \delta W = dU + pd\forall \tag{8.15a}$$

On per unit mass basis, Eq. (8.15a) reduces to

$$\delta q = du + \delta w = du + pdv \tag{8.15b}$$

When the heat is supplied to a system, a part of it is utilized in doing some work, whereas, the remaining part is expended in increasing its internal energy.

3. For control volume undergoing a process

In a control volume, both energy and mass interactions between system and surroundings take place. For control volume or flow processes, the total energy is the sum of internal energy, flow work, kinetic, and potential energies, that is,

$$dE = \underbrace{dU}_{\substack{\text{Internal}\\\text{energy}}} + \underbrace{d(p\forall)}_{\substack{\text{Flow}\\\text{energy}}} + \underbrace{\dot{m}VdV}_{\substack{\text{Kinetic}\\\text{energy}}} + \underbrace{\dot{m}gdz}_{\substack{\text{Potential}\\\text{energy}}} \tag{8.16}$$

The sum of internal energy and flow work (flow energy) is a property known as *enthalpy*, that is,

$$H = U + p\forall \tag{8.17}$$

Using Eqs (8.13) and (8.17), Eq. (8.16) reduces to

$$\delta Q - \delta W = dH + \dot{m}VdV + \dot{m}gdz \tag{8.18a}$$

For flow processes, the first law of thermodynamics in per unit mass flow rate form

$$\delta q - \delta w = dh + VdV + gdz \tag{8.18b}$$

On integration,

$$q - w = h_2 - h_1 + \frac{V_2^2 - V_1^2}{2} + g(z_2 - z_1) \tag{8.18c}$$

Equation (8.18) is popularly known as *steady flow energy equation* (SFEE). The subscripts 1 and 2 represent inlet and outlet of the control volume respectively.

It is relevant at this stage to describe a property known as *specific heat*. Physically, specific heat is the measure of heat storage capacity of a substance. It is defined as the amount of heat required to raise the temperature of a unit mass of substance by 1°C. For a gas, this can be accomplished at a constant pressure as well as at a constant volume. The specific heats at constant volume and constant pressure, respectively, are defined as

$$c_v = \left(\frac{\partial q}{\partial T}\right)_v \tag{8.19}$$

$$c_p = \left(\frac{\partial q}{\partial T}\right)_p \tag{8.20}$$

At constant volume, Eq. (8.15b) reduces to

$$\delta q = du \tag{8.21}$$

From Eqs (8.19) and (8.21),

$$c_v = \left(\frac{\partial u}{\partial T}\right)_v \tag{8.22}$$

The specific enthalpy is the sum of specific internal energy and flow work, that is,

$$h = u + pv \tag{8.23}$$

Differentiating Eq. (8.23),

$$du = dh - (pdv + vdp) \tag{8.24}$$

From Eqs (8.15b) and (8.24), the first law of thermodynamics for a closed system is expressed as

$$\delta q = dh - vdp \tag{8.25}$$

From Eqs (8.20) and (8.25)

$$c_p = \left(\frac{\partial h}{\partial T}\right)_p \tag{8.26}$$

Isentropic Process

In compressible flow, the processes of expansion and compression are usually idealized with isentropic process. The expression for isentropic process is derived herewith.

Rewriting Eqs (8.15b) and (8.25),

$$\delta q = du + pdv \tag{8.15b}$$

$$\delta q = dh - vdp \tag{8.25}$$

For isentropic process $\delta q = 0$ and from definition, $du = c_v dT$ and $dh = c_p dT$. The aforementioned equations reduce to

$$c_v dT + pdv = 0 \tag{8.27}$$

$$c_p dT - vdp = 0 \tag{8.28}$$

Eliminating dT from Eq. (8.28) using Eq. (8.27)

$$c_p\left(-p\frac{dv}{c_v}\right) - vdp = 0 \tag{8.29}$$

The ratio of specific heats is represented by $\gamma = c_p/c_v$ and dividing the aforementioned equation by pv

$$\gamma\frac{dv}{v} + \frac{dp}{p} = 0 \tag{8.30}$$

On integration

$$\gamma \ln v + \ln p = C_1 \quad \Rightarrow \quad \ln(pv^\gamma) = C_1 \tag{8.31}$$

or $\quad pv^\gamma = C \quad$ or $\quad p/\rho^\gamma = C \quad$ (8.32)

The isentropic process is represented by Eq. (8.32).

Second Law of Thermodynamics

The first law of thermodynamics tells that heat energy can be converted into work. However, it does not tell how much heat can be converted into work. The second law of thermodynamics quantifies the conversion of heat into work or the conversion of work into heat. Accordingly, there are two statements of second law of thermodynamics:

Clausius statement (Conversion of work into heat)

It is impossible for a device to transfer heat from a low-temperature body to high-temperature body without doing any work.

Clausius statement forms the basis for the working of heat pumps and refrigerators.

Kelvin–Planck statement (Conversion of heat into work)

It is impossible for a device to operate in a cycle receiving heat from a source and converting it to an equal amount of work.

Kelvin–Planck statement forms the basis for the working of heat engines. This means it is impossible for a heat engine to convert 100 per cent of the heat received from a temperature source into work. Some amount of heat has to be rejected to the sink. The index of heat unavailable for the conversion into work is a property known as *entropy*.

The first law of thermodynamics gives the concept of energy, whereas, the second law of thermodynamics gives the concept of entropy. Entropy plays an important role in understanding the different types of compressible flows discussed in this chapter. The compressible flows described in the chapter are either constant entropy processes or the processes accompanied with the change in entropy.

A Carnot engine operates between two temperature reservoirs and it is known that no heat engine has thermal efficiency higher than this engine. Figure 8.2(a) shows the block diagram of Carnot engine operating between

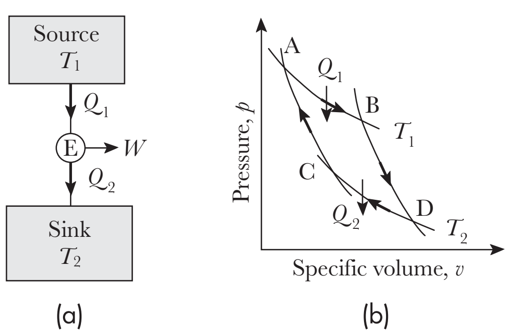

Fig. 8.2 Carnot engine (a) Block diagram (b) p–v diagram

source (high-temperature body) and sink (low-temperature body). The Carnot cycle consists of four processes, shown on p–v diagram in Fig. 8.2(b), namely,

process AB—isothermal heat addition
process BC—isentropic expansion process
process CD—isothermal heat rejection
process DA—isentropic compression process

Applying first law to the Carnot cycle

$$Q_1 - Q_2 = W \tag{8.33}$$

The cycle efficiency is given by

$$\eta = \frac{W}{Q_1} \tag{8.34}$$

From Eq. (8.33),

$$\eta = \frac{Q_1 - Q_2}{Q_1} = 1 - \frac{Q_2}{Q_1} \tag{8.35}$$

First law of thermodynamics for closed system (Eq. 8.21)

$$dQ = dU + dW \quad \Rightarrow \quad dQ = mc_v dT - pd\forall \tag{8.36}$$

For an isothermal process ($p\forall = C$ and $dT = 0$), Eq. (8.36) reduces to

$$dQ = C\frac{d\forall}{\forall} \tag{8.37}$$

Integrating Eq. (8.37) for process AB

$$Q_1 = p_A \forall_A \ln\left(\frac{\forall_B}{\forall_A}\right) \quad \Rightarrow \quad Q_1 = mRT_1 \ln\left(\frac{\forall_B}{\forall_A}\right) \tag{8.38}$$

Similarly for process CD

$$Q_2 = mRT_2 \ln\left(\frac{\forall_C}{\forall_D}\right) \tag{8.39}$$

For isentropic expansion and compression processes,

$$\frac{\forall_B}{\forall_C} = \left(\frac{T_2}{T_1}\right)^{\frac{1}{\gamma-1}} \quad \text{and} \quad \frac{\forall_A}{\forall_D} = \left(\frac{T_2}{T_1}\right)^{\frac{1}{\gamma-1}} \tag{8.40}$$

$$\frac{\forall_B}{\forall_C} = \frac{\forall_A}{\forall_D} \quad \text{and} \quad \frac{\forall_B}{\forall_A} = \frac{\forall_C}{\forall_D} \tag{8.41}$$

Using Eqs (8.38), (8.39), and (8.40), Eq. (8.35) can be written as

$$\eta = 1 - \frac{Q_2}{Q_1} = 1 - \frac{T_2}{T_1} \quad \Rightarrow \quad \frac{Q_2}{Q_1} = \frac{T_2}{T_1} \tag{8.42}$$

$$\frac{Q_1}{T_1} = \frac{Q_2}{T_2} \quad \Rightarrow \quad \frac{Q_1}{T_1} + \frac{-Q_2}{T_2} = 0 \tag{8.43}$$

This means the quantity Q/T is independent of path and hence, it is a property known as *entropy*. More appropriately, it is defined as

$$\Delta s = \oint \frac{dQ}{T} \quad \text{or} \quad \Delta s = \sum \frac{Q}{T} \tag{8.44}$$

Figure 8.3 shows that heat can be transferred from high-temperature region to low-temperature region only. Heat cannot flow on its own from a low-temperature region to a high-temperature region. If Q is the rate of heat transfer between a high-temperature body (T_1) and low-temperature body (T_2). Then, the second law for each case can be written as

$$\Delta s = \frac{-Q}{T_1} + \frac{Q}{T_2} > 0 \tag{8.45}$$

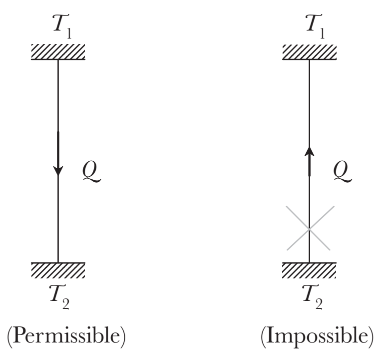

Fig. 8.3 Direction of heat flow

If Q amount of heat is to be transfered from a low-temperature body to a high-temperature body without doing any work, the entropy change comes out to be negative

$$\Delta s = \frac{Q}{T_1} + \frac{-Q}{T_2} < 0 \tag{8.46}$$

In accordance to the second law of thermodynamics, the change in entropy cannot be negative. Therefore, heat cannot be transferred from a low-temperature region to a high-temperature region at its own, as shown in Fig. 8.3.

A corollary of the second law of thermodynamics is that the entropy can never decrease, that is,

$$\boxed{\Delta s \geq 0} \tag{8.47}$$

Third Law of Thermodynamics

Entropy is a measure of disorder or randomness in a system. It is well known that molecules of a gas are loosely packed and are free to move randomly due to weak intermolecular forces. Molecular velocity is a function of temperature. From kinetic theory of gases, the velocity of molecules is directly proportional to the square root of temperature. This implies that during the heating process, the system randomness increases, resulting in an increase of entropy, whereas, the entropy decreases during the cooling process. In solids, on the other hand, the atoms occupy fixed positions in a lattice structure. The solid phase, thus, has least entropy among other phases at a given temperature. Figure 8.4 shows the phase diagram of a pure substance. This is evident from the third law of thermodynamics which states that *the entropy of a pure crystal is zero at absolute zero temperature.*

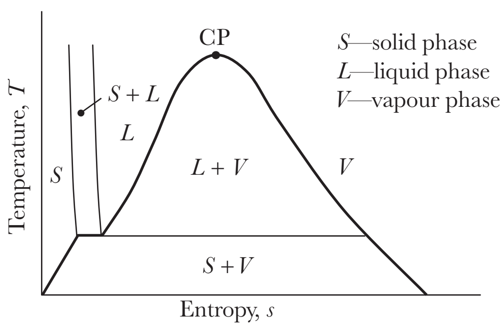

Fig. 8.4 Phase diagram of a pure substance

The third law sets a reference for the entropy.

Example 8.1 A total of 2 kg of air undergoes an isentropic expansion process in an insulated piston-cylinder assembly. The initial pressure and volume of the gas is 500 kPa and 0.05 m³. If the final volume of the air is 0.1 m³ and change in internal energy is −10 kJ/kg, determine its net heat transfer.

Solution:

Given data: $m = 2\,\text{kg}$, $p_1 = 500\,\text{kPa}$, $\forall_1 = 0.05\,\text{m}^3$, $\forall_2 = 0.1\,\text{m}^3$, $u_2 - u_1 = -10\,\text{kJ/kg}$

The final pressure is obtained from the isentropic relationship,

$$p_1\forall_1^\gamma = p_2\forall_2^\gamma \;\Rightarrow\; p_2 = p_1\left(\frac{\forall_1}{\forall_2}\right)^\gamma \;\Rightarrow\; p_2 = 500\left(\frac{0.05}{0.1}\right)^{1.4}$$

$$\Rightarrow\; p_2 = 189.46\,\text{kPa}$$

From the first law of thermodynamics for closed system,

$$\delta Q = dU + pd\forall$$

Integrating the aforementioned equation from state 1 to state 2,

$$Q_{12} = m(u_2 - u_1) + \int_1^2 pd\forall$$

Since the process is isentropic $p\forall^{\gamma} = C$

$$Q_{12} = m(u_2 - u_1) + C\int_1^2 \frac{d\forall}{\forall^{\gamma}}$$

$$Q_{12} = m(u_2 - u_1) + C\left(\frac{V_2^{-\gamma+1} - V_1^{-\gamma+1}}{-\gamma+1}\right) \Rightarrow Q_{12}$$

$$= m(u_2 - u_1) + \left(\frac{p_1V_1 - p_2V_2}{\gamma - 1}\right)$$

Substituting the numerical values to obtain the net heat transfer

$$Q_{12} = 2\times -10 + \left(\frac{500\times 0.05 - 189.46\times 0.1}{1.4 - 1}\right) \Rightarrow Q_{12} = -4.865\,\text{kJ}$$

Example 8.2 It was reported by a group of students that the power cycle developed by them consumes 100 kW of heat energy to produce a net work output of 48 kW. If the temperature of the source supplying this heat energy is maintained at 600 K and the heat rejection is done at 300 K, determine whether the developed power cycle is thermodynamically feasible.

Solution:

Given data: $T_1 = 600\,\text{K}$, $T_2 = 300\,\text{K}$, $Q_1 = 100\,\text{kW}$, $W = 48\,\text{kW}$

The efficiency of the power cycle is given by

$$\eta = \frac{W}{Q_1} \Rightarrow \eta = \frac{48}{100} \Rightarrow \eta = 0.48$$

The maximum thermal efficiency any power cycle can have is given by

$$\eta_{\max} = 1 - \frac{T_2}{T_1} \Rightarrow \eta_{\max} = 1 - \frac{300}{600} \Rightarrow \eta = 0.5$$

Since $\eta < \eta_{\max}$, the developed power cycle is thermodynamically feasible.

8.2 VELOCITY OF SOUND

A wave can be thought of as a movement of disturbance in a medium. In compressible flow, the sound wave motion in a medium is of concern. In solids, where atoms are closely packed, disturbance moves at a faster rate as compared to that

in liquids and gases. In liquids, a displaced molecule displaces a neighbouring molecule. In gases, displaced fluid mass compresses the neighbouring fluid mass causing localized increase in its density. A wave can be classified as *compression wave* and *rarefaction wave*. If the wave is at a higher pressure than the fluid medium in which it is propagating, the wave is known as compression wave. The rarefaction wave has a lower pressure than that of the medium in which it is propagating.

Now, it is desired to derive an expression for the velocity of sound wave. There are two ways of doing that: (a) by drawing an analogy from propagation of sound wave in solids and (b) propagation of sound waves in a gaseous medium. The first method is described below.

Consider a solid bar, it is acted upon by force F on its left face so that the compressive stress, f, is developed inside the rod and because of this the bar undergoes a change in its length, ΔL, as shown in Fig. 8.5.

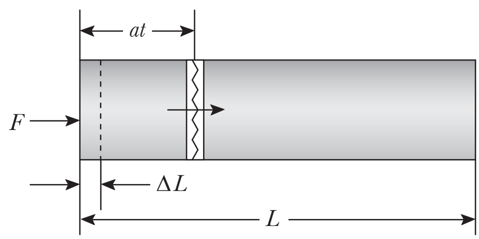

Fig. 8.5 Sound wave travelling in a solid rod

The strain at an instant 't' is defined as

$$\text{Strain} = \frac{\Delta L}{at} \tag{8.48}$$

where, a is the velocity of sound.

From Hooke's law, Young's modulus

$$E = \frac{\text{Stress}}{\text{Strain}} = \frac{f}{\Delta L/at} \tag{8.49}$$

Change in rod length per unit time is termed as the particle velocity, V. Equation (8.49) reduces to

$$V = \frac{f}{E/a} \tag{8.50}$$

Applying momentum balance,

$$F \times t = \rho A at \times V \tag{8.51}$$

or
$$V = \frac{f}{\rho a} \tag{8.52}$$

From Eqs (8.50) and (8.52), the sound velocity is

$$a = \sqrt{\frac{E}{\rho}} \tag{8.53}$$

In gases, the pressure is analogous to compressive stress and bulk's modulus of elasticity, K, is analogous to Young's modulus. Therefore, the velocity of sound in gases is given by

$$a = \sqrt{\frac{K}{\rho}} \tag{8.54}$$

where, $K = -\forall \dfrac{dp}{d\forall} = -v\dfrac{dp}{dv} = \rho \dfrac{dp}{d\rho}$

The velocity of sound is thus given by

$$\boxed{a = \sqrt{\frac{dp}{d\rho}}} \tag{8.55}$$

The following is an alternative method for obtaining this expression:

Consider an infinitesimal pressure wave moving into the stagnant fluid ($V = 0$) at the velocity of sound, as shown in Fig. 8.6. The fluid pressure, temperature, and density are p, T, and ρ, respectively. As a consequence of its movement the velocity becomes 'dV' at the upstream side. The pressure, temperature, and density become $p + dp$, $T + dT$, and $\rho + d\rho$, respectively, in the upstream of the wave. For the sake of analysis, a wave moving with sound velocity is superimposed on the existing pressure wave, so that the wave becomes stationary.

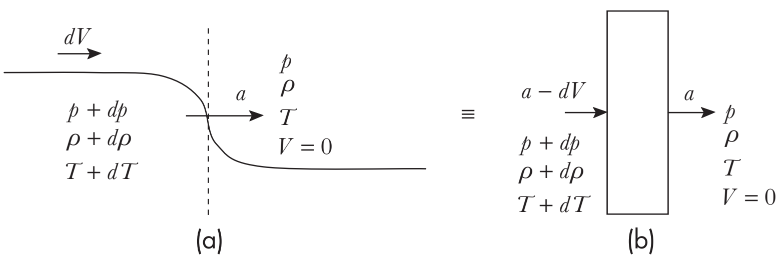

Fig. 8.6 An infinitesimal pressure wave (a) Moving (b) Stationary

The fluid velocities on the right hand side of the stationary wave is 'a' and $(a - dV)$ on the left side. Applying continuity on the stationary wave,

$$\rho A a = (\rho + d\rho) A (a - dV) \tag{8.56}$$

On simplification,

$$dV = a\left(\frac{d\rho}{\rho + d\rho}\right) \tag{8.57}$$

Applying momentum balance to the stationary wave,

$$(p + dp)A - pA = \dot{m}(a - (a - dV)) \tag{8.58}$$

or
$$dp = \rho a dV \tag{8.59}$$

Eliminating dV from the equation using Eq. (8.57) and simplifying

$$dp = \rho a^2\left(\frac{d\rho}{\rho + d\rho}\right) \tag{8.60}$$

For small strength, $\rho + d\rho \approx \rho$, Eq. (8.60) gives the sound velocity as

$$a = \sqrt{\frac{dp}{d\rho}} \tag{8.61}$$

For an isentropic process, $pv^\gamma = C$ or $p = \rho^\gamma C$. To find the derivative with respect to fluid density for an isentropic process, taking log and then differentiating to get

$$\frac{dp}{d\rho} = \frac{\gamma p}{\rho} \tag{8.62}$$

Hence, the velocity of sound for an isentropic process using the *ideal gas equation* is given by

$$a = \sqrt{\gamma RT} \tag{8.63a}$$

$$a = \sqrt{\frac{\gamma R_o T}{M_w}} \tag{8.63b}$$

where, M_w is the molecular mass of a given gas. From Eq. (8.63b), it is evident that the speed of sound is more in lower molecular weight gases.

8.2.1 Mach Number

Mach number, M, is defined as *the square-root of the ratio of inertia force to elastic force*

$$M = \sqrt{\frac{\text{Inertia force}}{\text{Elastic force}}} = \sqrt{\frac{(\rho AV)V}{KA}} \tag{8.64}$$

or
$$M = \sqrt{\frac{\rho V^2}{K}} = \sqrt{\frac{\rho V^2}{\rho dp/d\rho}} = \frac{V}{a} = \frac{\text{Fluid velocity}}{\text{Sound velocity}} \tag{8.65}$$

Mach number is, thus, also defined as *the ratio of fluid velocity to the velocity of sound in that medium (fluid)*.

On the basis of Mach number, the flow classification is done in the following manner:

1. For $M < 0.3$, the flow is considered as *incompressible* as the change in density is insignificant (see Section 8.7 for details).
2. For $0.3 < M < 0.8$, the flow is termed as *subsonic flow*.
3. For $0.8 < M < 1.2$, the flow is *transonic flow*. In fact, at $M = 1$ the flow is termed as *sonic flow*.
4. For $1.2 < M < 5.0$, the flow is *supersonic flow*.
5. For $5.0 < M < 11.0$, the flow is termed as *hypersonic flow*.
6. For $M > 11.0$, the flow is termed as *hypervelocity flow*.

The same is shown in Fig. 8.7.

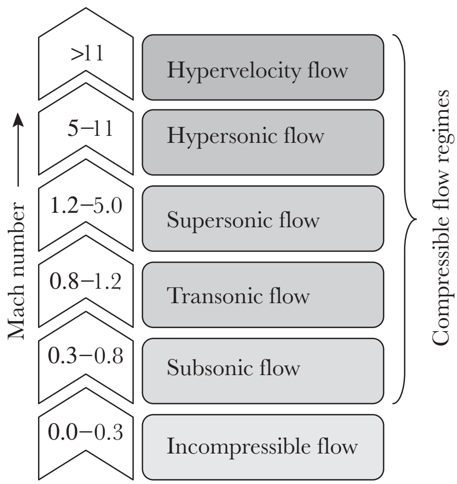

Fig. 8.7 Classification of compressible flows based on Mach number

8.2.2 Mach Cone

Different patterns of sound waves are obtained depending on whether a point source emanating sound wave is stationary or moving. Figure 8.8 shows such patterns for stationary and moving point source and position of wavefronts at time intervals Δt, $2\Delta t$, and $3\Delta t$. When the point source is stationary, the sound wavefronts are concentric, as shown in Fig. 8.8(a).

When the point source is moving with a velocity less than sound velocity, the patterns obtained are shown in Fig. 8.8(b). If it moves with a velocity greater than sound speed, which means it will break the sound barrier and will move

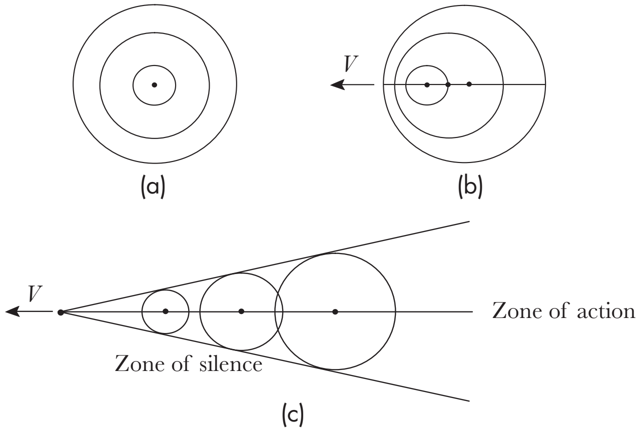

Fig. 8.8 Sound wavefronts emanating from (a) Stationary point source $V = 0$ (b) Point source moving at subsonic velocity $V < a$ (c) Point source moving at supersonic velocity $V > a$

ahead of the disturbance as shown in Fig. 8.8(c). The wavefronts in such a case form a conical surface tangential to the wavefronts known as Mach cone. The half angle of the Mach cone is known as Mach angle (α) given by

$$\sin\alpha = \frac{a\Delta t}{V\Delta t} = \frac{1}{M} \tag{8.66}$$

The region inside the Mach cone is known as *zone of action*, whereas the region outside is termed as *zone of silence*. It can be observed that as source moves away, the intensity of sound reduces.

8.3 STAGNATION AND CRITICAL QUANTITIES

Let us recall the definition of stagnation state, that is, if the fluid is brought to rest isentropically, the stagnation state is said to be achieved. To achieve the stagnation state let us consider the fluid entering a very large settling chamber through a valve, whose walls are thermally insulated, as shown in Fig. 8.9. The velocity of the fluid inside the chamber will be essentially zero. Consequently,

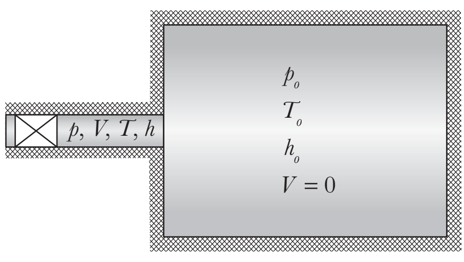

Fig. 8.9 Settling chamber connected to pipe fitted with a valve

the pressure, temperature, and density inside the chamber will increase as the kinetic energy of the fluid gets converted into the pressure energy. Thus, the quantities pressure, temperature, and density are termed as stagnation pressure, stagnation temperature, and stagnation density, respectively.

Applying steady flow energy equation between the inlet of the chamber and the inside of the chamber,

$$\cancelto{0}{q}-\cancelto{0}{w}=h_2-h_1+\frac{\cancelto{0}{V_2^2}-V_1^2}{2}+g(z_2\cancelto{0}{-z_1}) \tag{8.67}$$

Equation (8.67) reduces to

$$\boxed{h_o=h+\frac{V^2}{2}} \tag{8.68}$$

The subscript o in Eq. (8.68) indicates zero velocity (stagnation state). For a perfect gas, the enthalpy is dependent on temperature alone.

$$c_pT_o = c_pT+\frac{V^2}{2} \tag{8.69}$$

$$T_o=T+\frac{V^2}{2c_p}=T+T_v \tag{8.70}$$

where, $T_v = V^2/2c_p$ is termed as the *velocity temperature.*

Dividing Eq. (8.70) by T,

$$\frac{T_o}{T}=1+\frac{V^2}{2c_pT} \tag{8.71}$$

The specific heat at constant pressure can be written in terms of $\gamma(=c_p/c_v)$ and specific gas constant $\mathrm{R}(=c_p-c_v)$, as $c_p=\dfrac{\gamma \mathrm{R}}{\gamma-1}$. In addition, $a=\sqrt{\gamma \mathrm{R}T}$, Eq. (8.71) gives the stagnation temperature in terms of

$$\boxed{\frac{T_o}{T}=1+\frac{\gamma-1}{2}M^2} \tag{8.72}$$

The stagnation pressure and stagnation density can be evaluated from isentropic relations:

$$\boxed{\frac{p_o}{p}=\left(1+\frac{\gamma-1}{2}M^2\right)^{\frac{\gamma}{\gamma-1}}} \tag{8.73}$$

$$\boxed{\frac{\rho_o}{\rho}=\left(1+\frac{\gamma-1}{2}M^2\right)^{\frac{1}{\gamma-1}}} \tag{8.74}$$

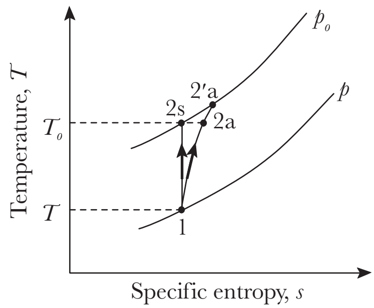

Fig. 8.10 *T–s* diagram showing the process to achieve stagnation state

Figure 8.10 shows the isentropic (1–2s) and adiabatic (1–2a) deceleration or compression processes on a *T–s* diagram for the block diagram shown in Fig. 8.9. Unlike isentropic process (1–2s), in adiabatic process (1–2a) the entropy increases; and hence, state points 2a and 2′a lie on the right-hand side of state point 2s. The stagnation state is defined by the existence of stagnation enthalpy or temperature and stagnation pressure together. The stagnation temperature or enthalpy can be achieved through adiabatic process but stagnation pressure cannot.

Figure 8.11 shows isentropic and adiabatic expansion and compression processes on a *T–s* diagram. It can be seen from the figure that for an actual adiabatic expansion or compression process the stagnation pressure does not remain constant but it drops to $p_{o,2a}$. It should also be remembered that during the compression process, the kinetic energy gets converted into pressure energy, which means that the flow velocity decreases during the compression process. The opposite happens in case of expansion where there is an increase in kinetic energy or flow velocity at the expense of pressure energy.

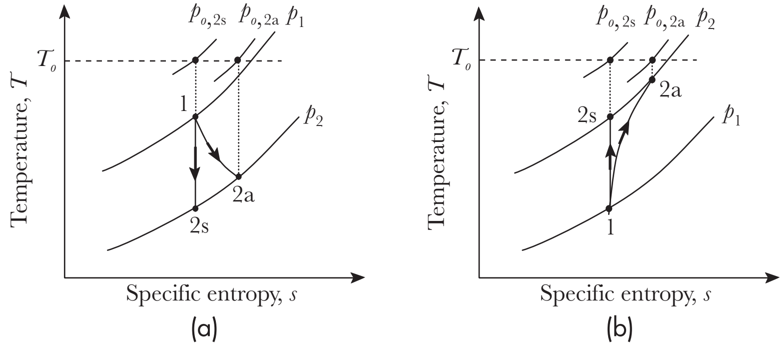

Fig. 8.11 *T–s* diagram showing (a) Expansion (b) Compression

The flow properties corresponding to critical Mach number (M = 1) or sonic condition are termed as *critical quantities*. They are denoted by usual

property symbol with asterisk in subscript. This means at $M = 1$, V becomes V_*, T becomes T_*, p becomes p_*, ρ becomes ρ_*, etc. At $M = 1$, $V = a$ or $V_* = a_*$.

Using Eq. (8.72), the critical temperature can be obtained in terms of stagnation temperature

$$\frac{T_*}{T_o} = \frac{2}{\gamma + 1} \tag{8.75}$$

The critical temperature in terms of any given temperature T can be obtained as

$$\frac{T_*}{T} = \frac{T_o/T}{T_o/T_*} = \frac{\left(1 + \frac{\gamma - 1}{2} M^2\right)}{\frac{\gamma + 1}{2}} \tag{8.76}$$

$$\frac{T_*}{T} = \frac{2}{\gamma + 1} + \frac{\gamma - 1}{\gamma + 1} M^2 \tag{8.77}$$

The critical pressure and critical density ratios can be evaluated from isentropic relations:

Critical pressure in terms of stagnation pressure

$$\frac{p_*}{p_o} = \left(\frac{2}{\gamma + 1}\right)^{\frac{\gamma}{\gamma - 1}} \tag{8.78}$$

Critical pressure in terms of given pressure

$$\frac{p_*}{p} = \left(\frac{2}{\gamma + 1} + \frac{\gamma - 1}{\gamma + 1} M^2\right)^{\frac{\gamma}{\gamma - 1}} \tag{8.79}$$

Critical density in terms of stagnation density

$$\frac{\rho_*}{\rho_o} = \left(\frac{2}{\gamma + 1}\right)^{\frac{1}{\gamma - 1}} \tag{8.80}$$

Critical density in terms of given density

$$\frac{\rho_*}{\rho} = \left(\frac{2}{\gamma + 1} + \frac{\gamma - 1}{\gamma + 1} M^2\right)^{\frac{1}{\gamma - 1}} \tag{8.81}$$

8.4 NON-DIMENSIONAL NUMBERS

This section deals with non-dimensional numbers used in compressible flow dynamics. The non-dimensionalization of fluid velocity (V) with some reference velocity is a useful way to understand the different facets of compressible flow.

Depending upon the reference velocity, different non-dimensional numbers are defined, as shown in Table 8.3.

Table 8.3 Non-dimensional numbers in compressible flow

Reference velocity	**Non-dimensional number**	**Definition**
Local sound velocity (a)	Mach number (M)	$M = \dfrac{V}{a}$
Critical fluid or sound velocity (V_* or a_*)	Mach number of II kind (M_*)	$M_* = \dfrac{V}{a_*}$
Maximum fluid velocity (V_{max})	Crocco number (Cr)	$Cr = \dfrac{V}{V_{max}}$

As mentioned earlier, the Mach number is defined as the ratio of fluid velocity to local sound velocity. Mach number of second kind is defined as the ratio of fluid velocity to the critical fluid or sound velocity.

$$M_* = \frac{V}{a_*} \tag{8.82}$$

To derive a relation between the two Mach numbers, multiply and divide the right-hand side (RHS) of Eq. (8.82) with local sound velocity, that is,

$$M_* = \frac{V}{a} \times \frac{a}{a_*} = M \times \frac{a}{a_*} \tag{8.83}$$

Squaring Eq. (8.83)

$$M_*^2 = M^2 \times \left(\frac{a}{a_*}\right)^2 \tag{8.84}$$

or $$M_*^2 = M^2 \frac{\gamma R T}{\gamma R T_*} \quad \Rightarrow \quad M_*^2 = M^2 \frac{T}{T_*} \tag{8.85}$$

Dividing numerator and denominator by T_o

or $$M_*^2 = M^2 \frac{T/T_o}{T_*/T_o} \quad \Rightarrow \quad M_*^2 = M^2 \frac{T_o/T_*}{T_o/T} \tag{8.86}$$

Substituting Eqs (8.72) and (8.75) in Eq. (8.86)

$$M_*^2 = \frac{\dfrac{\gamma+1}{2} M^2}{1 + \dfrac{\gamma-1}{2} M^2} \tag{8.87}$$

To physically interpret the significance of Mach number of II kind, Table 8.4 is drawn.

Table 8.4 Mach numbers

M	M_*
0	0
1	1
∞	$\sqrt{\dfrac{\gamma+1}{\gamma-1}}$

For extremely high-velocity flows, the Mach number attains an infinite value but the Mach number of second kind gives a finite value. Hence, the Mach number of second kind will be of use for very high flow velocities.

The maximum fluid velocity is attained if the fluid is expanded from stagnation conditions to the state when enthalpy becomes zero or absolute zero temperature is reached. The SFEE reduces to

$$h_o = \overset{0}{\cancel{h}} + \frac{V^2}{2} \tag{8.88}$$

Therefore, the maximum fluid velocity is given by

$$V_{\max} = \sqrt{2h_o} = \sqrt{2c_p T_o} \tag{8.89}$$

The non-dimensional number obtained by dividing fluid velocity by maximum fluid velocity is known as Crocco number.

$$\boxed{Cr = \frac{V}{V_{\max}}} \tag{8.90}$$

To derive a relation between the Crocco number and the Mach number, multiply and divide the RHS of Eq. (8.90) with local sound velocity, that is,

$$Cr = \frac{V}{a_*} \times \frac{a_*}{V_{\max}} = M_* \times \frac{a_*}{V_{\max}} \tag{8.91}$$

Squaring Eq. (8.91)

$$Cr^2 = M_*^2 \times \left(\frac{a_*}{V_{\max}}\right)^2 \tag{8.92}$$

or $$Cr^2 = M_*^2 \frac{\gamma R T_*}{2c_p T_o} \quad \Rightarrow \quad Cr^2 = M_*^2 \frac{\gamma-1}{2}\left(\frac{T_*}{T_o}\right) \tag{8.93}$$

Substituting Eqs (8.75) and (8.87) in Eq. (8.93)

$$Cr^2 = \frac{\frac{\gamma-1}{2}M^2}{1+\frac{\gamma-1}{2}M^2} \tag{8.94}$$

The variation of Mach number of II kind and Crocco number with Mach number for air has been shown in Fig. 8.12. It can be seen from the figure that there is a sharp increase in values of two numbers initially and after that the values of M_* and Cr are almost fixed to $\sqrt{6}$ and 1.0, respectively.

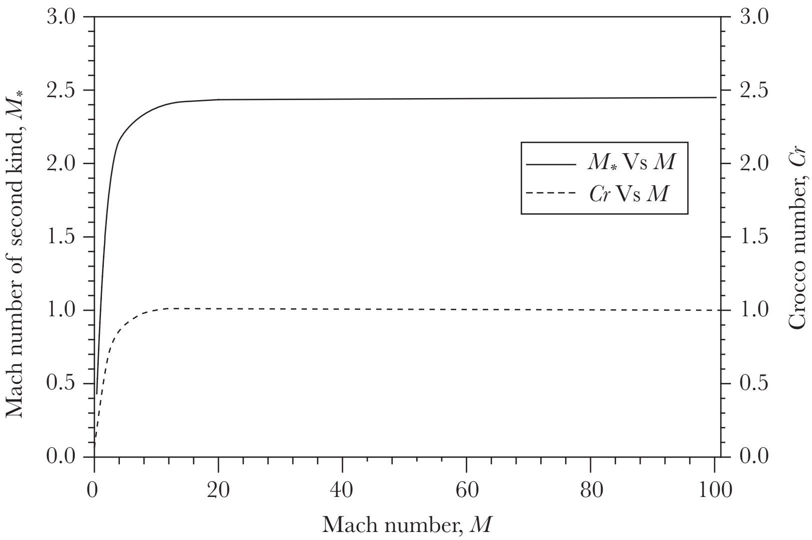

Fig. 8.12 Variation of M_* and Cr with Mach number

The stagnation and critical sound velocities can be computed using the stagnation and critical temperatures respectively.

$$a_o = \sqrt{\gamma R T_o}$$
$$a_* = \sqrt{\gamma R T_*} \tag{8.95}$$

Example 8.3 Compute the velocity temperature if the velocity of air is 100 m/s. In addition, determine the Mach number of an aircraft at which the velocity temperature of air at the inlet of aircraft engine is equal to half of static temperature.

Solution: By definition, the velocity temperature is given by

$$T_v = \frac{V^2}{2c_p} \Rightarrow T_v = \frac{100^2}{2 \times 1005} \Rightarrow T_v = 4.97°\text{C}$$

Since $T_v = T/2$, the velocity of air in terms of static temperature is

$$\frac{V^2}{2c_p} = \frac{T}{2} \quad \Rightarrow \quad V = \sqrt{c_p T}$$

Thus, the Mach number is

$$M = \frac{V}{a} \quad \Rightarrow \quad M = \sqrt{\frac{c_p T}{\gamma R T}} \quad \Rightarrow \quad M = \sqrt{\frac{\gamma R T}{(\gamma - 1)\gamma R T}}$$

$$\boxed{M = 1.58}$$

Example 8.4 In a steam power plant, the steam at a section of pipe has a pressure of 20 bar, temperature of 500°C and velocity of 100 m/s. Determine the Mach number, stagnation pressure and stagnation temperature. Take c_p = 2.2062 kJ/kg-K and c_v = 1.7013 kJ/kg-K, ρ =5.9621 kg/m³.

Solution: The stagnation temperature is computed using the steady flow energy equation:

$$T_o = T + \frac{V^2}{2c_p} \quad \Rightarrow \quad T_o = (500 + 273.15) + \frac{100^2}{2 \times 2206.2} \quad \Rightarrow \quad T_o = 775.41°\text{C}$$

The ratio of specific heats is $\gamma = \dfrac{2.2062}{1.7013} = 1.296.$

Specific gas constant R = 2206.2 − 1701.3 = 504.9 kJ/kg-K.

The stagnation pressure is calculated from the following isentropic relationship:

$$p_o = p\left(\frac{T_o}{T}\right)^{\frac{\gamma}{\gamma-1}} \quad \Rightarrow \quad p_o = 20 \times \left(\frac{775.41}{773.15}\right)^{\frac{1.296}{0.296}} \quad \Rightarrow \quad p_o = 20.257\,\text{bar}$$

Thus, the Mach number is

$$M = \frac{V}{a} \quad \Rightarrow \quad M = \frac{100}{\sqrt{1.296 \times 504.9 \times 773.15}} \quad \Rightarrow \quad M = 0.14$$

Example 8.5 In a large reservoir, air is maintained at a pressure of 10 bar and temperature of 200°C. Calculate the values of (a) stagnation enthalpy, (b) critical temperature, (c) velocity of sound at stagnation temperature, (d) maximum velocity, (e) critical sound velocity, and (f) critical fluid velocity. Assume isentropic flow for the calculation of these parameters.

Solution: The air may be assumed stagnant as the reservoir is large, that is, $p_o = 10$ bar and $T_o = 200$°C.

(a) Stagnation enthalpy

$$h_o = c_p T_o \quad \Rightarrow \quad h_o = 1.005 \times (200 + 273.15) \quad \Rightarrow \quad h_o = 475.5\,\text{kJ/kg}$$

(b) Critical temperature

$$T_* = \frac{2}{\gamma+1} T_o \quad \Rightarrow \quad T_* = \frac{2}{1.4+1} \times 473.15 \quad \Rightarrow \quad T_* = 394.3\,\text{K} = 121.15^\circ\text{C}$$

(c) Velocity of sound at stagnation temperature

$$a_o = \sqrt{\gamma R T_o} \quad \Rightarrow \quad a_o = \sqrt{1.4 \times 287 \times 473.15} \quad \Rightarrow \quad a_o = 436\,\text{m/s}$$

(d) Maximum velocity

$$V_{\max} = \sqrt{2h_o} \quad \Rightarrow \quad V_{\max} = \sqrt{2 \times 475.5 \times 10^3} \quad \Rightarrow \quad V_{\max} = 975.2\,\text{m/s}$$

(e) Critical sound velocity

$$a_* = \sqrt{\gamma R T_*} \quad \Rightarrow \quad a_* = \sqrt{1.4 \times 287 \times 394.3} \quad \Rightarrow \quad a_* = 398\,\text{m/s}$$

(f) Critical fluid velocity (corresponds to $M = 1$)

$$V_* = a_* \quad \Rightarrow \quad V_* = 398\,\text{m/s}$$

8.5 EFFECT OF MACH NUMBER ON FLOW COMPRESSIBILITY

The compressible fluid flow is not just the flow of compressible fluids. In fact, it is the variable density flow, which may occur due to change in pressure and temperature. Even the compressible fluids exhibit incompressible flow behaviour at low flow velocities. Likewise, the incompressible fluids may exhibit compressible flow behaviour under certain conditions. To prove this point, let us define *coefficient of pressure*, C_p as

$$C_p = \frac{p_o - p}{\frac{1}{2}\rho V^2} \tag{8.96}$$

For incompressible flow, the Bernoulli equation is (ignoring elevation effects, i.e., horizontal flow)

$$\frac{p}{\rho} + \frac{V^2}{2} = C \tag{8.97}$$

As $\quad V = 0 \quad \Rightarrow \quad p = p_o \quad \Rightarrow \quad C = p_o/\rho$

Equation (8.97) reduces to

$$\frac{p}{\rho} + \frac{V^2}{2} = \frac{p_o}{\rho} \tag{8.98}$$

This means for *incompressible flow*, $C_p = 1$.

Let us now find out the value of coefficient of pressure for isentropic compressible flow, the pressure ratio is

$$\frac{p_o}{p} = \left(1 + \frac{\gamma - 1}{2} M^2\right)^{\frac{\gamma}{\gamma-1}} \tag{8.73}$$

The expansion of $(1+x)^n$

$$(1+x)^n = 1 + nx + \frac{n(n-1)}{2!}x^2 + \frac{n(n-1)(n-2)}{3!}x^3 + \dots \tag{8.99}$$

where, $x = \frac{\gamma - 1}{2}M^2$ and $n = \frac{\gamma}{\gamma - 1}$.

From Eqs (8.73) and (8.99)

$$\frac{p_o}{p} = 1 + \frac{\gamma}{2}M^2 + \frac{\gamma}{8}M^4 + \frac{\gamma(2-\gamma)}{48}M^6 + \dots \tag{8.100}$$

Subtracting 1 from both sides and then dividing throughout by $\frac{\gamma}{2}M^2$

$$\frac{p_o - p}{\frac{\gamma}{2}M^2 p} = 1 + \frac{M^2}{4} + \frac{(2-\gamma)}{24}M^4 + \dots \tag{8.101}$$

In addition, $\frac{\gamma}{2}M^2 p = \frac{1}{2}\rho V^2$, the left-hand side (LHS) of Eq. (8.101) comes out to be coefficient of pressure. Hence, the coefficient of pressure for isentropic compressible flow

$$C_p = 1 + \frac{M^2}{4} + \frac{(2-\gamma)}{24}M^4 + \dots \tag{8.102}$$

Table 8.5 shows the effect of Mach number on the flow compressibility. The percentage deviation in the coefficient of pressure between the compressible and incompressible flows is a measure of compressibility.

Table 8.5 Effect of Mach number on flow compressibility

M	C_p	**Percentage deviation (%)**
0.1	1.0025	0.25
0.2	1.01	1.00
0.3	1.0227	2.27
0.4	1.0406	4.06
…	…	…
1.0	1.275	27.5

NOTE

It is clear from this analysis that the effects of compressibility cannot be ignored beyond Mach number of 0.3.

8.6 ISENTROPIC FLOW THROUGH VARYING AREA DUCTS

To see the effect of varying area on the compressible flow, let us do the following analysis:

On differentiating Eq. (8.68)

$$dh + VdV = 0 \tag{8.103}$$

From first law, $dq = dh - vdp$. Since the flow is isentropic, the heat transfer is zero, as $dq = Tds$:

$$dh = vdp \quad \Rightarrow \quad dh = dp/\rho \tag{8.104}$$

From Eqs (8.103) and (8.104)

$$dp = -\rho V dV \tag{8.105}$$

From the continuity equation ρAV = constant. Taking log and then differentiating,

$$\frac{d\rho}{\rho} + \frac{dA}{A} + \frac{dV}{V} = 0 \tag{8.106}$$

From Eqs (8.105) and (8.106)

$$\frac{dA}{A} = \frac{dp}{\rho V^2} - \frac{d\rho}{\rho} \quad \Rightarrow \quad \frac{dA}{A} = \frac{dp}{\rho V^2}\left(1 - V^2 \frac{d\rho}{dp}\right) \tag{8.107}$$

or

$$\frac{dA}{A} = \frac{dp}{\rho V^2}(1 - M^2) \tag{8.108}$$

Using Eq. (8.105)

$$\boxed{\frac{dA}{A} = -\frac{dV}{V}(1 - M^2)} \tag{8.109}$$

A *nozzle* is device that is used to accelerate the flow whereas *diffuser* is used to decelerate the flow. In a nozzle the change in velocity in the direction of flow is positive ($dV > 0$) while in case of diffuser this change is negative in flow of direction ($dV < 0$). To determine whether a particular variable area device is a *nozzle* or *diffuser* Eq. (8.109) is used, as shown in Table 8.6.

Table 8.6 Condition for nozzle and diffuser

Device	$\frac{dV}{V}$	**Mach number at entry, *M***	$\frac{dA}{A} = -\frac{dV}{V}(1 - M^2)$	**Shape**
Nozzle	Positive	Less than 1	Negative	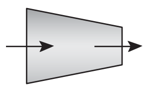
Nozzle	Positive	More than 1	Positive	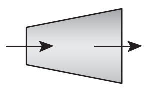
Diffuser	Negative	Less than 1	Positive	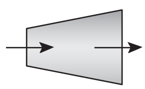
Diffuser	Negative	More than 1	Negative	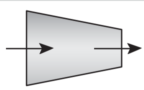

For a convergent–divergent device to act as nozzle or diffuser, the critical conditions must reach at the throat (area of minimum cross section). In addition, for convergent–divergent nozzle, the flow must be subsonic (i.e., Mach number should be less than unity) at the entrance. The convergent–divergent diffuser, on the other hand, must have supersonic flow (i.e., Mach number should be greater than unity) at the entrance. This has been shown in Fig. 8.13.

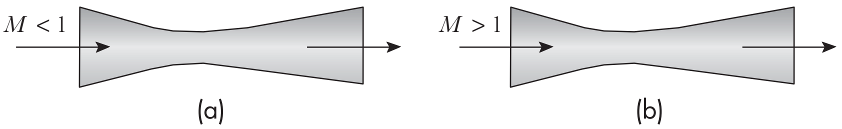

Fig. 8.13 Convergent–divergent (a) Nozzle (b) Diffuser

8.6.1 Critical Area Ratio

The critical properties have already been discussed in Section 8.3, which would be needed to calculate the critical area ratio for a nozzle or diffuser. The critical area is the cross-sectional area in variable area device where the fluid speed reaches sonic speed ($M = 1$).

Applying continuity equation in a variable area duct between the critical area and any given area,

$$\rho_* A_* V_* = \rho A V \quad \Rightarrow \quad \frac{A}{A_*} = \frac{\rho_*}{\rho} \times \frac{V_*}{V} \tag{8.110}$$

$$\frac{A}{A_*} = \frac{\rho_*}{\rho} \times \frac{1}{M_*} \tag{8.111}$$

From Eqs (8.81) and (8.87)

$$\frac{A}{A_*} = \left(\frac{2}{\gamma+1} + \frac{\gamma-1}{\gamma+1} M^2 \right)^{\frac{1}{\gamma-1}} \times \frac{1}{M} \left(\frac{2}{\gamma+1} + \frac{\gamma-1}{\gamma+1} M^2 \right)^{\frac{1}{2}} \tag{8.112}$$

Therefore, critical area ratio is given by

$$\boxed{\frac{A}{A_*} = \frac{1}{M} \left(\frac{2}{\gamma+1} + \frac{\gamma-1}{\gamma+1} M^2 \right)^{\frac{\gamma+1}{2(\gamma-1)}}} \tag{8.113}$$

Equation (8.113) is plotted in Fig. 8.14 with air ($\gamma = 1.4$) as the fluid medium. It can be seen that the critical area ratio is unity at sonic conditions. In other words, at the throat the Mach number turns unity.

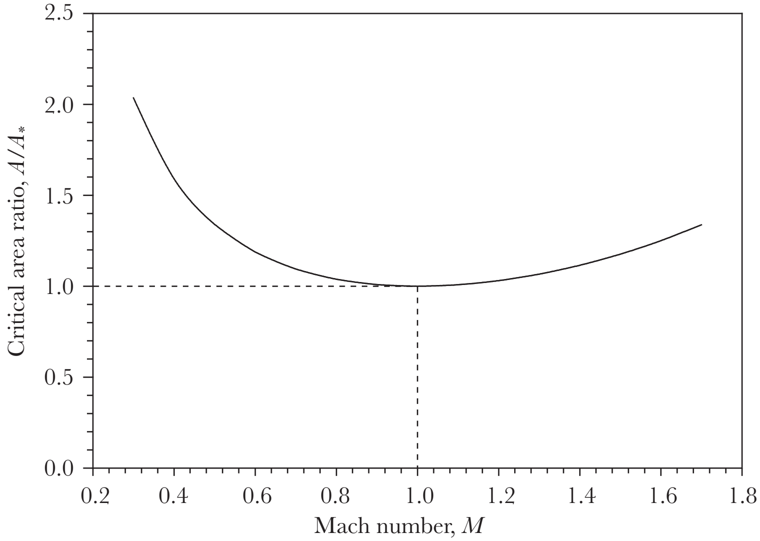

Fig. 8.14 Critical area ratio vs Mach number

8.6.2 Critical Impulse Function Ratio

Impulse function is defined as the sum of pressure force and inertia force. In a convergent–divergent nozzle, the difference in impulse functions at the exit and the entrance is known as *thrust*. The jet engines are characterized by the amount of thrust they produce.

By definition, impulse is,

$$F = pA + \rho AV^2 \tag{8.114}$$

or

$$F = pA\left(1 + \frac{\rho V^2}{p}\right) \Rightarrow F = pA\left(1 + \frac{\gamma V^2}{\gamma p/\rho}\right) \tag{8.115}$$

or

$$\boxed{F = pA(1 + \gamma M^2)} \tag{8.116}$$

The thrust force is the difference between the impulse functions at the outlet and the inlet of a duct.

$$\boxed{\tau = F_2 - F_1 = p_2 A_2\left(1 + \gamma M_2^2\right) - p_1 A_1\left(1 + \gamma M_1^2\right)} \tag{8.117}$$

The critical impulse function is the impulse function corresponding to unity Mach number, that is,

$$\boxed{F_* = p_* A_* (1 + \gamma)} \tag{8.118}$$

To get critical impulse function ratio, divide Eq. (8.116) by Eq. (8.118)

$$\frac{F}{F_*} = \frac{p}{p_*}\frac{A}{A_*}\frac{1+\gamma M^2}{1+\gamma} \tag{8.119}$$

From Eqs (8.79) and (8.113)

$$\frac{F}{F_*} = \left(\frac{2}{\gamma+1} + \frac{\gamma-1}{\gamma+1}M^2\right)^{-\frac{\gamma}{\gamma-1}} \frac{1}{M}\left(\frac{2}{\gamma+1} + \frac{\gamma-1}{\gamma+1}M^2\right)^{\frac{\gamma+1}{2(\gamma-1)}} \frac{1+\gamma M^2}{1+\gamma} \tag{8.120}$$

$$\frac{F}{F_*} = \frac{1+\gamma M^2}{M\sqrt{2(\gamma+1)\left(1+\frac{\gamma-1}{2}M^2\right)}} \tag{8.121}$$

8.6.3 Critical Mass Flow Rate

The critical mass flow rate through a duct is the maximum possible mass flow rate through it. The mass flow rate is given by

$$\dot{m} = \rho A V \quad \Rightarrow \quad \frac{\dot{m}}{A} = \rho V \quad \Rightarrow \quad \frac{\dot{m}}{A} = \frac{p}{RT}V \tag{8.122}$$

$$\frac{\dot{m}}{A} = \frac{\gamma p}{\sqrt{\gamma R T}}\frac{V}{a} \quad \Rightarrow \quad \frac{\dot{m}}{A} = \sqrt{\frac{\gamma}{R}}\frac{p/p_o}{\sqrt{T/T_o}}\frac{p_o}{\sqrt{T_o}}M \tag{8.123}$$

From Eqs (8.72) and (8.73) and rearranging

$$\frac{\dot{m}}{A}\frac{\sqrt{T_o}}{p_o}\sqrt{\frac{R}{\gamma}} = \frac{\left(1+\frac{\gamma-1}{2}M^2\right)^{-\frac{\gamma}{\gamma-1}}}{\left(1+\frac{\gamma-1}{2}M^2\right)^{-\frac{1}{2}}}M \tag{8.124}$$

The mass flow rate has been expressed in terms of Mach number

$$\frac{\dot{m}}{A}\frac{\sqrt{T_o}}{p_o}\sqrt{\frac{R}{\gamma}} = M\left(1+\frac{\gamma-1}{2}M^2\right)^{-\frac{\gamma+1}{2(\gamma-1)}} \tag{8.125}$$

To maximize the mass flow rate, differentiating Eq. (8.125) with respect to M and equating it to zero, that is,

$$\frac{d(\dot{m}/A)}{dM} = 0 \quad \Rightarrow \quad M = 1 \tag{8.126}$$

Thus, the critical mass flow rate is given by

$$\frac{\dot{m}}{A_*}\frac{\sqrt{T_o}}{p_o} = \sqrt{\frac{\gamma}{R}}\left(\frac{2}{\gamma+1}\right)^{\frac{\gamma+1}{2(\gamma-1)}} \tag{8.127}$$

With air ($\gamma = 1.4$ and R = 287 J/kg-K) as the fluid medium, the critical mass flow rate comes out to be

$$\frac{\dot{m}}{A_*}\frac{\sqrt{T_o}}{p_o} = 0.0404 \tag{8.128}$$

Alternatively, the critical mass flow rate can also be obtained by expressing the mass flow rate in terms of the pressure ratio as

$$\dot{m} = \rho AV \quad \Rightarrow \quad \frac{\dot{m}}{A} = \rho V \quad \Rightarrow \quad \frac{\dot{m}}{A} = \rho\sqrt{2(h_o - h)} \tag{8.129}$$

$$\frac{\dot{m}}{A} = \rho_o\left(\frac{p}{p_o}\right)^{\frac{1}{\gamma}}\sqrt{2c_pT_o\left(1-\frac{T}{T_o}\right)} \tag{8.130}$$

$$\Rightarrow \quad \frac{\dot{m}}{A} = \rho_o\left(\frac{p}{p_o}\right)^{\frac{1}{\gamma}}\sqrt{\frac{2\gamma RT_o}{\gamma-1}\left(1-\frac{T}{T_o}\right)} \tag{8.131}$$

$$\Rightarrow \quad \frac{\dot{m}}{A} = \frac{p_o}{RT_o}\left(\frac{p}{p_o}\right)^{\frac{1}{\gamma}}\sqrt{\frac{2\gamma RT_o}{\gamma-1}\left(1-\left(\frac{p}{p_o}\right)^{\frac{\gamma-1}{\gamma}}\right)} \tag{8.132}$$

The mass flow rate has been expressed in terms of pressure ratio

$$\Rightarrow \quad \frac{\dot{m}}{A}\frac{\sqrt{T_o}}{p_o}\sqrt{\frac{R}{\gamma}} = \sqrt{\frac{2}{\gamma-1}\left(\left(\frac{p}{p_o}\right)^{\frac{2}{\gamma}} - \left(\frac{p}{p_o}\right)^{\frac{\gamma+1}{\gamma}}\right)} \tag{8.133}$$

To maximize the mass flow rate, differentiating Eq. (8.133) with respect to p/p_o and equating it to zero, that is,

$$\frac{d(\dot{m}/A)}{d(p/p_o)} = 0 \quad \Rightarrow \quad \frac{p}{p_o} = \left(\frac{2}{\gamma+1}\right)^{\frac{\gamma}{\gamma-1}} \tag{8.134}$$

Thus, the critical mass flow rate is given by

$$\frac{\dot{m}}{A_*}\frac{\sqrt{T_o}}{p_o} = \sqrt{\frac{\gamma}{R}}\left(\frac{2}{\gamma+1}\right)^{\frac{\gamma+1}{2(\gamma-1)}} \tag{8.127}$$

Example 8.6 Deduce the following relations:

(a) $\dfrac{dT}{T} + \dfrac{\gamma-1}{2}M^2\dfrac{dV^2}{V^2} = 0$

(b) $\dfrac{F_*}{A_* p_o} = (\gamma+1)\left(\dfrac{2}{\gamma+1}\right)^{\frac{\gamma}{\gamma-1}}$

Solution:

(a) The stagnation temperature for an isentropic flow is given by

$$T_o = T\left(1 + \frac{\gamma - 1}{2}M^2\right)$$

Differentiating,

$$\cancelto{0}{dT_o} = \left(1 + \frac{\gamma - 1}{2}M^2\right)dT + Td\left(1 + \frac{\gamma - 1}{2}M^2\right)$$

$$0 = \left(1 + \frac{\gamma - 1}{2}M^2\right)dT + T\left(\frac{\gamma - 1}{2}dM^2\right)$$

Dividing throughout by T

$$\left(1 + \frac{\gamma - 1}{2}M^2\right)\frac{dT}{T} + \frac{\gamma - 1}{2}dM^2 = 0$$

$$\frac{dT}{T} + \frac{dT}{T}\frac{\gamma - 1}{2}M^2 + \frac{\gamma - 1}{2}dM^2 = 0$$

$$\frac{dT}{T} + \left(\frac{\gamma - 1}{2}\right)M^2\left(\frac{dT}{T} + \frac{dM^2}{M^2}\right) = 0$$

$$\frac{dT}{T} + \left(\frac{\gamma - 1}{2}\right)M^2\left(\frac{d(\gamma RT)}{\gamma RT} + \frac{dM^2}{M^2}\right) = 0$$

$$\frac{dT}{T} + \left(\frac{\gamma - 1}{2}\right)M^2\left(\frac{da^2}{a^2} + \frac{dM^2}{M^2}\right) = 0$$

$$\frac{dT}{T} + \left(\frac{\gamma - 1}{2}\right)M^2\left(\frac{M^2 da^2 + a^2 dM^2}{M^2 a^2}\right) = 0$$

$$\frac{dT}{T} + \left(\frac{\gamma - 1}{2}\right)M^2\frac{d(M^2 a^2)}{M^2 a^2} = 0$$

Since $Ma = V$

$$\frac{dT}{T} + \left(\frac{\gamma - 1}{2}\right)M^2\frac{dV^2}{V^2} = 0$$

(b) The impulse function is defined as the sum of inertia force and pressure force

$$F = pA + \rho AV^2$$

$$F = pA\left(1 + \frac{\rho V^2}{p}\right)$$

$$F = pA\left(1 + \frac{\gamma V^2}{\gamma p/\rho}\right)$$

$$F = pA(1 + \gamma M^2)$$

The critical impulse function corresponds to unity Mach number

$$F_* = p_* A_* (1+\gamma) \tag{1}$$

The critical pressure ratio is given by

$$p_* = p_o \left(\frac{2}{\gamma+1}\right)^{\frac{\gamma}{\gamma-1}} \tag{2}$$

Using Eqs (1) and (2),

$$\frac{F_*}{A_* p_o} = (\gamma+1)\left(\frac{2}{\gamma+1}\right)^{\frac{\gamma}{\gamma-1}}$$

8.6.4 Convergent Nozzles

Convergent nozzles are used to achieve subsonic or sonic flows. To study the flow characteristics of a nozzle, it is mandatory to fix the conditions at one end, while the conditions at the other end are varied. For this purpose, the nozzle inlet is connected to a very large tank where stagnation conditions are maintained. The back pressure at the nozzle exit is varied by means of a valve. This is shown in Fig. 8.15. The following are the salient points:

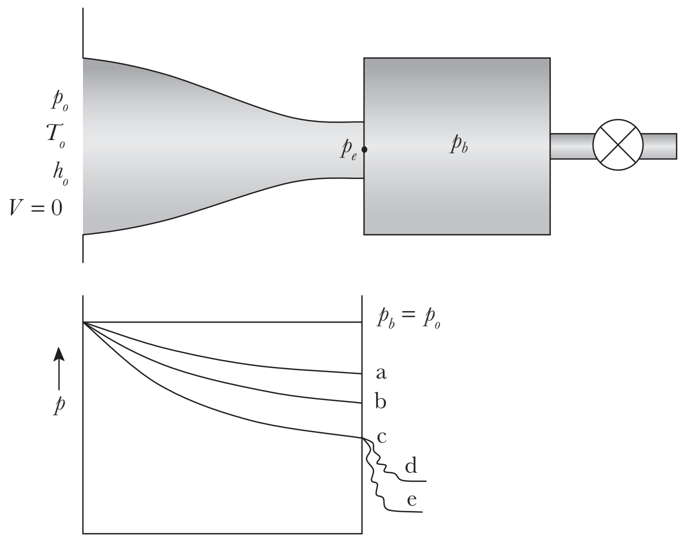

Fig. 8.15 Variation of pressure in a convergent nozzle

1. When the valve is closed, the back pressure will be same as that of the inlet stagnation pressure and as such there would be no flow.
2. As the valve is opened, the back pressure falls down and the flow through the nozzle starts taking place. The curves 'a' and 'b' in Fig. 8.15 correspond

to the back pressures above the critical pressure. The curve 'c' corresponds to the back pressure equal to the critical pressure.

3. It should be remembered that if the back pressure is reduced below the critical pressure, the nozzle exit pressure will not change. In fact, the expansion in the form of shock wave occurs immediately outside the nozzle, as shown in Fig. 8.16(a).

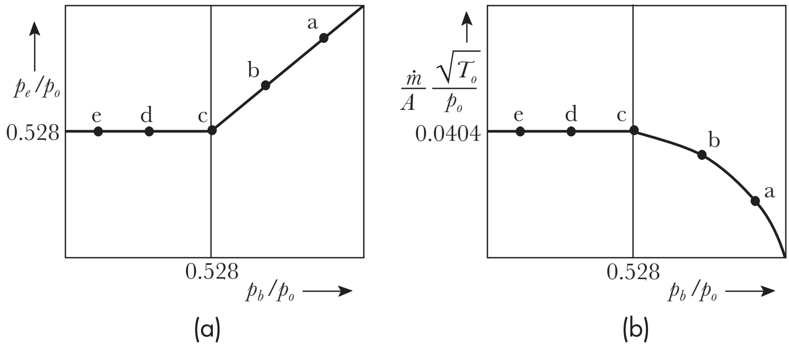

Fig. 8.16 Variation of (a) Nozzle exit pressure (b) Mass flow rate through a convergent nozzle

4. The mass flow rate through the convergent nozzle is increased with the reduction in back pressure until it reaches the critical pressure. Further reduction in back pressure will not cause any change in the mass flow rate, as shown in Fig. 8.16(b). The maximum mass flow rate through the nozzle is known as critical mass flow rate given by Eq. (8.127). The condition of maximum mass flow rate is known as *choking*.

Example 8.7 Air is discharged from a reservoir (p_o = 10 bar; T_o = 600 K) through a nozzle to an ambient pressure of 1.0 bar. If the flow rate is 0.5 kg/s, determine throat area, throat pressure, velocity at the throat, outlet area, Mach number, and maximum velocity for the isentropic flow.

Solution: Given that p_o = 10 bar, T_o = 600 K, p_e = 1 bar, and $\dot{m}$ = 0.5 kg/s

The throat area can be computed from the following relation:

$$\frac{\dot{m}}{A_*}\frac{\sqrt{T_o}}{p_o} = 0.0404 \quad \Rightarrow \quad A_* = \frac{0.5\times\sqrt{600}}{0.0404\times 10\times 10^5} \quad \Rightarrow \quad A_* = 3.03\,\text{cm}^2$$

The temperature and pressure at the throat are given by

$$\frac{T_*}{T_o} = \frac{2}{\gamma+1} \quad \Rightarrow \quad T_* = \frac{2\times 600}{1.4+1} \quad \Rightarrow \quad T_* = 500\,\text{K}$$

$$\frac{p_*}{p_o} = \left(\frac{2}{\gamma+1}\right)^{\frac{\gamma}{\gamma-1}} \quad \Rightarrow \quad p_* = \left(\frac{2}{1.4+1}\right)^{\frac{1.4}{0.4}}\times 10 \quad \Rightarrow \quad p_* = 5.28\,\text{bar}$$

From isentropic relation, the exit temperature can be found out

$$\frac{T_e}{T_*} = \left(\frac{p_e}{p_*}\right)^{\frac{\gamma-1}{\gamma}} \Rightarrow T_e = 500 \times \left(\frac{1}{5.28}\right)^{\frac{0.4}{1.4}} \Rightarrow T_e = 310.8\,\mathrm{K}$$

The Mach number can be determined from the following relations:

$$\frac{T_{o2}}{T_e} = 1 + \frac{\gamma-1}{2}M_e^2 \Rightarrow \frac{600}{310.8} = 1 + 0.2 \times M_e^2 \Rightarrow M_e = 2.157$$

Since the flow is isentropic, the stagnation temperature will remain the same $(T_{o2} = T_{o1})$.

The cross-sectional area at the nozzle exit can be obtained from

$$\frac{A_e}{A_*} = \frac{1}{M_e}\left(\frac{5+M_e^2}{6}\right)^3 \Rightarrow A_e = \frac{3.03}{2.157}\left(\frac{5+2.157^2}{6}\right)^3 \Rightarrow A_e = 5.84\,\mathrm{cm}^2$$

The maximum velocity is calculated from

$$V_{\max} = \sqrt{2h_o} = \sqrt{2c_pT_o} \Rightarrow V_{\max} = \sqrt{2 \times 1005 \times 600} \Rightarrow V_{\max} = 1098.2\,\mathrm{m/s}$$

Example 8.8 The diameters of a conical diffuser at the inlet and outlet are 200 mm and 400 mm, respectively. At the inlet, pressure is 80 kPa, temperature is 350 K, and velocity of air is 200 m/s. Compute the velocity and pressure at the outlet and the thrust experienced by the diffuser.

Solution: Section 1 is inlet, section 2 is outlet, and Section * is throat, as shown in Fig. 8.17.

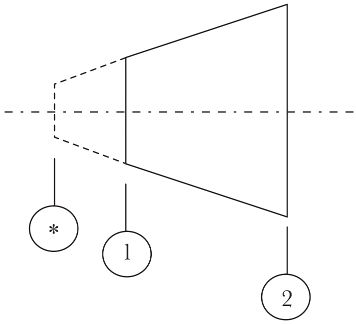

Fig. 8.17

Given that $p_1 = 80\mathrm{kPa}$, $T_1 = 350\mathrm{K}$, $V_1 = 200\,\mathrm{m/s}$, $d_1 = 0.2\,\mathrm{m}$, and $d_2 = 0.4\mathrm{m}$.

The cross-sectional areas at the inlet and outlet are

$$A_1 = \frac{\pi}{4} \times 0.2^2 \Rightarrow A_1 = 0.031416\,\mathrm{m}^2$$

$$A_2 = \frac{\pi}{4} \times 0.4^2 \Rightarrow A_2 = 0.125663\,\mathrm{m}^2$$

Mach number at the inlet

$$M_1 = \frac{200}{\sqrt{1.4\times 287\times 350}} \quad\Rightarrow\quad M_1 = 0.533$$

Stagnation temperature at the inlet

$$T_{o1} = T_1\left(1+\frac{\gamma-1}{2}M_1^2\right) \;\Rightarrow\; T_{o1} = 350\left(1+\frac{1.4-1}{2}\times 0.533^2\right) \;\Rightarrow\; T_{o1} = 370\,\mathrm{K}$$

Stagnation pressure at the inlet is obtained from isentropic relation:

$$p_{o1} = p_1\left(\frac{T_{o1}}{T_1}\right)^{\frac{\gamma}{\gamma-1}} \quad\Rightarrow\quad p_{o1} = 80\times\left(\frac{370}{350}\right)^{\frac{1.4}{0.4}} \quad\Rightarrow\quad p_{o1} = 97.17\,\mathrm{kPa}$$

Since the flow through the diffuser is assumed isentropic, there will not be any change in stagnation pressure and stagnation temperature,

$$p_{o2} = p_{o1} = 97.17\,\mathrm{kPa}$$

$$T_{o2} = T_{o1} = 370\,\mathrm{K}$$

Using the critical area ratio relation, the cross-sectional area at the throat can be computed,

$$\frac{A_1}{A_{*1}} = \frac{1}{M_1}\left(\frac{2}{\gamma+1}+\frac{\gamma-1}{\gamma+1}M_1^2\right)^{\frac{\gamma+1}{2(\gamma-1)}}$$

For air $\gamma = 1.4$, this relation reduces to

$$\frac{A_1}{A_{*1}} = \frac{1}{M_1}\left(\frac{5+M_1^2}{6}\right)^3 \quad\Rightarrow\quad \frac{A_1}{A_{*1}} = \frac{1}{0.533}\left(\frac{5+0.533^2}{6}\right)^3 = 1.28$$

$$\Rightarrow\quad A_{*1} = 0.0245\ \mathrm{m}^2$$

Using the same relation, the Mach number at the outlet can be found out as $A_{*1} = A_{*2}$

$$\frac{1}{M_2}\left(\frac{5+M_2^2}{6}\right)^3 = \frac{A_2}{A_{*2}} \quad\Rightarrow\quad \frac{1}{M_2}\left(\frac{5+M_2^2}{6}\right)^3 = 5.13$$

To find the Mach number at the outlet, the hit and trial method is used for solving the aforementioned non-linear equation,

$$M_2 = 0.1136$$

Temperature at the outlet

$$T_2 = \frac{T_{o2}}{\left(1+\frac{\gamma-1}{2}M_2^2\right)} \quad\Rightarrow\quad T_2 = \frac{370}{\left(1+\frac{1.4-1}{2}\times 0.1136^2\right)} \quad\Rightarrow\quad T_2 = 369\,\mathrm{K}$$

The velocity at the outlet of the diffuser is

$$V_2 = M_2 a_2 \quad\Rightarrow\quad V_2 = M_2\sqrt{\gamma R T_2} \quad\Rightarrow\quad V_2 = 0.1136\sqrt{1.4\times 287\times 369}$$

$$\Rightarrow\quad V_2 = 43.7\,\mathrm{m/s}$$

The outlet pressure

$$p_2 = \frac{p_{o2}}{(T_{o2}/T_2)^{\frac{\gamma}{\gamma-1}}} \Rightarrow p_2 = \frac{97.17}{(370/369)^{\frac{1.4}{1.4-1}}} \Rightarrow p_2 = 96.25\,\text{kPa}$$

The values impulse function at the inlet and outlet, respectively, are

$$F_1 = p_1A_1\left(1+\gamma M_1^2\right) \Rightarrow F_1 = 80\times 0.031416\times(1+1.4\times 0.533^2)$$

$$\Rightarrow F_1 = 3.51\,\text{kN}$$

$$F_2 = p_2A_2\left(1+\gamma M_2^2\right) \Rightarrow F_2 = 96.25\times 0.12566\times(1+1.4\times 0.1136^2)$$

$$\Rightarrow F_2 = 12.31\,\text{kN}$$

The thrust acting on the diffuser is the difference of impulse functions at inlet and outlet

$$\tau = F_2 - F_1 \Rightarrow \tau = 8.8\,\text{kN}$$

Example 8.9 Solve Example 8.8, using gas tables (Appendix B).

Solution: Section 1 is inlet, section 2 is outlet, and section * is throat, as shown in Fig. 8.16.

Given that $p_1 = 80\,\text{kPa}$, $T_1 = 350\,\text{K}$, $V_1 = 200\,\text{m/s}$, $d_1 = 0.2\,\text{m}$, and $d_2 = 0.4\,\text{m}$

The cross-sectional areas at the inlet and outlet are

$$A_1 = \frac{\pi}{4}\times 0.2^2 \Rightarrow A_1 = 0.031416\,\text{m}^2$$

$$A_2 = \frac{\pi}{4}\times 0.4^2 \Rightarrow A_2 = 0.125663\,\text{m}^2$$

Mach number at the inlet

$$M_1 = \frac{200}{\sqrt{1.4\times 287\times 350}} \Rightarrow M_1 = 0.533$$

using isentropic tables of Appendix B (Table B1), the ratio of static temperature to stagnation temperature at the inlet at $M_1 = 0.533$.

Using linear interpolation between $M = 0.52$ and $M = 0.54$

$$\frac{T_1}{T_{o1}} = 0.94869 + \frac{0.533-0.52}{0.54-0.52}(0.94489-0.94869) \Rightarrow \frac{T_1}{T_{o1}} = 0.94622$$

$$\Rightarrow T_{o1} = 369.89\,\text{K}$$

Similarly, the stagnation pressure at the inlet can also be obtained:

$$\frac{p_1}{p_{o1}} = 0.83165 + \frac{0.533-0.52}{0.54-0.52}(0.82005-0.83165) \Rightarrow \frac{p_1}{p_{o1}} = 0.82411$$

$$\Rightarrow p_{o1} = 97.07\,\text{kPa}$$

Since the flow through the diffuser is assumed isentropic, there will not be any change in stagnation pressure and stagnation temperature,

$$p_{o2} = p_{o1} = 97.07\,\text{kPa}$$

$$T_{o2} = T_{o1} = 369.89\,\text{K}$$

The critical area ratio from gas tables

$$\frac{A_1}{A_{*1}} = 1.27494 + \frac{0.533-0.52}{0.54-0.52}(1.24056-1.27494) \Rightarrow \frac{A_1}{A_{*1}} = 1.252593$$

$$\Rightarrow A_{*1} = 0.02508\,\text{m}^2$$

Since $A_{*1} = A_{*2}$, the critical area ratio at the exit

$$\frac{A_2}{A_{*2}} = \frac{0.125663}{0.02508} \Rightarrow \frac{A_2}{A_{*2}} = 5.01$$

Corresponding to the aforementioned critical area ratio, the Mach number at the exit from the table using linear interpolation between $\frac{A_2}{A_{*2}} = 5.81685$ and $\frac{A_2}{A_{*2}} = 4.85833$

$$M_2 = 0.1 + \frac{5.01-5.81865}{4.85833-5.81865}(0.12-0.1) \Rightarrow M_2 = 0.1168$$

Temperature at the outlet corresponding to aforementioned Mach number, using linear interpolation between $M = 0.1$ and $M = 0.12$.

$$\frac{T_2}{T_{o2}} = 0.998 + \frac{0.1168-0.1}{0.12-0.1}(0.99713-0.998) \Rightarrow \frac{T_2}{T_{o2}} = 0.997269$$

$$\Rightarrow T_2 = 368.87\,\text{K}$$

Similarly, the stagnation pressure at the inlet can also be obtained:

$$\frac{p_2}{p_{o2}} = 0.99303 + \frac{0.1168-0.1}{0.12-0.1}(0.98998-0.99303) \Rightarrow \frac{p_2}{p_{o2}} = 0.990468$$

$$\Rightarrow p_2 = 96.145\,\text{kPa}$$

The velocity at the outlet of the diffuser is

$$V_2 = M_2 a_2 \Rightarrow V_2 = M_2\sqrt{\gamma R T_2}$$

$$\Rightarrow V_2 = 0.1168\sqrt{1.4\times 287\times 368.87}$$

$$\Rightarrow V_2 = 44.96\,\text{m/s}$$

The values impulse function at the inlet and outlet, respectively, are

$$F_1 = p_1 A_1\left(1+\gamma M_1^2\right) \Rightarrow F_1 = 80\times 0.031416\times(1+1.4\times 0.533^2)$$

$$\Rightarrow F_1 = 3.51\,\text{kN}$$

$$F_2 = p_2 A_2\left(1+\gamma M_2^2\right) \Rightarrow F_2 = 96.145\times 0.12566\times(1+1.4\times 0.1168^2)$$

$$\Rightarrow F_2 = 12.31\,\text{kN}$$

The thrust acting on the diffuser is the difference of impulse functions at inlet and outlet

$$\tau = F_2 - F_1 \quad \Rightarrow \quad \tau = 8.8\,\text{kN}$$

8.6.5 Convergent–Divergent Nozzles

The convergent–divergent nozzle, also known as de Laval nozzle, is used to attain high Mach number flow or supersonic flow. The flow characteristics of such a nozzle are shown in Figs 8.18 and 8.19, where the variations in pressure and mass flow rate through the nozzle have been presented.

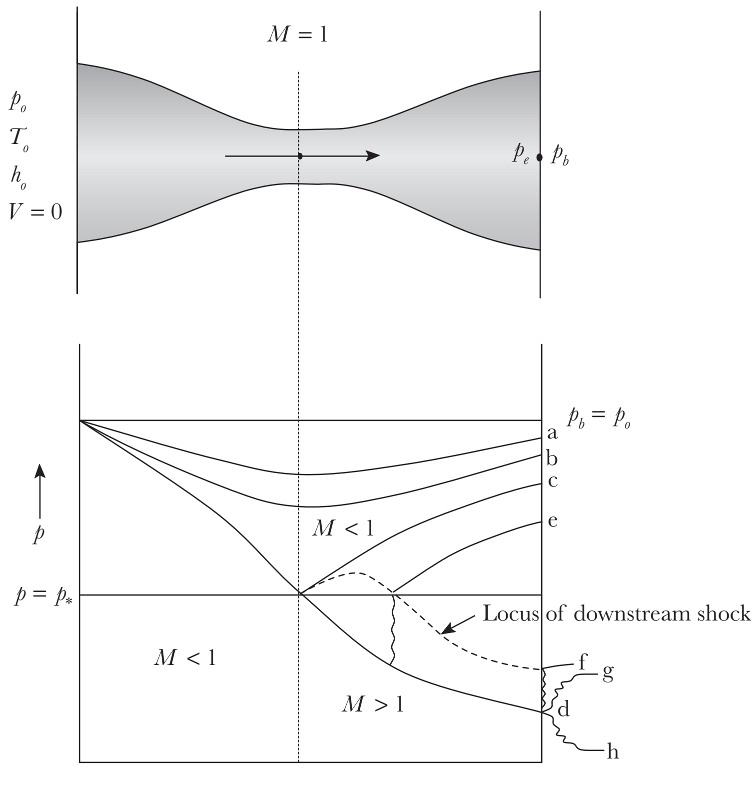

Fig. 8.18 Variation of pressure along the length of convergent–divergent nozzle

The following observations are made:

1. As long as the back pressure is equal to the stagnation pressure at the entrance, there will not be any flow.
2. As the back pressure is reduced the flow starts to occur. The mass flow rates increase with the reduction in back pressure until the pressure reaches 'c'. Till this point the converging part acts as a nozzle and diverging part as diffuser. This point signifies that the critical conditions have reached the throat. Further reduction in back pressure does not result rise in mass flow rate further. The nozzle is choked from this point onwards.

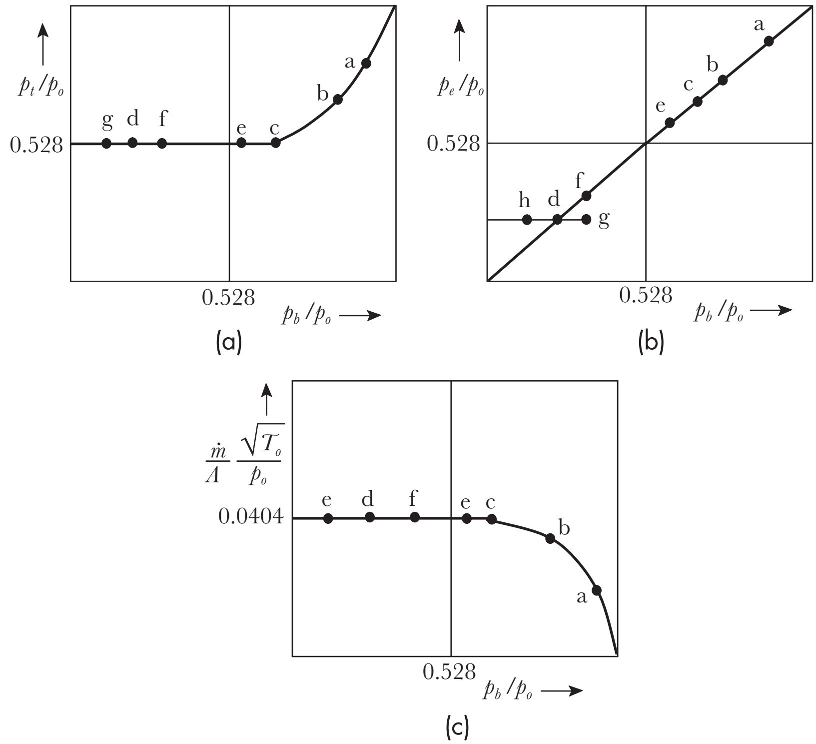

Fig. 8.19 Variation of (a) Throat pressure (b) Exit pressure (c) Mass flow rate through a convergent nozzle

3. Although mass flow rate becomes maximum at back pressure reduction beyond point 'c' onwards. The back pressure lower than that corresponding to 'c' will result in a shock wave in the diverging section. This shock wave moves towards the exit plane of the nozzle as the back pressure approaches the design pressure (pressure corresponding to point 'd'). At the upstream and downstream of the shock, the flow is isentropic. At the upstream of the shock, in the diverging section also acts as the nozzle and at the downstream of the shock the diverging section acts as diffuser.
4. Corresponding to point 'd', the back pressure becomes the exit design pressure of the nozzle. Corresponding to this point, the flow is isentropic throughout the length of the nozzle. Both convergent as well as divergent section acts as nozzle.
5. Now refer to Fig. 8.19(a), the throat pressure decreases with decrease in back pressure until the critical conditions are reached at the throat. The throat pressure remains the same as critical pressure for any value of back pressure lower than back pressure corresponding to 'c'.

6. Figure 8.19(b) shows that the pressure at exit plane of the nozzle decreases with the decrease in back pressure until pressure approaches the design point 'd'. At back pressure slightly higher than the design value of back pressure the shock wave occurs at the exit plane (point 'g'). If the back pressure reduces beyond that at point 'd', the expansion takes place immediately outside the exit plane of the nozzle.
7. Figure 8.19(c) shows that the mass flow first increases with the decrease in back pressure until the critical conditions are reached at the throat (i.e., the back pressure reaches the pressure at point 'c'). Further reduction in back pressure does not have any impact on the mass flow rate. The flow nozzle beyond point 'c' is termed as *choked flow*.

8.7 COMPRESSIBLE FLOW THROUGH CONSTANT AREA DUCT

It has been seen in the previous sections that the flow through variable area ducts (especially nozzles and diffusers) can be approximated to isentropic owing to (a) physical dimensions (small length and large diameter), which ensures small frictional effects, and (b) no heat transfer across the wall (insulated). It has already been mentioned in Section 8.1 that the flow is reversible if the system and its surroundings can be restored to its initial state after undergoing a process. No real process is reversible in nature. There are certain physical characteristics that make the flows irreversible and they are known as *irreversibilites*. Both friction and heat transfer are considered as irreversibilities. Their absence may approximate the flow reversible. Absence of heat transfer is termed as adiabatic. The reversible adiabatic process is also known as isentropic process. In this section, the flow through constant area ducts with irreversibilities will be analysed. The irreversibilities are in form of friction and heat transfer through duct walls. As such, the entropy in such cases does not remain constant. To avoid complications, the compressible flow with friction and compressible flow with heat transfer in a frictionless duct are dealt with separately. The former is known as *Fanno flow* and the latter is known as *Rayleigh flow*.

8.7.1 Fanno Flow

Fanno flow, named after Gino Girolamo Fanno (1882–1962 AD) an Italian mechanical engineer, is the adiabatic flow inside a constant area frictional duct, as shown in Fig. 8.20(a). Such a flow is seen in adiabatic capillary tube (expansion device) of a vapour compression refrigeration system. Due to friction, the entropy will not remain constant. As per the second law of thermodynamics, the entropy always increases. In line with the second law of thermodynamics, it should be noted that during the adiabatic subsonic flow inside the constant area duct, the friction will tend to expand the gas

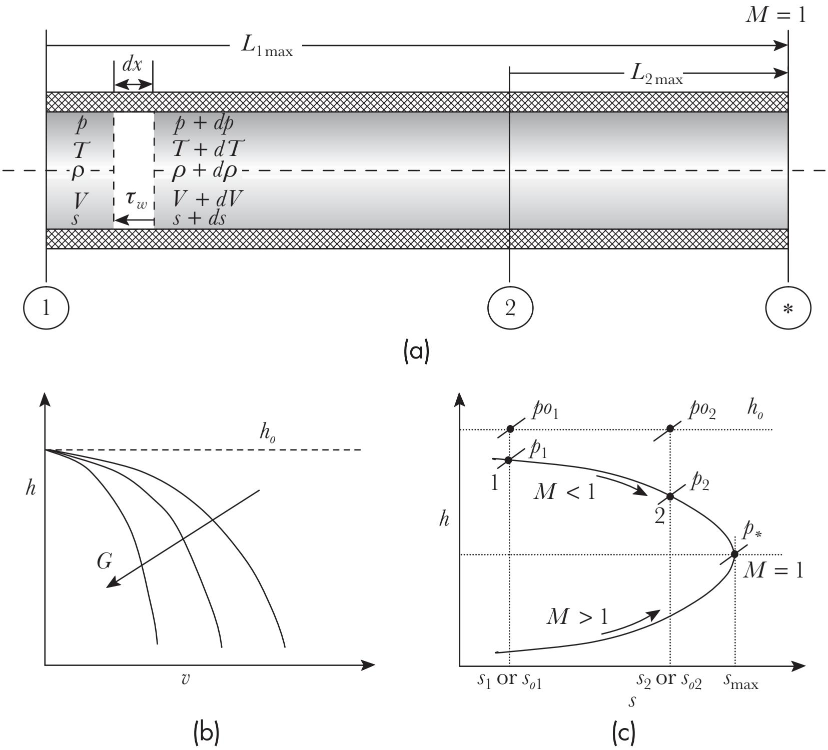

Fig. 8.20 Fanno flow (a) Insulated duct (b) *h–v* plot (c) *h–s* plot

and there is an increase in kinetic energy at the expense of pressure energy. On the other hand, if the adiabatic flow inside the duct is supersonic, the friction will tend to compress the flow and there is a gain in pressure energy. The flow, in each case, will ultimately reach to sonic conditions at the exit of the duct.

If stagnation conditions are prevailing at the inlet and the exit is connected to an exhaust chamber, which is maintained at pressure known as back pressure, the inlet conditions are fixed and back pressure is varied as done in Section 8.6.4. Like variable area duct, the increase in pressure difference across the constant area duct will increase the mass flow rate through it. The mass flow rate will not increase infinitely with the increase in pressure difference. As the back pressure reaches the critical pressure, the maximum mass flow rate is reached. Further reduction in back pressure will not have any effect on the mass flow rate. The condition is known as *choking* and mass flow rate is known as *choked mass flow rate* or *critical mass flow rate*. In fact, the mass flow rate and the pressure at the exit plane of the duct will cease to change. Further expansion occurs in the form of a shock wave immediately after the duct exit plane inside the exhaust chamber.

From continuity equation, the mass flux or mass velocity is given by

$$G = \frac{\dot{m}}{A} = \rho V \tag{8.135}$$

From the steady flow energy equation (Eq. 8.18),

$$h = h_o - \frac{V^2}{2} \quad \Rightarrow \quad h = h_o - \frac{G^2}{2\rho^2} \quad \Rightarrow \quad h = h_o - \frac{G^2 v^2}{2} \tag{8.136}$$

Equation (8.136) represents a parabola on h–v diagram, as shown in Fig. 8.20(b). It is better to represent this process on more popular h–s diagram. The Fanno line has been drawn for subsonic and supersonic compressible flows on the h–s diagram in Fig. 8.20(c).

The variation of other properties such as temperature, pressure, velocity, density, and impulse function during the adiabatic flow within the friction duct as a function of independent variables friction factor and Mach number is done by considering a control volume inside the duct of length dx, as shown in Fig. 8.20(a):

Taking log and then differentiating the continuity equation,

$$G = \rho V = \text{constant} \quad \Rightarrow \quad \frac{d\rho}{\rho} + \frac{dV}{V} = 0 \quad \Rightarrow \quad \boxed{\frac{d\rho}{\rho} = -\frac{dV^2}{2V^2}} \tag{8.137}$$

Taking log and then differentiating the equation of state (ideal gas law)

$$p = \rho RT \quad \Rightarrow \quad \boxed{\frac{dp}{p} = \frac{d\rho}{\rho} + \frac{dT}{T}} \tag{8.138}$$

Taking log and then differentiating the Mach number relation:

$$M = \frac{V}{a} \quad \Rightarrow \quad M^2 = \frac{V^2}{\gamma RT} \quad \Rightarrow \quad \boxed{\frac{dM^2}{M^2} = \frac{dV^2}{V^2} - \frac{dT}{T}} \tag{8.139}$$

Taking log and then differentiating the SFEE:

$$h + \frac{V^2}{2} = h_o \quad \Rightarrow \quad dh + d\left(\frac{V^2}{2}\right) = 0 \quad \Rightarrow \quad c_p dT + \frac{dV^2}{2} = 0 \tag{8.140}$$

$$\frac{\gamma RT}{\gamma - 1}\frac{dT}{T} + \frac{dV^2}{2} = 0 \quad \Rightarrow \quad a^2 \frac{dT}{T} + \frac{\gamma - 1}{2} dV^2 = 0 \tag{8.141}$$

$$\frac{dT}{T} + \frac{\gamma - 1}{2} M^2 \frac{dV^2}{V^2} = 0 \tag{8.142}$$

Eliminating $\frac{dT}{T}$ from Eqs (8.139) and (8.142) and simplifying

$$\boxed{\frac{dV^2}{V^2} = \frac{1}{\left(1 + \frac{\gamma - 1}{2} M^2\right)} \frac{dM^2}{M^2}} \tag{8.143}$$

From Eqs (8.137) and (8.143)

$$\frac{d\rho}{\rho} = -\frac{1}{2}\frac{1}{\left(1+\frac{\gamma-1}{2}M^2\right)}\frac{dM^2}{M^2} \tag{8.144}$$

Using Eqs (8.137), (8.138), (8.139), (8.143), and (8.144)

$$\frac{dp}{p} = \frac{1}{2}\frac{1}{\left(1+\frac{\gamma-1}{2}M^2\right)}\frac{dM^2}{M^2} - \frac{dM^2}{M^2} \tag{8.145}$$

Applying momentum on the control volume drawn in Fig. 8.20(a)

$$pA - (p+dp)A - \tau_w(\pi D dx) = \dot{m} dV \tag{8.146}$$

Expressing wall shear stress in terms of friction factor

$$-dpA - \left(\frac{f}{8}\rho V^2\right)(\pi D dx) = (\rho A V) dV \tag{8.147}$$

$$dp + f\frac{\rho V^2}{2}\frac{dx}{D} + \rho V^2 \frac{dV}{V} = 0 \tag{8.148}$$

Using $V^2 = M^2 a^2 \quad \Rightarrow \quad V^2 = \frac{\gamma p}{\rho} M^2$ and $\frac{dV}{V} = \frac{1}{2}\frac{dV^2}{V^2}$

$$dp + \frac{1}{2}\gamma p M^2 f\frac{dx}{D} + \frac{1}{2}\gamma p M^2 \frac{dV^2}{V^2} = 0 \tag{8.149}$$

$$\frac{dp}{p} + \frac{1}{2}\gamma M^2 f\frac{dx}{D} + \frac{1}{2}\gamma M^2 \frac{dV^2}{V^2} = 0 \tag{8.150}$$

From Eqs (8.143) and (8.148)

$$\frac{dp}{p} + \frac{1}{2}\gamma M^2 f\frac{dx}{D} + \frac{1}{2}\frac{\gamma M^2}{\left(1+\frac{\gamma-1}{2}M^2\right)}\frac{dM^2}{M^2} = 0 \tag{8.151}$$

Substituting Eq. (8.145) in Eq. (8.151) and simplifying

$$\frac{dM^2}{M^2} = \frac{\gamma M^2}{1-M^2}\left(1+\frac{\gamma-1}{2}M^2\right) f\frac{dx}{D} \tag{8.152}$$

or

$$f\frac{dx}{D} = \frac{1-M^2}{\gamma M^4\left(1+\frac{\gamma-1}{2}M^2\right)} dM^2 \tag{8.153}$$

Integrating Eq. (8.153) to calculate the maximum length of the duct for which the Mach number reaches unity at the exit section:

$$\int_0^{L_{max}} \frac{f}{D} dx = \int_{M^2}^{1} \frac{1-M^2}{\gamma M^4 \left(1+\frac{\gamma-1}{2}M^2\right)} dM^2 \tag{8.154}$$

Using partial fractions for the RHS integral,

$$\frac{f}{D} L_{max} = \frac{1-M^2}{\gamma M^2} + \frac{\gamma+1}{2\gamma} \ln \left\{ \frac{\frac{\gamma+1}{2}M^2}{1+\frac{\gamma-1}{2}M^2} \right\} \tag{8.155}$$

The rise in entropy is calculated using first and second laws of thermodynamics as

$$dq = dh - vdp \quad \Rightarrow \quad Tds = c_p dT - vdp \tag{8.156}$$

$$\Rightarrow \quad ds = c_p \frac{dT}{T} - \frac{v}{T} dp \tag{8.157}$$

From ideal gas law, $\frac{v}{T} = \frac{\mathrm{R}}{p}$

$$\Rightarrow \quad ds = c_p \frac{dT}{T} - \mathrm{R}\frac{dp}{p} \tag{8.158}$$

Integrating the Eq. (8.158) between state points 1 and 2,

$$s_2 - s_1 = c_p \ln\left(\frac{T_2}{T_1}\right) - \mathrm{R}\ln\left(\frac{p_2}{p_1}\right) \tag{8.159}$$

Integrating the same equation between stagnation states,

$$s_{o2} - s_{o1} = c_p \ln\left(\frac{T_{o2}}{T_{o1}}\right) - \mathrm{R}\ln\left(\frac{p_{o2}}{p_{o1}}\right) \tag{8.160}$$

However, the stagnation temperature is constant, Eq. (8.160) reduces to

$$s_2 - s_1 = s_{o2} - s_{o1} = \mathrm{R}\ln\left(\frac{p_{o1}}{p_{o2}}\right) \tag{8.161}$$

The fall in stagnation pressure is the measure of rise in entropy.

The ratio of stagnation pressures can be evaluated from Eq. (8.73),

$$\frac{p_{o1}}{p_{o2}} = \frac{p_1}{p_2} \left(\frac{1+\frac{\gamma-1}{2}M_1^2}{1+\frac{\gamma-1}{2}M_2^2} \right)^{\frac{\gamma}{\gamma-1}} \tag{8.162}$$

The pressure ratio p_1/p_2 can be evaluated using the continuity equation and the perfect gas relation:

$$\rho_1 V_1 = \rho_2 V_2 \quad \Rightarrow \quad \frac{p_1}{RT_1} V_1 = \frac{p_2}{RT_2} V_2 \tag{8.163}$$

$$\frac{p_1}{p_2} = \sqrt{\frac{T_1}{T_2}} \frac{M_2}{M_1} \quad \Rightarrow \quad \frac{p_1}{p_2} = \sqrt{\frac{T_o/T_2}{T_o/T_1}} \frac{M_2}{M_1} \tag{8.164}$$

Using Eq. (8.72),

$$\frac{p_1}{p_2} = \frac{M_2}{M_1}\left(\frac{1+\frac{\gamma-1}{2}M_2^2}{1+\frac{\gamma-1}{2}M_1^2}\right)^{\frac{1}{2}} \tag{8.165}$$

Substituting Eq. (8.165) in Eq. (8.162)

$$\frac{p_{o1}}{p_{o2}} = \frac{M_2}{M_1}\left(\frac{1+\frac{\gamma-1}{2}M_1^2}{1+\frac{\gamma-1}{2}M_2^2}\right)^{\frac{\gamma+1}{2(\gamma-1)}} \tag{8.166}$$

Hence, the change in entropy is given by

$$s_2 - s_1 = \mathrm{R}\ln\left(\frac{M_2}{M_1}\left(\frac{1+\frac{\gamma-1}{2}M_1^2}{1+\frac{\gamma-1}{2}M_2^2}\right)^{\frac{\gamma+1}{2(\gamma-1)}}\right) \tag{8.167}$$

The increase in entropy for choked Fanno flow is obtained by substituting $M_2 = 1$ and $M_1 = M$

$$s_* - s = \mathrm{R}\ln\left(\frac{1}{M}\left(\frac{1+\frac{\gamma-1}{2}M^2}{\frac{\gamma+1}{2}}\right)^{\frac{\gamma+1}{2(\gamma-1)}}\right) \tag{8.168}$$

Example 8.10 The air is flowing in an insulated pipe of diameter 40 mm with Mach numbers at the entry and at the exit are 0.3 and 0.6, respectively. Determine the length of the pipe if the friction factor is 0.02.

Solution: This problem is related to the Fanno flow category as the pipe is insulated (adiabatic) and having friction factor of 0.02. (Fig. 8.21).

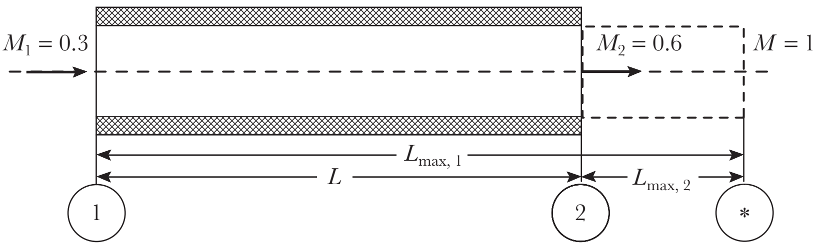

Fig. 8.21

The maximum length of the duct for section 1

$$L_{max,1} = \frac{D}{f}\left[\frac{1-M_1^2}{\gamma M_1^2} + \frac{\gamma+1}{2\gamma}\ln\left\{\frac{\frac{\gamma+1}{2}M_1^2}{1+\frac{\gamma-1}{2}M_1^2}\right\}\right]$$

$$L_{max,1} = \frac{0.04}{0.02}\left[\frac{1-0.3^2}{1.4\times0.3^2} + \frac{2.4}{2.8}\ln\left\{\frac{1.2\times0.3^2}{1+0.2\times0.3^2}\right\}\right] \Rightarrow L_{max,1} = 10.6\,\text{m}$$

The maximum length of the duct for section 2

$$L_{max,2} = \frac{D}{f}\left[\frac{1-M_2^2}{\gamma M_2^2} + \frac{\gamma+1}{2\gamma}\ln\left\{\frac{\frac{\gamma+1}{2}M_2^2}{1+\frac{\gamma-1}{2}M_2^2}\right\}\right]$$

$$L_{max,2} = \frac{0.04}{0.02}\left[\frac{1-0.6^2}{1.4\times0.6^2} + \frac{2.4}{2.8}\ln\left\{\frac{1.2\times0.6^2}{1+0.2\times0.6^2}\right\}\right] \Rightarrow L_{max,2} = 0.981\,\text{m}$$

The length of the pipe is

$$L = L_{max,2} - L_{max,1} \quad\Rightarrow\quad L = 10.6 - 0.981 \quad\Rightarrow\quad L = 9.619\,\text{m}$$

Example 8.11 Repeat Example 8.10 using gas tables.

Solution: This problem is related to the Fanno flow category as the pipe is insulated (adiabatic) and having friction factor of 0.02. (Fig. 8.21). Mach numbers at the entry and exit are 0.3 and 0.6, respectively.

Use Table B2 of appendix B, for $M = 0.3$

$$\frac{fL_{max,1}}{D} = 5.29925 \quad\Rightarrow\quad L_{max,1} = \frac{5.29925\times0.04}{0.02} \quad\Rightarrow\quad L_{max,1} = 10.5985\,\text{m}$$

For $M = 0.6$

$$\frac{fL_{max,2}}{D} = 0.49082 \quad\Rightarrow\quad L_{max,2} = \frac{0.49082\times0.04}{0.02} \quad\Rightarrow\quad L_{max,2} = 0.98164\,\text{m}$$

The length of the pipe is

$$L = L_{\max,2} - L_{\max,1} \quad \Rightarrow \quad L = 10.5985 - 0.98164 \quad \Rightarrow \quad L = 9.6186\,\text{m}$$

8.7.2 Rayleigh Flow

Rayleigh flow, named after John Strutt, 3rd Baron Rayleigh (1842–1919 AD) an English physicist, is the compressible flow accompanied with heat transfer in a constant area frictionless duct, as shown in Fig. 8.22(a).

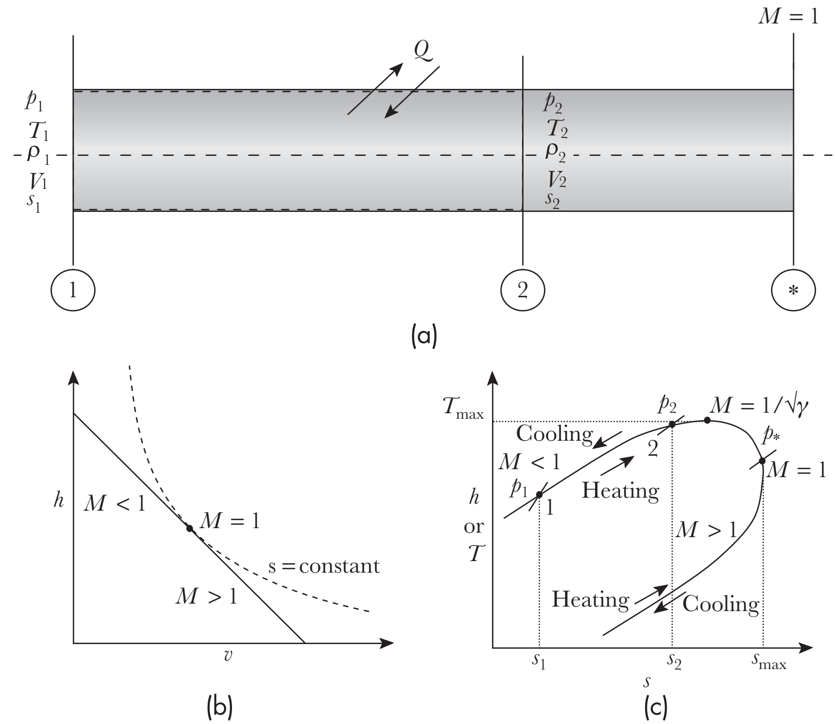

Fig. 8.22 Rayleigh flow (a) Duct (b) *h–v* plot (c) *h–s* plot

The irreversibility, which is responsible for change in flow Mach number in the frictionless duct, is the heat exchange with the surroundings.

Application of steady flow energy equation on the frictionless duct yields the following by choosing an infinitesimal control volume in the frictionless duct:

$$dq - \underbrace{\cancel{dw}}_{0} = dh + VdV + \underbrace{\cancel{gdz}}_{0} \tag{8.169}$$

The effect of gravity can be neglected as the duct is horizontal and also, there is no work done. Integrating Eq. (8.169) between sections 1 and 2 of the duct,

$$q = h_2 - h_1 + \frac{V_2^2 - V_1^2}{2} \quad \Rightarrow \quad q = h_{o2} - h_{o1} \tag{8.170}$$

The heat transfer leads to the change in stagnation enthalpy. The main difference between the Fanno flow and Rayleigh flow is that in Rayleigh flow, the stagnation enthalpy does not remain constant on account of heat exchange with the surroundings.

The application of momentum equation between sections 1 and 2 of the duct gives the following:

$$(p_1 - p_2)A = \dot{m}(V_2 - V_1) \tag{8.171}$$

From mass balance between sections 1 and 2

$$G = \frac{\dot{m}}{A} \quad \Rightarrow \quad G = \rho_1 V_1 = \rho_2 V_2 \quad \Rightarrow \quad \rho V = \text{constant} \tag{8.172}$$

The momentum equation reduces to

$$p_1 + \rho_1 V_1^2 = p_2 + \rho_2 V_2^2 \quad \Rightarrow \quad p + \rho V^2 = \text{constant} \tag{8.173}$$

In terms of G and v, Eq. (8.173) reduces to

$$p = C - G^2 v \tag{8.174}$$

Equation (8.174) has been plotted on the p–v diagram for a given G and an arbitrary constant C in Fig. 8.22(b). The equation represents a straight line known as Rayleigh line, and the heating and cooling decides the direction of the Rayleigh line. For the sake of better understanding, the Rayleigh line has been plotted on a more familiar diagram known as Mollier diagram or h–s diagram, that is, Fig. 8.22(c). The h–s diagram will be similar to the T–s diagram due to the assumption that the flowing gas has been assumed as a perfect gas. Like Fanno line, the Rayleigh line too has two branches; the upper branch is meant for subsonic flow while the lower branch is for supersonic flow. The line gets skewed due to heat transfer. If the flow inside the duct is accompanied with heating, the temperature and the entropy will tend to rise whether the flow is subsonic or supersonic. On the contrary, cooling will lead to reduction in both. Further, the heating process will try to accelerate the subsonic flow in a frictionless duct, whereas, deceleration happens if the flow is supersonic. The Mach number would ultimately reach unity in either case. Cooling, on the other hand, will cause deceleration during subsonic flow and acceleration during the supersonic flow in frictionless duct.

In order to find out the values of Mach number corresponding to maximum entropy and maximum temperature, the following procedure has been adopted:

1. The equation for entropy as a function of temperature and velocity is to be evolved for Rayleigh flow.
2. The derivative *ds/dT* and *dT/ds* are obtained and are equated to zero for maximum value of entropy and temperature respectively.
3. The values of Mach number corresponding to maximum entropy and the maximum temperature will then be obtained.

The entropy change can be obtained from the following equation:

$$ds = c_p \frac{dT}{T} - R\frac{dp}{p} \tag{8.175}$$

Using the equation of state,

$$ds = c_p \frac{dT}{T} - R\left(\frac{d\rho}{\rho} + \frac{dT}{T}\right) \Rightarrow ds = c_v \frac{dT}{T} - R\frac{d\rho}{\rho} \tag{8.176}$$

From continuity equation,

$$ds = \frac{R}{\gamma - 1}\frac{dT}{T} + R\frac{dV}{V} \Rightarrow \frac{ds}{dT} = \frac{R}{T(\gamma - 1)} + \frac{R}{V}\frac{dV}{dT} \tag{8.177}$$

The derivative *dV/dT* can be found out in following manner:

From the equation of state and the continuity equation,

$$\frac{dp}{p} = -\frac{dV}{V} + \frac{dT}{T} \tag{8.178}$$

Differentiating the Rayleigh line equation

$$dp = -\rho V dV \tag{8.179}$$

From the two aforementioned equations,

$$\frac{dT}{dV} = \frac{T}{V} - \frac{V}{R} \tag{8.180}$$

Substituting Eq. (8.180) in Eq. (8.177)

$$\frac{ds}{dT} = \frac{R}{T(\gamma - 1)} + \frac{R}{V\left(\frac{T}{V} - \frac{V}{R}\right)} \Rightarrow \frac{ds}{dT} = \frac{R(-V^2 + \gamma RT)}{T(\gamma - 1)(RT - V^2)} \tag{8.181}$$

For maximum entropy, $\frac{ds}{dT} = 0 \Rightarrow V^2 = \gamma RT \Rightarrow V^2 = a^2 \Rightarrow M = 1$

For maximum temperature or enthalpy, $\frac{dT}{ds}=0 \Rightarrow V^2 = RT \Rightarrow V^2 = \frac{a^2}{\gamma} \Rightarrow$ $M = 1/\sqrt{\gamma}$.

Ratio of Properties

Using the momentum equation, that is, Eq. (8.173), to obtain the pressure ratio between the two sections,

$$p_1 + p_1\gamma M_1^2 = p_2 + p_2\gamma M_2^2 \tag{8.182}$$

$$\frac{p_1}{p_2} = \frac{1+\gamma M_2^2}{1+\gamma M_1^2} \tag{8.183}$$

The ratio of pressures between any section and critical section is obtained by substituting $M_2 = 1$.

$$\frac{p}{p_*} = \frac{1+\gamma}{1+\gamma M^2} \tag{8.184}$$

The stagnation pressure ratio between sections 1 and 2 can be obtained by applying the chain rule.

$$\frac{p_{o1}}{p_{o2}} = \frac{p_{o1}}{p_1} \times \frac{p_1}{p_2} \times \frac{p_2}{p_{o2}} \tag{8.185}$$

$$\frac{p_{o1}}{p_{o2}} = \left(1+\frac{\gamma-1}{2}M_1^2\right)^{\frac{\gamma}{\gamma-1}} \times \left(\frac{1+\gamma M_2^2}{1+\gamma M_1^2}\right) \times \left(1+\frac{\gamma-1}{2}M_2^2\right)^{-\frac{\gamma}{\gamma-1}} \tag{8.186}$$

$$\frac{p_{o1}}{p_{o2}} = \left(\frac{1+\gamma M_2^2}{1+\gamma M_1^2}\right)\left(\frac{1+\frac{\gamma-1}{2}M_1^2}{1+\frac{\gamma-1}{2}M_2^2}\right)^{\frac{\gamma}{\gamma-1}} \tag{8.187}$$

The ratio of stagnation pressures between any section and critical section is obtained by substituting $M_2 = 1$.

$$\frac{p_o}{p_{o*}} = \left(\frac{1+\gamma}{1+\gamma M^2}\right)\left(\frac{1+\frac{\gamma-1}{2}M^2}{\frac{\gamma+1}{2}}\right)^{\frac{\gamma}{\gamma-1}} \tag{8.188}$$

From perfect gas relation, the temperature ratio between the two sections 1 and 2 can be obtained.

$$\frac{T_1}{T_2} = \frac{p_1}{p_2} \times \frac{\rho_2}{\rho_1} \quad \Rightarrow \quad \frac{T_1}{T_2} = \frac{p_1}{p_2} \times \frac{V_1}{V_2} \tag{8.189}$$

$$\frac{T_1}{T_2} = \frac{p_1}{p_2} \times \frac{M_1 a_1}{M_2 a_2} \quad \Rightarrow \quad \frac{T_1}{T_2} = \frac{p_1}{p_2} \times \frac{M_1}{M_2}\sqrt{\frac{T_1}{T_2}} \tag{8.190}$$

Substituting Eq. (8.183) in Eq. (8.190) and simplifying to get the temperature ratio in terms of Mach numbers,

$$\frac{T_1}{T_2} = \left(\frac{1+\gamma M_2^2}{1+\gamma M_1^2}\right)^2 \times \left(\frac{M_1}{M_2}\right)^2 \tag{8.191}$$

The ratio of temperatures between any section and critical section is obtained by substituting $M_2 = 1$.

$$\frac{T}{T_*} = M^2 \left(\frac{1+\gamma}{1+\gamma M^2}\right)^2 \tag{8.192}$$

The stagnation temperature ratio is obtained in a similar manner as stagnation pressure ratio.

$$\frac{T_{o1}}{T_{o2}} = \left(\frac{M_1}{M_2}\right)^2 \left(\frac{1+\gamma M_2^2}{1+\gamma M_1^2}\right)^2 \left(\frac{1+\frac{\gamma-1}{2}M_1^2}{1+\frac{\gamma-1}{2}M_2^2}\right) \tag{8.193}$$

The ratio of stagnation pressures between any section and critical section is obtained by substituting $M_2 = 1$.

$$\frac{T_o}{T_{o*}} = M^2 \left(\frac{1+\gamma}{1+\gamma M^2}\right)^2 \left(\frac{1+\frac{\gamma-1}{2}M^2}{\frac{\gamma+1}{2}}\right) \tag{8.194}$$

Change in entropy due to heat transfer can be obtained by integrating Eq. (8.175),

$$s_2 - s_1 = c_p \ln\left(\frac{T_2}{T_1}\right) - R\ln\left(\frac{p_2}{p_1}\right) \quad \Rightarrow \quad s_2 - s_1$$

$$= c_p \ln\left\{\frac{T_2/T_1}{(p_2/p_1)^{\gamma-1/\gamma}}\right\} \tag{8.195}$$

Substituting temperature and pressure ratios to obtain the entropy in terms of Mach numbers,

$$\frac{s_2 - s_1}{c_p} = \ln\left\{\left(\frac{M_2}{M_1}\right)^2 \left(\frac{1+\gamma M_1^2}{1+\gamma M_2^2}\right)^{\frac{\gamma+1}{\gamma}}\right\} \tag{8.196}$$

The change in entropy between any section and critical section is obtained by substituting $M_2 = 1$.

$$\frac{s - s_*}{c_p} = \ln\left\{M^2 \left(\frac{1+\gamma}{1+\gamma M^2}\right)^{\frac{\gamma+1}{\gamma}}\right\} \tag{8.197}$$

Example 8.12 The ratio of stagnation temperatures of air at the exit to the entry of a combustor of constant cross section is 2.5. If the parameters at the entrance are $p_1 = 5$ bar, $T_1 = 350$ K, and $M_1 = 0.3$, determine (a) temperature, pressure, and Mach number at the combustor exit, (b) change in stagnation pressure, (c) change in entropy, and (d) specific heat added.

Solution: Given that $T_{o2}/T_{o1} = 2.5$, $T_1 = 350$ K, $p_1 = 5$ bar, and $M_1 = 0.3$.

Figure 8.23 is drawn for the sake of better understanding of the problem.

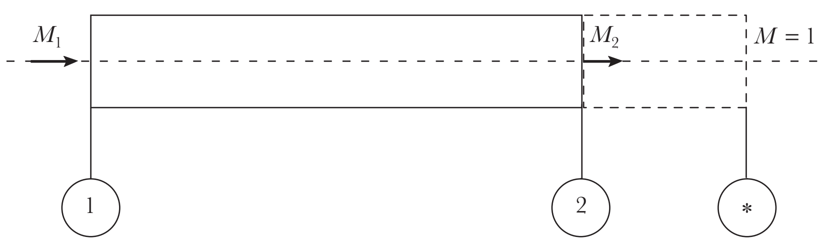

Fig. 8.23

The stagnation quantities at the inlet

$$T_{o1} = T_1\left(1+\frac{\gamma-1}{2}M_1^2\right) \Rightarrow T_{o1} = 350\left(1+\frac{1.4-1}{2}\times 0.3^2\right)$$

$$\Rightarrow T_{o1} = 356.3\,\text{K}$$

Therefore, stagnation temperature at the outlet

$$T_{o2} = 2.5T_{o1} \Rightarrow T_{o2} = 890.8\,\text{K}$$

$$p_{o1} = p_1\left(\frac{T_{o1}}{T_1}\right)^{\frac{\gamma}{\gamma-1}} \Rightarrow p_{o1} = 5\left(\frac{356.3}{350}\right)^{\frac{1.4}{0.4}} \Rightarrow p_{o1} = 5.322\,\text{bar}$$

The ratio of stagnation pressures between outlet and inlet

$$\frac{T_{o2}}{T_{o1}}=\frac{T_{o2}/T_{o*}}{T_{o1}/T_{o*}} \quad\Rightarrow\quad 2.5=\frac{M_2^2\left(\dfrac{1+\gamma}{1+\gamma M_2^2}\right)^2\left(\dfrac{1+\dfrac{\gamma-1}{2}M_2^2}{\dfrac{\gamma+1}{2}}\right)}{0.3^2\left(\dfrac{1+1.4}{1+1.4\times 0.3^2}\right)^2\left(\dfrac{1+0.2\times 0.3^2}{\dfrac{1.4+1}{2}}\right)}$$

$$\Rightarrow\quad M_2^2\left(\frac{1+1.4}{1+1.4M_2^2}\right)^2\left(\frac{1+0.2M_2^2}{1.2}\right)=0.86715 \quad\Rightarrow\quad M_2=0.6487$$

The pressure and temperature at the combustor outlet can be obtained from the following relations:

$$\frac{p_2}{p_1}=\frac{1+\gamma M_1^2}{1+\gamma M_2^2} \quad\Rightarrow\quad p_2=5\times\frac{1+1.4\times 0.3^2}{1+1.4\times 0.6487^2} \quad\Rightarrow\quad p_2=3.54\,\text{bar}$$

$$\frac{T_2}{T_1}=\left(\frac{1+\gamma M_1^2}{1+\gamma M_2^2}\right)^2\times\left(\frac{M_2}{M_1}\right)^2 \quad\Rightarrow\quad T_2=350\times 0.708^2\times\left(\frac{0.6487}{0.3}\right)^2$$

$$\Rightarrow\quad T_2=820.3\,\text{K}$$

Change in entropy

$$\Delta s=c_p\ln\left\{\frac{T_2/T_1}{(p_2/p_1)^{\gamma-1/\gamma}}\right\} \quad\Rightarrow\quad \Delta s=1005\ln\left\{\frac{820.3/350}{(3.54/5)^{\frac{0.4}{1.4}}}\right\}$$

$$\Rightarrow\quad \Delta s=955.15\,\text{J/kg-K}$$

Heat addition

$$Q=c_p(T_{o2}-T_{o1}) \quad\Rightarrow\quad Q=1005(890.8-356.3) \quad\Rightarrow\quad Q=537.17\,\text{kJ/kg}$$

Example 8.13 Repeat Example 8.12, using gas tables.

Solution: Given that $T_{o2}/T_{o1}=2.5$, $T_1=350\,\text{K}$, $p_1=5\,\text{bar}$, and $M_1=0.3$

From Table B1 of Appendix B,

For $M=0.3$

$$\frac{T_1}{T_{o1}}=0.98232 \quad\Rightarrow\quad T_{o1}=356.3\,\text{K}$$

Similarly, the stagnation pressure at the inlet can also be obtained:

$$\frac{p_1}{p_{o1}}=0.93947 \quad\Rightarrow\quad p_{o1}=5.322\,\text{bar}$$

Therefore, stagnation temperature at the outlet

$$T_{o2} = 2.5T_{o1} \quad \Rightarrow \quad T_{o2} = 890.75\,\text{K}$$

The ratio of stagnation pressures between the outlet and inlet (Table B3)

$$\frac{T_{o2}}{T_{o1}} = \frac{T_{o2}/T_{o*}}{T_{o1}/T_{o*}} \quad \Rightarrow \quad \frac{T_{o2}}{T_{o*}} = \frac{T_{o2}}{T_{o1}} \times \frac{T_{o1}}{T_{o*}}$$

$$\Rightarrow \quad \frac{T_{o2}}{T_{o*}} = 2.5 \times 0.34686 \quad \Rightarrow \quad \frac{T_{o2}}{T_{o*}} = 0.86715$$

In the same table corresponding to $T_{o2}/T_{o*} = 0.86715$, the exit Mach number is obtained by applying linear interpolation between $T_o/T_{o*} = 0.859203$ and $T_o/T_{o*} = 0.877084$

$$M_2 = 0.64 + \frac{0.86715 - 0.859203}{0.877084 - 0.859203}(0.66 - 0.64) \quad \Rightarrow \quad M_2 = 0.6489$$

The pressure and temperature at the combustor outlet can be obtained from the following relations:

$$\frac{p_2}{p_1} = \frac{p_2/p_*}{p_1/p_*} \quad \Rightarrow \quad \frac{p_2}{p_1} = \frac{1.52532 + \dfrac{0.6489 - 0.64}{0.66 - 0.64}(1.490831 - 1.52532)}{2.131439}$$

$$\Rightarrow \quad \frac{p_2}{p_1} = 0.7084 \quad \Rightarrow \quad p_2 = 3.542\,\text{bar}$$

$$\frac{T_2}{T_1} = \frac{T_2/T_*}{T_1/T_*} \quad \Rightarrow \quad \frac{T_2}{T_1} = \frac{0.952976 + \dfrac{0.6489 - 0.64}{0.66 - 0.64}(0.968155 - 0.952976)}{0.408873}$$

$$\Rightarrow \quad \frac{T_2}{T_1} = 2.34726 \quad \Rightarrow \quad T_2 = 821.54\,\text{K}$$

Change in entropy

$$\Delta s = c_p \ln\left\{\frac{T_2/T_1}{(p_2/p_1)^{\gamma-1/\gamma}}\right\} \quad \Rightarrow \quad \Delta s = 1005 \ln\left\{\frac{2.34726}{(0.7084)^{\frac{0.4}{1.4}}}\right\}$$

$$\Rightarrow \quad \Delta s = 956.5\,\text{J/kg-K}$$

Heat addition

$$Q = c_p(T_{o2} - T_{o1}) \quad \Rightarrow \quad Q = 1005(890.75 - 356.3) \quad \Rightarrow \quad Q = 537.122\,\text{kJ/kg}$$

8.8 SHOCK WAVES

A shock wave may be defined as a highly localized irreversibility as the flow undergoes a sudden transition from supersonic to subsonic state, which occurs within the distance of mean free path. This is caused due to changes in certain

conditions in the downstream of the flow. It should be remembered that the shock would occur only when the flow is taking place at supersonic speed. Within the shock, the flow crosses the sound barrier. Thus, it is characterized by sudden drop in velocity and abrupt rise in pressure. In addition, there is rise in temperature and density in the downstream of the shock as well. Since it is irreversible, the entropy rise takes place across it. The shocks may be classified as normal, oblique, attached, and detached, as shown in Fig. 8.24. Normal shocks are perpendicular to the flow, whereas, oblique shocks are inclined at an angle other than 90°.

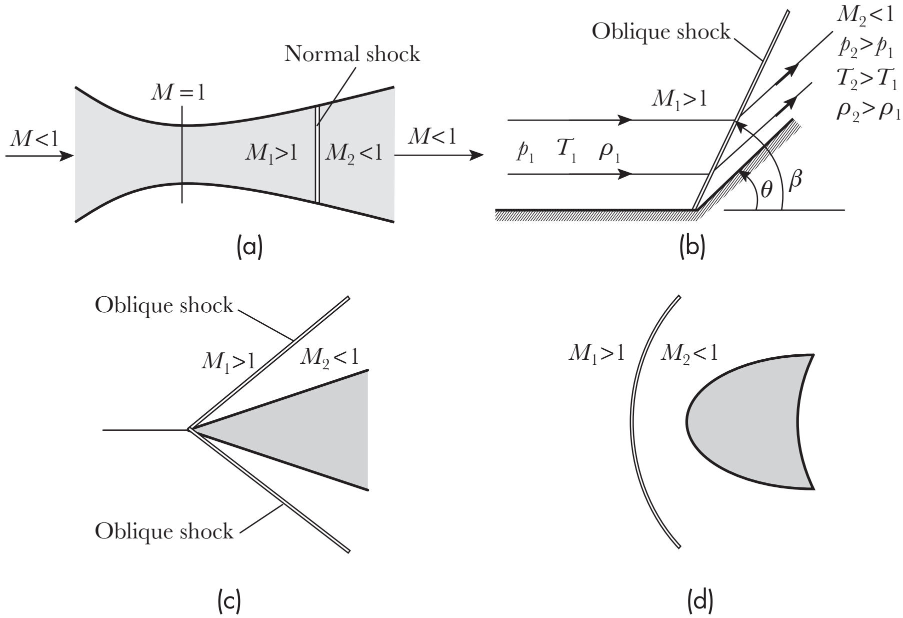

Fig. 8.24 Types of shocks (a) Normal (b) Oblique (c) Attached (d) Detached

In this section, analysis of only normal shock has been presented with the help of Fig. 8.25.

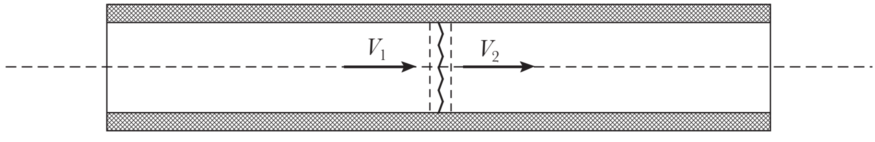

Fig. 8.25 Normal shock in a frictionless and adiabatic duct

The following are the general characteristics of a shock wave:

1. The thickness of the shock is negligibly small such that it may be assumed to take place at a constant area.

2. The flow in a shock is considered as frictionless owing to its negligible thickness.
3. The flow in a shock may be assumed adiabatic.
4. There is no external work and body forces (gravity) are negligibly small.

The governing equations for the normal shock can be evolved by considering a normal shock in a constant area adiabatic and frictionless duct.

Mass conservation

$$\frac{\dot{m}}{A} = \rho_1 V_2 = \rho_1 V_2 \tag{8.198}$$

Momentum conservation

$$(p_1 - p_2)A = \dot{m}(V_2 - V_1) \tag{8.199}$$

$$\left.\begin{aligned} p_1 + \rho_1 V_1^2 &= p_2 + \rho_2 V_2^2 \\ p_1\left(1+\gamma M_1^2\right) &= p_2\left(1+\gamma M_2^2\right) \end{aligned}\right\} \tag{8.200}$$

Energy conservation

$$0 = h_2 - h_1 + \frac{V_2^2 - V_1^2}{2} \tag{8.201}$$

$$h_1 + \frac{V_1^2}{2} = h_2 + \frac{V_2^2}{2} \quad \Rightarrow \quad h_{o1} = h_{o2} \tag{8.202}$$

8.8.1 Prandtl–Meyer Relation

Prandtl–Meyer relation establishes the relationship between the velocities at the upstream and downstream of a shock. As the flow transforms from supersonic to subsonic state, the flow crosses the sound barrier and the sonic or critical conditions occur within the shock. The application of energy conservation principle suggests that the stagnation enthalpy remains constant throughout the shock.

$$h_{o1} = h_{o*} = h_{o2} \tag{8.203}$$

$$h_{o1} = h_1 + \frac{V_1^2}{2} \quad \Rightarrow \quad h_{o1} = c_p T_1 + \frac{V_1^2}{2} \tag{8.204}$$

$$h_{o1} = \frac{\gamma R T_1}{\gamma - 1} + \frac{V_1^2}{2} \quad \Rightarrow \quad h_{o1} = \frac{a_1^2}{\gamma - 1} + \frac{V_1^2}{2} \tag{8.205}$$

Similarly, stagnation enthalpy downstream of the shock is given by

$$h_{o2} = \frac{a_2^2}{\gamma - 1} + \frac{V_2^2}{2} \tag{8.206}$$

The critical stagnation enthalpy can be obtained by replacing the sound fluid velocity by critical sound velocity, that is,

$$h_{o*} = \frac{a_*^2}{2}\left(\frac{\gamma+1}{\gamma-1}\right) \tag{8.207}$$

Now using Eqs (8.205) and (8.206) in Eq. (8.203),

$$\frac{a_1^2}{\gamma-1} + \frac{V_1^2}{2} = \frac{a_*^2}{2}\left(\frac{\gamma+1}{\gamma-1}\right) \tag{8.208}$$

$$\frac{a_2^2}{\gamma-1} + \frac{V_2^2}{2} = \frac{a_*^2}{2}\left(\frac{\gamma+1}{\gamma-1}\right) \tag{8.209}$$

Using the momentum Eq. (8.199) and continuity Eq. (8.198),

$$(p_1 - p_2)\frac{A}{\dot{m}} = V_2 - V_1 \quad \Rightarrow \quad \frac{p_1}{\rho_1 V_1} - \frac{p_2}{\rho_2 V_2} = V_2 - V_1 \tag{8.210}$$

$$\frac{a_1^2}{V_1} - \frac{a_2^2}{V_2} = V_2 - V_1 \tag{8.211}$$

Eliminating the upstream and downstream sound velocities from Eq. (8.211) using Eq. (8.208) in Eq. (8.209)

$$\left.\begin{aligned} &a_*^2 = V_1 V_2 \\ &\text{or} \\ &M_1^* M_2^* = 1 \end{aligned}\right\} \tag{8.212}$$

Equation (8.212) is known as the *Prandtl–Meyer equation.*

8.8.2 Mach Number Downstream of the Shock

Mach number is usually known at the upstream of the shock. The Mach number downstream of the shock in terms of the known upstream Mach number is computed in the following manner:

From the critical temperature ratio given by Eq. (8.75),

$$T_* = \frac{2}{\gamma+1} T_o \tag{8.213}$$

Multiplying both sides by γR

$$\gamma R T_* = \frac{2}{\gamma+1}\gamma R T_o \quad \Rightarrow \quad a_*^2 = \frac{2}{\gamma+1}\gamma R T_o \tag{8.214}$$

From Prandtl–Meyer equation,

$$V_1V_2 = \frac{2}{\gamma+1}\gamma RT_o \quad \Rightarrow \quad M_1M_2 = \frac{2}{\gamma+1}\frac{T_o}{\sqrt{T_1T_2}} \tag{8.215}$$

Squaring and rearranging,

$$M_2^2 = \frac{1}{M_1^2}\left(\frac{2}{\gamma+1}\right)^2\left(\frac{T_o}{T_1}\right)\left(\frac{T_o}{T_2}\right) \tag{8.216}$$

Using Eq. (8.72),

$$M_2^2 = \frac{1}{M_1^2}\left(\frac{2}{\gamma+1}\right)^2\left(1+\frac{\gamma-1}{2}M_1^2\right)\left(1+\frac{\gamma-1}{2}M_2^2\right) \tag{8.217}$$

On rearrangement, the Mach number downstream of the shock is given by

$$\boxed{M_2^2 = \frac{1+\dfrac{\gamma-1}{2}M_1^2}{\gamma M_1^2-\dfrac{\gamma-1}{2}}} \quad \Rightarrow \quad \boxed{M_2^2 = \frac{M_1^2+\dfrac{2}{\gamma-1}}{\dfrac{2\gamma}{\gamma-1}M_1^2-1}} \tag{8.218}$$

8.8.3 Ratio of Various Quantities across the Shock

The objective behind the present analysis is to determine the quantities downstream of the shock in terms of upstream Mach number. From momentum equation, the pressure ratio across the shock is given by

$$\frac{p_2}{p_1} = \frac{1+\gamma M_1^2}{1+\gamma M_2^2} \tag{8.219}$$

Substituting Eq. (8.218) in Eq. (8.219)

$$\frac{p_2}{p_1} = \frac{\left(1+\gamma M_1^2\right)\left(\dfrac{2\gamma}{\gamma-1}M_1^2-1\right)}{\dfrac{2\gamma}{\gamma-1}M_1^2-1+\gamma M_1^2+\dfrac{2\gamma}{\gamma-1}} \tag{8.220}$$

The pressure ratio is reduced to

$$\boxed{\frac{p_2}{p_1} = \frac{2\gamma}{\gamma+1}M_1^2-\frac{\gamma-1}{\gamma+1}} \tag{8.221}$$

It should be noted that the flow through the shock is analogous to Fanno flow, where the irreversibility is not the friction but the shock itself. The stagnation enthalpy remains unchanged before and after the shock as the flow through shock is considered adiabatic. Since the fluid is assumed to be a perfect gas, the

stagnation temperature will also be constant. Using Eq. (8.72) for stagnation temperatures across the shock, the temperature ratio is, thus, given by

$$\frac{T_2}{T_1} = \frac{T_{o1}/T_1}{T_{o2}/T_2} \quad \Rightarrow \quad \frac{T_2}{T_1} = \frac{1+\dfrac{\gamma-1}{2}M_1^2}{1+\dfrac{\gamma-1}{2}M_2^2} \tag{8.222}$$

Substituting Eq. (8.218) in Eq. (8.221)

$$\frac{T_2}{T_1} = \frac{\left(1+\dfrac{\gamma-1}{2}M_1^2\right)\left(\gamma M_1^2 - \dfrac{\gamma-1}{2}\right)}{\gamma M_1^2 - \dfrac{\gamma-1}{2} + \dfrac{\gamma-1}{2}\left(1+\dfrac{\gamma-1}{2}M_1^2\right)} \tag{8.223}$$

The temperature ratio, thus, reduces to

$$\boxed{\frac{T_2}{T_1} = \frac{\left(1+\dfrac{\gamma-1}{2}M_1^2\right)\left(\gamma M_1^2 - \dfrac{\gamma-1}{2}\right)}{\left(\dfrac{\gamma+1}{2}\right)^2 M_1^2}} \tag{8.224}$$

The density ratio across the shock is evaluated by using the ideal gas equation:

$$\frac{\rho_2}{\rho_1} = \frac{p_2}{p_1} \times \frac{T_1}{T_2} \tag{8.225}$$

Substituting Eqs (8.221) and (8.224) in Eq. (8.225)

$$\frac{\rho_2}{\rho_1} = \frac{2}{(\gamma+1)}\left(\gamma M_1^2 - \frac{\gamma-1}{2}\right) \times \frac{\left(\dfrac{\gamma+1}{2}\right)^2 M_1^2}{\left(1+\dfrac{\gamma-1}{2}M_1^2\right)\left(\gamma M_1^2 - \dfrac{\gamma-1}{2}\right)} \tag{8.226}$$

The density ratio is, therefore, given by

$$\boxed{\frac{\rho_2}{\rho_1} = \frac{\dfrac{\gamma+1}{2}M_1^2}{1+\dfrac{\gamma-1}{2}M_1^2}} \tag{8.227}$$

In accordance to continuity equation, the velocity ratio across the shock will be the inverse of density ratio

$$\boxed{\frac{V_2}{V_1} = \frac{1+\dfrac{\gamma-1}{2}M_1^2}{\dfrac{\gamma+1}{2}M_1^2}} \tag{8.228}$$

The stagnation pressure ratio across the shock is determined as:

$$\frac{p_{o2}}{p_{o1}} = \frac{p_{o2}}{p_2} \times \frac{p_2}{p_1} \times \frac{p_1}{p_{o1}} \tag{8.229}$$

$$\frac{p_{o2}}{p_{o1}} = \left(\frac{1 + \frac{\gamma - 1}{2} M_2^2}{1 + \frac{\gamma - 1}{2} M_1^2} \right)^{\frac{\gamma}{\gamma - 1}} \left(\frac{2\gamma}{\gamma + 1} M_1^2 - \frac{\gamma - 1}{\gamma + 1} \right) \tag{8.230}$$

Substituting Eq. (8.218) in Eq. (8.220) and simplifying

$$\frac{p_{o2}}{p_{o1}} = \left(\frac{\frac{\gamma + 1}{2} M_2^2}{1 + \frac{\gamma - 1}{2} M_1^2} \right)^{\frac{\gamma}{\gamma - 1}} \left(\frac{2\gamma}{\gamma + 1} M_1^2 - \frac{\gamma - 1}{\gamma + 1} \right)^{-\frac{1}{\gamma - 1}} \tag{8.231}$$

The stagnation to static pressure ratio across the shock is determined by

$$\frac{p_{o2}}{p_1} = \frac{p_{o2}}{p_2} \times \frac{p_2}{p_1} \tag{8.232}$$

$$\frac{p_{o2}}{p_1} = \left(1 + \frac{\gamma - 1}{2} M_2^2 \right)^{\frac{\gamma}{\gamma - 1}} \left(\frac{2\gamma}{\gamma + 1} M_1^2 - \frac{\gamma - 1}{\gamma + 1} \right) \tag{8.233}$$

The rise in entropy can be evaluated in a similar fashion as done in case of Fanno flow, that is,

$$s_2 - s_1 = -\mathrm{R} \ln\left(\frac{p_{o2}}{p_{o1}} \right) \Rightarrow \frac{\Delta s}{R} = -\ln\left(\frac{p_{o2}}{p_{o1}} \right) \tag{8.234}$$

The variation of entropy with Mach number has been plotted in Fig. 8.26. The following conclusions can be drawn:

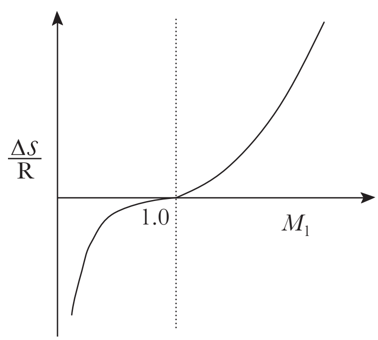

Fig. 8.26 Entropy variation with Mach number

1. There is no change in entropy for $M_1 = 1$.
2. When $M_1 < 1$, there is a decrease in entropy, which is not possible as it violates second law of thermodynamics. Hence, it can be concluded that in the subsonic flow occurrence of shock is impossible.
3. High value of Mach number in supersonic regime yields higher rise in entropy.

8.8.4 Rankine–Hugoniot Relation

The Rankine–Hugoniot equation relates the pressure ratio with the density ratio for the flow through a normal shock. This can be obtained by eliminating M_x^2 from Eqs (8.221) and (8.225).

$$\frac{p_2}{p_1} = \frac{2\gamma}{\gamma+1}\left(\frac{2(\rho_2/\rho_1)}{(\gamma+1)-(\gamma-1)(\rho_2/\rho_1)}\right) - \frac{\gamma-1}{\gamma+1} \tag{8.235}$$

On simplification,

$$\frac{p_2}{p_1} = \frac{\dfrac{\gamma+1}{\gamma-1}\dfrac{\rho_2}{\rho_1} - 1}{\dfrac{\gamma+1}{\gamma-1} - \dfrac{\rho_2}{\rho_1}} \quad \text{or} \quad \frac{\rho_2}{\rho_1} = \frac{1 + \dfrac{\gamma+1}{\gamma-1}\dfrac{p_2}{p_1}}{\dfrac{\gamma+1}{\gamma-1} + \dfrac{p_2}{p_1}} \tag{8.236}$$

Equation (8.236) is known as Rankine–Hugoniot equation and is plotted in Fig. 8.27, and a comparison has been made with the isentropic flow process.

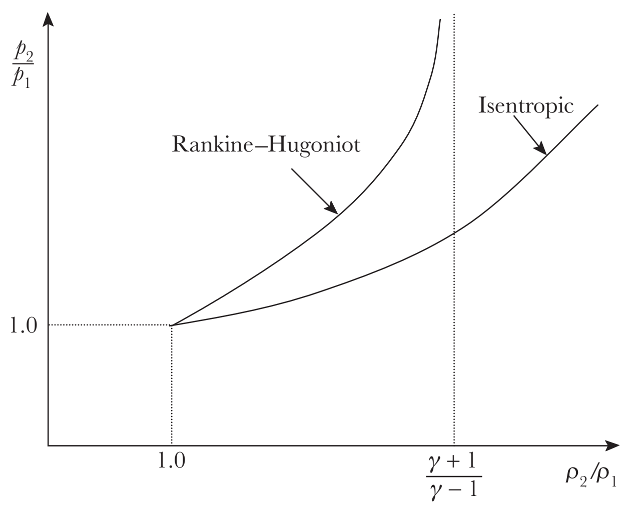

Fig. 8.27 Comparison of pressure variation with density in a shock with an isentropic process

The pressure rises infinitely as soon as the density ratio reaches $\dfrac{\gamma+1}{\gamma-1}$. However, there is no such abrupt rise in pressure if the process is isentropic or reversible adiabatic. The shock, which is a form of irreversibility, is responsible for the abrupt rise in pressure.

8.8.5 Shock Strength

Shock strength is defined as the ratio of rise in pressure to the pressure upstream of the shock. Mathematically,

$$\xi = \frac{p_2 - p_1}{p_1} \Rightarrow \xi = \frac{p_2}{p_1} - 1 \tag{8.237}$$

From Eq. (8.221),

$$\xi = \frac{2\gamma}{\gamma+1}\left(M_1^2 - 1\right) \tag{8.238}$$

The shock strength can also be expressed in terms of pressure and density ratios using Rankine–Hugoniot equation:

$$\xi = \frac{\dfrac{2\gamma}{\gamma-1}\left(\dfrac{\rho_2}{\rho_1} - 1\right)}{\dfrac{2}{\gamma-1} - \left(\dfrac{\rho_2}{\rho_1} - 1\right)} \tag{8.239}$$

The shocks that have $\xi \approx 0$ are termed as *shocks of vanishing strength* or *weak shocks*. For such shocks, $M_1 \approx 1, \dfrac{\rho_2}{\rho_1} \approx 1, \dfrac{p_2}{p_1} \approx 1, \dfrac{T_2}{T_1} \approx 1, \dfrac{p_{o2}}{p_{o1}} \approx 1$ and $\dfrac{\Delta s}{R} \approx 0$.

The *strong shocks* occur as a result of very high upstream Mach number, M_x. If $M_x \to \infty$, the downstream Mach number M_y [from Eq. (8.218)] approaches to

$$M_2^2 = \lim_{M_1 \to \infty}\left(\frac{\dfrac{1}{M_1^2} + \dfrac{\gamma-1}{2}}{\gamma - \dfrac{1}{M_1^2}\dfrac{\gamma-1}{2}}\right) \Rightarrow M_2 = \sqrt{\frac{\gamma-1}{2\gamma}} \tag{8.240}$$

As $M_1 \to \infty \Rightarrow M_2 \to \sqrt{\dfrac{\gamma-1}{2\gamma}}, \dfrac{\rho_2}{\rho_1} \to \dfrac{\gamma+1}{\gamma-1}, \dfrac{p_2}{p_1} \to \infty$, and $\dfrac{T_2}{T_1} \to \infty$.

Example 8.14 The parameters of air measured at upstream of a normal shock wave are $M_1 = 2.0$, $p_1 = 1\,\text{bar}$, and $T_1 = 300\,\text{K}$. Determine the Mach number, pressure, and temperature downstream of the shock.

Solution:

General relation	For air	Values
$M_2^2 = \dfrac{M_1^2 + \dfrac{2}{\gamma-1}}{\dfrac{2\gamma}{\gamma-1}M_1^2 - 1}$	$M_2^2 = \dfrac{M_1^2+5}{7M_1^2-1}$	$M_2 = 0.577$
$\dfrac{p_2}{p_1} = \dfrac{2\gamma}{\gamma+1}M_1^2 - \dfrac{\gamma-1}{\gamma+1}$	$\dfrac{p_2}{p_1} = \dfrac{7M_1^2-1}{6}$	$p_2 = 4.5$ bar
$\dfrac{T_2}{T_1} = \dfrac{\left(1+\dfrac{\gamma-1}{2}M_1^2\right)\left(\gamma M_1^2 - \dfrac{\gamma-1}{2}\right)}{\left(\dfrac{\gamma+1}{2}\right)^2 M_1^2}$	$\dfrac{T_2}{T_1} = \dfrac{\left(1+0.2M_1^2\right)\left(1.4M_1^2-0.2\right)}{(1.2)^2 M_1^2}$	$T_2 = 506.2$ K

Example 8.15 The air flow through a convergent–divergent nozzle having throat area equals to one-fourth of outlet area. A normal shock wave occurs in the diverging section of the nozzle. In addition, the static pressure at outlet is 0.5 times the stagnation pressure at inlet. The flow may be assumed isentropic throughout the nozzle except through the shock. Determine (a) Mach numbers before and after the shock and (b) the area of cross section of the nozzle at normal shock.

Solution: Figure 8.28 has been drawn to show the variation of pressure along the length nozzle.

Given that $p_2 = 0.5 p_{o1}$, $A_t = \dfrac{A_2}{4}$

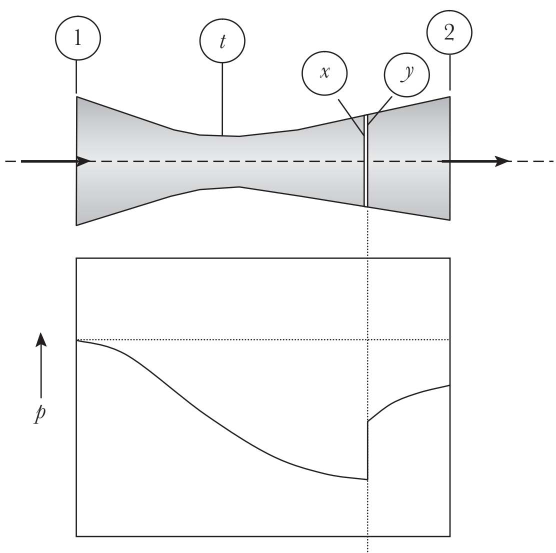

Fig. 8.28

The critical area for C–D nozzle is always at throat. Hence, the critical area for inlet section and the upstream shock must be equal to the area of the throat.

$$A_{*1} = A_t = A_{*x}$$

In addition, the critical area for exit plane and the downstream shock will be the same, that is,

$$A_{*2} = A_{*y}$$

Since, $\dfrac{\dot{m}\sqrt{T_o}}{A_* p_o} = \text{constant} \quad \Rightarrow \quad A_{*1} p_{o1} = A_{*2} p_{o2} \quad \Rightarrow \quad \dfrac{A_2}{4} p_{o1} = A_{*2} p_{o2}$

$$\frac{A_2}{4} \cdot \frac{p_2}{0.5} = A_{*2} p_{02}$$

$$\frac{p_{o2}}{p_2} \times \frac{A_{*2}}{A_2} = 0.5$$

Substituting the critical area ratio and stagnation to static pressure ratio relations,

$$\left(1 + \frac{\gamma - 1}{2} M_2^2\right)^{\frac{\gamma}{\gamma-1}} \times M_2 \left(\frac{2}{\gamma+1} + \frac{\gamma-1}{\gamma+1} M_2^2\right)^{-\frac{\gamma+1}{2(\gamma-1)}} = 0.5$$

Substituting $\gamma = 1.4$

$$\left(1 + 0.2 M_2^2\right)^{\frac{7}{2}} \times \frac{M_2}{\left(\dfrac{5 + M_2^2}{6}\right)^3} = 0.5$$

The solution of this non-linear equation is $M_2 = 0.287$.

The critical area ratio for exit section is

$$\frac{A_2}{A_{*2}} = \frac{1}{M_2}\left(\frac{5 + M_2^2}{6}\right)^3 \quad \Rightarrow \quad \frac{A_2}{A_{*2}} = \frac{1}{0.287}\left(\frac{5 + 0.287^2}{6}\right)^3 = 2.11$$

$$\frac{4A_{*1}}{A_{*2}} = 2.11 \quad \Rightarrow \quad \frac{A_{*1}}{A_{*2}} = 0.5275 \tag{1}$$

Applying critical area ratio relation on the upstream and downstream and of the shock,

$$\frac{A_x}{A_{*x}} = \frac{1}{M_x}\left(\frac{5 + M_x^2}{6}\right)^3 \tag{2}$$

$$\frac{A_y}{A_{*y}} = \frac{1}{M_y}\left(\frac{5 + M_y^2}{6}\right)^3 \tag{3}$$

In addition, $A_x = A_y$ as the shock is extremely thin. Dividing Eq. (3) by Eq. (2)

$$\frac{A_{*x}}{A_{*y}} = \frac{M_x}{M_y}\left(\frac{5 + M_y^2}{5 + M_x^2}\right)^3 = \frac{A_{*1}}{A_{*2}} \tag{4}$$

From Eqs (1) and (4),

$$\frac{M_x}{M_y}\left(\frac{5+M_y^2}{5+M_x^2}\right)^3 = 0.5275 \tag{5}$$

The ratio of Mach numbers across the shock is

$$M_y^2 = \frac{M_x^2 + \dfrac{2}{\gamma - 1}}{\dfrac{2\gamma}{\gamma - 1}M_x^2 - 1}$$

Substituting $\gamma = 1.4$ (for air)

$$M_y^2 = \frac{M_x^2 + 5}{7M_x^2 - 1} \tag{6}$$

Squaring Eq. (5) and substituting the value of M_y^2 from Eq. (6)

$$\frac{M_x^2}{\dfrac{M_x^2+5}{7M_x^2-1}}\left(\frac{5+\dfrac{M_x^2+5}{7M_x^2-1}}{5+M_x^2}\right)^6 = 0.278256$$

$$\frac{M_x^2\left(7M_x^2-1\right)}{\left(M_x^2+5\right)}\left(\frac{5\left(7M_x^2-1\right)+\left(M_x^2+5\right)}{\left(M_x^2+5\right)\left(7M_x^2-1\right)}\right)^6 = 0.278256$$

The solution of this non-linear equation is $M_x = 2.43$.

Substituting the value of M_x in Eq. (6)

$$M_y = \sqrt{\frac{2.43^2+5}{7\times 2.43^2 - 1}} \quad \Rightarrow \quad M_y = 0.52$$

To determine the value of cross-sectional area at the shock, Eq. (2) or Eq. (3) can be used.

$$\frac{A_x}{A_t} = \frac{1}{0.52}\left(\frac{5+0.52^2}{6}\right)^3 \quad \Rightarrow \quad A_x = 1.303A_t$$

8.9 COMPRESSIBLE FLOW OVER AN AIRFOIL

It has been observed that even if the free stream flow is subsonic, the flow over an airfoil may not remain subsonic always, due its profile or shape. In fact, at a particular free stream Mach number the flow becomes sonic at the point of minimum pressure on the airfoil. This free stream Mach number is termed as *critical Mach number* (M_{cr}). The pressure is maximum and the velocity is zero at the leading edge (LE), that is, at the stagnation point. While moving along the surface of the airfoil from leading edge to point C (say), there is a reduction in pressure and gain in velocity, as shown in Fig. 8.29.

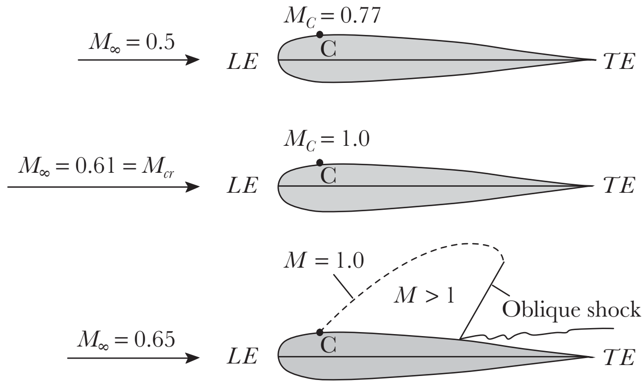

Fig. 8.29 Mach number variation over an airfoil

Point C is the point of minimum pressure on the airfoil surface. Towards trailing edge (TE) from point C, would actually result in pressure recovery to some extent and after which the flow separation may take place depending upon the angle of attack. The airfoil sections corresponding to zero angle of attack for different free stream Mach numbers have been shown in Fig. 8.29. The Mach number at point C increases with the increase in free stream Mach number. At critical free stream Mach number, the Mach number at point C turns unity. If the free stream Mach number is slightly increased beyond critical Mach number, a finite region of supersonic flow appears on the surface of the airfoil. In the figure, the supersonic region is shown only on the upper side. However, the region exists on either side of the airfoil.

Another phenomenon associated with the change in Mach number over the airfoil from subsonic to supersonic value is the sudden increase in the drag coefficient (as high as 10 times or even more), shown in Fig. 8.30. This rise in

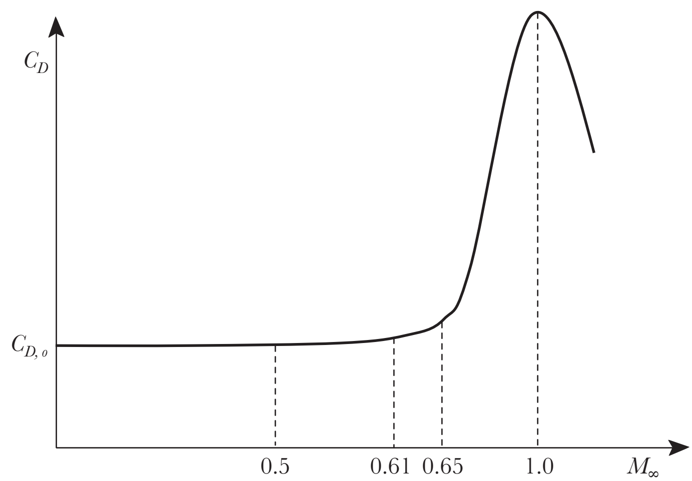

Fig. 8.30 Typical drag coefficient-free stream Mach number characteristics of an airfoil

drag is due to the wide region of supersonic flow on either side of the airfoil, which finally terminates into shock waves. It is known that the shocks are characterized by a sudden rise in pressure, which causes the flow to separate from the surface leading to a sudden increase in the drag. As the free stream Mach number reaches unity, the drag coefficient reaches a very high value capable of damaging the aircraft (commonly termed as flight crossing the 'sound barrier'), if the jet engine is not powerful enough.

POINTS TO REMEMBER

- The flow can be considered as compressible when the value of Mach number is greater than 0.3. Below that the flow can be treated as incompressible.
- Simply looking at a diverging or converging duct, one cannot say whether it is a nozzle or diffuser. The Mach number at the inlet of varying area duct makes it a nozzle or diffuser. A diverging duct is a diffuser, if the Mach number at the inlet is less than 1, whereas, the same duct acts as a nozzle if the Mach number at the inlet is greater than 1.
- A convergent–divergent device will act as a nozzle if the flow at the inlet is subsonic and the critical conditions must reach at the throat. In addition, the back pressure must be equal to the design pressure, that is, when the flow in the divergent part of the nozzle is shock-free.
- In Fanno flow or the adiabatic flow through the constant area frictional duct, the friction causes the flow to accelerate with subsonic conditions at the inlet. On the other hand, the friction causes the flow to decelerate with supersonic inlet conditions.
- In Rayleigh flow or the diabatic flow through the constant area frictional duct, heat addition causes the flow to accelerate, whereas, cooling causes it to decelerate with subsonic conditions at the inlet. On the other hand, heating causes the flow to decelerate and cooling causes it to accelerate with supersonic inlet conditions.
- A shock wave is a highly localized irreversibility in which the flow undergoes a sudden transition from supersonic state to subsonic state causing a tremendous rise in pressure. The shock strength is defined as the ratio of rise in pressure to the pressure upstream of the shock.
- The mass flow rate through a duct increases with the increase in pressure difference across it. A point is reached when increasing the pressure difference will not result in an increase in the mass flow rate. That condition is known as choking and the flow is said to be choked. This happens when the flow at the exit achieves the unity Mach number or sonic conditions.
- The critical Mach number in case of flow over an airfoil is the free stream Mach number at which the flow turns sonic at the point of minimum pressure. If the free stream Mach number is increased beyond the critical Mach number, there is a sudden overshoot in drag coefficient.

SUGGESTED READINGS

Anderson Jr., J.D., *Fundamentals of Aerodynamics*, 5th Ed., McGraw-Hill Education, New Delhi, 2013.

Balachandran, P., *Fundamentals of Compressible Fluid Dynamics*, Prentice Hall India, New Delhi, 2006.

Borgnakke C., R.E. Sonntag, *Fundamentals of Thermodynamics*, 7th Ed., John Wiley & Sons, New Delhi, 2009.

Rathakrishnan, E., *Gas Dynamics*, 5th Ed., Prentice Hall India, New Delhi, 2013.

Yahya, S.M., *Fundamentals of Compressible Flow*, *New Age International*, New Delhi, 2003.

MULTIPLE-CHOICE QUESTIONS

8.1 The speed of sound cannot be expressed as

(a) $\sqrt{\dfrac{dp}{d\rho}}$ (c) $\sqrt{\dfrac{\gamma\rho}{P}}$

(b) $\sqrt{\dfrac{\gamma\rho}{P}}$ (d) $\sqrt{\gamma RT}$

8.2 Crocco number can be defined as

(a) $\dfrac{V}{V_*}$ (c) $\dfrac{V}{V_{\max}}$

(b) $\dfrac{V}{a_0}$ (d) $\dfrac{V}{a}$

8.3 The critical pressure ratio for air is

(a) 0.582 (c) 0.528

(b) 1.4 (d) infinity

8.4 The temperature after expansion will be higher for the

(a) reversible adiabatic process (c) reversible isothermal process

(b) adiabatic process (d) none of these

8.5 Which among the following is unachievable?

(a) Stagnation pressure (c) Stagnation enthalpy

(b) Stagnation temperature (d) All of these

8.6 Convergent–divergent nozzles are used for application where the flow requirement is

(a) sonic (c) supersonic

(b) subsonic (d) transonic

8.7 Impulse function is the algebraic sum of

(a) pressure force and viscous force (c) inertia force and pressure force

(b) inertia force and viscous force (d) buoyant force and viscous force

8.8 A gas of 3 kg with $c_v = 750$ J/kg-K and $\gamma = 1.4$ has its temperature raised by 30°C isentropically. The change in enthalpy is

(a) 67.0 kJ (c) 31.5 kJ

(b) 94.5 kJ (d) 22.3 kJ

8.9 In a normal shock in air, the density ratio across is 3.0. The corresponding pressure ratio is
(a) 3 (c) 5.7
(b) 0.61 (d) 1.5

8.10 Air from a reservoir is to be passed through a supersonic nozzle so that the jet will have a Mach number 2.0. If the static temperature of the jet is not to be less than 27°C, the minimum temperature of the air in the reservoir should be
(a) 48.6°C (c) 267°C
(b) 167°C (d) 367°C

8.11 In a flow through convergent nozzle, the ratio of back pressure to the inlet pressure is given by $\frac{p_b}{p_1} = \left(\frac{2}{\gamma+1}\right)^{\frac{\gamma}{\gamma-1}}$. If the back pressure is lower than p_b given in equation, then
(a) flow in the nozzle is supersonic (c) shock appears at the exit plane of the nozzle
(b) a shock wave appears inside the nozzle (d) gases expand outside the nozzle and a shock appears outside the nozzle

8.12 In a normal shock wave in air, one of the Mach number is 3. The other Mach number is
(a) 2.65 upstream of the shock (c) 0.02 upstream of the shock
(b) 0.475 downstream of the shock (d) 3.75 upstream of the shock

8.13 In Fanno flow, the shock wave appears at the exit plane of a tube if
(a) $p_{exit} < p_{smax}$ (c) $p_{exit} = p_{smax}$
(b) $p_{exit} > p_{smax}$ (d) $p_{exit} >> p_{smax}$

8.14 The stagnation pressure remains constant in
(a) isentropic flow through the nozzle (c) Fanno flow
(b) flow through shock (d) Rayleigh flow

8.15 An aircraft is flying at a speed of 600 m/s. The ratio of its Mach numbers while flying at standard sea-level conditions ($T = 20°C$) and at an altitude of 20 km ($T = -56°C$) atmosphere conditions is
(a) 0.5976:1 (c) 2.19:1
(b) 1.16:1 (d) 1.35:1

8.16 Mach angle α is given by
(a) $\cos^{-1}(M)$ (c) $\cos^{-1}(1/M)$
(b) $\sin^{-1}(1/M)$ (d) $\sin^{-1}(M)$

8.17 The type of nozzle preferred in supersonic aircraft engines is
(a) convergent nozzle (c) convergent–divergent nozzle
(b) divergent nozzle (d) any of these

8.18 In a convergent–divergent nozzle, the flow is choked when the
(a) back pressure equals the critical pressure (c) back pressure greater than throat pressure
(b) back pressure less than critical pressure (d) throat pressure equals the critical pressure

8.19 Stagnation properties at a point in a flow field are obtained
(a) by limiting local velocity zero
(b) by limiting local velocity to be zero isentropically
(c) at critical Mach number
(d) none of these

8.20 When there is a sudden increase in drag coefficient on an airfoil as the free stream Mach number is increased beyond critical Mach number,
(a) flow over the airfoil turns sonic
(b) flow separation occurs due to the formation of shock
(c) creation of supersonic region occurs on the airfoil surface
(d) none of these

REVIEW QUESTIONS

8.1 Distinguish between the following:
(a) Adiabatic and isentropic processes
(b) Reversible and cyclic processes
(c) Rayleigh and Fanno flow
(d) Incompressible and compressible flows
(e) Static and stagnation quantities

8.2 Why are there two statements for the second law of thermodynamics?

8.3 Why is the knowledge of thermodynamics a prerequisite for the understanding of compressible flows?

8.4 In a multistage compression system, why is there a need of intercooling?

8.5 Why does the shock always occur in the divergent section of a convergent–divergent nozzle?

8.6 What causes choking during the compressible flow in a duct?

8.7 What causes the subsonic flow to accelerate in an insulated frictional duct?

8.8 What are shock waves? Discuss the variation in properties across the shock.

8.9 Why is critical Mach number less than unity for the flow over an airfoil?

8.10 What is the cause of sudden shoot in drag coefficient for the flow over an airfoil when Mach number exceeds its critical value?

UNSOLVED PROBLEMS

8.1 A total of 1kg of a gas undergoes an isobaric process in an insulated piston cylinder assembly from an initial state of 500 kPa, 0.2 m^3. If the final volume of the gas is 0.1m^3, determine the work done.

[Ans: −50 kJ]

8.2 A reversible heat engine operates between hot and cold reservoirs to produce the work output of 50 kW. The engine rejects heat at the rate 1500 kJ/min to the cold reservoir maintained at a temperature of 25°C. Determine the minimum theoretical temperature of hot reservoir.

[Ans: 894 K]

8.3 An air conditioning system fitted in a house pumps out 600 MJ heat per day to maintain the inside temperature at 25°C when the outside temperature is 45°C. Determine the minimum theoretical work per day required to run the air conditioner.

[Ans: 40.27 MJ per day]

8.4 For an isentropic flow, derive the following expressions

(a) $M^* = \left(\dfrac{T}{T^*}\right)^{1/2} M$

(b) $M^*_{\max} = \left(\dfrac{\gamma+1}{\gamma-1}\right)^{1/2}$

(c) $\dfrac{A}{A_*} = \left(\dfrac{(\gamma-1)/2}{1-(p/p_o)^{(\gamma-1)/\gamma}}\right)^{1/2} \left(\dfrac{2}{\gamma+1}\right)^{(\gamma+1)/2(\gamma-1)} \left(\dfrac{p}{p_o}\right)^{-1/\gamma}$

8.5 Determine the Mach angle for a supersonic flight cruising at a speed of 500 m/s in air at a temperature of −60°C.

[Ans: 35.8°]

8.6 In a duct, air is flowing with a velocity of 280 m/s, pressure 1.03 bar, and temperature 300 K. Compute:
(a) stagnation pressure and temperature
(b) stagnation pressure treating flow to be incompressible.

[Ans: (a) 1.58 bar, 339 K (b) 1.5004 bar]

8.7 At an altitude of 10 km (T = 223.25 K, p = 0.265 bar), an aircraft is cruising at a velocity of 800 km/h. The cross-sectional area of the diffuser inlet of aircraft engine is 0.6 m^2. Determine the Mach number, mass flow rate of air, the stagnation pressure, and temperature at diffuser inlet.

[Ans: 0.742, 55.14 kg/s, 0.3818 bar, 247.8 K]

8.8 A large tank supplies an inert gas to an experimental set-up at atmospheric pressure through a converging–diverging nozzle. The pressure and temperature inside the tank are 60 bar and 800 K. The exit area of the nozzle is 80 mm^2 and is designed to discharge at an exit Mach number of 3. Determine the pressure at exit of the nozzle and mass flow rate through it. Take γ = 1.66, R = 2077 J/kg-K.

[Ans: 1.87 bar, 0.08935 kg/s]

8.9 Air is expanded through a nozzle from 8 bar in a settling chamber of a supersonic wind tunnel to 4 bar in the test section. Estimate the stagnation temperature required in settling chamber to obtain a velocity of 400 m/s in the test section.

[Ans: 443.66 K]

8.10 A convergent–divergent nozzle of throat area 0.1 m^2 and exit area 0.4 m^2 is connected to an air reservoir (p_o = 2 bar, T_o = 330 K) at its inlet. Inside the divergent part of the nozzle, a normal shock occurs where the cross-sectional area is 0.3 m^2. Determine
(a) the static and stagnation pressure on the upstream and downstream of the shock
(b) the static and stagnation pressures and temperatures at the nozzle exit.

[Ans: (a) Upstream side: 0.0946 bar and 2 bar; Downstream side: 0.733 bar and 0.917 bar (b) 0.844 bar, 0.917 bar, 322.2 K, 329.9 K]

8.11 Air at $M = 1.8$, $p = 0.8$ bar, and $T = 373$ K enters an insulated duct of diameter 250 mm, undergoes a normal shock at a location where the Mach number is 1.3. The flow continues to the duct exit where $M = 1$. Determine the shock location, loss of stagnation pressure, mass flow rate, and change in entropy upstream side of the shock, across the shock and downstream side of the shock. Take $f = 0.01$.

[Ans: 4.42 m from the inlet, 0.08 bar, 25.56 kg/s, 85.91 J/kg-K, 6.813 J/kg-K, 11.877 J/kg-K]

8.12 A pipe of diameter 50 mm and length 10 m is connected to a reservoir containing air at its inlet. The air is discharged to the outside atmospheric conditions: $M = 0.8$, $p = 1.01$bar, and $T = 300$ K. Determine stagnation temperature and stagnation pressure at the inlet of pipe/inside the reservoir. Take $f = 0.015$.

[Ans: 338.4 K, 2.4295 bar]

8.13 At an inlet section of tubular combustion chamber, the velocity, temperature, and pressure of air–fuel mixture are 72 m/s, 500 K, and 5 bar. For outlet Mach number of 0.4, determine the outlet temperature and the fuel consumption if the calorific value of the fuel is 40 MJ/kg. Assuming that the properties of mixture remain same before and after combustion. Use standard air properties for fuel–air mixture.

[Ans: 2964 K, 0.0642 kg]

8.14 The heat rejected by the compressed air in a duct is 60 kJ/kg. The following are the conditions at the entry of the duct: $V_1 = 700$ m/s, $T_1 = 298$ K, and $p_1 = 4$ bar. Determine the duct outlet temperature and Mach number.

[Ans: 392.3 K, 1.633]

8.15 Use gas tables to solve Example 8.15.

Answers to Multiple-choice Questions

8.1 (b)	8.2 (c)	8.3 (c)	8.4 (b)	8.5 (a)
8.6 (c)	8.7 (c)	8.8 (b)	8.9 (c)	8.10 (c)
8.11 (d)	8.12 (b)	8.13 (a)	8.14 (a)	8.15 (b)
8.16 (b)	8.17 (c)	8.18 (d)	8.19 (b)	8.20 (b)

DESIGN OF EXPERIMENTS

Experiment 8.1 Diameter of Expanding Air Jet

Objective

To measure the diameter of the air jet at different axial distances from the issuing nozzle.

Experimental Set-up

When the jet of air is issued from a nozzle, its diameter keeps on increasing as one moves away from it. The jet diffuses into the surrounding air on account of pressure difference between the core and the surroundings. The purpose of the experiment is to find out the jet diameter at different axial locations from the nozzle exit. This experiment has its significance while utilizing the impact of jet for a specific purpose. The position of nozzle significantly affects the outcome of the process. The experimental set-up, shown in Fig. E8.1, requires a blower with an appropriate issuing nozzle (e.g., hair dryer) and a Pitot tube with a traversing mechanism.

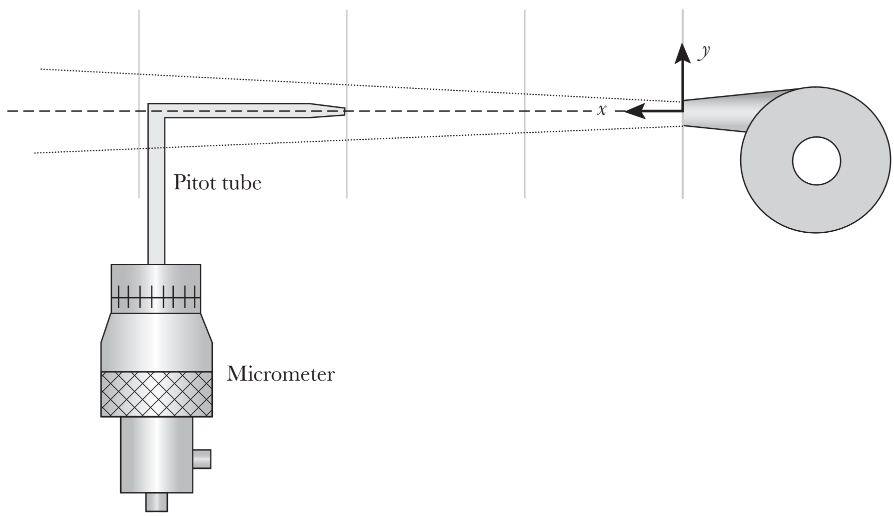

Fig. E8.1 Experimental set-up

Procedure

1. Start the blower.
2. Place the Pitot tube at specified axial location.
3. Use micrometer to traverse the probe (Pitot tube) across the jet. The upper and lower bound of the jet is characterized by zero velocity (no deflection in its manometer).
4. Repeat the experiment for different axial locations.

Observation Table

Axial distance from nozzle exit x (cm)	**Pitot tube micrometre reading, y (mm)**	**Pitot tube reading V (m/s)**	**Diameter of the jet $d = y_1 - y_n$ (mm)**
x_1	y_1		
	y_2		
	y_3		
	…		
x_2	y_1		
	y_2		
	y_3		
	…		
…			

Results and Discussion

1. Plot the jet diameter along the axial distance and discuss the behaviour.

Conclusions

Draw conclusions on the results obtained.

Experiment 8.2 Compressible Flow through Convergent–Divergent Nozzle

Objective

To locate the shock position inside the convergent–divergent (C–D) nozzle and to determine the choked mass flow rate for the given C–D nozzle

Experimental Set-up

The study of flow characteristics through a nozzle requires upstream flow conditions to be fixed at stagnation conditions, which can be achieved in a big pressure chamber. The arrangement should be such that the pressure inside the chamber should not fall with the opening of back pressure valve at downstream (i.e, p_o and T_o are constant). The back pressure valve is opened slightly and the pressure probe is traversed through the centre line of the test nozzle for the measurement of pressure using rack-and-pinion arrangement, shown in Fig. E8.2. The probe is connected to the pressure gauge on the other side. When the valve is slightly opened the critical conditions at the throat will not reach. The convergent part will act as nozzle and divergent as diffuser. With the opening of back pressure valve further, the critical conditions will be reached at the throat and the mass flow rate becomes maximum inside the nozzle. This condition is termed as *choking*. When the back pressure is less than the design pressure, a shock will occur in divergent part of the nozzle. This shock will move towards the exit as the pressure approaches the design exit pressure.

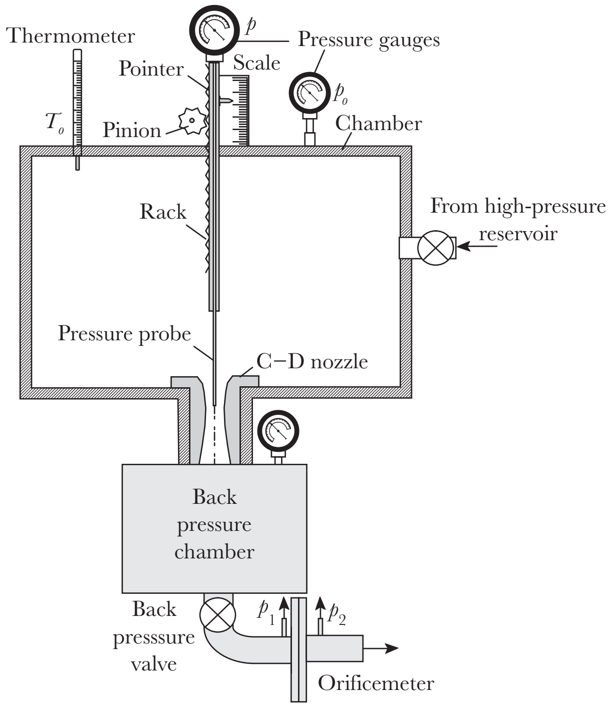

Fig. E8.2 Schematic diagram of experimental set-up

The shocks are characterized by sudden jump in pressure, which can easily be detected by the traversing pressure probe.

Procedure

1. Install the convergent–divergent nozzle in the test section of high-pressure chamber.
2. Pressurize the chamber by opening the valve that connects it to the high-pressure reservoir. Set the desired pressure inside the chamber.
3. Slightly open the back pressure valve such that a difference in pressure in the two chambers is created.
4. Traverse the pressure probe and record the pressure reading at different points throughout the axis of C–D nozzle. In addition, compute the mass flow rate using the orifice meter pressure readings.
5. Note down the pointer reading where there is a sudden jump in pressure.
6. Repeat the experiment for different back pressures.

Observation Table

1. Stagnation pressure, p_o = ______________________________ kPa
2. Stagnation temperature , T_o = ______________________________°C
3. Pipe diameter where orifice meter is fitted, d_1 = ______________ mm
4. Orifice diameter d_2 = ___________________________________ mm
5. Discharge coefficient of the given orifice meter, C_d = _________________

Back pressure p_b (kPa)	Orifice meter readings		Mass flow rate $m = \frac{C_d A_2}{\sqrt{1-(d_2/d_1)^4}}\sqrt{\frac{p_1 - p_2}{\rho}}$ (kg/s)	Pointer reading, y (mm)	Pressure along the centre line p (kPa)	Position of the shock from nozzle inlet y_{shock} (mm)
	p_1	p_2				
p_{b1}				y_1		
				y_2		
				y_3		
				…		
p_{b2}						
…						

Results and Discussion

1. Plot the pressure profile along the length of C–D nozzle for different back pressure readings and discuss the behaviour.
2. Choked mass flow rate, m_{choked} = ____________________ kg/s.

Conclusions

Draw conclusions on the results obtained.

CHAPTER 9

Fluid Machinery

LEARNING OBJECTIVES

After studying this chapter, the reader will be able to:

- Understand the fundamentals of different types of hydraulic machines, namely, turbines, pumps, etc.
- Develop the governing equations for different turbines and pumps
- Draw and comprehend the significance of characteristic curves for various turbines and pumps
- Familiarize oneself with the components and working principle of other miscellaneous hydraulic machinery, namely, hydraulic ram, fluid coupling, crane, etc.
- Design simple experiments to obtain the performance characteristic curves for hydraulic turbines and pumps

This chapter deals with detailed analyses of machines which either run on fluid power or run to power fluid. The machines which either utilize fluid power for the mechanical power generation (turbines) or which use external power to energize the fluid (pump or compressor) are known as *fluid machines*. The focus is mainly on various kinds of incompressible flow machines such as pumps and turbines and their performance characteristics. These hydraulic machines have a wide range of applications ranging from hydroelectric power generation to the pumping of underground water for domestic, agricultural, and industrial purpose.

For the sake of completeness, a section on miscellaneous machines, such as hydraulic crane, ram, fluid coupling, and torque converter, has also been included. These machines utilize the hydraulic power to serve specific purposes; for example, cranes are used in displacing or lifting heavy loads and are extensively used in construction activities, fluid coupling, and torque converters are used for smooth power transmission in automobiles, etc.

9.1 CLASSIFICATION OF FLUID MACHINES

Fluid machines can be broadly categorized into power-producing machines and power-absorbing machines, as shown in Fig. 9.1. Turbines and windmills come under the category of *power-producing machines* where power is extracted

from a high-pressure fluid. Pumps and compressors consume power to increase the pressure energy of the fluid, hence are termed as *power-absorbing machines*. The windmill and compressor use air as the working fluid whereas turbines and pumps use water as the working fluid. In this chapter, the discussion is restricted to turbines and pumps. Turbines can further be classified as impulse and reaction turbines. The *impulse turbine* got its name from the definition of impulse, which is, the force applied for a small fraction of time. In impulse turbine the water jet issued from the nozzle interacts momentarily with the buckets mounted on a rotating wheel. Pelton turbine is an impulse turbine. The *reaction turbine* works on the principle of the degree of reaction (explained later). Francis and Kaplan/propeller turbines are reaction turbines. Pumps are classified as centrifugal and reciprocating pumps. In *centrifugal pumps*, the centrifugal force of rotating blades is utilized to increase the pressure energy of water. The reciprocating pump has the piston–cylinder mechanism and the fluid gets activated to high pressure by the movement of piston.

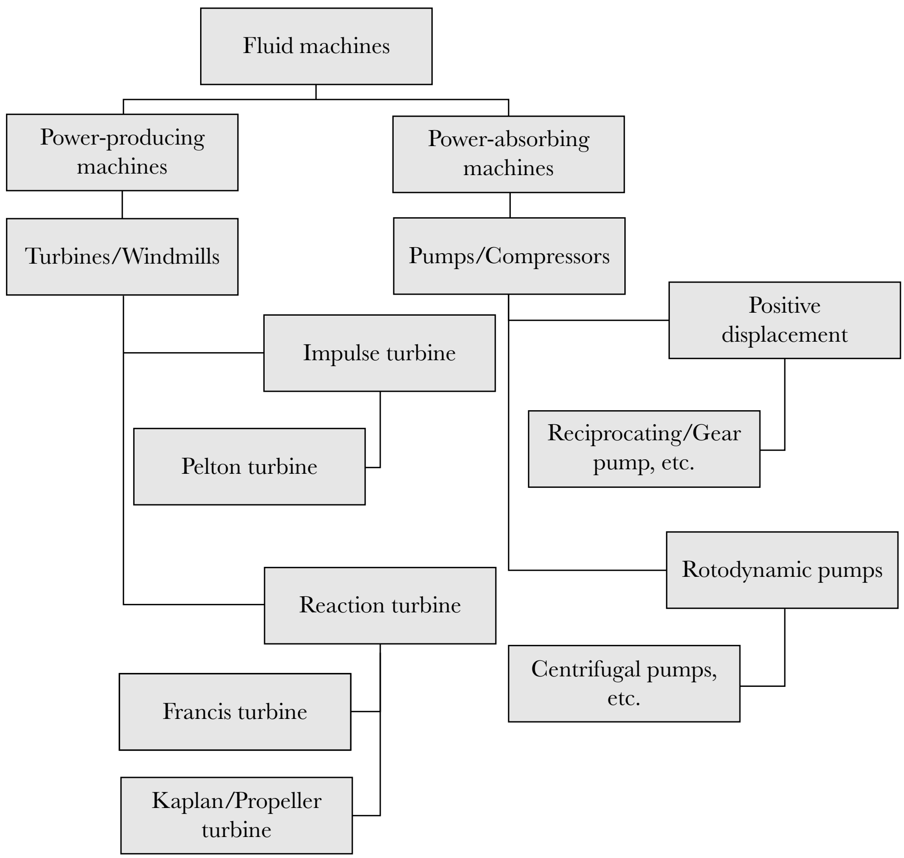

Fig. 9.1 General classification of fluid machines

9.2 CLASSIFICATION OF HYDRAULIC TURBINES

Turbines that use water as the working fluid for the production of power are known as hydraulic turbines. A general classification has already been explained in Section 9.1, where the turbines are categorized as impulse and reaction. This classification is based on the interaction of fluid with turbine blades. However, the turbines can further be classified on the basis of head available at the inlet, specific speed, and according to flow direction. There are three main turbines named after their inventors, namely, Pelton, Francis, and Kaplan. These classifications have been elaborated in Table 9.1.

Table 9.1 Classification of hydraulic turbines

Turbine	**Action of water**	**Flow direction**	**Available head**	**Specific speed**
Pelton	Impulse	Tangential flow	$H > 300\,\text{m}$	8–50
Francis	Reaction	Mixed flow	$50\,\text{m} < H < 300\,\text{m}$	50–250
Kaplan/Propeller	Reaction	Axial flow	$H < 50\,\text{m}$	250–850

The turbines can be classified under different headings:

1. Action of water on the runner (the rotating element of turbine)—impulse and reaction
2. Direction of flow—tangential flow, radial flow, axial flow, and mixed (radial + axial) flow
3. Available head—high head ($H > 300\,\text{m}$), medium head ($50\,\text{m} < H < 300\,\text{m}$), and low head ($H < 50\,\text{m}$)
4. *Specific speed* is the speed of geometrically similar turbine which produces unit power when operated under unit head—low, medium, and high specific speed turbines

9.3 HEADS AND EFFICIENCIES

In fluid mechanics, the term head indicates the energy in units of distance. There are two types of heads as far as turbines are concerned—gross head and net head. Gross head indicates the difference in head and tail race levels. Net head is the actual head available at the turbine inlet and is computed as gross head minus frictional losses in the penstock.

Efficiency is usually defined as the ratio of output to the input. Figure 9.2 has been drawn to explain the losses in different components of the hydroelectric power plant. The power input to the system is in the form of hydraulic energy of the stored water (equivalent to the net head) and the output is in the form of electrical energy.

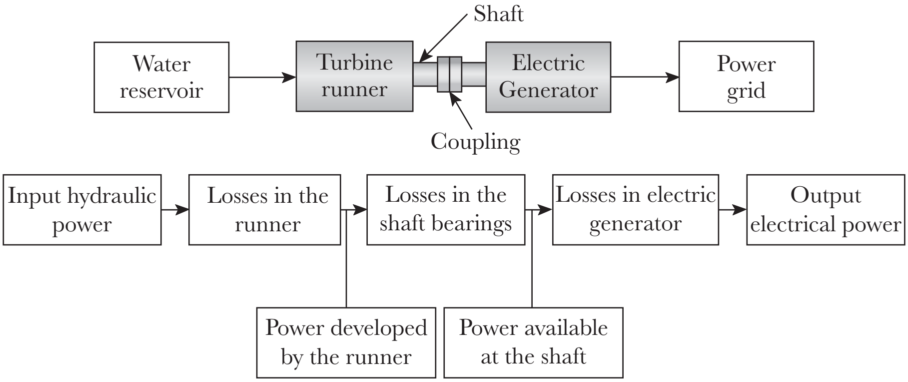

Fig. 9.2 Flow of power through different components of hydroelectric power plant

The output of the plant signifies its power-generation capacity usually expressed in megawatts (MWe). The last character 'e' in the unit indicates the electrical output of the plant. The different type of efficiencies associated with the performance of different components of hydroelectric power plant is shown in Table 9.2. The various components are turbine runner, shaft, and electrical generator. The efficiency of individual component is the ratio of its output to its input. The *hydraulic efficiency* is defined as the ratio of power developed by the turbine runner to power available at turbine inlet. The power developed by the runner is different from the power available at the turbine shaft by an amount equal to the mechanical losses (friction losses) in bearings.

Table 9.2 Turbine efficiencies

Efficiency	**Definition**	**Formula**
Hydraulic efficiency	$\eta_h = \dfrac{\text{Power developed by the runner}}{\text{Power available at turbine inlet}}$	$\eta_h = \dfrac{P_{\text{runner}}}{\rho Q gH}$
Volumetric efficiency	$\eta_v = \dfrac{\text{Actual discharge}}{\text{Total discharge}}$	$\eta_v = \dfrac{Q - \Delta Q}{Q}$
Mechanical efficiency	$\eta_m = \dfrac{\text{Power available at the shaft}}{\text{Power developed by the runner}}$	$\eta_m = \dfrac{P_{\text{shaft}}}{P_{\text{runner}}}$
Generator efficiency	$\eta_g = \dfrac{\text{Output electrical power}}{\text{Power available at the shaft}}$	$\eta_g = \dfrac{P_o}{P_{\text{shaft}}}$
Overall efficiency	$\eta_o = \dfrac{\text{Output electrical power}}{\text{Power available at turbine inlet}}$	$\eta_o = \dfrac{P_o}{\rho Q gH}$

Hence, *mechanical efficiency* is the ratio of power available at the shaft to the power developed by the runner. An electric generator cannot convert 100% mechanical power to electrical power. The ratio of the electrical power produced by the generator to mechanical power available at turbine–generator shaft is known as *generator efficiency*. The *volumetric efficiency* is defined as the ratio of actual discharge to the total discharge. Some of the water may not come in contact with the runner blades and goes to the sump untouched. If ΔQ represents the water which goes without coming in contact with the runner blades and Q is the total discharge. The *overall efficiency*, as the name suggests, is the efficiency of whole turbine-generator system which can be obtained by dividing the power output of generator to the hydraulic power input to turbine. It can also be obtained by multiplying all the efficiencies, namely hydraulic, mechanical, electrical, and volumetric efficiencies.

9.4 IMPACT OF JET

When a high-velocity jet impinges on a surface (fixed or moving), it exerts a force known as impact of jet. The computation of this force on the runner helps in determining the power produced by the runner. In this section, the jet impact (force) is computed for the following different cases:

9.4.1 Stationary Flat Vertical Plate

If the friction is ignored, the magnitude of the jet velocity will not change before and after the impact, there will be a change in direction only. The force on the plate is calculated by applying the momentum Eq. (9.1) on the control volume (CV) as shown in Fig. 9.3. For steady state flow conditions, the term with time derivative will be zero.

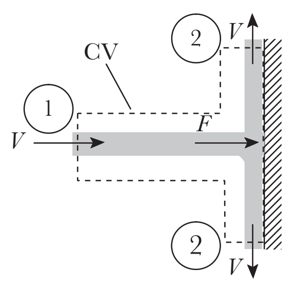

Fig. 9.3 Jet striking a fixed flat vertical plate

$$\sum F = \cancelto{0}{\frac{\partial}{\partial t}\int_{CV} \vec{V}\rho d\forall} + \int_{CS} \vec{V}\rho\vec{V}.d\vec{A} \tag{9.1}$$

Equation (9.1) in x and y component form for steady flow can be written as

$$\sum F_x = \int_{A_2} V_{x_2} d\dot{m}_2 - \int_{A_1} V_{x_1} d\dot{m}_1 \tag{9.2a}$$

$$\sum F_y = \int_{A_2} V_{y_2} d\dot{m}_2 - \int_{A_1} V_{y_1} d\dot{m}_1 \tag{9.2b}$$

where $\dot{m}$ represents the mass flow rate. Subscripts 1 and 2 represent inlet and outlet of the CV as shown in Fig. 9.3.

Considering y-direction momentum,

$$\sum F_y = \int_{CS} \rho V_y \vec{V}.d\vec{A}$$

$$\Rightarrow \quad F_y = \rho V_{y_2}(V_{y_2} A_2 \cos 0°) + \rho(-V_{y_2})(V_{y_2} A_2 \cos 0°) \quad \Rightarrow \quad \boxed{F_y = 0} \tag{9.3}$$

(as there is no inflow in y-direction, that is, $V_{y_1} = 0$)

Considering x-direction momentum,

$$\sum F_x = \int_{CS} \rho V_x \vec{V}.d\vec{A}$$

$$\Rightarrow \quad F_x = -\rho V_{x_1}(V_{x_1} A_1 \cos 180°) \quad \Rightarrow \quad \boxed{F = \rho A V^2} \tag{9.4}$$

(as there is no outflow in x-direction, that is, $V_{x_2} = 0$)

For a given liquid jet, the impact force is directly proportional to the jet's cross-sectional area and the square of jet velocity. This means a slight increase in jet velocity V results in substantial increase in impact force F. The force varies linearly with the jet's cross-sectional area.

9.4.2 Stationary Flat Inclined Plate

Let us consider a more generalized case when the plate is held inclined at an angle θ, as shown in Fig. 9.4. In such a case the force exerted normal to the plate surface exerted by the jet is obtained in a manner similar to that in Section 9.4.1. In this case, the angle between the velocity and area vectors is $(90°-\theta)$.

$$F = \rho A V^2 \cos(90° - \theta) \quad \Rightarrow \quad \boxed{F = \rho A V^2 \sin\theta} \tag{9.5}$$

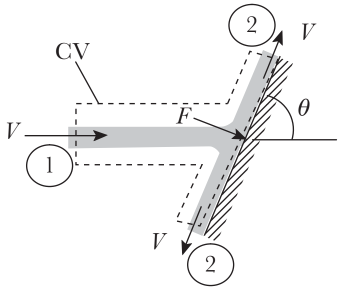

Fig. 9.4 Jet striking a fixed flat inclined plate

The following cases will evolve:

(a) When $\theta = 0 \quad \Rightarrow \quad$ horizontal $\quad \Rightarrow \quad F = 0$

(b) When $\theta = 90° \quad \Rightarrow \quad$ vertical $\quad \Rightarrow \quad F = \rho A V^2$

9.4.3 Stationary Curved Plate

Consider a fixed curved plate, as shown in Fig. 9.5, with a jet entering and leaving the plate tangentially. The force components in *x*- and *y*-directions exerted by the jet are computed as follows:

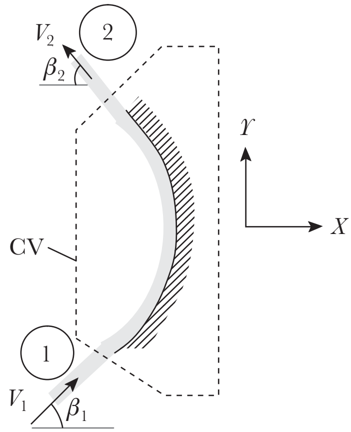

Fig. 9.5 Jet striking a fixed curved plate

From continuity equation, the mass flow rate is constant throughout, $\dot{m} = \dot{m}_1 = \dot{m}_2 = \text{constant}$

$$F_x = \dot{m}(V_1 \cos\beta_1 + V_2 \cos\beta_2) \tag{9.6}$$

$$F_y = \dot{m}(V_1 \sin\beta_1 - V_2 \sin\beta_2) \tag{9.7}$$

If the surface is highly polished, $V_1 = V_2 = V$ and if the plate is semicircular $\beta_1 = \beta_2 = 0°$, then $F_x = 2\dot{m}V$ and $F_y = 0$.

9.4.4 Moving Flat Plates

In this case, a number of flat plates are mounted on a wheel and the jet strikes at the middle of plate (Fig. 9.6), which causes the rotation of the wheel. The force exerted by the jet in the *x*-direction is given by

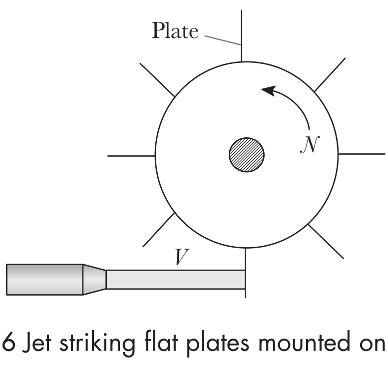

Fig. 9.6 Jet striking flat plates mounted on wheel

$$F = \rho AV(V-u) \tag{9.8}$$

where V is the jet velocity and u is the tangential velocity of the wheel at the middle of the plate. If D is the diameter of the wheel at the middle of the plate, the plate velocity is given by

$$u = \frac{\pi DN}{60} \tag{9.9}$$

where N is the rotational speed of the wheel in rpm.

The power developed by the wheel is

$$P_d = F_x \times u \quad \Rightarrow \quad P_d = \rho AV(V-u)u \tag{9.10}$$

The power input to the wheel is the kinetic energy of the impinging jet

$$P_{in} = \frac{1}{2}\dot{m}V^2 \quad \Rightarrow \quad P_{in} = \frac{1}{2}\rho AV^3 \tag{9.11}$$

The efficiency is given by

$$\eta = \frac{P_d}{P_{in}} \quad \Rightarrow \quad \eta = \frac{2u(V-u)}{V^2} \tag{9.12}$$

To maximize the efficiency,

$$\frac{d\eta}{du} = 0 \quad \Rightarrow \quad u = \frac{V}{2}$$

$$\Rightarrow \quad \eta_{max} = 0.5 \tag{9.13}$$

9.4.5 Moving Curved Plate

In Fig. 9.7, the jet at a velocity V_1 at an angle α_1 strikes a curved blade moving with velocity u. Since the blade is moving, the jet enters the blade only at a reduced velocity known as relative velocity V_{r1}. This velocity is tangential to the blade. The following velocities result from this:

V = absolute velocity of the jet

V_r = relative velocity

u = blade velocity

V_w = whirl velocity (horizontal component of absolute jet velocity, V)

V_f = flow velocity (vertical component of absolute jet velocity, V)

The subscript 1 is used for blade entry and subscript 2 for blade exit.

The force exerted by the jet in x-direction is obtained by multiplying the mass flow rate with the change in horizontal components of absolute jet velocities (i.e., whirl velocities) at entry and exit, respectively.

$$F_x = \dot{m}(V_{w1} - V_{w2}) \tag{9.14}$$

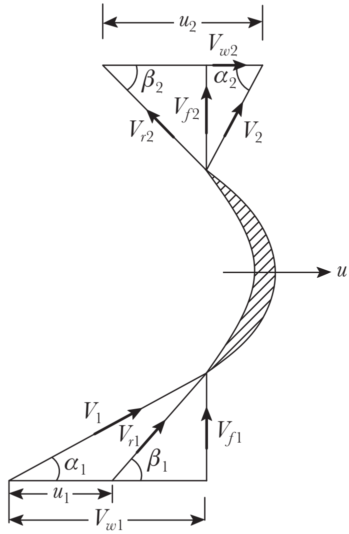

Fig. 9.7 Jet striking moving curved blade

Similarly, the force exerted by the jet in y-direction is obtained by multiplying the mass flow rate with change in the vertical components of absolute jet velocities (i.e., flow velocities) at entry and exit, respectively.

$$F_y = \dot{m}(V_{f1} - V_{f2}) \tag{9.15}$$

From inlet velocity triangle

$$V_1^2 = V_{w1}^2 + V_{f1}^2 \quad \Rightarrow \quad V_1^2 = V_{w1}^2 + V_{r1}^2 - (V_{w1} - u_1)^2 \tag{9.16}$$

Simplifying Eq. (9.16),

$$V_{w1}u_1 = \left(V_1^2 - V_{r1}^2 + u_1^2\right)/2 \tag{9.17}$$

Similarly from outlet velocity triangle

$$V_{w2}u_2 = \left(V_2^2 - V_{r2}^2 + u_2^2\right)/2 \tag{9.18}$$

Subtracting Eq. (9.18) from Eq. (9.17)

$$V_{w1}u_1 - V_{w2}u_2 = \frac{V_1^2 - V_2^2}{2} + \frac{V_{r2}^2 - V_{r1}^2}{2} + \frac{u_1^2 - u_2^2}{2} \tag{9.19}$$

Dividing throughout by g

$$\frac{V_{w1}u_1 - V_{w2}u_2}{g} = \frac{V_1^2 - V_2^2}{2g} + \frac{V_{r2}^2 - V_{r1}^2}{2g} + \frac{u_1^2 - u_2^2}{2g} \tag{9.20}$$

Equation (9.20) is the *fundamental equation of hydraulic machines* also known as *Euler turbine equation*. The left-hand side of this equation is known as *Euler's head* which is the actual head developed by a turbine.

$$H_{eu} = \frac{V_{w1}u_1 - V_{w2}u_2}{g} \tag{9.21}$$

It is clear from *Euler's equation* that the head developed is independent of the shape of the path taken by the water from entry to the exit. The *degree of reaction* is defined as the ratio of energy transfer taking place in the rotor/runner to the total energy transfer. The first term of the *Euler's equation* does not take place in the rotor of the hydraulic machine. Therefore, the degree of reaction is given by

$$R = \frac{\dfrac{V_{r2}^2 - V_{r1}^2}{2g} + \dfrac{u_1^2 - u_2^2}{2g}}{\dfrac{V_1^2 - V_2^2}{2g} + \dfrac{V_{r2}^2 - V_{r1}^2}{2g} + \dfrac{u_1^2 - u_2^2}{2g}} \tag{9.22}$$

Example 9.1 A nozzle issues a water jet of diameter 5 cm, which strikes a vertical fixed plate. The head available at centre line of the nozzle is 50 m. Determine the force exerted by the jet if velocity coefficient is 0.96.

Solution:

Given data:

Jet diameter, $D = 0.05$ m Head, $H = 50$ m

Coefficient of velocity, $C_v = 0.96$

Cross-sectional area of striking jet,

$$A = \frac{\pi}{4}D^2 \quad \Rightarrow \quad A = \frac{\pi}{4} \times 0.05^2 \quad \Rightarrow \quad A = 1.963 \times 10^{-3}\,\text{m}^2$$

Velocity of jet issued from the nozzle is given by

$$V = C_v\sqrt{2gH} \quad \Rightarrow \quad V = 0.96 \times \sqrt{2 \times 9.81 \times 50} \quad \Rightarrow \quad V = 30.06\,\text{m/s}$$

Force exerted by the jet on the plate

$$F = \rho A V^2 \quad \Rightarrow \quad F = 1000 \times 0.001963 \times 30.06^2 \quad \Rightarrow \quad F = 1.773\,\text{kN}$$

Example 9.2 If the vertical plate in Example 9.1 is moving at a velocity of 3 m/s, determine the force exerted jet on the plate, the work done by the jet and the efficiency of jet.

Solution: From Example 9.1

Velocity of jet issued from the nozzle, $V = 30.06$ m/s

Cross-sectional area of striking jet, $A = 1.963 \times 10^{-3}\,\text{m}^2$

And, given that velocity of the plate, $u = 3$ m/s

Force exerted by the jet on the plate

$$F = \rho A(V-u)^2 \quad \Rightarrow \quad F = 1000\times 0.001963\times 27.06^2 \quad \Rightarrow \quad F = 1.437\,\text{kN}$$

Work done by the jet

$$W_j = F\times u \quad \Rightarrow \quad W_j = 1.473\times 3 \quad \Rightarrow \quad W_j = 4.312\,\text{kW}$$

Efficiency of the jet

$$\eta = \frac{\text{Output of jet}}{\text{Input of jet}} \quad \Rightarrow \quad \eta = \frac{\text{Work done/s}}{\text{K.E of jet/s}} \quad \Rightarrow \quad \eta = \frac{F\times u}{\frac{1}{2}mV^2}$$

$$\eta = \frac{4312}{\frac{1}{2}\times(1000\times 0.001963\times 30.06)\times 30.06^2} \quad \Rightarrow \quad \eta = 0.1617 \text{ or } 16.17\%$$

9.5 PELTON TURBINE

Pelton turbine is a high head and low discharge impulse turbine, as shown in Fig. 9.8. It was invented by an American engineer *Lester Allan Pelton* (1829–1908). Pelton turbine works on the principle of conversion of available hydraulic energy first into kinetic energy of the jet and then into mechanical energy of the rotating wheel or *runner*, also known as *Pelton wheel*. The pressure energy gets converted into kinetic energy inside the *nozzle*. As a result, a high-velocity water jet comes out of the nozzle and strikes the *splitter* provided in the middle of each *bucket*.

The buckets are mounted on the *runner periphery* by means of nuts and bolts. The sharp edge of the splitter divides the water jet into two streams. The jet streams, after splitting, smoothly glide over the inner polished surface of the two halves of the *bucket*. Thus, the hydraulic power of the jet gets transmitted to the *runner* through the *buckets* without shocks. The *runner* starts rotating about its axis due to the impact of jet. The jet streams after hitting the *bucket* are directed to the tail race via *undercut* provided at the bottom of the bucket. The undercut also avoids back-hitting of the incoming bucket. Thus, the jet interacts with the *buckets* successively resulting in power transmission to the turbine *runner*. The *runner* is enclosed in a *casing* to avoid splashing of water. The *casing* does not serve any hydraulic purpose as the pressure inside the *casing* remains the same, that is, atmospheric pressure, before and after the jet impact.

9.5.1 Governing Mechanism

To control the flow of water in the Pelton turbine, three mechanisms are put in place namely *braking nozzle mechanism*, *deflector plate mechanism*, and *spearhead governing mechanism*. The *braking nozzle*, when activated, directs the jet to hit at the

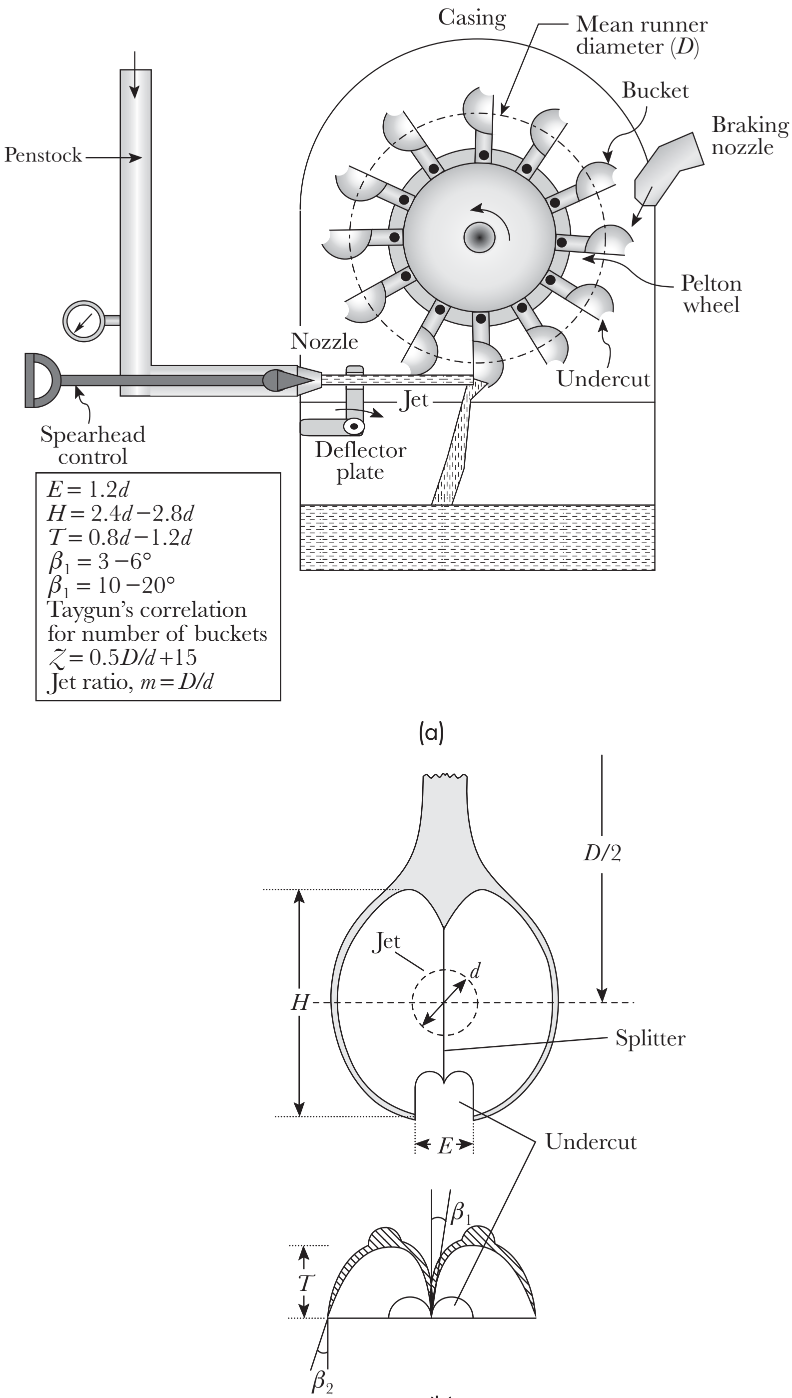

Fig. 9.8 Pelton turbine (a) Schematic (b) Bucket

back of *buckets* and hence, the *runner* speed is brought under control. The *deflector plate mechanism* is activated when the turbine needs to be stopped suddenly in the case of emergency. The plate deflects the jet away from the runner. The *spearhead mechanism* is used to control the small variation in turbine speed. The speed of any turbine varies with the change in load. The turbine is coupled with the electrical generator. In fact, it is the load on the generator that varies depending upon the consumption of power. Higher the load on turbine generator, lower will be the turbine speed. The other two mechanisms, namely braking nozzle and deflector plate mechanisms, are activated only when there is a sudden drop in the load leading to an alarming increase in turbine speed.

The *spearhead mechanism* is used to keep the speed of the turbine constant by controlling the flow of water into the turbine. The spearhead moves back and forth into the nozzle causing the change in the area of flow inside the nozzle. When the load is increased, the spearhead is moved back allowing more water to enter into the runner. Under low load conditions the spearhead is moved towards the nozzle opening to reduce the supply of water into the runner. The movement of the spear rod is controlled by a *governing mechanism*, as shown in Fig. 9.9. The oil pressure is maintained in the hydraulic circuit by means of a gear pump with its inlet connected to the *sump*. It has a governor which is connected to the turbine shaft by means of a belt drive. As the turbine speed increases due to fall in load, the fly balls of the governor fly out due to increased centrifugal force. This causes the sleeve of the governor to move up. A lever is connected with the sleeve at one end and to the relay valve at another through a fulcrum placed in the middle. The upward movement of the sleeve causes the downward movement of

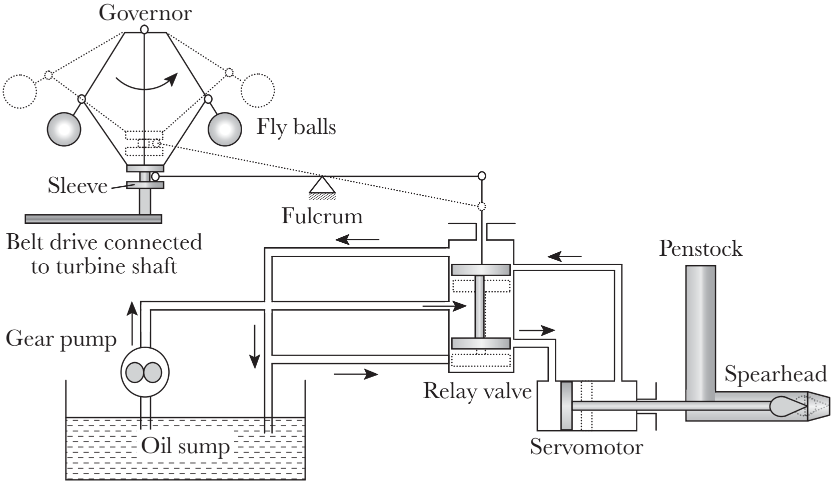

Fig. 9.9 Governing mechanism for Pelton turbine

the relay valve. The movement of the relay valve causes the oil to enter in the *servomotor*, which has a piston–cylinder arrangement. The high-pressure oil pushes the piston, which is connected to the spear rod. The spear rod, as a result, moves towards the nozzle opening thereby decreasing the flow of water into the turbine runner, thus, reducing the power developed by the turbine. The reverse happens as the speed of the turbine reduces.

9.5.2 Velocity Triangles and Output Power

The velocity triangles at the inlet and exit of Pelton turbine runner are shown in Fig. 9.10. Only half of the blade is shown in the figure as it is symmetric about the splitter of bucket. The triangle at the inlet is a straight line. The blade velocity u remains constant at the inlet and outlet sections as the two sections lie in the same plane at $D/2$ distance from the runner axis (refer Fig. 9.8).

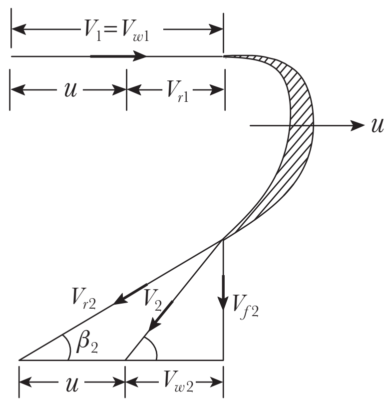

Fig. 9.10 Velocity triangles at inlet and outlet of pelton turbine blade

The force exerted by the jet is obtained by multiplying the mass flow rate and change in horizontal components of the absolute jet velocities at inlet and outlet sections of the blade,

$$F_x = \dot{m}\left[V_{w1} - (-V_{w2})\right] \tag{9.23}$$

The power developed by the runner is

$$P_d = \rho Q(V_{w1} + V_{w2})u \tag{9.24}$$

The power input is in the form of kinetic energy of the jet

$$P_{\text{in}} = \frac{1}{2}\rho Q V_1^2 \tag{9.25}$$

The hydraulic efficiency is the ratio of power developed by the runner and the power available at its inlet, that is,

$$\eta_h = \frac{2u(V_{w1} + V_{w2})}{V_1^2} \tag{9.26}$$

Table 9.3 shows different velocity ratios as it is often convenient to express the velocities in terms of non-dimensional coefficients.

Table 9.3 Velocity ratios

Coefficients	**Definition**	**Remarks**
Coefficient of velocity	$C_v = \frac{V_1}{\sqrt{2gH}}$	It is the ratio of actual jet velocity to the theoretical jet velocity. The jet velocity at the nozzle tip is different from the jet velocity striking the bucket as the jet diameter increases a little as it leaves the nozzle tip.
Speed ratio	$K_u = \frac{u}{\sqrt{2gH}}$	The speed ratio is obtained by dividing the tangential blade velocity with the theoretical velocity of jet at the nozzle tip.
Flow ratio	$K_f = \frac{V_f}{\sqrt{2gH}}$	The flow ratio is obtained by dividing the flow velocity with the theoretical velocity of jet at the nozzle tip.
Bucket friction coefficient	$K = \frac{V_{r2}}{V_{r1}}$	The bucket friction coefficient is taken as unity when the blade surface is highly polished. During the prolonged usage, its value falls below 1.

Using the inlet and outlet velocity triangles, the whirl velocities can be expressed in terms of known velocities, that is, V_1 and u.

From the inlet velocity triangle $V_{w1} = V_1$ and $V_{r1} = V_1 - u$.

From the outlet velocity triangle,

$$V_{w2} = V_{r2}\cos\beta_2 - u \tag{9.27}$$

or
$$V_{w2} = KV_{r1}\cos\beta_2 - u \tag{9.28}$$

or
$$V_{w2} = K(V_1 - u)\cos\beta_2 - u \tag{9.29}$$

Substituting V_{w1} and V_{w2} in Eq. (9.26) and simplifying

$$\eta_h = \frac{2u(V_1 - u)(1 + K\cos\beta_2)}{V_1^2} \tag{9.30}$$

or
$$\boxed{\eta_h = 2\frac{u}{V_1}\left(1 - \frac{u}{V_1}\right)(1 + K\cos\beta_2)} \tag{9.31}$$

Equation (9.31) represents a parabolic relation between η_h and u/V_1, as shown in Fig. 9.11. The hydraulic efficiency is zero when $u/V_1 = 0$ and when $u = V_1$. Under no-load conditions, the tangential blade velocity is equal to the absolute velocity of the striking jet, $u = V_1$. The velocity of Pelton turbine corresponding to no-load condition is termed as *runaway speed*. The efficiency can be maximised by differentiating Eq. (9.31) with respect to u and equating it to zero, that is,

$$\frac{d\eta_h}{du} = 0 \quad \Rightarrow \quad \frac{u}{V_1} = \frac{1}{2} \quad \Rightarrow \quad \boxed{\eta_{h,\max} = \frac{1 + K\cos\beta_2}{2}} \tag{9.32}$$

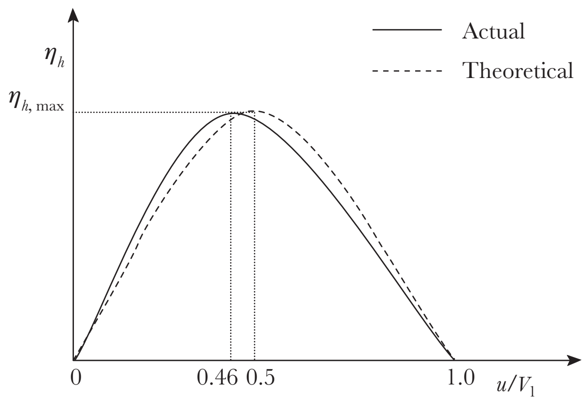

Fig. 9.11 Efficiency versus velocity ratio

Theoretically efficiency becomes maximum when $u/V_1 = 0.5$. In actual practice, the maximum efficiency occurs at a slightly lower value of u/V_1, that is, 0.46. The reason for this is that some of the power is lost in overcoming the following:

1. Friction between the runner and air present in the casing
2. Friction in the bearings of the turbine shaft

The power production from a Pelton turbine can be increased by the following modifications:

1. Use of more than one jet on a Pelton wheel. Maximum number of jets can be up to 4.
2. More than one runner can be mounted on the turbine shaft.
3. Number of turbine units can be increased. This will be a costly affair.

Example 9.3 The water fed from a reservoir to a power house is 6 m³/s at a total head of 250 m through a single penstock of 500 m long. The turbine has four Pelton wheels with two nozzles each. The efficiency of power transmission through the penstock

is 90% and overall efficiency is 85%. The coefficient of velocity for each nozzle may be assumed as 0.95 and the friction factor as 0.02. Determine the (a) power output of the plant (b) diameter of each nozzle (c) penstock diameter. Assume that all the nozzles have same diameter.

Given data:

Total head, $H_T = 250\,\text{m}$	Transmission efficiency, $\eta_t = 0.9$
Total discharge, $Q = 6\,\text{m}^3/\text{s}$	Overall efficiency, $\eta_o = 0.9$
Length of penstock, $L = 500\,\text{m}$	Coefficient of velocity, $C_v = 0.95$
No. of wheels, $n = 4$	Friction factor, $f = 0.02$
No. of nozzles, $z = 2$	

Solution:

(a) The power output is given by

$$P_o = \eta_o \frac{1}{2}\rho Q V_1^2$$

where V_1 is the velocity of the jet issued from each nozzle given by

$$V_1 = C_v\sqrt{2gH}$$

where H is the net head available at the turbine inlet, which can be calculated by subtracting the friction losses in penstock from the total head, that is,

$$H = H_T - h_f$$

In terms of transmission efficiency, the net head is calculated as

$$H = \eta_t H_T \quad \Rightarrow \quad H = 0.9\times 250 = 225\,\text{m}$$

$$\Rightarrow \quad V_1 = 0.95\sqrt{2\times 9.81\times 225} \quad \Rightarrow \quad V_1 = 63.11\,\text{m/s}$$

Therefore, the power output is

$$P_o = 0.85\times\frac{1}{2}\times 1000\times 6\times 63.11^2 \quad \Rightarrow \quad P_o = 10.156\,\text{MW}$$

(b) Diameter of each nozzle, d

Total number of nozzles = 4 × 2 = 8

Discharge through each nozzle, $q = Q/8 = 6/8 = 0.75\ \text{m}^3/\text{s}$,

which can also be computed as the product of nozzle area and the jet velocity.

$$\frac{\pi}{4}d^2V_1 = q \quad \Rightarrow \quad d = 0.123\,\text{m}$$

(c) Diameter of penstock, D

The head loss due to friction in the penstock (which is the difference between total and net heads) is calculated using Darcy–Weisbach equation

$$h_f = f\frac{L}{D}\frac{V^2}{2g} \quad \Rightarrow \quad h_f = 8f\frac{L}{\pi^2 D^5}\frac{Q^2}{g}$$

$$\Rightarrow \quad D = 1.035\,\text{m}$$

Example 9.4 A 30 MW power plant uses a double overhung Pelton turbine under the net head of 400 m at its inlet. Find the jet diameter, mean runner diameter, runner speed, and specific speed of the turbine. Assume generator efficiency 95%, mechanical efficiency 95%, hydraulic efficiency 90%, coefficient of velocity 0.95, speed ratio 0.46, and jet ratio 10.

Given data:

Net head, $H = 400\,\text{m}$	Hydraulic efficiency, $\eta_h = 0.90$
Power output, $P_o = 30\,\text{MW}$	Mechanical efficiency, $\eta_m = 0.95$
Jet ratio, $m = D/d = 10$	Generator efficiency, $\eta_g = 0.95$
Speed ratio, $K_u = 0.46$	Coefficient of velocity, $C_v = 0.95$

Solution: A double overhung Pelton turbine has been shown in Fig. 9.12. Power output of each runner is, therefore, given as

$$P_{ro} = \frac{P_o}{2\times\eta_g} \quad\Rightarrow\quad P_{ro} = 15.79\,\text{MW}$$

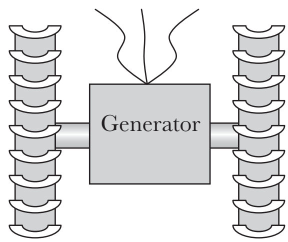

Fig. 9.12 Double overhung wheel

The overall efficiency is the product of hydraulic and mechanical efficiencies

$$\eta_o = \eta_h\eta_m \quad\Rightarrow\quad \eta_o = 0.855$$

The jet velocity is calculated as

$$V_1 = C_v\sqrt{2gH} \quad\Rightarrow\quad V_1 = 84.16\,\text{m/s}$$

Using the expression of power output, the discharge can be computed

$$P_{ro} = \eta_o \frac{1}{2}\rho Q V_1^2 \quad\Rightarrow\quad Q = 5.21\,\text{m}^3/\text{s}$$

The jet diameter is calculated as

$$\frac{\pi}{4}d^2 V_1 = Q \quad\Rightarrow\quad d = 0.28\,\text{m}$$

From the jet ratio, the mean runner diameter, $D = m \times d \quad\Rightarrow\quad D = 2.8\,\text{m}$

The tangential velocity of the runner

$$u = K_u\sqrt{2gH} \quad\Rightarrow\quad u = 40.75\,\text{m/s}$$

It is also expressed in terms of runner speed and its diameter

$$u = \frac{\pi D N}{60} \quad\Rightarrow\quad N = 278\,\text{rpm}$$

The specific speed for a turbine is given by

$$N_s = \frac{N\sqrt{P_{ro}}}{H^{5/4}} \quad\Rightarrow\quad N_s = 19.53$$

9.6 REACTION TURBINE

A turbine solely working on the principle of reaction is shown in Fig. 9.13. Water enters through the turbine axis and the reaction due to the jet leaving the nozzle causes it to rotate in the opposite direction. However, such an arrangement is not useful for mass production of electrical power. The reaction turbines work partly on reaction and partly utilize the impulsive action of the flow stream. Francis and Kaplan turbines fall under the category of reaction turbine.

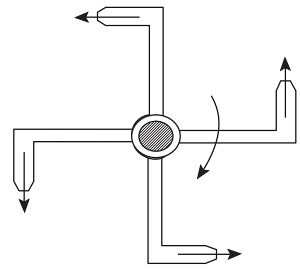

Fig. 9.13 Reaction turbine

The impulse turbine requires a high head and low discharge to operate. The discharge is constrained by the nozzle diameter. In addition, the nozzle converts the available pressure head proportionally to the kinetic head. Low heads produce low kinetic energy jets. Therefore, for low and medium heads, the use of impulse turbines is not feasible. This is the main reason behind the development of other types of turbines. If the head available is low, the power output of a turbine can be increased by increasing the discharge accordingly. The power output is given by

$$P_o = \eta_o \rho Q g H \tag{9.33}$$

In a reaction turbine, water enters the runner all around its periphery. The discharge through the reaction turbine is calculated as

$$Q = A_f \times V_f \tag{9.34}$$

To study the effect of flow velocity V_f, the following outlet velocity triangles are possible:

The hydraulic energy, which goes as waste into the tail race, is in the form of kinetic energy head at the runner exit, that is, $V_2^2/2g$. To present the effect of this loss, three different cases are shown in Fig. 9.14. The loss is least in the case of Fig. 9.14(b) as the magnitude of the absolute velocity at the runner exit V_2 is least when the flow leaves the runner blade radially. Further, the velocity V_2 can

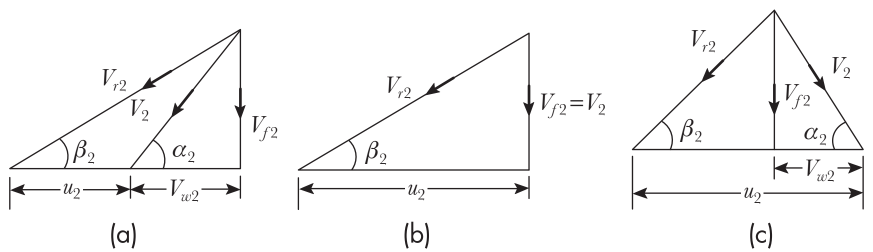

Fig. 9.14 Outlet velocity triangles for a reaction turbine

be minimized by choosing a smaller value of exit blade angle (~β_2 = 15°). It is for this reason that all the reaction turbines are designed to achieve radial flow at the runner exit.

The only way to increase the discharge is to increase the area of flow. The area of flow in a reaction turbine is given by

$$A_f = k\pi BD \tag{9.35}$$

where factor k takes into account the reduction in flow area due to thickness of the blades.

Its value is unity if the blades' thickness is negligibly small. B is the width of the runner and D is the runner diameter. To increase the discharge, diameter D cannot be increased much due to stress consideration. Hence, the only option to increase the discharge is to increase the width B. This change leads to the change in flow of direction in the runner from mixed (radial + axial) to axial. This has been shown in Fig. 9.15.

9.6.1 Francis Turbine

Francis turbine is a mixed flow reaction turbine, named after its inventor *James Bicheno Francis* (1815–1892), a British–American engineer. In the turbine, water enters the runner radially and leaves it axially. It is a medium flow and medium head turbine. A typical Francis turbine, shown in Fig. 9.16, consists of a spiral casing, wicket gates or guide vanes, the runner, and draft tube. The water through the penstock enters into the spiral casing and then into the runner through the wicket gates and finally it is discharged to the tail race through the draft tube. In Francis turbine, unlike Pelton turbine, the expansion of fluid (conversion of pressure energy into kinetic energy) is not just limited to one component but it occurs in a series of components. In Pelton turbine, the expansion of fluid takes place inside the nozzle only, whereas in Francis turbine the expansion partly takes place inside the spiral casing, partly in the wicket gates (guide vanes), and remaining inside the runner. The spiral-shaped (area reducing in the flow of direction) casing is designed to evenly distribute water into the runner periphery facilitating the jets emerging through the guide vanes to strike the runner blades with the same velocity. The guide vanes or wicket gates are provided at the runner inlet to guide as well as to control the flow of water into the runner. The guide vanes have airfoil shape to achieve smooth streamline flow at the runner entry. This will result in a shock-free flow into the runner. The exploded view of guide vanes and runner is shown in Fig. 9.16(b). The water stream from the guide vanes enters into the runner and glides over the runner blades to produce rotation of the runner. The draft tube is required in the reaction turbines to achieve the maximum output from them. The draft tubes have been discussed in Section 9.6.3. The velocity triangles for the Francis turbine runner have already

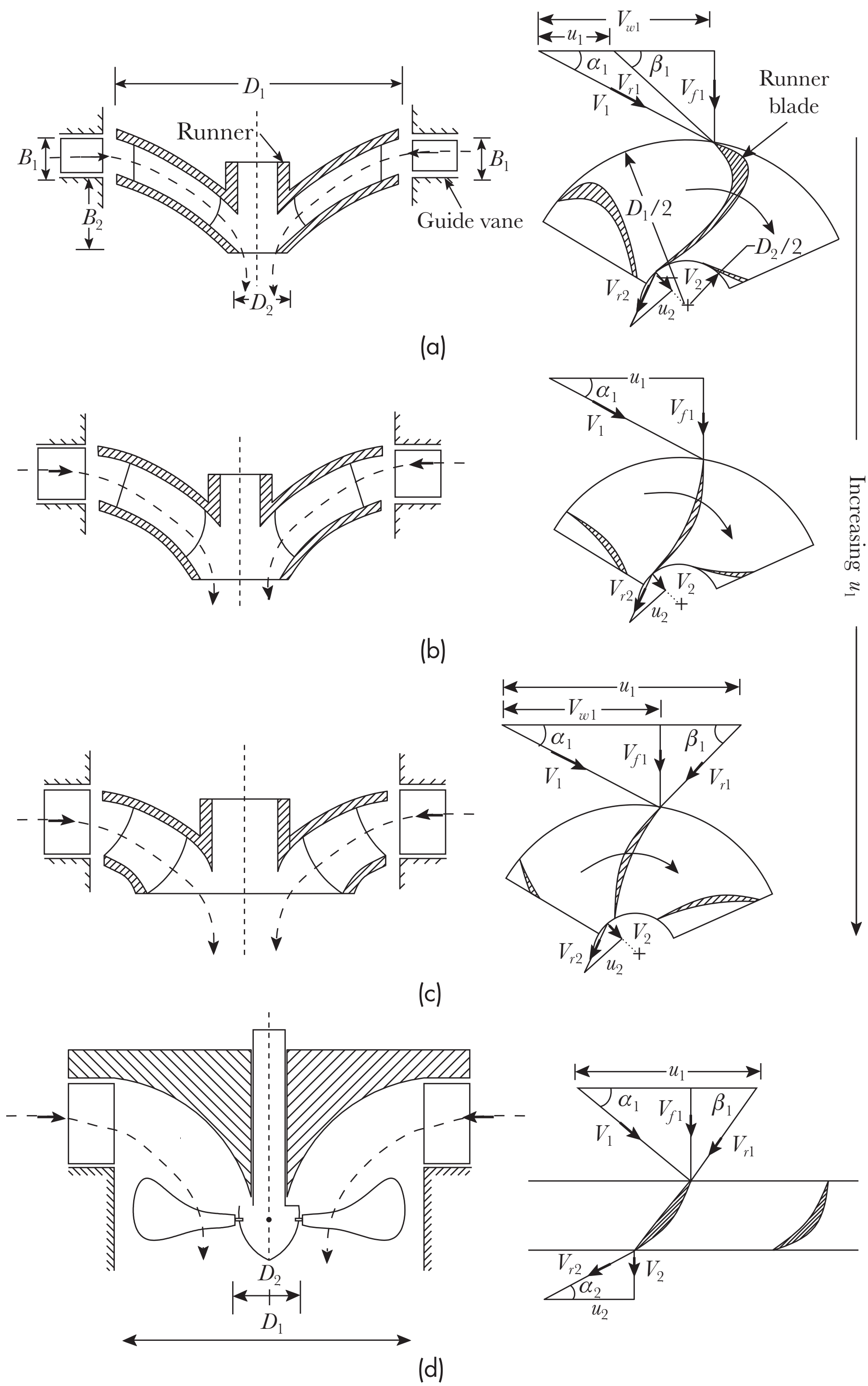

Fig. 9.15 Reaction turbine runners (a) Low-speed Francis (b) Medium-speed Francis (c) High-speed Francis (d) Kaplan

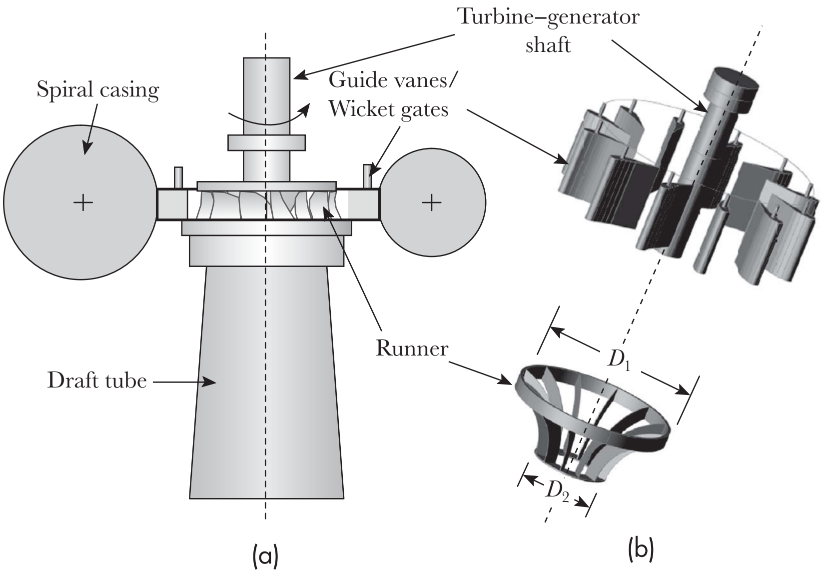

Fig. 9.16 Francis turbine (a) Schematic diagram (b) Exploded view

been explained in detail in the description of reaction turbines.

The discharge through the Francis turbine runner is given by

$$Q = k\pi B_1 D_1 V_{f1} = k\pi B_2 D_2 V_{f2} \tag{9.36}$$

Another way of finding the discharge is

$$Q = (\pi D_1 - Zt)B_1 D_1 V_{f1} = (\pi D_1 - Zt)B_2 D_2 V_{f2} \tag{9.37}$$

where Z is the number of blades and t is the blade thickness.

The hydraulic efficiency for the Francis turbine is

$$\eta_h = \frac{V_{w1}u_1}{gH} \tag{9.38}$$

Applying energy balance at the inlet and exit of the runner, considering only outgoing kinetic energy loss,

$$\rho Q gH = \rho Q V_{w1} u_1 + \frac{1}{2}\rho Q V_2^2 \tag{9.39}$$

$$V_{w1}u_1 = gH - \frac{1}{2}V_2^2 \tag{9.40}$$

The expression of hydraulic efficiency reduces to

$$\eta_h = 1 - \frac{V_2^2}{2gH} \tag{9.41}$$

Equation (9.41) is only valid for frictionless vanes/blades.

Example 9.5 A Francis turbine of specific speed 100 develops 20 MW under a head of 200 m. The hydraulic and overall efficiencies are 0.9 and 0.85, respectively. The flow takes place with constant flow velocity of 10 m/s. The ratio of width to diameter of wheel at the inlet is 0.2 and the area occupied by the thickness of blades is 7% area of flow. Calculate guide vane angle, peripheral velocity, and whirl velocity at inlet. In addition determine the energy loss, when the pressure at inlet and outlet of the runner is 12 and 0.2 bar, respectively, and height of the runner at the inlet and the outlet is 6 and 1 m, respectively, above the tail race.

Given data:

Net head, $H = 200\,\text{m}$	Hydraulic efficiency, $\eta_h = 0.90$
Power output, $P_o = 20\,\text{MW}$	Overall efficiency, $\eta_o = 0.85$
Flow velocity, $V_f = 10\,\text{m/s}$	Blade thickness coefficient, $k = 1 - 0.07 = 0.93$
Specific speed, $N_s = 100$	Width to diameter ratio, $B/D = 0.2$
Pressure at inlet, $p_1 = 12\,\text{bar}$	Pressure at outlet, $p_2 = 0.2\,\text{bar}$
Runner height at inlet, $z_1 = 6\,\text{m}$	Runner height at outlet, $z_2 = 1\,\text{m}$

Solution: The speed of runner can be calculated from the expression of specific speed of the turbine

$$N = \frac{N_s H^{5/4}}{\sqrt{P_o}} \quad \Rightarrow \quad N = 531.8\,\text{rpm}$$

The discharge can be calculated from the expression of output power

$$P_o = \eta_o \rho Q g H \quad \Rightarrow \quad Q = 12\,\text{m}^3/\text{s}$$

The discharge through a Francis turbine is given by

$$Q = k\pi B_1 D_1 V_{f1} \quad \Rightarrow \quad D_1 = 1.43\,\text{m} \quad \Rightarrow \quad B_1 = 0.286\,\text{m}$$

The tangential or peripheral velocity at inlet is given by,

$$u_1 = \frac{\pi D_1 N}{60} \quad \Rightarrow \quad u_1 = 39.82\,\text{m/s}$$

The whirl velocity can be computed using the expression for hydraulic efficiency

$$\eta_h = \frac{V_{w1} u_1}{gH} \quad \Rightarrow \quad V_{w1} = 44.34\,\text{m/s}$$

The inlet velocity triangle has been shown in Fig. 9.17. Using this triangle, the guide vane angle and inlet blade angle are calculated as

$$\tan\alpha_1 = \frac{V_{f1}}{V_{w1}} \quad \Rightarrow \quad \alpha_1 = 12.7°$$

$$\tan\beta_1 = \frac{V_{f1}}{V_{w1} - u_1} \quad \Rightarrow \quad \beta_1 = 65.67°$$

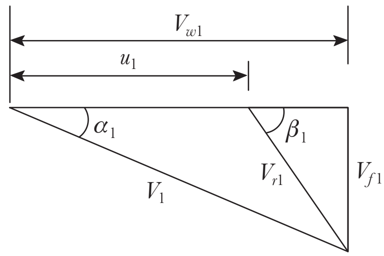

Fig. 9.17 Inlet velocity triangle

Example 9.6 An outward flow reaction turbine has the inner and outer diameters as 1.50 and 2.0 m, respectively, and is rotating at 300 rpm operating under an effective head of 50 m. The runner has 30 vanes 10 mm thick at inlet and 20 mm thick at the outlet. The width of the passage is 30 cm throughout. The discharge through the turbine is 10 m³/s. Determine (a) the blade angles at inlet and outlet and (b) power developed by the runner.

Given data:

Net head, $H = 50$ m	Runner speed, $N = 300$ rpm
Discharge, $Q = 10\,\text{m}^3/\text{s}$	No. of runner blades, $n = 30$
Blade thickness at inlet, $t_1 = 0.01$ m	Blade thickness at outlet, $t_2 = 0.02$ m
Runner width at inlet, $B_1 = 0.3$ m	Runner width at outlet, $B_2 = 0.3$ m
Runner diameter at inlet, $D_1 = 1.5$ m	Runner diameter at outlet, $D_2 = 2.0$ m

Solution: The discharge through the runner, taking blade thickness into consideration, can be expressed as

$$Q = (\pi B_1 D_1 - nB_1 t_1)V_{f1} = (\pi B_2 D_2 - nB_2 t_2)V_{f2} \tag{1}$$

The flow velocities at inlet and outlet, using Eq. (1), are given by

$$V_{f1} = 7.554\,\text{m/s}$$

$$V_{f2} = 5.865\,\text{m/s}$$

The peripheral velocities at inlet and outlet are given by

$$u_1 = \frac{\pi D_1 N}{60} \Rightarrow u_1 = 23.56\,\text{m/s}$$

$$u_2 = \frac{\pi D_2 N}{60} \Rightarrow u_2 = 31.4\,\text{m/s}$$

It is known that in a reaction turbine, the flow is radial at the outlet [Fig. 9.18(a)], that is,

$$\tan\beta_2 = \frac{V_{f2}}{u_2} \Rightarrow \beta_2 = 10.58°$$

The energy balance across the runner gives

$$\frac{V_{w1}u_1}{g} = H - \frac{V_2^2}{2g}, \quad \text{where} \quad V_2 = V_{f2}$$

Thus, the whirl velocity at inlet is

$$\Rightarrow \quad V_{w1} = 20.1 \text{m/s}$$

The velocity triangle at inlet will take the shape as shown in Fig. 9.18(b)

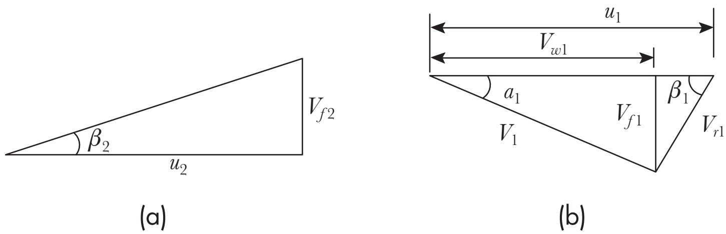

Fig. 9.18 Velocity triangles (a) Outlet (b) Inlet

The inlet blade angle can be computed by considering the inlet velocity triangle,

$$\tan\beta_1 = \frac{V_{f1}}{u_1 - V_{w1}} \quad \Rightarrow \quad \beta_1 = 65.39°$$

The power developed by the turbine runner is

$$P_d = \rho Q g \frac{V_{w1} u_1}{g} \quad \Rightarrow \quad P_d = 4.736 \, \text{MW}$$

The hydraulic efficiency is

$$\eta_h = \frac{V_{w1}u_1}{gH} \quad \Rightarrow \quad \eta_h = 96.5\%$$

9.6.2 Kaplan Turbine

The Kaplan turbine is an axial flow propeller water turbine with the runner resembling the propeller of a ship. The blades of its runner are of adjustable type to give maximum efficiency. If the runner blades are fixed to the boss, the turbine is simply known as *propeller turbine*. It was developed in 1913 by the Austrian professor *Viktor Kaplan* (1876–1934). The turbine is designed for high discharge and low head. Figure 9.19 shows a typical Kaplan turbine, which has a similar arrangement as that of a Francis turbine. The water from the penstock enters into the runner through the spiral casing and guide vanes. The water stream glides over the runner blades transferring the energy to the runner which in turn causes its rotation. A whirl chamber is provided between the guide vanes and the runner to transform the flow from radial to axial.

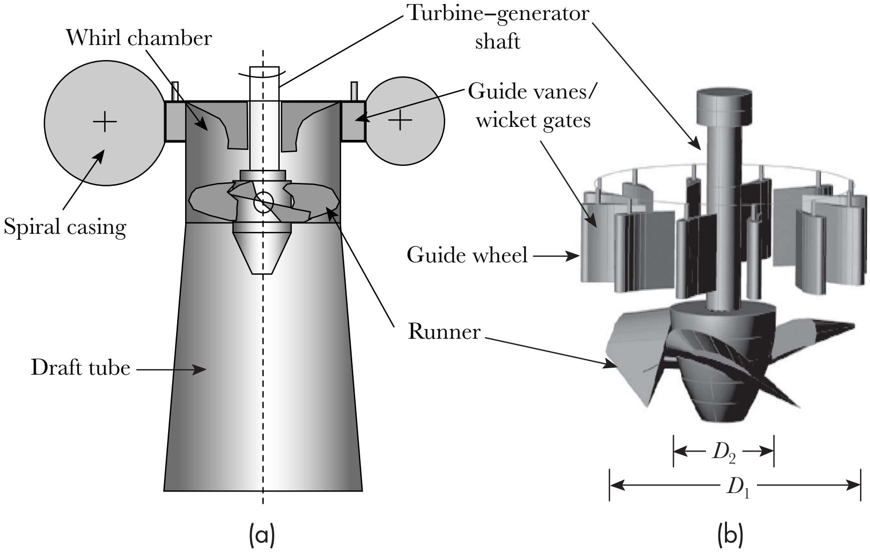

Fig. 9.19 Kaplan turbine (a) Schematic diagram (b) 3D view

The water enters into the turbine runner as free vortex. The number of vanes/blades usually varies from 3 to 4 and the maximum number is limited to 6. The velocity triangles for the Kaplan turbine have already been discussed in detail in the description of reaction turbine.

The tangential velocity, u, at the inlet and outlet remains the same as the inlet and exit section is at the same radial distance from the axis of the runner. The efficiency is calculated in a similar way as it is done in the case of Francis turbine using Eq. (9.38). The blades of Kaplan turbine are adjusted during varying load conditions to give the maximum efficiency, as shown in Fig. 9.20.

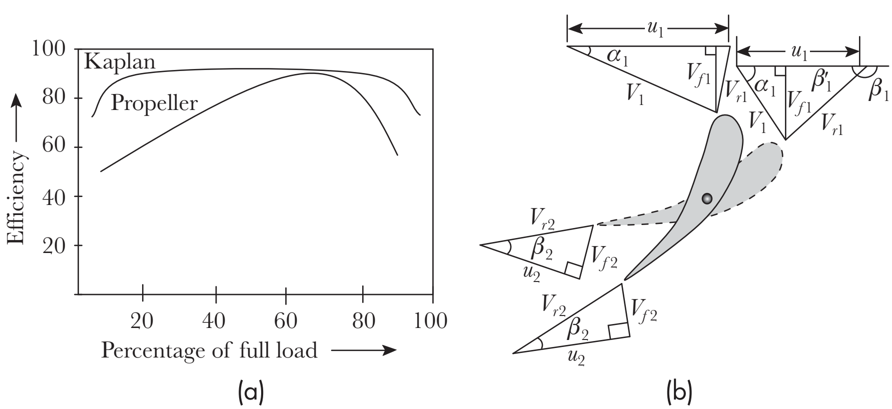

Fig. 9.20 (a) Performance at part loads (b) Velocity triangles at different blade orientations

The efficiency for the Kaplan turbine is almost constant for any load, whereas the efficiency of propeller turbine is not same for all loads. The maximum efficiency for Kaplan turbine can be as high as 94%. Figure 9.20(b) shows the velocity triangles for different blade orientations of a Kaplan turbine.

Example 9.7 A Kaplan turbine develops 5000 kW under the net head of 5 m. The speed ratio and flow ratio are 2 and 0.5, respectively. The outer diameter of the runner is thrice its inner diameter. Compute the runner diameters and runner speed, if overall efficiency is 0.92.

Given data:

Net head, $H = 5\,\text{m}$	Speed ratio, $K_u = 2$
Diameters ratio, $D_1/D_2 = 3$	Flow ratio, $K_f = 0.5$
Power output, $P_o = 5000\,\text{kW}$	Overall efficiency, $\eta_o = 0.92$

Solution: From the definition of overall efficiency, the discharge

$$Q = \frac{P_o}{\eta_o \rho g H} \quad \Rightarrow \quad Q = 110.8\,\text{m}^3/\text{s}$$

The flow velocity and tangential blade velocity can be computed from the definitions of flow and speed ratios, respectively, as

$$V_f = K_f\sqrt{2gH} \quad \Rightarrow \quad V_f = 4.95\,\text{m/s}$$

$$u = K_u\sqrt{2gH} \quad \Rightarrow \quad u = 19.81\,\text{m/s}$$

The area of flow is obtained by dividing the discharge by the flow velocity:

$$A_f = \frac{Q}{V_f} \quad \Rightarrow \quad A_f = 22.38\,\text{m}^2$$

If the area occupied by blade thickness is ignored, the flow area will be equal to the area of annular space available between the hub and blade tips, that is,

$$\frac{\pi}{4}\left(D_1^2 - D_2^2\right) = A_f \quad \Rightarrow \quad \frac{\pi}{4}\left(8D_2^2\right) = A_f$$

$$\Rightarrow \quad D_2 = 3.56\,\text{m} \quad \Rightarrow \quad D_1 = 10.68\,\text{m}$$

The runner speed is computed from peripheral blade velocity

$$N = \frac{60u}{\pi D_1} \quad \Rightarrow \quad N = 35.4\,\text{rpm}$$

Example 9.8 A Kaplan turbine operates under a head of 4 m. The runner speed is 100 rpm. The turbine has four 50 cm long airfoil shaped blades with mean blade circle radius as 1.5 m. The chord of the blade is inclined at 30° to the direction of motion and is of 2.5 m length. The flow velocity is 5 m/s. Calculate the power developed by the turbine and its efficiency, if lift and drag coefficients for the given angle of incidence are 0.7 and 0.05, respectively.

Given data:

Net head, $H = 4\,\text{m}$	Runner speed, $N = 100\,\text{rpm}$
Blade length, $b = 0.5\,\text{m}$	Runner diameter, $D_1 = 2 \times 1.5\,\text{m}$
Chord length, $l = 2.5\,\text{m}$	Blade angle, $\beta_1 = 30°$
Flow velocity, $V_{f1} = 5\,\text{m/s}$	Lift coefficient, $C_L = 0.7$
Drag coefficient, $C_D = 0.05$	Number of blades, $z = 4$

Solution: The Kaplan turbine runner blade and the forces on it have been shown in Fig. 9.21.

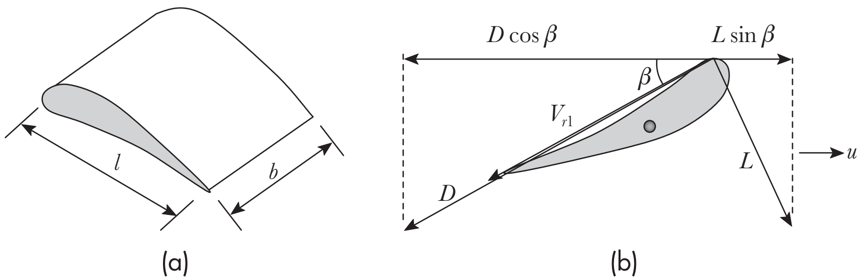

Fig. 9.21 (a) Runner blade (b) Drag and lift on runner blade

The net force acting on the blade in x-direction, responsible for the rotation of runner is given by

$$F_x = L\sin\beta - D\cos\beta$$

$$\Rightarrow \quad F_x = C_L \frac{1}{2}\rho V_{r1}^2 A \sin\beta - C_D \frac{1}{2}\rho V_{r1}^2 A\cos\beta$$

The projected blade area is the product of b and l and the relative velocity is computed from the inlet triangle

$$V_{r1} = \frac{V_{f1}}{\sin\beta} \quad \Rightarrow \quad V_{r1} = 10\,\text{m/s}$$

The required force is

$$\Rightarrow \quad F_x = \frac{1}{2}\rho V_{r1}^2 A(C_L \sin\beta - C_D \cos\beta) \quad \Rightarrow \quad F_x = 19.17\,\text{kN}$$

Power developed by turbine is

$$P_d = z \times F_x \times u \quad \Rightarrow \quad P_d = z \times F_x \times \frac{\pi D N}{60} \quad \Rightarrow \quad P_d = 1204\,\text{kW}$$

The discharge through the turbine is

$$Q = \frac{\pi}{4}[D_1^2 - (D_1 - b)^2]V_{f1} \quad \Rightarrow \quad Q = 34.375\,\text{m}^3\text{/s}$$

The hydraulic efficiency is

$$\eta_h = \frac{P_d}{\rho Q gH} \quad \Rightarrow \quad \eta_h = 89.3\%$$

9.6.3 Draft Tube

The draft tube, which is installed at the exit of the runner, is an essential part of reaction turbines. It is employed to produce a negative pressure (vacuum) at the exit of the runner, which results in an increased pressure difference across the runner. Higher pressure difference means more expansion work. Thus, the use of draft tube results in an increased output.

The draft tube has a diverging shape and is placed at the turbine exit where the pressure is below atmospheric pressure. In order to discharge the water at atmospheric pressure, the slight divergence in the draft tube is provided to recover the pressure from negative to zero gauge (atmospheric) pressure. Figure 9.22 shows a simple divergent-type draft tube connecting the runner exit to the tail race. Applying Bernoulli's equation between sections 1 and 3,

$$\frac{p_1}{\rho g} + \frac{V_1^2}{2g} + z_1 = \frac{p_3}{\rho g} + \frac{V_3^2}{2g} + z_3 + h_f \tag{9.42}$$

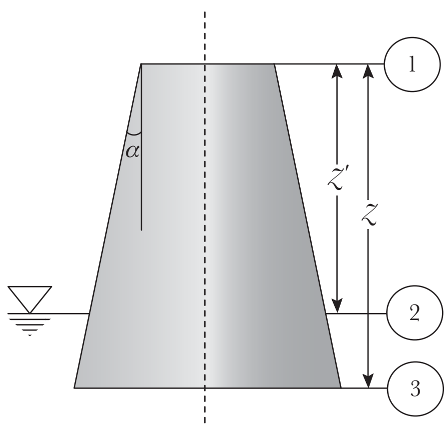

Fig. 9.22 Draft tube

From hydrostatics, the pressure at section 3 is greater than that at section 2 by an amount given by

$$p_3 = p_2 + \rho g(z - z') \tag{9.43}$$

Since, $p_2 = p_{\text{atm}}$ and using Eqs (9.42) and (9.43)

$$\frac{p_1}{\rho g} = \frac{p_{\text{atm}}}{\rho g} - \left(\frac{V_1^2 - V_3^2}{2g} + z + h_f \right) \tag{9.44}$$

This proves the point that the draft tube produces negative pressure at its entry. The quantity in the bracket of Eq. (9.44) is equivalent to the amount of pressure head recovered. The water leaves the turbine at a pressure equal to the pressure available outside the draft tube. The efficiency of the draft tube is defined in following manner:

$$\eta_d = \frac{\left(V_1^2/2g - V_3^2/2g \right) - h_f}{\left(V_1^2/2g - V_3^2/2g \right)} \tag{9.45}$$

where h_f is the head loss due to friction.

The following are the two important issues associated with the draft tube:

1. In the divergent passage, the pressure rises with a fall in velocity or the pressure energy is recovered at the cost of kinetic energy. The semi-angle of divergence α should be small to avoid flow separation near the wall of the draft tube. This angle is usually kept between 4° and 5°.
2. The expansion takes place inside the turbine, that is, the pressure energy gets converted into kinetic energy until the pressure becomes negative at the runner exit or at the draft tube entrance. Hence, there is a possibility that the pressure may fall below the vapour or saturation pressure corresponding to the fluid temperature. As a result, this leads to the onset of vaporization. The vapour bubbles form and move with the fluid stream. As soon as they reach the high-pressure region or near a solid surface, they burst. The intensity of the burst is sometimes so strong that it will lead to the erosion of the surface. This erosion is in the form of cavities and pits and thus, the phenomenon is known as *cavitation*.

The following are the draft tubes available in various geometries:

Straight type This is the simplest type of draft tube which resembles the frustum of a cone, as shown in Fig. 9.23(a). The cone angle is limited to 8–10° to avoid losses due to separation, as discussed above. It usually finds its application in vertical axis Francis turbine. Its maximum efficiency is 90%.

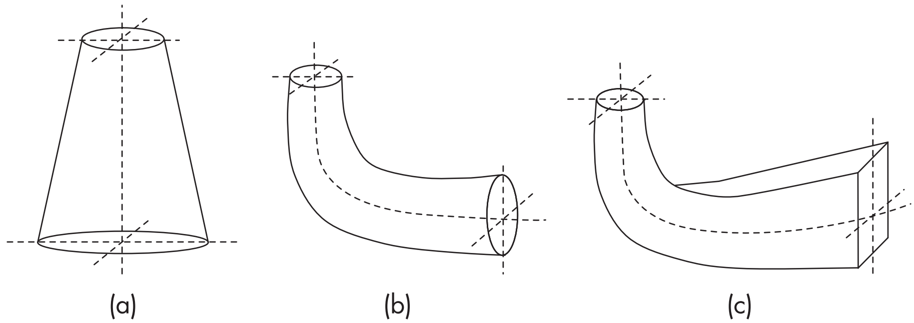

Fig. 9.23 Types of draft tubes (a) Straight (b) Simple elbow (c) Elbow with varying cross-section

Simple elbow type This type of draft tube, as shown in Fig. 9.23(b) is usually employed to keep the vertical length of draft tube short to save the cost of excavation. In this case also, the cone angle is kept small to avoid flow separation. The draft tube efficiency is low due to additional bend losses. It is about 60%.

Elbow type with varying cross-section Such a draft tube is shown in Fig. 9.23(c). To improve the efficiency of simple elbow-type draft tube, the following modifications are made:

1. There is transition from circular cross-section at inlet to the rectangular cross-section at outlet.
2. Further, the horizontal part is given an upward inclination so that the water is discharged at the tail race level and to prevent the entry of air from the draft tube exit.

Example 9.9 An elbow-type draft tube has a circular section of 1.5 m^2 at the entry and rectangular cross-section of 15 m^2 at the exit. The turbine is placed 2 m above tail race level. If the velocity at the inlet of the draft tube is 15 m/s, estimate the
(a) negative pressure head at the inlet to the draft tube
(b) efficiency of the draft tube
Assume friction losses in the draft tube to be 10% of the inlet velocity head.

Given data:

Inlet velocity, $V_1 = 15$ m/s	Friction head loss, $h_f = 0.1V_1^2/2g$
Area at inlet, $A_1 = 1.5$ m^2	Area at outlet, $A_2 = 15$ m^2

Solution: The elbow type draft tube has been shown in Fig. 9.24. Applying Bernoulli's equation at the inlet and outlet of draft tube:

$$\frac{p_1}{\rho g} + \frac{V_1^2}{2g} + z_1 = \frac{p_2}{\rho g} + \frac{V_2^2}{2g} + z_2 + h_f$$

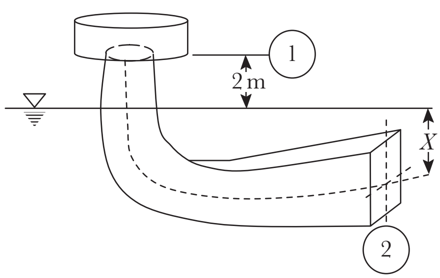

Fig. 9.24 Elbow-type draft tube

From hydrostatics,

$$\frac{p_2}{\rho g} = \frac{p_{atm}}{\rho g} + X \quad \Rightarrow \quad \frac{p_2}{\rho g} = 10.3 + X$$

In addition, $z_1 - z_2 = 2 + X$.

From continuity equation,

$$V_2 = \frac{A_1 V_1}{A_2} \quad \Rightarrow \quad V_2 = 1.5\,\text{m/s}$$

Therefore, pressure head at inlet,

$$\frac{p_1}{\rho g} = \frac{p_2}{\rho g} + \frac{V_2^2 - V_1^2}{2g} + z_2 - z_1 + 0.1\frac{V_1^2}{2g} \quad \Rightarrow \quad \frac{p_1}{\rho g} = -1.906\,\text{m}$$

Efficiency of the draft tube

$$\eta_d = \frac{\left(V_1^2/2g - V_2^2/2g\right) - h_f}{\left(V_1^2/2g - V_2^2/2g\right)} \quad \Rightarrow \quad \eta_d = 89.9\%$$

9.6.4 Governing Mechanism of Reaction Turbines

The governing mechanism of reaction turbines, as shown in Fig. 9.25, is similar to that of Pelton turbine. The only difference is the spearhead control mechanism is replaced by guide vane/wicket gate mechanism of the reaction turbine.

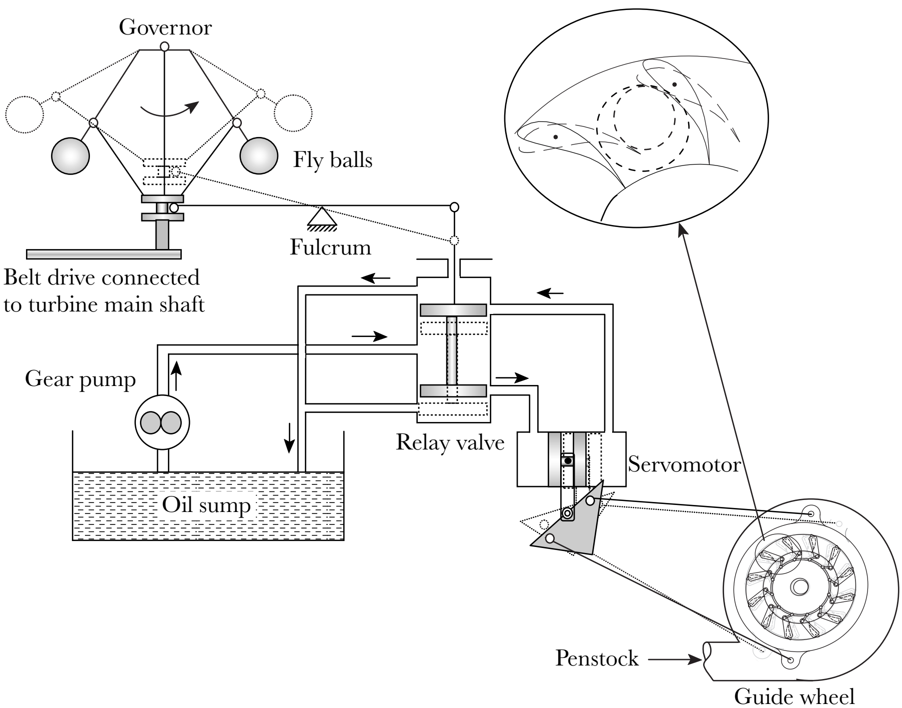

Fig. 9.25 Governing mechanism for a reaction turbine

The solid lines show the positions of different links at a normal speed of the turbine whereas the dotted lines show their positions at a higher speed. The governing mechanism, as described earlier, brings the speed of turbine within desired limits. The magnified view of the vanes of the guide wheel shows that the area of the guide vanes is reduced automatically to control the quantity of water entering into the runner. This brings the speed of the runner to the desired value.

9.7 UNIT QUANTITIES

The unit quantities play a pivotal role in understanding the performance of a turbine operating under the heads other than the design head. The other parameters such as power output, turbine speed, and discharge are related to the head. The unit quantities make an attempt to compare and correlate these parameters by reducing them corresponding to the unit head. This exercise is done with an assumption that the hydraulic efficiency of turbine remains constant even if the head is changed from the designed value. Thus, the velocity triangles for a given head and the unit head will be similar, as shown in Fig. 9.26.

As efficiency is assumed constant for any head,

$$\eta_h = \eta_{hu} \quad \Rightarrow \quad \frac{V_w u}{gH} = \frac{V_{wu} u_u}{g(1)} \quad \Rightarrow \quad \frac{u_u}{u} = \frac{V_w}{V_{wu}} \frac{1}{H} \tag{9.46}$$

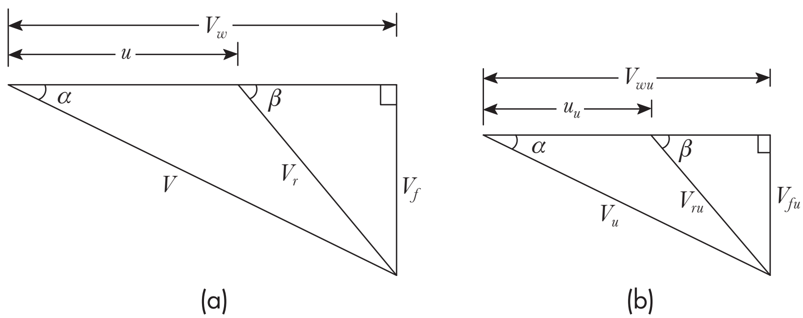

Fig. 9.26 Velocity triangles for (a) Any head, *H* (b) Unit head

From the similarity of triangles, $\frac{V_w}{V_{wu}} = \frac{u}{u_u}$, Eq. (9.46) reduces to

$$\frac{u_u}{u} = \frac{1}{\sqrt{H}} \quad \text{since } u \text{ is a function of } N \quad \Rightarrow \quad \boxed{N_u = \frac{N}{\sqrt{H}}} \tag{9.47}$$

Equation (9.47) is for *unit speed*, which may be defined as the speed of the turbine operating under unit head.

The *unit discharge* is defined as the discharge of a turbine operating under unit head.

$$Q = \pi BDV_f \quad \Rightarrow \quad Q_u = \pi BDV_{fu} \quad \text{or} \quad \frac{Q_u}{Q} = \frac{V_{fu}}{V_{fu}} \tag{9.48}$$

From the similarity of triangles, $\dfrac{V_f}{V_{fu}} = \dfrac{u}{u_u}$, Eq. (9.48) reduces to

$$\frac{Q_u}{Q} = \frac{1}{\sqrt{H}} \quad \Rightarrow \quad \boxed{Q_u = \frac{Q}{\sqrt{H}}} \tag{9.49}$$

The *unit power* of a turbine is the power output of a turbine operating under unit head.

$$P = \eta_o \rho Q g H \quad \Rightarrow \quad P_u = \eta_o \rho Q_u g(1) \quad \text{or} \quad \frac{P_u}{P} = \frac{Q_u}{Q}\frac{1}{H} \tag{9.50}$$

From Eq. (9.50)

$$\frac{P_u}{P} = \frac{1}{\sqrt{H}}\frac{1}{H} \quad \Rightarrow \quad \boxed{P_u = \frac{P}{H^{3/2}}} \tag{9.51}$$

Similarly, the *unit force* and *unit torque* can be defined. The force of the impact is calculated as the product of mass flow rate and change in whirl velocity.

$$F = \rho Q V_w \quad \Rightarrow \quad F_u = \rho Q V_{wu} \tag{9.52}$$

$$\frac{F_u}{F} = \frac{V_{wu}}{V_{wu}} \quad \Rightarrow \quad \boxed{F_u = \frac{F}{H}} \tag{9.53}$$

The torque is the product force and radius of the runner

$$\frac{T_u}{T} = \frac{F_u \times D/2}{F \times D/2} \quad \Rightarrow \quad \boxed{T_u = \frac{T}{H}} \tag{9.54}$$

The unit quantities help in predicting the performance of a turbine under heads other than designed head. Table 9.4 shows heads and the corresponding parameters.

Table 9.4 Heads and the corresponding parameters

Head	**Corresponding parameters**				
Designed head, H	N	Q	P	F	T
Changed head, H'	N'	Q'	P'	F'	T'

To establish the relation between them, the concept of unit quantities is used as,

$$N_u = \frac{N}{\sqrt{H}} = \frac{N'}{\sqrt{H'}} \quad \Rightarrow \quad \boxed{N' = N\sqrt{\frac{H'}{H}}} \tag{9.55}$$

$$Q_u = \frac{Q}{\sqrt{H}} = \frac{Q'}{\sqrt{H'}} \quad \Rightarrow \quad \boxed{Q' = Q\sqrt{\frac{H'}{H}}} \tag{9.56}$$

$$P_u = \frac{P}{H^{3/2}} = \frac{P'}{H'^{3/2}} \quad \Rightarrow \quad \boxed{P' = P\left(\frac{H'}{H}\right)^{3/2}} \tag{9.57}$$

$$F_u = \frac{F}{H} = \frac{F'}{H'} \quad \Rightarrow \quad \boxed{F' = F\frac{H'}{H}} \tag{9.58}$$

$$T_u = \frac{T}{H} = \frac{T'}{H'} \quad \Rightarrow \quad \boxed{T' = T\frac{H'}{H}} \tag{9.59}$$

The *unit quantities* help in predicting the performance of a turbine operating under any head other than designed head. This is based on the assumption that efficiency remains constant even if there is a change in the available head. The term *specific speed*, N_s, has already been defined in the beginning of the chapter, as the speed of a geometrically similar turbine which produces unit power when operated under unit head. To derive the expression for specific speed, the following procedure is adopted:

The tangential speed of the runner of geometrically similar turbine is equal to the tangential speed of the actual turbine operating under unit head.

$$u_s = u_u \quad \Rightarrow \quad \frac{\pi D_s N_s}{60} = \frac{\pi D N_u}{60} \quad \Rightarrow \quad \boxed{N_s = \frac{D}{D_s} N_u} \tag{9.60}$$

The ratio of the power outputs of the actual turbine and the geometrically similar turbine is given by

$$\frac{P_u}{P_s} = \frac{\eta_o \rho Q_u g(1)}{\eta_o \rho Q_s g(1)} \quad \Rightarrow \quad \frac{P_u}{P_s} = \frac{Q_u}{Q_s} \quad \Rightarrow \quad \frac{P_u}{P_s} = \frac{\pi B D V_{fu}}{\pi B_s D_s V_{fu}} \tag{9.61}$$

It should be noted that $P_s = 1$ and $B/D = n$ (a constant), Eq. (9.61) reduces to

$$P_u = \left(\frac{D}{D_s}\right)^2 \quad \Rightarrow \quad \frac{P_u}{P_s} = \frac{\pi B D V_{fu}}{\pi B_s D_s V_{fu}} \tag{9.62}$$

Using the expression of unit power, Eq. (9.61) reduces to

$$\frac{D}{D_s} = \sqrt{\left(\frac{P}{H^{3/2}}\right)} \quad \Rightarrow \quad \boxed{\frac{D}{D_s} = \frac{\sqrt{P}}{H^{3/4}}} \tag{9.63}$$

From Eqs (9.60) and (9.63) and using the expression for unit speed

$$N_s = \frac{\sqrt{P}}{H^{3/4}} \frac{N}{\sqrt{H}} \Rightarrow \boxed{N_s = \frac{N\sqrt{P}}{H^{5/4}}} \tag{9.64}$$

Example 9.10 An impulse turbine produces 6000 kW while operating under the head of 300 m. The runner speed is 300 rpm and the overall efficiency is 85%. Determine the values of unit speed, unit discharge, and unit power. If the available head falls to 150 m, find the changed values of speed, discharge, and power.

Given data:

Original head, $H = 300$ m	Runner speed, $N = 240$ rpm
Power produced, $P_o = 6000$ kW	Changed head, $H' = 150$ m
Overall efficiency, $\eta_o = 0.85$	

Solution: The concept of unit speed is applied to evaluate the quantities at changed head with an assumption that overall efficiency remains constant.

From the expression of overall efficiency, the discharge is given by

$$Q = \frac{P_o}{\eta_o \rho g H} \Rightarrow Q = 2.4\,\text{m}^3/\text{s}$$

From the expression of unit quantities,

$$Q_u = \frac{Q}{\sqrt{H}} = \frac{Q'}{\sqrt{H'}} \Rightarrow Q' = Q\sqrt{\frac{H'}{H}} \Rightarrow Q' = 1.697\,\text{m}^3/\text{s}$$

$$N_u = \frac{N}{\sqrt{H}} = \frac{N'}{\sqrt{H'}} \Rightarrow N' = N\sqrt{\frac{H'}{H}} \Rightarrow N' = 212.1\,\text{rpm}$$

$$P_u = \frac{P}{H^{3/2}} = \frac{P'}{H'^{3/2}} \Rightarrow P' = P\left(\frac{H'}{H}\right)^{3/2} \Rightarrow P' = 2121.3\,\text{kW}$$

9.8 PERFORMANCE CHARACTERISTICS OF TURBINES

A fluid machine is designed to operate under a given set of conditions. However, in practice it has to undergo off-design conditions due to change in load or available head. The performance of the machine for the off-design conditions needs to be predetermined. For this purpose, the data representing these conditions is obtained by performing tests on either model or prototype. The data is represented by means of curves known as *characteristics* of the machine. The characteristics of turbines are broadly classified as follows:

1. Main characteristics (or constant head curves)
2. Operating characteristics (or constant speed curves)
3. Muschel curves (or isoefficiency or constant efficiency curves)

9.8.1 Main Characteristics

To obtain the main characteristics of a turbine, the head is kept constant and the variations in other parameters with speed are recorded. The parameters and the corresponding unit quantities are calculated and plotted against the unit speed for different gate openings (G).

The following are the observations from Fig. 9.27:

1. For any gate opening, there is no change in discharge with the change in speed in case of Pelton turbine. The reason is that the discharge is controlled inside the nozzle using spearhead mechanism in a Pelton turbine. For a given gate opening, the discharge from the nozzle is constant. The load is dictated by the generator coupled with the turbine in actual practice based on the demand of a power requirement in a locality. Otherwise, in a laboratory, the load is applied on the turbine runner by means of dynamometer. With the application of load, there is a reduction in the

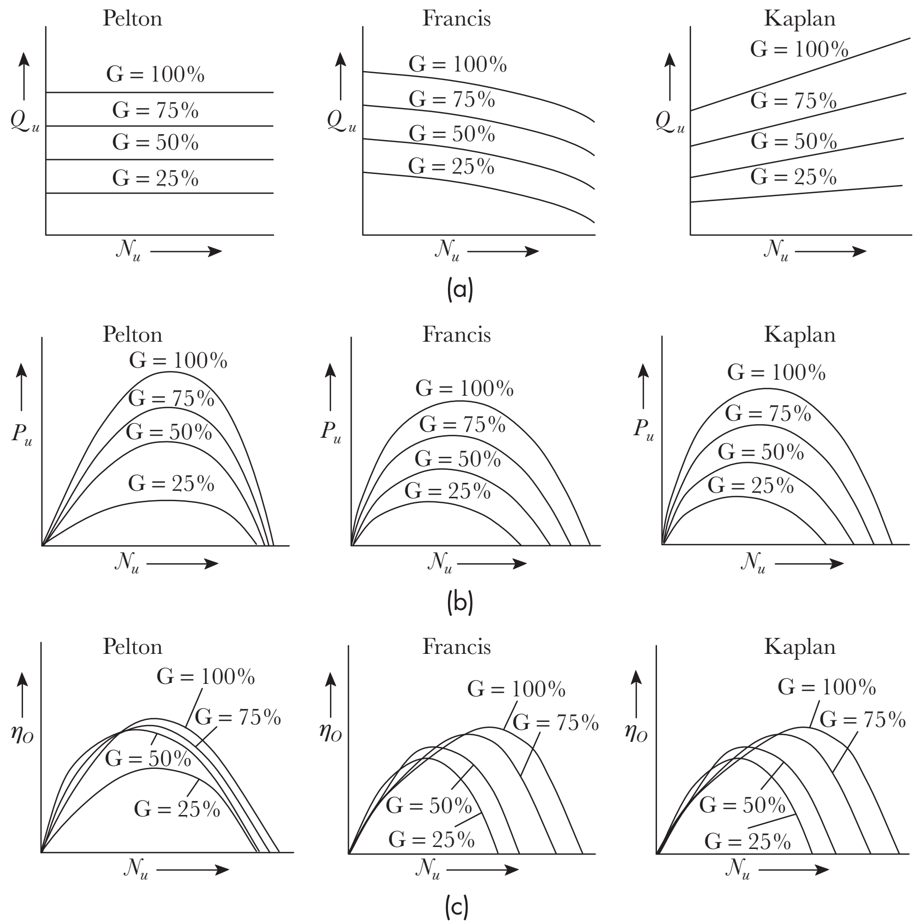

Fig. 9.27 Main characteristics (a) Q_u versus N_u (b) P_u versus N_u (c) η_o versus N_u

speed of the runner and the discharge remains fixed as the position of spear is fixed for a particular gate opening. Further, the casing of Pelton turbine does not play any hydraulic role or there is no change in pressure inside the casing. Therefore, the discharge remains undisturbed.

2. In case of Francis turbine, water enters radially into the runner. As the speed of the runner is increased the corresponding centrifugal force, which acts radially outward, will also increase and will act as a barrier to the flow entering into it. That is, why the discharge decreases with the increase in turbine speed.
3. In case of Kaplan turbine, water enters and leaves the turbine runner axially. The discharge increases with the increase in runner speed because of the fact that increased speed causes an increase in centrifugal force. The water is pushed towards the wall resulting into a low pressure region near the turbine shaft. This region gets filled by drawing more quantity of water from the whirl chamber, thus resulting in an increased discharge.
4. It has been seen earlier in the description of Pelton wheel, there exists a parabolic relation between the power output as well as the hydraulic efficiency and the tangential speed of the runner u. Similarly, it can be shown such a relation does exist in the reaction turbines as well. The power output is higher for larger gate openings as power output is a function of discharge.

9.8.2 Operating Characteristics

The constant speed curves are also known as operating characteristics because of the fact that the turbine is required to operate at a constant speed to produce a constant frequency electrical power while the available head at the turbine inlet keeps on changing from day to day and from season to season. The typical operating characteristics of a water turbine are shown in Fig. 9.28.

It should be noted that these characteristics are drawn by varying the load in such a way that for a given head the turbine speed remains constant. Following are the observations:

1. A turbine starts rotating only after a particular value of discharge Q_0. Lower than this value, the discharge is not enough to start the turbine. Hence, both power output and the efficiency are zero till this value of discharge. Beyond this point, power output varies linearly with discharge as power developed by the runner is proportional to discharge. Hydraulic efficiency, on the other hand, increases with discharge but the behaviour is non-linear. The non-linearity can be attributed to non-linearity in different types of losses such as mechanical, volumetric, etc. (Fig. 9.28a).

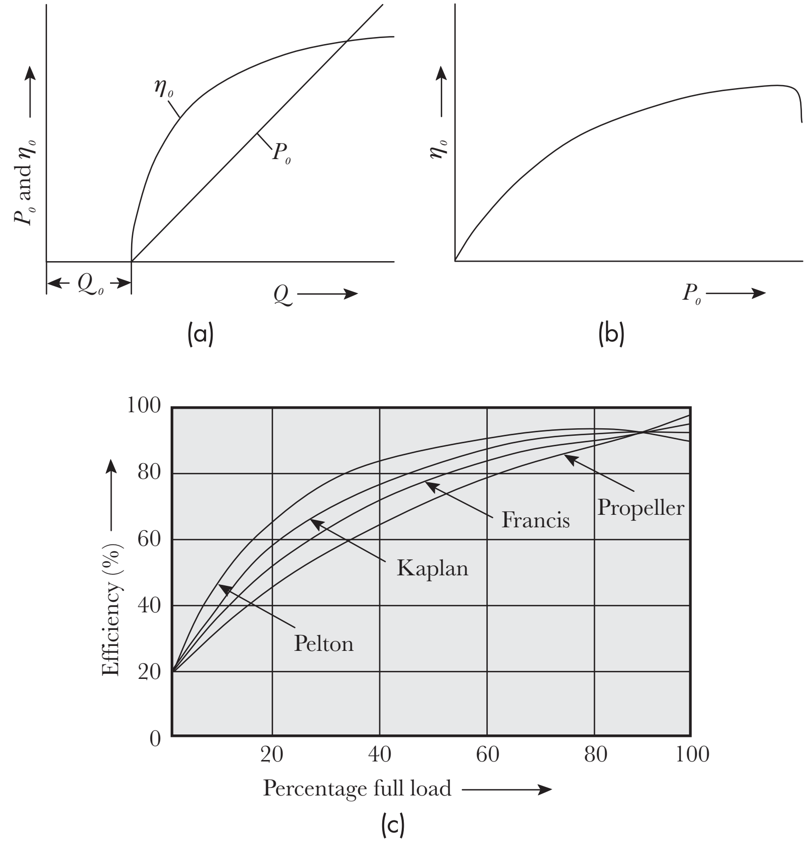

Fig. 9.28 Operating characteristics (a) η_h versus Q and P_o versus Q (b) η_h versus P_o (c) η_h versus percentage full load

2. The variation of efficiency with power output is also non-linear, as shown in Fig. 9.28(b). There is a sudden drop in efficiency after it has attained a maximum value. Higher the available head higher will be the power output. Similarly, higher the discharge higher will be the power output. Power output is thus dependent on both discharge as well as the available head. The sudden drop in efficiency may be due to the increase in input (available head and/or discharge).
3. Figure 9.28(c) shows the variation in efficiency with the percentage full load for all types of turbines. With the increase in load, the efficiency increases in all turbines. Pelton turbine gives the highest efficiency for different loads. The efficiency of Kaplan turbine approaches that of Pelton turbine. Francis turbine gives a satisfactory performance. Propeller turbine performs badly at varying loads.

9.8.3 Muschel Characteristics

Muschel characteristics or isoefficiency curves are obtained from the data collected for plotting main and operating characteristic curves. The primary objective of these curves is to locate the regions of constant efficiencies. A simple procedure has been depicted in Fig. 9.29. The discharge versus speed characteristics and efficiency versus speed characteristics for different gate openings for a given turbine (Kaplan turbine in the present case) are taken into consideration. The constant efficiency line, say for $\eta_o = 0.2$, is drawn on efficiency versus speed characteristics. This line intersects the curves for various gate openings. The lines from these points of intersections are projected vertically upwards to intersect the corresponding gate opening curves on discharge versus speed characteristics. The points of intersection of vertical

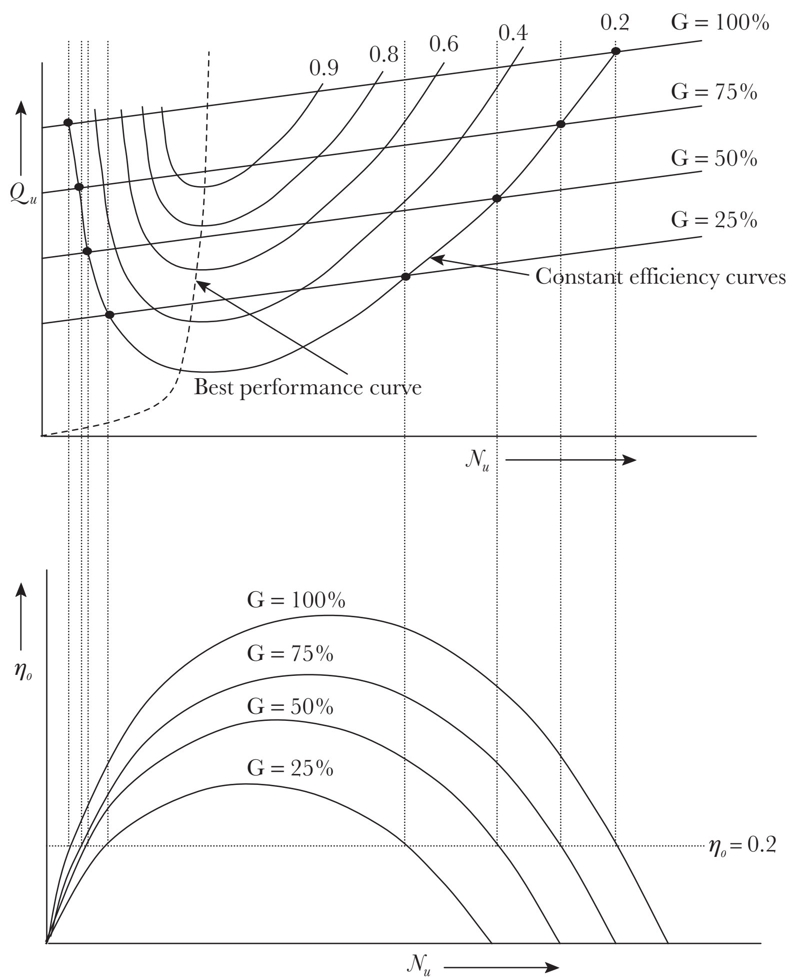

Fig. 9.29 Muschel characteristics

projectors and the discharge-speed curves are joined together by means of a smooth line. This smooth line is the constant efficiency curve corresponding to $\eta_o = 0.2$. In a similar fashion, the constant efficiency curves for higher values can be plotted, as shown in the diagram.

9.9 HYDROELECTRIC POWER PLANT

The hydroelectric power plant, as shown in Fig. 9.30, consists of a water reservoir (2) with a dam (3) on one side. The free surface of water in the reservoir is known as head race (1). At the bottom of the dam a pipe, known as penstock (6), is used to transmit high-pressure water to the turbine through a surge tank (5). The surge tank is provided to take care of pressure pulse known as *water hammer* generated inside the penstock due to the sudden closure of valve at turbine inlet during low load conditions.

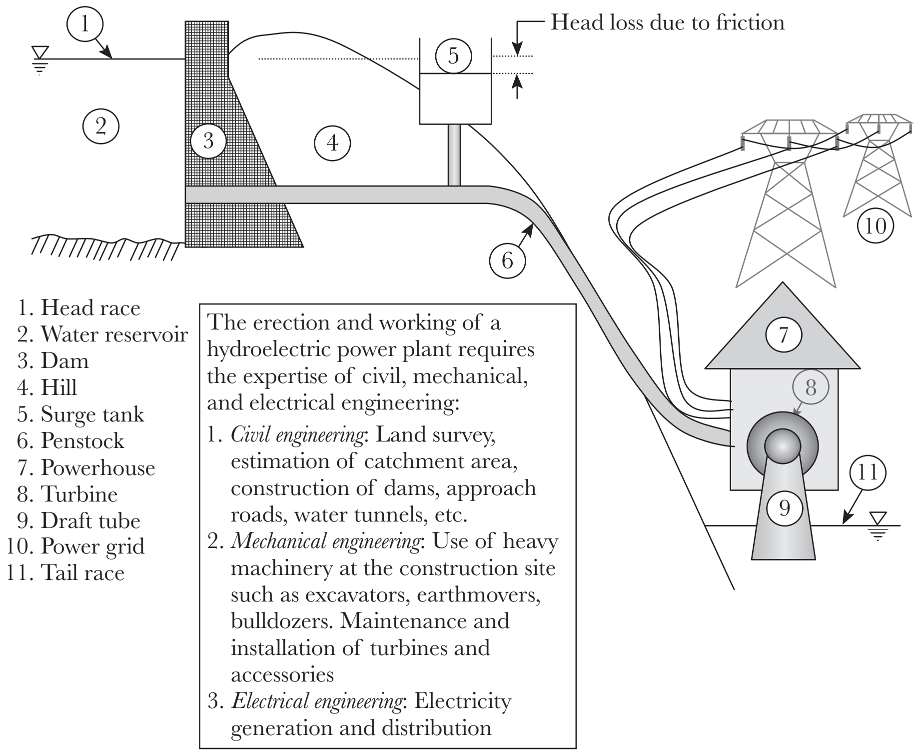

Fig. 9.30 Schematic diagram of hydroelectric power plant

On the other hand if the load is increased, the excess water is compensated through the surge tank. The flow of water needs to be regulated as per the changing load during the day. It should be noted that there will be a difference in the level of water in the reservoir and in surge tank, which is equivalent to

frictional losses in the section of penstock between reservoir and surge tank. The power house (7) consists of turbine (8) coupled with the electric generator (not shown in the figure). The turbine rotates due to the dynamic action of high-pressure water entering through the penstock. The turbine in turn rotates the three-phase electric generator, which produces electric power. The generated power is transmitted to various localities through a number of substations by means of the grid (10). The water after doing work in the turbine is rejected to the tail race (11) through the draft tube (9).

9.10 PUMPS

Pumps are used to increase the pressure energy/potential energy of liquid by doing mechanical work on the given fluid. The rotating element of a pump is known as *impeller*. The mechanical work to the pumps is supplied by an electric motor or an engine coupled with its impeller. The pumps are generally classified into *positive displacement pumps* and *non-positive displacement* or *rotodynamic pumps*.

In a *positive displacement pump*, there is no flow reversal, that is, the liquid is sucked into a chamber. From there it is activated by a mechanical member to a high pressure or potential region. Examples are reciprocating pump, gear pump, screw pump, peristaltic pump, rotary vane pump, etc. The fluid volume is, thus, positively displaced. In a *rotodynamic pump*, the dynamic action of rotating fluid element increases the pressure energy of water. The flow reversal may occur at some place inside the pump. The example is centrifugal pump. In this section, one pump from each category will be discussed in detail and they are centrifugal pump and reciprocating pumps.

9.10.1 Centrifugal Pump

It is a rotodynamic pump which uses a rotating impeller to increase the pressure energy of a fluid. Centrifugal pumps are the most commonly used pump to transport liquids through a pipe network. These pumps are similar in construction to Francis turbine but differ in functioning. In centrifugal pumps, the fluid enters axially and laves radially into the volute casing through the diffuser. The shape of the impeller resembles the runner of Francis turbine. Centrifugal pumps are used for low heads and high discharge. They are classified on the basis of the following factors:

1. Type of casing
2. Number of stages
3. Working head
4. Flow direction
5. Specific speed

This classification has been shown in Table 9.5.

Table 9.5 Classification of centrifugal pumps

Type of casing	Number of stages	Working head	Flow direction (Specific speed)
Volute	Single stage	Low head ($H < 15\,\text{m}$)	Radial flow (10–70)
Vortex chamber	Multistage	Medium head ($15\,\text{m} < H < 45\,\text{m}$)	Mixed flow (70–135)
Diffuser		High head ($H > 45\,\text{m}$)	Axial flow (100–425)

Types of Casing

A centrifugal pump may have the following types of casing:

Volute casing is of a spiral shape with uniformly increasing cross-sectional area, as shown in Fig. 9.31. This increasing area serves twin purposes: (a) accommodates the increased quantity of water towards the pipe delivery, which will ensure that the jet leaves the impeller blade with the same velocity (b) the kinetic energy of the flowing water gets converted into pressure energy.

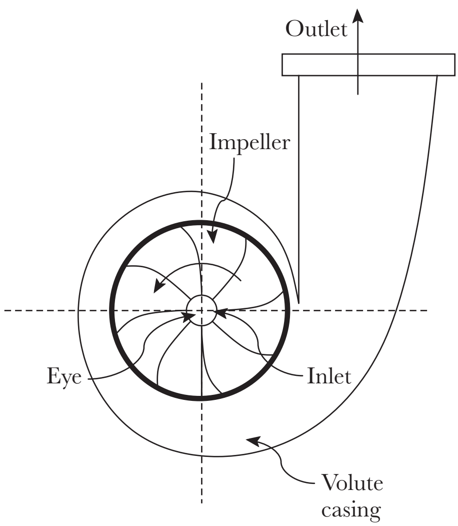

Fig. 9.31 Volute pump

Vortex chamber is formed by providing a uniform radial clearance between the impeller and volute casing known as vortex or whirl pool chamber. The basic idea behind this arrangement is that increased area causes a reduction in velocity and increase in pressure. The provision of this chamber enhances the efficiency of the pump (Fig. 9.32).

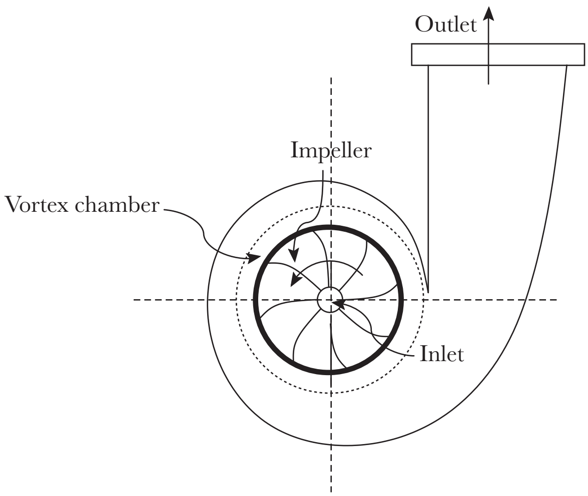

Fig. 9.32 Vortex pump

Diffuser pump has a guide wheel between the impeller and the casing. The area of flow between the guide vanes is such that it increases in the outward radial direction which facilitates an increase in pressure. That is why the guide wheel in the pump is termed as diffuser. Since the pump resembles Francis turbine, it is also known as *turbine pump*. The water is made to enter the guide vanes at a proper angle to avoid losses due to shocks. If the operating conditions change frequently, the use of such pumps is not recommended at such places (Fig. 9.33).

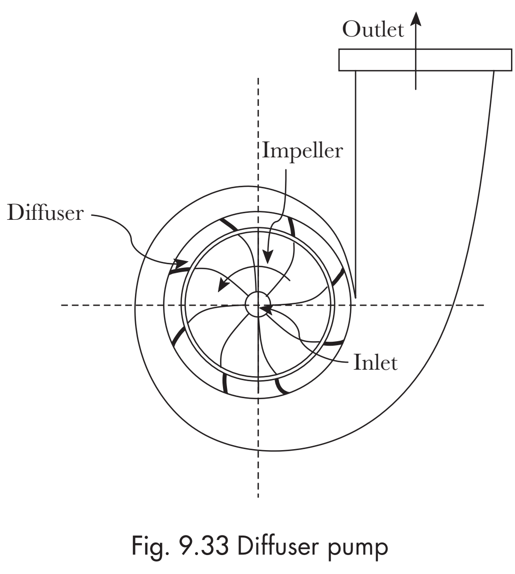

Fig. 9.33 Diffuser pump

Number of Stages

On the basis of number of stages, pumps can be classified as single-stage and multistage pumps. A single-stage pump has one impeller whereas multistage pumps have more than one impeller. As mentioned earlier, the centrifugal pumps are low head and high-discharge pumps. The multistaging is done to increase the pressure at the delivery (outlet). Multistage pumps can have series as well as parallel arrangements. In former case, the objective is to achieve a high head, whereas in the latter case very high discharge is the aim. The series arrangement can be obtained either by using multiple impellers mounted on the same shaft and housed in the same casing, as shown in Fig. 9.34 or by connecting individual pumps such that the outlet of one is the inlet of other. Multistage pumps are usually provided with guide vanes whereas single-stage pumps are of volute or vortex type.

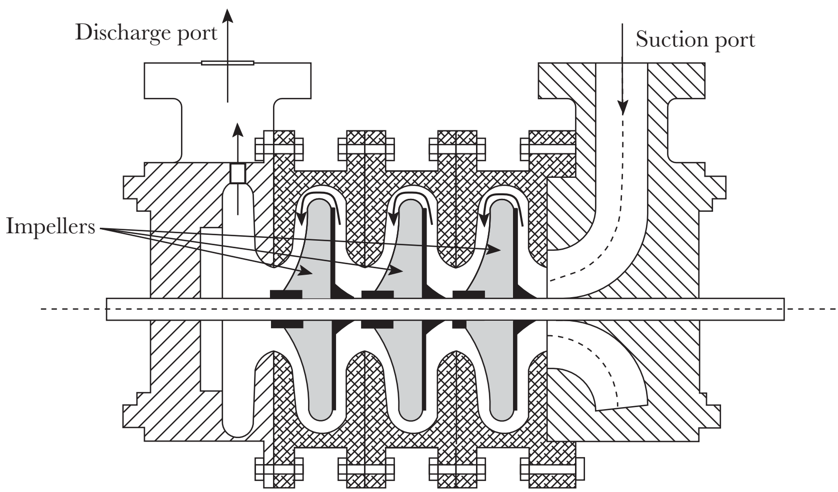

Fig. 9.34 Multistage pump-series arrangement

In multistage parallel arrangement, outlets of individual pumps are connected to a single delivery pipe. Thus, discharge at the outlet of delivery pipe is the sum of discharges of individual pumps.

Flow Direction

On the basis of direction of flow, the pumps are classified as radial flow, mixed flow, and axial flow pumps. The half-sectional views of these pumps along with flow directions are shown in Fig. 9.35. In radial flow pump, fluid enters and leaves the pump impeller radially. In mixed flow pump, fluid enters the pump impeller axially and leaves it radially. In axial flow pump, fluid enters and leaves the impeller axially.

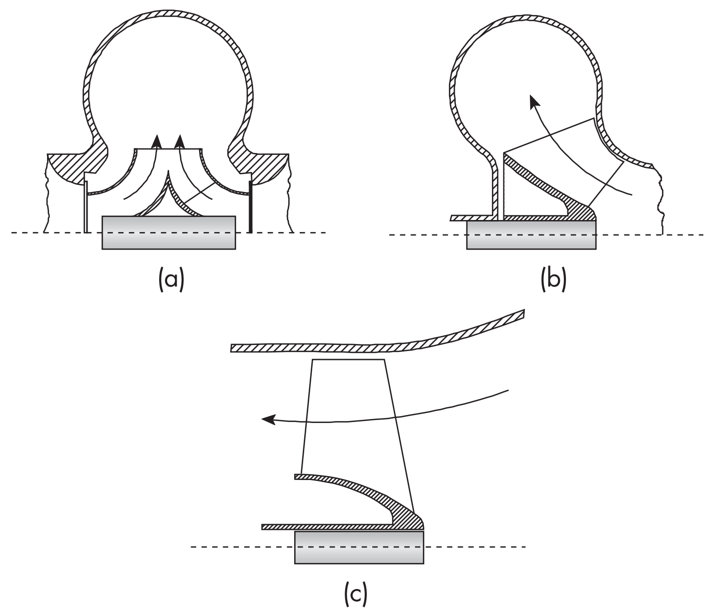

Fig. 9.35 Pumps (a) Radial flow (b) Mixed flow (c) Axial flow

Specific Speed

The *specific speed* of a pump is defined as the speed of geometrically similar pump which delivers unit discharge at unit head. The tangential speed of the pump having impeller diameter D is given by

$$u = \frac{\pi DN}{60} \quad \Rightarrow \quad N \propto \frac{u}{D} \quad \Rightarrow \quad N \propto \frac{\sqrt{H}}{D} \tag{9.65}$$

as u is proportional to the square root of head developed from the definition of speed ratio.

The discharge through the pump is

$$Q = \pi BDV_f \quad \Rightarrow \quad Q \propto D^2 V_f \quad \text{as} \quad B/D = n \quad \Rightarrow \quad D \propto \sqrt{\frac{Q}{V_f}} \tag{9.66}$$

since V_f is proportional to the square root of head developed from the definition of flow ratio. Thus,

$$D \propto \frac{\sqrt{Q}}{H^{1/4}} \tag{9.67}$$

From Eqs (9.65) and (9.67)

$$N \propto \frac{H^{3/4}}{\sqrt{Q}} \quad \Rightarrow \quad N = \frac{CH^{3/4}}{\sqrt{Q}} \tag{9.68}$$

where C is the constant of proportionality.

From the definition of specific speed of pump, $N = N_s$ if $Q = 1$ and $H = 1 \Rightarrow$ $C = N_s$

$$N_s = N\frac{\sqrt{Q}}{H^{3/4}} \tag{9.69}$$

Working Principle of Centrifugal Pump

A centrifugal pump, as shown in Fig. 9.36(a), as described earlier is used to increase the pressure energy of water and is connected to the tank and sump by means of delivery and suction pipes, respectively. The pump creates a negative pressure at the suction side causing the water to be sucked from the sump. The priming valve is provided at the top of the casing to prime the pump. *Priming* is the process of filling the casing of the pump with water before starting the pump. If the casing is not filled with water, it will have air inside. The head developed is proportional to the density of fluid. Since air has very low density, the head created is too small to lift water from the sump. The rotating element of the pump as discussed earlier is known as *impeller*, which is coupled to the shaft of the driving motor or engine. An impeller may be shrouded or unshrouded (open), as shown in Fig. 9.36(b). Open impellers are less efficient than shrouded ones due to back leakage and turbulence caused by the motion of open blades close to the fixed casing. However, they are less prone to blockage by mud or weeds. The shrouded impellers

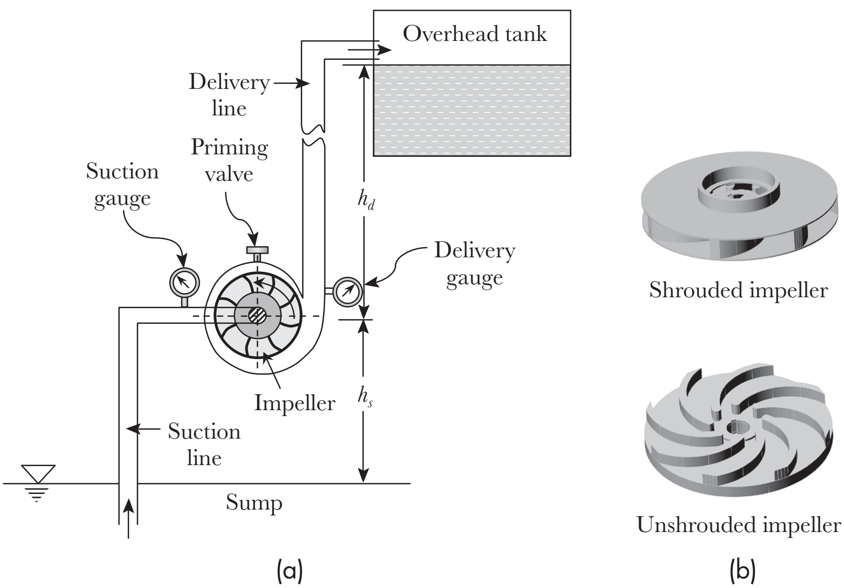

Fig. 9.36 Single-stage centrifugal pump (a) Schematic diagram (b) Impellers

are considerably more robust and less inclined to be damaged by stones or other objects passing through. The cost to manufacture open impellers is less as compared to shrouded impellers. The shrouded impellers have higher efficiency.

To understand the functioning of pump, the knowledge of following various types of pump heads is a must:

Static head It is the vertical distance between the levels of water in the overhead tank and the sump.

$$H_s = h_s + h_d \tag{9.70}$$

where h_s is the suction head and h_d is the delivery head.

Total head It is the necessary head developed by a pump to deliver water from the sump level to the delivery tank level.

$$H = h_s + h_d + h_{fs} + h_{fd} + \frac{V_d^2}{2g} \tag{9.71}$$

where h_s is the suction head, h_d is the delivery head, h_{fs} and h_{fd} are the friction head loss in suction and delivery pipes respectively, and V_d is the discharge velocity.

Manometric head It is the pressure head rise across the impeller. It is called manometric head as a manometer measures the difference in pressure between these two points. If the gauges are installed as close to the pump as possible, the difference in their reading will give the manometric head.

$$H_m = H_{md} - H_{ms} \tag{9.72}$$

where H_{ms} can be evaluated by applying Bernoulli's equation between sump level and the pump centre line and H_{md} by applying Bernoulli's equation between the pump centre line and level of water in the delivery tank, as

$$H_{ms} = \frac{p_s}{\rho g} \Rightarrow H_{ms} = \frac{p_{\text{atm}}}{\rho g} - \frac{V_s^2}{2g} - h_s - h_{fs} \tag{9.73}$$

$$H_{md} = \frac{p_d}{\rho g} \Rightarrow H_{md} = \frac{p_{\text{atm}}}{\rho g} + h_d + h_{fd} \tag{9.74}$$

Therefore, the manometric head is given by

$$H_m = h_s + h_d + h_{fs} + h_{fd} + \frac{V_s^2}{2g} \tag{9.75}$$

If the diameters of the suction and delivery pipes are same, the velocity inside the suction and delivery pipes will also be the same as per the continuity equation. In such a case, the manometric head will be same as the total head.

Centrifugal head It is also known as Euler's head. It is the head imparted by impeller to the fluid. Since centrifugal pump is similar in construction to Francis turbine, the impeller blades are designed in such a way that the flow at the inlet of impeller is radial, that is, $V_{w1} = 0$ or $\alpha_1 = 0$.

$$H_{eu} = \frac{V_{w2}u_2}{g} \Rightarrow H_{eu} = \frac{V_2^2 - V_1^2}{2g} + \frac{V_2^2 - V_1^2}{2g} + \frac{V_{r1}^2 - V_{r2}^2}{2g} \tag{9.76}$$

The phenomenon of *cavitation* is also present in centrifugal pumps. In these pumps, cavitation is likely to occur at the suction (inlet) of pump where the pressure is negative (less than atmospheric pressure). Therefore, in order to avoid cavitation, the absolute pressure at the suction must not be less than the vapour pressure. The pump position above the sump level can be adjusted to avoid cavitation. The limiting value of suction lift is obtained by applying the Bernoulli's equation between the pump centre line and the sump level and replacing the suction pressure with vapour pressure as (refer Eq. 9.73)

$$\frac{p_s}{\rho g} = \frac{p_{atm}}{\rho g} - \frac{V_s^2}{2g} - h_s - h_{fs} \tag{9.77}$$

The limiting value of suction lift beyond which the cavitation may occur is given by

$$h_{s,\,lim} = \frac{p_{atm}}{\rho g} - \frac{p_v}{\rho g} - \frac{V_s^2}{2g} - h_{fs} \tag{9.78}$$

The net positive suction head, NPSH, is defined as the suction head available at pump inlet above the head corresponding to vapour pressure $(p_v/\rho g)$ at the pump inlet.

$$\text{NPSH} = \frac{p_s}{\rho g} + \frac{V_s^2}{2g} - \frac{p_v}{\rho g} \tag{9.79}$$

From Eq. (9.77), the NSPH can be written as shown:

$$\text{NPSH} = \frac{p_{atm}}{\rho g} - \frac{p_v}{\rho g} - h_s - h_{fs} \tag{9.80}$$

Thoma's cavitation parameter is defined as the ratio of net positive suction head to the manometric or total head developed by the pump

$$\sigma = \frac{\text{NPSH}}{H} \Rightarrow \sigma = \frac{\left(\frac{p_{atm}}{\rho g} - \frac{p_v}{\rho g} - h_s - h_{fs}\right)}{H} \tag{9.81}$$

Thoma's cavitation factor becomes critical if the head corresponding to vapour pressure is replaced by the absolute suction pressure head.

$$\sigma_c = \frac{\left(\frac{p_{atm}}{\rho g} - \frac{p_s}{\rho g} - h_s - h_{fs}\right)}{H} \tag{9.82}$$

The cavitation in a pump does not occur if $\sigma > \sigma_c$ ($p_v < p_s$). Smaller values of suction lift are recommended. It has also been seen that, in order to avoid cavitation, sometimes the pump is installed below the sump level, that is, h_s becomes negative.

Efficiencies of a Centrifugal Pump

In centrifugal pump, electric motor transmits power to the pump through a coupling mounted on their shafts. In fact, the power transmission in a centrifugal pump takes place through a number of intermediate units. More precisely, the electric power received by the motor's stator is transmitted to its rotor by induction. The motor shaft is keyed to the rotor which is connected to the shaft of the pump by means of a coupling. The pump's shaft is keyed to its impeller. The impeller transmits the power to the fluid. The outputs of individual units to their inputs form the genesis of the following efficiencies:

Manometric efficiency It is the ratio of manometric head to Euler's head.

$$\eta_{\text{mano}} = \frac{H_{\text{mano}}}{H_{\text{eu}}} \Rightarrow \eta_{\text{mano}} = \frac{gH_{\text{mano}}}{V_{w2}u_2} \tag{9.83}$$

Mechanical efficiency It is the ratio of power available at the impeller (rate of work done by impeller on fluid) to the power available at the shaft of the pump.

$$\eta_m = \frac{\text{Power available at impeller}}{\text{Shaft power}} \Rightarrow \eta_m = \frac{\rho Q\, gH_{\text{eu}}}{P_{\text{shaft}}} \tag{9.84}$$

Overall efficiency It is the ratio of pump's power output to its power input.

$$\eta_o = \frac{\text{Output power}}{\text{Input power}} \Rightarrow \eta_o = \frac{\rho Q\, gH_{\text{mano}}}{P_{\text{shaft}}} \tag{9.85}$$

Thus, overall efficiency is the product of manometric and mechanical efficiencies.

Effect of Blade Curvature

The impeller's blade outlet angle plays an important role in determining the performance of the centrifugal pump. It can be seen from Fig. 9.37 that changing the outlet blade angle β_2 changes the outlet velocity triangle. The following cases result:

1. If $\beta_2 < 90°$, the blade is termed *forward curved blade* and it rotates at a low speed.
2. If $\beta_2 = 90°$, the blade is termed *radial blade* and it rotates at a medium speed.
3. If $\beta_2 > 90°$, the blade is termed *backward curved blade* and it rotates at a high speed.

The head developed by the pump can be expressed in terms of discharge Q, using Eq. (9.76).

$$H_{\text{eu}} = \frac{V_{w2}u_2}{g} \Rightarrow H_{\text{eu}} = \frac{u_2}{g}(u_2 - V_{f2}\cot\beta'_2) \tag{9.86}$$

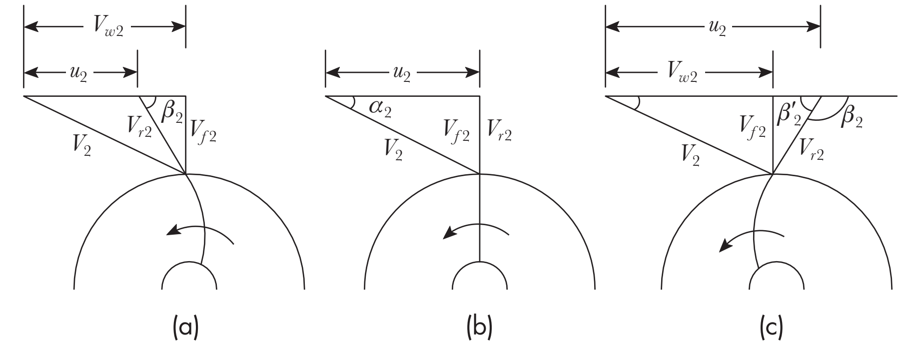

Fig. 9.37 Outlet velocity triangles (a) Forward curved blade (b) Radial blade (c) Backward curved blade

where $V_{f2} = \dfrac{Q}{\pi B_2 D_2}$. Hence Eq. (9.86) can be written as

$$H_{\text{eu}} = \frac{u_2}{g}\left(u_2 - \frac{Q}{\pi B_2 D_2}\cot\beta'_2\right) \tag{9.87}$$

Using Eq. (9.87), H_{eu} versus Q has been plotted for different outlet blades angles in Fig. 9.38(a), which represents a theoretical relationship between them. In case of radial blades, the head developed is independent of the discharge. In pumps with forward curved blades, the head increases with the increase in discharge. On the other hand, in pumps with backward curved blades head decreases with discharge. In actual practice, because of losses the behaviour is not as simple as it looks in Fig. 9.38(a). The actual variation of H_{eu} with Q is shown in Fig. 9.38(b) and power requirement for forward, radial and backward curved blades is shown in Fig. 9.38(c). For both radial and forward curved blades, there is an increase in power with the rise in the flow rate whereas for backward blades, the power decreases

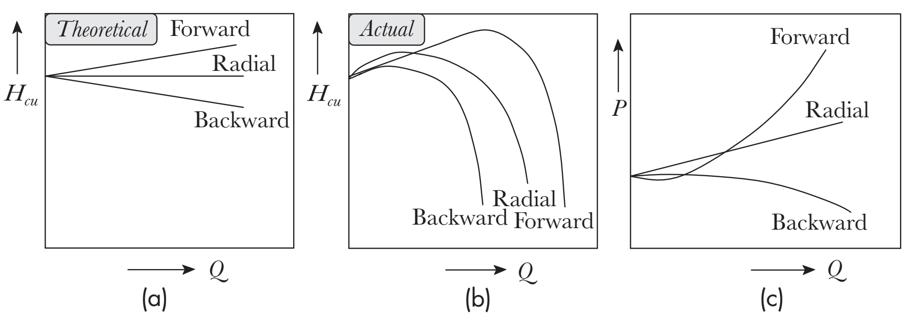

Fig. 9.38 Characteristic curves (a) Theoretical H_{eu} versus Q (b) Actual H_{eu} versus Q (c) P versus Q characteristics

with discharge. The maximum power occurs at low values of discharge in case of pumps with backward curved blades. Power requirement for such pumps decreases with increase in discharge. This allows the electric motor that runs the pump to be safely used at the high discharge. On the other hand, in case of radial and forward curved blade pumps, if motor is rated for maximum power, then most of the time it will remain underutilized. If a lower power rated motor is employed, the increase in discharge beyond design point will result in overloading and burning of the motor. This is why the pumps with backward blades are more common than those with radial or forward blades.

9.10.3 Pump Characteristics

Like turbines, the pump characteristics are also classified as follows:

1. Main characteristics
2. Operating characteristics
3. Constant efficiency curves
4. Constant head discharge curves

The main characteristics are obtained by fixing the pump speed at some arbitrary value as the pump is normally designed to run at a constant speed. This is evident from the fact that the pump is run with the help of an electric induction motor which runs at a constant speed. Therefore, it is advantageous to know the performance of a pump at different speeds. The operating characteristics of a pump are the main characteristics corresponding to design speed of the pump. Figure 9.39(a) shows the typical main characteristics of a pump at a given speed. The design head of a pump is the head corresponding to maximum efficiency. Figure 9.39(b) shows the variation of head, power, and discharge with speed. The head has parabolic variation with speed, power input has cubic variation with speed and discharge has linear variation with speed.

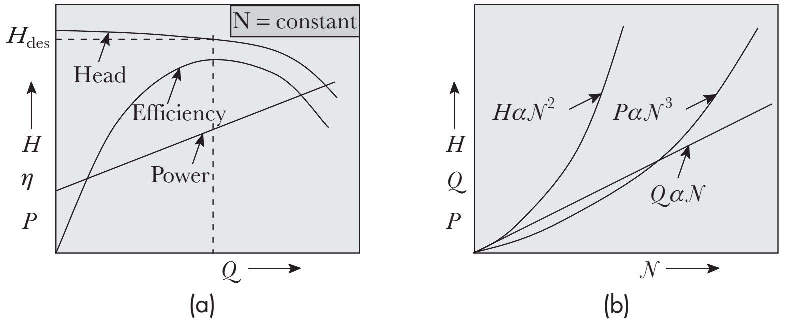

Fig. 9.39 Pump characteristics: Parameters variation with (a) Discharge (b) Speed

The constant efficiency or Muschel curves can be obtained in a similar fashion as they have been obtained for turbines in Section 9.8.3.

Example 9.11 The impeller of a centrifugal pump has an internal diameter of 200 mm and external diameter 400 mm. The widths of the impeller at entry and exit are 20 and 10 mm, respectively. The discharge of water through the impeller is 20 L/s. The impeller rotates at 1440 rpm and the blade angle at the outlet is 30°. Determine the pressure head rise in the impeller neglecting friction losses.

Given data:

Internal diameter, $D_1 = 200$ mm	External diameter, $D_2 = 400$ mm
Inlet width, $B_1 = 20$ mm	Outlet width, $B_2 = 10$ mm
Impeller speed, $N = 1440$ rpm	Discharge, $Q = 0.02$ m³/s
Outlet blade angle, $\beta_2 = 30°$	

Solution: Applying energy balance across the impeller.

Head at the outlet = Head at the inlet + Euler's head (head generated by the impeller)

$$\frac{p_2}{\rho g} + \frac{V_2^2}{2g} + z_2 = \frac{p_1}{\rho g} + \frac{V_1^2}{2g} + z_1 + \frac{V_{w2} u_2}{g}$$

The difference between inlet and outlet can be neglected, that is, $z_1 = z_2$. The pressure rise in the impeller is the

$$\Rightarrow \quad \frac{p_2 - p_1}{\rho g} = \frac{V_1^2 - V_2^2}{2g} + \frac{V_{w2} u_2}{g}$$

From the outlet velocity triangle (Fig. 9.40) of the centrifugal impeller,

$$V_{w2} = u_2 - V_{f2} \cot \beta_2$$

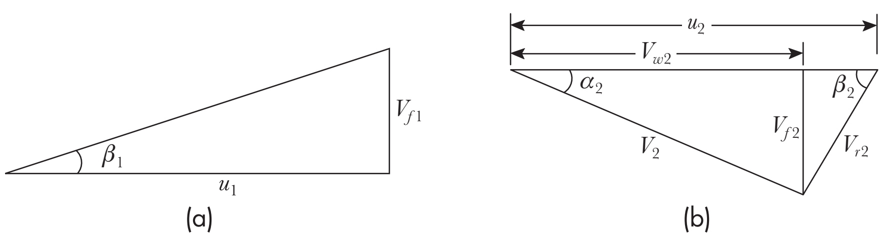

Fig. 9.40 Velocity triangles (a) Inlet (b) Outlet

where

$$u_2 = \frac{\pi D_2 N}{60} \quad \Rightarrow \quad u_2 = 30.16 \text{ m/s}$$

$$V_{f2} = \frac{Q}{\pi B_2 D_2} \quad \Rightarrow \quad V_{f2} = 1.59 \text{ m/s}$$

Therefore, $V_{w2} = 27.4$ m/s.

The absolute velocity at the outlet can be obtained from the outlet velocity,

$$V_2^2 = V_{w2}^2 + V_{f2}^2 \quad \Rightarrow \quad V_2 = 27.446\,\text{m/s}$$

From the inlet velocity triangle, $V_1 = V_{f1}$

$$V_{f1} = \frac{Q}{\pi B_1 D_1} \quad \Rightarrow \quad V_{f1} = 1.59\,\text{m/s}$$

Therefore, the pressure rise in impeller is

$$\frac{p_2 - p_1}{\rho g} = \frac{V_1^2 - V_2^2}{2g} + \frac{V_{w2} u_2}{g} \quad \Rightarrow \quad \frac{p_2 - p_1}{\rho g} = 46\,\text{m} \quad \Rightarrow \quad \Delta p = 451\,\text{kPa}$$

Example 9.12 The static lift of a centrifugal pump is 50 m of which 5 m is suction lift. The diameter for suction and delivery pipes is 250 mm. The head loss due to friction loss in suction and delivery pipes is 1.5 and 7.5 m, respectively. The pump has an impeller of diameter 500 mm and width 50 mm at outlet and is running at 1440 rpm. The exit blade angle is 15°. If manometric efficiency is 85%, determine the discharge and pressure at suction and delivery.

Given data:

Static head, $H_s = 50\,\text{m}$	Suction lift, $h_s = 5\,\text{m}$
Outlet diameter, $D_2 = 0.5\,\text{m}$	Outlet width, $B_2 = 50\,\text{mm}$
Friction loss in suction pipe, $h_{fs} = 1.5\,\text{m}$	Friction loss in delivery pipe, $h_{fd} = 7.5\,\text{m}$
Pipe diameters, d_s or $d_d = 0.25\,\text{m}$	Outlet blade angle, $\beta_2 = 15°$
Overall efficiency, $\eta_{\text{mano}} = 0.85$	Impeller speed, $N = 1440\,\text{rpm}$

Solution: A schematic diagram for the problem has been shown in Fig. 9.41.

Net or manometric head,

$$H_m = H_s + h_{fs} + h_{fd} \quad \Rightarrow \quad H_m = 59\,\text{m}$$

The peripheral velocity at outlet

$$u_2 = \frac{\pi D_2 N}{60} \quad \Rightarrow \quad u_2 = 37.7\,\text{m/s}$$

From the expression of manometric efficiency, the whirl velocity at the outlet is

$$V_{w2} = \frac{gH_m}{\eta_{\text{mano}} u_2} \quad \Rightarrow \quad V_{w2} = 18.06\,\text{m/s}$$

From the outlet velocity triangle

$$V_{f2} = (u_2 - V_{w2}) \tan \beta_2 \quad \Rightarrow \quad V_{f2} = 5.26\,\text{m/s}$$

Discharge,

$$Q = \pi B_2 D_2 V_{f2} \quad \Rightarrow \quad Q = 0.41\,\text{m}^3/\text{s}$$

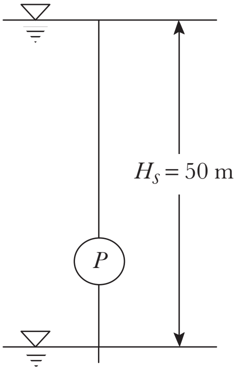

Fig. 9.41 Schematic diagram

Since the diameters of the two pipes are same, the velocity will also be same. The velocity delivery pipe,

$$V_d = \frac{4Q}{\pi d_d^2} \Rightarrow V_d = 8.35\,\text{m/s} = V_s$$

The pump should be able to generate a head equal to delivery lift and to overcome friction in the delivery pipe,

$$\frac{p_d}{\rho g} + \frac{V_d^2}{2g} = H_d + h_{fd} \Rightarrow \frac{p_d}{\rho g} = 48.9\,\text{m} \Rightarrow p_d = 480\,\text{kPa (gauge)}$$

Similarly, energy balance at suction gives

$$\frac{p_s}{\rho g} = \frac{p_{\text{atm}}}{\rho g} - \frac{V_s^2}{2g} - h_s - h_{fs} \Rightarrow \frac{p_s}{\rho g} = -10.05\,\text{m} \Rightarrow p_s = -98\,\text{kPa (gauge)}$$

The gauge reading in the atmosphere is zero.

Pump Affinity Laws

The pump affinity laws are used to predict the performance of rotodynamic pumps. The performance of geometrically similar pump impellers operating under dynamically similar conditions is estimated by applying the dimensional analysis (refer chapter 10). The performance of a pump is described by three important parameters H, Q, and P, as mentioned in the previous section.

The following is the step-by-step procedure:

1. Non-dimensionalizing the parameters H, Q, and P by dividing corresponding dimensions in terms of impeller diameter D and impeller speed N.

Total head $\dfrac{H}{V^2/g}$ or $\dfrac{H}{N^2D^2/g}$ or $\dfrac{gH}{N^2D^2}$ and it should be constant for the two geometrically similar pumps, that is,

$$\frac{H_1}{N_1^2D_1^2} = \frac{H_2}{N_2^2D_2^2} = \text{constant} \quad \text{or} \quad \boxed{\frac{H_2}{H_1} = \frac{N_2^2D_2^2}{N_1^2D_1^2}} \tag{9.88}$$

Discharge $\dfrac{Q}{ND^3}$ and it should be constant for the two geometrically similar pumps, that is,

$$\frac{Q_1}{N_1D_1^3} = \frac{Q_2}{N_2D_2^3} = \text{constant} \quad \text{or} \quad \boxed{\frac{Q_2}{Q_1} = \frac{N_2D_2^3}{N_1D_1^3}} \tag{9.89}$$

Power $\dfrac{P}{\rho QgH}$ or $\dfrac{P}{\rho(ND^3)g(N^2D^2/g)}$ or $\dfrac{P}{\rho N^3D^5}$ and it should be constant for the two geometrically similar pumps, that is,

$$\frac{P_1}{N_1^3D_1^5} = \frac{P_2}{N_2^3D_2^5} = \text{constant} \quad \text{or} \quad \boxed{\frac{P_2}{P_1} = \frac{N_2^3D_2^5}{N_1^3D_1^5}} \tag{9.90}$$

2. Making either impeller diameter D constant or impeller speed N constant

First law D = constant

Equations (9.88), (9.89), and (9.90) give

$$\frac{H_2}{H_1} = \frac{N_2^2}{N_1^2}; \quad \frac{Q_2}{Q_1} = \frac{N_2}{N_1}; \quad \frac{P_2}{P_1} = \frac{N_2^3}{N_1^3} \tag{9.91}$$

Second law N = constant

Equations (9.88), (9.89), and (9.90) give

$$\frac{H_2}{H_1} = \frac{D_2^2}{D_1^2}; \quad \frac{Q_2}{Q_1} = \frac{D_2^3}{D_1^3}; \quad \frac{P_2}{P_1} = \frac{D_2^5}{D_1^5} \tag{9.92}$$

Example 9.13 A centrifugal pump having an impeller diameter 350 mm runs at a speed of 600 rpm under normal operating conditions. It was tested at 600 rpm and the following head and discharge data is obtained:

Discharge, L/s	Head, m
400	4.5
250	7.2
190	8.0
125	8.6
0	10.5

Generate the pump curves for the speeds of 500 and 400 rpm.

Solution: Since speed is not constant, first law of pump affinity is used to find out the discharge and corresponding head using the head and discharge data for 600 rpm pump speed.

Pump speed, rpm	Discharge, L/s $Q_2 = \frac{N_2}{N_1} Q_1$	Head, m $H_2 = \frac{N_2^2}{N_1^2} H_1$
500	333.33	3.13
	208.33	5.00
	158.33	5.56
	104.17	5.97
	0.00	7.29
400	266.67	2.00
	166.67	3.20
	126.67	3.56
	83.33	3.82
	0.00	4.67

These data points are plotted in Fig. 9.42.

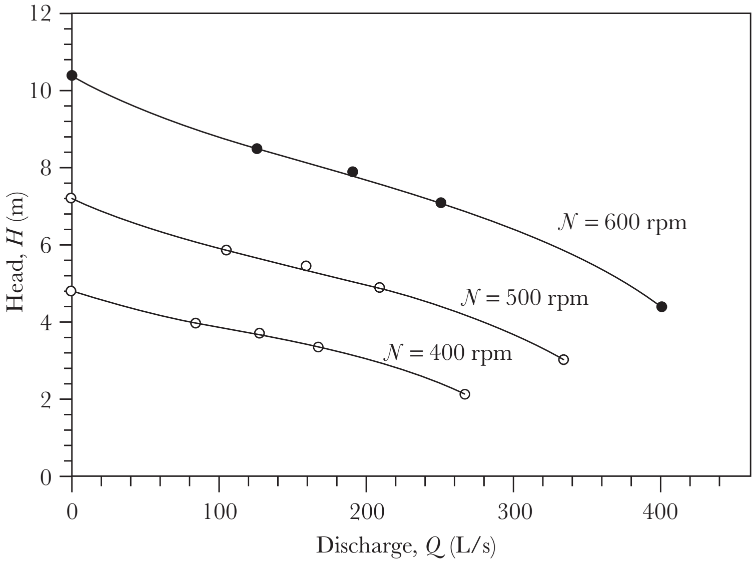

Fig. 9.42

Example 9.14 A centrifugal pump of impeller diameter 250 mm running at 1400 rpm requires 15 kW to deliver 30 L/s at a head of 30 m. Determine its new discharge, head, power required if the impeller diameter is reduced to 150 mm.

Given data:

$Q_1 = 30\,\text{L/s}$	$D_1 = 250\,\text{mm}$
$H_1 = 30\,\text{m}$	$D_2 = 150\,\text{mm}$
$P_1 = 15\,\text{kW}$	$N = 1400\,\text{rpm}$

Solution: Since there is no mention to speed change, second law of pump affinity can be applied comfortably.

The new head is

$$H_2 = \frac{D_2^2}{D_1^2}H_1 \quad \Rightarrow \quad H_2 = \left(\frac{150}{250}\right)^2 \times 30 \quad \Rightarrow \quad H_2 = 10.8\,\text{m}$$

The discharge is

$$Q_2 = \frac{D_2^3}{D_1^3}Q_1 \quad \Rightarrow \quad Q_2 = \left(\frac{150}{250}\right)^3 \times 30 \quad \Rightarrow \quad Q_2 = 6.48\,\text{L/s}$$

The power required is

$$\frac{P_2}{P_1} = \frac{D_2^5}{D_1^5} \quad \Rightarrow \quad P_2 = \left(\frac{150}{250}\right)^5 \times 15 \quad \Rightarrow \quad P_2 = 1.16\,\text{kW}$$

9.10.2 Reciprocating Pump

The reciprocating pump is a positive displacement pump which consists of a piston–cylinder arrangement, as shown in Fig. 9.43. The pump is run by means of an induction motor. The rotational motion of motor shaft is converted into reciprocating motion by means of a crank and connecting rod mechanism. The water from the sump is drawn into the cylinder due to backward movement of the piston. The backward movement of the piston forces the suction valve to lift up allowing water to enter into the cylinder. The delivery valve, on the other hand will be pulled down during the suction stroke of the piston.

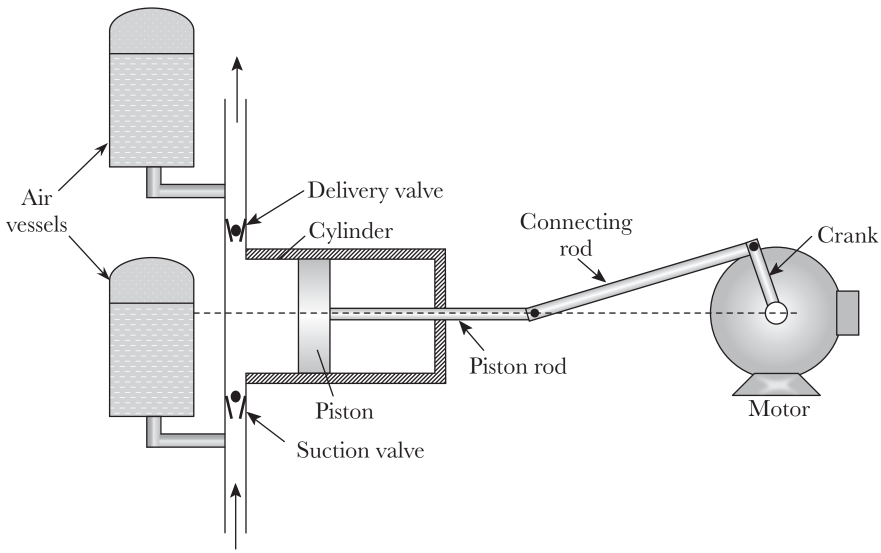

Fig. 9.43 Schematic diagram of a single-acting reciprocating pump

The water inside the cylinder is activated to high pressure by the forward movement of the piston. The forward motion of the piston causes delivery valve to open and suction valve to close. The pump shown in Fig. 9.43 is a *single-acting pump* as only one face of the piston is exposed to the fluid. As such the flow at the delivery side is intermittent or pulsating. If both the faces of piston are exposed to the fluid the pump is known as *double-acting pump*. In such pumps, the discharge at the delivery is continuous. The air vessels are fitted to suction and delivery sides to make the flow continuous.

The air vessels, as the name indicates, has air which gets compressed as the water is drawn into the chamber due to the piston movement. The compressed air in the air vessel at suction side pushes the water into the cylinder during the suction stroke. The compressed air in the air vessel at delivery side pushes the water into delivery line when the delivery valve is closed and, thus, making

the flow continuous in delivery line. The air vessel at delivery side is provided only with the single-acting pump. The air vessel at suction reduces the chances of cavitation, longer suction pipes can be used and the pump can be run at a higher speed. The air vessel on delivery side, on the other hand, helps in removing pulsation in the flow and helps in reducing friction losses resulting in saving of power.

The reciprocating pumps are useful for high head and low discharge applications. Due to rubbing surfaces, the maintenance cost is too high and because of this they have limited applications.

The theoretical discharge through a single-acting pump is calculated using the following relation:

$$Q_{\text{th}} = \frac{LAN}{60} \tag{9.93}$$

where L is the stroke length, A is the cylinder bore area, and N is the speed in rpm. For double-acting pump, the theoretical discharge becomes

$$Q_{\text{th}} = \frac{LAN}{60} + \frac{L(A - A_p)N}{60} \tag{9.94}$$

where A_p is the cross-sectional area of the piston rod, which is very small as compared to A. Ignoring A_p,

$$Q_{\text{th}} = \frac{2LAN}{60} \tag{9.95}$$

Theoretical work done by the pump is given by,

$$\dot{W}_{\text{th}} = \rho g Q_{\text{th}} H_s \tag{9.96}$$

Considering all the losses (friction + leakage), the actual input power to the pump is given by

$$P_{\text{in}} = \frac{\rho g Q_{\text{th}} H_s}{\eta} \Rightarrow P_{\text{in}} = \frac{\rho g Q_{\text{th}} (h_s + h_d)}{\eta} \tag{9.97}$$

The difference between the theoretical and actual discharge is known as *slip*. It may be due to leakage loss and time delay in opening and closing of the valves. It is given by

$$\text{Slip} = Q_{\text{th}} - Q_{\text{act}} \tag{9.98}$$

The percentage slip is given by

$$\%\ \text{slip} = \frac{Q_{\text{th}} - Q_{\text{act}}}{Q_{\text{th}}} \times 100 \Rightarrow \%\ \text{slip} = (1 - C_d) \times 100 \tag{9.99}$$

It has been observed that the slip is negative sometimes. The following are the reasons for *negative slip*:

1. The delivery pipe is short.
2. The suction pipe is long.
3. The pump is running at a very high speed.

In any or all of the above cases, the inertia force in the suction line becomes larger than the pressure force above the delivery valve. This results in simultaneous opening of both the valves. Hence, the actual discharge becomes more than the theoretical discharge.

The performance of a reciprocating pump is represented on an indicator diagram, which is a plot between the pressure and volume. The area of the indicator diagram gives the work done. Since area of the cylinder is constant, the volume of the cylinder is a function of piston displacement alone. In addition, the working fluid in a pump is liquid (constant density fluid). The pressure on y-axis can be represented in terms of head. A typical indicator diagram of a reciprocating pump has been shown in Fig. 9.44(b). The piston displacement can be expressed in terms of crank angle [Fig. 9.44(a)]

$$x = r - r\cos\theta = r - r\cos\omega t \tag{9.100}$$

where ω is the angular speed in rad/s.

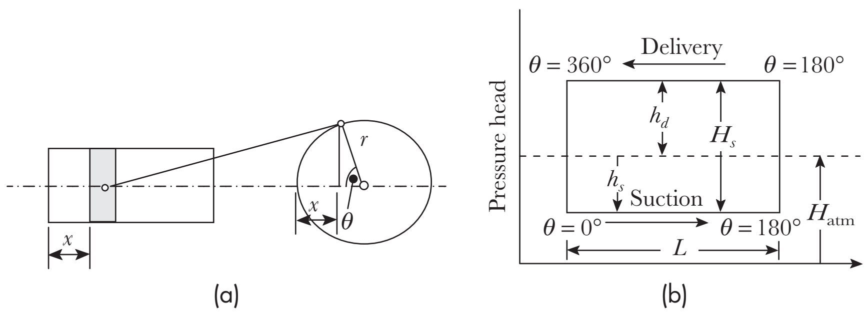

Fig. 9.44 (a) Piston displacement and crank angle (b) Indicator diagram

Effect of Piston Acceleration

To determine the effect of piston acceleration on the net work done, the piston velocity and acceleration can be found out by differentiating the piston displacement once and twice, respectively. The piston velocity is, therefore, given by

$$V = \frac{dx}{dt} = \frac{d}{dt}(r - r\cos\omega t) \quad \Rightarrow \quad V = \omega r \sin\omega t \tag{9.101}$$

The piston acceleration is, therefore, given by

$$\alpha = \frac{d^2x}{dt^2} = \frac{d}{dt}(\omega r \sin \omega t) \quad \Rightarrow \quad \alpha = \omega^2 r \cos \omega t \tag{9.102}$$

The fluid velocity in the delivery or suction pipe can be obtained by applying continuity equation, that is,

$$v = \frac{AV}{a} = \frac{A}{a}\omega r \sin \omega t \tag{9.103}$$

where a is the cross-sectional area of suction/delivery pipe.

The fluid acceleration in suction/delivery pipe is

$$\beta = \frac{dv}{dt} \quad \Rightarrow \quad \beta = \frac{A}{a}\omega^2 r \cos \omega t \tag{9.104}$$

The inertia force in suction/delivery pipe is

$$F = m\beta \quad \Rightarrow \quad F = \rho a l \frac{A}{a}\omega^2 r \cos \omega t \tag{9.105}$$

Intensity of pressure due to accelerating fluid is

$$p = F/a \quad \Rightarrow \quad p = \rho l \frac{A}{a}\omega^2 r \cos \theta \tag{9.106}$$

The accelerating head is

$$h_a = \frac{p}{\rho g} \quad \Rightarrow \quad h_a = l \frac{A}{a}\frac{\omega^2 r}{g}\cos \theta \tag{9.107}$$

At the beginning of stroke, $\theta = 0°$

$$h_a = l \frac{A}{a}\frac{\omega^2 r}{g} \tag{9.108}$$

At the middle of stroke, $\theta = 90°$

$$h_a = 0 \tag{9.109}$$

At the end of stroke, $\theta = 180°$

$$h_a = -l \frac{A}{a}\frac{\omega^2 r}{g} \tag{9.110}$$

Thus, the maximum value of suction and delivery side accelerating heads are given by

$$\left.\begin{aligned} h_{as} &= l_s \frac{A}{a_s}\frac{\omega^2 r}{g} \\ h_{ad} &= l_d \frac{A}{a_d}\frac{\omega^2 r}{g} \end{aligned}\right\} \tag{9.111}$$

The accelerating head is linearly related to the crank radius which, from Eq. (9.100), is a function of piston displacement. Hence, the accelerating head varies linearly with the piston displacement, as shown in Fig. 9.45, on the indicator diagram. The net change in area is zero. Hence, there is no change in net work done due to the piston acceleration.

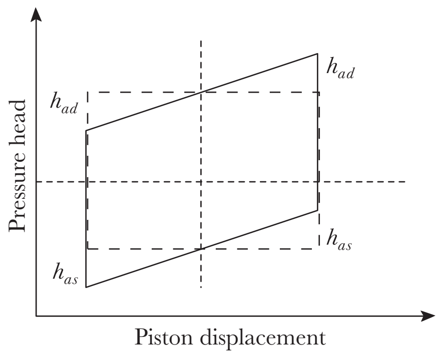

Fig. 9.45 Effect of piston acceleration

Effect of Friction

The friction causes the work done to increase. The head loss due to friction in suction and delivery pipes can be obtained from Darcy–Weisbach equation. The head loss due to friction and the piston displacement shows a parabolic behaviour.

$$\left.\begin{aligned} h_{fs} &= f\frac{l_s}{d_s}\frac{v_s^2}{2g} \\ h_{fd} &= f\frac{l_d}{d_d}\frac{v_d^2}{2g} \end{aligned}\right\} \Rightarrow \left.\begin{aligned} h_{fs} &= f\frac{l_s}{d_s}\frac{1}{2g}\left(\frac{A}{a_s}wr\sin\theta\right)^2 \\ h_{fd} &= f\frac{l_d}{d_d}\frac{1}{2g}\left(\frac{A}{a_d}wr\sin\theta\right)^2 \end{aligned}\right\} \tag{9.112}$$

Equation (9.112) has been plotted on the indicator diagram in Fig. 9.46(a). The work done to overcome the friction on suction and delivery side is the area of the parabolic shaded region which is given by

$$\left.\begin{aligned} w_{fs} &= \frac{2}{3}h_{fs}L \\ w_{fd} &= \frac{2}{3}h_{fd}L \end{aligned}\right\} \tag{9.113}$$

The combined effect of friction and piston acceleration has been shown on the indicator diagram in Fig. 9.46(b). The maximum speed of the pump is limited by taking the phenomenon of cavitation or flow separation into consideration at the

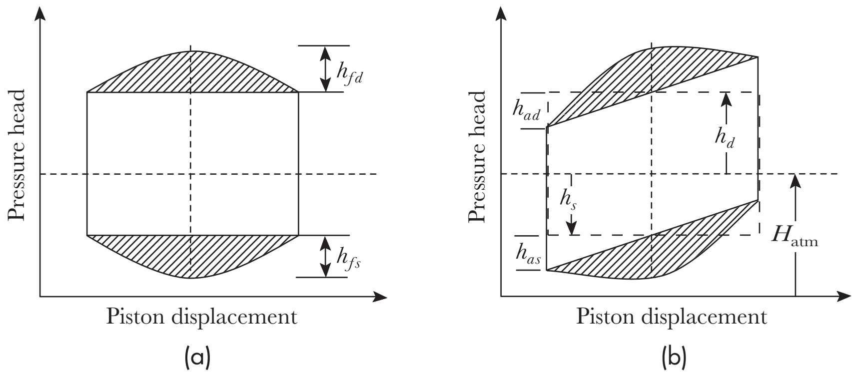

Fig. 9.46 Indicator diagram (a) Effect of piston acceleration (b) Combined effect of piston acceleration and friction

beginning of suction stroke. If H_{sep} represents the head corresponding to vapour pressure, the limiting value of speed can be calculated by equating it with the head corresponding to absolute pressure at the beginning of suction stroke, that is,

$$H_{atm} - h_s - h_{as} \geq H_{sep} \tag{9.114}$$

The work saved by the use of air vessels is shown in Example 9.15.

Example 9.15 Show that work saved by fitting air vessels at suction and delivery sides is 84.8% in a single-acting reciprocating pump.

Solution: For a single-acting reciprocating pump, flow velocity through the suction/delivery pipe of cross-section area a is

$$v = \frac{A}{a}\omega r \sin\theta$$

Head loss due to friction (Darcy's equation)

$$h_f = f\frac{l}{2gd}\left(\frac{A}{a}\omega r \sin\theta\right)^2$$

Work done in overcoming friction without air vessel

$$w_f = \frac{2}{3}h_f L \;\Rightarrow\; 4w_f = \frac{2}{3}\left[f\frac{l}{2gd}\left(\frac{A}{a}\omega r \sin 90^\circ\right)^2\right]L$$

$$\Rightarrow\; w_f = \frac{2}{3}L\frac{fl}{2gd}\left(\frac{A}{a}\omega r\right)^2$$

With the installation of air vessels to the suction and delivery of the pump, the flow velocity through the suction and delivery pipes becomes uniform, which is equal to the mean velocity given by

$$\bar{v} = \frac{Q}{a} = \frac{LAN}{60a} \;\Rightarrow\; \bar{v} = \frac{(2r)A}{60a}\frac{60\omega}{2\pi} \;\Rightarrow\; \bar{v} = \frac{A}{a}\frac{\omega r}{\pi}$$

Head loss due to friction in this case becomes

$$h_f = f\frac{l}{2gd}\left(\frac{A}{a}\frac{\omega r}{\pi}\right)^2$$

Thus, the shaded region (corresponding to friction loss) formed on indicator diagram is no more a parabola rather it's a rectangle as the velocity inside the pipe have become uniform. Thus, work done in overcoming friction with air vessel is

$$w_f = h_f L \quad \Rightarrow \quad w_f = L\frac{fl}{2gd}\left(\frac{A}{a}\frac{\omega r}{\pi}\right)^2$$

Percentage work saved is given by

$$\text{Percentage work saved} = \frac{(w_f)_{\text{without air vessel}} - (w_f)_{\text{with air vessel}}}{(w_f)_{\text{without air vessel}}} \times 100$$

$$\text{Percentage work saved} = \frac{2/3 - 1/\pi^2}{2/3} \times 100 = 84.8\%$$

Example 9.16 The stroke and bore of a single cylinder reciprocating engine running at 60 rpm are 400 mm and 200 mm, respectively. The 20 m long delivery pipe has a diameter of 75 mm. Determine the power saved by installing an air vessel in the delivery pipe, if pipe friction factor is 0.008.

Solution:

Given data:

Cylinder bore, $D = 0.2$ m	Delivery pipe diameter, $d = 0.075$ m
Delivery pipe length, $l = 200$ m	Stroke length, $L = 0.4$ m
Friction factor, $f = 0.008$	Speed, $N = 60$ rpm

Discharge through a single-acting pump is given by

$$Q = \frac{LAN}{60} \quad \Rightarrow \quad Q = \frac{L(\pi D^2/4)N}{60}$$

$$\Rightarrow \quad Q = \frac{0.4(\pi \times 0.2^2/4) \times 60}{60} \quad \Rightarrow \quad Q = 0.01257\,\text{m}^3/\text{s}$$

Friction head loss without air vessel is

$$h_f = f\frac{l}{d}\frac{v^2}{2g} \quad \Rightarrow \quad h_f = f\frac{l}{2gd}\left(\frac{A}{a}\omega r\right)^2$$

$$h_f = 0.008 \times \frac{20}{2 \times 9.81 \times 0.075} \times \left(\frac{0.2^2}{0.075^2} \times \frac{2\pi \times 60}{60} \times 0.2\right)^2 \quad \Rightarrow \quad h_f = 86.8\,\text{m}$$

Friction head loss with air vessel is

$$h_f = f\frac{l}{d}\frac{\bar{v}^2}{2g} \quad\Rightarrow\quad h_f = f\frac{l}{2gd}\left(\frac{A}{a}\frac{\omega r}{\pi}\right)^2$$

$$h_f = 0.008\times\frac{20}{2\times 9.81\times 0.075}\times\left(\frac{0.2^2}{0.075^2}\times\frac{2\pi\times 60}{60\pi}\times 0.2\right)^2 \quad\Rightarrow\quad h_f = 8.79\,\text{m}$$

Power saved by the use of air vessel is given by

$$P_{\text{saved}} = \rho Q g\left(\frac{2}{3}h_{f\,\text{without air vessel}} - h_{f\,\text{with air vessel}}\right)$$

$$P_{\text{saved}} = 1000\times 0.01257\times 9.81\times\left(\frac{2}{3}\times 86.8 - 8.79\right) \quad\Rightarrow\quad P_{\text{saved}} = 6.051\,\text{kW}$$

Example 9.17 A single-acting reciprocating pump, discharging water at a height of 20 m, has 250 mm bore and 500 mm stroke and is running at 100 rpm. The delivery pipe is 30 m long and has 10 cm diameter. If an air vessel is provided on the delivery side at a length of 2 m from the cylinder, calculate the pressure head at beginning and middle of the delivery stroke. Take friction factor $f = 0.025$.

Given data:

Delivery head, $h_d = 20$ m	Delivery pipe diameter, $d = 0.1$ m
Cylinder bore, $D = 0.25$ m	Stroke length, $L = 0.5$ m
Delivery pipe length, $l = 30$ m	Position of air vessel, $l_{ad} = 2$ m
Friction factor, $f = 0.025$	Speed, $N = 50$ rpm

Solution: An indicator diagram for delivery side has been shown in Fig. 9.47. The discharge of water through the pump is

$$Q_{\text{th}} = \frac{LAN}{60} \quad\Rightarrow\quad Q_{\text{th}} = \frac{\pi}{4}D^2L\frac{N}{60}$$

$$\Rightarrow\quad Q_{\text{th}} = 0.02\,\text{m}^3/\text{s}$$

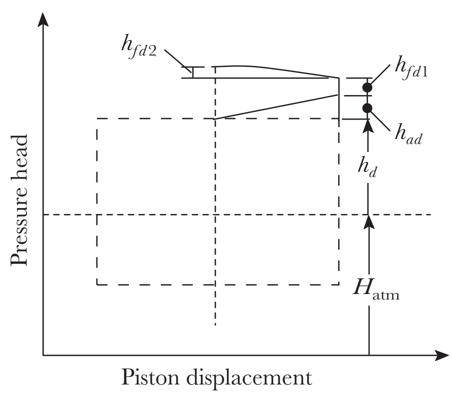

Fig. 9.47 Delivery side friction and acceleration head variation

Rotational speed is

$$\omega = \frac{2\pi N}{60} \quad \Rightarrow \quad \omega = 5.235\,\text{rad/s}$$

Total pressure head on delivery side of piston is

$$h_{td} = h_d + h_{ad} + h_{fd}$$

Due to the installation of air vessel on the delivery side, the acceleration pressure head is reduced as instead of total delivery pipe length only pipe length up to the air vessel is taken into consideration. In addition, at the beginning of a delivery stroke, the friction head is reduced by a bit as length above the air vessel is taken into consideration. However, at the middle of stroke, total delivery pipe length will be used for the computation of friction head and the acceleration head is zero.

The velocity in the delivery pipe is

$$V = \frac{Q_{\text{th}}}{a} \quad \Rightarrow \quad V = \frac{4Q_{\text{th}}}{\pi d^2} \quad \Rightarrow \quad V = 2.61\,\text{m/s}$$

At the *beginning of delivery stroke*, the total head is

$$h_{td} = h_d + h_{ad} + h_{fd1}$$

where $h_{fd1} = f\dfrac{l'}{d}\dfrac{V^2}{2g}$ as $l' = 28\,\text{m} \quad \Rightarrow \quad h_{fd1} = 2.43\,\text{m}$

The acceleration head is

$$h_{ad} = l_{ad}\frac{A}{a}\frac{\omega^2 r}{g} \quad \text{as } r = L/2 = 0.25\,\text{m} \quad \Rightarrow \quad h_{ad} = 8.73\,\text{m}$$

Therefore, total pressure head at the beginning of delivery stroke is

$$h_{td} = h_d + h_{ad} + h_{fd1} \quad \Rightarrow \quad h_{td} = 31.16\,\text{m (gauge)}$$

At the *middle of delivery stroke*, the total head is

$$h_{td} = h_d + h_{fd1} + h_{fd2} \quad \text{or} \quad h_{td} = h_d + h_{fd}$$

where $h_{fd} = f\dfrac{l}{d}\dfrac{V^2}{2g} \quad \Rightarrow \quad h_{fd} = 2.6\,\text{m}$

Therefore, total pressure head at the middle of delivery stroke is

$$h_{td} = h_d + h_{fd} \quad \Rightarrow \quad h_{td} = 22.6\,\text{m (gauge)}$$

Example 9.18 Determine the maximum speed of a single-acting reciprocating pump if separation head is 3 m of water (abs). The pump is placed 3 m above the sump level and it delivers water to a tank placed 15 m above its centre line. The pump has 100 mm bore and 180 mm stroke. The diameter of suction and deliver pipe is 40 mm whereas the length of suction pipe is 4 m and that of delivery pipe 18 m.

Given data:

Delivery head, $h_d = 15\,\text{m}$	Suction lift, $h_s = 3\,\text{m}$
Cylinder bore, $D = 0.1\,\text{m}$	Stroke length, $L = 0.18\,\text{m}$
Delivery pipe length, $l_d = 18\,\text{m}$	Delivery pipe diameter, $d_d = 0.04\,\text{m}$
Suction pipe length, $l_s = 4\,\text{m}$	Suction pipe diameter, $d_s = 0.04\,\text{m}$
Separation head, $H_{se} = 3\,\text{m abs}$	Atmospheric head, $H_{\text{atm}} = 10.3\,\text{m abs}$

Solution: The minimum pressure during suction stroke occurs at the beginning of suction stroke, as shown in Fig. 9.48. The minimum pressure at the beginning of suction stroke should not fall below separating head. This will avoid cavitation, that is,

$$H_{\text{atm}} - h_s - h_{as} \geq H_{\text{sep}}$$

or

$$h_{as} \leq H_{\text{atm}} - h_s - H_{\text{sep}}$$

$$\frac{l_s}{g}\frac{A}{a}\left(\frac{2\pi N}{60}\right)^2 r \leq H_{\text{atm}} - h_s - H_{\text{sep}}$$

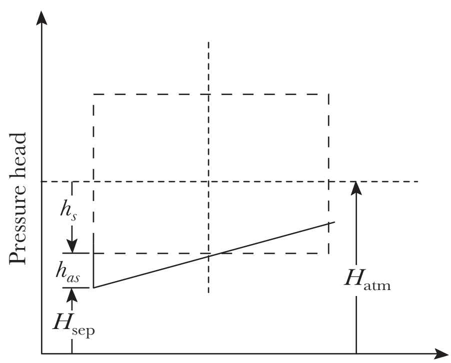

Fig. 9.48 Condition to avoid cavitation

The maximum limiting velocity is obtained by considering the sign of equality only.

$$\frac{l_s}{g}\frac{A}{a}\left(\frac{2\pi N}{60}\right)^2 r = H_{\text{atm}} - h_s - H_{\text{sep}} \quad \Rightarrow \quad 0.0025152\,\text{N}^2$$

$$= 4.3 \quad \Rightarrow \quad N = 41.35\,\text{rpm}$$

9.11 MISCELLANEOUS FLUID MACHINES

This section is dedicated to the fluid machines, which uses the fluid power to perform certain operations. In this section, the description of fluid machines such as hydraulic crane, hydraulic ram, fluid coupling, and torque converter has been presented.

9.11.1 Hydraulic Crane

The *crane*, as shown in Fig. 9.49, consists of two main components the *mast* and the *jigger*. The *jib* and *tie* are attached with the *mast* which is free to rotate about its axis. The jib can move up and down to adjust the radius of action for the load to be lifted whereas tie is fixed to the mast. The *jigger* is composed of two sets of pulleys, one fixed while other is moving, wound around by a strong cable. The hooked end of the cable passes over the *guide pulley* through *movable pulley* to be attached with the load. A *heavy metal ball* is provided just above the *hook* to keep the *cable* or *rope* intact with the *guide pulley* under no-load conditions. The *ram*, fixed to the movable pulley from one side, slides in a fixed cylinder due to hydraulic action of the high-pressure fluid. The amount of fluid pressure applied depends upon the magnitude of the load to be lifted.

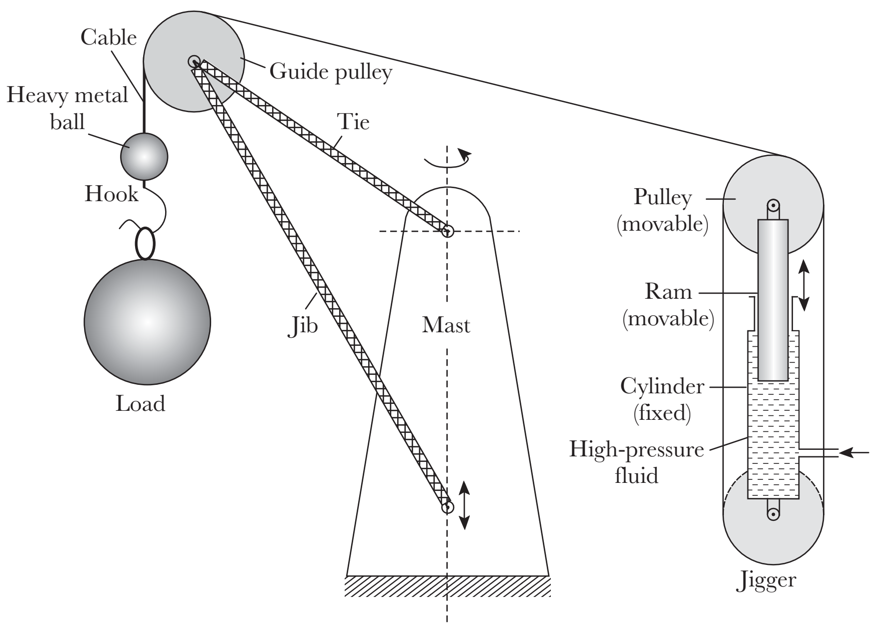

Fig. 9.49 Schematic diagram hydraulic crane

9.11.2 Hydraulic Ram

The hydraulic ram is a mechanical device that is used to pump small quantity of water from a supply tank to a height greater than the height of supply tank, without the use of external power. The schematic diagram of hydraulic ram, as shown in Fig. 9.50, consists of supply tank and chamber fitted with air vessel. The chamber has two valves, one for throwing out waste water (known as waste valve) and the other operates between the chamber and the air vessel.

With the opening of inlet valve, the water rushes into the chamber. The pressure starts building up with more and more water accumulating inside the chamber

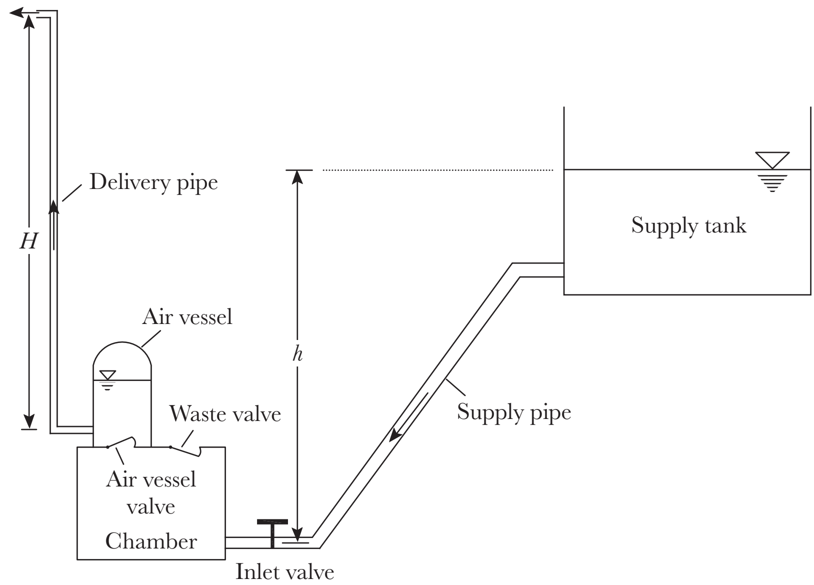

Fig. 9.50 Schematic diagram of hydraulic ram

leading to a sudden closure of waste valve. During the closing of waste valve some water gets spilled out as waste. The sudden closure causes the pressure inside the chamber to further shoot up, forcing the bottom valve of air vessel to open. The water entering from the bottom of air vessel compresses the available air. The pressure, thus, starts building up inside the air vessel. The high-pressure air pushes the water to go out through the delivery pipe with simultaneous closure of the bottom valve.

The ram efficiency is given by

$$\eta_{\text{ram}} = \frac{\text{Power delivered by ram}}{\text{Power input to ram}} = \frac{\rho q g H}{\rho Q g h} \tag{9.115}$$

where Q is the discharge of the water supplied and q is the discharge of water at the delivery. For useful output from the hydraulic ram, the diameter of delivery pipe is smaller than that of supply pipe.

9.11.3 Fluid Coupling

A coupling is a mechanical device which transmits power from one shaft to another. A conventional mechanical coupling (flange or flexible) connects the two shafts by means of nuts and bolts. The *fluid coupling*, on the other hand, is based on hydrokinetic transmission principle by utilising the clinging property of fluid, without any mechanical contact. Fluid couplings are used in automotive, mining, power generation, material handling, oil and gas, marine, mobile equipment, and other transportation-related applications.

The fluid coupling, as shown in Fig. 9.51, consists of two bladed wheels mounted on different shafts aligned axially and housed in a leak-proof casing called *shell*.

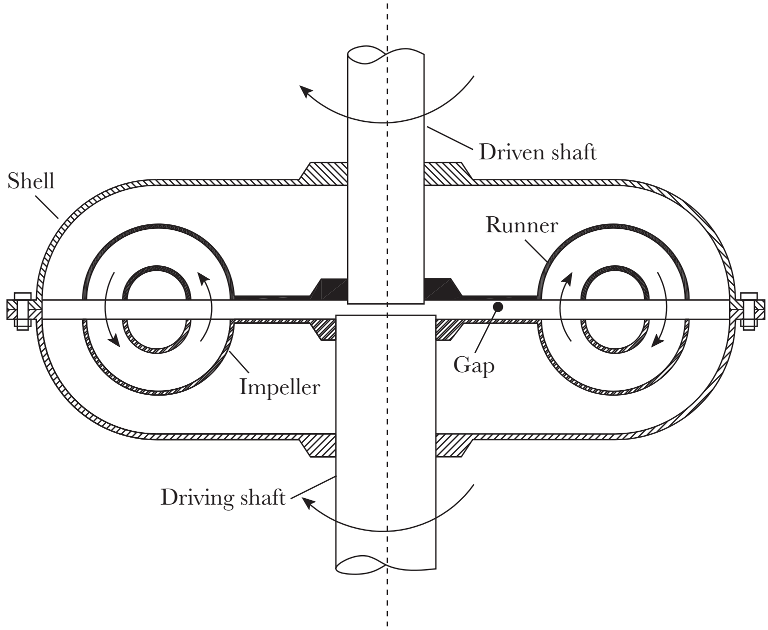

Fig. 9.51 Fluid coupling

The bladed wheel on the driver shaft is termed as *impeller* whereas that on the driven shaft is termed as *runner*. The shell, which houses the impeller and runner arrangement, is filled with a pressurized fluid such as oil or water through which power is transmitted hydraulically in a wear-free manner. The rotating impeller causes the rotating fluid to move out radially in linear direction under the action of centrifugal force through the vanes of the impeller. In the course of its movement, the fluid is thrown upwards towards the vanes of the runner crossing the gap. The fluid gets adhered to the runner vanes causing it to rotate in the same direction. In this way, the power from the impeller gets transmitted to the runner. It should be remembered that to rotate the runner, the inertia of the runner due to the load attached to it, needs to be overcome by the hydraulic energy of the clinging fluid. The higher the input speed, the greater is the amount of mechanical energy transmitted to runner. By varying the amount of fluid inside the shell, start-up behaviour and the amount of power transmitted to the runner, that is, the speed of runner shaft can be controlled. If the runner is required to remain idle even when the impeller is running, the fluid is brought to such a low level that it does not have enough energy to overcome the runner's inertia. Fluids having low viscosity are recommended for the fluid couplings as the losses due to internal friction for such fluids are low. Fluid couplings are very much efficient as loss in torque from impeller to runner is typically only 2–4% due to internal friction of the fluid. Since there is no mechanical contact between the impeller and runner wheel, it does not cause torsional vibration and driveline shock resulting in long life of the equipment.

9.11.4 Torque Converter

The *torque converter* is a special type of fluid coupling which, in addition to transmitting power from one shaft to another, is capable of multiplying torque. Nowadays, it is widely used as a replacement for *clutch* in the automobile industry. It is preferred over a conventional clutch simply due to smooth engagement and disengagement of driver shaft with the driven shaft. There is no direct contact between the parts resulting in efficient power transmission and less maintenance. The torque converter mainly differs from the fluid coupling by an additional component known as *stator*, which is interposed between the impeller and the runner. The stator, as the name indicates, remains stationary. Its function is to alter the return flow from the runner to the impeller. For higher torque multiplication, the multiple runners and stators are employed. Each set of runner and stator is designed to produce a unique torque multiplication factor. The higher torque multiplication is usually required by heavy vehicles.

Example 9.19 A hydraulic ram is supplied with water at 50 L/s under a head of 5 m. It lifts the water at a rate of 5 L/s to a tank 30 m above the ram. The delivery pipe has a length and diameter of 100 m and 50 mm, respectively. Determine its efficiency. Neglect friction losses.

Given data:

Discharge supplied to ram, $Q = 0.05\,\text{m}^3/\text{s}$	Delivery pipe length, $l = 100\,\text{m}$
Discharge at the delivery, $q = 0.005\,\text{m}^3/\text{s}$	Delivery head, $H = 30\,\text{m}$
Supply head, $h = 5\,\text{m}$	Delivery pipe diameter, $d = 0.05\,\text{m}$

Solution: The efficiency of hydraulic ram is

$$\eta_{\text{ram}} = \frac{qH}{Qh} \quad \Rightarrow \quad \eta_{\text{ram}} = \frac{0.005 \times 30}{0.05 \times 5} \quad \Rightarrow \quad \eta_{\text{ram}} = 60\,\%$$

Example 9.20 A total of 600 L/s of an oil having specific gravity 0.8 at a pressure of 500 kPa is supplied to a hydraulic crane to lift a load of 20 kN to a height of 10 m. What is its efficiency?

Given data:

Pressure of oil, $p = 5 \times 10^5\,\text{N/m}^2$	Load lifted, $W = 2 \times 10^4\,\text{N}$
Volume of oil supplied, $Q = 0.06\,\text{m}^3$	Height, $H = 10\,\text{m}$

Solution: Energy input to the hydraulic crane $= p \times Q = 5 \times 10^5 \times 0.06 = 3 \times 10^4\,\text{Nm}$.

The work done by the crane in lifting the load = load × height raised $= W \times H = 2 \times 10^5\,\text{Nm}$

$$\eta_{\text{crane}} = \frac{\text{work done by crane}}{\text{energy input}} = \frac{WH}{pQ} \quad \Rightarrow \quad \eta_{\text{ram}} = \frac{2 \times 10^5}{3 \times 10^4} \quad \Rightarrow \quad \eta_{\text{ram}} = 66.7\,\%$$

POINTS TO REMEMBER

- Hydraulic turbines are mainly classified into impulse and reaction turbines. The main difference between these two lies in the action of water jet on the runner blades. In impulse turbine, the jet interacts with the runner blades for a very small duration of time and there is no change in pressure before and after the jet impingement. In reaction turbine, it is the reaction of jet interaction with runner blades that becomes important. The pressure gets transformed into kinetic energy during the course of journey of water stream through the runner.
- Pelton turbine is a tangential flow impulse turbine designed for high head and low-discharge conditions. Francis turbine is a mixed flow reaction turbine designed for medium head and medium discharge whereas Kaplan turbine is an axial flow reaction turbine designed for low head and high discharge.
- Draft tube is generally used with reaction turbines to recover the pressure energy at turbine exit so that the water coming out of the runner can be discharged into the tail race at atmospheric pressure. Thereby, increasing the hydraulic efficiency of the turbine.
- Pumps are mainly classified into positive displacement and non-positive displacement pumps. In positive displacement pumps, the fluid is positively displaced by a mechanical element (piston or gear tooth) and there is no flow reversal. In non-displacement or rotodynamic pumps, a rotating element (impeller) activates the fluid to high pressure. There will be flow reversal if the pump is stopped.
- The centrifugal pumps are similar to Francis turbine in construction and opposite in operation.
- The phenomenon of cavitation is common in hydraulic machines especially in reaction turbines and centrifugal pumps. The term cavitation is derived from the word cavity (hole/pit). Cavitation is, thus, the erosion of blade/casing surfaces. Whenever there is a fall in liquid pressure below the vapour pressure, the vapour bubbles are formed in the liquid bulk. These vapour bubbles when burst or collapse near the solid surface causes its erosion.
- In reciprocating pumps, the difference in the theoretical and the actual discharge is termed as slip. The slip is usually positive but in some cases it is found to be negative also. This may happen when the inertia force in the suction is greater than the pressure force above the deliver valve. This occurs when delivery pipe is short or suction pipe is long or pump is running at high speed.
- The torque converter is a type of fluid coupling where, in addition to transmitting power from one shaft to another, is capable of multiplying torque.
- Hydraulic ram pumps water to small heights making use of available water head without the use of any external agency.
- Hydraulic crane lifts heavier objects exploiting mechanical advantage as per Pascal's law.

SUGGESTED READINGS

Agarwal S.K., *Fluid Mechanics and Machinery*, Tata McGraw-Hill Education, New Delhi, 2006.

Douglas, J.F., J.M. Gasoriek, J.A. Swaffield, and L.B. Jack, *Fluid Mechanics*, 5th Ed., Prentice Hall, 2006.

Husain, Z., Z. Abdullah, and Z. Alimuddin, *Basic Fluid Mechanics and Hydraulic Machines*, B.S. Publications, Hyderabad, 2008.

MULTIPLE-CHOICE QUESTIONS

9.1 The speed of hydraulic turbine under no-load conditions with guide vanes fully open is known as ________________

(a) specific speed (c) runaway speed
(b) unit speed (d) critical speed

9.2 Multistage centrifugal pumps are used to attaina

(a) high discharge (c) high head
(b) low discharge (d) low head

9.3 The delivery valve is kept ________________ before starting the centrifugal pump

(a) fully closed (c) fully open
(b) partially closed (d) partially open

9.4 The casing of centrifugal pump is of diverging shape to

(a) minimize friction loss (c) maximize efficiency
(b) minimize kinetic energy loss (d) avoid cavitation

9.5 Which of the following hydraulic turbines has the highest specific speed?

(a) Pelton (c) Kaplan
(b) Francis (d) Any of these

9.6 Which of the following hydraulic turbine requires a large amount of discharge?

(a) Pelton (c) Kaplan
(b) Francis (d) Any of these

9.7 Which of the following hydraulic turbine requires a high head at its inlet?

(a) Pelton (c) Kaplan
(b) Francis (d) Any of these

9.8 A draft tube is used with

(a) impulse (c) both of these
(b) reaction (d) none of these

9.9 A draft tube usually has a divergent shape

(a) to increase the work output (c) to guide water to tail race
(b) for pressure recovery (d) all of these

9.10 The divergence angle of the draft tube is kept small

(a) to avoid flow separation (c) for gradual conversion of kinetic energy into pressure energy
(b) to minimize losses (d) all of these

9.11 Chances of cavitation is maximum at the
(a) runner inlet
(b) guide vanes
(c) draft tube inlet
(d) penstock

9.12 Foot valves are provided in the suction line of pumps
(a) to retain water inside the pump casing
(b) to avoid priming
(c) to keep the casing free of air
(d) all of these

9.13 In fluid couplings, the low viscosity fluid is recommended as
(a) slip will be low
(b) low viscosity fluid is cheaper
(c) it will exert pressure on the wall of shell
(d) none of these

9.14 A fluid coupling is generally used with
(a) an ordinary gear box
(b) an epicyclic gear box
(c) a compound gear box
(d) none of these

9.15 Stator in torque converters
(a) redirects the fluid returning from the runner before striking the impeller again
(b) helps in reducing fluid's inertia and hence increases efficiency
(c) absorbs shocks and vibrations
(d) all of these

9.16 In cranes, a heavy metal ball is attached to the hook
(a) to keep cable taut with the guide pulley in the absence of load
(b) to give stability to crane while lifting
(c) to counterbalance the load to be lifted
(d) all of these

9.17 In Fig. 9.52, curves A, B, and C, respectively, correspond to
(a) Kaplan, Francis, and Pelton turbines
(b) Kaplan, Pelton, and Francis turbines
(c) Pelton, Francis, and Kaplan turbines
(d) Francis, Kaplan, and Pelton turbines

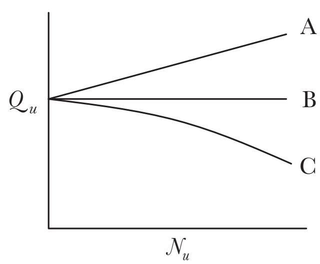

Fig. 9.52

9.18 In Francis turbine, the discharge decreases with the speed due to
(a) buoyancy force
(b) inertia force
(c) gravity force
(d) centrifugal force

9.19 Which pump would you recommend for highly viscous fluids?
(a) Centrifugal pump
(b) Reciprocating pump
(c) Screw pump
(d) Gear pump

9.20 Prior to running reciprocating pumps, air vessels are filled with
(a) water (c) compressed air
(b) air (d) vacuum

REVIEW QUESTIONS

9.1 Differentiate between the following:
(a) Impulse and reaction turbines
(b) Radial and axial flow machines
(c) Positive displacement and non-positive displacement machines
(d) Unit speed and specific speed
(e) Main and operating characteristics
(f) Fluid coupling and torque converter
9.2 What are different speed regulation mechanisms in Pelton turbine?
9.3 Discuss the role wicket gates in a reaction turbine.
9.4 Why the blades are made radial at runner outlet in reaction turbines?
9.5 Why does a draft tube have diverging section?
9.6 Unlike propeller turbine, at any given load Kaplan turbine operates at constant and higher efficiency. Why?
9.7 What is the significance of isoefficiency curves?
9.8 Why are centrifugal pumps usually designed with backward curved blades?
9.9 Why is priming needed in centrifugal pumps?
9.10 Why is the casing of the centrifugal pump spiral in shape?
9.11 Describe the role of diffuser in a centrifugal pump.
9.12 What limits the suction lift in a reciprocating pump?
9.13 What is slip? What are the conditions of negative slip in a reciprocating pump?
9.14 Explain the phenomenon of cavitation and discuss the techniques to avoid it.
9.15 Discuss the purpose of providing air vessels with reciprocating pumps.
9.16 Why is low-viscosity oil preferred in fluid coupling?

UNSOLVED PROBLEMS

9.1 A jet with a velocity V impinges a curved plate moving at velocity u in the direction of jet, as shown in Fig. 9.53, show that power of the jet is given by

$$P_{\text{jet}} = \rho A u (V - u)^2 (1 + \cos\theta)$$

where ρ is the density of the jet fluid, A is the cross-sectional area of the jet.

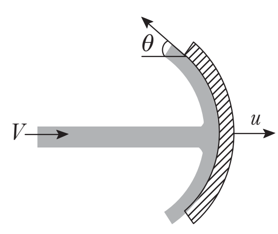

Fig. 9.53

9.2 A 15 mm diameter jet of water impinges normally at the centre of rectangular plate of size 100 mm × 100 mm × 4 mm with a velocity of 5 m/s. The top edge of the plate is hinged. Determine the force required to apply at the bottom edge to keep the plate vertical. What would be the angle by which the plate is deflected in the absence of resisting force? The density of plate material is 7850 kg/m^3.

[Ans: 2.209 N, 55.1°]

9.3 Pelton wheel runner produces 20 MW under a head of 450 m when running at a speed of 600 rpm. If the mean runner diameter is 10 times the diameter of jet, determine the number of jets, diameter of each jet, diameter of wheel, and discharge. The overall efficiency, coefficient of velocity, and speed ratio are 0.85, 0.98, and 0.47, respectively.

[Ans: 4, 0.1406 m, 1.406 m, 5.33 m^3/s]

9.4 A Pelton turbine produces 8 MW of power under net head of 440 m. The turbine has two jets. The buckets deflect the jet by an angle of 165°. If the bucket friction coefficient is 0.85, compute the following:
(a) Discharge
(b) Diameter of each jet
(c) The total force exerted by the jets on the wheel in the tangential direction
(d) Power produced by the runner
(e) Hydraulic efficiency

The overall efficiency, coefficient of velocity and speed ratio may be assumed 0.85, 0.98, and 0.47, respectively.

[Ans: (a) 2.18 m^3/s (b) 12.35 cm (c) 188.1 kN (d) 8.214 MW (e) 90.9%]

9.5 The following data is provided to design a Pelton turbine: available head $H = 400$ m, turbine speed $N = 800$ rpm, power available at the shaft $P_{shaft} = 15$ MW, jet ratio $m = 8$ and overall efficiency $\eta_o = 0.82$. Determine the Pelton wheel diameter, jet diameter and number of jets required, if speed ratio $K_u = 0.46$ and velocity coefficient $C_v = 0.96$.

[Ans: 0.973 m, 0.1216 m, 5]

9.6 An outward flow reaction turbine operates under a head of 45 m and discharge of 10 m^3/s. The speed of the runner is 450 rpm. At the runner blade inlet, the speed and flow ratios are 0.7 and 0.2, respectively. If the overall and hydraulic efficiencies are 82 and 90%, respectively, compute the following:
(a) The power developed
(b) Inlet blade angle
(c) Inlet guide vane angle at the
(d) Specific speed
(e) Runner diameter and width at the inlet

[Ans: (a) 3.258 MW (b) 74° (c) 17.3° (d) 220.38 (e) 0.883 m, 0.607 m]

9.7 Show that for an inward flow reaction turbine with axial discharge and flow velocity constant, the hydraulic efficiency is given by the following expression:

$$\eta_h = \frac{1}{1 + \dfrac{\tan\alpha_1 \tan\beta_1}{2}}$$

where symbols have their usual meanings.

9.8 A Kaplan turbine develops 15 MW at a head of 30 m and at a rotational speed of 300 rpm. The outer diameter of the blades is 2.25 m and the hub diameter is 0.75 m. If the overall efficiency is 85% and the hydraulic efficiency is 92%, determine water discharge, vane angle and blade angle at the inlet.

[Ans: 59.96 m³/s, 65.7°, 31.5°]

9.9 The inner and outer diameters of the runner of a Kaplan turbine are 3 m and 6 m respectively. It develops 30 MW while operating under an effective head of 30 m. The turbine has an overall efficiency 0.82 and is running at 200 rpm. Determine the discharge of water and inlet and outlet runner blade angles at the root and at the tip of the blades, if hydraulic efficiency is 0.9.

[Ans: 124.3 m³/s, 14.3° and 10.56° (at the root), 5.71° and 5.32° (at the tip)]

9.10 A reaction turbine has an exit velocity of 10 m/s. The turbine outlet is connected with tail race by means of a straight conical draft tube. The velocity head at the exit of draft tube is 2 m. For cavitation not to occur, the minimum pressure head in the turbine is set at 3 m (abs). Estimate the maximum height at which the turbine should be placed above tail race. The atmospheric pressure can be taken as 10.3 m of water.

[Ans: 4.203 m]

9.11 The diameter and width of the impeller at outlet of a centrifugal pump is 750 and 75 mm, respectively. The pump delivers water at a rate of 1.0 m³/s against a head of 60 m. The hydraulic efficiency of the pump is 85%. The leakage loss is 4% of the discharge and external mechanical loss is 10 kW. If the impeller speed is 1440 rpm compute the blade angle at outlet and overall efficiency.

[Ans: 7.57°, 83.8%]

9.12 The suction lift of a diffuser pump is 3 m and the height of the delivery tank above the pump is 12 m. The radial velocity of water through the impeller is 3 m/s. The blades of the impeller are curved back at 45° and the water enters the blades radially. The velocity of water in the delivery pipe is 1.75 m/s. The manometric efficiency of the pump is 0.85. Neglecting friction and other losses in the pipe and impeller, find the following:
(a) Tangential velocity of the impeller at the outlet
(b) Kinetic head at the outlet of the impeller
(c) Pressure rise in the impeller
(d) Angle of guide vanes

[Ans: (a) 14.81 m/s (b) 7.57 m (c) 10.72 m of water (d) 14.25°]

9.13 The manometric head developed by a three-stage centrifugal pump running at 450 rpm is 60 m. The width and diameter of each impeller at the outlet are 60 mm and 750 mm, respectively, with outlet blade angle 45°. Determine its manometric efficiency, if discharge through the pump is 0.3 m³/s.

[Ans: 71.45%]

9.14 A single-acting single cylinder reciprocating pump has stroke length of 400 mm and the piston diameter of 400 mm. The pump runs at 20 rpm. The suction and

delivery heads are 4 and 20 m, respectively; the length of suction and delivery pipes are 6 and 25 m, respectively, and the diameter of each pipe is 200 mm. Estimate the power required to drive the pump, if the friction factor is 0.02.

[Ans: 3.94 kW]

9.15 A double acting reciprocating pump raises the water level by 20 m and the discharge is 100 L/s. The diameter of the piston is 250 mm and the stroke is 600 mm. The velocity of water in the delivery pipe is 1.4 m/s. The friction losses amount to 0.2 m in the suction pipe and 1.8 m in the delivery pipe. Taking efficiency of the pump as 90% and the slip 2%, find the speed and the power input of the pump.

[Ans: 103.9 rpm, 24.6 kW]

9.16 Show that work saved by fitting air vessels at suction and delivery sides is 39.2% in a double-acting pump.

9.17 A centrifugal pump of impeller diameter 200 mm running at 1800 rpm requires 10 kW to deliver 20 L/s at a head of 30 m. Determine its new discharge, head, power required if the impeller diameter is reduced to 100 mm.

[Ans: 2.5 L/s, 7.5 m, 0.3125 kW]

9.18 Determine discharge, speed, and power of ¼ scale model of Francis turbine operating under the head of 50 m if prototype is running at a speed of 200 rpm produces 20 MW under the head of 75 m.

[Ans: 1.54 m^3/s, 653.2 rpm, 0.68 MW]

Answers to Multiple-choice Questions

9.1 (c)	9.2 (c)	9.3 (a)	9.4 (b)	9.5 (a)
9.6 (c)	9.7 (a)	9.8 (b)	9.9 (d)	9.10 (d)
9.11 (c)	9.12 (d)	9.13 (a)	9.14 (b)	9.15 (a)
9.16 (a)	9.17 (b)	9.18 (d)	9.19 (d)	9.20 (b)

DESIGN OF EXPERIMENTS

Experiment 9.1 Performance Characteristics of a Hydraulic Turbine

Objective

To obtain the performance characteristic curves for the given Pelton turbine.

Experimental Set-up

A Pelton turbine is an impulse turbine where the high-speed water jet strikes the buckets mounted on the periphery of the wheel, as shown in Fig. E9.1. The impact of the impinging jet causes the wheel to rotate.

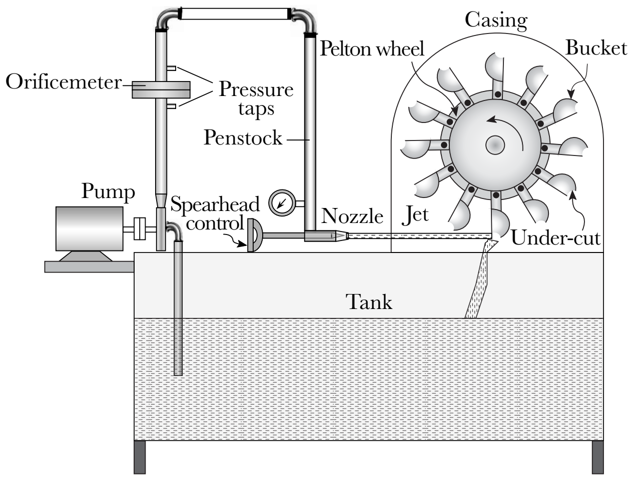

Fig. E9.1 Schematic diagram of Pelton turbine test rig

Thus, the kinetic energy of the jet gets converted into the mechanical work (rotational energy) inside the Pelton turbine. No pressure change occurs at the turbine blades (bucket), and so the turbine doesn't require a casing for operation. However, the casing is provided around the wheel for avoiding the splashing of water. The conduit bringing high-pressure water to the impulse wheel is called the penstock. The role of the pump in the present set-up is to generate a sufficient head to run the turbine. The purpose of the spearhead control is to alter the flow rate of water into the turbine. The power developed by the turbine is measured by means of a rope dynamometer. In hydroelectric power plant, the turbine coupled with the electrical generator is employed to produce the electricity.

The power input to the turbine is given by

$$P_{\text{in}} = \frac{1}{2}\dot{m}V^2 = \rho Q g H \tag{E9.1}$$

where H is the head available at the turbine inlet ≈ head developed by the pump.

The discharge in the penstock is measured by means of an orificemeter and is given by the

$$Q = C_d \frac{A_1 A_2}{\sqrt{A_1^2 - A_2^2}} \sqrt{2\left(\frac{p_1 - p_2}{\rho}\right) - 2g\Delta z} \tag{E9.2}$$

The output brake-power is measured by the rope dynamometer mounted on the turbine shaft, is given by

$$P_{\text{out}} = \frac{2\pi NT}{60} = \frac{\pi D_e NF}{60} \tag{E9.3}$$

where D_e is the effective diameter of the brake drum and F is the effective load on the brake drum and N is the speed of the turbine in rpm.

The turbine efficiency is defined as the ratio of power available at the brake drum to the hydraulic power available at turbine inlet,

$$\eta = \frac{P_{\text{out}}}{P_{\text{in}}} \tag{E9.4}$$

The specific speed of a turbine is defined as the speed of geometrically similar turbine, which produces unit power while operating under unit head

$$N_s = \frac{N\sqrt{P_{\text{out}}}}{H^{5/4}} \tag{E9.5}$$

The speed and power in Eq. (E9.5) corresponds to the maximum efficiency.

Procedure

1. Prime the centrifugal pump, which is used to generate high-pressure head in the penstock.
2. Start the pump and keep the gate valve fully open.
3. Note down the pressure gauge readings (orificemeter + turbine inlet), tachometer reading for no-load conditions.
4. For constant head readings, keep the delivery valve of the pump fully open.
5. Load the turbine by operating the screw of the rope dynamometer.
6. Record the speed corresponding to applied load values (spring balance readings of the dynamometer).
7. For constant speed readings, keep the turbine speed at a certain value for each value of applied load. The speed adjustment can be done by controlling the delivery valve of the pump.
8. Record the inlet pressure reading (inlet head) corresponding to applied values of load (spring balance readings of the dynamometer).

Observation Table

1. Diameter of the brake drum, D ____________ m
2. Diameter of the rope, d ____________ m
3. Effective diameter, $D_e = D + d$ ____________ m
4. Diameter of the orifice, d_2 ____________ m
5. Diameter of the pipe (in which the orifice is fitted), d_1 ____________ m
6. Discharge coefficient of the orifice, C_d ____________
7. Inter-tap spacing (orifice), Δz ____________ m

(a) Constant Head (Main Characteristics)

Head at inlet, H = _______________ m

S. no.	Runner speed	Inlet pressure	Head at the inlet	Orificemeter			Discharge	Input power	Load on brake drum		Torque	Output power	Efficiency
	N (rpm)	p kg/cm^2	$H = p/\rho g$ (m)	p_1 kg/cm^2	p_2 kg/cm^2	Δp kg/cm^2	Q (m^3/s)	P_{in} (kW)	Spring balance (kg)	Effective load F (N)	$T = F \times D_e/2$ (N-m)	(kW)	(%)

(b) Constant Speed (Operating Characteristics)

Constant speed = ________________ rpm

S. no.	Runner speed	Inlet pressure	Head at the inlet	Orificemeter			Discharge	Input power	Load on brake drum		Torque	Output power	Efficiency
	N (rpm)	p kg/cm^2	$H = p/\rho g$ (m)	p_1 kg/cm^2	p_2 kg/cm^2	Δp kg/cm^2	Q (m^3/s)	P_{in} (kW)	Spring balance (kg)	Effective load F (N)	$T = F \times D_e/2$ (N-m)	(kW)	(%)

Results and Discussion

1. Draw and discuss the main characteristic curves of
   (a) Q_u versus N_u
   (b) P_u versus N_u
   (c) η versus N_u
2. Draw and discuss the operating characteristic curves of
   (a) P_o versus Q
   (b) η_o versus Q
   (c) η_o versus P_o
3. Draw and discuss the Muschel or isoefficiency curves

Conclusion

Draw conclusions on the results obtained.

Experiment 9.2 Performance Characteristics of a Hydraulic Pump

Objective

To obtain the performance characteristics of a centrifugal pump.

Experimental Set-up

A centrifugal pump test rig, shown in Fig. E9.2, consists of a centrifugal pump, an electric motor, measuring and sump tanks, energy metre, and pressure gauges. Centrifugal pump is a rotodynamic pump, where the fluid is sucked through the eye of the impeller (rotating element) of the pump. Due to the centrifugal action of the rotating impeller, the fluid is pushed radially outward into the spiral casing, where the fast moving fluid is decelerated and as such the pressure of the fluid is increased. The pressure in the suction and delivery line is measured by means of suction and delivery gauges, respectively. The discharge through the pump is measured by means of water collected in the measuring tank for a given height and corresponding time taken to reach that height is measured using a stop clock.

The power input to the motor, which runs the pump by means of a belt and pulley arrangement, is measured by energy metre. Centrifugal pumps are suitable for smaller heads at larger discharge. The flow rate is changed only by adjusting the speed of the driver motor.

The performance of a pump is characterized by its net head H, which is defined as the change in head between the suction side and the delivery side of the pump. H_{net} is expressed in equivalent column height of water. The net head developed by the pump is given by

$$H_{\text{net}} = \frac{p_d - p_s}{\rho g} + \frac{V_d^2 - V_s^2}{2g} + z_d - z_s \tag{E9.6}$$

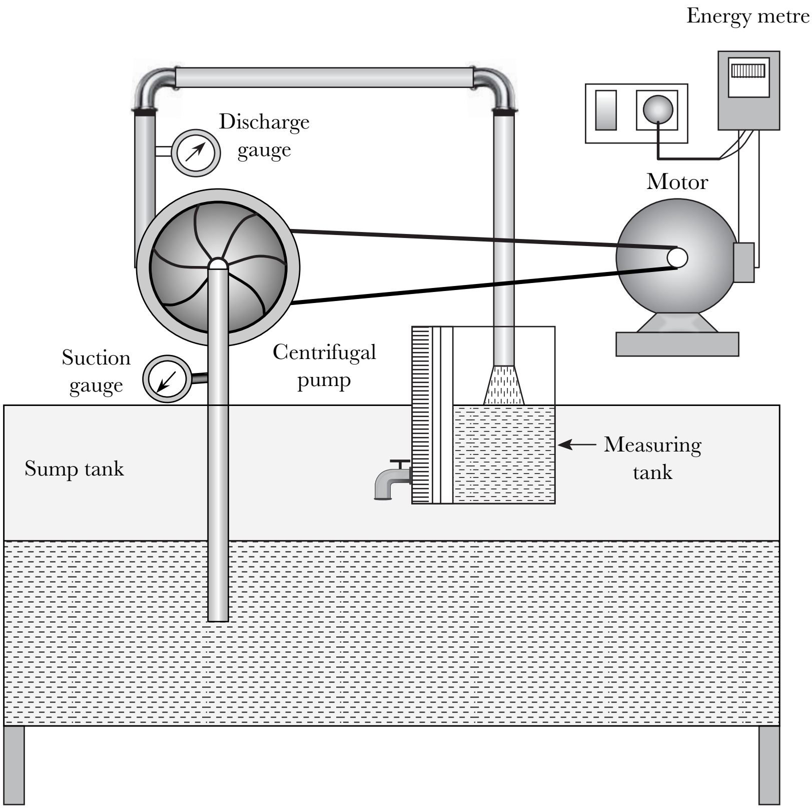

Fig. E9.2 Schematic diagram of centrifugal pump test rig

The velocity of water can be calculated using discharge and area of the pipes. The discharge produced by the pump can be determined using the collecting tank and stopwatch set-up and is given by

$$Q = \frac{Ah}{t} \tag{E9.7}$$

where

A = area of the collecting tank

h = level rise in glass tube fitted on the measuring tank

t = time taken to rise h meters

The net head is proportional to the useful power actually delivered to the fluid in the pump. It is defined as,

$$P_o = \rho Q g H_{\text{net}} \tag{E9.8}$$

The input electrical energy to the motor can be determined using the watt hour energy metre. The expression for power is,

$$E_{\text{in}} = \frac{3600 \times n \times 1000}{k \times t} \tag{E9.9}$$

where

n = number of flashes on energy metre

k = energy metre constant, flash/kWh

t = time taken for n flashes, (sec)

In pump terminology the external energy supplied to the pump is called the brake horsepower (bhp) of the pump, which can be calculated by considering the transmission efficiency.

$$P_{in} = \eta_{trans} \times E_{in} \tag{E9.10}$$

The pump efficiency pump is defined as the ratio of useful power to supplied power,

$$\eta = \frac{P_o}{P_{in}} \tag{E9.11}$$

The specific speed of a pump is defined as the speed of geometrically similar pump, which generates unit head at unit discharge

$$N_s = \frac{N\sqrt{Q}}{H^{3/4}} \tag{E9.12}$$

Procedure

1. Prime the pump and keep the delivery valve closed fully.
2. Start the pump. Select a speed to run the motor.
3. Open the delivery valve fully.
4. Note down the pressure gauge readings for the delivery valve opening.
5. Measure the discharge using the rise in water level in collecting tank and stopwatch.
6. Note the time for n (say, 5) revolutions/flashes of energy metre disk.
7. Vary the discharge using delivery valve and maintain the speed constant (point 2).
8. Record pressure gauge readings, time for 5 flashes of energy metre and discharge for each delivery valve setting (6 sets at least).
9. Perform the above procedure for the other two sets of pump speed.

Observation Table

1. Measuring tank dimensions _____ m × _____ m × ____ m
2. Elevation difference between gauges, $z_d - z_s$ ________________________ m
3. Energy metre constant, k ________________ (flash/kWh)
4. Transmission efficiency, η_{trans} ___________________________
5. Diameter of suction and delivery pipes ________________________ m

Results and Discussion

1. Calculate the power developed and efficiency
2. Draw the performance characteristics of
   (a) H_{net} versus Q
   (b) P_o versus Q
   (c) η versus Q

Conclusion

Draw conclusions on the results obtained.

S. no.	**Discharge**			**Pressure head**			**Datum head**	**Net head**	**Power developed**	**Power input**	**Pump efficiency**	**Speed**	**Time (5 flashes of energy metre)**
	h	t	Q	p_s	p_d	$H = \frac{p_d - p_s}{\rho g}$	$z_d - z_s$	H_{net}	P_o	P_{in}	η	N	
	m	s	m^3/s	kg/cm^2	kg/cm^2	m	m	m	*W*	*W*	%	rpm	s
1.													
2.													
3.													
…													

CHAPTER 10 Dimensional Analysis and Similitude

LEARNING OBJECTIVES

After studying this chapter, the reader will be able to:

- Apply Rayleigh's indicial and Buckingham-pi techniques of dimensional analysis
- Understand the importance of dimensional analysis from the classic example of G.I. Taylor's method for energy estimation during a nuclear explosion
- Predict the performance of full-scale prototype using the results of tests performed on models

In the previous chapters, the theoretical basis for the analyses of flow problems and design of heavy fluid structures and machines has been developed. In this chapter, the role of dimensional analysis in identifying different parameters involved in a system and then establishing a possible functional relationship between them will be discussed. It should be noted that the derived relationship is of qualitative nature. For quantitative assessment of the unknown factors, relevant experiments should be conducted. The importance of dimensional analysis can be judged from the classic example of G.I. Taylor's dimensional analysis for the estimation of energy released during nuclear explosion explained later in this chapter.

Similitude, on the other hand, is the absolute similarity between a system (prototype) and its geometric replica (model). The tests are conducted on the scale down models and the results are predicted for the actual prototypes. The results of these studies are necessary before initiating the full-scale construction of prototype, which involves huge capital investments.

The dimensional analysis and similitude has numerous applications in aviation, automotive sector, ship building industries, and construction of dams, bridges, and high-rise buildings.

10.1 DIMENSIONAL ANALYSIS

Sometimes it is almost impossible to get an analytical solution of a physical problem involving the real fluids. In addition, the analytical solutions are based on a number of assumptions, which deviates from the real situation.

Dimensional analysis helps in relating the parameters qualitatively. However, it does not establish the exact relationship. In these methods, the parameters are usually related in power law form involving a number of constants. The power law form relates the dependent variable with the product of independent variables, each raised to some unknown exponents. In order to obtain the exact relationship, the experiments should be performed on the actual physical system. The generated experimental data is used to evaluate the numerical values of the constants. Thus, dimensional analysis is a very useful tool for planning, presentation, and interpretation of experimental data.

In the words of American Nobel laureate in Physics, P.W. Bridgman (1882–1961 AD), a pioneer of the theory on dimensional analysis:

> '*The principal use of dimensional analysis is to deduce from a study of the dimensions of the variables in any physical system certain limitations on the form of any possible relationship between those variables. The method is of great generality and mathematical simplicity.*'

In quantitative analysis of physical problems, the mathematical relationship between the numerical values of the physical quantities ($x_1, x_2, x_3, \ldots, x_n$) involved is expressed in terms of general physical equation of the form

$$x_n = f(x_1, x_2, x_3, \ldots, x_{n-1}) \tag{10.1}$$

where, x_n is called *dependent* variable and all others are termed as *independent* variables.

The aforementioned physical equation must follow *the principle of dimensional homogeneity*, which states that

> '*Each term of the equation must have the same dimensions.*'

For example, the total head at a point in a hydraulic circuit or pipe network is the sum of pressure, velocity, and datum heads.

$$H = \frac{p}{\rho g} + \frac{V^2}{2g} + z \tag{10.2}$$

The total head H has the dimension of length [L], each term on the right-hand side must have the dimension of length as per the principle of dimensional homogeneity. Let us verify the dimension of each term on the right side using Table 10.1.

Pressure head	$\frac{p}{\rho g}$	$\frac{[\mathrm{ML^{-1}T^{-2}}]}{[\mathrm{ML^{-3}}][\mathrm{LT^{-2}}]} = [\mathrm{L}]$
Velocity head	$\frac{V^2}{2g}$	$\frac{[\mathrm{LT^{-1}}]^2}{[\mathrm{LT^{-2}}]} = [\mathrm{L}]$
Datum head	z	$[\mathrm{L}]$

Table 10.1 Physical quantities with their dimensions and units

Type	Quantities	Symbol	Dimensions	SI unit	SI unit symbol
Base	Mass	m	M	Kilogram	kg
	Length	l, x, d, etc.	L	Metre	m
	Time	t	T	Second	s
	Electric current	I, i	I	Ampere	A
	Temperature	T	Θ	Kelvin	K
	Amount of substance	n	N	Mole	mol
	Luminous intensity	I_v	J	Candela	cd
Derived	Area	A	L^2	Square metre	m^2
	Volume	$\forall$	L^3	Cubic metre	m^3
	Angle	θ	–	Radians	rad
	Velocity	V	LT^{-1}	Metre/second	m/s
	Angular velocity	ω	T^{-1}	Radian/second	rad/s
	Acceleration	a	LT^{-2}	Metre/second^2	m/s^2
	Discharge	Q	L^3T^{-1}	Metre^3/second	m^3/s
	Density	ρ	ML^{-3}	Kilogram/Metre^3	kg/m^3
	Dynamic viscosity	μ	$ML^{-1}T^{-1}$	Kilogram/ Metre-second	kg/m-s
	Kinematic viscosity	υ	L^2T^{-1}	Metre^2/second	m^2/s
	Momentum	P	MLT^{-1}	Kilogram-metre/ second	kg-m/s
	Force	F	MLT^{-2}	Newton	N
	Impulse	I	MLT^{-1}	Newton-second	N-s
	Pressure	p	$ML^{-1}T^{-2}$	Newton/metre^2 or Pascal	N/m^2 or Pa
	Stress	σ	$ML^{-1}T^{-2}$	Newton/metre^2 or Pascal	N/m^2 or Pa
	Strain	ε	–	–	–
	Energy, work	E, W	ML^2T^{-2}	Newton-metre or Joule	N-m or J
	Power	P	ML^2T^{-3}	Joule/s or Watt	J/s or W
	Specific enthalpy	h	L^2T^{-2}	Joule/kilogram	J/kg
	Specific entropy	s	$L^2T^{-2}\Theta^{-1}$	Joule/kilogram-Kelvin	J/kg-K
	Specific heat	c	$L^2T^{-2}\Theta^{-1}$	Joule/kilogram-Kelvin	J/kg-K

Each term has the dimension of length. The left-hand side and right-hand side of Eq. (10.2) have the same dimensions, thus, this equation satisfies the principle of dimensional homogeneity.

10.1.1 Dimensions

Dimension is defined as any measurable property used to describe the physical state of a body or a system. The magnitude of a dimension is described by *units* of measurement. SI (International System of Units), FPS (foot-pound-second), CGS (centimetre-gram-second), and MKS (metre-kilogram-second) systems are the commonly used systems for units of measurement. In fact, SI system is the most acceptable international system for units of measurement.

The physical parameters or quantities are categorized into base or fundamental and derived dimensions. The base or fundamental quantities have their own dimensions and units. There are seven such base quantities, whose dimensions are represented by a single *Sans Serif Roman* capital letter. The following are the definitions of some important base quantities used in fluid mechanics:

Mass *Kilogram* is the SI unit of mass that is equal to the mass of the international prototype of the kilogram, which is an artifact made of platinum-iridium kept at the *Bureau International des Poids et Mesures* (BIPM) under certain specified conditions.

Time *Second* is the SI unit of time, which is the duration of 9192631770 periods corresponding to the transition between the two hyperfine levels of the ground state of the Cesium 133 atom at rest at absolute zero temperature.

Length *Metre* is the SI unit of length, which is the length of the path travelled by light in vacuum during a time interval of 1/299792458 (speed of light in vacuum) of a second.

Temperature Kelvin is the SI unit of temperature, which is the fraction 1/273.16 of the thermodynamic temperature of the triple point of water (0.01°C).

The derived quantities, as the name indicates, are derived from the base quantities. In other words, all quantities other than base quantities are derived quantities. The derived quantities can always be expressed in terms of the base quantities relating them by definition or as per some physical laws governing them. The dimensions of the derived quantities are, thus, written as products of the dimensions of base quantities with appropriate power. Table 10.1 shows the base and derived quantities and their dimensions.

10.1.2 Rayleigh's Indicial Method

This *power series* or *indicial* method of dimensional analysis was developed by the Nobel Laureate John William Strutt, 3rd Baron Rayleigh (1842–1919 AD), an *English physicist*. It is based on the *principle of dimensional homogeneity* of all

the parameters or quantities or variables involved in a physical problem. The following is the step-by-step procedure:

1. The dependent variable is identified and expressed as some function of independent variables with each independent variable raised to an unknown exponent.
2. Each variable is then written in terms of its fundamental dimensions.
3. Using the principle of dimensional homogeneity, the powers of each fundamental dimension on either side of the equation are compared.
4. A set of simultaneous linear equations is obtained in terms of unknown exponents.
5. These simultaneous equations are solved to obtain the numerical values of unknown exponents.

The Rayleigh method has been demonstrated in solved Examples 10.1, 10.2, and 10.3. This method becomes tedious if the variables involved are large in number. In such cases, Buckingham-pi theorem, described in the subsequent section, is more convenient to use.

Example 10.1 A pressure wave propagating with a velocity u through a liquid is dependent upon the elastic modulus (bulk) of the liquid K and its mass density ρ. Use Rayleigh's indicial method to obtain a functional relationship among the parameters.

Solution: Velocity u is the dependent variable influenced by independent variables bulk modulus K and density ρ. Expressing velocity in power law form,

$$u = \mathrm{C}K^{\mathrm{a}}\rho^{\mathrm{b}} \tag{1}$$

where a, b, and C are the dimensionless constants.

The fundamental dimensions of the parameters involved

$$u = \mathrm{LT^{-1}}, \quad K = \mathrm{ML^{-1}T^{-2}}, \quad \rho = \mathrm{ML^{-3}}$$

Substituting these dimensions in Eq. (1),

$$[\mathrm{LT^{-1}}] = [\mathrm{M^0L^0T^0}]\,[\mathrm{ML^{-1}T^{-2}}]^{\mathrm{a}}\,[\mathrm{ML^{-3}}]^{\mathrm{b}}$$

$$[\mathrm{M^0LT^{-1}}] = [\mathrm{M}]^{\mathrm{a+b}}\,[\mathrm{L}]^{\mathrm{-a-3b}}\,[\mathrm{T}]^{\mathrm{-2a}}$$

Equating the power indices (exponents) of M, L, and T, the following three equations are evolved:

$$\mathrm{M:}\quad \mathrm{a + b = 0}$$

$$\mathrm{L:}\quad \mathrm{-a - 3b = 1}$$

$$\mathrm{T:}\quad \mathrm{-2a = -1}$$

Solving these simultaneous equations,

$$\mathrm{a = 1/2}$$

$$\mathrm{b = -1/2}$$

Substituting these constants in Eq. (1) to obtain the functional relation between velocity, density, and bulk's modulus

$$u = \mathrm{C}\sqrt{\frac{K}{\rho}}$$

The constant C can be evaluated from the experiments.

Example 10.2 The rise in a fluid level inside a capillary tube H depends on its specific weight γ, surface tension σ, and radius of the capillary tube R. Deduce the following relationship using Rayleigh indicial method:

$$\frac{H}{R} = f\left(\frac{\sigma}{\gamma R^2}\right)$$

Solution: The capillary rise H is a dependent variable, whereas, specific weight γ, surface tension σ, and radius of the capillary tube R are independent variables. The fundamental dimensions of these parameters are

$$H = [\mathrm{L}]$$
$$\gamma = [\mathrm{ML^{-2}T^{-2}}]$$
$$\sigma = [\mathrm{MT^{-2}}]$$
$$R = [\mathrm{L}]$$

Relating the dependent parameter with the independent parameters by power law form

$$H = \mathrm{C_1}\gamma^{\mathrm{a}}\sigma^{\mathrm{b}}R^{\mathrm{c}} \tag{1}$$

$$[\mathrm{L}] = [\mathrm{M^0L^0T^0}]\ [\mathrm{ML^{-2}\,T^{-2}}]^{\mathrm{a}}[\mathrm{MT^{-2}}]^{\mathrm{b}}[\mathrm{L}]^{\mathrm{c}}$$

$$[\mathrm{M^0L\,T^0}] = [\mathrm{M}]^{\mathrm{a+b}}[\mathrm{L}]^{-2\mathrm{a}+\mathrm{c}}[\mathrm{T}]^{-2\mathrm{a}-2\mathrm{b}}$$

Equating the power indices (exponents) of M, L, and T, the following three equations are evolved:

M: $\mathrm{a + b = 0}$

L: $\mathrm{-2a + c = 1}$

T: $\mathrm{-2a - 2b = 0 \quad \rightarrow \quad a + b = 0}$

Since there are three variables and only two equations, expressing any two variables in terms of third variable is shown as

$$\mathrm{a = -b}$$
$$\mathrm{c = 1 - 2b}$$

Substituting the aforementioned constants in Eq. (1)

$$H = \mathrm{C_1}\gamma^{-\mathrm{b}}\sigma^{\mathrm{b}}R^{1-2\mathrm{b}}$$

$$\frac{H}{R} = \mathrm{C_1}\frac{1}{\gamma^{\mathrm{b}}}\sigma^{\mathrm{b}}\frac{1}{R^{2\mathrm{b}}}$$

$$\frac{H}{R} = \mathrm{C_1}\left(\frac{\sigma}{\gamma R^2}\right)^{\mathrm{b}}$$

$$\frac{H}{R} = f\left(\frac{\sigma}{\gamma R^2}\right)$$

Example 10.3 Derive an expression for the drag force F_{D} on a sphere of diameter D moving with a uniform velocity u in a fluid of density ρ and dynamic viscosity μ.

Solution: The drag force F_D is a dependent variable, whereas, sphere diameter D, fluid density ρ, fluid velocity u, and fluid viscosity μ are independent variables. The fundamental dimensions of these parameters are

Drag force $F_D = [MLT^{-2}]$
Diameter $D = [L]$
Velocity $u = [LT^{-2}]$
Density $\rho = [ML^{-3}]$
Dynamic viscosity $\mu = [ML^{-1}T^{-1}]$

The relation in power law form is

$$F_D = C_1 D^a u^b \rho^c \mu^d \tag{1}$$

$$[MLT^{-2}] = [M^0L^0T^0][L]^a[LT^{-1}]^b[ML^{-3}]^c[ML^{-1}T^{-1}]^d$$

$$[MLT^{-2}] = [M]^{c+d}[L]^{a+b-3c-d}[T]^{-b-d}$$

Equating the exponents

M: $c + d = 1 \;\rightarrow\; c = 1 - d$
T: $-b - d = -2 \;\rightarrow\; b = 2 - d$
L: $a + b - 3c - d = 1 \;\rightarrow\; a = 2 - d$

Substituting in Eq. (1)

$$F_D = C_1 D^{2-d} u^{2-d} \rho^{1-d} \mu^d$$

$$F_D = C_1 \frac{D^2}{D^d}\frac{u^2}{u^d}\frac{\rho}{\rho^d}\mu^d$$

$$F_D = C_1 \rho u^2 D^2 \left[\frac{\mu}{\rho u D}\right]^d$$

$$F_D = \rho u^2 D^2 f\left[\frac{\mu}{\rho u D}\right]$$

$$F_D = \rho u^2 D^2 f_1(\mathrm{Re})$$

10.1.3 Buckingham-pi Theorem

Buckingham-pi theorem got its name after its founder Edgar Buckingham (1867–1940 AD), an American physicist. This method not only helps in establishing a functional relationship between the independent and dependent variables, but also reduces the total number of parameters.

Statement

Given n variables that are expressible in terms of r independent dimensions, then there are no more than (n − r) independent dimensionless variables.

If there are n number of total variables, such that there exists a functional relationship between them, that is,

$$f(x_1, x_2, x_3, \ldots, x_n) = 0 \tag{10.3}$$

The following steps are involved in the Buckingham-pi method:

1. List all the variables and express each of them in terms of fundamental dimensions namely, mass [M], length [L], time [T], temperature [Θ], etc., as shown in Table 10.1.
2. Let the parameters collectively contain r number of fundamental dimensions.
3. The number of repeating variables must be equal to the total number of fundamental dimensions.
4. The number of dimensionless π-groups $= n - r$.
5. The number of parameters involved is now reduced by r and the functional relationship needs to be established between only $(n - r)$ π-groups, that is,

$$f(\pi_1, \pi_2, \pi_3, \ldots, \pi_{n-r}) = 0 \tag{10.4}$$

Suppose x_1, x_2, and x_3 are the repeating variables, then the following π-groups can be determined:

$$\left.\begin{aligned} \pi_1 &= x_1^{a_1} x_2^{b_1} x_3^{c_1} x_4 \\ \pi_2 &= x_1^{a_2} x_2^{b_2} x_3^{c_2} x_5 \\ &\ldots \\ \pi_{n-r} &= x_1^{a_{n-m}} x_2^{b_{n-m}} x_3^{c_{n-m}} x_n \end{aligned}\right\} \tag{10.5}$$

The following points must be remembered while selecting repeating variables:

1. The repeating variables chosen must contain all the fundamental dimensions collectively.
2. No two of the selected repeating variables have the same dimensions.
3. The dependent variable is generally not taken as a repeating variable.
4. The chosen repeating variables must represent variables from each of the following categories—geometric, kinematic, and dynamic. In geometric variables any one which is the most suitable among parameters such as diameter, length, or height may be chosen. Kinematic means motion. The most relevant among kinematic variables such as velocity, acceleration, and discharge may be selected. The variables such as density, viscosity fall under dynamic category.

Buckingham-pi method has been demonstrated in Examples 10.4 and 10.5.

Example 10.4 Using Buckingham-pi theorem, establish a functional relationship for drop in pressure across a pipe of length L and diameter d with average wall roughness

height e. The fluid having density ρ and viscosity μ is flowing through the pipe with a velocity V.

Solution: The pressure drop is a function of the following parameters:

$$\Delta p = f(\rho, \mu, V, d, L, e) \tag{1}$$

The following are the fundamental dimensions of all the parameters involved:

$$\Delta p = [ML^{-1}T^{-2}]$$

$$\rho = [ML^{-3}]$$

$$\mu = [ML^{-1}T^{-1}]$$

$$V = [LT^{-1}]$$

$$d = [L]$$

$$L = [L]$$

$$e = [L]$$

Number of variables $n = 7$

Number of fundamental dimensions = 3 (i.e., M, L, and T)

Number of repeating variables (same as number of fundamental dimensions) $r = 3$

Thus, number of dimensionless terms (π-terms), $n - r = 7 - 3 = 4$

Hence, the number of variables is now reduced from 7 to 4 only.

Selection of repeating variables on the basis of rules discussed in Section 10.1.3:

Selecting ρ, μ, and d as repeating variables

Determining π-*terms:*

$$\pi_1 = \rho^a \mu^b d^c \Delta p$$

$$[M^0L^0T^0] = [ML^{-3}]^a [ML^{-1}T^{-1}]^b [L]^c [ML^{-1}T^{-2}]$$

Using the principle of dimensional homogeneity, that is, the power of each fundamental dimension must be the same on either side of equation.

T: $b = -2$

M: $a + b = -1 \quad \rightarrow \quad a = 1$

L: $3a + b - c = -1 \quad \rightarrow \quad c = 2$

Substituting the constants to get the first π-term

$$\pi_1 = \frac{\rho d^2 \Delta p}{\mu^2}$$

$$\pi_2 = \rho^a \mu^b d^c V$$

$$[M^0L^0T^0] = [ML^{-3}]^a [ML^{-1}T^{-1}]^b [L]^c [LT^{-1}]$$

Using the principle of dimensional homogeneity

T: $b = -1$

M: $a + b = 0 \quad \rightarrow \quad a = 1$

L: $3a + b - c = 1 \quad \rightarrow \quad c = 1$

Substituting the constants to get the second π-term

$$\pi_2 = \frac{\rho V d}{\mu}$$

$$\pi_3 = \rho^a \mu^b d^c L$$

$$[M^0 L^0 T^0] = [ML^{-3}]^a [ML^{-1}T^{-1}]^b [L]^c [L]$$

Using the principle of dimensional homogeneity

T: $b = 0$

M: $a + b = 0 \quad \rightarrow \quad a = 0$

L: $3a + f b - c = 1 \quad \rightarrow \quad c = -1$

Substituting the constants to get the third π-term

$$\pi_3 = \frac{L}{d}$$

The last π-term

$$\pi_4 = \rho^a \mu^b d^c e$$

$$[M^0 L^0 T^0] = [ML^{-3}]^a [ML^{-1}T^{-1}]^b [L]^c [L]$$

Using the principle of dimensional homogeneity

T: $b = 0$

M: $a + b = 0 \quad \rightarrow \quad a = 0$

L: $3a + b - c = 1 \quad \rightarrow \quad c = -1$

Substituting the constants to get the fourth π-term

$$\pi_4 = \frac{e}{d}$$

Therefore, the relation between dependent and independent parameters represented by Eq. (1), is now reduced as

$$\pi_1 = f_1(\pi_2, \pi_3, \pi_4)$$

$$\frac{\rho d^2 \Delta p}{\mu^2} = f_1\left(\frac{\rho V d}{\mu}, \frac{L}{d}, \frac{e}{d}\right)$$

Dividing π_1 by π_2^2 to get a new dimensionless term on the LHS to obtain the following

$$\frac{\Delta p}{\rho V^2} = f_2\left(\frac{\rho V d}{\mu}, \frac{L}{d}, \frac{e}{d}\right)$$

The aforementioned equation takes the following form when the LHS is divided by ½ and the dimensionless ratio *L/d* is taken out of the function f_2:

$$\frac{\Delta p}{(1/2)\rho V^2} = \frac{L}{d} f_3\left(\frac{\rho V d}{\mu}, \frac{e}{d}\right)$$

The aforementioned relation is nothing but the well-known Darcy–Weisbach equation, that is,

$$\Delta p = \frac{L}{d} f_3\left(\mathrm{Re}, \frac{e}{d}\right)\left(\frac{1}{2}\rho V^2\right)$$

where, the function $f_3(\mathrm{Re}, e/d)$ is the friction factor, which can be obtained from Moody's chart.

Example 10.5 The lift L is produced by an airplane wing of chord length l at an angle of attack α, when kept in a fluid with velocity V, density ρ, and viscosity μ. If the speed of sound in fluid is a, establish a relationship among involved variables.

Solution: The lift L is a function of independent parameters listed in the problem statement:

$$L = f(V, l, \rho, \mu, a, \alpha) \tag{1}$$

The following are the fundamental dimensions of all the parameters involved

$$L = [\mathrm{MLT^{-2}}]$$

$$\rho = [\mathrm{ML^{-3}}]$$

$$\mu = [\mathrm{ML^{-1}T^{-1}}]$$

$$V = [\mathrm{LT^{-1}}]$$

$$l = [\mathrm{L}]$$

$$a = [\mathrm{LT^{-1}}]$$

$$\alpha = [\mathrm{M^0L^0T^0}]$$

Number of variables $n = 7$
Number of fundamental dimensions = 3 (i.e., M, L, T)
Number of repeating variables (same as number of fundamental dimensions) $r = 3$
Thus, number of dimensionless terms (π-terms), $n - r = 7 - 3 = 4$.
Hence, the number of variables is now reduced from 7 to 4 only.

Selection of repeating variables on the basis of rules discussed in Section 10.1.3:

Selecting ρ, V, and l as repeating variables

Determining π*-terms:*

$$\pi_1 = \rho^{\mathrm{a}} V^{\mathrm{b}} l^{\mathrm{c}} L$$

$$[\mathrm{M^0L^0T^0}] = [\mathrm{ML^{-3}}]^{\mathrm{a}} [\mathrm{LT^{-1}}]^{\mathrm{b}} [\mathrm{L}]^{\mathrm{c}} [\mathrm{MLT^{-2}}]$$

Using the principle of dimensional homogeneity, that is, the power of each fundamental dimension must be the same on either side of the equation.

T: $-\mathrm{b} - 2 = -2 \rightarrow \mathrm{b} = -2$
M: $\mathrm{a} + 1 = 0 \rightarrow \mathrm{a} = -1$
L: $-3\mathrm{a} + \mathrm{b} + \mathrm{c} + 1 = 0 \rightarrow \mathrm{c} = -2$

Substituting the constants to get the first π-term

$$\pi_1 = \frac{L}{\rho V^2 l^2}$$

$$\pi_2 = \rho^a V^b l^c \mu$$

$$[M^0L^0T^0] = [ML^{-3}]^a [LT^{-1}]^b [L]^c [ML^{-1}T^{-1}]$$

Using the principle of dimensional homogeneity, that is, the power of each fundamental dimension must be the same on either side of the equation.

T: $-b - 1 = 0 \rightarrow b = -1$

M: $a + 1 = 0 \rightarrow a = -1$

L: $-3a + b + c - 1 = 0 \rightarrow c = -1$

Substituting the constants to get the second π-term

$$\pi_2 = \frac{\mu}{\rho V l}$$

$$\pi_3 = \rho^a V^b l^c a$$

$$[M^0L^0T^0] = [ML^{-3}]^a [LT^{-1}]^b [L]^c [LT^{-1}]$$

Using the principle of dimensional homogeneity, that is, the power of each fundamental dimension must be the same on either side of the equation.

T: $-b - 1 = 0 \rightarrow b = -1$

M: $a = 0$

L: $-3a + b + c + 1 = 0 \rightarrow c = 0$

Substituting the constants to get the third π-term

$$\pi_3 = \frac{a}{V}$$

The fourth π-term will be same as angle of attack (dimensionless).

$$\pi_4 = \alpha$$

Therefore, the relation between dependent and independent parameters represented by Eq. (1), is now reduced as

$$\pi_1 = f_1(\pi_2, \pi_3, \pi_4)$$

$$\frac{L}{\rho V^2 l^2} = f_1\left(\frac{\mu}{\rho V l}, \frac{a}{V}, \alpha\right)$$

The aforementioned equation may be reduced to

$$C_L = \frac{L}{(1/2)\rho V^2 A} = f_2(\mathrm{Re}, M, \alpha)$$

where, C_L is the lift coefficient.

10.1.4 Taylor Analysis

The utility of dimensional analysis can be judged from its successful predictions in various fields, for example, aviation, shipping, automotive sector, etc. G.I. Taylor, a British physicist, used dimensional analysis for estimating the energy released during a nuclear explosion. The analysis was based on the released photographs of Trinity test in New Mexico in 1945 (Fig. 10.1). The analysis provided a close estimate of the energy released during the actual test. G.I. Taylor's analysis[1,2] is based on the assumptions that shock wave (fire ball) is spherical in shape and it emanates from a small space. The radius of the fire ball R is a function of time t, energy released E, and the density of the surrounding medium, that is, air ρ.

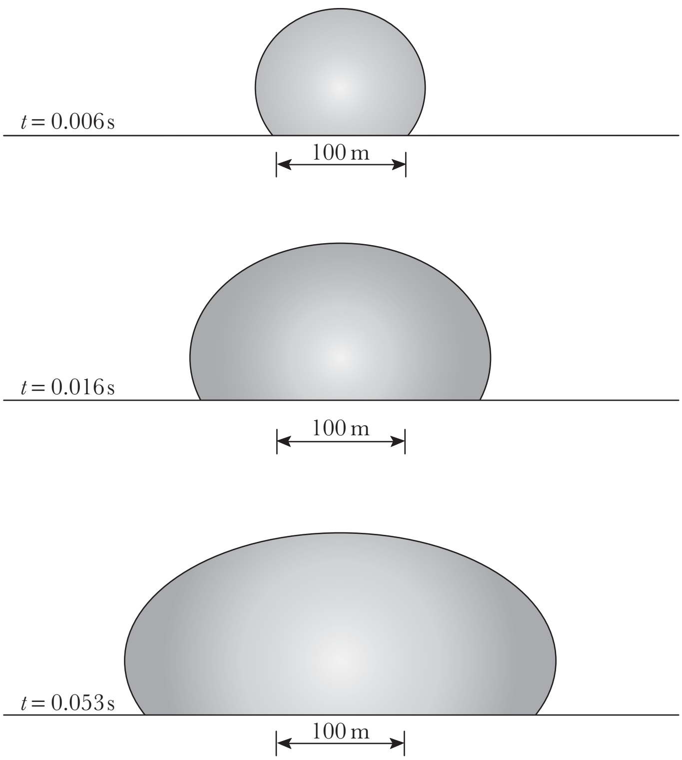

Fig. 10.1 Schematic diagram showing progression of nuclear explosion

1. G.I. Taylor, The formation of a blast wave by a very intense explosion: Theoretical discussion. Proc. Roy. Soc. A 201 (1950), pp. 493–509 [Reprinted in The Scientific Papers of Sir Geoffrey Ingram Taylor, Vol. 3, G.K. Batchelor, ed., Cambridge University Press, Cambridge, pp. 510–521].
2. G.I. Taylor, The formation of a blast wave by a very intense explosion: II. The atomic explosion of 1945. Proceedings of the Royal Society A 201, 1950, pp. 493–509 [Reprinted in The scientific papers of Sir Geoffrey Ingram Taylor, G.K. Batchelor. ed., Vol. 3, Cambridge University Press, pp. 510–521].

The fundamental dimensions of these parameters are

$$R = [\mathrm{L}]$$
$$E = [\mathrm{ML^2T^{-2}}]$$
$$\rho = [\mathrm{ML^{-3}}]$$
$$t = [\mathrm{T}]$$

Relating the dependent parameter with the independent parameters by power law form,

$$R = \mathrm{C_1} E^{\mathrm{a}} \rho^{\mathrm{b}} t^{\mathrm{c}} \tag{10.6}$$

$$[\mathrm{L}] = [\mathrm{M^0L^0T^0}]\ [\mathrm{ML^2T^{-2}}]^{\mathrm{a}} [\mathrm{ML^{-3}}]^{\mathrm{b}} [\mathrm{T}]^{\mathrm{c}}$$

$$[\mathrm{M^0L\,T^0}] = [\mathrm{M}]^{\mathrm{a+b}} [\mathrm{L}]^{\mathrm{2a-3b}} [\mathrm{T}]^{\mathrm{-2a+c}}$$

Equating the power indices (exponents) of M, L, and T, the following three equations are evolved:

M: $\mathrm{a + b = 0}$
L: $\mathrm{2a - 3b = 1}$
T: $\mathrm{-2a + c = 0}$

Solving these equations to obtain exponents a, b, and c:

$$\boxed{\mathrm{a = 1/5}}$$
$$\boxed{\mathrm{b = -1/5}}$$
$$\boxed{\mathrm{c = 2/5}}$$

Substituting these constants in Eq. (10.6)

$$R = \mathrm{C_1}\left(\frac{Et^2}{\rho}\right)^{1/5}$$

The energy released is, thus, given by

$$E = \mathrm{C}\frac{\rho R^5}{t^2}$$

where, constant $\mathrm{C} = 1/\mathrm{C_1^5}$.

Assuming the constant C = 1, the expression for energy released during explosion is given by

$$\boxed{E = \frac{\rho R^5}{t^2}}$$

At $t = 0.006$ s, the radius of the fireball $R = 80$ m (approx.), the energy released

$$E = \frac{1.2 \times 80^5}{0.006^2} \Rightarrow \boxed{E = 1.092 \times 10^8\ \mathrm{MJ}}$$

10.2 SIMILITUDE

Real-life problems usually involve a number of phenomena occurring simultaneously, for example, fluid-structure interaction, fluid-thermal coupling, etc. This makes the analytical solution of such complex problems very difficult. In addition, numerical solution requires extraordinary skills and computational facilities. Further, conducting experiments on full-scale models involve huge finances and meticulous planning. For example, it is not feasible to construct a full-scale model of a dam/high-rise building/spacecraft just for experimental purpose. The design has to be foolproof so that the chances of failure are the least. One way of dealing with such problems is to conduct the experimental tests on the scale-down models before going for construction or manufacturing. This will save time and money and ensure the safe design of the actual structure or machine.

The structure or machine of actual size is known as *prototype*, whereas, its geometric replica is termed as *model*. It should be noted that the model is not always smaller than its prototype. When the prototype is of miniature type, the model is usually scaled-up to carry out experimental tests. It should also be remembered that while testing a model, the use of the same fluid is not necessary. The *similitude* is defined as complete similarity between the model and its prototype. The complete similarity is achieved only when the two are geometrically, kinematically, and dynamically similar, as shown in Fig. 10.2.

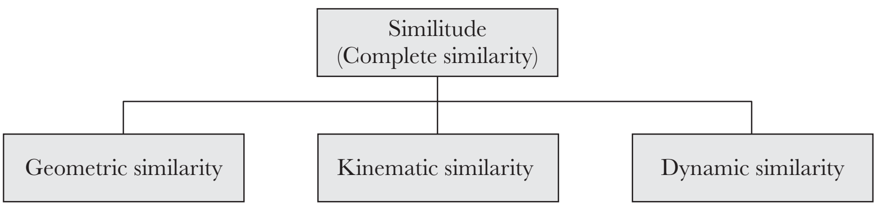

Fig. 10.2 Organization chart for defining similitude

The model and prototype of an airfoil section has been shown in Fig. 10.3. The model, as can be seen from the figure, is the geometric replica of its prototype. The two are subjected to different velocities in a fixed ratio. The prototype and model are subjected to different forces, namely, pressure force (F_p), viscous force (F_v), and gravity force (F_g). Their directions are also shown in Fig. 10.3.

10.2.1 Geometric Similarity

The geometric similarity is also known as similarity of shapes, as shown in Fig. 10.3. The model and prototype are said to be similar if the ratios of the corresponding dimensions are equal, that is,

$$\frac{l_m}{l_p} = l_r \tag{10.7}$$

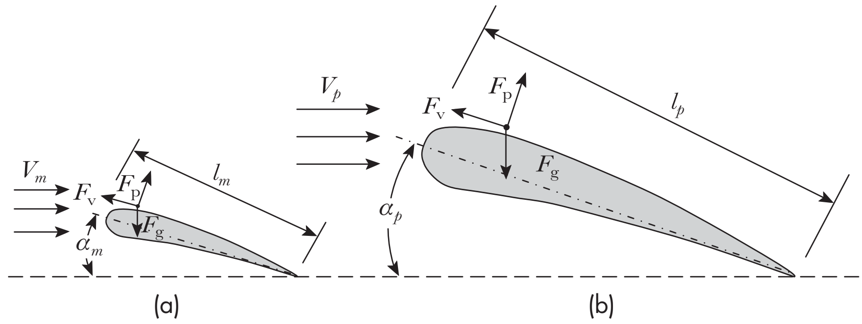

Fig. 10.3 Airfoil section (a) Model (b) Prototype

where, l_m and l_p are the corresponding length dimensions of model and prototype, respectively, and l_r is known as the *length scale factor* or *model ratio*.

Attaining geometric similarity seems easier but the fact is that it is almost impossible to attain. The reason is that the surface roughness needs to be scaled down or scaled up in the same proportion, which may not be possible. However, for the sake of convenience the geometric similarity does not include surface roughness.

10.2.2 Kinematic Similarity

The similarity of fluid motion on model and prototype is termed as kinematic similarity. The motion is defined in terms of velocity and acceleration. Both these quantities involve distance and time. For distance, the *length scale factor* is used as described in Eq. (10.7). For time, the *time scale factor* is defined in a similar way:

$$t_r = \frac{t_m}{t_p} \tag{10.8}$$

Similarly, the *velocity scale factor*

$$V_r = \frac{V_m}{V_p} \quad \Rightarrow \quad V_r = \frac{l_m/t_m}{l_p/t_p} \quad \Rightarrow \quad V_r = \frac{l_r}{t_r} \tag{10.9}$$

and, the *acceleration scale factor*

$$a_r = \frac{a_m}{a_p} \quad \Rightarrow \quad a_r = \frac{l_m/t_m^2}{l_p/t_p^2} \quad \Rightarrow \quad a_r = \frac{l_r}{t_r^2} \tag{10.10}$$

The physical meaning of kinematic similarity is that the fluid motion represented by the patterns formed by streamlines on model and prototype will be similar at a given instance.

10.2.3 Dynamic Similarity

Dynamic similarity pertains to similarity of forces acting on the model and the prototype. According to this, the ratio of magnitude of forces on the corresponding points at the surface of the prototype and model must be constant. Table 10.2 shows the forces that may encounter in fluid flow.

Table 10.2 Forces in fluid flow

Force	Formulae
Inertia force, F_i	$F_i = m \times a \Rightarrow F_i = \rho l^3 \times V^2/l \Rightarrow F_i = \rho l^2 V^2$
Viscous force, F_v	$F_v = \tau \times A \Rightarrow F_v = \mu \frac{V}{l} \times l^2 \Rightarrow F_v = \mu V l$
Pressure force, F_p	$F_p = p \times A \Rightarrow F_p = p l^2$
Gravity force, F_g	$F_g = mg \Rightarrow F_g = \rho l^3 g$
Elastic force, F_e	$F_e = E l^2$
Surface tension force, F_σ	$F_\sigma = \sigma l$

The ratios of inertia force to other forces are the famous non-dimensional numbers used in fluid mechanics. Table 10.3 presents these non-dimensional numbers.

On the basis of equivalence of these non-dimensional numbers, the dynamic similarity is established between the model and the prototype. Depending upon the type of flow, the equivalence of the particular non-dimensional number is applied:

Reynolds model law This law is applicable for the flow conditions where the effects of viscous forces are predominant. For dynamic similarity in such cases, the Reynolds number for model and prototype must be the same.

$$\mathrm{Re}_m = \mathrm{Re}_p \quad \Rightarrow \quad \left(\frac{\rho V l}{\mu}\right)_m = \left(\frac{\rho V l}{\mu}\right)_p \tag{10.11}$$

Froude model law This law is applicable when the flow is gravity-driven flow, that is, flow in open channels and flow in tilted pipes. For dynamic similarity in such cases, the Froude number for model and prototype must be the same.

$$Fr_m = Fr_p \quad \Rightarrow \quad \left(\frac{V}{\sqrt{gl}}\right)_m = \left(\frac{V}{\sqrt{gl}}\right)_p \tag{10.12}$$

Table 10.3 Non-dimensional numbers

Force	Definition	Formula	Application
Reynolds number, Re	$\mathrm{Re} = \dfrac{\text{Inertia force}}{\text{Viscous force}}$	$\mathrm{Re} = \dfrac{\rho Vl}{\mu}$	• Finds application in internal as well as external flows • Helps in identifying whether the flow is laminar or turbulent
Froude number, *Fr*	$Fr = \sqrt{\dfrac{\text{Inertia force}}{\text{Gravity force}}}$	$Fr = \dfrac{V}{\sqrt{gl}}$	• Finds application in open channel flows • Helps in identifying whether the flow is subcritical or supercritical
Mach number, *M*	$M = \sqrt{\dfrac{\text{Inertia force}}{\text{Elastic force}}}$	$M = \dfrac{V}{\sqrt{E/\rho}}$	• Finds application in compressible flows • Helps in identifying whether the flow is subsonic or supersonic
Euler number, *Eu*	$Eu = \sqrt{\dfrac{\text{Inertia force}}{\text{Pressure force}}}$	$Eu = \dfrac{V}{\sqrt{p/\rho}}$	• Finds application in flows with pressure or pressure difference is important
Weber number, *We*	$We = \sqrt{\dfrac{\text{Inertia force}}{\text{Surface tension force}}}$	$We = \dfrac{V}{\sqrt{\sigma/\rho l}}$	• Finds application in two-phase flows, droplet dynamics, etc.

Euler model law This law is applicable where the pressure forces are predominant. For dynamic similarity in such cases, the Euler number for model and prototype must be the same.

$$Fr_m = Fr_p \quad \Rightarrow \quad \left(\frac{V}{\sqrt{p/\rho}}\right)_m = \left(\frac{V}{\sqrt{p/\rho}}\right)_p \tag{10.13}$$

Mach model law This law is applicable for compressible flows. As the density varies due to pressure, there is elastic compression and the corresponding force is known as elastic force. For dynamic similarity in such cases, the Mach number for model and prototype must be the same.

$$M_m = M_p \quad \Rightarrow \quad \left(\frac{V}{\sqrt{E/\rho}}\right)_m = \left(\frac{V}{\sqrt{E/\rho}}\right)_p \tag{10.14}$$

Weber model law This law is applicable for the cases where the surface tension force is significant. The surface tension comes into picture whenever the liquid and the vapour phases come in contact. This force acts at the liquid–vapour interface, for example, bubble and droplet dynamics. For dynamic similarity in such cases, the Weber number for model and prototype must be the same.

$$We_m = We_p \quad \Rightarrow \quad \left(\frac{V}{\sqrt{\sigma/\rho l}}\right)_m = \left(\frac{V}{\sqrt{\sigma/\rho l}}\right)_p \tag{10.15}$$

Let us consider the example of the wing of an aircraft having airfoil section, shown in Fig. 10.2. It is required to test the model of the aircraft wing in a wind tunnel and obviously the model should be set at the same angle of attack as that of the prototype. The question is—at what air velocity should the model be tested so that the lift produced by the prototype at a given speed and angle of attack can be predicted? To find the solution to this problem, the following steps are to be taken:

1. To attain the dynamic similarity between the model and the prototype, the Reynolds model law must be satisfied,

$$\frac{\rho_m V_m l_m}{\mu_m} = \frac{\rho_p V_p l_p}{\mu_p} \tag{10.16}$$

   The air velocity at which the model will be tested inside the wind tunnel is obtained from Eq. (10.16):

$$V_m = \frac{\mu_m}{\mu_p}\frac{l_p}{l_m}\frac{\rho_p}{\rho_m}V_p \tag{10.17}$$

2. In addition, the dynamic similarity requires equivalence of lift coefficients for the model and the prototype.

$$\frac{L_p}{(1/2)\rho_p V_p^2 l_p^2} = \frac{L_m}{(1/2)\rho_m V_m^2 l_m^2} \tag{10.18}$$

Therefore, lift produced by the prototype at the same angle of attack is obtained from Eq. (10.18):

$$L_p = \frac{\rho_p}{\rho_m}\left(\frac{V_p}{V_m}\right)^2\left(\frac{l_p}{l_m}\right)^2 L_m \tag{10.19}$$

Example 10.6 A dam is to be constructed across a river, 25 m wide, to discharge the water at the rate of 150 m³/s under a head of 5 m. Determine the dimensions for the dam's laboratory model if the available discharge at the test section is 30 L/s.

Solution: Using Froude model law,

$$Fr_m = Fr_p \quad \Rightarrow \quad \frac{V_m}{\sqrt{gh_m}} = \frac{V_p}{\sqrt{gh_p}} \quad \Rightarrow \quad \frac{V_m}{V_p} = \sqrt{\frac{h_m}{h_p}}$$

The velocity ratio is the square root of depth ratio,

$$V_r = \sqrt{h_r}$$

Ratio of flow area

$$\frac{A_m}{A_p} = \frac{b_m h_m}{b_p h_p} \quad \Rightarrow \quad A_r = b_r h_r$$

From the geometric similarity,

$$\frac{b_m}{b_p} = \frac{h_m}{h_p} \quad \Rightarrow \quad b_r = h_r$$

Discharge ratio

$$\frac{Q_m}{Q_p} = \frac{A_m V_m}{A_p V_p} \quad \Rightarrow \quad Q_r = A_r V_r \quad \Rightarrow \quad Q_r = h_r^{2.5}$$

Substituting the values to get the value of

$$h_r = \left(\frac{30\times 10^{-3}}{150}\right)^{1/2.5} \quad \Rightarrow \quad h_r = 0.03314$$

The head required for the dam's model

$$h_m = h_r h_p \quad \Rightarrow \quad h_m = 0.03314\times 5 \quad \Rightarrow \quad h_m = 16.57\,\text{cm}$$

The width of the dam's model

$$b_m = b_r b_p \quad \Rightarrow \quad b_m = 0.03314\times 25 \quad \Rightarrow \quad b_m = 82.85\,\text{cm}$$

Example 10.7 To design an aircraft for the flight velocity of 350 km/h under atmospheric conditions, a 1/5-th model of the aircraft is to be tested in a wind tunnel, the pressure used in wind tunnel is 5 times the atmospheric pressure.

(a) Determine the air velocity for testing the model.
(b) What would the drag on the actual aircraft be if the drag on the model is 400 N?

Solution: Since the aircraft is to be designed for low velocity, that is, 350 km/h. The sound velocity at 25°C is 1245 km/h and the corresponding Mach number is less than 0.3. Effect of compressibility does not come into picture, only Reynolds model law would be sufficient for designing of the aircraft.

$$\mathrm{Re}_m = \mathrm{Re}_p \quad \Rightarrow \quad \frac{\rho_m V_m l_m}{\mu_m} = \frac{\rho_p V_p l_p}{\mu_p} \quad \Rightarrow \quad \frac{V_m}{V_p} = \frac{\mu_m}{\mu_p}\frac{\rho_p}{\rho_m}\frac{l_p}{l_m}$$

The velocity ratio is, thus, given by

$$V_r = \frac{\mu_r}{\rho_r l_r}$$

Since pressure does not affect the viscosity significantly, $\mu_r = 1$, the air density varies with the variation in pressure. Considering isothermal conditions, p/ρ = constant.

$$\frac{\rho_m}{\rho_p} = \frac{p_m}{p_p} \quad \Rightarrow \quad \rho_r = p_r \quad \Rightarrow \quad \rho_r = 5$$

Thus, the velocity ratio is

$$V_r = \frac{\mu_r}{\rho_r l_r} \quad \Rightarrow \quad V_r = \frac{1}{5 \times 1/5} \quad \Rightarrow \quad V_r = 1$$

The velocity of air at which the model to be tested inside the wind tunnel is

$$V_m = V_r V_p \quad \Rightarrow \quad V_m = 350\,\text{km/h}$$

The ratio of drag forces

$$D_r = \frac{D_m}{D_p} = \rho_r l_r^2 V_r^2 \quad \because \quad D = \frac{1}{2}\rho V^2 A$$

Therefore, the drag on the actual aircraft is

$$D_p = \frac{D_m}{\rho_r l_r^2 V_r^2} \quad \Rightarrow \quad D_p = \frac{400}{5 \times (1/5)^2 \times 1^2} \quad \Rightarrow \quad D_p = 2000\,\text{N}$$

10.2.4 Distorted Models

One may come across some practical problems where the application of strict adherence to similitude principles may not be possible. For example, in order to model rivers, estuaries, ports, dams, etc., where there is a longitudinal slope and large areal spread (basin), the same geometric scaling will lead to unexpected erroneous results. In such cases, distorted scale modelling is recommended. The vertical flow dimension (depth) is scaled by Froude model law while length and width are scaled to the available space where the river model is to be built. The horizontal scales are of the order of 1/200–1/1000, whereas, vertical scale is of the order of 1/100 (see Example 10.8).

Example 10.8 To model a river, the horizontal scale is 1:500 and vertical scale is 1:50, determine (a) model bed slope if prototype bed slope is 0.0003 (b) river flow velocity and discharge if the corresponding values for the model are 1 m/s and 30 L/s, respectively.

Solution: This problem demonstrates the use of a distorted model to model the river flow.

Given that h_r = 1/50 and b_r = 1/500

The length ratio is the same as the width ratio to attain geometric similarity, that is, l_r = 1/500

(a) Slope ratio

$$\frac{i_m}{i_p} = \frac{h_m/l_m}{h_p/l_p} \quad \Rightarrow \quad i_r = \frac{h_r}{l_r} \quad \Rightarrow \quad i_r = \frac{1/50}{1/500} \quad \Rightarrow \quad i_r = 10$$

Thus, the bed slope for the river model is

$$i_m = i_r i_p \quad \Rightarrow \quad i_m = 0.003$$

(b) Velocity ratio is obtained from Froude model law

$$\frac{V_m}{V_p} = \sqrt{\frac{h_m}{h_p}} \quad \Rightarrow \quad V_r = \sqrt{h_r} \quad \Rightarrow \quad V_r = \sqrt{1/50} \quad \Rightarrow \quad V_r = 0.1414$$

The flow velocity of river

$$V_p = V_m / V_r \quad \Rightarrow \quad V_m = 1/0.1414 \quad \Rightarrow \quad V_m = 7.07 \text{ m/s}$$

Ratio of flow area

$$\frac{A_m}{A_p} = \frac{b_m h_m}{b_p h_p} \quad \Rightarrow \quad A_r = b_r h_r$$

Discharge ratio

$$\frac{Q_m}{Q_p} = \frac{A_m V_m}{A_p V_p} \quad \Rightarrow \quad Q_r = A_r V_r \quad \Rightarrow \quad Q_r = b_r h_r^{1.5} \quad \Rightarrow \quad Q_r = \frac{1}{500}\left(\frac{1}{50}\right)^{1.5}$$

The discharge through river

$$Q_p = Q_m / Q_r \quad \Rightarrow \quad Q_p = 500 \times 50^{1.5} \times 0.03 \quad \Rightarrow \quad Q_p = 5303.3 \text{m}^3\text{/s}$$

POINTS TO REMEMBER

- Dimensional analysis helps in developing a functional relationship between the dependent and independent variables of a system. However, it does not establish the exact relationship. For exact relation, experiments are conducted to find out the unknown factors using regression analysis.
- There are two commonly used methods of dimensional analysis are Rayleigh method and Buckingham-pi method. Buckingham-pi method is more advantageous due to reduction in the number of variables by forming non-dimensional groups.
- Similitude is the complete similarity between an actual system (prototype) and its geometric replica (model). The model must comply with the prototype on the basis on geometric, kinematic, and dynamic similarities.
- Geometric similarity is the similarity in shapes, kinematic similarity is the similarity in motion, and dynamic similarity is the similarity of the forces acting on them.
- The distorted models are used when it is difficult to adhere to uniform scaling in all the dimensions. In such cases, the scaling factor is different for vertical and horizontal directions.

SUGGESTED READINGS

Douglas, J.F., J.M. Gasiorek, J.A. Swaffield, *Fluid Mechanics*, 3rd Ed., Addison-Wesley Longman, Delhi, 1999.

Massey, B., *Mechanics of Fluids*, 8th Ed., Taylor and Francis, Noida, 2010.

Subramanya, K., *Theory and Applications of Fluid Mechanics*, Tata McGraw Hill Education Pvt. Ltd., New Delhi, 1993.

Taylor, B.N., A. Thompson, *The International Systems of Units* (*SI*), 2008 Ed., NIST Special Publications 330, 2008.

MULTIPLE-CHOICE QUESTIONS

10.1 Pascal-second is the unit of

(a) drag
(b) kinematic viscosity
(c) dynamic viscosity
(d) pressure

10.2 Froude number is the ratio of inertia force to

(a) viscous force
(b) buoyancy force
(c) gravity force
(d) surface tension force

10.3 Kinematic similarity is the similarity of

(a) motion
(b) dimensions
(c) forces
(d) all of these

10.4 Dynamic similarity is similarity of

(a) forces
(b) dimensions
(c) motion
(d) all of these

10.5 Is the true geometric similarity possible?

(a) Yes
(b) No
(c) Can't say
(d) Sometimes it's possible

10.6 If Reynolds number and Froude number for model and prototype, to be tested on the same fluid, are equal then the scale of the model is

(a) V_r
(b) $\sqrt{V_r}$
(c) $\dfrac{1}{\sqrt{V_r}}$
(d) 1.0

10.7 What will be the discharge ratio in a distorted model of harbour if horizontal and vertical scales are L_r and h_r, respectively?

(a) $L_r h_r$
(b) $L_r^{1/2} h_r$
(c) $L_r h_r^{1/2}$
(d) $L_r h_r^{3/2}$

10.8 Distorted models are used for

(a) large prototype
(b) prototype with large difference in horizontal and vertical dimensions
(c) large prototype with complex geometry
(d) none of these

10.9 Which law of similarity is trait for two phase flow in a horizontal tube?

(a) Reynolds model law
(b) Froude model law
(c) Euler model law
(d) Mach model law

10.10 A $\frac{1}{20}$ size model of a boat has a drag of 0.2 N while testing at a speed of 2 m/s inside the laboratory with the fluid used for prototype. What will be corresponding resistance in the actual boat?

(a) 0.16 kN (c) 16 kN
(b) 1.6 kN (d) 160 kN

REVIEW QUESTIONS

10.1 What do you understand by dimensional homogeneity?
10.2 What is the significance of dimensional analysis?
10.3 What is similitude? What are different types of similarities between the model and its prototype?
10.4 Why is it impossible to achieve geometric similarity between a model and its prototype?
10.5 Discuss the need for distorted models.

UNSOLVED PROBLEMS

10.1 Using Rayleigh method, show that the discharge Q through the triangular notch having vertex angle θ and head h is given by

$$\frac{Q}{\sqrt{gh}} = h^2 f\left(\theta, \frac{V}{\sqrt{gh}}\right)$$

where V is the velocity of approach and g is the acceleration due to gravity.

10.2 If the power P developed by a hydraulic turbine is found to depend on water density ρ, speed of rotation N(rpm), runner diameter D, head available at turbine inlet H and acceleration due to gravity g, develop a functional relationship among the parameters using Rayleigh method.

$$\left[\textbf{Ans: } \boldsymbol{P = K\rho N^3 D^5 f\left(\frac{H}{D}, \frac{g}{N^2 D}\right)}\right]$$

10.3 Using Buckingham-pi method, show that the frictional torque T of a disc of diameter D rotating with speed N in a viscous fluid having dynamic viscosity μ and density ρ is given by

$$\frac{T}{\rho N^2 D^5} = f\left(\frac{\mu}{\rho N D^2}\right)$$

10.4 Obtain the functional relationship using Buckingham-pi method for discharge Q through a triangular notch which depends upon the head h above it, height H and top width B of the notch, and fluid properties dynamic viscosity μ, density ρ, surface tension σ, and acceleration due to gravity g.

$$\left[\textbf{Ans: } \boldsymbol{\frac{Q}{\sqrt{g}h^{5/2}} = f\left(\frac{H}{h}, \frac{B}{h}, \frac{\mu}{\sqrt{g}\rho h^{3/2}}, \frac{\sigma}{\rho g h^2}\right)}\right]$$

10.5 Apply Buckingham-pi method to derive an expression for the shear stress τ_w at the bed of a rough channel having flow depth h, average roughness height e, the flow velocity V, fluid density ρ, and dynamic viscosity μ.

$$\left[\textbf{Ans: } \frac{\tau_w}{\rho V^2} = f\left(\frac{e}{h}, \frac{\mu}{\rho V h}\right)\right]$$

10.6 Determine the velocity of water at 50°C through a smooth pipe of diameter 150 mm, if the water flow is dynamically similar to the air flowing at a velocity 150 m/s through the pipe of 100 mm diameter at 25°C.

[Ans: 3.54 m/s]

10.7 An aircraft is to fly at 1440 km/h at a height of 10 km above the sea level (where the temperature is –50°C and pressure is 26.5 kPa). A 1/20th scale model is tested in a pressurized wind tunnel in which air is 25°C. For complete dynamic similarity, what pressure and velocity should be used in the wind tunnel? (For air $\mu \alpha T^{1.5}/(T + 117)$, $K = \gamma p$, $p = \rho RT$, where the temperature T is in K, γ is the ratio of specific heats).

[Ans: 1036.2 kPa, 462.4 m/s]

10.8 A 10 km long canal having flow depth of 5 m, width 100 m, and bed slope 0.002 is to be modelled inside the laboratory space of 20 m keeping vertical scale 1/5. The average discharge through the canal is 10,000 m³/s. Determine the discharge and dimensions of the canal model. [*Hint*: Use distorted model theory]

[Ans: Q = 56.5 L/s, b = 0.2 m, h = 0.1 m, i = 0.02]

Answers to Multiple-choice Questions

10.1 (c)	10.2 (c)	10.3 (a)	10.4 (a)	10.5 (b)
10.6 (d)	10.7 (d)	10.8 (b)	10.9 (d)	10.10 (b)

Features of the Book

DESIGN OF EXPERIMENTS

Experiment 4.1 Verification of Bernoulli's

Objective
To verify the Bernoulli's equation

Theory
Bernoulli's equation is the energy conservation equation, whicl energy of a flow system is constant. The condition for the apı equation is that the flow should be incompressible, non-viscous In addition, there should be no heat transfer and work done.

Experiment 4.2 Verification of Momentum Equation

Objective
To verify the linear momentum equation using the impact of jı

Theory
The force generated by impinging jet on a plate can be theoret momentum equation. In the proposed design, a water jet symm of the plate has been considered. Let us assume a control volur stream on the plate surface due to jet impingement with subscr the outlet, as shown in Fig. E4.2. From continuity equation (ini

Design of Experiments

Each chapter includes a section Design of Experiments where two experiments are detailed, complete with the experimental set-up, tabulation formats, and the step-by-step procedure enabling the students to apply the concepts discussed in the chapter.

Points to Remember

Given at the end of each chapter, it enables quick recapitulation of the important concepts discussed in the chapter.

POINTS TO REMEMBER

- Reynolds transport equation is a tool to convert system analy volume analysis. It relates the rate of change of an extensive system to the rate of change of the corresponding intensive control volume.
- N–S equations are the most versatile equations in fluid dynam used for solving almost all types of flow problems, that is, st uniform, non-uniform, viscous, non-viscous, incompressible one dimensional and multidimensional.
- The momentum equation is based on Newton's second law of helpful in determining the forces and reactions in flow systems impinging jets, thrust calculations.
- Bernoulli's equation is a condensed form of N–S equation appli incompressible, inviscid, and one-dimensional flow problems. ' equation can be modified to incorporate the work done by appl balance across the external work agency.
- In Couette flow, the incompressible viscous flow between tl plates is studied with one plate moving while the other is m The pressure gradient affects the magnitude of flow velociti two plates. The favourable pressure gradient causes flow velo whereas the adverse pressure gradient retards the flow.

Example 4.2 In Fig. 4.5, water enters a bend diameter 30 cm fitted with nozzle of diameter 15 c at the end at a pressure 15 kPa (gauge). The dischar through the bend is 90 L/s. Determine the horizon component of force acting at the inlet.

Solution: From continuity equation,

$$Q = A_1V_1 = A_2V_2$$

The velocities at sections 1 and 2,

$$V_1 = \frac{Q}{A_1} = \frac{4Q}{\pi d_1^2} \Rightarrow V_1 = \frac{4\times 0.09}{\pi(0.3)^2} \Rightarrow V_1 =$$

Solved Examples

Numerous simple and relevant solved examples are provided at the end of each section to augment the understanding of concepts.

Figures and Graphs

Each chapter is interspersed with numerous simple illustrations and graphical representations that complement the discussions in the text.

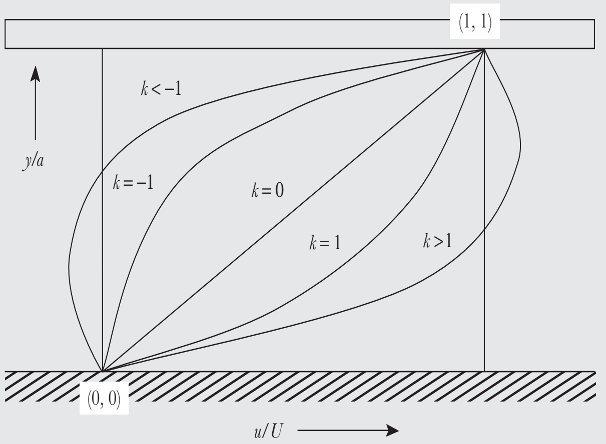

Fig. 4.21 Velocity profiles for different k's

Table 4.1 Velocity profiles for different pressure gradients

Cases	Velocity profile	Description
$k = 0$ i.e., $\frac{dp}{dx} = 0$	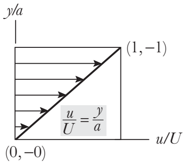	In absence of pressure gradient, the flu between the plates is stationary until th upper plate is moved with a velocity, U There won't be any slip (or any relativ motion) between the plate surface and th contacting fluid. The velocity varies linear between the two plates.
$k = -1$ i.e., $\frac{dp}{dx} > 0$	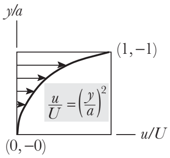	In the presence of adverse pressure gradie ($dp/dx > 0$), pressure increases in the flow c direction, thus it acts as a barrier to the flow. A such, the velocities at different y's between th plates reduce as compared to the case whe there was no pressure gradient. The veloci profile for this case is a parabola with verte (0, 0) and axis as the x-axis.
Large negative values of k		In presence of very strong adverse pressu gradient $dp/dx >> 0$, the flow velocities ne

Tables

Tabular presentation of data helps to quickly grasp the information and also serves as a ready-reckoner.

APPENDIX A

Properties of Common Fluids

Table A1 Thermophysical properties of common gases at 25°C temperature and 101.325 kPa pressure

Gas	ρ (kg/m³)	c_v (kJ/kg-K)	c_p (kJ/kg-K)	μ (kg/m-s) × 10^{-6}	γ	R (kJ/kg-K)
Air	1.184	0.71806	1.0066	18.492	1.4018	0.28854
CO_2	1.8081	0.65749	0.85085	14.932	1.2941	0.19336
N_2	1.1453	0.74314	1.0413	17.812	1.4013	0.29816
O_2	1.3089	0.65845	0.91963	20.459	1.3967	0.26118
Argon	1.6339	0.31239	0.52156	22.559	1.6696	0.20917
NH_3	0.70355	1.6448	2.1645	10.093	1.316	0.5197
CH_4	0.65691	1.7086	2.2317	11.186	1.3062	0.5231
C_2H_6	1.2386	1.4721	1.7576	9.3541	1.1939	0.2855
C_3H_8	1.832	1.4887	1.6909	8.1463	1.1359	0.2022
C_4H_{10}	2.4497	1.5693	1.7348	7.4054	1.1055	0.1655

Source: REFPROP 9.0 refrigerant property database developed by the National Institute of Standards and Technology (NIST).

Table A2 Properties of air at standard atmospheric pressure (101.325 kPa)

T (°C)	ρ (kg/m³)	c_v (kJ/kg-K)	c_p (kJ/kg-K)	μ (kg/m-s) × 10^{-6}
−50	1.5840	0.7163	1.0062	14.6500
−40	1.5156	0.7164	1.0060	15.1890
−30	1.4530	0.7165	1.0059	15.7180
−20	1.3953	0.7166	1.0058	16.2390
−10	1.3421	0.7169	1.0058	16.7530
0	1.2927	0.7171	1.0060	17.2590
10	1.2469	0.7175	1.0061	17.7570
20	1.2043	0.7178	1.0064	18.2490
30	1.1644	0.7183	1.0068	18.7340
40	1.1272	0.7188	1.0072	19.2120
50	1.0922	0.7194	1.0077	19.6840

(*Contd*)

Table A2 Properties of air at standard atmospheric pressure (*Contd*)

T (°C)	ρ (kg/m^3)	c_v (kJ/kg-K)	c_p (kJ/kg-K)	μ (kg/m-s) $\times 10^{-6}$
60	1.0594	0.7201	1.0083	20.1500
70	1.0284	0.7208	1.0090	20.6090
80	0.9993	0.7217	1.0097	21.0640
90	0.9717	0.7226	1.0106	21.5120
100	0.9456	0.7236	1.0115	21.9560
110	0.9209	0.7246	1.0125	22.3940
120	0.8975	0.7258	1.0136	22.8270
130	0.8752	0.7270	1.0148	23.2550
140	0.8540	0.7283	1.0160	23.6790
150	0.8338	0.7297	1.0174	24.0980

Source: REFPROP 9.0 refrigerant property database developed by the National Institute of Standards and Technology (NIST).

Table A3 Properties of air at 25°C

p (MPa)	ρ (kg/m^3)	c_v (kJ/kg-K)	c_p (kJ/kg-K)	μ (kg/m-s) $\times 10^{-6}$
0.1	1.1685	0.7181	1.0065	18.4920
0.5	5.8495	0.7191	1.0131	18.5580
1.0	11.7150	0.7203	1.0213	18.6430
1.5	17.5950	0.7215	1.0295	18.7310
2.0	23.4880	0.7228	1.0377	18.8200
2.5	29.3910	0.7240	1.0460	18.9120
3.0	35.3030	0.7252	1.0543	19.0060
3.5	41.2220	0.7263	1.0626	19.1020
4.0	47.1450	0.7275	1.0708	19.2010
4.5	53.0710	0.7286	1.0790	19.3030
5.0	58.9980	0.7298	1.0873	19.4070
5.5	64.9220	0.7309	1.0954	19.5140
6.0	70.8430	0.7320	1.1035	19.6230
6.5	76.7580	0.7331	1.1116	19.7350
7.0	82.6640	0.7342	1.1196	19.8500
7.5	88.5600	0.7352	1.1275	19.9680
8.0	94.4430	0.7363	1.1353	20.0880
8.5	100.3100	0.7373	1.1430	20.2120
9.0	106.1600	0.7383	1.1506	20.3380
9.5	111.9900	0.7393	1.1582	20.4670
10.0	117.8000	0.7403	1.1655	20.5990

Source: REFPROP 9.0 refrigerant property database developed by the National Institute of Standards and Technology (NIST).

Table A4 Properties of water at standard atmospheric pressure (101.325 kPa)

T (°C)	ρ **(kg/m³)**	c_p **(kJ/kg-K)**	μ **(kg/m-s)** $\times 10^{-6}$
0.01	999.84	4.2194	1790.90
5.00	999.97	4.2050	1518.10
10.00	999.70	4.1952	1305.90
15.00	999.10	4.1885	1137.50
20.00	998.21	4.1841	1001.60
25.00	997.05	4.1813	890.08
30.00	995.65	4.1798	797.35
35.00	994.03	4.1793	719.32
40.00	992.22	4.1794	652.98
45.00	990.21	4.1801	596.07
50.00	988.04	4.1813	546.85
55.00	985.69	4.1830	503.98
60.00	983.20	4.1850	466.40
65.00	980.55	4.1873	433.26
70.00	977.76	4.1901	403.89
75.00	974.84	4.1932	377.74
80.00	971.79	4.1968	354.35
85.00	968.61	4.2007	333.34
90.00	965.31	4.2052	314.41
95.00	961.89	4.2102	297.28
99.97	958.37	4.2156	281.82

Source: REFPROP 9.0 refrigerant property database developed by the National Institute of Standards and Technology (NIST).

Table A5 Properties of saturated water

T(°C)	p_{sat}(MPa)	ρ_f (kg/m³)	ρ_g (kg/m³)	h_f (kJ/kg)	h_g (kJ/kg)	s_f (kJ/kg-K)	s_g (kJ/kg-K)	c_{pf} (kJ/kg-K)	c_{pg} (kJ/kg-K)	μ_f (×10⁻⁶) (kg/m-s)	μ_g (×10⁻⁶) (kg/m-s)	σ (N/m)
0.01	0.00061	999.79	0.00485	0.000612	2500.9	0.0000	9.1555	4.220	1.884	1791.2	9.2163	0.075646
5	0.00087	999.92	0.00680	21.02	2510.1	0.0763	9.0248	4.206	1.889	1518.3	9.3357	0.074942
10	0.00123	999.65	0.00941	42.02	2519.2	0.1511	8.8998	4.196	1.895	1306	9.4612	0.074221
15	0.00171	999.06	0.01284	62.98	2528.3	0.2245	8.7803	4.189	1.900	1137.6	9.5919	0.073486
20	0.00234	998.16	0.01731	83.91	2537.4	0.2965	8.6660	4.184	1.906	1001.6	9.7272	0.072736
25	0.00317	997.00	0.02308	104.83	2546.5	0.3672	8.5566	4.182	1.912	890.11	9.8669	0.071972
30	0.00425	995.61	0.03042	125.73	2555.5	0.4368	8.4520	4.180	1.918	797.36	10.0100	0.071194
35	0.00563	993.99	0.03967	146.63	2564.5	0.5051	8.3517	4.180	1.925	719.31	10.1570	0.070402
40	0.00738	992.18	0.05124	167.53	2573.5	0.5724	8.2555	4.180	1.931	652.97	10.3080	0.069596
45	0.00960	990.17	0.06557	188.43	2582.4	0.6386	8.1633	4.180	1.939	596.05	10.4610	0.068777
50	0.01235	988.00	0.08315	209.34	2591.3	0.7038	8.0748	4.182	1.947	546.83	10.6160	0.067944
55	0.01576	985.66	0.10456	230.26	2600.1	0.7680	7.9898	4.183	1.955	503.96	10.7740	0.067098
60	0.01995	983.16	0.13043	251.18	2608.8	0.8313	7.9081	4.185	1.965	466.38	10.9350	0.066238
65	0.02504	980.52	0.16146	272.12	2617.5	0.8937	7.8296	4.188	1.975	433.24	11.0970	0.065366
70	0.03120	977.73	0.19843	293.07	2626.1	0.9551	7.7540	4.190	1.986	403.87	11.2600	0.064481
75	0.03860	974.81	0.24219	314.03	2634.6	1.0158	7.6812	4.193	1.999	377.72	11.4260	0.063583
80	0.04741	971.77	0.29367	335.01	2643.0	1.0756	7.6111	4.197	2.012	354.33	11.5920	0.062673
85	0.05787	968.59	0.35388	356.01	2651.3	1.1346	7.5434	4.201	2.027	333.33	11.7600	0.061750
90	0.07018	965.30	0.42390	377.04	2659.5	1.1929	7.4781	4.205	2.043	314.4	11.9290	0.060816
95	0.08461	961.88	0.50491	398.09	2667.6	1.2504	7.4151	4.210	2.061	297.28	12.0990	0.059870

(Contd)

Table A5 Properties of saturated water (*Contd*)

T(°C)	p_{sat}(MPa)	ρ_f (kg/m³)	ρ_g (kg/m³)	h_f (kJ/kg)	h_g (kJ/kg)	s_f (kJ/kg-K)	s_g (kJ/kg-K)	c_{pf} (kJ/kg-K)	c_{pg} (kJ/kg-K)	μ_f ($\times 10^{-6}$) (kg/m-s)	μ_g ($\times 10^{-6}$) (kg/m-s)	σ (N/m)
100	0.10142	958.35	0.59817	419.17	2675.6	1.3072	7.3541	4.216	2.080	281.74	12.2690	0.058912
110	0.14338	950.95	0.82693	461.42	2691.1	1.4188	7.2381	4.228	2.124	254.7	12.6120	0.056962
120	0.19867	943.11	1.12210	503.81	2705.9	1.5279	7.1291	4.244	2.177	232.05	12.9560	0.054968
130	0.27028	934.83	1.49700	546.38	2720.1	1.6346	7.0264	4.262	2.239	212.9	13.3010	0.052932
140	0.36154	926.13	1.96670	589.16	2733.4	1.7392	6.9293	4.283	2.311	196.54	13.6470	0.050856
150	0.47616	917.01	2.54810	632.18	2745.9	1.8418	6.8371	4.307	2.394	182.46	13.9920	0.048741
160	0.61823	907.45	3.25960	675.47	2757.4	1.9426	6.7491	4.335	2.488	170.24	14.3370	0.046591
170	0.79219	897.45	4.12220	719.08	2767.9	2.0417	6.6650	4.368	2.594	159.55	14.6810	0.044406
180	1.00280	887.00	5.15880	763.05	2777.2	2.1392	6.5840	4.405	2.713	150.14	15.0250	0.042190
190	1.25520	876.08	6.39540	807.43	2785.3	2.2355	6.5059	4.447	2.844	141.78	15.3700	0.039945
200	1.55490	864.66	7.861	852.27	2792.0	2.3305	6.4302	4.496	2.990	134.32	15.7150	0.037675
220	2.31960	840.22	11.61	943.58	2800.9	2.5177	6.2840	4.615	3.329	121.52	16.4110	0.033067
240	3.34690	813.37	16.749	1037.60	2803.0	2.7020	6.1423	4.772	3.754	110.85	17.1250	0.028394
260	4.69230	783.63	23.712	1135.00	2796.6	2.8849	6.0016	4.986	4.308	101.68	17.8770	0.023689
280	6.41660	750.28	33.165	1236.90	2779.9	3.0685	5.8579	5.289	5.073	93.506	18.7000	0.018993
300	8.58790	712.14	46.168	1345.00	2749.6	3.2552	5.7059	5.750	6.220	85.896	19.6510	0.014360
320	11.28400	667.09	64.638	1462.20	2700.6	3.4494	5.5372	6.537	8.159	78.408	20.8460	0.009864
340	14.60100	610.67	92.759	1594.50	2621.8	3.6601	5.3356	8.208	12.236	70.431	22.5540	0.005626
360	18.66600	527.59	143.90	1761.70	2481.5	3.9167	5.0536	15.004	27.356	60.329	25.7240	0.001877
374.14	22.09000	317.00	317.00	–	–	–	–	–	–	43.13	43.1300	0.000

Source: REFPROP 9.0 refrigerant property database developed by the National Institute of Standards and Technology (NIST).

APPENDIX B

Perfect Gas Tables ($\gamma = 1.4$)

Table B1 Isentropic flow

M	T/T_o	p/p_o	ρ/ρ_o	A/A^*	F/F^*	$(A/A^*).(p/p_o)$	M^*
0.00	1.00000	1.00000	1.00000	Indefinite	Indefinite	Indefinite	0.00000
0.02	0.99992	0.99972	0.99980	28.94114	22.83364	28.93304	0.02191
0.04	0.99968	0.99888	0.99920	14.47950	11.43462	14.46330	0.04381
0.06	0.99928	0.99748	0.99820	9.66293	7.64285	9.63862	0.06570
0.08	0.99872	0.99553	0.99681	7.25763	5.75288	7.22521	0.08758
0.10	0.99800	0.99303	0.99502	5.81685	4.62363	5.77631	0.10944
0.12	0.99713	0.98998	0.99284	4.85833	3.87473	4.80968	0.13126
0.14	0.99610	0.98640	0.99027	4.17540	3.34317	4.11862	0.15306
0.16	0.99491	0.98228	0.98731	3.66473	2.94743	3.59980	0.17482
0.18	0.99356	0.97765	0.98398	3.26889	2.64223	3.19582	0.19654
0.20	0.99206	0.97250	0.98028	2.95345	2.40040	2.87222	0.21822
0.22	0.99041	0.96685	0.97620	2.69649	2.20464	2.60709	0.23984
0.24	0.98861	0.96070	0.97177	2.48340	2.04344	2.38581	0.26141
0.26	0.98666	0.95408	0.96698	2.30406	1.90880	2.19827	0.28291
0.28	0.98456	0.94700	0.96185	2.15126	1.79503	2.03724	0.30435
0.30	0.98232	0.93947	0.95638	2.01968	1.69794	1.89743	0.32572
0.32	0.97993	0.93150	0.95058	1.90537	1.61440	1.77486	0.34701
0.34	0.97740	0.92312	0.94446	1.80528	1.54200	1.66648	0.36822
0.36	0.97473	0.91433	0.93803	1.71705	1.47888	1.56995	0.38935
0.38	0.97193	0.90516	0.93130	1.63882	1.42356	1.48339	0.41039
0.40	0.96899	0.89561	0.92427	1.56910	1.37487	1.40531	0.43133
0.42	0.96592	0.88572	0.91697	1.50668	1.33185	1.33450	0.45218
0.44	0.96272	0.87550	0.90940	1.45058	1.29371	1.26998	0.47293
0.46	0.95940	0.86496	0.90157	1.39998	1.25981	1.21093	0.49357
0.48	0.95595	0.85413	0.89349	1.35421	1.22962	1.15667	0.51410
0.50	0.95238	0.84302	0.88517	1.31269	1.20268	1.10662	0.53452

(*Contd*)

Table B1 Isentropic flow (*Contd*)

M	T/T_o	p/p_o	ρ/ρ_o	A/A^*	F/F^*	$(A/A^*).(p/p_o)$	M^*
0.52	0.94869	0.83165	0.87663	1.27494	1.17860	1.06031	0.55483
0.54	0.94489	0.82005	0.86788	1.24056	1.15705	1.01732	0.57501
0.56	0.94098	0.80823	0.85892	1.20919	1.13777	0.97730	0.59507
0.58	0.93696	0.79621	0.84978	1.18053	1.12050	0.93995	0.61501
0.60	0.93284	0.78400	0.84045	1.15432	1.10504	0.90500	0.63481
0.62	0.92861	0.77164	0.83096	1.13034	1.09120	0.87222	0.65448
0.64	0.92428	0.75913	0.82132	1.10839	1.07883	0.84141	0.67402
0.66	0.91986	0.74650	0.81153	1.08829	1.06777	0.81240	0.69342
0.68	0.91535	0.73376	0.80162	1.06988	1.05792	0.78503	0.71268
0.70	0.91075	0.72093	0.79158	1.05304	1.04915	0.75917	0.73179
0.72	0.90606	0.70803	0.78143	1.03765	1.04137	0.73468	0.75076
0.74	0.90129	0.69507	0.77119	1.02359	1.03449	0.71147	0.76958
0.76	0.89644	0.68207	0.76086	1.01078	1.02844	0.68942	0.78825
0.78	0.89152	0.66905	0.75046	0.99912	1.02314	0.66846	0.80677
0.80	0.88652	0.65602	0.73999	0.98855	1.01853	0.64851	0.82514
0.82	0.88146	0.64300	0.72947	0.97900	1.01455	0.62949	0.84335
0.84	0.87633	0.63000	0.71891	0.97039	1.01115	0.61135	0.86140
0.86	0.87114	0.61703	0.70831	0.96269	1.00829	0.59401	0.87929
0.88	0.86589	0.60412	0.69768	0.95583	1.00591	0.57743	0.89703
0.90	0.86059	0.59126	0.68704	0.94978	1.00399	0.56157	0.91460
0.92	0.85523	0.57848	0.67640	0.94449	1.00248	0.54636	0.93201
0.94	0.84982	0.56578	0.66576	0.93992	1.00136	0.53178	0.94925
0.96	0.84437	0.55317	0.65513	0.93605	1.00059	0.51779	0.96633
0.98	0.83887	0.54067	0.64452	0.93284	1.00014	0.50436	0.98325
1.00	0.83333	0.52828	0.63394	0.93026	1.00000	0.49144	1.00000
1.02	0.82776	0.51602	0.62339	0.92829	1.00014	0.47901	1.01658
1.04	0.82215	0.50389	0.61289	0.92691	1.00053	0.46706	1.03300
1.06	0.81651	0.49189	0.60243	0.92609	1.00116	0.45554	1.04925
1.08	0.81085	0.48005	0.59203	0.92582	1.00200	0.44444	1.06533
1.10	0.80515	0.46835	0.58170	0.92608	1.00305	0.43373	1.08124
1.12	0.79944	0.45682	0.57143	0.92685	1.00429	0.42340	1.09699
1.14	0.79370	0.44545	0.56123	0.92812	1.00569	0.41343	1.11256
1.16	0.78795	0.43425	0.55112	0.92988	1.00726	0.40380	1.12797
1.18	0.78218	0.42322	0.54108	0.93212	1.00897	0.39449	1.14321

(*Contd*)

Table B1 Isentropic flow (*Contd*)

M	T/T_o	p/p_o	ρ/ρ_o	A/A^*	F/F^*	$(A/A^*).(p/p_o)$	M^*
1.20	0.77640	0.41238	0.53114	0.93481	1.01081	0.38550	1.15828
1.22	0.77061	0.40171	0.52129	0.93797	1.01278	0.37679	1.17319
1.24	0.76481	0.39123	0.51154	0.94157	1.01486	0.36837	1.18792
1.26	0.75900	0.38093	0.50189	0.94561	1.01705	0.36021	1.20249
1.28	0.75319	0.37083	0.49234	0.95008	1.01933	0.35232	1.21690
1.30	0.74738	0.36091	0.48290	0.95498	1.02170	0.34466	1.23114
1.32	0.74158	0.35119	0.47357	0.96030	1.02414	0.33725	1.24521
1.34	0.73577	0.34166	0.46436	0.96603	1.02666	0.33006	1.25912
1.36	0.72997	0.33233	0.45526	0.97218	1.02925	0.32308	1.27286
1.38	0.72418	0.32319	0.44628	0.97874	1.03189	0.31632	1.28645
1.40	0.71839	0.31424	0.43742	0.98571	1.03459	0.30975	1.29987
1.42	0.71262	0.30549	0.42869	0.99308	1.03733	0.30337	1.31313
1.44	0.70685	0.29693	0.42007	1.00085	1.04012	0.29718	1.32623
1.46	0.70110	0.28856	0.41158	1.00902	1.04295	0.29117	1.33917
1.48	0.69537	0.28039	0.40322	1.01759	1.04581	0.28532	1.35195
1.50	0.68966	0.27240	0.39498	1.02656	1.04870	0.27964	1.36458
1.52	0.68396	0.26461	0.38688	1.03594	1.05162	0.27412	1.37705
1.54	0.67828	0.25700	0.37890	1.04571	1.05456	0.26874	1.38936
1.56	0.67262	0.24957	0.37105	1.05588	1.05752	0.26352	1.40152
1.58	0.66699	0.24233	0.36332	1.06645	1.06049	0.25844	1.41353
1.60	0.66138	0.23527	0.35573	1.07743	1.06348	0.25349	1.42539
1.62	0.65579	0.22839	0.34827	1.08881	1.06647	0.24867	1.43710
1.64	0.65023	0.22168	0.34093	1.10060	1.06948	0.24398	1.44866
1.66	0.64470	0.21515	0.33372	1.11280	1.07249	0.23942	1.46008
1.68	0.63919	0.20879	0.32664	1.12540	1.07550	0.23497	1.47135
1.70	0.63371	0.20259	0.31969	1.13842	1.07851	0.23064	1.48247
1.72	0.62827	0.19656	0.31287	1.15186	1.08152	0.22642	1.49345
1.74	0.62285	0.19070	0.30617	1.16572	1.08453	0.22230	1.50429
1.76	0.61747	0.18499	0.29959	1.18000	1.08753	0.21829	1.51499
1.78	0.61211	0.17944	0.29315	1.19471	1.09053	0.21438	1.52555
1.80	0.60680	0.17404	0.28682	1.20986	1.09351	0.21056	1.53598
1.82	0.60151	0.16879	0.28061	1.22543	1.09649	0.20684	1.54626
1.84	0.59626	0.16369	0.27453	1.24145	1.09946	0.20321	1.55642
1.86	0.59104	0.15873	0.26857	1.25792	1.10242	0.19967	1.56644

(*Contd*)

Table B1 Isentropic flow (*Contd*)

M	T/T_o	p/p_o	ρ/ρ_o	A/A^*	F/F^*	$(A/A^*).(p/p_o)$	M^*
1.88	0.58586	0.15392	0.26272	1.27483	1.10536	0.19622	1.57633
1.90	0.58072	0.14924	0.25699	1.29220	1.10829	0.19285	1.58609
1.92	0.57561	0.14470	0.25138	1.31002	1.11120	0.18955	1.59572
1.94	0.57054	0.14028	0.24588	1.32832	1.11410	0.18634	1.60523
1.96	0.56551	0.13600	0.24049	1.34708	1.11698	0.18320	1.61460
1.98	0.56051	0.13184	0.23521	1.36632	1.11984	0.18014	1.62386
2.00	0.55556	0.12780	0.23005	1.38605	1.12268	0.17714	1.63299
2.02	0.55064	0.12389	0.22499	1.40626	1.12551	0.17422	1.64201
2.04	0.54576	0.12009	0.22004	1.42697	1.12831	0.17136	1.65090
2.06	0.54091	0.11640	0.21519	1.44818	1.13110	0.16857	1.65967
2.08	0.53611	0.11282	0.21045	1.46991	1.13387	0.16584	1.66833
2.10	0.53135	0.10935	0.20580	1.49214	1.13661	0.16317	1.67687
2.12	0.52663	0.10599	0.20126	1.51490	1.13933	0.16056	1.68530
2.14	0.52194	0.10273	0.19681	1.53819	1.14204	0.15801	1.69362
2.16	0.51730	0.09956	0.19247	1.56202	1.14471	0.15552	1.70183
2.18	0.51269	0.09649	0.18821	1.58640	1.14737	0.15308	1.70992
2.20	0.50813	0.09352	0.18405	1.61133	1.15001	0.15069	1.71791
2.22	0.50361	0.09064	0.17998	1.63681	1.15262	0.14836	1.72579
2.24	0.49912	0.08785	0.17600	1.66287	1.15521	0.14608	1.73357
2.26	0.49468	0.08514	0.17211	1.68951	1.15777	0.14384	1.74125
2.28	0.49027	0.08251	0.16830	1.71673	1.16032	0.14166	1.74882
2.30	0.48591	0.07997	0.16458	1.74455	1.16284	0.13952	1.75629
2.32	0.48158	0.07751	0.16095	1.77297	1.16533	0.13742	1.76366
2.34	0.47730	0.07512	0.15739	1.80200	1.16780	0.13537	1.77093
2.36	0.47305	0.07281	0.15391	1.83165	1.17025	0.13336	1.77811
2.38	0.46885	0.07057	0.15052	1.86194	1.17268	0.13140	1.78519
2.40	0.46468	0.06840	0.14720	1.89286	1.17508	0.12947	1.79218
2.42	0.46056	0.06630	0.14395	1.92444	1.17746	0.12758	1.79907
2.44	0.45647	0.06426	0.14078	1.95667	1.17981	0.12574	1.80587
2.46	0.45242	0.06229	0.13768	1.98958	1.18214	0.12393	1.81258
2.48	0.44841	0.06038	0.13465	2.02316	1.18445	0.12215	1.81921
2.50	0.44444	0.05853	0.13169	2.05744	1.18673	0.12042	1.82574
2.52	0.44051	0.05674	0.12879	2.09241	1.18899	0.11871	1.83219
2.54	0.43662	0.05500	0.12597	2.12809	1.19123	0.11705	1.83855

(*Contd*)

Table B1 Isentropic flow (*Contd*)

M	T/T_o	p/p_o	ρ/ρ_o	A/A^*	F/F^*	$(A/A^*).(p/p_o)$	M^*
2.56	0.43277	0.05332	0.12321	2.16450	1.19344	0.11541	1.84483
2.58	0.42895	0.05169	0.12051	2.20164	1.19563	0.11381	1.85103
2.60	0.42517	0.05012	0.11787	2.23952	1.19780	0.11223	1.85714
2.62	0.42143	0.04859	0.11530	2.27815	1.19995	0.11069	1.86318
2.64	0.41772	0.04711	0.11278	2.31756	1.20207	0.10918	1.86913
2.66	0.41406	0.04568	0.11032	2.35774	1.20417	0.10770	1.87501
2.68	0.41043	0.04429	0.10792	2.39871	1.20625	0.10624	1.88081
2.70	0.40683	0.04295	0.10557	2.44048	1.20830	0.10482	1.88653
2.72	0.40328	0.04165	0.10328	2.48306	1.21033	0.10342	1.89218
2.74	0.39976	0.04039	0.10104	2.52647	1.21235	0.10205	1.89775
2.76	0.39627	0.03917	0.09885	2.57072	1.21433	0.10070	1.90325
2.78	0.39282	0.03799	0.09671	2.61581	1.21630	0.09938	1.90868
2.80	0.38941	0.03685	0.09463	2.66177	1.21825	0.09808	1.91404
2.82	0.38603	0.03574	0.09259	2.70861	1.22017	0.09681	1.91933
2.84	0.38268	0.03467	0.09059	2.75633	1.22208	0.09556	1.92455
2.86	0.37937	0.03363	0.08865	2.80496	1.22396	0.09433	1.92970
2.88	0.37610	0.03263	0.08675	2.85451	1.22582	0.09313	1.93479
2.90	0.37286	0.03165	0.08489	2.90498	1.22766	0.09195	1.93981
2.92	0.36965	0.03071	0.08307	2.95639	1.22948	0.09079	1.94477
2.94	0.36647	0.02980	0.08130	3.00877	1.23128	0.08965	1.94966
2.96	0.36333	0.02891	0.07957	3.06211	1.23307	0.08853	1.95449
2.98	0.36022	0.02805	0.07788	3.11644	1.23483	0.08743	1.95925
3.00	0.35714	0.02722	0.07623	3.17176	1.23657	0.08635	1.96396
3.02	0.35410	0.02642	0.07461	3.22811	1.23829	0.08529	1.96861
3.04	0.35108	0.02564	0.07303	3.28548	1.23999	0.08424	1.97319
3.06	0.34810	0.02489	0.07149	3.34389	1.24168	0.08322	1.97772
3.08	0.34515	0.02416	0.06999	3.40337	1.24334	0.08221	1.98219
3.10	0.34223	0.02345	0.06852	3.46392	1.24499	0.08122	1.98661
3.12	0.33934	0.02276	0.06708	3.52555	1.24662	0.08025	1.99097
3.14	0.33648	0.02210	0.06568	3.58830	1.24823	0.07930	1.99527
3.16	0.33365	0.02146	0.06430	3.65216	1.24982	0.07836	1.99952
3.18	0.33085	0.02083	0.06296	3.71717	1.25139	0.07744	2.00372
3.20	0.32808	0.02023	0.06165	3.78333	1.25295	0.07653	2.00786
3.22	0.32534	0.01964	0.06037	3.85065	1.25449	0.07564	2.01195

(*Contd*)

Table B1 Isentropic flow (*Contd*)

M	T/T_o	p/p_o	ρ/ρ_o	A/A^*	F/F^*	$(A/A^*).(p/p_o)$	M^*
3.24	0.32263	0.01908	0.05912	3.91917	1.25601	0.07476	2.01599
3.26	0.31995	0.01853	0.05790	3.98889	1.25752	0.07390	2.01998
3.28	0.31729	0.01799	0.05671	4.05982	1.25901	0.07305	2.02392
3.30	0.31466	0.01748	0.05554	4.13200	1.26048	0.07221	2.02781
3.32	0.31206	0.01698	0.05440	4.20543	1.26193	0.07139	2.03165
3.34	0.30949	0.01649	0.05329	4.28014	1.26337	0.07059	2.03545
3.36	0.30694	0.01602	0.05220	4.35613	1.26479	0.06979	2.03920
3.38	0.30443	0.01557	0.05113	4.43344	1.26620	0.06901	2.04290
3.40	0.30193	0.01512	0.05009	4.51207	1.26759	0.06824	2.04656
3.42	0.29947	0.01470	0.04908	4.59204	1.26897	0.06749	2.05017
3.44	0.29702	0.01428	0.04808	4.67338	1.27033	0.06674	2.05374
3.46	0.29461	0.01388	0.04711	4.75610	1.27167	0.06601	2.05727
3.48	0.29222	0.01349	0.04616	4.84022	1.27300	0.06529	2.06075
3.50	0.28986	0.01311	0.04523	4.92576	1.27432	0.06458	2.06419
3.52	0.28751	0.01274	0.04433	5.01274	1.27562	0.06388	2.06759
3.54	0.28520	0.01239	0.04344	5.10118	1.27691	0.06320	2.07094
3.56	0.28291	0.01204	0.04257	5.19110	1.27818	0.06252	2.07426
3.58	0.28064	0.01171	0.04172	5.28251	1.27944	0.06185	2.07754
3.60	0.27840	0.01138	0.04089	5.37545	1.28068	0.06120	2.08077
3.62	0.27618	0.01107	0.04008	5.46992	1.28191	0.06055	2.08397
3.64	0.27398	0.01076	0.03929	5.56596	1.28313	0.05992	2.08713
3.66	0.27180	0.01047	0.03852	5.66357	1.28433	0.05929	2.09026
3.68	0.26965	0.01018	0.03776	5.76279	1.28552	0.05867	2.09334
3.70	0.26752	0.00990	0.03702	5.86362	1.28670	0.05807	2.09639
3.72	0.26542	0.00963	0.03629	5.96610	1.28787	0.05747	2.09941
3.74	0.26333	0.00937	0.03558	6.07025	1.28902	0.05688	2.10238
3.76	0.26127	0.00912	0.03489	6.17608	1.29016	0.05630	2.10533
3.78	0.25922	0.00887	0.03421	6.28362	1.29128	0.05573	2.10824
3.80	0.25720	0.00863	0.03355	6.39290	1.29240	0.05516	2.11111
3.82	0.25520	0.00840	0.03290	6.50392	1.29350	0.05461	2.11395
3.84	0.25322	0.00817	0.03227	6.61673	1.29459	0.05406	2.11676
3.86	0.25126	0.00795	0.03165	6.73133	1.29567	0.05352	2.11954
3.88	0.24932	0.00774	0.03104	6.84775	1.29674	0.05299	2.12228
3.90	0.24740	0.00753	0.03044	6.96602	1.29779	0.05247	2.12499

(*Contd*)

Table B1 Isentropic flow (*Contd*)

M	T/T_o	p/p_o	ρ/ρ_o	A/A^*	F/F^*	$(A/A^*).(p/p_o)$	M^*
3.92	0.24550	0.00733	0.02986	7.08616	1.29883	0.05195	2.12767
3.94	0.24362	0.00714	0.02929	7.20819	1.29987	0.05144	2.13032
3.96	0.24176	0.00695	0.02874	7.33214	1.30089	0.05094	2.13294
3.98	0.23992	0.00676	0.02819	7.45803	1.30190	0.05045	2.13553
4.00	0.23810	0.00659	0.02766	7.58588	1.30290	0.04996	2.13809
4.02	0.23629	0.00641	0.02714	7.71572	1.30389	0.04948	2.14062
4.04	0.23450	0.00624	0.02663	7.84758	1.30487	0.04901	2.14312
4.06	0.23274	0.00608	0.02613	7.98148	1.30583	0.04854	2.14560
4.08	0.23099	0.00592	0.02564	8.11744	1.30679	0.04808	2.14804
4.10	0.22925	0.00577	0.02516	8.25549	1.30774	0.04763	2.15046
4.12	0.22754	0.00562	0.02470	8.39566	1.30868	0.04718	2.15285
4.14	0.22584	0.00547	0.02424	8.53798	1.30960	0.04674	2.15522
4.16	0.22416	0.00533	0.02379	8.68246	1.31052	0.04630	2.15756
4.18	0.22250	0.00520	0.02335	8.82913	1.31143	0.04587	2.15987
4.20	0.22085	0.00506	0.02292	8.97803	1.31233	0.04545	2.16215
4.22	0.21922	0.00493	0.02250	9.12917	1.31322	0.04503	2.16442
4.24	0.21760	0.00481	0.02209	9.28259	1.31410	0.04462	2.16665
4.26	0.21601	0.00468	0.02169	9.43832	1.31497	0.04421	2.16886
4.28	0.21442	0.00457	0.02129	9.59637	1.31583	0.04381	2.17105
4.30	0.21286	0.00445	0.02090	9.75678	1.31668	0.04341	2.17321
4.32	0.21131	0.00434	0.02052	9.91958	1.31752	0.04302	2.17535
4.34	0.20977	0.00423	0.02015	10.08480	1.31836	0.04264	2.17747
4.36	0.20825	0.00412	0.01979	10.25246	1.31919	0.04225	2.17956
4.38	0.20674	0.00402	0.01944	10.42259	1.32000	0.04188	2.18163
4.40	0.20525	0.00392	0.01909	10.59522	1.32081	0.04151	2.18368
4.42	0.20378	0.00382	0.01875	10.77039	1.32161	0.04114	2.18571
4.44	0.20232	0.00372	0.01841	10.94811	1.32241	0.04078	2.18771
4.46	0.20087	0.00363	0.01808	11.12843	1.32319	0.04042	2.18970
4.48	0.19944	0.00354	0.01776	11.31136	1.32397	0.04007	2.19166
4.50	0.19802	0.00346	0.01745	11.49695	1.32474	0.03972	2.19360
4.52	0.19662	0.00337	0.01714	11.68522	1.32550	0.03938	2.19552
4.54	0.19522	0.00329	0.01684	11.87620	1.32625	0.03904	2.19742
4.56	0.19385	0.00321	0.01654	12.06992	1.32700	0.03871	2.19930
4.58	0.19248	0.00313	0.01625	12.26642	1.32773	0.03838	2.20116
4.60	0.19113	0.00305	0.01597	12.46573	1.32846	0.03805	2.20300

(*Contd*)

Table B1 Isentropic flow (*Contd*)

M	T/T_o	p/p_o	ρ/ρ_o	A/A^*	F/F^*	$(A/A^*).(p/p_o)$	M^*
4.62	0.18979	0.00298	0.01569	12.66787	1.32919	0.03773	2.20482
4.64	0.18847	0.00291	0.01542	12.87288	1.32990	0.03741	2.20662
4.66	0.18716	0.00284	0.01515	13.08080	1.33061	0.03710	2.20841
4.68	0.18586	0.00277	0.01489	13.29165	1.33131	0.03679	2.21017
4.70	0.18457	0.00270	0.01464	13.50547	1.33201	0.03648	2.21192
4.72	0.18330	0.00264	0.01438	13.72230	1.33269	0.03618	2.21365
4.74	0.18203	0.00257	0.01414	13.94215	1.33338	0.03588	2.21536
4.76	0.18078	0.00251	0.01390	14.16508	1.33405	0.03558	2.21705
4.78	0.17954	0.00245	0.01366	14.39111	1.33472	0.03529	2.21872
4.80	0.17832	0.00239	0.01343	14.62027	1.33538	0.03500	2.22038
4.82	0.17710	0.00234	0.01320	14.85261	1.33603	0.03472	2.22202
4.84	0.17590	0.00228	0.01298	15.08815	1.33668	0.03444	2.22365
4.86	0.17471	0.00223	0.01276	15.32693	1.33732	0.03416	2.22526
4.88	0.17352	0.00218	0.01254	15.56899	1.33796	0.03389	2.22685
4.90	0.17235	0.00213	0.01233	15.81437	1.33859	0.03361	2.22842
4.92	0.17120	0.00208	0.01213	16.06309	1.33921	0.03335	2.22998
4.94	0.17005	0.00203	0.01192	16.31519	1.33983	0.03308	2.23153
4.96	0.16891	0.00198	0.01173	16.57072	1.34044	0.03282	2.23306
4.98	0.16778	0.00193	0.01153	16.82970	1.34104	0.03256	2.23457
5.00	0.16667	0.00189	0.01134	17.09217	1.34164	0.03230	2.23607

Table B2 Fanno flow

M	F/F^*	T/T^*	p_o/p_o^*	p/p^*	fL_{max}/D
0.00	Indefinite	1.20000	Indefinite	Indefinite	Indefinite
0.02	22.83364	1.19990	28.94213	54.77006	1778.44988
0.04	11.43462	1.19962	14.48149	27.38175	440.35221
0.06	7.64285	1.19914	9.66591	18.25085	193.03108
0.08	5.75288	1.19847	7.26161	13.68431	106.71821
0.10	4.62363	1.19760	5.82183	10.94351	66.92156
0.12	3.87473	1.19655	4.86432	9.11559	45.40796
0.14	3.34317	1.19531	4.18240	7.80932	32.51130
0.16	2.94743	1.19389	3.67274	6.82907	24.19783
0.18	2.64223	1.19227	3.27793	6.06618	18.54265

(*Contd*)

Table B2 Fanno flow (*Contd*)

M	F/F^*	T/T^*	p_o/p_o^*	p/p^*	fL_{max}/D
0.20	2.40040	1.19048	2.96352	5.45545	14.53327
0.22	2.20464	1.18850	2.70760	4.95537	11.59605
0.24	2.04344	1.18633	2.49556	4.53829	9.38648
0.26	1.90880	1.18399	2.31729	4.18505	7.68757
0.28	1.79503	1.18147	2.16555	3.88199	6.35721
0.30	1.69794	1.17878	2.03507	3.61906	5.29925
0.32	1.61440	1.17592	1.92185	3.38874	4.44674
0.34	1.54200	1.17288	1.82288	3.18529	3.75195
0.36	1.47888	1.16968	1.73578	3.00422	3.18012
0.38	1.42356	1.16632	1.65870	2.84200	2.70545
0.40	1.37487	1.16279	1.59014	2.69582	2.30849
0.42	1.33185	1.15911	1.52890	2.56338	1.97437
0.44	1.29371	1.15527	1.47401	2.44280	1.69152
0.46	1.25981	1.15128	1.42463	2.33256	1.45091
0.48	1.22962	1.14714	1.38010	2.23135	1.24534
0.50	1.20268	1.14286	1.33984	2.13809	1.06906
0.52	1.17860	1.13843	1.30339	2.05187	0.91742
0.54	1.15705	1.13387	1.27032	1.97192	0.78662
0.56	1.13777	1.12918	1.24029	1.89755	0.67357
0.58	1.12050	1.12435	1.21301	1.82820	0.57568
0.60	1.10504	1.11940	1.18820	1.76336	0.49082
0.62	1.09120	1.11433	1.16565	1.70261	0.41720
0.64	1.07883	1.10914	1.14515	1.64556	0.35330
0.66	1.06777	1.10383	1.12654	1.59187	0.29785
0.68	1.05792	1.09842	1.10965	1.54126	0.24978
0.70	1.04915	1.09290	1.09437	1.49345	0.20814
0.72	1.04137	1.08727	1.08057	1.44823	0.17215
0.74	1.03449	1.08155	1.06814	1.40537	0.14112
0.76	1.02844	1.07573	1.05700	1.36470	0.11447
0.78	1.02314	1.06982	1.04705	1.32605	0.09167
0.80	1.01853	1.06383	1.03823	1.28928	0.07229
0.82	1.01455	1.05775	1.03046	1.25423	0.05593
0.84	1.01115	1.05160	1.02370	1.22080	0.04226
0.86	1.00829	1.04537	1.01787	1.18888	0.03097
0.88	1.00591	1.03907	1.01294	1.15835	0.02179
0.90	1.00399	1.03270	1.00886	1.12913	0.01451

(*Contd*)

Table B2 Fanno flow (*Contd*)

M	F/F^*	T/T^*	p_o/p_o^*	p/p^*	fL_{max}/D
0.92	1.00248	1.02627	1.00560	1.10114	0.00891
0.94	1.00136	1.01978	1.00311	1.07430	0.00482
0.96	1.00059	1.01324	1.00136	1.04854	0.00206
0.98	1.00014	1.00664	1.00034	1.02379	0.00049
1.00	1.00000	1.00000	1.00000	1.00000	0.00000
1.02	1.00014	0.99331	1.00033	0.97711	0.00046
1.04	1.00053	0.98658	1.00131	0.95507	0.00177
1.06	1.00116	0.97982	1.00291	0.93383	0.00384
1.08	1.00200	0.97302	1.00512	0.91335	0.00658
1.10	1.00305	0.96618	1.00793	0.89359	0.00994
1.12	1.00429	0.95932	1.01131	0.87451	0.01382
1.14	1.00569	0.95244	1.01527	0.85608	0.01819
1.16	1.00726	0.94554	1.01978	0.83826	0.02298
1.18	1.00897	0.93861	1.02484	0.82103	0.02814
1.20	1.01081	0.93168	1.03044	0.80436	0.03364
1.22	1.01278	0.92473	1.03657	0.78822	0.03943
1.24	1.01486	0.91777	1.04323	0.77258	0.04547
1.26	1.01705	0.91080	1.05041	0.75743	0.05174
1.28	1.01933	0.90383	1.05810	0.74274	0.05820
1.30	1.02170	0.89686	1.06630	0.72848	0.06483
1.32	1.02414	0.88989	1.07502	0.71465	0.07161
1.34	1.02666	0.88292	1.08424	0.70122	0.07850
1.36	1.02925	0.87596	1.09396	0.68818	0.08550
1.38	1.03189	0.86901	1.10419	0.67551	0.09259
1.40	1.03459	0.86207	1.11493	0.66320	0.09974
1.42	1.03733	0.85514	1.12616	0.65122	0.10694
1.44	1.04012	0.84822	1.13790	0.63958	0.11419
1.46	1.04295	0.84133	1.15015	0.62825	0.12146
1.48	1.04581	0.83445	1.16290	0.61722	0.12875
1.50	1.04870	0.82759	1.17617	0.60648	0.13605
1.52	1.05162	0.82075	1.18994	0.59602	0.14335
1.54	1.05456	0.81393	1.20423	0.58583	0.15063
1.56	1.05752	0.80715	1.21904	0.57591	0.15790
1.58	1.06049	0.80038	1.23438	0.56623	0.16514
1.60	1.06348	0.79365	1.25024	0.55679	0.17236
1.62	1.06647	0.78695	1.26663	0.54759	0.17954

(*Contd*)

Table B2 Fanno flow (*Contd*)

M	F/F^*	T/T^*	p_o/p_o^*	p/p^*	fL_{max}/D
1.64	1.06948	0.78027	1.28355	0.53862	0.18667
1.66	1.07249	0.77363	1.30102	0.52986	0.19377
1.68	1.07550	0.76703	1.31904	0.52131	0.20081
1.70	1.07851	0.76046	1.33761	0.51297	0.20780
1.72	1.08152	0.75392	1.35674	0.50482	0.21474
1.74	1.08453	0.74742	1.37643	0.49686	0.22162
1.76	1.08753	0.74096	1.39670	0.48909	0.22844
1.78	1.09053	0.73454	1.41755	0.48149	0.23519
1.80	1.09351	0.72816	1.43898	0.47407	0.24189
1.82	1.09649	0.72181	1.46101	0.46681	0.24851
1.84	1.09946	0.71551	1.48365	0.45972	0.25507
1.86	1.10242	0.70925	1.50689	0.45278	0.26156
1.88	1.10536	0.70304	1.53076	0.44600	0.26798
1.90	1.10829	0.69686	1.55526	0.43936	0.27433
1.92	1.11120	0.69073	1.58039	0.43287	0.28061
1.94	1.11410	0.68465	1.60617	0.42651	0.28681
1.96	1.11698	0.67861	1.63261	0.42029	0.29295
1.98	1.11984	0.67262	1.65972	0.41421	0.29901
2.00	1.12268	0.66667	1.68750	0.40825	0.30500
2.02	1.12551	0.66076	1.71597	0.40241	0.31091
2.04	1.12831	0.65491	1.74514	0.39670	0.31676
2.06	1.13110	0.64910	1.77502	0.39110	0.32253
2.08	1.13387	0.64334	1.80561	0.38562	0.32822
2.10	1.13661	0.63762	1.83694	0.38024	0.33385
2.12	1.13933	0.63195	1.86902	0.37498	0.33940
2.14	1.14204	0.62633	1.90184	0.36982	0.34489
2.16	1.14471	0.62076	1.93544	0.36476	0.35030
2.18	1.14737	0.61523	1.96981	0.35980	0.35564
2.20	1.15001	0.60976	2.00497	0.35494	0.36091
2.22	1.15262	0.60433	2.04094	0.35017	0.36611
2.24	1.15521	0.59895	2.07773	0.34550	0.37124
2.26	1.15777	0.59361	2.11535	0.34091	0.37631
2.28	1.16032	0.58833	2.15381	0.33641	0.38130
2.30	1.16284	0.58309	2.19313	0.33200	0.38623
2.32	1.16533	0.57790	2.23332	0.32767	0.39109
2.34	1.16780	0.57276	2.27440	0.32342	0.39589

(*Contd*)

Table B2 Fanno flow (*Contd*)

M	F/F^*	T/T^*	p_o/p_o^*	p/p^*	fL_{max}/D
2.36	1.17025	0.56767	2.31638	0.31925	0.40062
2.38	1.17268	0.56262	2.35928	0.31516	0.40529
2.40	1.17508	0.55762	2.40310	0.31114	0.40989
2.42	1.17746	0.55267	2.44787	0.30720	0.41443
2.44	1.17981	0.54777	2.49360	0.30332	0.41891
2.46	1.18214	0.54291	2.54031	0.29952	0.42332
2.48	1.18445	0.53810	2.58801	0.29579	0.42768
2.50	1.18673	0.53333	2.63672	0.29212	0.43198
2.52	1.18899	0.52862	2.68645	0.28852	0.43621
2.54	1.19123	0.52394	2.73723	0.28498	0.44039
2.56	1.19344	0.51932	2.78906	0.28150	0.44451
2.58	1.19563	0.51474	2.84197	0.27808	0.44858
2.60	1.19780	0.51020	2.89598	0.27473	0.45259
2.62	1.19995	0.50571	2.95109	0.27143	0.45654
2.64	1.20207	0.50127	3.00733	0.26818	0.46044
2.66	1.20417	0.49687	3.06472	0.26500	0.46429
2.68	1.20625	0.49251	3.12327	0.26186	0.46808
2.70	1.20830	0.48820	3.18301	0.25878	0.47182
2.72	1.21033	0.48393	3.24395	0.25575	0.47551
2.74	1.21235	0.47971	3.30611	0.25278	0.47915
2.76	1.21433	0.47553	3.36952	0.24985	0.48274
2.78	1.21630	0.47139	3.43418	0.24697	0.48627
2.80	1.21825	0.46729	3.50012	0.24414	0.48977
2.82	1.22017	0.46323	3.56737	0.24135	0.49321
2.84	1.22208	0.45922	3.63593	0.23861	0.49660
2.86	1.22396	0.45525	3.70584	0.23592	0.49995
2.88	1.22582	0.45132	3.77711	0.23326	0.50326
2.90	1.22766	0.44743	3.84977	0.23066	0.50652
2.92	1.22948	0.44358	3.92383	0.22809	0.50973
2.94	1.23128	0.43977	3.99932	0.22556	0.51290
2.96	1.23307	0.43600	4.07625	0.22307	0.51603
2.98	1.23483	0.43226	4.15466	0.22063	0.51912
3.00	1.23657	0.42857	4.23457	0.21822	0.52216
3.02	1.23829	0.42492	4.31599	0.21585	0.52516
3.04	1.23999	0.42130	4.39895	0.21351	0.52813
3.06	1.24168	0.41772	4.48347	0.21121	0.53105
3.08	1.24334	0.41418	4.56959	0.20895	0.53393

(*Contd*)

Table B2 Fanno flow (*Contd*)

M	F/F^*	T/T^*	p_o/p_o^*	p/p^*	fL_{max}/D
3.10	1.24499	0.41068	4.65731	0.20672	0.53678
3.12	1.24662	0.40721	4.74667	0.20453	0.53958
3.14	1.24823	0.40378	4.83769	0.20237	0.54235
3.16	1.24982	0.40038	4.93039	0.20024	0.54509
3.18	1.25139	0.39702	5.02481	0.19814	0.54778
3.20	1.25295	0.39370	5.12096	0.19608	0.55044
3.22	1.25449	0.39041	5.21887	0.19405	0.55307
3.24	1.25601	0.38716	5.31857	0.19204	0.55566
3.26	1.25752	0.38394	5.42008	0.19007	0.55822
3.28	1.25901	0.38075	5.52343	0.18812	0.56074
3.30	1.26048	0.37760	5.62865	0.18621	0.56323
3.32	1.26193	0.37448	5.73576	0.18432	0.56569
3.34	1.26337	0.37139	5.84479	0.18246	0.56812
3.36	1.26479	0.36833	5.95577	0.18063	0.57051
3.38	1.26620	0.36531	6.06873	0.17882	0.57287
3.40	1.26759	0.36232	6.18370	0.17704	0.57521
3.42	1.26897	0.35936	6.30070	0.17528	0.57751
3.44	1.27033	0.35643	6.41976	0.17355	0.57978
3.46	1.27167	0.35353	6.54092	0.17185	0.58203
3.48	1.27300	0.35066	6.66419	0.17016	0.58424
3.50	1.27432	0.34783	6.78962	0.16851	0.58643
3.52	1.27562	0.34502	6.91723	0.16687	0.58859
3.54	1.27691	0.34224	7.04705	0.16526	0.59072
3.56	1.27818	0.33949	7.17912	0.16367	0.59282
3.58	1.27944	0.33677	7.31346	0.16210	0.59490
3.60	1.28068	0.33408	7.45011	0.16055	0.59696
3.62	1.28191	0.33141	7.58910	0.15903	0.59898
3.64	1.28313	0.32877	7.73045	0.15752	0.60098
3.66	1.28433	0.32616	7.87421	0.15604	0.60296
3.68	1.28552	0.32358	8.02040	0.15458	0.60491
3.70	1.28670	0.32103	8.16907	0.15313	0.60684
3.72	1.28787	0.31850	8.32023	0.15171	0.60874
3.74	1.28902	0.31600	8.47393	0.15030	0.61062
3.76	1.29016	0.31352	8.63020	0.14892	0.61247
3.78	1.29128	0.31107	8.78907	0.14755	0.61431
3.80	1.29240	0.30864	8.95059	0.14620	0.61612
3.82	1.29350	0.30624	9.11477	0.14487	0.61791

(*Contd*)

Table B2 Fanno flow (*Contd*)

M	F/F^*	T/T^*	p_o/p_o^*	p/p^*	fL_{max}/D
3.84	1.29459	0.30387	9.28167	0.14355	0.61968
3.86	1.29567	0.30151	9.45131	0.14225	0.62142
3.88	1.29674	0.29919	9.62373	0.14097	0.62315
3.90	1.29779	0.29688	9.79897	0.13971	0.62485
3.92	1.29883	0.29460	9.97707	0.13846	0.62653
3.94	1.29987	0.29235	10.15806	0.13723	0.62820
3.96	1.30089	0.29011	10.34197	0.13602	0.62984
3.98	1.30190	0.28790	10.52886	0.13482	0.63146
4.00	1.30290	0.28571	10.71875	0.13363	0.63307
4.02	1.30389	0.28355	10.91168	0.13246	0.63465
4.04	1.30487	0.28140	11.10770	0.13131	0.63622
4.06	1.30583	0.27928	11.30684	0.13017	0.63776
4.08	1.30679	0.27718	11.50915	0.12904	0.63929
4.10	1.30774	0.27510	11.71465	0.12793	0.64080
4.12	1.30868	0.27304	11.92340	0.12683	0.64230
4.14	1.30960	0.27101	12.13543	0.12574	0.64377
4.16	1.31052	0.26899	12.35079	0.12467	0.64523
4.18	1.31143	0.26699	12.56951	0.12362	0.64668
4.20	1.31233	0.26502	12.79164	0.12257	0.64810
4.22	1.31322	0.26306	13.01722	0.12154	0.64951
4.24	1.31410	0.26112	13.24629	0.12052	0.65090
4.26	1.31497	0.25921	13.47890	0.11951	0.65228
4.28	1.31583	0.25731	13.71509	0.11852	0.65364
4.30	1.31668	0.25543	13.95490	0.11753	0.65499
4.32	1.31752	0.25357	14.19838	0.11656	0.65632
4.34	1.31836	0.25172	14.44557	0.11560	0.65763
4.36	1.31919	0.24990	14.69652	0.11466	0.65893
4.38	1.32000	0.24809	14.95127	0.11372	0.66022
4.40	1.32081	0.24631	15.20987	0.11279	0.66149
4.42	1.32161	0.24453	15.47236	0.11188	0.66275
4.44	1.32241	0.24278	15.73879	0.11097	0.66399
4.46	1.32319	0.24105	16.00921	0.11008	0.66522
4.48	1.32397	0.23933	16.28366	0.10920	0.66643
4.50	1.32474	0.23762	16.56219	0.10833	0.66764
4.52	1.32550	0.23594	16.84486	0.10746	0.66882
4.54	1.32625	0.23427	17.13170	0.10661	0.67000

(*Contd*)

Table B2 Fanno flow (*Contd*)

M	F/F^*	T/T^*	p_o/p_o^*	p/p^*	fL_{max}/D
4.56	1.32700	0.23262	17.42277	0.10577	0.67116
4.58	1.32773	0.23098	17.71812	0.10494	0.67231
4.60	1.32846	0.22936	18.01779	0.10411	0.67345
4.62	1.32919	0.22775	18.32185	0.10330	0.67457
4.64	1.32990	0.22616	18.63032	0.10249	0.67569
4.66	1.33061	0.22459	18.94328	0.10170	0.67679
4.68	1.33131	0.22303	19.26076	0.10091	0.67788
4.70	1.33201	0.22148	19.58283	0.10013	0.67895
4.72	1.33269	0.21995	19.90953	0.09936	0.68002
4.74	1.33338	0.21844	20.24091	0.09860	0.68107
4.76	1.33405	0.21694	20.57703	0.09785	0.68211
4.78	1.33472	0.21545	20.91795	0.09711	0.68315
4.80	1.33538	0.21398	21.26371	0.09637	0.68417
4.82	1.33603	0.21252	21.61437	0.09564	0.68518
4.84	1.33668	0.21108	21.96999	0.09492	0.68618
4.86	1.33732	0.20965	22.33061	0.09421	0.68717
4.88	1.33796	0.20823	22.69631	0.09351	0.68814
4.90	1.33859	0.20683	23.06712	0.09281	0.68911
4.92	1.33921	0.20543	23.44311	0.09212	0.69007
4.94	1.33983	0.20406	23.82434	0.09144	0.69102
4.96	1.34044	0.20269	24.21086	0.09077	0.69196
4.98	1.34104	0.20134	24.60272	0.09010	0.69289
5.00	1.34164	0.20000	25.00000	0.08944	0.69380

Table B3 Rayleigh flow

M	T/T^*	p/p^*	T_o/T_o^*	p_o/p_o^*
0.00	0	2.400000	0	1.267876
0.02	0.002301	2.398657	0.001918	1.267522
0.04	0.009175	2.394636	0.007648	1.26646
0.06	0.020529	2.387965	0.017119	1.2647
0.08	0.036212	2.378687	0.030215	1.262256
0.10	0.05602	2.366864	0.046777	1.259146
0.12	0.079698	2.352572	0.066606	1.255394
0.14	0.106946	2.335903	0.089471	1.251029

(*Contd*)

Table B3 Rayleigh flow (*Contd*)

M	T/T^*	p/p^*	T_o/T_o^*	p_o/p_o^*
0.16	0.137429	2.31696	0.11511	1.246083
0.18	0.170779	2.29586	0.143238	1.240592
0.20	0.206612	2.272727	0.173554	1.234596
0.22	0.244523	2.247696	0.205742	1.228136
0.24	0.284108	2.220906	0.239484	1.221255
0.26	0.324957	2.192502	0.274459	1.214
0.28	0.366674	2.16263	0.310353	1.206416
0.30	0.408873	2.131439	0.34686	1.198549
0.32	0.451187	2.099076	0.383689	1.190446
0.34	0.493273	2.065689	0.420565	1.182153
0.36	0.534816	2.031419	0.457232	1.173714
0.38	0.575526	1.996406	0.493456	1.165175
0.40	0.615148	1.960784	0.529027	1.156577
0.42	0.653456	1.924681	0.563758	1.14796
0.44	0.690255	1.888218	0.597485	1.139364
0.46	0.725383	1.851509	0.630068	1.130825
0.48	0.758707	1.814662	0.66139	1.122377
0.50	0.790123	1.777778	0.691358	1.114053
0.52	0.819554	1.740947	0.719897	1.105882
0.54	0.846948	1.704255	0.746952	1.097892
0.56	0.872274	1.667779	0.772486	1.090109
0.58	0.895523	1.631588	0.796478	1.082556
0.60	0.916704	1.595745	0.818923	1.075253
0.62	0.935843	1.560306	0.839825	1.068221
0.64	0.952976	1.52532	0.859203	1.061475
0.66	0.968155	1.490831	0.877084	1.055031
0.68	0.981439	1.456876	0.893502	1.048904
0.70	0.992895	1.423488	0.908499	1.043104
0.72	1.002598	1.390692	0.922122	1.037642
0.74	1.010624	1.358511	0.934423	1.032528
0.76	1.017057	1.326964	0.945456	1.027769
0.78	1.02198	1.296064	0.955279	1.023372
0.80	1.025477	1.265823	0.963948	1.019343
0.82	1.027633	1.236247	0.971524	1.015687
0.84	1.028533	1.207341	0.978066	1.012407
0.86	1.02826	1.179106	0.983633	1.009507

(*Contd*)

Table B3 Rayleigh flow (*Contd*)

M	T/T^*	p/p^*	T_o/T_o^*	p_o/p_o^*
0.88	1.026894	1.151543	0.988283	1.006989
0.90	1.024516	1.124649	0.992073	1.004856
0.92	1.021201	1.098418	0.995058	1.003109
0.94	1.017023	1.072846	0.997293	1.001749
0.96	1.012052	1.047925	0.998828	1.000778
0.98	1.006357	1.023646	0.999715	1.000194
1.00	1.000000	1.000000	1.000000	1.000000
1.02	0.993043	0.976976	0.99973	1.000194
1.04	0.985543	0.954563	0.998947	1.000778
1.06	0.977555	0.932749	0.997692	1.00175
1.08	0.969129	0.911522	0.996006	1.00311
1.10	0.960313	0.890869	0.993924	1.004858
1.12	0.951151	0.870777	0.99148	1.006995
1.14	0.941687	0.851233	0.988708	1.009519
1.16	0.931958	0.832224	0.985638	1.01243
1.18	0.922	0.813736	0.982299	1.015729
1.20	0.911848	0.795756	0.978717	1.019415
1.22	0.901532	0.778271	0.974916	1.023488
1.24	0.891081	0.761267	0.970922	1.027949
1.26	0.880522	0.744731	0.966754	1.032798
1.28	0.869878	0.728651	0.962433	1.038035
1.30	0.859174	0.713012	0.957979	1.04366
1.32	0.848428	0.697804	0.953407	1.049675
1.34	0.837661	0.683013	0.948734	1.056081
1.36	0.826888	0.668628	0.943976	1.062878
1.38	0.816127	0.654636	0.939145	1.070068
1.40	0.805391	0.641026	0.934254	1.077652
1.42	0.794694	0.627786	0.929315	1.085631
1.44	0.784046	0.614905	0.924338	1.094008
1.46	0.773459	0.602373	0.919333	1.102785
1.48	0.762942	0.590179	0.91431	1.111963
1.50	0.752504	0.578313	0.909276	1.121545
1.52	0.742152	0.566765	0.904238	1.131534
1.54	0.731894	0.555525	0.899205	1.141932
1.56	0.721735	0.544583	0.894181	1.152742
1.58	0.71168	0.533931	0.889173	1.163967

(*Contd*)

Table B3 Rayleigh flow (*Contd*)

M	T/T^*	p/p^*	T_o/T_o^*	p_o/p_o^*
1.60	0.701735	0.52356	0.884186	1.175611
1.62	0.691903	0.513461	0.879225	1.187676
1.64	0.682188	0.503626	0.874292	1.200168
1.66	0.672593	0.494047	0.869394	1.213089
1.68	0.66312	0.484715	0.864531	1.226443
1.70	0.653771	0.475624	0.859709	1.240235
1.72	0.644549	0.466766	0.854929	1.25447
1.74	0.635454	0.458134	0.850195	1.269151
1.76	0.626487	0.449721	0.845507	1.284284
1.78	0.617649	0.441521	0.840868	1.299873
1.80	0.608941	0.433526	0.836279	1.315925
1.82	0.600363	0.425731	0.831743	1.332443
1.84	0.591914	0.41813	0.827259	1.349434
1.86	0.583595	0.410717	0.822829	1.366903
1.88	0.575404	0.403486	0.818455	1.384856
1.90	0.567342	0.396432	0.814136	1.4033
1.92	0.559407	0.38955	0.809873	1.42224
1.94	0.551599	0.382834	0.805666	1.441683
1.96	0.543917	0.376279	0.801517	1.461635
1.98	0.53636	0.369882	0.797424	1.482104
2.00	0.528926	0.363636	0.793388	1.503096
2.02	0.521614	0.357539	0.78941	1.524618
2.04	0.514422	0.351584	0.785488	1.546678
2.06	0.50735	0.34577	0.781624	1.569283
2.08	0.500396	0.34009	0.777816	1.592441
2.10	0.493558	0.334541	0.774064	1.616159
2.12	0.486835	0.329121	0.770368	1.640446
2.14	0.480225	0.323824	0.766727	1.66531
2.16	0.473727	0.318647	0.763142	1.690759
2.18	0.467338	0.313588	0.759611	1.716801
2.20	0.461058	0.308642	0.756135	1.743446
2.22	0.454884	0.303807	0.752712	1.770702
2.24	0.448815	0.299079	0.749342	1.798578
2.26	0.442849	0.294455	0.746024	1.827083
2.28	0.436985	0.289934	0.742758	1.856227
2.30	0.43122	0.28551	0.739543	1.88602

(*Contd*)

Table B3 Rayleigh flow (*Contd*)

M	T/T^*	p/p^*	T_o/T_o^*	p_o/p_o^*
2.32	0.425554	0.281183	0.736379	1.916471
2.34	0.419984	0.276949	0.733264	1.947589
2.36	0.414509	0.272807	0.730199	1.979386
2.38	0.409127	0.268752	0.727182	2.011871
2.40	0.403836	0.264784	0.724213	2.045055
2.42	0.398635	0.260899	0.721291	2.078948
2.44	0.393523	0.257096	0.718415	2.113561
2.46	0.388497	0.253372	0.715585	2.148905
2.48	0.383556	0.249725	0.7128	2.184991
2.50	0.378698	0.246154	0.710059	2.221831
2.52	0.373923	0.242656	0.707362	2.259436
2.54	0.369228	0.239229	0.704708	2.297818
2.56	0.364611	0.235871	0.702096	2.336987
2.58	0.360073	0.232582	0.699525	2.376958
2.60	0.35561	0.229358	0.696995	2.417741
2.62	0.351222	0.226198	0.694506	2.459349
2.64	0.346907	0.223101	0.692055	2.501795
2.66	0.342663	0.220066	0.689644	2.545091
2.68	0.33849	0.217089	0.687271	2.58925
2.70	0.334387	0.214171	0.684935	2.634285
2.72	0.33035	0.211309	0.682636	2.680211
2.74	0.326381	0.208503	0.680374	2.727039
2.76	0.322476	0.20575	0.678146	2.774784
2.78	0.318636	0.20305	0.675954	2.823459
2.80	0.314858	0.200401	0.673796	2.87308
2.82	0.311142	0.197802	0.671672	2.923659
2.84	0.307486	0.195251	0.669582	2.975211
2.86	0.303889	0.192749	0.667523	3.027751
2.88	0.300351	0.190293	0.665497	3.081293
2.90	0.296869	0.187882	0.663502	3.135853
2.92	0.293443	0.185515	0.661538	3.191445
2.94	0.290072	0.183192	0.659604	3.248086
2.96	0.286754	0.18091	0.6577	3.30579
2.98	0.28349	0.17867	0.655825	3.364573
3.00	0.280277	0.176471	0.653979	3.424452
3.02	0.277115	0.17431	0.652161	3.485442

(*Contd*)

Table B3 Rayleigh flow (*Contd*)

M	T/T^*	p/p^*	T_o/T_o^*	p_o/p_o^*
3.04	0.274002	0.172188	0.650371	3.547559
3.06	0.270938	0.170104	0.648608	3.610821
3.08	0.267922	0.168056	0.646872	3.675243
3.10	0.264954	0.166044	0.645162	3.740844
3.12	0.262031	0.164067	0.643478	3.807639
3.14	0.259153	0.162124	0.641819	3.875646
3.16	0.25632	0.160215	0.640185	3.944883
3.18	0.25353	0.158339	0.638575	4.015368
3.20	0.250783	0.156495	0.636989	4.087118
3.22	0.248078	0.154681	0.635427	4.160151
3.24	0.245414	0.152899	0.633888	4.234486
3.26	0.24279	0.151146	0.632371	4.310142
3.28	0.240206	0.149423	0.630877	4.387137
3.30	0.237661	0.147729	0.629405	4.465489
3.32	0.235154	0.146062	0.627954	4.545219
3.34	0.232684	0.144423	0.626525	4.626346
3.36	0.230251	0.142811	0.625116	4.708889
3.38	0.227854	0.141225	0.623727	4.792868
3.40	0.225492	0.139665	0.622359	4.878303
3.42	0.223166	0.13813	0.62101	4.965214
3.44	0.220873	0.136619	0.619681	5.053622
3.46	0.218614	0.135133	0.61837	5.143548
3.48	0.216387	0.133671	0.617078	5.235012
3.50	0.214193	0.132231	0.615805	5.328035
3.52	0.212031	0.130815	0.614549	5.422639
3.54	0.209899	0.12942	0.613312	5.518846
3.56	0.207799	0.128048	0.612091	5.616676
3.58	0.205728	0.126696	0.610888	5.716153
3.60	0.203686	0.125366	0.609701	5.817298
3.62	0.201674	0.124056	0.608531	5.920134
3.64	0.19969	0.122766	0.607378	6.024684
3.66	0.197734	0.121495	0.60624	6.13097
3.68	0.195806	0.120244	0.605117	6.239015
3.70	0.193904	0.119012	0.60401	6.348844
3.72	0.192029	0.117799	0.602919	6.460479

(*Contd*)

Table B3 Rayleigh flow (*Contd*)

M	T/T^*	p/p^*	T_o/T_o^*	p_o/p_o^*
3.74	0.190179	0.116603	0.601842	6.573945
3.76	0.188356	0.115425	0.60078	6.689265
3.78	0.186557	0.114265	0.599732	6.806464
3.80	0.184783	0.113122	0.598698	6.925566
3.82	0.183034	0.111996	0.597678	7.046596
3.84	0.181308	0.110886	0.596672	7.16958
3.86	0.179605	0.109792	0.595679	7.294542
3.88	0.177926	0.108715	0.594699	7.421508
3.90	0.176269	0.107652	0.593732	7.550504
3.92	0.174634	0.106605	0.592778	7.681556
3.94	0.173021	0.105573	0.591837	7.81469
3.96	0.17143	0.104556	0.590908	7.949932
3.98	0.16986	0.103553	0.589991	8.08731
4.00	0.16831	0.102564	0.589086	8.226849
4.02	0.166781	0.101589	0.588193	8.368578
4.04	0.165272	0.100628	0.587311	8.512525
4.06	0.163783	0.09968	0.586441	8.658716
4.08	0.162313	0.098745	0.585582	8.807179
4.10	0.160862	0.097823	0.584733	8.957944
4.12	0.15943	0.096914	0.583896	9.111038
4.14	0.158016	0.096018	0.583069	9.26649
4.16	0.156621	0.095133	0.582253	9.42433
4.18	0.155243	0.09426	0.581447	9.584586
4.20	0.153883	0.0934	0.580651	9.747289
4.22	0.15254	0.092551	0.579865	9.912467
4.24	0.151214	0.091713	0.579089	10.08015
4.26	0.149905	0.090886	0.578323	10.25037
4.28	0.148612	0.090071	0.577566	10.42316
4.30	0.147335	0.089266	0.576818	10.59854
4.32	0.146075	0.088472	0.57608	10.77656
4.34	0.14483	0.087688	0.57535	10.95723
4.36	0.1436	0.086914	0.57463	11.1406
4.38	0.142386	0.086151	0.573918	11.32669
4.40	0.141186	0.085397	0.573215	11.51554
4.42	0.140001	0.084653	0.572521	11.70717

(*Contd*)

Table B3 Rayleigh flow (*Contd*)

M	T/T^*	p/p^*	T_o/T_o^*	p_o/p_o^*
4.44	0.138831	0.083919	0.571834	11.90163
4.46	0.137675	0.083194	0.571156	12.09894
4.48	0.136532	0.082478	0.570487	12.29914
4.50	0.135404	0.081772	0.569825	12.50226
4.52	0.134289	0.081074	0.569171	12.70834
4.54	0.133188	0.080385	0.568525	12.9174
4.56	0.132099	0.079705	0.567886	13.12949
4.58	0.131024	0.079033	0.567255	13.34464
4.60	0.129961	0.07837	0.566632	13.56288
4.62	0.128911	0.077715	0.566015	13.78425
4.64	0.127874	0.077068	0.565406	14.00879
4.66	0.126848	0.076429	0.564804	14.23653
4.68	0.125835	0.075797	0.564209	14.4675
4.70	0.124833	0.075174	0.563621	14.70174
4.72	0.123843	0.074558	0.563039	14.9393
4.74	0.122864	0.073949	0.562464	15.1802
4.76	0.121897	0.073348	0.561896	15.42449
4.78	0.120941	0.072754	0.561334	15.6722
4.80	0.119995	0.072167	0.560779	15.92337
4.82	0.119061	0.071588	0.56023	16.17803
4.84	0.118137	0.071015	0.559687	16.43624
4.86	0.117224	0.070448	0.55915	16.69801
4.88	0.116321	0.069889	0.558619	16.96341
4.90	0.115428	0.069336	0.558094	17.23245
4.92	0.114545	0.06879	0.557575	17.50519
4.94	0.113672	0.06825	0.557062	17.78167
4.96	0.112809	0.067716	0.556554	18.06192
4.98	0.111955	0.067188	0.556052	18.34598
5.00	0.111111	0.066667	0.555556	18.6339

Table B4 Normal shock

M_1	M_2	p_{o2}/p_{o1}	ρ_2/ρ_1	p_2/p_1	T_2/T_1	p_{o2}/p_1
1.00	1.00000	1.00000	1.00000	1.00000	1.00000	1.89293
1.02	0.98052	0.99999	1.03344	1.04713	1.01325	1.93790

(*Contd*)

Table B4 Normal shock (*Contd*)

M_1	M_2	p_{o2}/p_{o1}	ρ_2/ρ_1	p_2/p_1	T_2/T_1	p_{o2}/p_1
1.04	0.96203	0.99992	1.06709	1.09520	1.02634	1.98442
1.06	0.94445	0.99975	1.10092	1.14420	1.03931	2.03245
1.08	0.92771	0.99943	1.13492	1.19413	1.05217	2.08194
1.10	0.91177	0.99893	1.16908	1.24500	1.06494	2.13285
1.12	0.89656	0.99821	1.20338	1.29680	1.07763	2.18513
1.14	0.88204	0.99726	1.23779	1.34953	1.09027	2.23877
1.16	0.86816	0.99605	1.27231	1.40320	1.10287	2.29372
1.18	0.85488	0.99457	1.30693	1.45780	1.11544	2.34998
1.20	0.84217	0.99280	1.34161	1.51333	1.12799	2.40750
1.22	0.82999	0.99073	1.37636	1.56980	1.14054	2.46628
1.24	0.81830	0.98836	1.41116	1.62720	1.15309	2.52629
1.26	0.80709	0.98568	1.44599	1.68553	1.16566	2.58753
1.28	0.79631	0.98268	1.48084	1.74480	1.17825	2.64996
1.30	0.78596	0.97937	1.51570	1.80500	1.19087	2.71359
1.32	0.77600	0.97575	1.55055	1.86613	1.20353	2.77840
1.34	0.76641	0.97182	1.58538	1.92820	1.21624	2.84438
1.36	0.75718	0.96758	1.62018	1.99120	1.22900	2.91152
1.38	0.74829	0.96304	1.65494	2.05513	1.24181	2.97981
1.40	0.73971	0.95819	1.68966	2.12000	1.25469	3.04924
1.42	0.73144	0.95306	1.72430	2.18580	1.26764	3.11980
1.44	0.72345	0.94765	1.75888	2.25253	1.28066	3.19149
1.46	0.71574	0.94196	1.79337	2.32020	1.29377	3.26431
1.48	0.70829	0.93600	1.82777	2.38880	1.30695	3.33823
1.50	0.70109	0.92979	1.86207	2.45833	1.32022	3.41327
1.52	0.69413	0.92332	1.89626	2.52880	1.33357	3.48942
1.54	0.68739	0.91662	1.93033	2.60020	1.34703	3.56667
1.56	0.68087	0.90970	1.96427	2.67253	1.36057	3.64501
1.58	0.67455	0.90255	1.99808	2.74580	1.37422	3.72445
1.60	0.66844	0.89520	2.03175	2.82000	1.38797	3.80497
1.62	0.66251	0.88765	2.06526	2.89513	1.40182	3.88658
1.64	0.65677	0.87992	2.09863	2.97120	1.41578	3.96928
1.66	0.65119	0.87201	2.13183	3.04820	1.42985	4.05305
1.68	0.64579	0.86394	2.16486	3.12613	1.44403	4.13791
1.70	0.64054	0.85572	2.19772	3.20500	1.45833	4.22383
1.72	0.63545	0.84736	2.23040	3.28480	1.47274	4.31083
1.74	0.63051	0.83886	2.26289	3.36553	1.48727	4.39890

(*Contd*)

Table B4 Normal shock (*Contd*)

M_1	M_2	p_{o2}/p_{o1}	ρ_2/ρ_1	p_2/p_1	T_2/T_1	p_{o2}/p_1
1.76	0.62570	0.83024	2.29520	3.44720	1.50192	4.48804
1.78	0.62104	0.82151	2.32731	3.52980	1.51669	4.57825
1.80	0.61650	0.81268	2.35922	3.61333	1.53158	4.66952
1.82	0.61209	0.80376	2.39093	3.69780	1.54659	4.76185
1.84	0.60780	0.79476	2.42244	3.78320	1.56173	4.85524
1.86	0.60363	0.78569	2.45373	3.86953	1.57700	4.94970
1.88	0.59957	0.77655	2.48481	3.95680	1.59239	5.04521
1.90	0.59562	0.76736	2.51568	4.04500	1.60792	5.14178
1.92	0.59177	0.75812	2.54633	4.13413	1.62357	5.23940
1.94	0.58802	0.74884	2.57675	4.22420	1.63935	5.33808
1.96	0.58437	0.73954	2.60695	4.31520	1.65527	5.43782
1.98	0.58082	0.73021	2.63692	4.40713	1.67132	5.53860
2.00	0.57735	0.72087	2.66667	4.50000	1.68750	5.64044
2.02	0.57397	0.71153	2.69618	4.59380	1.70382	5.74333
2.04	0.57068	0.70218	2.72546	4.68853	1.72027	5.84727
2.06	0.56747	0.69284	2.75451	4.78420	1.73686	5.95226
2.08	0.56433	0.68351	2.78332	4.88080	1.75359	6.05829
2.10	0.56128	0.67420	2.81190	4.97833	1.77045	6.16537
2.12	0.55829	0.66492	2.84024	5.07680	1.78745	6.27351
2.14	0.55538	0.65567	2.86835	5.17620	1.80459	6.38268
2.16	0.55254	0.64645	2.89621	5.27653	1.82188	6.49290
2.18	0.54977	0.63727	2.92383	5.37780	1.83930	6.60417
2.20	0.54706	0.62814	2.95122	5.48000	1.85686	6.71648
2.22	0.54441	0.61905	2.97837	5.58313	1.87456	6.82983
2.24	0.54182	0.61002	3.00527	5.68720	1.89241	6.94423
2.26	0.53930	0.60105	3.03194	5.79220	1.91040	7.05967
2.28	0.53683	0.59214	3.05836	5.89813	1.92853	7.17616
2.30	0.53441	0.58329	3.08455	6.00500	1.94680	7.29368
2.32	0.53205	0.57452	3.11049	6.11280	1.96522	7.41225
2.34	0.52974	0.56581	3.13620	6.22153	1.98378	7.53185
2.36	0.52749	0.55718	3.16167	6.33120	2.00249	7.65250
2.38	0.52528	0.54862	3.18690	6.44180	2.02134	7.77419
2.40	0.52312	0.54014	3.21190	6.55333	2.04033	7.89691
2.42	0.52100	0.53175	3.23665	6.66580	2.05947	8.02068
2.44	0.51894	0.52344	3.26117	6.77920	2.07876	8.14549
2.46	0.51691	0.51521	3.28546	6.89353	2.09819	8.27133

(*Contd*)

Table B4 Normal shock (*Contd*)

M_1	M_2	p_{o2}/p_{o1}	ρ_2/ρ_1	p_2/p_1	T_2/T_1	p_{o2}/p_1
2.48	0.51493	0.50707	3.30951	7.00880	2.11777	8.39821
2.50	0.51299	0.49901	3.33333	7.12500	2.13750	8.52614
2.52	0.51109	0.49105	3.35692	7.24213	2.15737	8.65510
2.54	0.50923	0.48318	3.38028	7.36020	2.17739	8.78509
2.56	0.50741	0.47540	3.40341	7.47920	2.19756	8.91613
2.58	0.50562	0.46772	3.42631	7.59913	2.21788	9.04820
2.60	0.50387	0.46012	3.44898	7.72000	2.23834	9.18131
2.62	0.50216	0.45263	3.47143	7.84180	2.25896	9.31545
2.64	0.50048	0.44522	3.49365	7.96453	2.27972	9.45064
2.66	0.49883	0.43792	3.51565	8.08820	2.30063	9.58685
2.68	0.49722	0.43070	3.53743	8.21280	2.32168	9.72411
2.70	0.49563	0.42359	3.55899	8.33833	2.34289	9.86240
2.72	0.49408	0.41657	3.58033	8.46480	2.36425	10.00173
2.74	0.49256	0.40965	3.60146	8.59220	2.38576	10.14209
2.76	0.49107	0.40283	3.62237	8.72053	2.40741	10.28349
2.78	0.48960	0.39610	3.64307	8.84980	2.42922	10.42592
2.80	0.48817	0.38946	3.66355	8.98000	2.45117	10.56939
2.82	0.48676	0.38293	3.68383	9.11113	2.47328	10.71389
2.84	0.48538	0.37649	3.70389	9.24320	2.49554	10.85943
2.86	0.48402	0.37014	3.72375	9.37620	2.51794	11.00600
2.88	0.48269	0.36389	3.74341	9.51013	2.54050	11.15361
2.90	0.48138	0.35773	3.76286	9.64500	2.56321	11.30225
2.92	0.48010	0.35167	3.78211	9.78080	2.58607	11.45192
2.94	0.47884	0.34570	3.80117	9.91753	2.60908	11.60263
2.96	0.47760	0.33982	3.82002	10.05520	2.63224	11.75438
2.98	0.47638	0.33404	3.83868	10.19380	2.65555	11.90715
3.00	0.47519	0.32834	3.85714	10.33333	2.67901	12.06096
3.02	0.47402	0.32274	3.87541	10.47380	2.70263	12.21581
3.04	0.47287	0.31723	3.89350	10.61520	2.72639	12.37169
3.06	0.47174	0.31180	3.91139	10.75753	2.75031	12.52860
3.08	0.47063	0.30646	3.92909	10.90080	2.77438	12.68655
3.10	0.46953	0.30121	3.94661	11.04500	2.79860	12.84553
3.12	0.46846	0.29605	3.96395	11.19013	2.82298	13.00554
3.14	0.46741	0.29097	3.98110	11.33620	2.84750	13.16659
3.16	0.46637	0.28597	3.99808	11.48320	2.87218	13.32866
3.18	0.46535	0.28106	4.01488	11.63113	2.89701	13.49178

(*Contd*)

Table B4 Normal shock (*Contd*)

M_1	M_2	p_{o2}/p_{o1}	ρ_2/ρ_1	p_2/p_1	T_2/T_1	p_{o2}/p_1
3.20	0.46435	0.27623	4.03150	11.78000	2.92199	13.65592
3.22	0.46336	0.27148	4.04794	11.92980	2.94713	13.82110
3.24	0.46240	0.26681	4.06422	12.08053	2.97241	13.98731
3.26	0.46144	0.26222	4.08032	12.23220	2.99785	14.15455
3.28	0.46051	0.25771	4.09625	12.38480	3.02345	14.32283
3.30	0.45959	0.25328	4.11202	12.53833	3.04919	14.49214
3.32	0.45868	0.24892	4.12762	12.69280	3.07509	14.66248
3.34	0.45779	0.24463	4.14306	12.84820	3.10114	14.83385
3.36	0.45691	0.24043	4.15833	13.00453	3.12734	15.00626
3.38	0.45605	0.23629	4.17345	13.16180	3.15370	15.17969
3.40	0.45520	0.23223	4.18841	13.32000	3.18021	15.35417
3.42	0.45436	0.22823	4.20321	13.47913	3.20687	15.52967
3.44	0.45354	0.22431	4.21785	13.63920	3.23369	15.70620
3.46	0.45273	0.22045	4.23234	13.80020	3.26065	15.88377
3.48	0.45194	0.21667	4.24668	13.96213	3.28778	16.06237
3.50	0.45115	0.21295	4.26087	14.12500	3.31505	16.24200
3.52	0.45038	0.20929	4.27491	14.28880	3.34248	16.42266
3.54	0.44962	0.20570	4.28880	14.45353	3.37006	16.60436
3.56	0.44887	0.20218	4.30255	14.61920	3.39780	16.78709
3.58	0.44814	0.19871	4.31616	14.78580	3.42569	16.97085
3.60	0.44741	0.19531	4.32962	14.95333	3.45373	17.15564
3.62	0.44670	0.19197	4.34294	15.12180	3.48192	17.34146
3.64	0.44600	0.18869	4.35613	15.29120	3.51027	17.52831
3.66	0.44530	0.18547	4.36918	15.46153	3.53878	17.71620
3.68	0.44462	0.18230	4.38209	15.63280	3.56743	17.90512
3.70	0.44395	0.17919	4.39486	15.80500	3.59624	18.09507
3.72	0.44329	0.17614	4.40751	15.97813	3.62521	18.28605
3.74	0.44263	0.17314	4.42002	16.15220	3.65433	18.47806
3.76	0.44199	0.17020	4.43241	16.32720	3.68360	18.67110
3.78	0.44136	0.16731	4.44466	16.50313	3.71302	18.86518
3.80	0.44073	0.16447	4.45679	16.68000	3.74260	19.06029
3.82	0.44012	0.16168	4.46879	16.85780	3.77234	19.25642
3.84	0.43951	0.15895	4.48067	17.03653	3.80223	19.45359
3.86	0.43891	0.15626	4.49243	17.21620	3.83227	19.65180
3.88	0.43832	0.15362	4.50407	17.39680	3.86246	19.85103
3.90	0.43774	0.15103	4.51559	17.57833	3.89281	20.05129

(*Contd*)

Table B4 Normal shock (*Contd*)

M_1	M_2	p_{o2}/p_{o1}	ρ_2/ρ_1	p_2/p_1	T_2/T_1	p_{o2}/p_1
3.92	0.43717	0.14848	4.52699	17.76080	3.92332	20.25259
3.94	0.43661	0.14598	4.53827	17.94420	3.95398	20.45491
3.96	0.43605	0.14353	4.54944	18.12853	3.98479	20.65827
3.98	0.43550	0.14112	4.56049	18.31380	4.01575	20.86266
4.00	0.43496	0.13876	4.57143	18.50000	4.04688	21.06808
4.02	0.43443	0.13643	4.58226	18.68713	4.07815	21.27453
4.04	0.43390	0.13415	4.59298	18.87520	4.10958	21.48201
4.06	0.43338	0.13191	4.60359	19.06420	4.14116	21.69053
4.08	0.43287	0.12972	4.61409	19.25413	4.17290	21.90007
4.10	0.43236	0.12756	4.62448	19.44500	4.20479	22.11065
4.12	0.43186	0.12544	4.63478	19.63680	4.23684	22.32226
4.14	0.43137	0.12335	4.64496	19.82953	4.26904	22.53489
4.16	0.43089	0.12131	4.65505	20.02320	4.30140	22.74856
4.18	0.43041	0.11930	4.66503	20.21780	4.33391	22.96326
4.20	0.42994	0.11733	4.67491	20.41333	4.36657	23.17899
4.22	0.42947	0.11540	4.68470	20.60980	4.39939	23.39576
4.24	0.42901	0.11350	4.69438	20.80720	4.43236	23.61355
4.26	0.42856	0.11163	4.70397	21.00553	4.46549	23.83237
4.28	0.42811	0.10980	4.71346	21.20480	4.49877	24.05223
4.30	0.42767	0.10800	4.72286	21.40500	4.53221	24.27311
4.32	0.42723	0.10623	4.73217	21.60613	4.56580	24.49503
4.34	0.42680	0.10450	4.74138	21.80820	4.59955	24.71798
4.36	0.42638	0.10280	4.75050	22.01120	4.63345	24.94195
4.38	0.42596	0.10112	4.75953	22.21513	4.66750	25.16696
4.40	0.42554	0.09948	4.76847	22.42000	4.70171	25.39300
4.42	0.42514	0.09787	4.77733	22.62580	4.73608	25.62007
4.44	0.42473	0.09628	4.78609	22.83253	4.77060	25.84818
4.46	0.42433	0.09473	4.79477	23.04020	4.80527	26.07731
4.48	0.42394	0.09320	4.80337	23.24880	4.84010	26.30747
4.50	0.42355	0.09170	4.81188	23.45833	4.87509	26.53867
4.52	0.42317	0.09022	4.82031	23.66880	4.91022	26.77089
4.54	0.42279	0.08878	4.82866	23.88020	4.94552	27.00415
4.56	0.42241	0.08735	4.83692	24.09253	4.98097	27.23843
4.58	0.42205	0.08596	4.84511	24.30580	5.01657	27.47375
4.60	0.42168	0.08459	4.85321	24.52000	5.05233	27.71010
4.62	0.42132	0.08324	4.86124	24.73513	5.08824	27.94747

(*Contd*)

Table B4 Normal shock (*Contd*)

M_1	M_2	p_{o2}/p_{o1}	ρ_2/ρ_1	p_2/p_1	T_2/T_1	p_{o2}/p_1
4.64	0.42096	0.08192	4.86919	24.95120	5.12430	28.18588
4.66	0.42061	0.08062	4.87706	25.16820	5.16053	28.42532
4.68	0.42026	0.07934	4.88486	25.38613	5.19690	28.66579
4.70	0.41992	0.07809	4.89258	25.60500	5.23343	28.90729
4.72	0.41958	0.07685	4.90023	25.82480	5.27012	29.14982
4.74	0.41925	0.07564	4.90780	26.04553	5.30696	29.39339
4.76	0.41891	0.07445	4.91531	26.26720	5.34396	29.63798
4.78	0.41859	0.07329	4.92274	26.48980	5.38111	29.88360
4.80	0.41826	0.07214	4.93010	26.71333	5.41842	30.13026
4.82	0.41794	0.07101	4.93739	26.93780	5.45588	30.37794
4.84	0.41763	0.06991	4.94461	27.16320	5.49349	30.62665
4.86	0.41731	0.06882	4.95177	27.38953	5.53126	30.87640
4.88	0.41701	0.06775	4.95885	27.61680	5.56919	31.12718
4.90	0.41670	0.06670	4.96587	27.84500	5.60727	31.37898
4.92	0.41640	0.06567	4.97283	28.07413	5.64551	31.63182
4.94	0.41610	0.06465	4.97972	28.30420	5.68390	31.88569
4.96	0.41581	0.06366	4.98654	28.53520	5.72244	32.14059
4.98	0.41552	0.06268	4.99330	28.76713	5.76114	32.39652
5.00	0.41523	0.06172	5.00000	29.00000	5.80000	32.65347

APPENDIX C

Uncertainty Analysis

The uncertainty or error in the measured quantity is the least count of the instrument. A measured parameter is generally represented by

$$x = x \pm \delta x \tag{C.1}$$

where $\pm\delta x$ represents the error band in the measured parameter.

The uncertainty in a dependent parameter y which is a function of n number of independent measured parameters $x_1, x_2, x_3, \ldots, x_n$ is the root mean square of uncertainties in the independent parameters. The following is the procedure:

Let a parameter be calculated using certain measured quantities as,

$$y = y(x_1, x_2, x_3, \ldots, x_n) \tag{C.2}$$

Then uncertainty in y is given as

$$\delta y = \sqrt{\left(\frac{\partial y}{\partial x_1}\delta x_1\right)^2 + \left(\frac{\partial y}{\partial x_2}\delta x_2\right)^2 + \left(\frac{\partial y}{\partial x_3}\delta x_3\right)^2 + \cdots + \left(\frac{\partial y}{\partial x_n}\delta x_n\right)^2} \tag{C.3}$$

where, $\delta x_1, \delta x_2, \delta x_3, \ldots, \delta x_n$ are the possible errors in measurements of $x_1, x_2, x_3, \ldots, x_n$, δy is absolute uncertainty, and $\frac{\delta y}{y}$ is relative uncertainty.

Case I: Addition/Subtraction of Parameters

If two parameters x_1 and x_2 have the uncertainties δx_1 and δx_2, respectively, the uncertainty in their sum or difference is given by

$$y = x_1 \pm x_2 \tag{C.4}$$

Using Eq. (C.3),

$$\delta y = \sqrt{(\delta x_1)^2 + (\delta x_2)^2} \tag{C.5}$$

Case II: Multiplication of Parameters

If two parameters x_1 and x_2 have the uncertainties δx_1 and δx_2, respectively, the uncertainty in their sum or difference is given by

$$y = x_1 \cdot x_2 \tag{C.6}$$

Using Eq. (C.3),

$$\frac{\delta y}{y} = \sqrt{\left(\frac{\delta x_1}{x_1}\right)^2 + \left(\frac{\delta x_2}{x_2}\right)^2} \tag{C.7}$$

Example

Let $$y = \frac{x_1^2 x_2 x_3^{1/2}}{x_4^3} \tag{1}$$

$$\delta y = \sqrt{\left(\frac{\partial y}{\partial x_1}\delta x_1\right)^2 + \left(\frac{\partial y}{\partial x_2}\delta x_2\right)^2 + \left(\frac{\partial y}{\partial x_3}\delta x_3\right)^2 + \left(\frac{\partial y}{\partial x_4}\delta x_4\right)^2} \tag{2}$$

Partial derivatives are as follows:

$$\frac{\partial y}{\partial x_1} = 2x_1 \frac{x_2 x_3^{1/2}}{x_4^3} \quad \Rightarrow \quad \frac{\partial y}{\partial x_1} = 2\frac{y}{x_1}$$

$$\frac{\partial y}{\partial x_2} = \frac{x_1^2 x_3^{1/2}}{x_4^3} \quad \Rightarrow \quad \frac{\partial y}{\partial x_2} = \frac{y}{x_2}$$

$$\frac{\partial y}{\partial x_3} = \frac{1}{2}\frac{x_1^2 x_2 x_3^{-1/2}}{x_4^3} \quad \Rightarrow \quad \frac{\partial y}{\partial x_3} = \frac{1}{2}\frac{y}{x_3}$$

$$\frac{\partial y}{\partial x_4} = -3\frac{x_1^2 x_2 x_3^{1/2}}{x_4^4} \quad \Rightarrow \quad \frac{\partial y}{\partial x_3} = -3\frac{y}{x_4}$$

Using Eq. (C.3)

$$\frac{\delta y}{y} = \sqrt{\left(2\frac{\delta x_1}{x_1}\right)^2 + \left(\frac{\delta x_2}{x_2}\right)^2 + \left(\frac{1}{2}\frac{\delta x_3}{x_3}\right)^2 + \left(-3\frac{\delta x_4}{x_4}\right)^2} \tag{3}$$

APPENDIX D Scalar, Vector, and Tensor Quantities

Any physical quantity is termed as *scalar* if it has only magnitude. Such quantities have only one piece of information and in this case it is the magnitude. Examples are distance, speed, pressure, temperature, etc.

A *vector* quantity has both magnitude as well as direction. Thus, it is characterized by two pieces of information, that is, magnitude and direction. Examples are velocity, acceleration, force, momentum, etc. Velocity vector $\vec{V}$ can be represented by

$$\vec{V} = u\hat{i} + v\hat{j} + w\hat{k} \tag{D.1}$$

where u, v, and w are the velocity components (magnitudes) in x, y, and z directions, respectively, $\hat{i}$, $\hat{j}$, and $\hat{k}$ are the unit vectors (vectors having unity magnitude) in x, y, and z directions, respectively. Thus, they represent directions only (illustrated in Fig. D1).

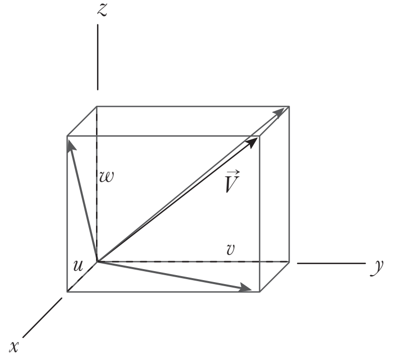

Fig. D1 Velocity vector

A *tensor* has three pieces of information: magnitude, direction, and the plane of action. A tensor quantity can be thought of an array or matrix of magnitudes and their position in the matrix represents the direction as well as plane of action. In fact, scalars and vectors can be thought of tensors having

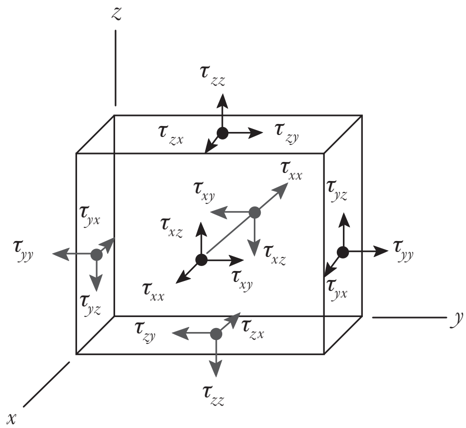

Fig. D2 Stress tensor

ranks 0 and 1, respectively. Examples are stress tensor, strain tensor, etc. The *stress tensor* (shown in Fig. D2) is given by

$$\tau_{ij} = \begin{bmatrix} \tau_{xx} & \tau_{xy} & \tau_{xz} \\ \tau_{yx} & \tau_{yy} & \tau_{yz} \\ \tau_{zx} & \tau_{zy} & \tau_{zz} \end{bmatrix} \tag{D.2}$$

Equation (D.1) can be also be represented in the form of a matrix

$$\vec{V} = \begin{bmatrix} u \\ v \\ w \end{bmatrix} \tag{D.3}$$

Glossary

Absolute pressure The actual pressure at a point. It is obtained by adding atmospheric pressure to the pressure indicated by the gauge (positive or negative).

Adhesion The force of attraction between dissimilar molecules.

Adiabatic process The process in which there is no heat transfer between the system and its surroundings. *A reversible adiabatic process* is also known as *isentropic process*.

Aerodynamic force The resultant force acting on a body when a fluid flows over it. Its horizontal component parallel to the flow stream is known as *drag* and vertical component perpendicular to the flow stream is known as *lift*.

Angle of attack The angle between the chordline of an airfoil and the direction of flow stream.

Angular momentum conservation principle States that the rate of change of angular momentum of a body is directly proportional to net torque applied on it.

Barometer A device used to measure the atmospheric pressure.

Boundary layer The thin viscous region near the solid surface when a fluid flows over it. Velocity varies from within the boundary layer from 0 to 99 percent of free stream velocity.

Boundary layer separation Occurs only when fluid flow takes place on a curved body. The pressure does not remain constant along the body due to change in the flow area above it. Velocity increases and pressure decreases due to reduction in flow area in the upstream side of the curved body in the direction of flow.

Boundary layer thickness The perpendicular distance above the solid surface where fluid velocity approaches 99 percent of free stream velocity.

Buoyancy The phenomenon of experiencing an upward force when a body is immersed (fully or partially) in a fluid. This upward force is called *buoyant force* and is equal to the weight of the volume of fluid displaced by the immersed body.

Cavitation The formation of cavities on the blade/casing surface of a runner or impeller. Cavitation occurs due to the fall in pressure below saturation pressure of the liquid inside a fluid machine causing it to evaporate. The vapour bubbles formed collapse near the solid surface causing it to erode.

Centre of buoyancy The centre of gravity of the submerged portion of a floating body.

Centre of gravity The point where the weight of the body is supposed to be concentrated.

Centre of pressure The point on the submerged surface where the resultant hydrostatic pressure force acts.

Channel bed slope The slope of channel bed in the direction of flow. Slopes are of three types: (a) *mild slope* is the one at which the uniform flow through it remains subcritical, (b) *critical slope* is the slope at which uniform flow is critical, and (c) *steep slope* is the slope at which the uniform flow is supercritical.

Chemical equilibrium The uniformity of concentration or chemical composition everywhere in the system.

Choking Referred to as the condition of maximum mass flow rate through a duct.

Circulation Defined as the *line integral* of the tangential component of the fluid velocity around a closed path.

Clausius statement *It is impossible for a device to transfer heat from a low temperature body to high temperature body without doing any work*. Clausius statement forms the basis for the working of heat pumps and refrigerators.

Closed system or control mass A system which does not allow mass to cross its boundary. However, energy interactions are allowed to take place across its boundary. Quantity of mass within the system is fixed.

Cohesion The force of attraction between similar molecules.

Compressibility factor A useful thermodynamic parameter for modifying the ideal gas law to account for the real gas behaviour.

Compressible flow A variable density flow. At Mach numbers greater than 0.3, the compressibility effects become significant.

Compression wave The wave which is at a higher pressure than the fluid medium in which it is propagating.

Contact angle ϕ The angle formed between the solid surface and the tangent to the liquid droplet periphery at the point of contact with (a) $\phi < 90^o$ for *wetting* or *hydrophilic surface* and (b) $\phi > 90^o$ for *non-wetting* or *hydrophobic surface*.

Contraction coefficient The ratio of cross-sectional area at *vena-contracta* to pipe's cross-sectional area.

Correction factors These are employed for the compensation of error induced due to the use of *average velocity* in the calculation of momentum flux and kinetic energy. *Momentum correction factor* is the ratio of actual momentum flux to the average momentum flux whereas *energy correction factor* is the ratio of actual kinetic energy to the average

kinetic energy. The momentum and energy correction factors are always greater than unity. For steady and uniform flows their values are unity.

Critical condition The state of fluid corresponding to unity Mach number.

Critical depth The depth of flow in an open channel corresponding to which specific energy is minimum.

Critical flow A type of open channel flow where *Froude number* is equal to unity.

Critical Mach number In case of flow over an airfoil is the free stream Mach number at which the flow turns sonic at the point of minimum pressure.

Crocco number The ratio of fluid velocity to maximum fluid velocity (square root of twice of stagnation enthalpy).

Cyclic process The process in which both initial and final states are same.

d'Alembert's paradox The discrepancy in potential flow and viscous flow past cylinder. In potential flow, fluid is ideal and there is no viscous boundary layer formation. Thus, in the upstream side velocity increases and pressure decreases whereas in the downstream side dropped pressure is fully recovered at the expense of kinetic energy. Hence, there exists two stagnation points on the surface of the cylinder. However, in actual practice, the boundary layer forms on the cylinder and gets separated in the downstream side due to adverse pressure gradient. It is found that there exists only one stagnation point on the upstream side. On the downstream side there is a low pressure wake due to non-recovery of pressure. This inconsistency is known as *d'Alembert's paradox*.

Darcy friction factor This is four times the value of the skin friction coefficient.

Degree of reaction The ratio of energy transfer taking place in the rotor/runner to the total energy transfer.

Density Defined as mass per unit volume.

Dimension Any measurable property used to describe the physical state of a body or a system.

Discharge coefficient The ratio of actual discharge to theoretical discharge. Usually, its value is less than unity.

Displacement thickness The measure of mass flow rate deficit within boundary layer region. It is the distance by which a surface be displaced to compensate the mass flow rate deficit.

Drag coefficient The ratio of total drag force to dynamic force (dynamic pressure times frontal area).

Dynamics The study of bodies in motion. *Dynamics* has two sub-categories, namely *kinematics* and *kinetics*.

Energy conservation principle This is the same as the *first law of thermodynamics* which states that energy can neither be created nor destroyed but it can be transformed from one form to another. That is, total energy of a system is constant. For one-dimensional steady flow, the equation which represents the energy conservation principle is the *steady flow energy equation*. For one-dimensional incompressible, inviscid and steady flow, the energy conservation principle is represented by *Bernoulli's equation*.

Energy grade line or total energy line This is employed for graphical representation of mechanical energy level at any point in a pipe network. The energy grade line represents the summation of pressure, velocity and datum heads.

Energy thickness The measure of kinetic energy deficit within boundary layer region.

Entropy A measure of disorderliness or randomness in a system. A gas has more randomness compared to a liquid whereas liquids have more randomness compared to solids. Randomness (i.e., molecular motion or diffusion) is a function of temperature. Higher the temperature higher will be the degree of randomness. Thus, as per third law of thermodynamics *entropy of a perfect crystal is zero at absolute zero temperature*.

Equilibrium This implies a state of balance within the system.

Equipotential line The line of constant *potential function*. The velocity component in a given direction is the partial derivative of potential function in that direction. These lines are always perpendicular to the *streamlines*.

Euler number The square root of the ratio of inertia force to pressure force.

Eulerian approach Uses the concept of control volume to analyse any flow problem with the assumption of fluid being continuum.

Extensive property A property dependent on the size of the system, for example, mass, volume, etc.

External flow The flow which takes place over a solid body for example, flow over an aircraft, submarines, vehicles, etc.

Fanno flow This is adiabatic flow through a constant area frictional duct.

First law of thermodynamics This is the energy conservation principle and its consequence is the property known as *internal energy*. It states that *energy can neither be created nor destroyed but it can be transformed from one form to another*. This means that heat can be converted into work and work can be converted to heat.

Flow lines Conventional imaginary lines depicting the flow, for example, *streamline*, *pathline*, *streakline*, and *timeline*.

Flow-tangency condition This is applicable to the flow of ideal fluid over a solid body. The velocity is tangential at every point on the solid surface/boundary and there is no component of flow velocity normal to the surface.

Fluids Defined as the substances that deform continuously and indefinitely under the action of shear stress. Unlike solids, fluids offer no resistance to the applied shear. Both liquids and gases fall under the category of fluids.

Froude number Defined as the square root of the ratio of inertia force to gravity force.

Gauge pressure The pressure above atmospheric pressure. It is also known as *positive* pressure. It is the pressure indicated by the pressure measuring device or gauge.

Generator efficiency The ratio of the electrical power produced by the generator to mechanical power available at turbine-generator shaft.

Gradually varied flow The flow in open channel when the change in depth occurs gradually over a comparatively long distance.

Hydraulic diameter The ratio of four times of area of cross-section to wetted perimeter of cross-section.

Hydraulic drop A type of rapidly varied flow in which there is a sudden drop in flow depth (depth falls below the *critical depth*).

Hydraulic efficiency The ratio of power developed by the turbine runner to power available at turbine inlet.

Hydraulic grade line The line drawn along the pipe, which represents the summation of pressure and datum heads.

Hydraulic jump A type of rapidly varied flow in which there is a sudden rise in flow depth (depth rises above the *critical depth*).

Hydraulic mean depth The ratio of cross-sectional area of a channel to its wetted-perimeter.

Hydraulically smooth and rough pipes They are classified on the basis of viscous sub-layer thickness and average internal surface roughness height. If the average roughness height exceeds the thickness of viscous sublayer, the pipe is termed as *hydraulically rough* whereas if average roughness height is less than the thickness of viscous it is termed as *hydraulically smooth*.

Ideal fluid The fluid which has constant density (incompressible) and zero viscosity (non-viscous/inviscid). No fluid is an ideal fluid as every fluid has got viscosity. Liquids are more viscous than gases.

Ideal gas A gas that follows ideal gas law. No gas is an ideal gas.

Impulse function Defined as the sum of pressure force and inertia force. The difference in impulse functions at the exit and the entrance of a duct is known as *thrust*.

Impulse turbine Works on the impulse (impact) of jet impinging the buckets mounted on the runner periphery causing it to rotate.

Incompressible flow The flow in which there is no change in density of fluid. In general, the flow of incompressible fluids (liquids) is incompressible flow. However, at low Mach numbers ($M < 0.3$), even the flow of compressible fluids (gases) is considered incompressible.

Internal flow The flow which takes place in the region enclosed by solid surface for example, flow inside the pipes, ducts, and closed conduits.

Intensive property This property is independent of mass of the system, for example, temperature, pressure, and density. Intensity property is equal to extensive property per unit mass.

Irreversible process The process in which a system and its surroundings cannot be restored to its initial state. There are certain physical characteristics which make the flows irreversible and they are known as irreversibilites for example, friction, heat transfer through a finite temperature difference, and occurrence of shock wave during the flow.

Isenthalpic process Constant enthalpy process.

Isentropic process Constant entropy process. It is also known as reversible adiabatic process.

Isobaric process Constant pressure process.

Isochoric process Constant volume process.

Isolated system A system which is completely isolated with no mass or energy interactions taking place with the surroundings.

Isothermal process Constant temperature process.

Kelvin–Planck statement *It is impossible for a device to operate in a cycle receiving heat from a source and converting it to an equal amount of work*. Kelvin–Planck statement forms the basis for the working of heat engines.

Kinematics This deals with motion only, which is characterized by velocity or/and acceleration.

Kinetics This also takes care of forces that cause motion.

Knudsen number Defined as the ratio of mean free path of molecules to the characteristic dimension of the flow channel. Its value ascertains whether to treat fluid as a *continuum* (continuous medium) or not. If $Kn < 0.01$, the fluid can be treated as continuum whereas for $Kn > 10$, the flow is considered as free molecular flow.

Lagrangian approach This approach disregards concept of fluid as a continuum. The individual fluid particles are tracked and the fluid motion is defined by means of their positions and velocity vectors.

Laminar flow Highly ordered flow that is perceived as the movement of lamina (thin planes) one over another. The effect of viscous forces

is predominant over inertia forces and as such the value of Reynolds number is small.

Lift coefficient The ratio of lift force to dynamic force (dynamic pressure times frontal area).

Linear momentum conservation principle This is the same as *Newton's second law of motion* which states that the rate of change of linear momentum of a body is directly proportional to net force applied on it. In fluids, the equation which represents the momentum conservation principle is the *Navier–Stokes equation*.

Mach number Defined as the ratio of fluid velocity to sound velocity in that medium. It is also defined as the square root of the ratio of inertia force to elastic force.

Mach number of second kind Defined as the ratio of fluid velocity to the critical fluid or sound velocity.

Magnus effect The lateral force experienced by a rotating body in a flow stream. It can be observed in the deviation of trajectories of the spinning balls in table tennis, cricket, football, etc.

Major loss in pipes The main loss in fluid pressure due to friction in closed conduits or pipes. It is computed using *Darcy–Weisbach equation*.

Manometer The simplest of pressure measuring devices. It employs a liquid column in a glass tube and a graduated scale to measure the difference in pressure between any two points.

Mass conservation principle This principle states that mass of a system is conserved (constant). In a control volume, entering mass flow rate is equal to the sum of rate of mass accumulation and mass leaving it. The equation which represents the mass conservation principle is the *continuity equation*.

Matter Defined as anything that has mass and occupies space. Matter exists in two forms viz. solids and fluids (liquids and gases).

Mechanical efficiency The ratio of power available at the shaft to the power developed by the runner.

Mechanical equilibrium The equilibrium of forces, which means forces within the system must be balanced (net force within the system is zero).

Mechanics A field of physics that deals with the motion of bodies caused due to the action of forces. It has two sub-categories—*statics* and *dynamics*.

Metacentre The point of intersection of the normal axis of floating body and the line action of buoyancy force when it is tilted.

Minor losses in pipes Small losses in fluid pressure in a pipe due to bends, fittings, sudden expansion, sudden contraction, entry and exit.

Model The scale down or scaled up geometric replica of the actual system (prototype).

Momentum thickness The measure of momentum deficit within boundary layer region.

Net positive suction head Defined as the available suction head at pump inlet above the head corresponding to vapour pressure

Newton's law of viscosity States that in a fluid shear stress is directly proportional to strain rate. The constant of proportionality is known as *dynamic viscosity*. This law is equivalent to *Hooke's law* in solids which states that stress is directly proportional strain.

Newtonian fluids The fluids which follow Newton's law of viscosity.

Non-Newtonian fluids The fluids which do not follow the Newton's law of viscosity. *Psuedoplastics*, *dilatants*, *viscoplastics*, and *bingham plastics* are different categories of non-Newtonian fluids.

Non-uniform flow The flow in which the velocity does not remain the same at every point at a given instant.

Normal stress The normal component of applied force per unit area. It is also known as *pressure*.

No-slip condition This implies that there exists no slip (relative motion) between the fluid and the solid surface at the point of contact.

Open system or control volume This is a system that allows both mass and energy exchange to take place across its boundary. Volume of an open system is generally fixed; hence the name.

Overall efficiency This is the efficiency of overall turbine-generator system which can be obtained by dividing the power output of generator to the power input to turbine. It can also be obtained by multiplying all the efficiencies viz. hydraulic, mechanical, electrical, and volumetric efficiencies.

Pascal's law States that at a point, a static fluid exerts equal pressure in all directions. In other words, if the pressure is increased at any point, there is an increase in pressure by the same amount at every other point in the container.

Pathline Path traced by an individual fluid particle.

Perfect gas An ideal gas which has constant specific heat at all temperatures.

Piezometer A special type of manometer with one-end open to the atmosphere and other connected to a system containing a non-volatile pressurized liquid.

Positive displacement pump This has a mechanical member which activates the fluid to high pressure. It has an arrangement which makes sure that once the flow is pumped out of the casing it cannot return, that is, there is no flow reversal. The fluid volume is, thus, positively displaced. Examples are reciprocating pump, gear pump, screw pump, peristaltic pump, rotary vane pump, etc.

Potential flow The flow of ideal fluids. The name is derived from the velocity potential functions defined for different types of irrotational 2D flows.

Prandtl mixing length The distance travelled by a fluid particle across the flow stream before it loses its momentum and becomes a part of the bulk flow stream.

Pressure coefficient The ratio of pressure difference between a point on a solid surface and free stream to the dynamic pressure. It gives the pressure distribution over a solid surface in a flow stream.

Pressure drag or form drag The drag due to pressure difference across a curved body in the flow direction (see *boundary layer separation* and *d'Alembert's paradox*).

Pressure This is defined as the normal force per unit area. From kinetic theory of gases, it is also defined as the net force exerted by the molecules of a gas striking the walls of its container.

Principle of dimensional homogeneity States that dimensions of each term in an equation must be the same.

Process The change in state of a system.

Property It is the characteristic of a system. There are two types of properties namely *intensive property* and *extensive property*.

Prototype The actual system.

Rapidly varied flow The flow in open channel when the depth changes abruptly in a short distance along the channel length.

Rarefaction wave The wave which is at a lower pressure than the fluid medium in which it is propagating.

Rayleigh flow The flow accompanied with heat transfer in a constant area frictionless duct.

Reaction turbine Works on the principle of reaction of water jet. The leaving water jet causes a reaction on runner blades making it to rotate. Nonetheless, reaction turbines used for the production of electric power works partly on reaction and partly utilizes the impulsive action of the flow stream.

Reversible process The process in which both a system and its surroundings can be restored to its initial state. No real process is reversible in nature.

Reynolds number Defined as the ratio of inertia forced to viscous force. Its value ascertains whether the flow is *laminar* or *turbulent*. In a pipe flow the value of critical Reynolds number is 2,300 whereas for the flow over flat plate its value is 5×10^5.

Reynolds transport theorem A tool that relates a change in the extensive property in a system to the change in the corresponding intensive property for the control volume.

Rotodynamic pump or non-positive displacement pump The pump in which the dynamic action of rotating fluid element increases the pressure energy of water. The flow reversal may occur at some place inside the pump. The example is centrifugal pump.

Second law of thermodynamics Establishes that not all the heat energy can be converted to work. Some heat has to be rejected to the sink (unavailable energy). Its consequence is a property known as *entropy*, which is also known as the index of unavailable energy.

Semi-perfect gas An ideal gas having specific heats as some function of temperature.

Shock A highly localized irreversibility in a compressible flow as the flow undergoes a transition from supersonic flow regime to subsonic flow regime. They are characterized by sudden rise in pressure.

Shock strength Defined as the ratio of rise in pressure to the pressure upstream of the shock.

Similitude Defined as complete similarity (geometric, kinematic, and dynamic) between a model and its prototype.

Skin friction coefficient The ratio of wall shear stress to dynamic pressure.

Skin friction drag The drag due to viscous boundary layer formation over a body.

Slip Slip in a reciprocating pump is defined as the difference between the theoretical and actual discharge. It is due to leakage loss and time delay in opening and closing of the valves. Slip can be *negative* also if delivery pipe is short, suction pipe is long, and the pump is running at a very high speed.

Specific energy The total head or total energy per unit specific weight above the channel bed. For the uniform flow, in which there is no variation in depth along the channel length specific energy remains constant throughout the channel. For non-uniform or varied flow, if depth changes along the channel length, the specific energy varies accordingly.

Specific gravity Specific gravity of a fluid is defined as the ratio of density of a given fluid to that of a standard fluid at a specified condition. For liquids, the standard fluid is water having density 1,000 kg/m^3 at 4°C and for gases, the standard fluid is air having density 1.2 kg/m^3 at 20°C temperature and 1 atm pressure.

Specific heat The heat storage capacity of a material. It is defined as the amount of heat required to raise the temperature of unit mass of a substance by 1°C.

Specific speed Specific speed of a turbine is the speed of a geometrically similar turbine which produces unit power while operating under unit head.

Specific speed of a pump is the speed of a geometrically similar pump which delivers unit discharge at unit head.

Specific volume The reciprocal of density.

Specific weight Defined as the weight of unit volume of a substance.

Stability Defined as the tendency of a body to regain its original position after given a small tilt. If a body could not return to its original position instead topple is said to be *unstable*. If a body is stable at any tilt angle, it is said to be under *neutral equilibrium*. The stability criterion of fully submerged bodies differs from that of floating bodies. A submerged body is in stable equilibrium if *centre of gravity* lies below *centre of buoyancy* whereas in case of floating bodies, stability is achieved if *metacentre* lies above *centre of gravity*.

Stagnation condition The state of a fluid which is brought to rest isentropically.

Stagnation point The point of maximum pressure and zero velocity for the fluid flowing over a solid body.

Stalling A phenomenon associated with airfoils which is characterized by a sudden reduction in lift coefficient and large increase in drag as the *angle of attack* attains a large value. This happens due to the flow separation from the upper surface of the airfoil leading to the formation of large low pressure wake in the rear portion of the airfoil.

State Defined as the condition of a system described by its particular set of properties. Only one property is needed to fix the state of a pure substance when it is saturated; otherwise at least two properties are needed to fix the state of a pure substance if it is not saturated.

Statics Deals with stationary bodies or bodies at rest.

Steady flow The flow in which the fluid properties at a point do not change with time.

Streakline The line obtained by joining the current location of all the fluid particles that have passed through a fixed point in space.

Streamline This is tangential to the direction of flowing stream. The tangent drawn at any point on it gives the direction of velocity vector. Streamline is the line of constant *stream function*.

Stress Defined as the force per unit area. Physically, it is resistance offered by the material to the applied force. In the absence of applied force, material will have no stress.

Subcritical or tranquil flow A type of open channel flow where *Froude number* is less than unity.

Subsonic flow The flow at Mach numbers less than unity.

Supercritical flow A type of open channel flow where *Froude number* is greater than unity.

Supersonic flow The flow at Mach numbers greater than unity.

Surface tension The magnitude of pulling force per unit length at the solid-fluid/fluid-fluid interface.

System Defined as the part of universe consisting of a quantity of matter or region which is under investigation. Everything outside the system is *surroundings*. *System boundary* is the imaginary or real surface that separates system from its surroundings. There are three types of *systems*, viz. *closed system* (also referred as *system*) or *control mass*, *open system* or *control volume*, and *isolated system*.

Tangential stress The tangential component of force per unit area. It is also known as shear stress.

Thermal equilibrium The equilibrium of temperature, that is temperature of the system is same throughout.

Thermodynamic equilibrium This is the equilibrium of temperature, forces, and chemical composition of a system. Thermodynamic equilibrium is achieved when the system is in thermal, mechanical and chemical equilibria.

Third law of thermodynamics This gives the reference datum for entropy. It says that entropy of a perfect crystal is zero at absolute zero temperature.

Timeline The line obtained by joining the location of same set of fluid particles at any instant of time.

Total drag The sum of skin friction drag and pressure drag.

Transmission efficiency Transmission efficiency of a pipeline is the ratio of fluid power available at outlet to the power available at inlet. Maximum transmission efficiency of any pipeline is 66.67%.

Turbulent flow Chaotic or disordered flow where it is difficult to predict the motion of individual fluid particles. The motion is purely random as the effect of inertia forces is pretty high. Thus, it occurs at high value of Reynolds number.

Uniform flow The flow in which magnitude and direction of fluid velocity is same at every point in a flow field at a given instant. It occurs inside open channels where the flow cross-section and channel-bed slope are constant.

Unit quantities These play an important role in predicting the performance of a turbine operating under the heads other than the design head on the assumption that efficiency remains constant.

Unsteady or transient flow The flow in which there is variation in fluid properties with time.

Vacuum pressure The pressure below atmospheric pressure. It is also known as *negative* pressure. It is the pressure indicated by vacuum gauge.

Vapour pressure The pressure exerted by the vapour collected above the liquid surface in a closed container. The vapour pressure corresponding to the dynamic equilibrium is known as *saturation pressure*. For a pure substance, the two are same.

Varied flow This occurs inside open channels where the flow cross-section does not remain constant.

Velocity coefficient The ratio of jet velocity at vena contracta to the theoretical velocity of the jet.

Vena-contracta The area corresponding to the least flow cross-section.

Ventilation A technique to avoid the formation of low pressure region in the immediate downstream of the notch/weir with the help of tubes which allow the atmospheric air to fill the low pressure region.

Viscosity The internal resistance of the fluid to motion. There are two types of viscosities, namely dynamic viscosity and kinematic viscosity. *Dynamic viscosity* is the ratio of shear stress to shear strain rate. *Kinematic viscosity* is the ratio of dynamic viscosity to density. It is a measure of rate of momentum diffusion through the fluid.

Viscous or laminar sublayer A very thin viscous region within the turbulent boundary layer near the solid surface. In this layer, there is a sudden transition in fluid velocity and velocity profile may comfortably be assumed linear due to its small thickness.

Volumetric efficiency The ratio of actual discharge to the total discharge. Some of the water may not come in contact with the runner blades and goes to the sump untouched.

Vorticity Defined as the *curl* of velocity vector, which is equal to the twice of angular velocity.

Water hammer or hydraulic shock The sudden and transient increase in pressure due to an abrupt change in fluid velocity in pipe systems.

Weber number The square root of the ratio of inertia force to surface tension force.

Zeroeth law of thermodynamics This law states that if two bodies are in thermal equilibrium with a third body, all the bodies will be in thermal equilibrium. This law forms the basis of temperature measurement (thermometry).

INDEX

Index Terms	Links	
A		
Adverse pressure gradient	240	
Air vessels	516	
Airfoil	248	251
Alternate depths	348	
Angle of attack	247	251
Angular momentum conservation principle	164	
B		
Backwater curve	352	
Bazin formula	361	
Bernoulli's equation	178	180
Blade curvature	508	
Backward curved blade	508	
Forward curved blade	508	
Radial blade	508	
Blasius equation	225	
Bluff body	249	
Boundary layer	3	
Boundary layer thickness	213	
Displacement thickness	214	
Energy thickness	215	
Momentum thickness	215	
Boyle's law	383	
Bucket friction coefficient	473	
Buckingham-pi theorem	551	

Index Terms | Links

Index Terms	Links		
Buoyancy	68		
Archimedes' principle	68		
Bouyant force	68		
Centre of buoyancy	71		
Metacentre	71		
Metacentric height	72	73	

C

Index Terms	Links		
Calibration	44		
Carnot cycle	389		
Cavitation	507		
Centre of gravity	55		
Centre of pressure	55		
Centrifugal pump	500		
Channel-bed slope	352		
Critical	352		
Mild	352		
Steep	352		
Charles' law	383		
Chezy equation	340		
Choked flow	421		
Circulation	111		
Clausius statement	388		
Coefficient of pressure	130	133	405
Coefficient of velocity	473		
Compressibility factor	383		
Compressible flows	396		
Hypersonic	396		
Sonic	396		
Subsonic	396		
Supersonic	396		
Transonic	396		

Index Terms	Links	
Compression wave	393	
Computational fluid dynamics	21	
Finite difference method	22	
Finite element method	23	
Finite volume method	22	
Constriction meters	296	
Flow nozzle or nozzle meter	300	
Orificemeter	300	
Venturimeter	297	
Continuity equation	112	
Contraction coefficient	276	306
Control volume	150	
Coriolis flow meter	305	
Couette flow	188	
Critical depth	348	
Critical flow	336	349
Critical Mach number	446	
Critical Reynolds number	268	
Crocco number	402	

D

Index Terms	Links	
d'Alembert's paradox	133	245
Darcy–Weisbach equation	270	
Developing flow	264	
Dimension	548	
Discharge coefficient	299	307
Distorted models	565	
Draft tube	487	
Elbow type with varying cross-section	489	
Simple elbow type	489	
Straight type	488	

Index Terms	Links		
Drag	227	247	
Drag coefficient	249	447	
Pressure or form drag	245	249	
Skin friction coefficient	227		
Skin friction drag	246	249	
Drop-down curve	352		
E			
Eddies	266		
Eddy viscosity	267		
Efficiency	462		
Generator efficiency	463		
Hydraulic efficiency	462	473	
Manometric efficiency	508		
Mechanical efficiency	463	508	
Overall efficiency	463	508	
Volumetric efficiency	463		
Energy	384	385	
Energy conservation principle	168		
First law of thermodynamics	168		
Energy correction factor	196		
Energy grade line	291	338	
Enthalpy	386		
Entrance length	264		
Entropy	384	388	390
	391		
Equation of state	382		
Equilibrium	383		
Chemical	383		
Mechanical	383		
Thermal	383		
Thermodynamic	384		

Index Terms	**Links**	

Euler model law	562	
Euler turbine equation	468	
Euler’s equation	177	
Eulerian approach	97	98
Extensive property	150	
External flow	263	

F

Fanno flow	421	
Favourable pressure gradient	239	
Features of fluid motion	108	
Angular deformation	110	
Linear deformation	109	
Rotation	110	
Translation	108	
First area moment of inertia	56	
Flow lines	101	
Pathline	102	
Streakline	103	
Streamline	101	114
Timeline	104	
Flow net	116	
Flow ratio	473	
Flows	18	
Compressible	19	
External	20	
Incompressible	19	
Internal	20	
Inviscid	19	
Laminar	18	19
Multidimensional	20	
Non-uniform	20	

Index Terms	**Links**		
Flows (*Cont.*)			
One-dimensional	20		
Steady	20		
Subsonic	19		
Supersonic	19		
Three-dimensional	20		
Turbulent	18	19	
Two-dimensional	20		
Uniform	20		
Unsteady	20		
Viscous	19		
Fluid coupling	527		
Fluids	1	2	4
Newtonian	4		
Non-Newtonian	4	5	
Forced vortex	79		
Francis formula	361		
Francis turbine	478		
Friction equation	281		
Friction factor	194		
Froude model law	561		
Froude number	335	349	
Fully developed flow	264		

G

Gates	53	54
Gay-Lussac’s law	383	
Gravity driven	333	

H

Hagen–Poiseuille flow	191

Index Terms **Links**

Index Terms	Links	
Hardy Cross method	285	
Hooke’s law	2	
Hot-wire anemometer	304	
Hydraulic crane	526	
Hydraulic drop	354	
Hydraulic grade line	291	338
Hydraulic jump	354	
Hydraulic ram	526	
Hydraulic siphon	309	
Hydraulically rough surface	268	
Hydraulically smooth surface	268	
Hysteresis	42	

I

Ideal gas	383	
Ideal gas law	383	
Impulse function	409	
Impulse turbine	460	
Intensive property	150	
Internal energy	384	
Internal flow	263	

J

Joukowsky equation	312	

K

Kaplan turbine	483	
Kevin–Planck statement	388	
Knudsen number	3	

Index Terms **Links**

L

Lagrangian approach 97 98
Laminar boundary layer 213
Laminar flow 265 267
Laminar sublayer 265
Laws of thermodynamics 384
First law 384
Second law 388
Third law 391
Zeroth law 384
Lift 247
Lift coefficient 250
Lift and drag 136
Linear momentum conservation principle 154 164
Cauchy's equation 158
Generalized Hooke's law 156
Generalized stress tensor 157
Momentum equation 158
Newton's second law of motion 154 159
Newton's third law of motion 159
Pascal's law 156
Viscous stress tensor 156

M

Mach angle 397
Mach cone 396
Mach model law 562
Mach number 19 395
Mach number of second kind 401
Magnus effect 136
Major loss in a pipe 269

Index Terms	Links	

Manning equation	340	
Mass conservation principle	153	171
Continuity equation	153	172
Material acceleration	99	
Convective	99	
Local	99	
Material derivative	99	
Mean free path	3	
Mechanics	1	
Dynamics	1	
Kinematics	1	
Kinetics	1	
Statics	1	
Minor losses	272	
Entry loss	277	
Exit loss	275	
Loss due to sudden contraction	275	
Loss due to sudden expansion	272	
Losses in pipe fittings	278	
Momentum correction factor	197	
Moody chart	271	
Mouthpiece	307	

N

Navier–Stokes equation	176	
Newton's law of viscosity	2	
No slip condition	3	211
Non-Newtonian fluids	4	
Bingham plastic	5	
Dilatant	5	
Pseudoplastic	5	
Shear thickening fluid	5	

Index Terms	Links	

Non-Newtonian fluids (*Cont.*)
- Shear thinning fluid 5
- Viscoplastic 5

Non-positive displacement 500
Notches or Weirs 359
- Cippoletti weir 364
- Rectangular 360
- Stepped 362
- Suppressed weir 361
- Trapezoidal 363
- Triangular 362
- Unsuppressed weir 361

O

Optimum hydraulic cross-section 344
Orifice 306

P

Parshall fume 368
Particle Reynolds number 314
Pelton turbine 474
Perfect gas 383
Pipe resistance 281
Pitot-static tube 301
Point of separation 239 244
Positive displacement pump 500
Potential flow 120
- Blunt body 128
- Circular cylinder 131
- Doublet 125
- Rotating circular cylinder 134

Index Terms	**Links**		
Potential flow (*Cont.*)			
Sink flow	121		
Source flow	121		
Uniform flow	121		
Vortex flow	123		
Prandtl boundary layer equation	222		
Prandtl–Meyer equation	438		
Prandtl mixing length	268		
Pressure	35		
Absolute pressure	41		
Barometer	52		
Bellows type pressure gauge	42	43	
Bourdon tube pressure gauge	41	42	
Dead weight pressure tester	43		
Differential manometer	45		
Gauge pressure	41		
Hydrostatic pressure	39		
Inclined tube manometer	46	47	
Manometer	44		
Micromanometer	47		
Pascal's law	36		
Piezometer	44		
Vacuum pressure	41		
Pressure driven flow	263		
Priming	505		
Principle of dimensional homogeneity	546	549	
Process	382		
Adiabatic	382		
Cyclic	382	384	
Isenthalpic	382		
Isentropic	382	387	406
Isobaric	382		

Index Terms	**Links**
Process (*Cont.*)	
Isochoric	382
Isothermal	382
Reversible	382
Reversible adiabatic	382
Properties of fluids	6
Adhesion	13
Capillary effect	15
Cohesion	13
Contact angle	15
Density	7
Dynamic viscosity	10
Extensive property	6
Hydrophilic surface	15
Hydrophobic surface	15
Intensive property	6
Kinematic viscosity	10
Non-wetting surface	15
Saturation pressure	17
Specific gravity	7
Specific properties	7
Specific volume	7
Specific weight	8
Surface tension	13
Vapour pressure	17
Wetting surface	15
Pump affinity laws	513
First law	514
Second law	514
Pump heads	506
Centrifugal	507
Manometric	506

Pump heads (*Cont.*)
  Static 506
  Total 506

R

Rankine–Hugoniot equation 442
Rarefaction wave 393
Rayleigh flow 428
Rayleigh's indicial method 548
Reaction turbine 460 477
Reciprocating pump 516
  Double-acting 516
  Single-acting 516
Resistance coefficient 278
Reynolds experiment 104 144
Reynolds model law 561
Reynolds number 18
Reynolds stress 267
Reynolds transport theorem 150
Rotameter 303
Rotodynamic pump 500

S

Second area moment of inertia 56
Semi-perfect gas 383
Shock strength 443
Shock wave 435
  Attached 436
  Detached 436
  Normal 436
  Oblique 436

Index Terms	**Links**		
Shooting flow	336	350	
Similitude	559		
Dynamic similarity	561		
Geometric similarity	559		
Kinematic similarity	560		
Slip	517		
Slurry flow	314		
Colloidal dispersion	314		
Heterogeneous flow	314		
Homogeneous flow	314		
Pseudo-homogeneous flow	314		
Sound barrier	448		
Specific energy	337		
Specific heat	386		
Specific speed	461	493	504
Speed ratio	473		
Stability	69		
Neutral equilibrium	69		
Stable equilibrium	72		
Unstable equilibrium	69	72	
Stalling	250		
State	382		
Steady flow energy equation	386		
Steady uniform flow	334	335	
Steady varied flow	334		
Gradually varied flow	334	351	
Rapidly varied flow	334	354	
Stokes' theorem	111		
Stream function	114		
Streamlined body	245		
Subcritical flow	336	350	
Sudden contraction loss factor	276		

Index Terms	Links	
Sudden expansion loss factor	274	
Supercritical flow	336	350
System	6	150
Closed system	6	
Control mass	6	
Control volume	6	
Isolated system	6	
Open system	6	
Surroundings	6	
System boundary	6	
T		
Thrust	409	
Torque converter	529	
Tranquil flow	336	
Transmission efficiency	295	
Turbulent boundary layer	213	236
Turbulent flow	265	268
U		
Unit quantities	491	
Unit discharge	492	
Unit force	492	
Unit power	492	
Unit speed	491	
Unit torque	492	
Unsteady uniform flow	334	
Unsteady varied flow	334	
Gradually varied flow	334	
Rapidly varied flow	334	

Index Terms	**Links**	

V

Velocity coefficient	306	
Velocity potential function	115	
Equipotential lines	115	
Vena contracta	275	300
Venturi fume	365	
Viscous sub-layer	237	
Viscous sublayer	265	
von Karman momentum equation	231	
von Karman vortex street	244	
Vorticity	111	

W

Wake	244	
Water hammer	311	499
Weber model law	563	